3 February 2012 | $10

Science



2011 Visualization Challenge

AAAS

EDITORIAL

503 The Global Knowledge Society
Nina V. Fedoroff

NEWS OF THE WEEK

508 A roundup of the week's top stories

NEWS & ANALYSIS

512 The Limits of Avian Flu Studies in Ferrets
514 Donation Spurs a Cell Observatory—And Bigger Plans
515 Celebrated Exoplanet Vanishes in a Cloud of Dust—Or Maybe Not

NEWS FOCUS

516 China's Sequencing Powerhouse Comes of Age
520 Rebuilding Wetlands by Managing the Muddy Mississippi
522 Technology Is Turning U.S. Oil Around But Not the World's

SPECIAL FEATURE

525 2011 International Science & Engineering Visualization Challenge
>> For related online content, go to www.sciencemag.org/site/special/vis2011/; Science *Podcast*

LETTERS

537 Investing in Libya's Education
S. K. Sgaier
Invasive Species Unchecked by Climate
P. E. Hulme
Response
M. T. Burrows et al.
Proceed with Planning Despite Multiple Models
R. Dickinson
538 CORRECTIONS AND CLARIFICATIONS
538 TECHNICAL COMMENT ABSTRACTS

BOOKS *ET AL.*

540 American Anthrax
J. Guillemin, reviewed by D. A. Relman
541 Strings Attached
R. W. Grant, reviewed by T. Cowen

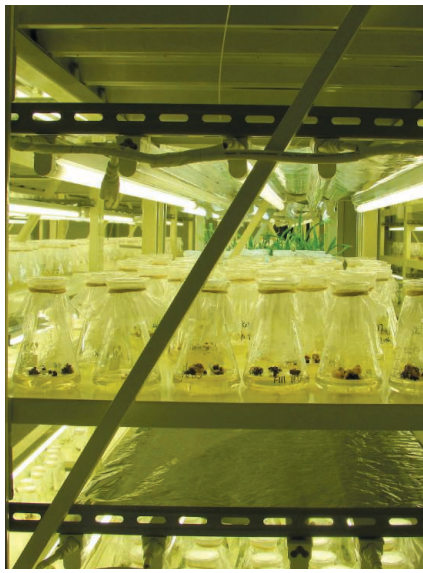
POLICY FORUM

542 Coercive Citation in Academic Publishing
A. W. Wilhite and E. A. Fong

PERSPECTIVES

544 Ready, Steady, Compete
M. C. Villeval
>> Report p. 579
545 Surviving in a Toxic World
A. J. Wolstenholme
>> Report p. 574
546 To Stop or Not to Stop?
N. D. Volkow and R. D. Baler
>> Report p. 601
548 Marching in Near Lock-Step
D. T. Rodbell
>> Report p. 570
549 Seeing the Superfluid Transition of a Gas
W. Zwerger
>> Report p. 564

CONTENTS continued >>



page 516



page 540



COVER

Computer illustration of streams of matter delineating the network of cosmic voids, each tens of millions of light years across. Matter accumulates where the voids meet, forming a cosmic web of walls, filaments, and clusters of galaxies. This illustration was awarded first place in the informational graphics category in the 2011 *Science*/NSF International Science & Engineering Visualization Challenge. The winning entries are featured in a special section starting on page 525 and at www.sciencemag.org/site/special/vis2011/.

Image: Miguel A. Aragon Calvo, Julieta Aguilera, Mark Subbarao

DEPARTMENTS

501 This Week in *Science*
504 Editors' Choice
506 *Science* Staff
605 New Products
606 *Science* Careers

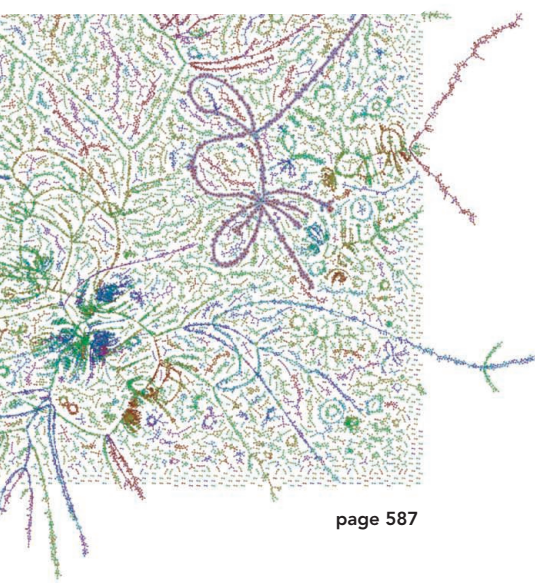
Published by AAAS



pages 546 & 601



pages 548 & 570



page 587

BREVIA

551 Nanoscopy in a Living Mouse Brain
S. Berning et al.
Super high-resolution microscopy resolves neuron dynamics in the cerebral cortex of a living mouse.

RESEARCH ARTICLES

552 High-Resolution View of the Yeast Meiotic Program Revealed by Ribosome Profiling
G. A. Brar et al.
During yeast sporulation, the production of most proteins is tightly regulated by both messenger RNA levels and translational control.

557 The Southern Ocean's Role in Carbon Exchange During the Last Deglaciation
A. Burke and L. F. Robinson
Radiocarbon measurements of deep-sea corals reveal the presence of old, carbon-rich water in the Southern Ocean.

REPORTS

561 Spin-Down of Radio Millisecond Pulsars at Genesis
T. M. Tauris
Numerical calculations show that processes responsible for spinning up millisecond pulsars may also lead them to slow down.

563 Revealing the Superfluid Lambda Transition in the Universal Thermodynamics of a Unitary Fermi Gas
M. J. H. Ku et al.
Thermodynamic quantities for the superfluid transition of a strongly interacting atomic Fermi gas were measured.
>> *Perspective p. 549*

567 Iron Catalysts for Selective Anti-Markovnikov Alkene Hydrosilylation Using Tertiary Silanes
A. M. Tondreau et al.
Iron catalysts offer a potentially cheaper route than platinum for certain commercially useful carbon-silicon compounds.

570 High-Latitude Forcing of the South American Summer Monsoon During the Last Glacial
L. C. Kanner et al.
High-latitude processes in the Northern and Southern Hemispheres both influence the South American Summer Monsoon.
>> *Perspective p. 548*

574 Natural Variation in a Chloride Channel Subunit Confers Avermectin Resistance in *C. elegans*
R. Ghosh et al.
Resistance to avermectin, an anti-nematode drug, is conferred by a deletion in a glutamate-gated chloride channel.
>> *Perspective p. 545*

579 Affirmative Action Policies Promote Women and Do Not Harm Efficiency in the Laboratory
L. Balafoutas and M. Sutter
Increasing the representation of competition-averse individuals does not alter overall output.
>> *Perspective p. 544*

582 Female Leadership Raises Aspirations and Educational Attainment for Girls: A Policy Experiment in India
L. Beaman et al.
The effects of female leaders on girls occur via policy changes in the short run and parental aspirations in the longer run.

587 Untangling Genomes from Metagenomes: Revealing an Uncultured Class of Marine Euryarchaeota
V. Iverson et al.
Reconstruction of whole genomes from a complex microbial community has revealed an evolutionary surprise.

590 Sequential Signaling Crosstalk Regulates Endomesoderm Segregation in Sea Urchin Embryos
A. J. Sethi et al.
Separation of deuterostome endoderm and mesoderm occurs through sequential interactions between Notch and Wnt signaling.

593 Growth of Western Australian Corals in the Anthropocene
T. F. Cooper et al.
Cores taken from massive corals indicate that temperature rather than ocean acidification has governed reef growth.
>> Science *Podcast*

597 Innate Response Activator B Cells Protect Against Microbial Sepsis
P. J. Rauch et al.
A specialized population of B lymphocytes is important for controlling bacterial infections and preventing sepsis.

601 Abnormal Brain Structure Implicated in Stimulant Drug Addiction
K. D. Ersche et al.
A neurological marker of addiction vulnerability occurs in sibling pairs who do not take drugs.
>> *Perspective p. 546*; Science *Podcast*

Published by AAAS

SCIENCEONLINE

SCIENCEXPRESS

www.sciencexpress.org

Field-Effect Tunneling Transistor Based on Vertical Graphene Heterostructures
L. Britnell et al.
Boron nitride or molybdenum disulfide layers sandwiched between graphene sheets act as tunneling barriers to minimize device leakage currents.
10.1126/science.1218461

Extremely Long-Lived Nuclear Pore Proteins in the Rat Brain
J. N. Savas et al.
Individual components of rat brain nuclear pores can be almost as old as the animal itself.
10.1126/science.1217421

ER Cargo Properties Specify a Requirement for COPII Coat Rigidity Mediated by Sec13p
A. Čopič et al.
Membrane curvature of cellular vesicles is generated by altering the symmetry of the cargo and the rigidity of coat proteins.
10.1126/science.1215909

Pollinator-Mediated Selection on Flower Color Allele Drives Reinforcement
R. Hopkins and M. D. Rausher
Butterfly behavior reduces hybridization and reinforces speciation among *Phlox* plants.
10.1126/science.1215198

Founder Effects Persist Despite Adaptive Differentiation: A Field Experiment with Lizards
J. J. Kolbe et al.
Introduced populations of anoles retain characteristics of their founders and acquire adaptations to their new environment.
10.1126/science.1209566

Adaptations of Avian Flu Virus Are a Cause for Concern
K. I. Berns et al.
10.1126/science.1217994

TECHNICALCOMMENTS

Comment on "Abiotic Pyrite Formation Produces a Large Fe Isotope Fractionation"
A. D. Czaja et al.
Full text at www.sciencemag.org/cgi/content/full/335/6068/538-c

Response to Comment on "Abiotic Pyrite Formation Produces a Large Fe Isotope Fractionation"
R. Guilbaud et al.
Full text at www.sciencemag.org/cgi/content/full/335/6068/538-d

SCIENCENOW

www.sciencenow.org

Highlights From Our Daily News Coverage

North Star May Be Wasting Away
Polaris could be casting off the equivalent of Earth's mass every year, observations suggest.
http://scim.ag/North_Star

Breaking the Law or Bending the Terminology?
One team of physicists skirts a fundamental limit on a phenomenon called diffraction—sort of.
http://scim.ag/Law_Diffraction

Killer Whale Menu Finally Revealed
Inuit hunters provide a glimpse of what these giant predators eat in the remote Arctic.
http://scim.ag/Killer_Whales

SCIENCESIGNALING

www.sciencesignaling.org

The Signal Transduction Knowledge Environment

31 January issue: http://scim.ag/ss013112

RESEARCH ARTICLE: PAS Kinase Promotes Cell Survival and Growth Through Activation of Rho1
C. M. Cardon et al.

PODCAST
J. Rutter and A. M. VanHook
Signaling through PAS kinases bypasses the pro-growth requirement of Tor2 in yeast.

RESEARCH ARTICLE: Myosin I Links PIP_3 Signaling to Remodeling of the Actin Cytoskeleton in Chemotaxis
C.-L. Chen et al.
Some myosin motor proteins use the phospholipid PIP_3 to link membrane and cytoskeletal dynamics.

ST NETWATCH: Mouse Genome Informatics
This site includes information about genes, phenotypes, and disease models.

SCIENCETRANSLATIONAL MEDICINE

www.sciencetranslationalmedicine.org

Integrating Medicine and Science

1 February issue: http://scim.ag/stm020112

RESEARCH ARTICLE: Massage Therapy Attenuates Inflammatory Signaling After Exercise-Induced Muscle Damage
J. D. Crane et al.
Massage abrogates inflammatory processes resulting from exercise-induced muscle damage.

RESEARCH ARTICLE: CXCL12-Induced Monocyte-Endothelial Interactions Promote Lymphocyte Transmigration Across an in Vitro Blood-Brain Barrier
S. Man et al.
In an in vitro model of the human blood-brain barrier, chemokine receptors regulate the transmigration of leukocytes.

REPORT: The Anti-Trypanosome Drug Fexinidazole Shows Potential for Treating Visceral Leishmaniasis
S. Wyllie et al.
Fexinidazole, a drug in clinical testing for African sleeping sickness, may prove useful for another neglected tropical disease.

MEETING REPORT: Using Health Information Technology to Engage Communities
L. K. Marriott et al.
The Internet can be used for personal health management and to facilitate partnerships and data-sharing in a community setting.

MEETING REPORT: Real-Time Assessment of Community Health Needs and Concerns
L. B. Cottler and R. Nagarajan
Interfacing the efforts of community health workers with Web-based systems will facilitate ongoing assessment of community needs.

MEETING REPORT: Meaningful Use of Electronic Behavioral Health Data in Primary Health Care
B. Tai et al.
Treatment of mental health and substance abuse issues requires the delivery of services through a primary-care–based integrated system.

MEETING REPORT: Geomapping Health-Related Data
S. Sayani
Geographical information systems can be used to analyze health data and drive improvements.

SCIENCECAREERS

www.sciencecareers.org/career_magazine

Free Career Resources for Scientists

The America Invents Act for Academic Scientists
J. Austin
Here is what academic scientists need to know about the biggest change to U.S. patent law in 60 years.
http://scim.ag/AmericaInvents

Game On: Education as Play
D. Strain
Game designer and former biologist Jeremy Friedberg won an honorable mention in this year's Science and Engineering Visualization Challenge.
http://scim.ag/JeremyFriedberg

Content Collection: Mentoring Advice
E. Pain
A good mentor at each career stage can greatly enhance your professional and personal achievement.
http://scim.ag/CC_Mentoring

SCIENCEPODCAST

www.sciencemag.org/multimedia/podcast

Free Weekly Show

On the 3 February *Science* Podcast: how corals respond to climate change, inherited factors for drug addiction, 2011 Visualization Challenge winners, and more.

SCIENCEINSIDER

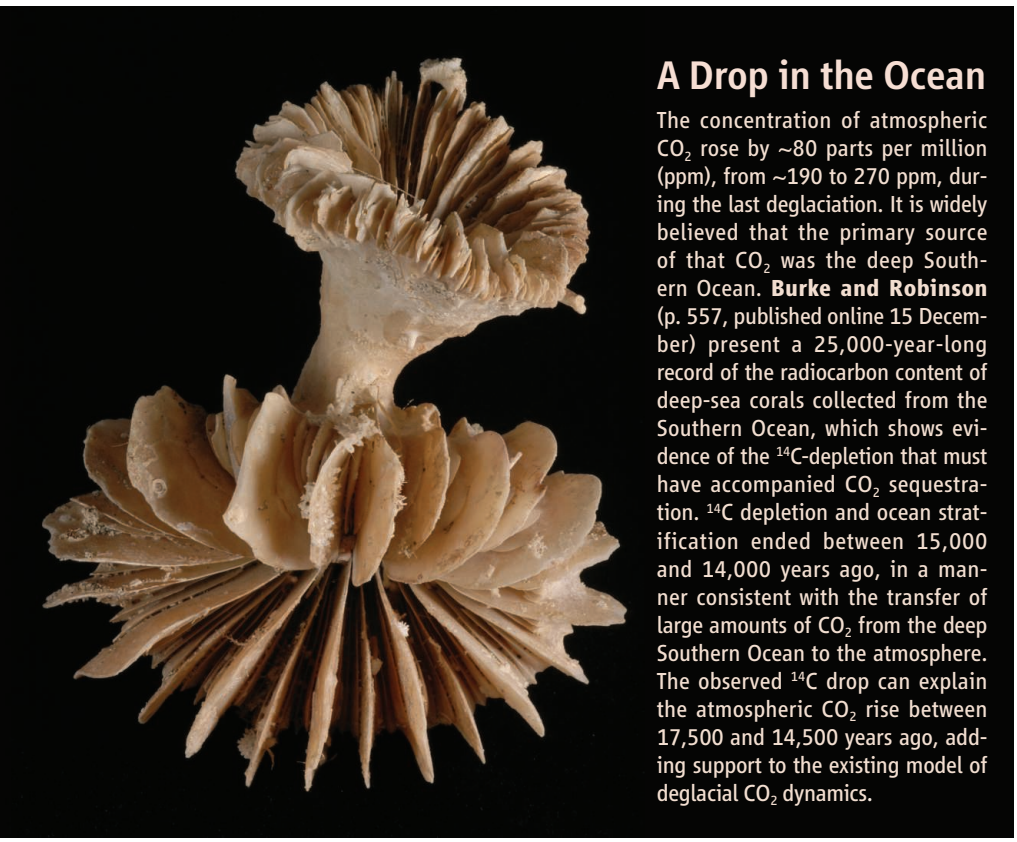
news.sciencemag.org/scienceinsider

Science Policy News and Analysis

SCIENCE (ISSN 0036-8075) is published weekly on Friday, except the last week in December, by the American Association for the Advancement of Science, 1200 New York Avenue, NW, Washington, DC 20005. Periodicals Mail postage (publication No. 484460) paid at Washington, DC, and additional mailing offices. Copyright © 2012 by the American Association for the Advancement of Science. The title SCIENCE is a registered trademark of the AAAS. Domestic individual membership and subscription (51 issues): $149 ($74 allocated to subscription). Domestic institutional subscription (51 issues): $990; Foreign postage extra: Mexico, Caribbean (surface mail) $55; other countries (air assist delivery) $85. First class, airmail, student, and emeritus rates on request. Canadian rates with GST available upon request, GST #1254 88122. Publications Mail Agreement Number 1069624. **Printed in the U.S.A.**

Change of address: Allow 4 weeks, giving old and new addresses and 8-digit account number. **Postmaster:** Send change of address to AAAS, P.O. Box 96178, Washington, DC 20090–6178. **Single-copy sales:** $10.00 current issue, $15.00 back issue prepaid includes surface postage; bulk rates on request. **Authorization to photocopy** material for internal or personal use under circumstances not falling within the fair use provisions of the Copyright Act is granted by AAAS to libraries and other users registered with the Copyright Clearance Center (CCC) Transactional Reporting Service, provided that $30.00 per article is paid directly to CCC, 222 Rosewood Drive, Danvers, MA 01923. The identification code for *Science* is 0036-8075. *Science* is indexed in the *Reader's Guide to Periodical Literature* and in several specialized indexes.

AAAS
ADVANCING SCIENCE, SERVING SOCIETY



A Drop in the Ocean

The concentration of atmospheric CO_2 rose by ~80 parts per million (ppm), from ~190 to 270 ppm, during the last deglaciation. It is widely believed that the primary source of that CO_2 was the deep Southern Ocean. **Burke and Robinson** (p. 557, published online 15 December) present a 25,000-year-long record of the radiocarbon content of deep-sea corals collected from the Southern Ocean, which shows evidence of the ^{14}C-depletion that must have accompanied CO_2 sequestration. ^{14}C depletion and ocean stratification ended between 15,000 and 14,000 years ago, in a manner consistent with the transfer of large amounts of CO_2 from the deep Southern Ocean to the atmosphere. The observed ^{14}C drop can explain the atmospheric CO_2 rise between 17,500 and 14,500 years ago, adding support to the existing model of deglacial CO_2 dynamics.

Monitoring Meiosis

During meiosis, or in yeast sporulation, haploid cells are generated from diploid cells. **Brar *et al.*** (p. 552, published online 22 December) performed a detailed analysis of messenger RNA (mRNA) abundance and protein synthesis over the course of sporulation. The production of most proteins was tightly regulated both at the mRNA level and by translational control. An unexpected complexity was observed as the cell passed through this key developmental transition, including increases in noncanonical translation from upstream regions of known RNA transcripts, which appear to be important in translational control.

Nailing Down the Superfluid Transition

A gas of fermions, the class of particle that protons, neutrons, and electrons belong to, can be found in contexts as different as neutron stars and a block of metal. When the interaction between fermions is on the brink of forming fermion pairs, the thermodynamics of the gas become dependent only on the gas temperature and density. **Ku *et al.*** (p. 563, published online 12 January; see the Perspective by **Zwerger**) measured this universal thermodynamics with high precision in an ultracold Fermi gas, observing the predicted transition into a superfluid state through the characteristic lambda-shaped transition in the gas's specific heat.

Probing Pulsar Rotation

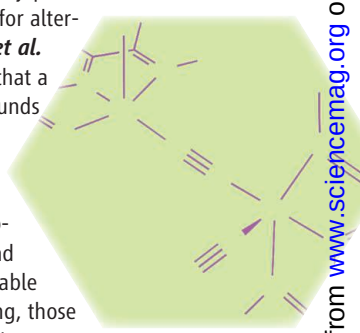
Pulsars are strongly magnetized, rapidly rotating neutron stars. Those with periods of the order of milliseconds obtain their fast spin by accreting mass from a companion star in a binary system. **Tauris** (p. 561) combined numerical stellar evolution calculations with a model of how accretion torques act on a neutron star. During the late accretion phase of millisecond pulsars, the termination stage of mass transfer results in a loss of more than 50% of their rotational energy. This effect may explain the observed pulsar spin distributions.

Monsoon Forcing

Dansgaard/Oeschger (D/O) events—the sudden, millennial-scale periods of warmth that punctuate the cold climate of the Last Glacial period, and Heinrich events—cold intervals characterized by tremendous discharges of icebergs into the North Atlantic, have been observed at many locations in the Northern Hemisphere but not extensively in the Southern Hemisphere. **Kanner *et al.*** (p. 570, published online 12 January; see the Perspective by **Rodbell**) present a stable isotope record from the central Peruvian Andes, which represents a record of the South American Summer Monsoon from 50,000 to 16,000 years ago and which contains the signals of D/O and Heinrich events. The Southern Hemisphere monsoon displayed an antiphase relationship to Northern Hemisphere monsoon intensity at the millennial scale, and Antarctic millennial-scale climate fluctuations influenced the South American Summer Monsoon.

An Iron Hand for Silicon

Carbon-silicon bonds are integral to the structure of the silicone materials widely used in adhesives, cosmetics, and numerous other industrial and consumer products. Generally, platinum-based catalysts have performed best in the hydrosilylation reactions that form these bonds, but the expense of the precious metal and, in some cases, by-product formation have motivated a search for alternatives. **Tondreau *et al.*** (p. 567) now show that a class of iron compounds readily catalyzes hydrosilylation of certain commercially important substrates with rates and selectivities comparable to, or even exceeding, those associated with platinum.



Girl Power

The potential of affirmative action policies to reduce overall outcomes because of lower individual performance has been discussed widely and at length. But do quotas or preferential treatment of applicants alter the pool of candidates? **Balafoutas and Sutter** (p. 579; see the Perspective by **Villeval**) used an existing laboratory-based task to assess the change in composition of winning candidates and the overall outcome as a function of three affirmative action policies. Policies designed to encourage more women to enter a competitive environment served to recruit enough high-performing individuals to ensure that the efficiency in performing the task was preserved. **Beaman *et al.*** (p. 582, published online 12 January) examined the effects of a constitutionally mandated reservation of village-council and council-leader positions for women in West Bengal after two election cycles (1998 and 2003). The program appeared to narrow the gender gap in aspirations of parents for their

Continued on page 502

CREDITS (TOP TO BOTTOM): DANN BLACKWOOD/U.S. GEOLOGICAL SURVEY; TONDREAU *ET AL.*

Downloaded from www.sciencemag.org on February 2, 2012

AAAS Travels

MONGOLIA
July 4-19, 2012
Discover expansive landscapes and the proud heritage of Mongolia. Explore the Orkhon Valley Cultural Lancscape, the Gun-Galuut Nature Reserve, and Gobi Desert, site of the Flaming Cliffs dinosaur site. Naadam Festival horse racing and activities will be a treat! $3,995 + air.



The Tibetan Plateau
July 22–August 7, 2012
Join us to explore the Top of the World this summer! Learn about rich cultural traditions, take the train across the Tibetan Plateau, and discover expansive natural areas, huge Pleistocene lakes, the cultural heart around Lhasa, wildlife, wildflowers and more! $4,195 + air.



For a detailed brochure, please call (800) 252-4910
All prices are per person twin share + air

Betchart Expeditions Inc.
17050 Montebello Road
Cupertino, California 95014
Email: AAASInfo@betchartexpeditions.com
www.betchartexpeditions.com



AAAS is here –
bringing educational infrastructure to the developing world.

AAAS is helping the Rwandan government rebuild its educational infrastructure. By providing materials such as the Project 2061 *Atlas of Science Literacy*, lesson plans from Science NetLinks, and access to *Science* digital libraries, AAAS is helping the people of Rwanda work toward a future built around science and technology. If you're not yet a AAAS member, join us. Together we can make a difference.

To learn more, visit
aaas.org/plusyou/rwanda

AAAS + U = Δ

Continued from page 501

children and of children for themselves; in addition, teenage girls spent more time in school and less on household chores. Beliefs and attitudes changed only after the second set of elections—that is, after a longer exposure to female role models—complementing the more rapid policy changes instituted by women council leaders after the first round of elections.

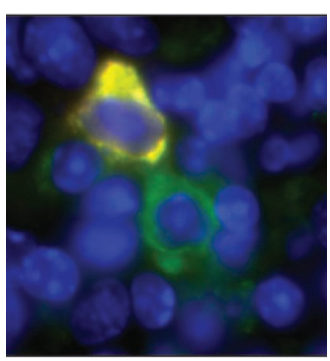
Mystery of an Unextreme Microbe

Metagenomics has given us glimpses into the huge diversity of microorganisms that are the engines of Earth's elemental cycling. These kinds of surveys can supply a good idea of the dominant organisms in ecosystems, but, because the majority of environmental microbes are difficult to culture and the most abundant organisms swamp metagenomes, it is difficult to discern the functional significance of other contributors. **Iverson *et al.*** (p. 587) sampled the Puget Sound and developed methods to reconstruct individual genomes from metagenomes, which allowed closure of a genome from the enigmatic marine group II *Euryarchaeota.* This Archaean is evidently motile, shows signs of extensive gene-swapping with bacteria, and offers some hints to the origin of proteorhodopsin—a molecule that some marine bacteria use to harvest energy from sunlight.

Heat or Acid?

The question of how tropical coral reefs will respond to increasing atmospheric greenhouse gas concentrations and concomitant climate change is widely debated. Model predictions and laboratory experiments suggest that decreasing carbonate saturation and decreasing pH may reduce calcification in carbonate-depositing organisms, including corals, yet field data are sparse, and recent declines in coral growth rates have been variously attributed to thermal stress or ocean acidification. **Cooper *et al.*** (p. 593) demonstrate that there has been no large-scale decline in calcification rates of massive *Porites* on coral reefs along the Indian Ocean coast of Western Australia. Instead, coral growth has increased significantly in the past 110 years, particularly at high latitudes. Thus, coral calcification appears to increase as ocean waters warm, but—at excessive temperatures—coral bleaching and reduced ocean carbonate saturation may lead to growth declines as observed on the Great Barrier Reef.

Immune Sentinels



A classic paradigm in immunology holds that the immune response occurs in two waves: Rapidly responding cells of the innate immune system help to contain the invading pathogen and alert lymphocytes. These cells of the adaptive immune system then help to clear the infection and go on to form long-lasting memory. However, some specialized populations of lymphocytes can also respond quickly to an infection and carry out functions that overlap with the innate immune system. Now, **Rauch *et al.*** (p. 597, published online 12 January) describe one such cell type—innate response activator (IRA) B cells. IRA B cells recognize bacterial liposaccharide through Toll-like receptor 4 and, in response, produce the cytokine GM-CSF, which activates other innate immune cells. Deletion of IRA B cells in mice impaired their ability to clear a bacterial infection and promoted septic shock.

Nature or Drug Abuse?

There are significant structural changes in striatal and prefrontal brain regions of stimulant drug-dependent individuals. However, it is not clear if these brain abnormalities predate drug-taking, rendering individuals vulnerable for the development of dependence, or if these changes are the effect of many years of drug use. **Ersche *et al.*** (p. 601; see the Perpective by **Volkow and Baler**) investigated brain abnormalities in both drug-dependent individuals and in their biological siblings who have never taken drugs of abuse and compared them with matched healthy volunteers. The brain abnormalities in the sibling pairs were associated with significant impairments in the regulation of behavior; an ability known to be compromised in drug dependence. Because these neural changes were observed in family members who do not take drugs, the changes are likely to represent neurological markers of vulnerability to addiction rather than consequences of chronic drug abuse.

CREDIT: RAUCH *ET AL.*

Downloaded from www.sciencemag.org on February 2, 2012



Nina V. Fedoroff is the president of AAAS, a Distinguished Professor of Biosciences at the King Abdullah University of Science and Technology in Saudi Arabia, and an Evan Pugh Professor at The Pennsylvania State University.

The Global Knowledge Society

KNOWLEDGE SOCIETIES REST ON A FOUNDATION OF EDUCATIONAL AND RESEARCH EXCELLENCE. The Internet, advances in communications technology, and the rapidly expanding global fiber optic network are necessary, but not sufficient. It takes people to train, to educate, to collaborate, and to innovate. Building the global knowledge society is the theme of the 2012 American Association for the Advancement of Science (AAAS) Annual Meeting in Vancouver (16 to 22 February). Bringing together scientists and educators from more than 50 nations, the meeting tackles global issues and new ways of building connections between developed and developing nations.

Science and technology have long figured in the efforts of societies to gain military advantage. Archimedes invented the defensive engines and burning glasses used to ward off the Roman attack on Syracuse in 214 BC. Leonardo da Vinci and Michelangelo were military engineers; Napoleon Bonaparte viewed himself as a scientist. Abraham Lincoln established the U.S. National Academy of Sciences during the Civil War in part to provide advice on military matters.



The emergence of scientists as peacemakers and diplomats is recent. Ongoing meetings between top Soviet and U.S. scientists are often credited with keeping the Cold War cold. Presaging the establishment of formal diplomatic relations, U.S. Presidential Science Advisor Frank Press traveled to China in 1978 to negotiate an Agreement for Cooperation in Science and Technology, signed by President Carter and Chinese leader Deng Xiaoping.

The use of science in crafting international relations—what we now call science diplomacy—got a boost in President Obama's 2009 Cairo speech, in which he announced that he would send "science envoys" to Muslim-majority nations. Nobel laureate Ahmed Zewail, former National Institutes of Health Director Elias Zerhouni, and former National Academy of Sciences President Bruce Alberts, now the Editor-in-Chief of *Science*, served ably as the inaugural envoys.

Although there is value in sending abroad representatives of the scientific community, an aspect of U.S. culture that commands wide respect, there are also broader objectives between peoples that cry out for the active involvement of many more scientists, engineers, and educators. Today, countries all over the world aspire to have high-skill, high-value economies, to become "knowledge societies" and "knowledge economies." The extraordinary value of knowledge is, of course, that there are no limits to its growth or the value it can generate.

Going beyond local benefit, it is increasingly important to create a global knowledge society. The array of challenges facing humanity in the 21st century is daunting: developing energy sources that do not contribute to climate warming, building an agriculture that can feed a population that will soon exceed 9 billion with less water and a smaller ecological footprint, improving access to public health measures and clean water, preserving what remains of our biodiversity, restoring degraded ecosystems, controlling population growth, and stimulating economic development. All of these challenges are global in their scope, profoundly interconnected, and dependent on scientific and technological input.

Today's communications technologies make it possible to teach and collaborate with anyone anywhere. Online educational resources and organizations devoted to creating partnerships and networks among scientists, engineers, and educators continue to proliferate.* But in the end, the task of creating a truly global knowledge society, of knitting together the scientific and technical communities of nations to solve humanity's common problems, falls to each and all of us.

– Nina V. Fedoroff

10.1126/science.1219498

*Examples: OpenCourseWare Consortium (www.ocwconsortium.org), Science Initiative Group (http://sig.ias.edu), Engineers Without Borders (www.ewb-usa.org), The Global Knowledge Initiative (http://globalknowledgeinitiative.org), Scientists Without Borders (www.scientistswithoutborders.org).

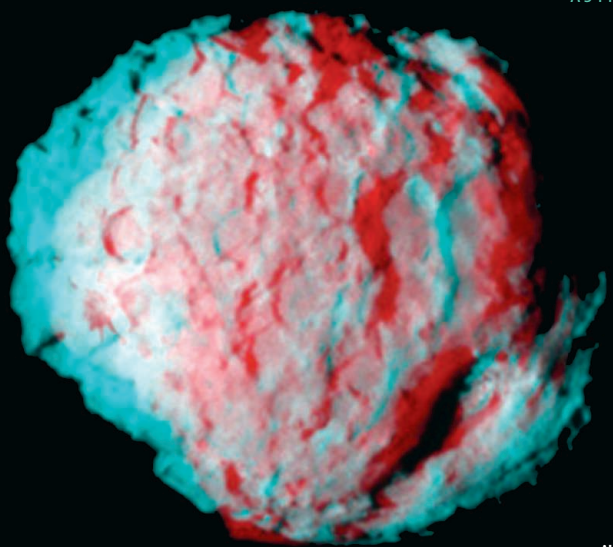
CREDITS: (TOP) DOUG MILLS/NEW YORK TIMES; (RIGHT) ISTOCKPHOTO.COM

Downloaded from www.sciencemag.org on February 2, 2012

Published by AAAS

EDITORS' CHOICE

EDITED BY KRISTEN MUELLER AND JAKE YESTON



ASTRONOMY

A Comet Dates Jupiter

In 2004, NASA's Stardust mission flew by comet Wild 2 and retrieved particles from the comet's coma, the tail of dust and gas that forms when a comet approaches the Sun. Two years later, those particles were brought to Earth and analyzed by international teams of scientists. Ogliore *et al.* describe mineralogical and isotope data for a fragment from the Stardust collection. This fragment, named Iris, resembles chondrules, the type of round, once-molten silicate particles typically found in meteorites. Iris probably formed in the inner solar nebula, and thus its presence in the coma of comet Wild 2 is a testament to the transport of particles from the inner, hotter parts of the solar nebula to the outer, colder ones, where comets originate. Iris formed at least 3 million years after the formation of the earliest solids in the solar system. Transport of material across the solar system must have occurred before Jupiter formed, as its growing embryo would have opened a gap in the protoplanetary disk, preventing outward transport past its orbit. Thus, unless transport occurred outside the plane of the protoplanetary disk or Jupiter was interior to Iris when this particle formed, the results imply that Jupiter formed 3 million years after the formation of the earliest solids. — MJC

Astrophys. J **745**, L19 (2012).

SOCIOLOGY

I Liked You From the Start

There is a tendency for people involved in a particular social network to be similar, but separating cause and effect can be difficult. To study the evolution of networks and behavior simultaneously, Lewis *et al*. used Facebook entries written by more than 1500 college students at a U.S. college over a 4-year period. From the time the students were freshmen until their senior year, network and profile information (including "friends" listings and taste in music, books, and movies) was tabulated. Students who liked certain kinds of movies (such as dark satire) or certain kinds of music (such as lite/classic rock) tended, more frequently than chance, to find others with similar tastes at the start. With the exception of a liking for classical/jazz music, preferences did not seem to be contagious. Although the authors acknowledge limitations of their study set, they conclude that ties strengthen among similar people, and our likes and dislikes do not tend to "rub off" on those around us. — BJ

Proc. Natl. Acad. Sci. U.S.A. **109**, 68 (2012).

GENETICS

Wrapped Up Right

All eukaryotic chromosomes have a centromere, which ensures that the genomic DNA is shared equally between daughter cells during cell division. Centromeres are defined by the presence of nucleosomes that contain a special histone H3 variant, CenH3. Accumulating evidence suggests that CenH3-containing nucleosomes have an unusual structure: Rather than consisting of the highly conserved octamer of histone proteins, which wraps up ~147 bp of DNA, they may instead form tetramers, which wrap only half as much DNA.

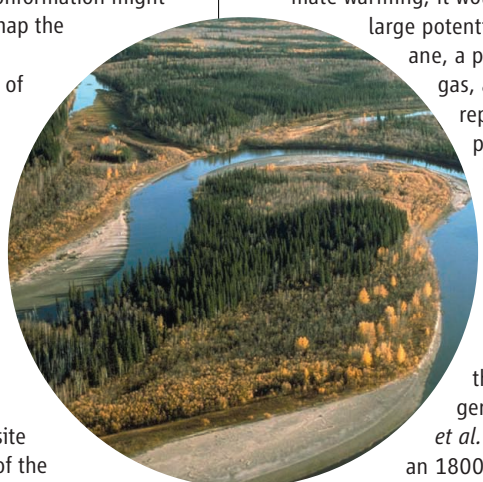
To understand how widespread this unusual centromeric nucleosome conformation might be, Krassovsky *et al.* fine-map the positions of budding yeast centromeres, which consist of a single CenH3 (known as Cse4) nucleosome binding site on each chromosome. Cse4 binds a region of DNA that is 80 bp in length, consistent with a tetramer nucleosome conformation. The highly AT-rich DNA sequence at the centromere and two protein-binding sites that flank the centromere site probably exclude binding of the canonical octamer nucleosome and recruit and stabilize the binding of the Cse4 nucleosome. Cse4 nucleosomes that become misincorporated at noncentromere sites, on the other hand, form octamers and are found in regions of high nucleosome turnover, the latter observation hinting how such excess Cse4, which could impede the function of the centromere, might be purged from the genome. — GR

Proc. Natl. Acad. Sci. U.S.A. **109**, 243 (2012).

CLIMATE SCIENCE

Here's Looking at You

Permafrost contains huge amounts of organic carbon. If it were to thaw in response to climate warming, it would constitute a very large potential source of methane, a powerful greenhouse gas, and therefore could represent a potent positive feedback to warming. The spatial extent and dynamic state of permafrost are difficult to determine, however, making it difficult to assess the prospective danger to climate. Minsley *et al.* present results from an 1800-km-long aerial electromagnetic survey of the Yukon Flats region of northeastern Alaska, which shows the configuration of permafrost to depths of 100 m in sediments deposited over the past 4 million years. In addition to providing a baseline for future studies, their data reveal important details about potential



CREDITS (TOP TO BOTTOM): NASA; U.S. FISH AND WILDLIFE SERVICE

Downloaded from www.sciencemag.org on February 2, 2012

Published by AAAS

connections between surface and groundwaters and the evolution of the permafrost over the past 1000 years. — HJS

Geophys. Res. Lett. **39**, 10.1029/2011GL050079 (2012).

CELL BIOLOGY

Push Me Pull You

A contractile ring composed of actin and myosin promotes cytokinesis—the final stage of cell division when daughter cells are physically separated from one another. The small GTPase RhoA regulates the contraction of this actomyosin ring. A Rho-family GTPase-activating protein (GAP), CYK-4 helps RhoA localize to the cleavage furrow, in part by binding to the guanine nucleotide exchange factor (GEF) for RhoA, ECT2. The cytokinetic role of the GAP domain of CYK-4, however, is unclear. Previously, Rac1 inactivation was proposed to be the primary function of the GAP domain. Now, working in *C. elegans* embryos, Loria *et al.* suggest that the CYK-4 GAP domain also contributes to activating RhoA during cytokinesis. Some defects in furrow ingression could be relieved by relaxation of the Rac1-dependent cortical actin network, bypassing to a certain extent the need for activated RhoA and a functional GAP domain in CYK-4. Cleavage furrow ingression thus reflects the balance of forces between the contractile ring and the cell cortex outside of the furrow region, allowing the cell to complete cytokinesis even when some of the cytokinetic machinery has been compromised. — SMH

Curr. Biol. **22**, 10.1016/j.cub.2011.12.019 (2012).

CHEMISTRY

Sacrifices at the Surface

There has been a thriving research discussion over the past decade about the tendency of certain dissolved ions to accumulate at the air/water interface of aerosols, and the associated implications for atmospheric chemistry. The driving framework of this sort of partitioning also has some bearing on how various salts affect aqueous protein solubility and conformational equilibria. A chemically intuitive explanation for the effect might suggest that surface migration is enthalpically unfavorable (as the ions remain only partially solvated) but is ultimately driven by the entropic enhancement associated with liberating the bulk water molecules that previously surrounded the ion completely. Otten *et al.* now present experimental studies of thiocyanate partitioning by temperature-dependent second harmonic generation spectroscopy (a surface-sensitive technique), together with theoretical simulations, that reverse the reasoning in this framework. The data point to an enthalpic gain and accompanying entropic sacrifice as the ions move from bulk to surface. The enthalpic gain is essentially attributed to full hydrogen bonding at water molecules driven away from the surface (where they previously were half exposed to uncoordinating air). The entropic loss, somewhat harder to account for, is attributed to suppression of collective capillary wave motions by the ions, engendering a more ordered surface. — JSY

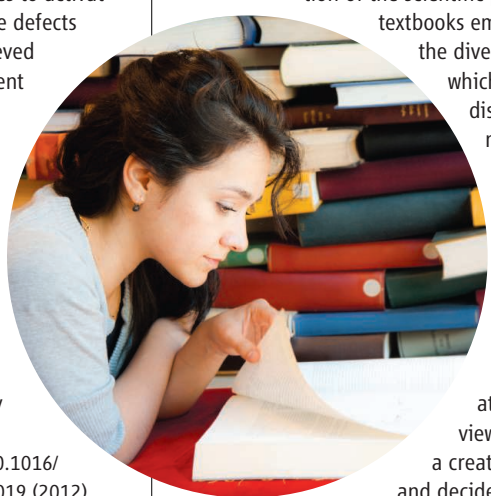
Proc. Natl. Acad. Sci. U.S.A. **109**, 701 (2012).

EDUCATION

Science Illustrated

U.S. college freshmen aspiring to a career in science often lose their enthusiasm. One cause may be introductory courses lacking an integration of the scientific process. If textbooks emphasized the diverse paths by which scientific discoveries are made, instead of simply stating outcomes derived from these discoveries, undergraduates Might view science as a creative endeavor and decide to stick with it. Duncan *et al*. examined figures in six introductory biology textbooks published in 2008 and tallied the number of figures presenting descriptive information (such as illustrations of ribosomal subunits) versus the number that illustrated a multistep process. On average, multistep scientific investigations were presented in fewer than 5% of the hundreds of figures in each book. The authors argue that this may contribute to a lack of appreciation of the nature of science by students. Shifting the balance of illustrations in scientific textbooks toward those presenting the design and interpretation of models, experiments, and field studies, and inclusion of the unexpected twists and turns involved in scientific discovery, could help undergraduates maintain their interest in scientific careers. — MM

J. Microbiol. Biol. Educ. **12**, 143 (2011).



CREDIT: ISTOCKPHOTO.COM

58,905
polysyllabic words reexamining *Ardipithecus ramidus.*

One more data point on why you should spend more time at membercentral.aaas.org. There you can enjoy members-only downloads, videos, webinars, blogs, discounts, and other content geared for people who aren't afraid of footnotes.

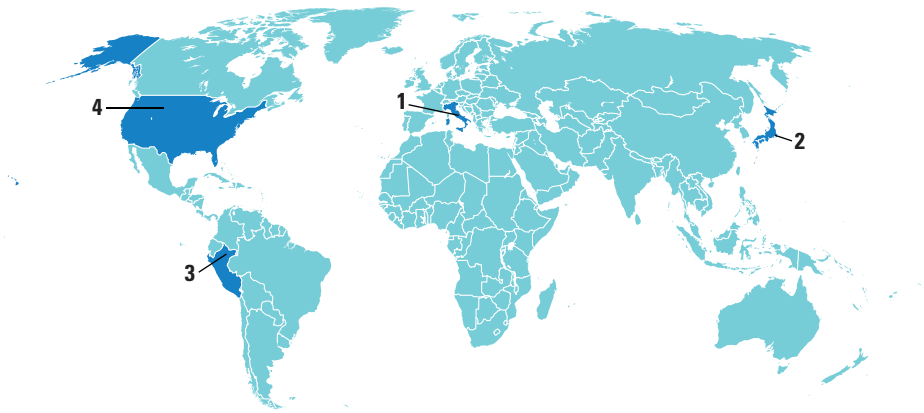
AAAS MEMBERCENTRAL

membercentral.aaas.org

Downloaded from www.sciencemag.org on February 2, 2012

Published by AAAS

AROUND THE WORLD



L'Aquila, Italy **1**

Italian Official Another Defendant in Earthquake Trial

The former head of Italy's civil protection department, Guido Bertolaso, will be investigated for manslaughter alongside seven scientists and technicians who are currently on trial for allegedly having carried out a superficial seismic risk analysis and giving a false sense of security to people in the central Italian town of L'Aquila only days before the deadly earthquake of 6 April 2009 struck, killing 308 people.

Bertolaso was implicated by a recording of a 30 March 2009 phone conversation



Shakeup. Former Italian Premier Silvio Berlusconi (*left*) and Guido Bertolaso survey earthquake damage near L'Aquila.

between himself and regional civil protection officer Daniela Stati, a day before the seven experts met to discuss a seismic "swarm" in the region that had lasted several months. In the conversation, Bertolaso told Stati that the experts, members of a government advisory body known as the National Commission for the Forecast and Prevention of Major Risks, were to meet up "not because we are frightened and worried" by the tremors but because "we want to reassure the public."

The trial started last September, but with nearly 300 witnesses scheduled to testify, it is likely to last until at least the autumn.
http://scim.ag/_Bertolaso

Tokyo **2**

Japanese Experts Question Safety Of—and Need for—Nuclear Power

Japan is preparing for the possibility of a summer without nuclear power as utilities and safety experts squabble over the safety of the country's remaining reactors. Of Japan's 54 nuclear reactors, only three are currently operating, and they must shut down for periodic inspection by the end of April.

In the wake of the Fukushima disaster, last summer the governing Democratic Party of Japan required "stress tests," analyses of a facility's ability to withstand natural disasters, to be part of periodic inspections. Based on that analysis, Japan's Nuclear and Industrial Safety Agency (NISA) has concluded that two reactors at a plant in Ohi on the Japanese sea coast have passed. Operator Kansai Electric Power is seeking approval to restart the two reactors.

But on 27 January, two members of a NISA advisory committee called the stress tests flawed, noting that the criteria for the tests should reflect new lessons from Fukushima, but that studies of the sequence of events that led to the disaster are still ongoing.

A new national energy policy is due by the end of the summer, and observers expect it could call for a phase-out of nuclear power. A sudden and permanent shut down of all reactors, however, would be a huge surprise.
http://scim.ag/nuclearjapan

Iquitos, Peru **3**

Andes Biodiversity Threatened

A survey of herbarium and museum records dating back a century, combined with remote sensing data about vegetation and climate, has shown that despite large national nature





At risk? The Cloud-forest Screech-owl (*top*) and the Black-faced Brush-finch are endemic to the Andes.

reserves in Peru and Bolivia, a surprising number of endemic species are still unprotected there. Duke University's Jennifer Swenson and her colleagues compiled location and habitat information from 7000 specimens representing about 700 endemic plants, amphibians, birds, and mammals living in 1.25 million square kilometers of the eastern slope of the Andes. They predicted the current ranges of these species using satellite information to identify similar habitats

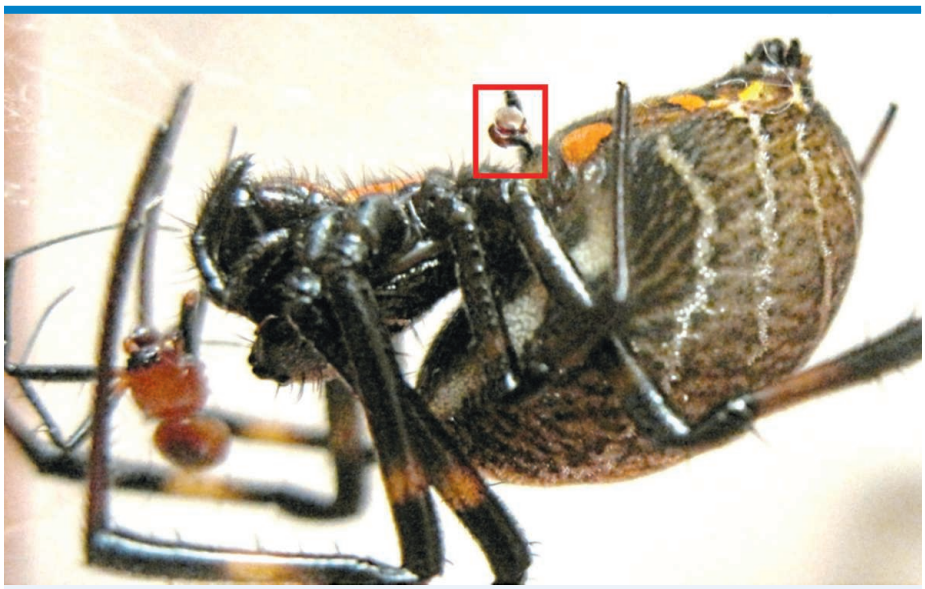
NOTED

>Light bulb moment: **Thomas Edison is still number one** when it comes to invention. The 2012 Lemelson-MIT Invention Index surveyed Americans aged 16 to 25 for their perceptions on invention. Asked to name who they thought was the greatest innovator of all time, 54% of the 1000 respondents named the inventor and holder of more than 1000 U.S. patents—taking a bite out of second-place holder and Apple Inc. co-founder Steve Jobs, who weighed in at 24%.

CREDITS (TOP TO BOTTOM): PHOTO BY ROSS MACLEOD; BRUCE E. YOUNG; LIVIO ANTICOLI/AP PHOTO

Downloaded from www.sciencemag.org on February 2, 2012

Published by AAAS



Spider Can Inseminate Female From Afar

The orb-web spider *Nephilengys malabarensis* is into rough sex—so rough that the male will often voluntarily break off his whole sex organ, or palp, while it's still lodged in the female's abdomen, rather than risk being eaten alive by her. Now a group of researchers think they know why evolution has allowed this dead-end dad to survive. They collected 25 pairs of spiders and introduced them to one another. After each pair had mated and the male's palp was left in the female, the researchers dissected the female and counted the sperm in her abdomen and the amount remaining in the embedded palp. That organ, they reported online 31 January in *Biology Letters*, continues to transfer sperm into the female long after the male has fled or been consumed. The longer it's embedded, the more sperm it transfers, and it's even more efficient when the male breaks it off himself to run away, rather than letting the female do it while eating him.

CREDITS (TOP TO BOTTOM): D. LI ET AL. *BIOLOGY LETTERS* (PUBLISHED ONLINE 2012) © 2012 THE ROYAL SOCIETY; © THE JAPAN PRIZE FOUNDATION; JASON SMITH/UNIVERSITY OF CHICAGO; N. LYDON/WIKIMEDIA COMMONS; © THE JAPAN PRIZE FOUNDATION

where the species might also live. Birds and mammals were most diverse at about 2700 meters, with amphibians thriving at approximately 1200 meters, the researchers reported last week in *BMC Ecology*. The report noted that about 80% of the areas most in need of preservation are vulnerable. "The current protected areas aren't doing the best job" of saving biodiversity, comments Toby Pennington, a botanist at the Royal Botanic Garden Edinburgh in Scotland.

Lead, South Dakota **4**

Nobelists Lobby for Gigantic Neutrino Experiment

Forty-two theoretical physicists, including three Nobel laureates, sent a letter 19 January to the U.S. Department of Energy (DOE), urging it to build an enormous particle detector that they say is key to the United States' future in particle physics. The Long Baseline Neutrino Experiment would lurk in the abandoned Homestake gold mine in Lead, South Dakota, and snare particles called neutrinos fired 1300 kilometers through Earth from Fermi National Accelerator Laboratory (Fermilab) in Batavia, Illinois. If built deep enough, so that background radiation levels are very low, the detector could search for very weak signals, such as signs that protons decay, and detect neutrinos from supernovae. "This project is absolutely crucial to having a world-leading program in the United States," says Jogesh Pati, of SLAC National Accelerator Laboratory in Menlo Park, California.

The letter doesn't guarantee that DOE will build the $1.5 billion detector. In July 2010, 38 theorists, including the same three Nobelists, wrote to Secretary of Energy Steven Chu urging DOE to run Fermilab's atom smasher, the Tevatron, through 2014. But with Europe's higher-energy Large Hadron Collider up and running, DOE decided to shutter Tevatron last September as scheduled.

THEY SAID IT

"I think that there are ways … to recognize the sanctity of life, but nonetheless to look at fertility clinics where there are cells that are sitting there that are not going to be used to create life. … I hope the president will find a way to agree that there ought to be federally funded research."

—Newt Gingrich on 19 July 2001 discussing embryonic stem (ES) cell research

"[Stem cell research] was the use of science to desensitize society over the killing of babies."

—Newt Gingrich 28 January. The next day, he vowed to ban ES research should he be elected president. **http://scim.ag/_Newt**

NEWSMAKERS

Leukemia Drug and Magnet Material Net Japan Prizes



Clockwise from top left: Druker, Rowley, Sagawa, and Lydon.

A trio of American researchers will share one of this year's Japan Prizes for bringing their work on a leukemia drug from a basic discovery to a clinical success, while a Japanese materials scientist is taking the other prize for a breakthrough with permanent magnets.

Janet Rowley of the University of Chicago, **Brian Druker** of the Oregon Health & Science University in Portland, and **Nicholas Lydon** of Blueprint Medicines in Cambridge, Massachusetts, jointly won the Healthcare and Medical Technology prize for developing a leukemia drug called imatinib, better known as Gleevec in the United States and Glivec elsewhere. Now used as a once-a-day pill, the drug has made chronic myelogenous leukemia (CML), once fatal within 3 to 5 years, "a manageable disease," Druker said at the prize announcement press conference 25 January. >>

Downloaded from www.sciencemag.org on February 2, 2012

Published by AAAS

>>NEWSMAKERS

Masato Sagawa, of Kyoto-based Intermetallics Co., won the prize in the field of Environment, Energy, and Infrastructure for work on the neodymium-iron-boron alloy which constitutes the high-performance permanent magnets at the heart of energy-efficient motors used in everything from hard disk drives to construction equipment.

The three healthcare laureates will equally share one $650,000 award; Sagawa alone gets an equal sum. All four will receive their awards at an April ceremony in Tokyo. **http://scim.ag/Japanprize**

White House Gives Up on NOAA Science Chief Nomination

The White House formally withdrew its nomination of geochemist **Scott Doney**, a senior scientist at the Woods Hole Oceanographic Institution in Massachusetts, to be chief scientist of the National Oceanic and Atmospheric Administration (NOAA) on 24 January. A U.S. Senate vote on Doney's nomination had been blocked for more than a year by Senator David Vitter (R–LA), who was unhappy with the Obama Administration's decision to impose a moratorium on offshore drilling in the wake of the April 2010 explosion of the *Deepwater Horizon* drilling rig in the Gulf of Mexico.

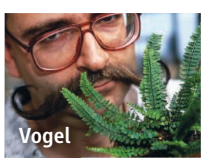
Under U.S. Senate rules, a single lawmaker can place a "hold" on a nomination, effectively preventing a vote. Doney's nomination had been approved by a Senate committee, but never got a vote in the full Senate after Vitter announced a hold in December 2010.


Doney

The withdrawal marks another setback for NOAA chief Jane Lubchenco. House Republicans have blocked her efforts to establish a new Climate Service within NOAA, and Doney's nomination marked an effort to raise the profile of the chief scientist's position. In October 2009, she announced a NOAA reorganization that included "reinstituting and elevating the role" to a presidential appointment.
http://scim.ag/DoneyNOAA

A Colorful Addition to a Berlin Museum

With his signature mustache and a tendency toward floral ties, Johannes Vogel will be hard to miss in the halls of Berlin's Natural History Museum. Vogel, an expert on fern genetics, took over as director of the museum on 1 February. He had been Keeper of Botany at London's Natural History Museum since 2004. Vogel says his top priority for the new job will be shaping the Berlin museum as a bridge between science and the public, in part by increasing the visibility of the behind-the-scenes research. "I want people to see the live part, the part that is yet to be discovered," he says. He'd also like to make the museum's 30-million zoological and geological samples more publicly accessible. "Amateur naturalists know more about some groups [of samples] than experts in the museum," says Vogel, whose job comes with the honorary title professor of biodiversity at nearby Humboldt University. Ideally, he says, the museum would set up a glass-walled "biodiversity discovery factory" in which automated scanners could process samples, categorizing known species and flagging new ones, in full view of visitors.

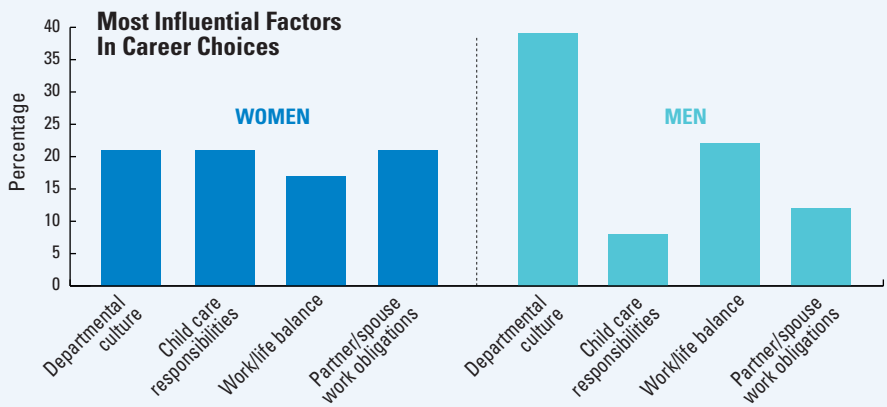

Vogel

Vogel is mildly famous for his family connections as well. His wife, botanist Sarah Darwin, is the great-great-granddaughter of naturalist Charles.

BY THE NUMBERS

$5.7 billion The amount the Swiss drug company Roche Holding AG has offered in a hostile takeover bid for the San Diego–based DNA sequencing company Illumina.

2% Percentage of plant collectors who have found more than 50% of the world's known species, according to a study in the *Proceedings of the Royal Society B*.



Making Choices

Women biochemists of all ages consider family-related factors to be as important as their professional surroundings in making career decisions, while their male counterparts place much more weight on working conditions. Some 1780 members of the American Society for Biochemistry and Molecular Biology answered a survey last year on the roles of gender and family in academic biochemistry. The survey, a first for the society, also found that the number of women in the academic workplace matches the number of men through the post-doctoral level but that men hold the lion's share of tenure-track and tenured positions.

Wolf Prize Winners Announced

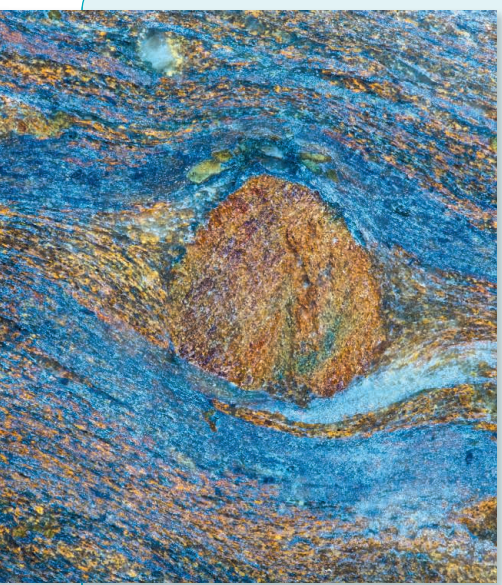
Two U.S. nanoscientists are among this year's Wolf Prize winners, which recognize researchers at the top of their fields in chemistry, physics, mathematics, medicine, agriculture, and the arts.

Like the other four scientists revealed on 19 January by Israel's Wolf Foundation, the chemistry duo honored—**Paul Alivisatos** of the Lawrence Berkeley National Laboratory in California and **Charles Lieber** of Harvard University—will take home a not-so small prize: $100,000. Alivisatos was recognized for his exploration of nanocrystal structure

CREDITS (TOP TO BOTTOM): PHOTO BY TOM KLEINDINST, WOODS HOLE OCEANOGRAPHIC INSTITUTION; © NATURAL HISTORY MUSEUM; ASBMB

Downloaded from www.sciencemag.org on February 2, 2012

Published by AAAS



Random Sample

Rock-a-Day Calendar


Stimpson

A British seismologist has a geologic twist on the classic nightstand "word-a-day" calendar: the daily rock. In 2010, scientist-turned-shutterbug Ian G. Stimpson of Keele University in the United Kingdom set out to photograph a different rock for each day of the year, a project he dubbed Rock 365. And, as of 2012, he's back at it, posting new daily rock photos to Flickr and to his blog, Hypocentre. "How do you get better than Rock 365?" he asks. "You leave it to the leap year and do Rock 366."

For inspiration, Stimpson has turned to his university's large rock collection, which includes sheared limestones, trilobite fossils, and garnet-bearing schists (pictured) gathered from around the world. Digging through the collection was a learning experience, even for the veteran rock buff. He stumbled across rocks he wasn't familiar with—sometimes to his detriment. He handled a sample of orpiment, for example, before learning that it was an arsenic sulfide mineral.

Toxins aside, Stimpson says his blogging marathon can be exhausting—not to mention inconvenient. At one point, he says, he found himself facing his own deadline while stranded in the airport at Casablanca, Morocco, without a geologic feature in sight. But when in doubt, look down: He turned his camera to the airport's granite floor. And this year, Stimpson plans to set sail on a cruise to the Baltic Sea for his 50th birthday. His solution for the days away from terra firma: A set of rocks, packed in his suitcase.

and design, while Lieber was noted for his work in building nanowires.

The other awardees include physicist **Jacob Bekenstein** of the Hebrew University of Jerusalem, a prominent black hole researcher. **Ronald Evans**, a hormone guru at the Salk Institute in San Diego, California, will receive the Wolf Prize in medicine. Mathematicians **Michael Aschbacher** of the California Institute of Technology in Pasadena and **Luis Caffarelli** of the University of Texas, Austin, will each also walk away with a prize. Perhaps the biggest name in the awards this year, however, isn't a scientist: Famous tenor **Placido Domingo** has also won in recognition of his long tenure in music.

FINDINGS

CDC Finds No Physical Cause For Mysterious Disease

A 6-year study of Morgellons disease—an odd sickness described by patients who say it causes colored fibers to emerge from the skin—came to a quiet end last week. Paid for by the U.S. government, a $580,000 report in *PLoS ONE* found no infectious organism, no toxin, no parasite—indeed, no physical cause of the disease. Instead, the report suggested it might be an epidemic of "delusional parasitosis."

Led by the U.S. Centers for Disease Control and Prevention (CDC), the investigation sought to learn what prompted a flurry of complaints starting in the early 2000s from patients who felt they were infected with bugs, harmed by toxins, or riddled with parasites that caused skin lesions and extrusions of fiber. Many also complained of fatigue or confusion. Several dozen members of Congress, including then-Senator Barack Obama, asked for an inquiry. Last week's report was the result. CDC teamed up with researchers from Kaiser Permanente of Northern California and others to comb through medical records and gather clinical samples. They found no communicable disease and primarily cotton fibers. This is good news, says CDC official Daniel Rutz: It means that people who have Morgellons do not need to worry about infecting relatives.

A Volcanic Trigger for Europe's Little Ice Age

For decades scientists have debated whether a fading of the sun or massive volcanic eruptions sent Europe into the icy grip of the Little Ice Age. This week a group of researchers reported new climate records and modeling that credits a burst of volcanic eruptions late in the 1200s with sole responsibility for triggering a centuries-long big chill across Europe.

In a paper published in *Geophysical Research Letters* on 31 January, geologist Gifford Miller of the University of Colorado, Boulder, and colleagues report carbon-dating of whole plant remains now emerging from beneath the ice cap on Canada's Baffin Island. The dating shows that the plants mostly died between 1275 and 1300 as Arctic ice suddenly expanded. That abrupt chill coincided with four massive volcanic eruptions in the tropics, suggesting the eruptions caused the cooling. And the group's climate modeling indicates that the volcanic cooling, which normally lasts just a few years,


Cold snap. Pieter Bruegel conveyed the icy cold of Europe circa 1565.

could have become locked in for centuries if it reordered ocean and sea-ice circulation in the North Atlantic.

The new data convince climate modeler Gavin Schmidt of the Goddard Institute for Space Studies in New York City, who was not part of the study, that volcanoes triggered the abrupt onset of the Little Ice Age. But the modeling suggesting how the cooling could persist for centuries, he says, needs more work.

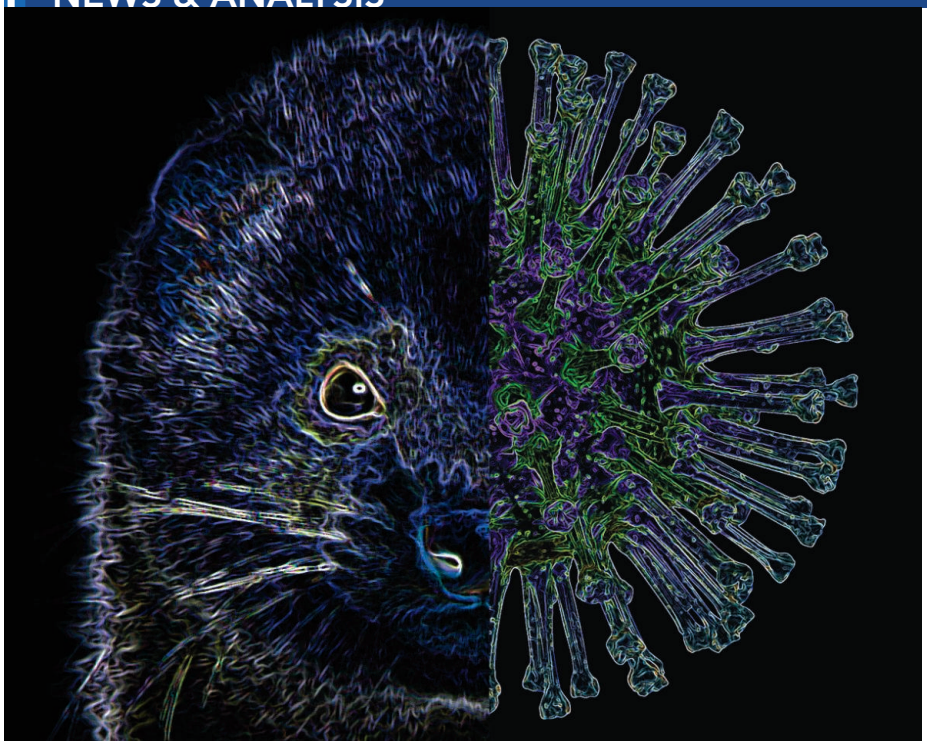
Science LIVE

Join us on 9 February for a live chat with experts about the **science of love** and the latest research into **human emotions**. **http://scim.ag/science-live**

CREDITS (TOP TO BOTTOM): © IAN G. STIMPSON 2010; COURTESY OF IAN GEOFFREY STIMPSON; © THE GALLERY COLLECTION/CORBIS

Downloaded from www.sciencemag.org on February 2, 2012

Published by AAAS



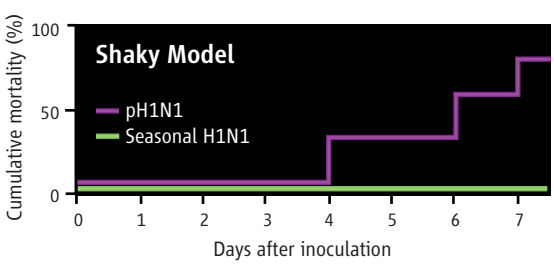
AVIAN INFLUENZA

The Limits of Avian Flu Studies in Ferrets

To publish or not to publish, that is *not* the question—or at least not the ultimate one. For the last few months, scientists, policymakers, and the public have intensely debated whether journals should reveal details of experiments by two labs that have engineered H5N1 avian influenza viruses that easily transmit among mammals—and could thus potentially spark a human flu pandemic. But there's another difficult quandary in this tug of war between scientific freedom and bioterror fears. Both research teams relied on experiments with ferrets. How concerned should people be that what happened in *Mustela putorius furo* with these mutant viruses will apply to humans?

Researchers widely agree that the ferret provides the best model to study influenza transmission in humans: This weasel-like animal uses the same cellular receptors for the virus, and strains that infect people spread among ferrets and cause similar symptoms. "We should not say, 'Well, it's just a ferret; let's forget about the results,' " says Ron Fouchier, a virologist at Erasmus MC in Rotterdam, the Netherlands, who led one of the groups behind the controversial studies. But even Fouchier emphasizes that, in many ways, the ferret model "is pretty shaky" and can lead to misleading conclusions, as it did with a study by his group when the 2009 pandemic H1N1 (pH1N1) virus emerged. "We always have to be really, really critical about what we do," Fouchier says. "We cannot say [because] it transmitted in ferrets, it must be transmissible in humans."

The H5N1 virus, which decimates chicken flocks, first surfaced in humans in 1997 but has rarely spread from person to person. The World Health Organization has tracked cases since 2003, and as of 24 January, 344 of the 583 people who had confirmed infections died from H5N1. That startlingly high 59% mortality likely overestimates the actual lethality of the virus, as many nonfatal or subclinical infections surely go undetected. Still, influenza investigators have feared that if this virus mutated and began spreading easily among people, it could wreak havoc, as we have no immunity to the avian hemagglutinin—the H5—glyco-protein on the viral surface that enables the virus to establish an infection.



False alarm. This ferret study triggered fears that the 2009 pandemic H1N1 was far deadlier than the seasonal strain.

The hubbub started at an influenza meeting in September, when Fouchier described how his lab had introduced five mutations to create a highly lethal H5N1 that passes between ferrets like "seasonal" strains of the virus that routinely infect humans. Fouchier and his co-workers have a paper accepted by *Science* about their experiment; they are still deciding what to include, in the wake of a December recommendation by the U.S. government's National Science Advisory Board for Biosecurity (NSABB) to redact methodological and other details. Similarly, Yoshihiro Kawaoka of the University of Wisconsin, Madison, and the University of Tokyo has an accepted manuscript on hold at *Nature* that describes how his lab combined H5N1 with pH1N1 to make a mutant that easily spreads between ferrets. The new virus effectively stitches the H5—which has properties that make it especially deadly—into the pandemic strain.

Few specifics are known about the work in either lab, but Kawaoka revealed an unexpected detail in a commentary online in *Nature* on 25 January, underscoring the confusion that swirls around these findings and the ferret model: His virus didn't kill the animals. So if nature or bioterrorists created a similar virus—or if it accidentally escaped from the lab, as some fear—does the ferret model predict it would have little chance of causing mayhem in humans? "Severity of infection, including lethality, is a complex biologic phenomenon involving pre-existing immunity to pathogens, individual susceptibility, pathogen dose, etc.," said Kawaoka in an e-mail reply to *Science*. "With all of these variables it is impossible to declaratively answer this question."

Kawaoka has firsthand experience with the difficulty of connecting the dots between ferrets and humans. During the relatively mild 2009 pandemic with H1N1, when many researchers worried that the newly discovered mashup of avian-swine-human influenza viruses might kill millions of humans who had little immunity to the bird component, his lab published a ferret study online in *Nature* on 13 July 2009 to help clarify the threat.

CREDITS (TOP IMAGE): COLLAGE: N. KEVITIYAGALA/*SCIENCE*; PHOTOS (LEFT TO RIGHT) ISTOCK; © PASIEKA/PHOTO RESEARCHERS INC.; (BOTTOM GRAPH) ADAPTED FROM J. M. A. VAN DEN BRAND *ET AL.*, JID **201** (1 APRIL 2010)

Downloaded from www.sciencemag.org on February 2, 2012

Published by AAAS

Seasonal strains of influenza uniformly spread between ferrets and rarely cause serious harm—which is a key reason the model has become so popular. In a comparison with seasonal strains, Kawaoka's group found that pH1N1 was more pathogenic in ferrets and caused "appreciable pathology" that was "reminiscent of infections with highly pathogenic H5N1 influenza viruses." A headline in the press release from the University of Wisconsin, Madison, read "Study suggests H1N1 virus more dangerous than suspected." *Science* had published a similar ferret study (http://scim.ag/ferretvirus) online a couple of weeks earlier (2 July 2009) by Fouchier's group that reached the same conclusions.

In another published experiment, the Fouchier group went a step further. They compared pH1N1, seasonal H1N1, and H5N1 in ferrets and found that the pandemic strain was indeed more lethal than seasonal H1N1 (see graph) and less than H5N1. Fouchier now says they made "a big mistake" by concluding that "pandemic H1N1 reaches further down the airway than seasonal flu, and, therefore, it's likely to become a severe pandemic."

As it turns out, neither team factored in that their young ferrets, by experimental design, had no influenza immunity. Long-lived humans, in contrast, acquire immunity from both strains in circulation and vaccines. The pH1N1 caused the least amount of harm in older people who had been exposed to variants of the 1918 pandemic strain, which shared similarities with the new one. But many children, who had scant preexisting immunity to flu, were hospitalized with lower respiratory disease. "The clinical picture we saw in the hospital was quite similar to what we saw in our ferret model," Fouchier says. But of course that's in hindsight.

The choice of influenza strains used in ferret experiments can also lead to conflicting results, as happened in a study by the U.S. Centers for Disease Control and Prevention (CDC) when pH1N1 emerged. In tandem with its online publication of the Dutch experiment in ferrets, *Science* ran a report (http://scim.ag/-H1N1) from CDC researchers that demonstrated that different strains of pH1N1 did not spread to all their ferrets. This "lack of efficient respiratory droplet transmission suggests that additional virus adaptation in mammals may be required to reach the high-transmissible phenotypes observed with seasonal H1N1 or the 1918 pandemic virus," they concluded. In the end, pH1N1 infected humans throughout the world with similar efficiency to seasonal strains.

CDC's Ruben Donis, who did not participate in that study but has done other flu experiments with ferrets, stresses that even a given strain represents a swarm of viruses, as flu mutates rapidly within each host. The specimen taken from a human may also differ if it is taken from the lung versus the nose. "There's all this fuzziness in every experiment we do," Donis says.

Further complicating analyses, these experiments typically involve few ferrets, as they require complex handling procedures and large cages in often tight biocontained facilities. "Go and look for the confidence intervals or the p-value [in ferret studies]," Donis says. "Nobody shows statistics. The statisticians laugh when you tell them you used three ferrets." This can often make potentially important results uninterpretable—which may help explain why a recent study he led, published online in *Virology* on 5 November 2011, did not spark an international uproar. In that experiment, his team created a mutant H5N1 that spread from infected ferrets to one of two animals in an adjacent cage.

"We have to be really, really careful to interpret our data in ferret transmission in a quantitative way," Fouchier says. "You cannot say if you got two out of four transmissions that your virus is 50% transmissible." His group's new study has little to say about the kinetics and efficiency of transmission of its mutant virus in humans. "I can't tell if this virus were released now to the world whether it would transmit efficiently," he stresses. "The only thing we say is it can be airborne."

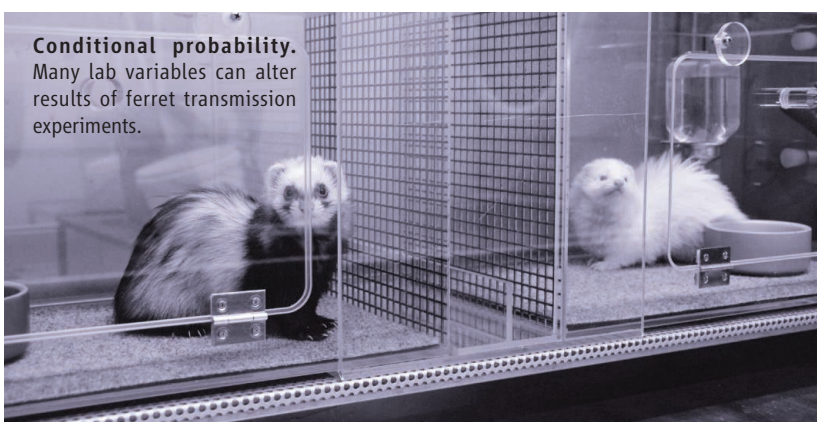
What's more, as Peter Palese and Taia Wang of the Mount Sinai School of Medicine in New York City point out in a perspective published online 25 January in the *Proceedings of the National Academy of Sciences*, some strains spread between ferrets but not humans. And pathogenicity of H5N1 clearly differs between the species, too. "Very few strains of H5N1 in the ferret are lethal," says influenza researcher and NSABB member Robert Webster of St. Jude Children's Research Hospital in Memphis, Tennessee.

In the pig, which shares the same receptors for influenza viruses used by both humans and birds, H5N1 is wimpier still, never causing serious illness. "You could argue that the ferret in the case of H5N1 is an outlier; it's just too susceptible to severe disease," CDC's Donis says. "Maybe the pig is a better model for H5N1 because, in reality, many, many people are exposed to H5N1 and very few get sick."

Laboratory conditions can alter outcomes, too, says Kanta Subbarao, who studies flu in ferrets and mice at the U.S. National Institute of Allergy and Infectious Diseases. Factors such as infecting the "index" animal via nose drops versus the trachea, the amount of virus used, the genetic differences in this outbred species, and the age of ferrets all can affect results. For technical reasons, no one quantifies the aerosolized droplets that presumably spread the virus in transmission experiments. "My take-home message when I speak of animal models for influenza is we should look at more than one model," Subbarao says.

Many influenza researchers hope the Fouchier and Kawaoka data can ultimately help clarify the factors that allow flu to spread in humans. "We desperately need to understand transmissibility," says Webster, who is glad the new studies were done. "People are starting to say these scientists are irresponsible for doing this work. We're never going to understand what transmissibility is unless we can work in the best model, and the best model we've got is this ferret—unless you would like to volunteer."

–JON COHEN



Conditional probability. Many lab variables can alter results of ferret transmission experiments.

CREDIT: SANDER HERFST/ERASMUS MC

Downloaded from www.sciencemag.org on February 2, 2012

Published by AAAS

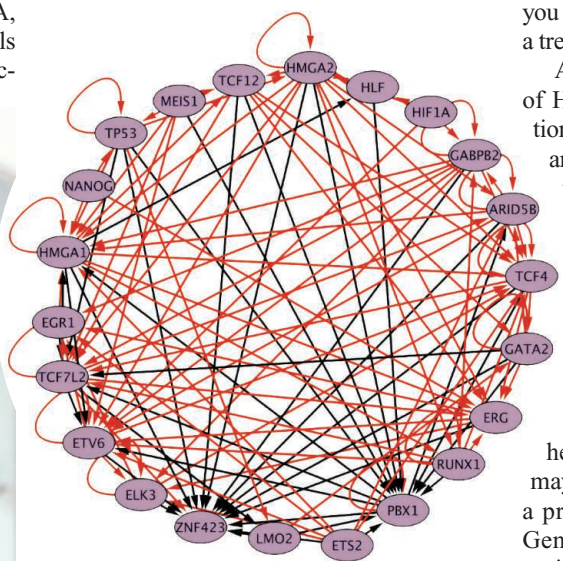
CELL BIOLOGY

Donation Spurs a Cell Observatory—And Bigger Plans

The Broad Institute in Cambridge, Massachusetts, received a $32.5 million gift last week to take on one of the biggest challenges in biology: mapping the molecular "circuitry" inside several kinds of mammalian cells. And Broad Director Eric Lander, a geneticist with a penchant for ambitious endeavors, is using the occasion to endorse a proposal floated by a few cell biologists for an even grander international effort—some call it the Human Circuits Project—that would chart the molecular and genetic connections in all human cell types.

Lander's team at Broad wants to build on ongoing work to trace how genes, RNA, proteins, and other biomolecules inside cells interact in pathways to make those cells function in healthy people or malfunction in disease. Lander, a leader of the Human Genome Project that completed its work 9 years ago, says that deciphering such cell wiring once looked impossible, as did sequencing the 3 billion bases of the human genome, but the goal has become more manageable. "More people are saying this is not a crazy notion at all. It is a finite task, and let's see some pilot projects to convince us that this can be done," he argues.





Observer. The Broad Institute's Aviv Regev will lead an effort to map molecular and genetic circuits inside cells, such as the gene transcription network (*above*) in differentiating blood stem cells.

Broad's new Klarman Cell Observatory is one such pilot. The Klarman Family Foundation—a Boston charity founded by financier Seth Klarman, who sits on Broad's board, and his wife, Beth—donated the money that will launch it. Broad officials say they chose the name because the project will bring together biologists from the institute and elsewhere to tackle the cell's inner workings, akin to how astronomers once gathered at telescope observatories to collect and analyze data. "It is a substantial challenge, but it is one in which groups around the world have been making a lot of progress in the past few years," says Broad computational biologist Aviv Regev, who will head the observatory. (The Klarman family, which has previously funded basic and clinical research on eating disorders, declined to give an interview.)

Regev says unraveling a cell's circuitry has become easier thanks to new tools, such as RNAi—short snippets of RNA that can be used to shut off genes—and a technique called ChIP-Seq, which uses cheap DNA sequencing to map sites along the genome where proteins bind to DNA. The $32.5 million donation will fund a 5-year program with three components, according to Regev. One is technology development, improving existing tools and making them available "not just in the observatory but to the wider community," Regev says. Another program will support small collaborative grants at the Broad Institute and beyond, including Israel, where the Klarman Foundation has a special interest.

The third component has a more specific goal: studying, Regev says, "as many layers of the circuitry as possible" in two to four mammalian cell types to build a comprehensive model of those cells. Researchers might, for example, expand work she and collaborators have done on mapping gene expression in immune dendritic cells exposed to pathogens and in blood stem cells as they mature into different types of blood cells.

Broad investigators hope the models they develop could eventually apply to any type of cell, Regev says. At that point it might be time for a Human Circuits Project, according to Lander. Work from Regev's team and others suggests "there's a modularity to circuitry," Lander says. "There's only a finite number of cell types, and there's only a finite number of states that they're in and a finite number of circuits, and they get reused." And like the human genome, which even now isn't 100% done, even a partial success would help: "If you had 50% of the circuit catalog, you'd have a tremendous amount."

A decade ago, the U.S. National Institutes of Health (NIH) funded a large collaboration with some similar aims, called the Alliance for Cellular Signaling, that attempted to map the signals sent from cell receptors to the nucleus in mouse cells. NIH shut the effort down early. "It was too ambitious" and struggled with balky cell types, data analysis, and demanding logistics, says geneticist Paul Sternberg of the California Institute of Technology in Pasadena, an adviser to the project.

If scientists want to turn to NIH for help with a Human Circuits Project, they may need to define it better. Peter Good, a program officer at the National Human Genome Research Institute, says he isn't entirely clear yet on what Lander means by cell circuits: "Different people think it means different things." Good notes that NIH already funds projects that appear to be related to Broad's goals, such as an effort called LINCS that is cataloging gene expression and other measures of response when cells are perturbed by various drugs and other small molecules.

The Allen Institute for Brain Science in Seattle and the Salk Institute and the University of California, San Diego, are also planning major efforts to study cell circuitry, notes UCSD computational biologist Trey Ideker. Ideker says that an international cell circuitry project could face challenges different from those encountered by the Human Genome Project. "It's a lot bigger and a lot less well defined," he says. But Ideker also believes such an effort is essential for moving forward with personalized genomic medicine: "To understand someone's genome, you're going to need the wiring diagram," he says.

–JOCELYN KAISER

CREDITS (LEFT TO RIGHT): IMAGE COURTESY OF MARIA NEMCHUK, BROAD COMMUNICATIONS; N. NOVERSHTERN *ET AL.*, *CELL* **144**, 2 (21 JANUARY 2011) © 2011 ELSEVIER INC.

Downloaded from www.sciencemag.org on February 2, 2012

Published by AAAS

ASTRONOMY

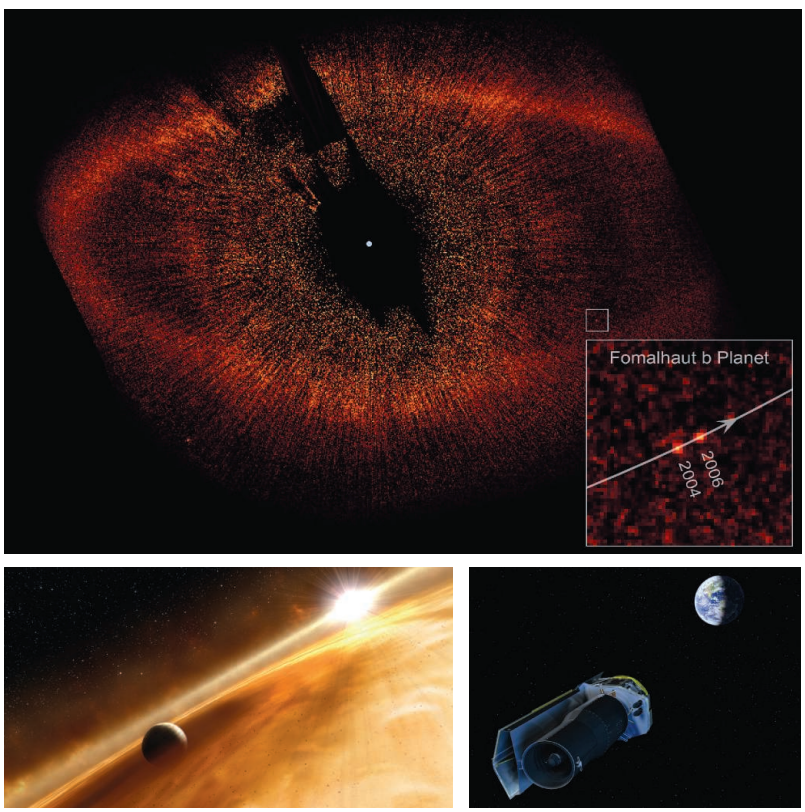
Celebrated Exoplanet Vanishes In a Cloud of Dust—Or Maybe Not

Every week, astronomers add new extrasolar planets to a roster that now numbers more than 700. But on rare occasions, a finding comes along that threatens to knock one of those discoveries off the list. Last week, Fomalhaut b, an exoplanet that once enjoyed celebrity status, faced an identity crisis after astronomers failed to spot it in a new round of observations. But the group that discovered the planet is sticking to its guns.

Located 25 light-years away, Fomalhaut b was reported in 2008 as one of the first exoplanets to be discovered through direct imaging. Its discoverers, led by Paul Kalas of the University of California, Berkeley, detected the object in optical-light images of a star called Fomalhaut, photographed by the Hubble Space Telescope. Even though the object was just a tiny speck on the rim of the disk spinning around the star, Kalas and colleagues determined through follow-up ground-based observations that it was gravitationally bound to Fomalhaut and was moving in what appeared to be a planetary orbit. Their findings were published in *Science* (28 November, p. 1345) and helped make the direct detection of extrasolar planets a runner-up for 2008's Breakthrough of the Year.

When Markus Janson, an astronomer at Princeton University, read about the discovery, he was puzzled that Kalas's observations had revealed the planet in the optical band but not at infrared wavelengths. "That's the opposite of what you would normally expect," Janson says, because a planet bright enough to be imaged directly would have to be warm enough to emit thermal energy detectable in the infrared. Janson also wondered why Kalas's observations showed that the planet lost nearly half of its brightness between 2004 and 2006.

So Janson applied for time on NASA's space-based Spitzer telescope—a powerful infrared imager—to look at Fomalhaut. Despite his hunch that the planet didn't exist, "I would have been happy to find something," Janson says. "Weird things happen in nature, and if we would have found something, that would have been fantastic because there's so much more you can say about an exoplanet with infrared data."



Planetary mirage? Optical images of Formalhaut (*top*) seemed to show a planet (artist's impression, *bottom left*). But infrared observations by Spitzer (*bottom right*) raise doubts.

Last September, with half of the Spitzer data analyzed and no sign of a planet in sight, Janson met informally with Kalas at an exoplanet conference in Wyoming. Kalas showed Janson the Hubble data and analysis on his laptop. Fomalhaut b's low mass—less than that of Jupiter—made it invisible in the infrared, Kalas explained. The reason it was still visible in the optical, he speculated, was that it had a large "circumplanetary dust ring" like that of Saturn.

Janson told Kalas he wasn't convinced. In his view, the Spitzer observations—which were several times as sensitive as the infrared observations Kalas's group had made—should have detected something. To be visible in optical light, Janson argued, the planet's ring would have to be several times wider than the planet itself and would have to be tilted to reflect the star's light into earthly telescopes—an improbable combination. "Toward the end, I said I wouldn't call this a planet myself," Janson says. After returning from the conference, he and his colleagues completed their analysis and wrote a paper that has just been accepted by *The Astrophysical Journal*.

Janson does not dispute that Kalas's group saw something. "There is certainly something in the system," he says. "It's just a lot more complex than a planet." One possibility, he says, is that the object is a large dust cloud arising from a recent collision of asteroids. As the cloud is dispersing, it's getting fainter—which would explain the halving of brightness between 2004 and 2006.

Kalas says the 2008 discovery paper took into account the puzzling dimensions that caught Janson's attention, and in fact considered—and rejected—the dust cloud hypothesis. For the object to be a dust cloud, "we would need to invoke a 'fortuitous' observation of a rare and short-lived event," Kalas says.

Kalas says Janson and his colleagues are wrong to dismiss the possibility of a large ring around the planet. "They ignore the recent discovery of Saturn's Phoebe ring, which is five to six times larger in size than the ring we proposed for Fomalhaut b," Kalas says. In other words, "Fomalhaut b may represent the first discovery of such a ring around an extrasolar planet."

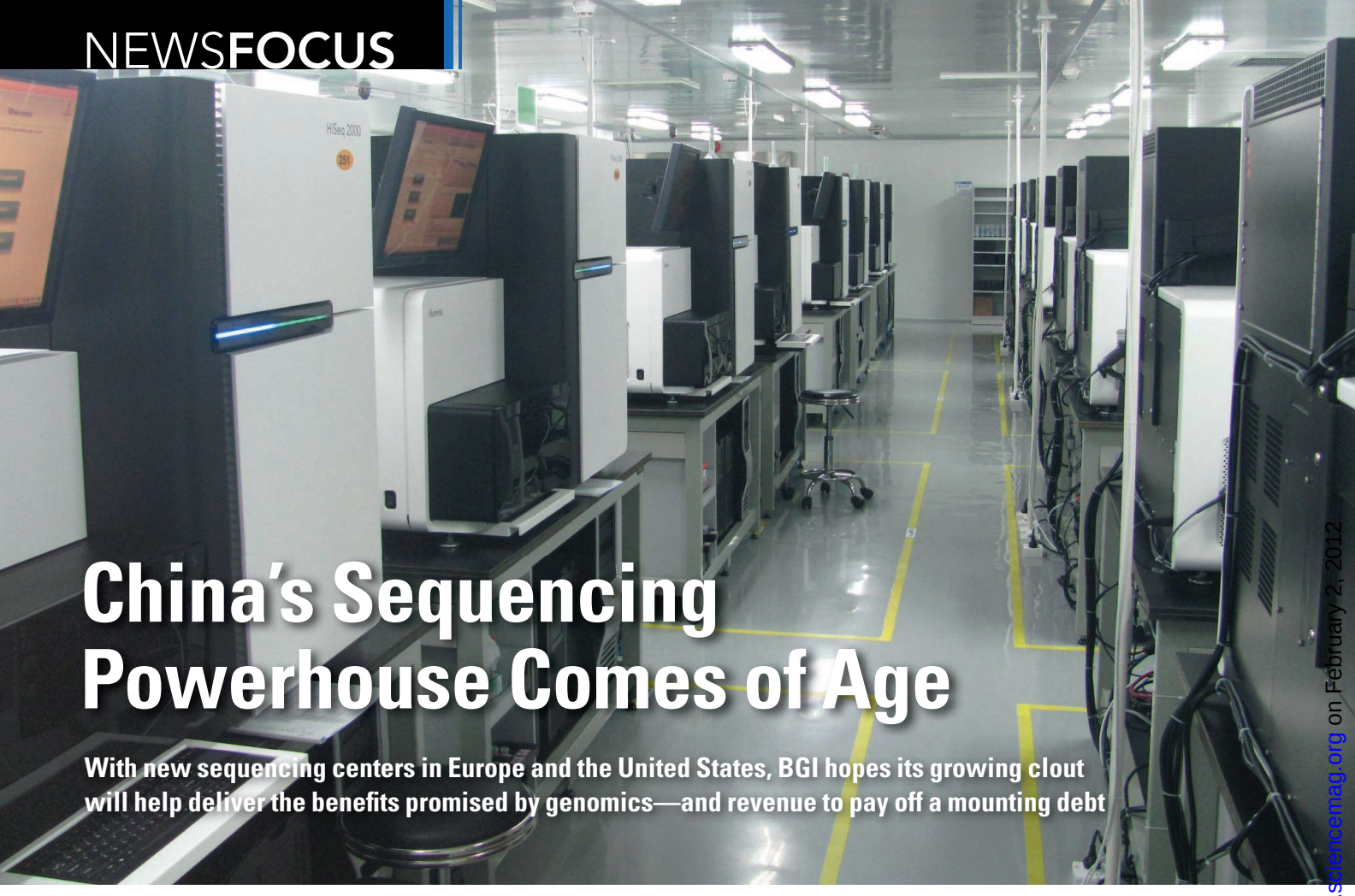
Others are not so sure. Alice Quillen, an astronomer at the University of Rochester in New York state who predicted in 2005 that a planet had to be lurking somewhere in Fomalhaut's circumstellar disk, strongly suspects that what Kalas and his colleagues found is not a planet. "In my opinion, it is a misinterpretation of speckles in noisy data," she says. "Real planets have yet to be discovered in the Fomalhaut system."

–YUDHIJIT BHATTACHARJEE

CREDITS (TOP TO BOTTOM): NASA, ESA, P. KALAS, J. GRAHAM, E. CHIANG, E. KITE (UC BERKELEY), M. CLAMPIN (NASA GSFC), M. FITZGERALD (LLNL), K. STAPELFELDT AND J. KRIST (NASA JPL); ESA, NASA, AND L. CALCADA (ESO FOR STSCI); NASA/JPL-CALTECH/R. HURT (SSC)

Downloaded from www.sciencemag.org on February 2, 2012

Published by AAAS



China's Sequencing Powerhouse Comes of Age

With new sequencing centers in Europe and the United States, BGI hopes its growing clout will help deliver the benefits promised by genomics—and revenue to pay off a mounting debt

SHENZHEN, CHINA—On the sidelines of a genomics conference here last November, immunologist Lennart Hammarström sat down for a preliminary discussion with officials of the genome sequencing powerhouse BGI-Shenzhen. Hammarström, of the Karolinska Institute in Stockholm, had concluded that the best way to identify genetic mutations behind primary immunodeficiency disorders would be to sequence patient genomes. He hoped to gauge BGI's interest in cooperating—and got more than he expected. After 2 hours they had agreed on a vision and decided, "Let's do it," he says. At the end of his presentation 2 days later, Hammarström donned a BGI T-shirt and with BGI Director Wang Jian signed an agreement under which the Shenzhen institute will sequence thousands of patient samples, the two sides will exchange graduate students, and Hammarström will head a new department of immunogenetics at BGI. Hammarström was awed by how quickly it all came together. "It's BGI speed, the speed of light," he says.

Such dealmaking is a central element of BGI's improbable emergence as a genomics superpower. Unlike other major sequencing centers that are attached to institutes with in-house biology expertise and long-standing scientific programs, BGI, since its inception in 1999, has focused on developing its sequencing and bioinformatics capabilities while turning to outside teams in crop science, human disease, and microbiology to help define its research objectives.

As a result, BGI has become the go-to organization for groups in need of sequencing. At the meeting, BGI inked deals with Johns Hopkins University in Baltimore, Maryland, to work on synthetic yeast and with the International Rice Research Institute (IRRI) in Los Baños, Philippines, to study genomic diversity of 3000 rice strains. Earlier last year, BGI agreed to collaborate to sequence 5000 cassava varieties and 10,000 autism patients and family members, and do heaps of sequencing for the international Human Variome Project (*Science*, 16 December 2011, p. 1487). And it's looking for partners on its own audacious goal to sequence a million human genomes, a million plant and animal genomes, and a million microbial genomes. To foster closer collaboration, BGI is establishing two sequencing centers in the United States and one in Europe, with more in the offing. The growing web of partnerships is turning BGI into the only genomics enterprise with a global footprint.

In building its empire, BGI has made a huge gamble. To fuel its growth, BGI has borrowed heavily from a $1.5 billion line of credit from a government-owned bank—debt it must start to pay back in 10 years. Elsewhere, governments have invested in genomics and sequencing centers with the expectation of future payoffs in medicine and other areas. But none has taken as entrepreneurial an approach as China has in counting on a single institute to recoup its investment.

Competitors are puzzled by the BGI phenomenon. "I don't think their model is very different in terms of interactions [with researchers]," says Richard Gibbs, director of the Human Genome Sequencing Center at Baylor College of Medicine in Houston, Texas, one of the big three sequencing centers funded by the U.S. National Human Genome Research Institute (NHGRI). Applying genomics to biomedicine is "pretty straightforward" in matching sequencing technology and expertise with funding and science, he says. Others worry that BGI's sheer size and mounting debt could skew priorities across the field if sequencing projects are determined by the likelihood of a payoff. Jack Gilbert, an environmental microbiologist at the University of Chicago

CREDIT: D. NORMILE/*SCIENCE*

Downloaded from www.sciencemag.org on February 2, 2012

Published by AAAS

Heavy artillery. BGI claims it has more sequencing capacity than the entire United States.

and Argonne National Laboratory in Illinois, collaborates with and admires BGI. Nonetheless, he worries, "If one organization dominates the market and has an agenda, this could be bad for innovation in science."

BGI officials say they are not bent on world domination. "I don't think this is the only [sequencing] model that fits the entire field and should not be the only model," says BGI Executive Director Wang Jun. But he adds that their approach to genomics "is probably a model no one else could easily follow."

As a research institute sponsored by the Shenzhen municipal government, BGI has set up private nonprofit institutes in Hong Kong, Europe, and the United States to manage its sequencing centers. It owns private companies that offer sequencing and clinical services. BGI also has a college in Shenzhen it hopes to turn into a university and an annual genomics conference, and it is launching a journal, *GigaScience*. Wang says they are simply trying to attract sufficient resources "to prove that the genome matters."



BGI's triumvirate. From left: Chair Yang Huanming, Director Wang Jian, and Executive Director Wang Jun.

Seizing the day

According to BGI brass, the center's rise was happenstance. "We went one step by one step," says Yang Huanming, BGI's charismatic chair. "I don't think BGI had a long-term strategy, but it did have long-term dreams and it has been opportunistic," adds Gane Ka-Shu Wong, a biosystems informaticist at the University of Alberta in Edmonton, Canada, who has been a BGI associate director from the start.

Yang, Wang Jian, and a handful of colleagues formed Beijing Genomics Institute in 1999 to give their homeland a foothold in sequencing. That year, backed by seed funding from the Chinese Academy of Sciences (CAS) and promises of further government support, Yang persuaded the international Human Genome Organisation to allow China to sequence 1% of the human genome. It was the only developing country in the landmark project, a fact that dominated news coverage in China when sequencing was completed in 2001.

As work on the human genome wound down, BGI faced a problem: It had 150 people, sequencing machines, and supercomputers but no continuing funding. To win grants, "we had to do something else," Yang says. They took aim at the rice genome, a project BGI initiated with Chinese partners. By the time they reported the draft sequence in *Science* in 2002, BGI's payroll had swelled to 300, and it was even hungrier for grants. "We decided we would take on any problem related to genomics," Yang says.

BGI joined with domestic partners and won grants for other sequencing projects deemed important for China's economy or prestige, including the chicken, silkworm, and panda genomes. And it expanded its overseas ties. BGI participated in the International HapMap Project, among others. In the process, it developed a recipe for success in its collaborations. For example, to tackle the pig genome, BGI took charge of sequencing and bioinformatics while Danish partners handled functional analysis. Every step of the way, Yang says, they sought to drive down costs, increase speed, and cover expenses.

In late 2003, riding political support for having quickly sequenced several strains of the SARS virus, BGI became a CAS insti-

Step by Step

14 July 1999 BGI founded with the goal of taking on 1% of the human genome, which the International Human Genome Project had awarded to China on 6 June.

15 February 2001 *Nature* publishes "Initial sequencing and analysis of the human genome."

5 April 2002 *Science* publishes BGI's sequence of the rice genome.

April 2003 BGI sequences several variants of the SARS virus, analyzing proteins and developing the first diagnostic reagent.

December 2004 BGI sends a team to help identify Indian Ocean tsunami victims using DNA.

23 October 2006 BGI holds its first International Genomics Conference.

April 2007 BGI-Shenzhen officially registered.

May 2008 BGI sends a team to Sichuan Province to aid in post-earthquake disease control.

6 November 2008 *Nature* publishes "The diploid genome sequence of an Asian individual."

20 March 2009 BGI opens a sequencing center in Hong Kong.

13 December 2009 *Nature* publishes the sequence of the giant panda genome.

January 2010 BGI purchases 128 Illumina HiSeq 2000 sequencing systems.

9 January 2010 BGI launches a 1000 plant and animal reference genome project and calls for worldwide collaboration.

2 July 2010 *Science* publishes "Sequencing of 50 Human Exomes Reveals Adaptation to High Altitude."

24 May 2011 BGI sequences a pathogenic *E. coli* strain ravaging Germany.

July through November 2011 BGI announces plans for sequencing centers in Copenhagen, Sacramento, and Philadelphia.

CREDITS: D. NORMILE/*SCIENCE* (3)

Downloaded from www.sciencemag.org on February 2, 2012

Published by AAAS

tute. But it was a poor match. "There was serious conflict between CAS and BGI," Yang says. CAS institutes have an academic structure, with senior scientists often heading small teams. BGI was building a large-scale sequencing operation staffed with an army of programmers and bioinformaticists. More important, Yang says there was little recognition of the importance of sequencing. There was "almost nothing" in funding for sequencing in China's 5-year plan that ended last year, he says.

Shenzhen's government came to the rescue. In 2007, the prosperous special economic zone, eager to expand its economic base beyond manufacturing, offered 20 million yuan ($3.2 million) per year for 4 years and found BGI a home in a former shoe factory. Conflicting visions split BGI's scientists. Some chose to remain under CAS as the Beijing Institute of Genomics while Yang and his supporters decamped to Shenzhen.

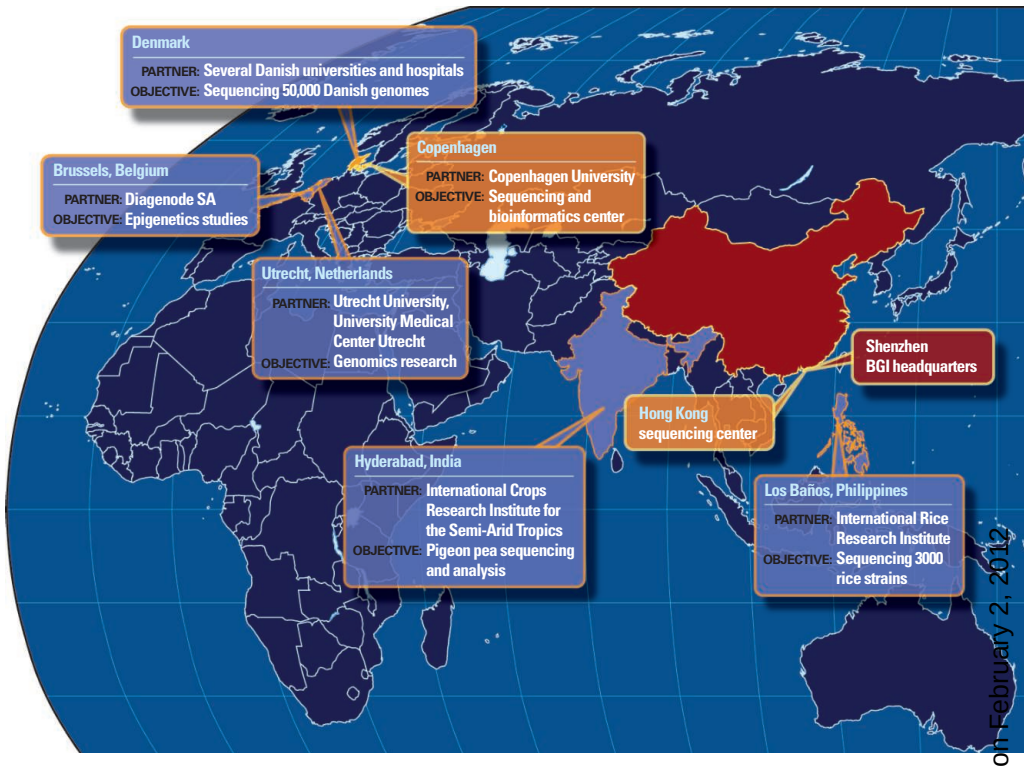
In early 2010, BGI hit the jackpot when the China Development Bank extended a 10 billion yuan ($1.58 billion) line of credit. The bank finances projects in line with central government policy, which includes support for biotech, Wang Jun says.

BGI immediately bought 128 Illumina HiSeq 2000 sequencers, each capable of sequencing a human genome in a week. In one stroke, BGI acquired more sequencing power than any other center in the world. Winning an arms race was not the objective, Wang Jun says. "We just did a rough calculation: If we sequence the major farm animals and sequence the major medical genomes, how many instruments do we need?" They also predicted that the Illumina machines would not be trumped by a new generation of sequencers for at least 3 years.

Massive sequencing capacity is one prong of BGI's strategy. It has also strived to blaze a trail in bioinformatics by developing free software for the community. "They've been astonishingly open in the whole [bioinformatics] effort," says Mark Edwards, a plant geneticist at Southern Cross University in Lismore, Australia.

Bioinformatics has become increasingly important as sequencing volume has grown.

Global Network

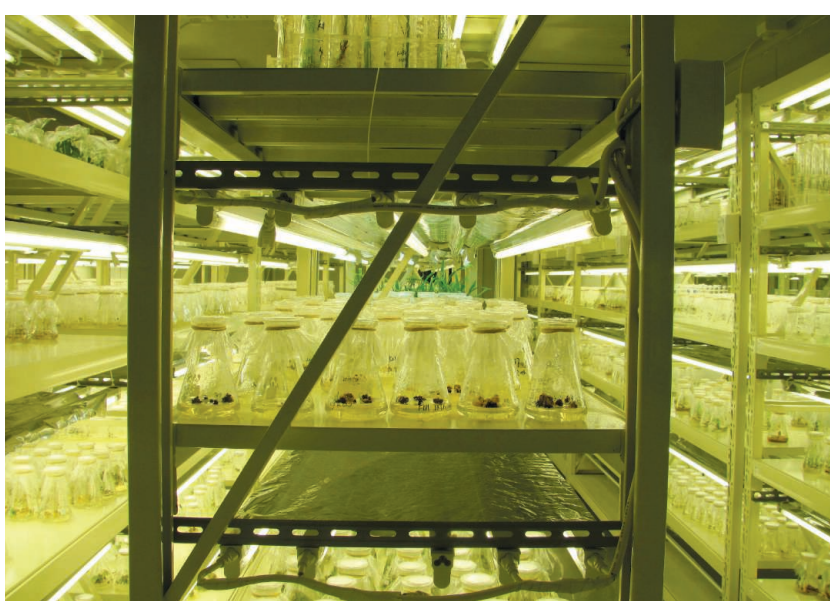


For example, a BGI-Danish project called LuCamp sequenced all exomes, the genome's coding regions, of 1000 patients with metabolic disorders and 1000 controls. The project "was the first of its kind," says team member Rasmus Nielsen, a computational biologist at the University of California, Berkeley. Earlier disease-related genomics efforts involved more limited sequencing and produced less data. Before starting, "you need to know how many samples and to what depth you have to sequence to maximize the statistical power to identify a particular gene or loci that is associated with a disease," says Li Yingrui, who headed BGI's bioinformatics for LuCamp. The project required simulations and new statistical models on scales not previously attempted. Sequencing was completed in 2010; the first report from the ongoing functional analysis appeared in *Nature Genetics* in October 2010.

Li's role in LuCamp highlights another facet of how BGI does things differently. When the project started in 2008, he was 21 years old and cutting master's degree courses, preferring to work on a real-world problem. "The textbooks are all behind the cutting edge," Li says.

When BGI put a student in charge of bioinformatics and staffed LuCamp with 20-somethings, its partners were understandably anxious. "We worried about whether they could deliver, given that most of the people working on the project were not trained scientists," Nielsen says. But the team delivered the goods.

Li eventually dropped out of grad school—"it was kind of a waste of time," he says—and now heads a 400-strong group at BGI exploring future technologies.



Room to grow. BGI is looking to agriculture and other fields to boost its revenues.

CREDIT: D. NORMILE/*SCIENCE*

Downloaded from www.sciencemag.org on February 2, 2012

Published by AAAS



CREDIT: D. NORMILE/*SCIENCE*

A package deal

The dramatic decline in sequencing costs, from $50,000 for a human genome 5 years ago to approaching $1000 today, was expected to spur a "democratization" of sequencing. Instead it is sparking more-ambitious sequencing plans with ever-more-complex logistics and bioinformatics. That plays to BGI's strength, which is "the integration of both the sequencing and the bioinformatics," Nielsen says. And it explains BGI's attraction to its growing stable of partners. For the rice project, after BGI sequences thousands of rice strains, IRRI intends to link biological characteristics to sequence data—in other words, connect phenotype to genotype. It aims to identify genes for desirable traits such as drought tolerance, pest resistance, and grain quality to improve commercial varieties. "BGI is the only one with the muscle" to carry out such a massive effort—sequencing 3000 strains and possibly 7000 more later—in a reasonable amount of time, says IRRI plant geneticist Hei Leung.



Early achiever. Li Yingrui, 25, leads a 400-strong team.

Hammarström, meanwhile, hopes to unravel the genetics of immune disorders. He and others have hunted for disease-related genes by looking at single-nucleotide polymorphisms in the genomic region associated with the major histocompatibility complex (MHC), a cell surface molecule that is key to the immune response. That approach has come up empty-handed, Hammarström says. Unraveling the genetics is tricky because many conditions are rare and likely involve multiple genes, hence the need for a huge number of samples. BGI will sequence the MHCs or exomes of 100,000 patients and controls in 5 years. The plan is "ambitious, yes, but within reach," Hammarström says.

The Center for Applied Genomics of Children's Hospital of Philadelphia (CHOP) is also partnering with BGI. CHOP and BGI had originally hoped to get NHGRI funding to set up a new sequencing center. When it became clear they would not win support, the two institutes dipped into their own resources to establish BGI@CHOP. Pediatrician Hakon Hakonarson, the center's director, says CHOP is already basing clinical decisions on the likely efficacy and side effects of medications by comparing patients' genotypes with samples in the hospital's biobank—the largest of its kind, with samples from most pediatric diseases along with data on medication, response, and side effects. Through whole-genome sequencing of samples, they expect to make more comprehensive and precise clinical decisions. "This is the future of medicine," Hakonarson says.

To execute this plan, BGI will set up a sequencing center at CHOP. It will start with 10 sequencers and could later add up to 40 more. One big advantage of the U.S. operation, Hakonarson says, is that BGI will have a better shot at winning National Institutes of Health grants. He envisions half of the sequencing capacity set aside for studies using CHOP's biobank and half for BGI's non-CHOP projects.

CHOP is one of three beachheads that BGI is establishing outside China. Over the past year, it has announced plans to also set up sequencing operations in Copenhagen and at the Sacramento campus of the University of California, Davis. Centers are being mulled for southern Europe, Japan, and Australia. Baylor's Gibbs welcomes BGI's American ventures. "We're thrilled that we've got more people in the mix," he says. He believes the U.S. centers have an advantage over BGI in expertise integrating sequencing, bioinformatics, and biology.

Day of reckoning

BGI may not be able to sustain its breakneck pace forever. Yang says that although BGI can sequence more economically than anyone, "we do not make money on it." Thanks in part to services such as prenatal screening and genetic typing for bone marrow or organ recipients, BGI had about 1 billion yuan ($158 million) in revenue in the year through March 2011—enough to break even, Wang Jian says. They pay interest on the debt but must start paying back principal in 10 years. To generate more income, BGI is expanding its applied research portfolio. It launched an agricultural department in 2009 to use genomic techniques to improve cultivars, particularly of overlooked crops such as foxtail millet. BGI is developing genetically modified minipigs as models for breast cancer and degenerative diseases such as Alzheimer's and atherosclerosis, and it has high hopes for payoffs from synthetic biology.

With partners in diverse fields, BGI could be better positioned than its rivals to benefit if genomics begins to produce long-promised rewards. "They're being very intelligent about picking their collaborators," says Richard Cotton, a geneticist at the University of Melbourne in Australia who works with BGI on the Human Variome Project. "In the next 10 years," Wang Jun predicts, "we will be able to develop something useful for ordinary people." That may allow BGI to begin paying down its massive loan.

BGI's day of reckoning is at least a decade away. For now, its bold ambitions are carrying the day. "They make you realize the sky is the limit," Hammarström says.

–DENNIS NORMILE

Downloaded from www.sciencemag.org on February 2, 2012

Published by AAAS



Water unleashed. The Mississippi pours through the 10-ton floodgate of the Morganza spillway.

CREDIT: PATRICK SEMANSKY/AP

ECOLOGY

Rebuilding Wetlands by Managing The Muddy Mississippi

When spillways were opened to divert the flooding Mississippi last spring, scientists studying the waters sought data that might help restore the river's eroding delta

The Mississippi delta is in trouble. The thick lobe of sediments at the river's mouth—called the Bird's Foot delta for the three tributaries radiating from the main river channel into the Gulf of Mexico like the flexing claws of a large bird—marks where the mighty river has poured into the Gulf of Mexico for the past 600 to 800 years. Seasonal flooding along the river once swept pulses of sand, silt, and clay to the coast, forming a foundation for the vast wetlands. But these days, a complex network of humanmade river channels, levees, and dams, intended to control the river and save coastal communities from flooding, has cut sediment supply to the delta in half. Rising sea levels due to climate change and lowering land surface from groundwater pumping and oil and gas extraction are also taking their toll.

The result of this perfect storm of problems is that the delta's coastal wetlands—one of the most storied ecosystems in the world—are now rapidly ebbing away. River-borne sediments took about 7000 years to build the roughly 21,000-square-kilometer Mississippi delta region, but the ocean has reclaimed much of it in only a century. "Land loss and gain is closely coupled to the course and management of the Mississippi River and its sediment load," says Alex Kolker, a geologist at Louisiana Universities Marine Consortium in Chauvin. Since 1900, he notes, about 4900 square kilometers of land have been lost—an area roughly the size of Delaware.

The shrinking delta is a critical problem, and not just for naturalists: Louisiana's coastal ecosystem is big business, home to commercial and recreational fishing industries worth $3.5 billion a year, and the wetlands harbor plant and animal species that attract more than $220 million in tourism each year. And as the deadly impact of 2005's hurricanes Katrina and Rita highlighted, robust wetlands and barrier islands could also act as a natural buffer for the coast against storm surges and waves.

Coastal managers and scientists have struggled to find ways to restore water flow through the wetlands and bring back the sediment. Oddly, a recent natural disaster, the 2011 Mississippi River floods, suggests that answers to the sediment-resupply problem may lie in some of the very coastal-management structures erected to chain the river. "No one had any idea, when [these structures] were put in place in the past century, that they could be used for rebuilding or restoring wetlands," says Jeffrey Nittrouer, a geologist at the University of Illinois, Urbana-Champaign.

The April and May 2011 floods along the Mississippi River—the second largest on record in the region, after the floods of 1927—claimed several lives and cost as much as $4 billion in damage. The toll would have been still higher, but to divert floodwaters bearing down on Baton Rouge and New Orleans, the U.S. Army Corps of Engineers controversially, and for the first time since 1973, decided to open the Morganza spillway.

The released water flooded some oyster farms and crops and threatened towns downstream. But to Kolker, Nittrouer, and others interested in preserving or rebuilding the Mississippi delta, opening that spillway did offer a rare opportunity to conduct a large-scale natural experiment in real time. Some coastal managers and researchers have suspected that properly managing the Mississippi's annual floodwaters might be the most effective way to bring the sediment back to the wetlands. The idea, Kolker says, would be to partially divert the Mississippi, timing those diversions "so that you open them widest during a large flood and then close them during low-flow periods."

But there's a lack of data concerning how diverting the river might affect the large loads of sediment the floodwaters carry. Or at least there was until researchers such as Kolker and Nittrouer, many aided by rapid-response grants from the U.S. National Science Foundation, scrambled last spring to document the impact of the spillway's flooding on the delta. "We knew this was going to be a large event," Kolker says. "The nice thing about a river flood is you can see it coming."

The natural experiment, as several research teams reported at the American Geophysical Union (AGU) meeting in December, gave mixed results: The floodwaters did carry enough sediment to help rebuild the wetlands, but that material didn't always stay where it could do the most good. However, Nittrouer notes, researchers gained valuable insights from the 2011 diversions—including ideas about how spillway design can help produce more targeted sediment deposits, and what volume of flow through the spillways might be required for effective wetland rebuilding.

Parting the waters

Before last year, Nittrouer and other scientists couldn't answer basic questions about what happens to the Mississippi's sediment during a large, managed flood. "There

Downloaded from www.sciencemag.org on February 2, 2012

Published by AAAS

are no real strong science publications on coastal management and diversions," Nittrouer says. For example, it wasn't clear if the released sediment would reach the wetlands or stay there, or even whether managed floodwaters actually carry enough sediment to make a difference. Even with managed diversions, the land might submerge faster than it could rebuild.

When the Army Corps flipped the switch on the Morganza spillway on 14 May 2011, some answers to those questions began to rush in. This spillway diverts waters from the main Mississippi channel into the broad, shallow Atchafalaya Basin, just to the west of the river, and daily satellite images soon revealed a huge plume of sediment making its way through the basin. Keeping an eye on those images, Nittrouer and his team set to work on the ground, mapping not only the plume's path but also the volume and distribution of the sediment at different depths within the water. They also assessed the distribution of sediment sizes in the water, from sand to silt to clay. Cores in existing wetlands, he says, reveal that sand is best for wetland- and delta-building, because the larger grains settle out of the water earlier, and sandy sediment is easier for plants to colonize.

Kolker, too, was tracking the progress of the floodwaters and the plume of sediment, using current meters, salinity, and temperature data. His team found that most of the sediments in the floodwaters diverted through the Atchafalaya Basin ultimately went out onto the shelf rather than remaining in the basin. It's a disappointing result, he says, although not really a surprise. But what was heartening, he adds, is the volume of sediment in the floodwaters: "What this means in terms of coastal restoration is that these floods bring in huge pulses of material—and we have to figure out ways to keep these materials in the nearshore zone."

Nittrouer says he was also encouraged by the volume of sediment his team found in the floodwaters. Another useful piece of information, he says, is the discovery that the design of the spillways themselves has a major bearing on the fate of the sediments. His team found that out by comparing the sediment plume that passed through the Morganza spillway with another plume: one that traveled through the Bonnet Carré spillway, 19 kilometers west of New Orleans, which the Army Corps also opened in May to divert floodwater into Lake Pontchartrain.

Both spillways have a forebay, a large pool where the floodwaters collect before the spillway is opened. The Morganza's forebay is many kilometers across—and acts like a big sediment trap, it turns out. Much of the floodwaters' sediment settled out into the forebay and never even made it to the Atchafalaya Basin, Nittrouer's team reported at the AGU meeting. By contrast, the Bonnet Carré's forebay is only 300 meters wide; sediment was shunted directly through the forebay and across the spillway into the lake. That's a key piece of information for possible restoration and management plans using diversions, Nittrouer notes. "The Bonnet Carré would be a design structure more analogous to a diversion plan," he says.



Muddy waters. A surge of sediment carried by the Mississippi and Atchafalaya rivers reached the gulf on 17 May 2011.

CREDIT: COURTESY OF MODIS RAPID RESPONSE TEAM/NASA

In one of the biggest surprises, Nittrouer says, measurements taken at the Bonnet Carré spillway revealed that even the uppermost 5 meters of water contained a significant amount of sediment, particularly sand. That's important, because the spillways decant only the top 10% to 20% of the floodwaters. Computer models of river diversions seriously underestimate that portion's sediment, Nittrouer says, because they average sediment concentrations across many tens of kilometers of river length instead of zooming in on how the twists and turns of the river affect sediment dynamics and sediment load. "What we found is that these local effects of sediment transport conditions … are extremely important for getting sediment out of these diversions," concludes Nittrouer, who helped organize the AGU session.

How to take such information and build it into models aiding coastal restoration management is now the challenge facing researchers. More data may be arriving soon: On 12 January, Louisiana's Coastal Protection and Restoration Authority (CPRA), created in 2006 to study how to combat the coastal erosion, released a draft of its 50-year plan to shore up Louisiana's coastline. A team of CPRA scientists, engineers, and administrators, with advice from an independent scientific board, spent 2 years analyzing nearly 400 proposed scientific projects, including restoration projects such as river diversions and marsh rebuilding, as well as risk-reduction projects, such as building new levees to protect against storm surge or floodproofing structures. The new draft selects 145 projects for funding, at a cost of $50 billion, divided equally between restoration and risk-reduction plans. Following a public-comment period that lasts through 25 February, the plan will move on to the Louisiana Legislature on 26 March.

"This whole attempt to reconstruct the Louisiana coastline is truly novel because of the scope and scale," says William Dennison, a marine scientist at the University of Maryland's Center for Environmental Science who chaired CPRA's independent science board. "The whole thing is a big experiment."

Nittrouer acknowledges that conclusions based on the data from the spillway openings are too preliminary to shape policy about diversions and coastal management. But it's a start. "Ultimately, if we're going to understand something about delivering water and sediment from the main channel to wetlands, it's important to get the timing and magnitude down," he says.

And the bottom line, he adds, is good news: Diverting enough sediment to kickstart wetland restoration won't necessarily require a flood on the scale of the 2011 disaster. Even with much smaller flows, the extensive network of flood-control devices along the Mississippi means that "you can efficiently and effectively route sediment outside of the main channel for the sake of constructing new coastal landscape. … It's something that you could reproduce in the future."

–CAROLYN GRAMLING

Downloaded from www.sciencemag.org on February 2, 2012

Published by AAAS



Saudi Arabia of the north. The new technologies of fracking and horizontal drilling are driving an oil boom in North Dakota.

OIL RESOURCES

Technology Is Turning U.S. Oil Around But Not the World's

The high price of oil is driving technological innovation that has reversed the decline in U.S. oil production, but the world will increasingly depend on OPEC and "non-oil" oil

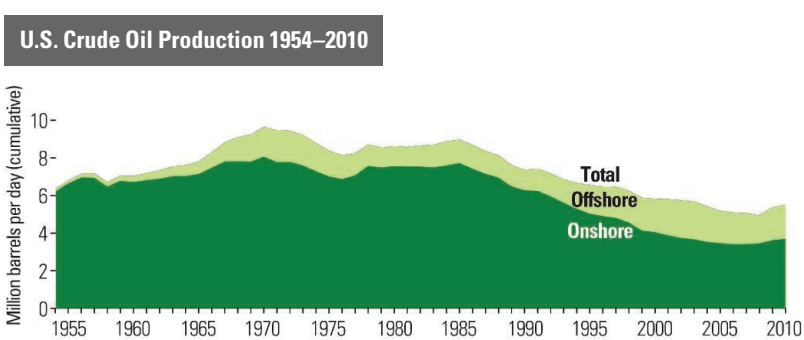
The 1 October 2011 *Wall Street Journal* headline was none too subtle: "How North Dakota Became Saudi Arabia." Blatant boosterism, perhaps, but not complete fantasy. Hard against the Canadian border, North Dakota has a full-blown oil boom under way. The state's oil production recently quadrupled in 3 years, making it the fourth largest oil-producing state in the world's third largest oil-producing country. And that gusher has been instrumental in reversing the 2-decade-long decline in U.S. oil production.

For technological optimists, North Dakota's oil boom demonstrates the future of oil outside of the Organization of Petroleum Exporting Countries (OPEC). Oil production "is a high-technology industry, [and] I don't think the innovation will come to an end," says Daniel Yergin, chair of IHS Cambridge Energy Research Associates (CERA) in Massachusetts.

New techniques such as the "fracking" that is now unlocking North Dakota's oil riches will frustrate the oil "peakists," Yergin writes in his recent book, *The Quest*. For at least 20 years, peakists have been warning of an imminent maxing out of world oil production. Yergin thinks not.

Instead, Yergin says, technological innovation driven by higher prices will make hard-to-extract North Dakota "tight oil," Canadian oil sands, and far-offshore deposits accessible and profitable. That opening of new, abundant sources will help put off the much-feared peak until "perhaps sometime around mid-century," Yergin writes.

Less-optimistic analysts remain unconvinced. "Technology does make a difference," says oil analyst Richard Nehring of Nehring Associates in Colorado Springs, Colorado. But "the question is how big that difference is going to be." Many think it will barely offset the declining output of aging fields. "You can definitely keep squeezing more out of what you've found, but everything gets harder," notes energy analyst David Greene of Oak Ridge National Laboratory in Tennessee. Because harder means slower, Yergin's mid-century timing of the peak remains dubious for many analysts. "We're getting pretty close to it right now," Nehring says.



Up, down, and up again. U.S. oil production peaked in 1970, declined through years of low prices, but lately rose again with high prices and new drilling technologies.

The big squeeze

For drillers outside of OPEC, cheap, easy oil is now a thing of the past. Fields that gushed oil on their discovery in the 1930s, '40s, and '50s are well on their way to a dribble. And discoveries of truly huge oil fields capable of easily delivering a half-billion barrels or more are now few and far between. That suggests to some that world production is about to peak.

U.S. oil production, once the world's largest, peaked in 1970. It has since been in decline except when it temporarily plateaued in the early 1980s as Alaskan oil was tapped and high oil prices drove a frenzy of drilling. Although prices rose again through the 2000s, U.S. production continued to decline as oil production outside of OPEC plateaued for the past 8 years or so.

For years, no one outside of OPEC seemed able to produce oil any faster, price incentives or not. But U.S. drillers have been getting serious. Some borrowed technology from the natural gas industry that frees up gas bound in nearly impermeable rock (*Science*, 25 June 2010, p. 1624). In such hydrofracturing or "fracking," wells are drilled down into layers of gas-bearing shale and bored horizontally for great distances; then high-pressure water is pumped in, cracking the surrounding rock. By raising production in North Dakota and elsewhere in the west, fracking of "tight oil" has now boosted U.S. oil production by almost half a million barrels a day.

U.S. drillers using other, incrementally improving technologies inched out into the once-inaccessible "ultradeep" waters of the Gulf of Mexico. Offshore oil production in shallow to deep waters had been declining since 2003. But with

CREDITS (TOP TO BOTTOM): JIM BLECHA/COURTESY OF WHITING PETROLEUM CORP.; U.S. ENERGY INFORMATION ADMINISTRATION/ANNUAL ENERGY REVIEW 2010

Downloaded from www.sciencemag.org on February 2, 2012

Published by AAAS

the newly developed ability to drill in waters deeper than 1500 meters, oil began to flow from these ultradeep waters in 2005. By 2009, ultradeep-water production had reversed the decline in Gulf of Mexico production and returned it to its peak of the early 2000s.

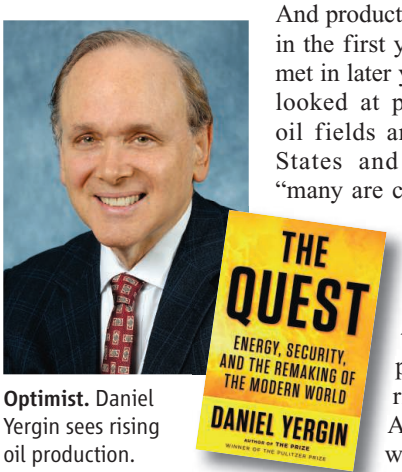
New, high-tech ways for getting at hard-to-extract oil haven't been limited to the United States. Rather than drilling for oil, Canadians have been digging for it in the so-called oil sands of Alberta, where subsurface sands come coated with a tarry substance that is convertible to oil. With refined technology, Canadians have been digging or steam-extracting more oil of late, hitting 1.5 million barrels per day in 2010. Yergin projects that oil sands production could double by 2020.

Unconventional sorts of oil such as tight oil and oil sands are "expanding the definition of oil," Yergin writes. Going further, he and various authorities now consider natural gas liquids (NGLs)—the lightweight hydrocarbons that condense from gas once it has left the ground—as part of the "liquids" that will meet the world's growing demand for anything like crude oil. Organizations such as the U.S. Energy Information Agency (EIA) and oil giant BP now even include biofuels in the liquids category. "I can't tell what it is that's going into my car's tank," says BP's senior U.S. economist, Mark Finley in Washington, D.C. "They all go into the mix."

Sufficiency or scarcity?

With high prices driving so much innovation, Yergin is optimistic. The headline of his 17 September 2011 *Wall Street Journal* article says it all: "There Will Be Oil." CERA has projected that the world's *liquids* production will grow from 93 million barrels per day (mb/d) in 2010 to about 110 mb/d in 2030, meeting expected demand. BP's Energy Outlook 2030, released last month, shows similar gains by 2030.

According to BP's projections, non-OPEC liquid supply will grow. Growth in production of U.S. and Brazilian biofuels and of oil from Canadian oil sands, Brazilian deep water, and U.S. tight oil will offset continued declines in aging non-OPEC fields. "We don't perceive a world facing a global resource constraint," says Finley. And tight oil and offshore oil will even hold off any further decline in U.S. crude oil production through at least 2035, according to an EIA report released late last month.



Optimist. Daniel Yergin sees rising oil production.

Peakists—along with other analysts who would decline that label—are far less sanguine. For starters, they would leave biofuels out of the discussion. Biofuels aren't oil, they note, and their development is even more uncertain than oil production is. For that matter, natural gas liquids are not part of the resource that has been the subject of the decades-long peak oil debate.

But beyond the creeping redefinition of oil, critics of projected production growth see an overabundance of optimism. True, there are trillions of barrels of oil left in the ground, they say, but how fast can it be produced? "It's about rates," Greene says. Perhaps the most fundamental rate in the debate is the growth rate's opposite number, the decline rate: how fast production in existing fields is falling. That's how fast new production must be added just to keep overall production steady. In his book, Yergin cites a CERA study that came up with a decline rate of 3%. But other estimates are more like 5%, including a 2008 estimate by the International Energy Agency in Paris.

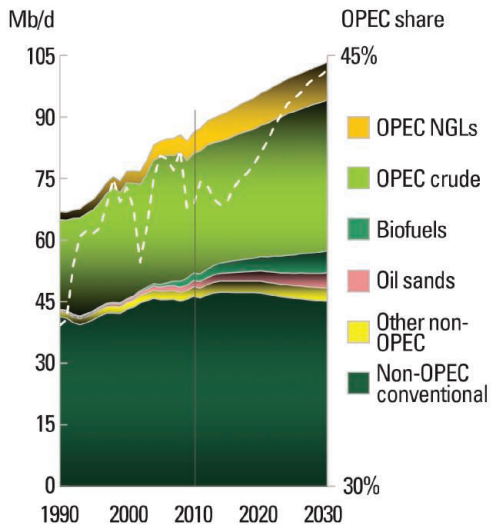
Whatever the decline rate, many projected rates of growth in oil supply are inflated by enthusiasm for new sources that have yet to prove themselves, says geologist Arthur Berman of Labyrinth Consulting Services in Sugar Land, Texas. Drillers, naturally enough, have been targeting the most promising tight-oil prospects first, he notes. But elsewhere, good productivity is likely to be frustratingly patchy. And production typically soars in the first year only to plummet in later years. Nehring has looked at prospective tight-oil fields around the United States and concluded that "many are called, but few are worth choosing."

Likewise, oil sands may have rocketed Canada to number two in proven oil reserves, right behind Saudi Arabia, but sands won't come close to compensating for the depletion of aging fields. Yergin writes that production could double there by 2020, to 3 mb/d; that would be only a few percent of world production. And there is nothing else in the world like Alberta's sands.

There are "world-class" amounts of oil in the deep offshore, Nehring concedes. But deep-water projects take 10 to 20 years to develop, he notes, spreading the contributions from the deep offshore over many years. So he calls the deep water "a plateau-prolonging source of oil."

All in all, peakists and other pessimists see the non-OPEC oil plateau of the past 8 years continuing. BP more or less agrees. Excluding biofuels, non-OPEC oil production in the BP outlook rises only about 3% by 2015 to a plateau that continues through 2030.

Liquids Supply by Type



OPEC ascendant. BP projects non-OPEC oil output (pink wedge and below) to plateau as OPEC's market share (dotted line) rises.

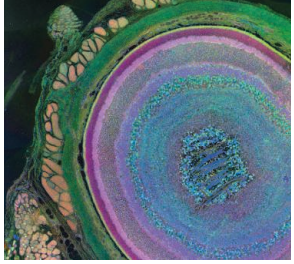
As in outlooks by other energy organizations, BP assumes that OPEC countries can and will increase production to meet any demand above what non-OPEC countries can cover. OPEC's production of natural gas liquids increases by more than 4 mb/d, or about 60% in the BP projection, but BP still sees a need for OPEC oil production to rise by almost 8 mb/d, or about 25%.

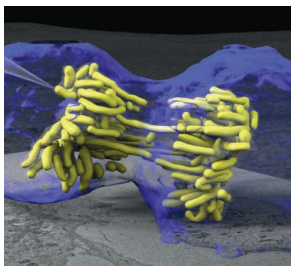
Six million barrels per day of that OPEC oil increase is slated to be split between Saudi Arabia and Iraq. In the past, Saudi Arabia has always increased its production capacity ahead of demand. But Iraq and other OPEC countries such as Venezuela and Iran have been far less reliable. "The challenges the world faces are much more above ground than below it," says Finley, referring to the political, social, and economic forces that already constrain production from abundant resources below ground. So that makes for three things to watch: the price of oil, the level of non-OPEC production, and the state of affairs in the OPEC countries.

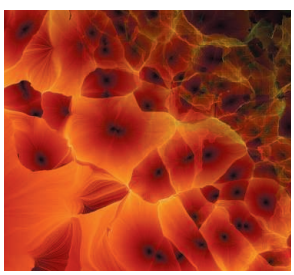
–RICHARD A. KERR

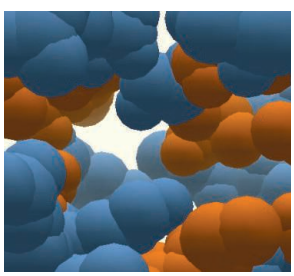
CREDITS (TOP TO BOTTOM): © BP; © JON CHOMITZ PHOTOGRAPHY; COURTESY OF PENGUIN BOOKS

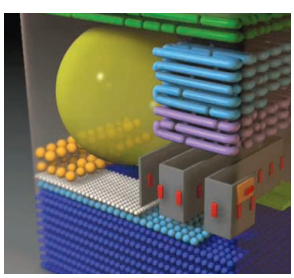
Downloaded from www.sciencemag.org on February 2, 2012











2011 International Science & Engineering Visualization Challenge

The spectacular orange-colored blossoms on the cover of this week's issue of *Science* are not what they appear to be. Turn to page 530, and you will find that the image is, in fact, a depiction of the network of voids in the cosmic web; each void can be tens of millions of light-years across. The eye-catching rendering is one of the winning entries in the 2011 International Science and Engineering Visualization Challenge.

Science and the U.S. National Science Foundation (NSF) have cosponsored this annual challenge for the past 9 years. The aim is to promote cutting-edge efforts to visualize scientific data, principles, and ideas—skills that are critical for communication among scientists and between scientists and the general public, especially students. Rapid technological change is opening new vistas in visualizing data: This year's winners include a cross-section of an eye in which different cell types are each colored a unique shade, an interactive game in which players try to mimic nature's amazing capacity for folding proteins, and a video that assembles a cell's jumble of components into an ordered assortment.

We received 212 entries from 33 countries. (U.S. entries came from 24 states and territories.) A committee of staff members from *Science* and NSF screened the entries and, in a new departure this year, those selected as finalists were posted on NSF's Web site, and visitors were invited to vote for their top choice in each category. A total of 3200 votes came in; entries that received the most votes were named the "People's Choice." Independently, an outside panel of experts in scientific visualization reviewed the finalists and selected the winners. The winning entries are featured on the following pages, in an online slideshow at http://scim.ag/y41Bht, and at www.nsf.gov/news/scivis. Some entries were put together by large teams, not all of whose members could be listed in print; the online presentations provide more details. Tarri Joyner and Zachariah Miller of NSF organized this year's challenge. Daniel Strain of *Science*'s News staff wrote the text that accompanies the images in this special section.

We encourage you to submit applications for next year's challenge, details of which will be available on NSF's Web site, and to join us in celebrating this year's winners.

COLIN NORMAN, NEWS EDITOR, *SCIENCE*

Downloaded from www.sciencemag.org on February 2, 2012

Judges

Donna Cox
National Center for Supercomputing Applications, University of Illinois

Alisa Zapp Machalek
National Institute of General Medical Sciences, National Institutes of Health, Bethesda, MD

Keith Powers
Powerful Concepts, Palo Alto, CA

Corinne Sandone
Johns Hopkins University School of Medicine, Baltimore, MD

Tierney Thys
National Geographic Explorer, Carmel, CA

Thomas Wagner
NASA, Washington, DC

Science

NSF

Published by AAAS

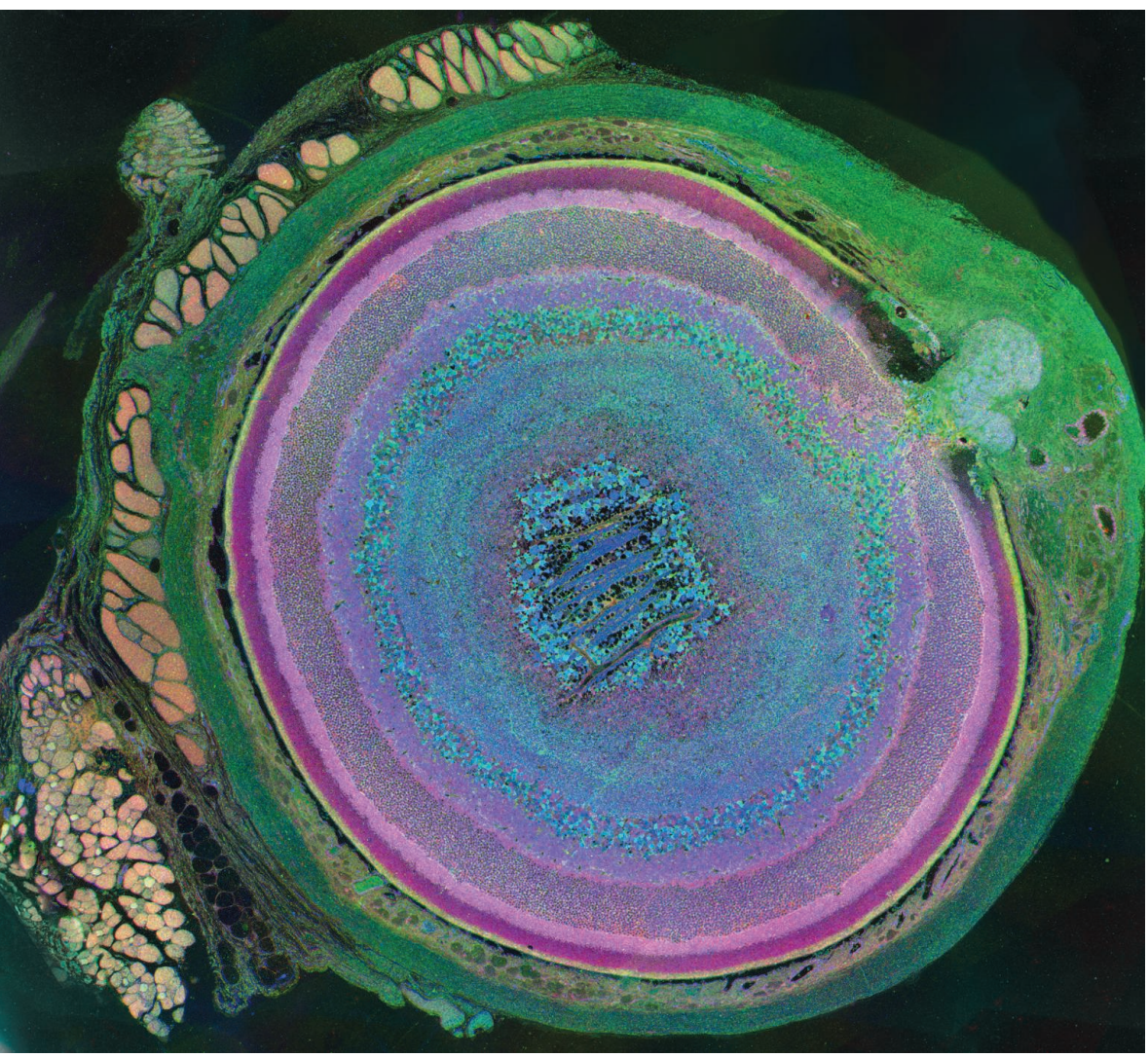
PHOTOGRAPHY

1ST PLACE
Metabolomic Eye
Bryan William Jones
University of Utah Moran Eye Center

Eyeballs—now in Technicolor. This photograph, taken by neuroscientist Bryan Jones of the University of Utah's Moran Eye Center (MEC) in Salt Lake City, may look like a piece of candy. But it's actually a metabolic look at the wide diversity of cells in the mouse eye—in all, 70 different types of cells, from muscles to retina, each colored a unique shade.

To map out the tissues in this mouse's eye, Jones turned to a technique called computational molecular phenotyping (CMP). This approach, pioneered by Robert Marc, also at MEC, takes advantage of the unique array of molecules in all cells in a tissue. "Within a cell type, there is a very narrowly regulated fingerprint that defines who that cell is and what that cell does," Jones says. In this case, he probed the relative concentrations of several common organic molecules.

Using a tool that cuts into biological material on the microscopic scale, Jones shaved into the eye, creating serial 120-nanometer-thick slices, thinner than the wavelength of light—much like licking a gobstopper, he says. Jones then stained those layers with specialized antibodies that bind to three molecules: taurine, glutamine, and glutamate, which he assigned to red, green, and blue color channels on a computer. The unique distributions of these molecules can be seen here in rainbow color. Muscle cells, located at the left edge of the image, look pale yellow, whereas scleral tissue, surrounding the entire orb, shows up green in this image.



In order to study the molecular fingerprints of specific tissues, scientists previously had to grind up entire organs and analyze the cells all together. That turned what might be a metabolically diverse organ into a homogenous mess, Jones says. But CMP highlights a tissue's complexity. "There's incredible diversity in a cell population normally thought to be homogenous." And mammal eyes aren't even the most complex retinas out there, he adds. Goldfish eyes, for instance, contain more than 200 separate cell types.

The photograph is certainly eye-catching, says challenge judge Alisa Zapp Machalek. "It was just what we were looking for," she says. "It was the perfect balance between a beautiful picture that tingles the eyeballs and something that is incredibly informative."

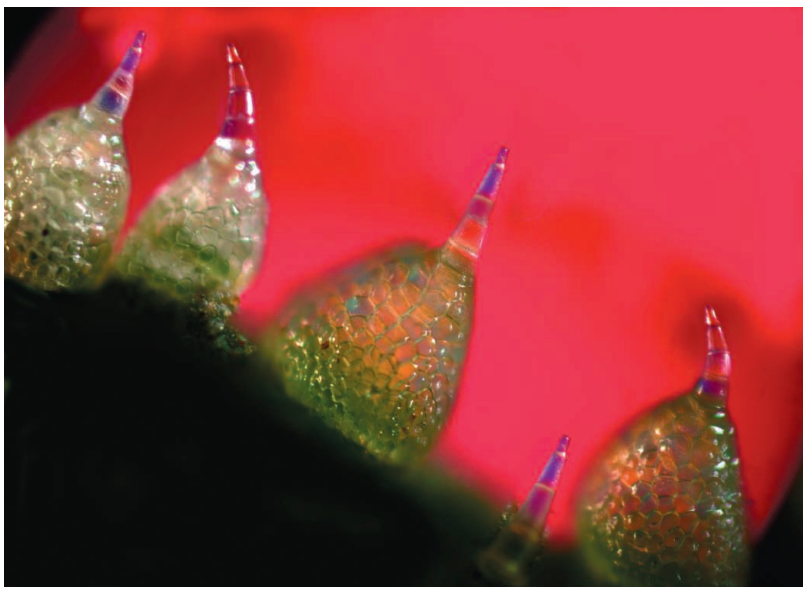
Downloaded from www.sciencemag.org on February 2, 2012

Published by AAAS

HONORABLE MENTION

Microscopic Image of Trichomes on the Skin of an Immature Cucumber

Robert Rock Belliveau



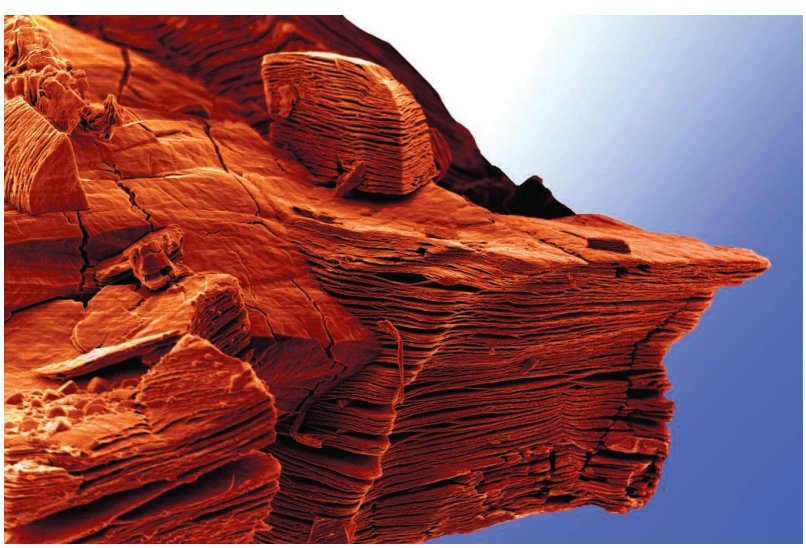
No, this photograph doesn't depict alien slugs stripped from a science-fiction film—just the surface of a young cucumber. It's a new perspective on an old vegetable. To take this close-up, vibrant shot, photographer Robert Belliveau employed a polarizing microscope. Unlike normal light microscopes, which use unpolarized light, these zooming tools adopt plane-polarized light and record the refraction of light as it passes through small objects to produce a sharp, colorful image.

The structures shown here at 800× magnification are trichomes. They coat the surface of still-growing cucumbers and look, to the naked eye, like a thin film of hair. That fuzziness, however, belies the structures' nasty streak. The tips of trichomes taper to a point that can pierce the mouths of predators, and their bulbous bases are filled with bitter-tasting and toxic molecules called cucurbitacins. It's a dangerous and strange landscape that humans normally don't get to see, says Belliveau, who has also turned his microscope on tomatoes and many other edible plants. "The microscopic world of plants, especially fruits and vegetables, is such an exotic world," he says. "It's actually otherworldly."

PEOPLE'S CHOICE

The Cliff of the Two-Dimensional World

Babak Anasori, Michael Naguib,
Yury Gogotsi, Michel W. Barsoum
Drexel University



This landscape, which looks like a red-rock bluff straight out of Utah, isn't a geologic feature. Instead, it's a nanostructured material made from ultrathin layers of titanium-based compounds and seen under an electron microscope.

To construct the small outcropping, Babak Anasori and colleagues at Drexel University in Philadelphia used a technique called exfoliation. They placed Ti_3AlC_2 powders in a solution of hydrofluoric acid and stripped away the aluminum atoms. What remained were stacked layers of Ti_3C_2, seen here in false color, resembling stratigraphic mineral layers. These exfoliated layers, which the team dubbed MXenes, are so thin they are two-dimensional. In other words, each strip is only five atomic layers thick. The team is the first to render such materials in 2D. The MXenes could be used in energy storage devices, sensors, solar cells, and other applications, the team writes. And they could give the majesty of Arches National Park in Utah some nanoscale competition.

Downloaded from www.sciencemag.org on February 2, 2012

Published by AAAS

ILLUSTRATION

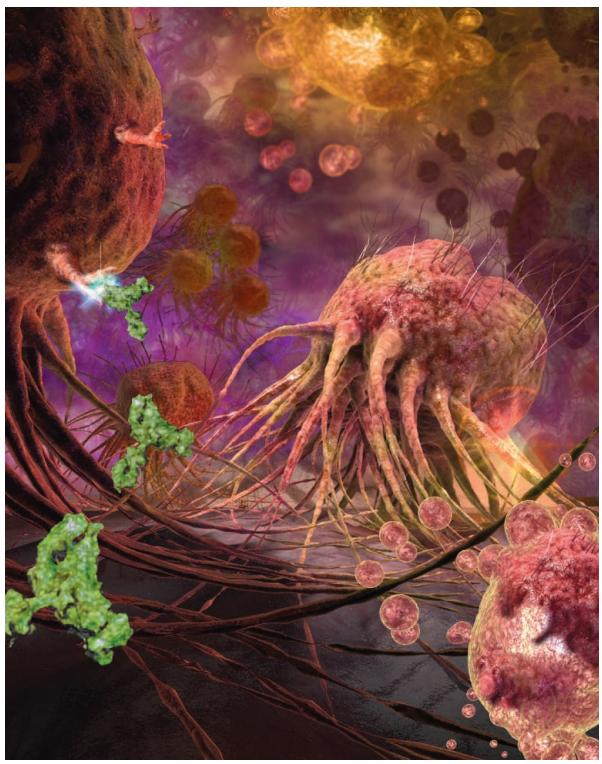
HONORABLE MENTION

Tumor Death-Cell Receptors on Breast Cancer Cell

Emiko Paul and Quade Paul, Echo Medical Media;
Ron Gamble, UAB Insight

Cancer cells get the monster movie treatment. If Emiko Paul of Echo Medical Media's illustration of breast cancer cells looks like something out of an H. P. Lovecraft short story, it's no accident. "We wanted to show something that was dramatic and very active," Paul says.

This image, modeled using 3D software then painted in Adobe Photoshop, depicts the war on cancer in a manner that makes clear who the bad guys are. Paul drew on microscopic images of breast cancer cells—seen here looking like creatures with long tentacles—for inspiration. But her illustration also depicts a possible weapon against these malignant tissues: an antibody developed by researchers at the University of Alabama, Birmingham, called TRA-8 (the green, globular structures). This molecule activates a protein on the surface of many cancer cells, which then triggers a chain of events that kills off those cells, much like a self-destruct switch. TRA-8, whose efficacy researchers are currently exploring, could be the garlic to cancer's vampire.





HONORABLE MENTION

Variable-Diameter Carbon Nanotubes

Joel Brehm
University of Nebraska, Lincoln

Nanostructures, as the name implies, are much too small to see. But using 3D modeling techniques and some guesswork, graphic artist Joel Brehm renders a handful of these ultrathin structures visible to the naked eye. Brehm's illustration focuses on the work of his colleague, Yongfen Lu, an engineer at the University of Nebraska, Lincoln. Lu and colleagues employ lasers to develop new methods for crafting thin tubes made from carbon. But not just any tubes. His team's method precisely varies the diameter and properties of these structures. The resulting tubes, seen here, widen, narrow, or even bulge out like pears along their length. These designs could improve transistors and sensors in a range of electronics, the team says.

The tricky part, Brehm says, was making the nanotubes look small even though they'd been blown up to poster size. To do that, he added a granular texture to the honeycombed stalks and also brightened their edges. Those small touches, he says, made the tubes look more like objects viewed through an electron microscope.

NOTE: There was no 1st place prize awarded in Illustration.

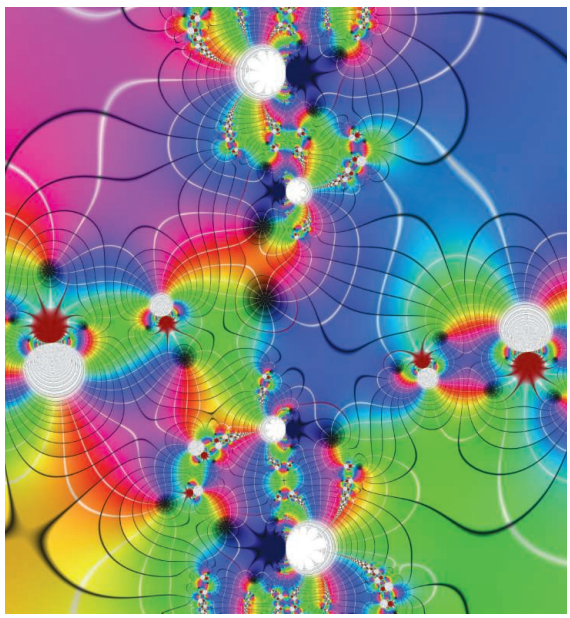
Downloaded from www.sciencemag.org on February 2, 2012

Published by AAAS

HONORABLE MENTION

Exploring Complex Functions Using Domain Coloring

Konstantin Poelke, Konrad Polthier
Free University of Berlin



Mathematicians discover their hippie sides. Forgoing long strings of digits and variables, researchers at the Free University of Berlin have taken a tie-dye approach to visualizing math equations. This illustration represents one example of a complex function. Such functions are mathematical relationships that incorporate both real numbers and what experts call imaginary numbers, such as the square root of –1.

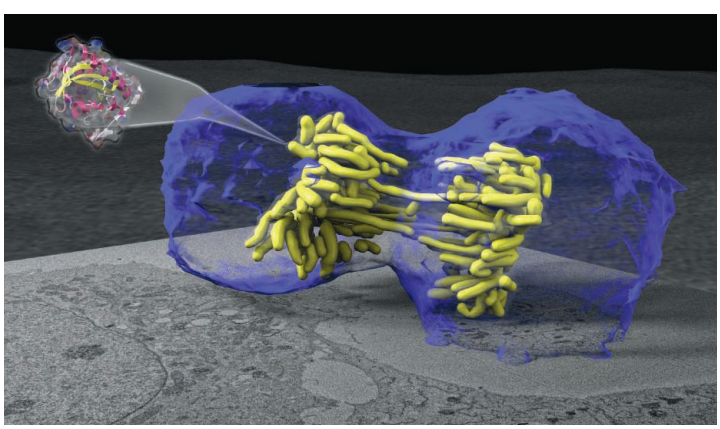
Unlike familiar sine waves or logarithmic curves, complex functions are four-dimensional, combining both inputs and outputs in two dimensions. To visualize these heady equations, Konstantin Poelke and his Ph.D. supervisor Konrad Polthier turned to and improved a technique called domain coloring. They assigned each complex number in their equation to a spot on a color wheel. The further numbers get from zero, the brighter they are (white regions, for instance, represent mathematical "singularities" that approach infinity). The result is like a topographic map, but it packs two dimensions of information (hue and brightness) into each point instead of the single dimension of altitude.

Such functions may fly right over the heads of many nonmath enthusiasts, Poelke says. But he hopes casual viewers will understand the basics of the relationships between the complex numbers shown here just by looking at the arrangement of the psychedelic shades.

PEOPLE'S CHOICE

Separation of a Cell

Andrew Noske and Thomas Deerinck
The National Center for Microscopy and Imaging Research; Horng Ou and Clodagh O'Shea, Salk Institute



From films like *Avatar* to hand-held video games, 3D is all the rage. Textbook graphics are not catching on. In this illustration, Andrew Noske of the National Center for Microscopy and Imaging Research at the University of California, San Diego, and colleagues create a visualization of mitosis that hops off the page.

The new and tactile view of a cell undergoing division comes thanks to a specialized protein called MiniSOG. This molecule, which Noske's team shows zipping toward the reader, is fluorescent and stands out crisply under an electron microscope. With some tweaking, it also binds tightly to a second protein closely associated with DNA. That gives scientists the ability to target and view in detail chromosomes as they peel apart during mitosis. The result is a far cry from the standard, flat images popular in biology textbooks, the team writes. And unlike the 3D glasses that accompany screenings of sci-fi films, this new visualization approach may be more than a gimmick, giving students a deeper look at a familiar phenomenon.

Downloaded from www.sciencemag.org on February 2, 2012

Published by AAAS

INFORMATIONAL POSTERS & GRAPHICS

1ST PLACE

The Cosmic Web

Miguel Angel Aragon-Calvo, Julieta Aguilera, Mark Subbarao
Johns Hopkins University



A spider's web catches flies. But the cosmic web depicted in the winning poster snares galaxies. Cosmologist Miguel Angel Aragon-Calvo of Johns Hopkins University in Baltimore, Maryland, and colleagues illustrate how an invisible network of matter creates space's familiar features: "This poster is [intended] to show the relationship between galaxies and the environment where they live," he says.

Galaxies don't grow out of nothing, Aragon-Calvo notes. Instead, their formation is decided by underlying but invisible accumulations of dark matter. Scientists suspect that this substance, which is still theoretical and remains impossible to observe, gives rise to most of the gravity in the universe. That gravity becomes the glue that holds galaxies together. So, in regions where dark matter is dense, galaxies begin to form, often grouping together in clusters or long walls.

In their poster, which from top to bottom represents about 240 million light-years, Aragon-Calvo and colleagues simulate that process. They explore the same patch of space from five different vantage points, traveling from the invisible to the visible. As the universe expands following the big bang, strings of dark matter condense along the edges of voids nearly tens of millions of light-years wide. These mostly empty regions of space can be seen at the far left of the poster (dark orange) bordered by bright filaments rich in matter. In the middle, weeping willow–like arcs follow the flow of matter over time. The lines converge at the present day, shown in red, and eventually spawn bright galaxies at the same points (far right). Depicting the entire "history of matter" in one poster is an ambitious task, but Aragon-Calvo hopes that viewers will come away with one message: "The universe has a rich structure." Just like a spider web.

This brightly colored illustration with accompanying text is "aesthetically beautiful," says challenge judge Corinne Sandone. And "I think it's fabulous that we can see some of the structure and to see it visualized as you move further and further into space."

HONORABLE MENTION

The Ebola Virus

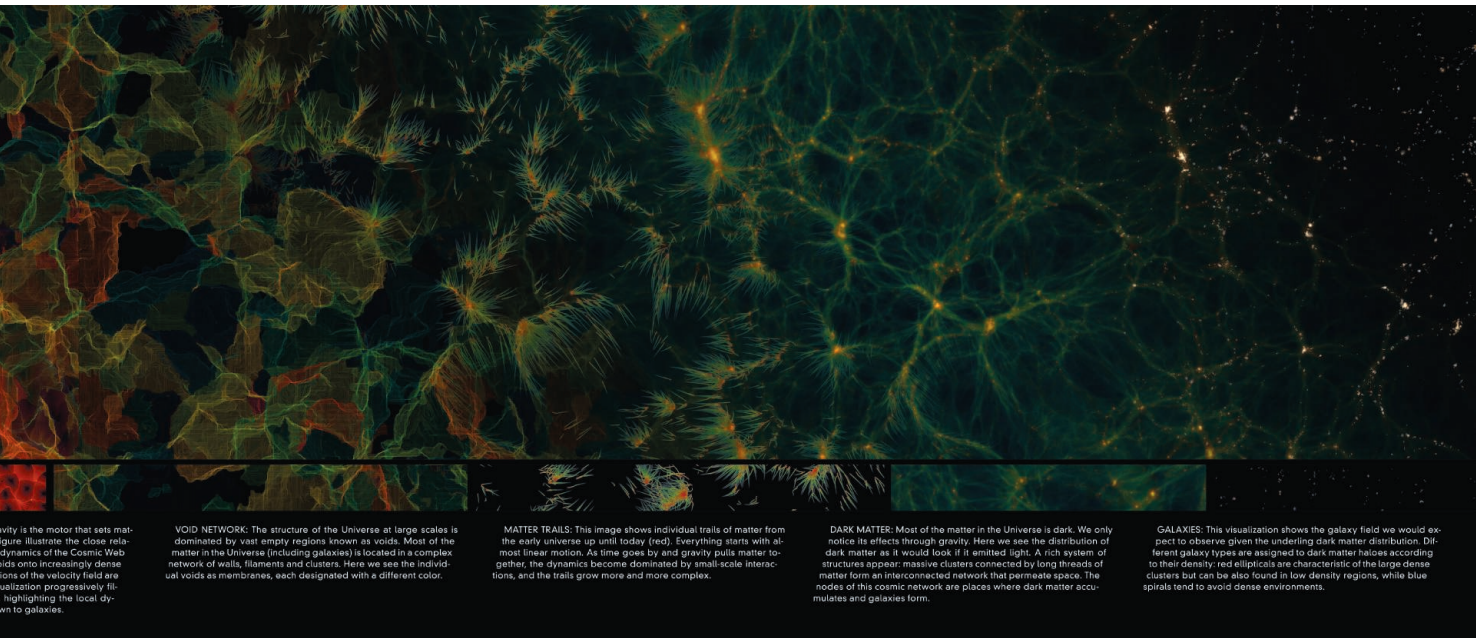
Ivan Konstantinov, Yury Stefanov, Alexander Kovalevsky, Anastasya Bakulina
Visual Science

Not all good science visualizations highlight the beauty of the natural world. Take this illustration by Ivan Konstantinov and colleagues at the Russia-based group Visual Science. His team drew on existing scientific information to depict the 3D structure of the Ebola virus, responsible for fatal outbreaks of hemorrhagic fever throughout much of Africa.

This virus, only 1400 nanometers in length, is no simple pathogen, Konstantinov says. His group previously patched together a similar 3D model of HIV. But Ebola is nearly 10 times larger, containing roughly 3 million lipids and protein molecules. The poster, too, provides a good look at how Ebola turns dangerous. Proteins coded by the virus's own genome are shown here in maroon. They're the pathogen's Velcro, clinging to the surface of target cells and giving the virus access to their interior. Anyone perusing this poster "can clearly understand that the Ebola virion is a very complex supramolecular structure, with various polypeptides, lipids, and RNA genome included," Konstantinov says. Not exactly the stuff of an Ansel Adams photograph, but an eye-catching sight nevertheless.

Downloaded from www.sciencemag.org on February 2, 2012

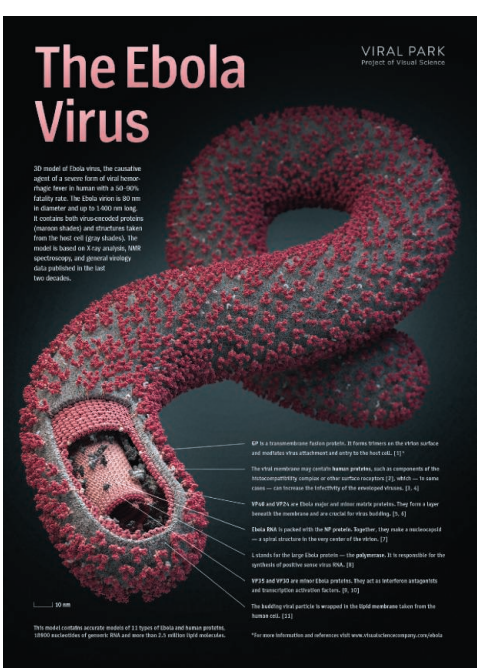
Published by AAAS



PEOPLE'S CHOICE

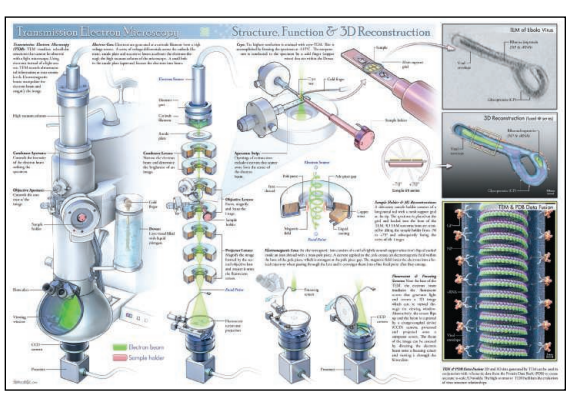
Transmission Electron Microscopy: Structure, Function & 3D Reconstruction

Fabian de Kok-Mercado, Victoria Wahl-Jensen, and Laura Bollinger
NIAID IRF



For anyone who's ever wanted to take apart a microscope to see how it works, this is the poster for you. Here, scientists at the National Institute of Allergy and Infectious Diseases Integrated Research Facility (IRF) in Frederick, Maryland, dismantle a transmission electron microscope (TEM) piece by piece—all without damaging expensive lab equipment. These instruments bombard tiny objects such as viruses or proteins with beams of electrons, capturing images too small for conventional light microscopes.

In their dissection, Fabian de Kok-Mercado and colleagues at IRF delve into deeper and deeper detail, moving from left to right. The researchers first display a TEM in its entirety. Then they follow the visualization tool down to its cryo-device (at right), which keeps organic samples cool for maximum clarity. In between, viewers themselves can track the formation of an electron beam from start to finish. It begins at the electron gun that creates the free particles using an electric current, then continues through a handful of lenses that condense, focus, and magnify the output. It's the ideal schematic for technology junkies who like to think small.



Downloaded from www.sciencemag.org on Febru

INTERACTIVE GAMES

1ST PLACE

Foldit

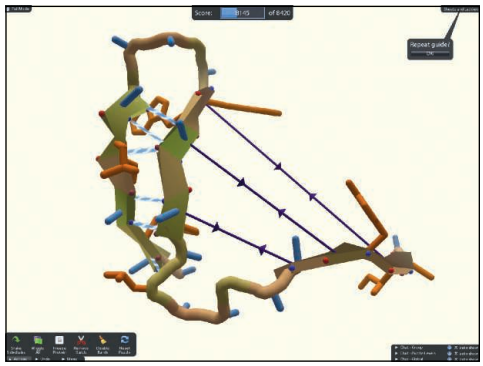
Seth Cooper, David Baker, Zoran Popović,
Firas Khatib, Jeff Flatten
Center for Game Science, University of Washington

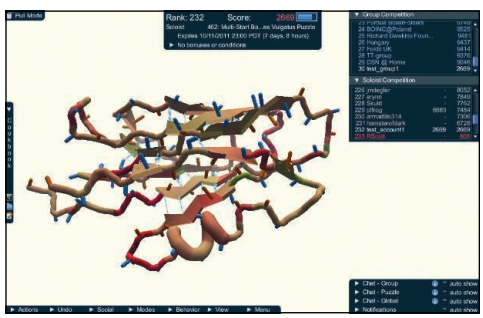
Call it origami for nerds. Foldit players rack up points for twisting, bending, and canoodling chains of amino acids to make realistic proteins. And, unlike rewards for blasting aliens or eating ghosts in Space Invaders or Pac-Man, the points in Foldit count toward science. Players are "spending their time not tending to an imaginary farm," says Seth Cooper of the University of Washington, Seattle, a member of the team that developed the game. "They're doing something with real implications."

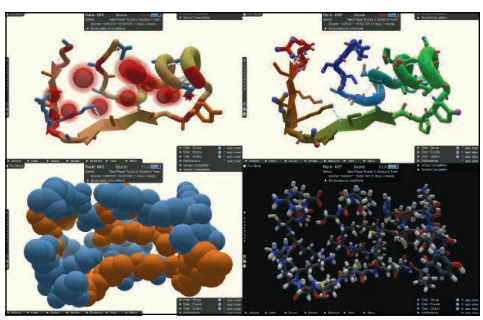
Foldit takes advantage of the human mind's savvy for solving spatial problems, Cooper says. Puzzles start with a snaking arrangement of amino acids, identical to the sequence of an actual protein. Players then have to fold that sequence into a complex 3D structure that fits the laws of chemistry. The closer players get to folding a realistic-looking molecule, the higher they score. Tiny warning blobs, for instance, pop up when water-insoluble amino acid side chains point to the outside of a protein. To make those blobs go away, competitors need to tuck the side chains into the molecule's interior.

But Foldit isn't just a fun exercise for puzzle fiends, Cooper says. It's also a great platform for turning at-home gamers into researchers. The efforts of Foldit's 200,000-plus players have helped researchers understand how a number of important proteins loop and scrunch inside cells. Players, for instance, recently resolved the 3D conformation of a protein critical to the functioning of the Mason-Pfizer monkey virus. Cooper and his colleagues published their results in 2011 in *Nature Structural & Molecular Biology*. The team also added a new feature: Gamers can play cellular architect and build proteins never before seen in nature. Scientists will then be able to draw on these player designs to construct brand-new molecules in the lab.

"I love the way Foldit crowd-sources the power of the people to solve real science problems, a feat that makes it a supremely useful citizen science project," says challenge judge Tierney Thys. And although the science of protein folding may be complicated, Foldit is accessible to a wide range of gamers, says challenge judge Thomas Wagner. And, he adds, "it was fun to play."







PEOPLE'S CHOICE

Velu the Welder

Muralitharan Vengadasalam, Ganesh Venkat, Vignesh Palanimuthu,
Fabian Herrera, Ashok Maharaja, Tata Consultancy Services



Learning to weld takes patience and nimble fingers. Some time spent on a Wii gaming console might not hurt, either. In this interactive challenge, the brainchild of developers at Tata Consultancy Services in Chennai, India, players step into a virtual apprentice workshop. They follow in the footsteps of Velu, a young Indian man getting a crash course in welding.

Although they've adapted their instructional game for the PC, Muralitharan Vengadasalam and colleagues suggest that Velu the Welder is best played on a Wii. The console's motion-sensing controller makes players feel like they're holding a real welding torch. First, Velu's stand-ins get a lesson in gas welding, completing basic welding moves on pieces of scrap metal. After that, they graduate to arc welding, joining metal pieces together to make a frame. The aim is to provide marketable skills to school dropouts in India. It's certainly a lot more productive than swinging a club in Wii golf.

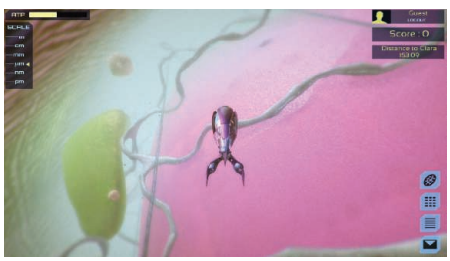
Downloaded from www.sciencemag.org on February 2, 2012

Published by AAAS

HONORABLE MENTION

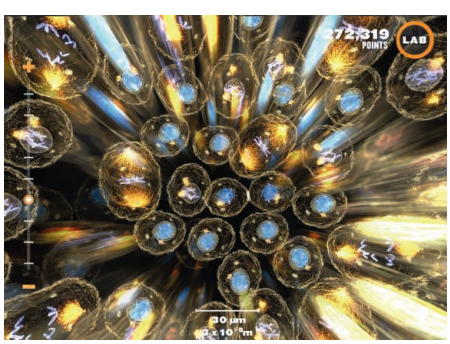
Meta!Blast 3D Interactive Application for Cell and Metabolic Biology. Level 1: The Cell

W. Schneller, P. J. Campell, M. Stenerson, D. Bassham, E. S. Wurtele
Iowa State University



Meta!Blast 3D may be the closest science education comes to Halo. While the game aims to teach novices about the cell, it's rooted, like the favorite Xbox shoot 'em up, in action. Gamers play a lab dishwasher who discovers that her entire study group—undergraduate adviser, grad students, and all—have been sucked into a photosynthetic cell. So it's time to pilot a microscopic craft around chloroplasts to the rescue. If that sounds exciting, wait until you have to dodge the ranging proteosomes that try to gobble your intracellular spaceship whole.

Adventure aside, Meta!Blast helps students "to understand that the cell is a very complex and beautiful world," says game designer Eve Wurtele, a biologist at Iowa State University in Ames. Case in point: your ship is powered by ATP. If you use too much of the cellular fuel, you sputter to a stop.



HONORABLE MENTION

Powers of Minus Ten

Laura Lynn Gonzalez
Green-Eye Visualization

Instead of playing Angry Birds on their iPads, high school–age students can use their hand-held devices to take a trip into the hand itself. In Powers of Minus Ten, developed by Laura Lynn Gonzalez of Green-Eye Visualization, players take a scavenger hunt through the skin on the human hand and into individual cells—just by flicking their fingers.

Gonzalez's game, also available on the PC, is loosely based on the famous 1968 short film *Powers of Ten*, which traveled from outer space, then deep into the human body. When players zip past the skin on the hand and enter a cell, they see animated chromosomes and proteins buzzing like Las Vegas street signs. Kids can tap on these cellular structures to learn more about them. The app is constantly evolving: Players will soon be able to delve inside the mitochondria and even zoom down to the atomic level, Gonzalez says.

Too often at this magnification, "people get lost," Gonzalez says. She hopes her interactive tour will help students learn their way around a cell. So, no angry birds but a lot of happy teachers.

HONORABLE MENTION

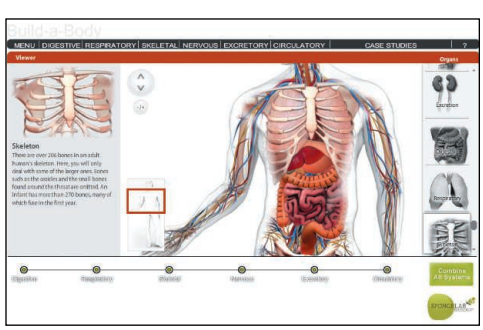
Build-a-Body

Jeremy Friedberg
Spongelab Interactive

Build-a-Body lets eighth- to 12th-graders play transplant surgeon—or, perhaps, Dr. Frankenstein. Gamers piece together the human body's systems by dragging and dropping organs into place. After plopping the small intestine into the abdomen, for example, you then score more points by figuring out how it joins to the large intestine looping around: "You're building [the body] from the ground up here," says game designer Jeremy Friedberg of Spongelab Interactive.

The game's a colorful introduction to the human body. But it doesn't stop once students have completed the systems. Build-a-Body also generates an evolving list of "case studies." Pop-up windows highlight the symptoms of various illnesses such as celiac disease, and players, now diagnostic physicians, decide what systems those diseases target.

Friedberg adds that Build-a-Body is just one piece of Spongelab's portfolio. The gaming group has also launched Build-a-Fish, Build-a-Worm, and Build-a-Frog. The quartet of games gives students the opportunity to compare differences and similarities between humans and their hopping, wriggling, or swimming kin.



Downloaded from www.sciencemag.org
ruary 2, 2012

Published by AAAS

VIDEO

1ST PLACE & PEOPLE'S CHOICE

Rapid Visual Inventory & Comparison of Complex 3D Structures

Graham Johnson, TSRI & grahamj.com;
Andrew Noske, NCMIR;
Bradley Marsh, IMB

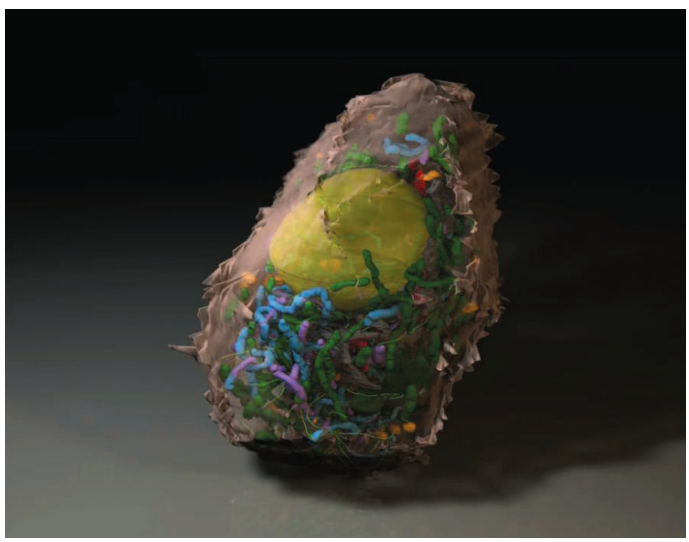
In this video, Ph.D. animator Graham Johnson of the Scripps Research Institute in San Diego, California, and colleagues take the normally jumbled pieces of a mouse pancreatic cell and stack them into neat piles. It's an organizational feat sure to please cleanliness-loving scientists. But the visualization also gives researchers and students a new look at the abundances and relative sizes of organelles, from mitochondria to insulin granules. "The cell is a lot more complicated-looking than most people think of it," Johnson says. "We wanted to clarify it."

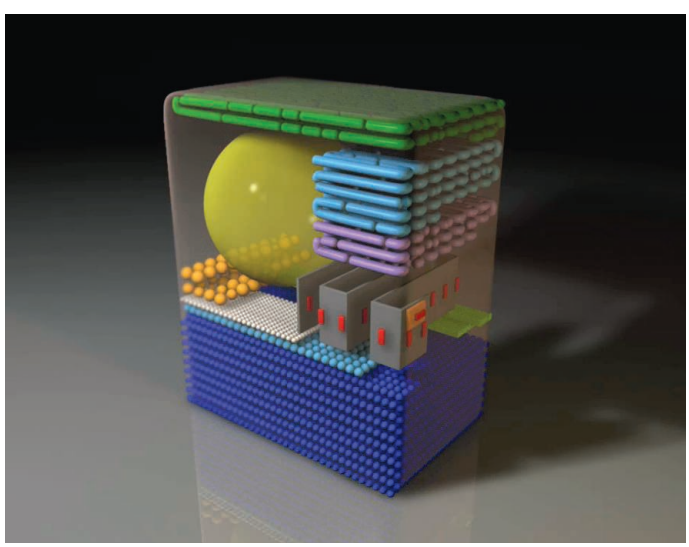
The video opens with a 3D model of a chaotic cell taken from the pancreas as seen in its natural state. Thousands of irregularly shaped organelles huddle around a central and bean-shaped nucleus. Then, Johnson and colleagues start to spring-clean. Drawing on data from the lab of team member Bradley Marsh, a cell biologist at the University of Queensland in Brisbane, Australia, the researchers simplify the cell's components and then sort them by organelle. They first group together the mitochondria (green) and insulin granules (blue), then clump these and other organelles together to form uniform columns and rows for easy comparison.

The resulting image looks less like a cell and more like a 3D abacus. But it also displays the relative volumes of these cellular factories and compartments. Surprisingly, for instance, mitochondria occupy only 7% of the cell volume, which is hard to see from the raw cell alone.

This visualization, Johnson says, represents the middle ground between the two standard depictions of the cell: the natural, or chaotic, cell and the cartoonish, or textbook, cell. That became clear when the team showed the video to school kids in Australia: "When they could see the random, video-game-looking cell morph into the type of cell that their teacher had been presenting to them from textbooks and the Internet," he says, "they really got excited."

The team "manages to weave into one short video an unbelievable amount of information," says challenge judge Tierney Thys. "From morphology to volumetrics and beyond, it presents completely different data sets in a seamless, accessible, and aesthetic manner."



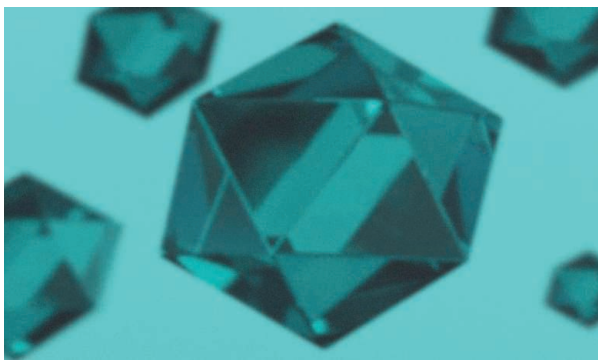


Downloaded from www.sciencemag.org on February 2, 2012

HONORABLE MENTION

High-Density Energy Storage Using Self-Assembled Materials

Christopher E. Wilmer, Omar K. Farha, Patrick E. Fuller
Northwestern University



In one of the most famous scenes in *2001: A Space Odyssey*, futuristic spaceships spin and twirl to *The Blue Danube* by Johann Strauss. Christopher Wilmer and colleagues at Northwestern University in Evanston, Illinois, kick off their video with that same whimsical waltz. Instead of spinning spaceships, however, their visualization shows hundreds of molecules floating around and joining to each other to form solid crystals. Wilmer, a big fan of Stanley Kubrick's 1968 film, had for years looked for an "excuse" to dramatize his research using Strauss's music: Kubrick "wanted to convey the majesty of space engineering," Wilmer says. "I also wanted to convey the majesty of self-assembly on the molecular scale."

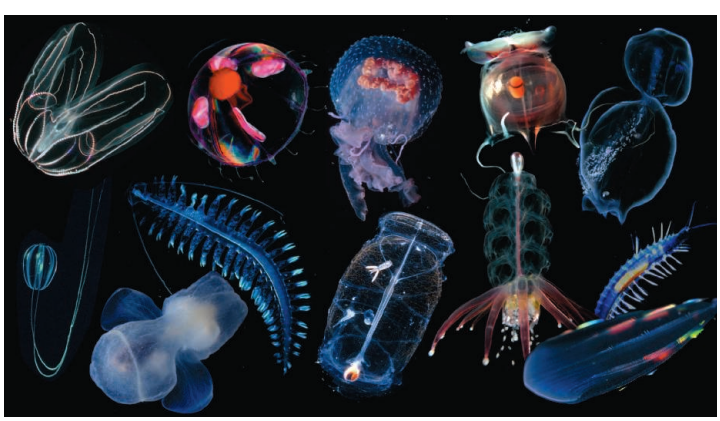
Wilmer's work focuses on how gaseous fuel molecules such as methane cling to solids. Unlike liquid gasoline, gaseous methane—a much cleaner energy source—is tough to squeeze into automobile gas tanks. But when scientists add special porous crystals to those tanks, methane begins to cluster inside the pores, greatly increasing the gas's density. His team employs computer algorithms to screen thousands of possible crystal structures to identify the ones best suited to concentrating methane and other gases. The topic isn't simple, but, with the help of this playfully animated video, Wilmer says he and his labmates have finally been able to explain their research to relatives. The homage to a sci-fi classic doesn't hurt.

HONORABLE MENTION

There's No Such Thing as a Jellyfish

Steven Haddock, Susan Von Thun
MBARI & jellywatch.org

Don't call them jellyfish. Portuguese man o' wars, comb jellies, and larvaceans may all look gooey and diaphanous, but they're also very different animals, according to this video by marine biologist Steven Haddock and colleagues at the Monterey Bay Aquarium Research Institute in Moss Landing, California. Creatures often lumped under the label "jellyfish" in truth reflect a startling diversity of sea life: "Jellyfish are not just horrible, ugly stinging blobs," Haddock says. "They're actually a lot of different shapes and sizes."



Haddock and his crew shot the creatures in this video from a deep-sea submersible below California's Monterey Bay. There are the long and billowing sea nettles belonging to a class of animals called Scyphozoa and Siphonophores such as the purple and sometimes deadly Portuguese man o' wars. Many of these organisms live as gigantic superorganisms, in which many individuals have specialized to take on different roles. Comb jellies are frequently covered in rows of beating hairlike cilia that propel them through the water. Then there are the larvaceans, pea-sized invertebrates that secrete balloonlike houses made from mucus. In all, the video is an effective PSA for the neglected creatures of the sea.

www.sciencemag.org on February 2, 2012

Published by AAAS





LETTERS

edited by Jennifer Sills

Investing in Libya's Education

HIGH LEVELS OF UNEMPLOYMENT (20 TO 30%) (*1*), RAMPANT CORRUPTION, and social and intellectual oppression caused Libya's youth to revolt against the Gaddafi regime. They now hope to play a role in rebuilding the country. They can start by insisting that the Libyan government realign and scale up its education system.

Libya's education system faces serious challenges. The country's infrastructure has been extensively damaged (*2*). Primary and secondary education is outdated, poor quality, and not designed to generate free-thinkers and leaders. Furthermore, higher education planning has not been strategic (*3*). Libya has many low-quality physicians (*4*), for example, and medical research outputs have been abysmal (*5*). Finally, in the absence of skills and job prospects, a group of young revolutionaries are refusing to lay down their arms, thereby posing a security challenge to the country.

To reform the education system, a task force with national and international experts should be established to focus on short-term and long-term needs. In the short term, the young armed men should be provided with opportunities to transition from being the armed guardians of the revolution to builders of a new nation. Vocational training should be offered to them followed by job opportunities in areas such as construction, communication, and energy. In the long term, both lower and higher education systems must be redesigned to meet global standards and train a new generation of thought-leaders and professionals. The number of university seats in areas such as medicine, agriculture, and engineering should be planned in line with national needs. Science and technology should be prioritized to foster innovation and create new areas of economic development (*6*). Above all, families and civil society organizations have a critical role to play in educating the youth in the principles of democracy and in fostering a transformative culture of free speech and open discourse.



A new song. Children sing a new national anthem at their school in Tripoli.

SEMA K. SGAIER

Bill & Melinda Gates Foundation, New Delhi, India. E-mail: Sema.Sgaier@gatesfoundation.org

References

1. Central Intelligence Agency (CIA), The World Factbook, Libya (www.cia.gov/library/publications/the-world-factbook/geos/ly.html).
2. News24, Libyan schools to teach anti-Gaddafi revolt (www.news24.com/Africa/News/Libyan-schools-to-teach-anti-Gaddafi-revolt-20120107).
3. European Commission–TEMPUS, "Higher Education in Libya" (European Commission, Brussels, Belgium, 2011); http://eacea.ec.europa.eu/tempus/participating_countries/reviews/libya_review_of_higher_education.pdf.
4. M. Daw, E. Elkhammas, *Libyan J. Med.* **3**, 1 (2008).
5. O. Bakoush, A. Al-Tubuly, N. Ashammakhi, E. Elkhammas, *Libyan J. Med.* **2**, 125 (2007).
6. InterAcademy Council, "Inventing a better future: A strategy for building worldwide capacities in science and technology" (InterAcademy Council, Amsterdam, Netherlands, 2004); www.interacademycouncil.net/File.aspx?id=27016.

Invasive Species Unchecked by Climate

IN THE REPORT "THE PACE OF SHIFTING CLIMATE in marine and terrestrial ecosystems" (M. T. Burrows *et al.*, 4 November 2011, p. 652), the dispersal rates of many species were revealed to be as much as an order of magnitude lower than the velocity of climate change in terrestrial and marine ecosystems. Such evidence implies a widespread risk that biodiversity will fail to rapidly track changes in thermal conditions through shifts in individual species distributions (*1*). Yet, in almost perverse irony, invasive alien species that pose a threat to biodiversity, human health, and/or food security are less likely to have trouble keeping up with the fast pace of global warming. The spread rates of alien invasive species in terrestrial and marine ecosystems are between 20 and 30 times as high as the maximum velocities of climate change (*2*). Maximum spread rates vary among invasive plants (*3*), birds (*4*), and insects (*5*), but are often an order of magnitude higher than future estimates of the velocity of climate change (*6*). Even these impressive spread rates are dwarfed by those observed for plant and animal pathogens in terrestrial and marine ecosystems (*7*). Thus, native biodiversity will not only be under pressure from rapid spatial shifts in worldwide temperatures, but will also be exposed to greater risks from alien invasive pests, pathogens, and weeds that can disperse even faster (*8*). Alien invasive species also have the capacity to evolve enhanced dispersal efficiency in novel environments (*9*); hence, they are less likely to face extinction risks under climate change (*10*). Furthermore, the range expansions of alien invasive species are facilitated by increasing human trade, transport, and travel (*11*). This makes it even more important for governments to design robust policy and regulatory frameworks to combat both the current and potential future threats of biological invasions (*12*).

PHILIP E. HULME

The Bio-Protection Research Centre, Lincoln University, P.O. Box 84, Canterbury, New Zealand. E-mail: philip.hulme@lincoln.ac.nz

CREDIT: ZOHRA BENSEMRA/REUTERS

Downloaded from www.sciencemag.org on February 2, 2012

References

1. I.-C. Chen, J. K. Hill, R. Ohlemüller, D. B. Roy, C. D. Thomas, *Science* **333**, 1024 (2011).
2. E. D. Grosholz, *Ecology* **77**, 1680 (1996).
3. P. Pysek, P. E. Hulme, *Ecoscience* **12**, 302 (2005).
4. T. M. Blackburn, J. L. Lockwood, P. Cassey, *Avian Invasions* (Oxford Univ. Press, Oxford, 2009).
5. A. M. Liebhold, P. C. Tobin, *Annu. Revi. Entomol*. **53**, 387 (2008).
6. S. R. Loarie *et al*., *Nature* **462**, 1052 (2009).
7. H. McCallum, D. Harvell, A. Dobson, *Ecol. Lett*. **6**, 1062 (2003).
8. G.-R. Walther *et al*., *Trends Ecol. Evol*. **24**, 686 (2009).
9. H. Kokko, A. López-Sepulcre, *Science* **313**, 789 (2006).
10. B. Sandel *et al*., *Science* **334**, 660 (2011).
11. P. E. Hulme, *J. Appl. Ecol*. **46**, 10 (2009).
12. P. E. Hulme, P. Pyšek, W. Nentwig, M. Vilá, *Science* **324**, 40 (2009).

Response

HULME POINTS OUT THAT OBSERVED RATES of range expansion by invasive alien species are higher than the median speed of isotherm movement over the past 50 years, which in turn has outpaced the rates of climate-associated range changes of marine and terrestrial species (*1*, *2*). This is not surprising, given the many ecological and anthropogenic processes that combine to facilitate the translocation of invasive species and the subsequent expansion of their populations (*3*, *4*). Successful alien species have been observed to rapidly expand their ranges until some limit, typically climate-imposed, is reached (*5*). Comparisons of climate-change–induced range shifts between native and alien species are meaningful only after the initial invasive spread has reached a stable range boundary.

A focus on regions with high velocities of climate change, and on regions such as the tropics where novel thermal niches are being created, should allow researchers to collect data to test hypotheses about the role of climate in driving range shifts of invasive and native species. It is important to remember that the distinctions among native and alien species will be blurred under rapid global change as both types expand their ranges into novel environments (*6*). This may be particularly true in the world's boreal oceans as melting sea ice facilitates new migratory passages between the Atlantic and Pacific Oceans. Moreover, as the ebb and flow of biodiversity intensifies under anthropogenic climate change, novel climates and communities of species will develop. Policy will not only have to address the threats of alien invasions, but also have to deal with rapid range shifts of native species and with the threats to species that are unable to adapt or move. Climate change is redefining management strategies and conservation goals and concepts (*7*).

MICHAEL T. BURROWS,[1]* DAVID S. SCHOEMAN,[2,3] CARLOS M. DUARTE,[4,5] MARY I. O'CONNOR,[6] LAUREN B. BUCKLEY,[7] CARRIE V. KAPPEL,[8] CAMILLE PARMESAN,[9] BENJAMIN S. HALPERN,[8] CHRIS BROWN,[10] KEITH M. BRANDER,[11] JOHN F. BRUNO,[7] JOHN M. PANDOLFI,[12] WILLIAM J. SYDEMAN,[13] PIPPA MOORE,[14,15] WOLFGANG KIESSLING,[16] ANTHONY J. RICHARDSON,[10,17,18] ELVIRA S. POLOCZANSKA[17]

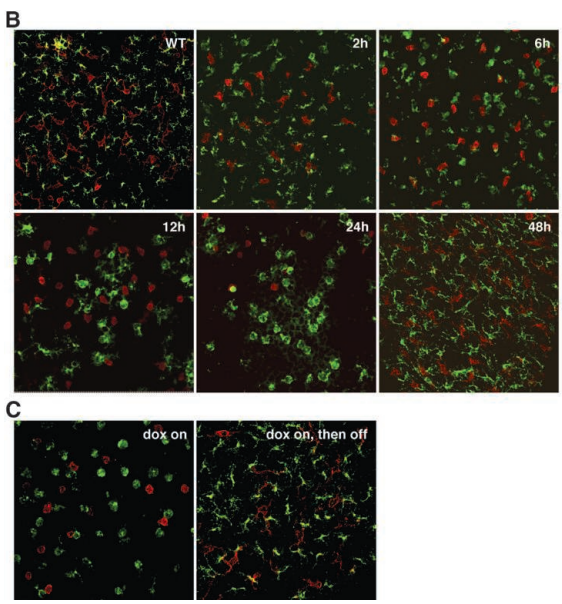
[1]Department of Ecology, Scottish Association for Marine Science, Scottish Marine Institute, Oban, Argyll, PA37 1QA, Scotland, UK. [2]Environmental Science Research Institute, School of Environmental Sciences, University of Ulster, Coleraine, BT52 1SA, Northern Ireland. [3]Department of Zoology, P.O. Box 77000, Nelson Mandela Metropolitan University, Port Elizabeth, 6031, South Africa. [4]The UWA Oceans Institute, University of Western Australia, 35 Stirling Highway, Crawley, WA 6009, Australia. [5]Department of Global Change Research, IMEDEA (UIB-CSIC), Instituto Mediterráneo de Estudios Avanzados, Esporles, 07190, Spain. [6]Department of Zoology and Biodiversity Research Centre, University of British Columbia, Vancouver, BC, Canada V6T 1Z4. [7]Department of Biology, The University of North Carolina at Chapel Hill, Chapel Hill, NC 27599-3280, USA. [8]National Center for Ecological Analysis and Synthesis, University of California Santa Barbara, 735 State Street, Suite 300, Santa Barbara, CA 93101, USA. [9]1 University Station C0930, Integrative Biology, University of Texas, Austin, TX 78712, USA. [10]School

CORRECTIONS AND CLARIFICATIONS

Editors' Choice: "A layer-by-layer amplifier" by M. S. Lavine (20 January, p. 265). The accompanying illustration was of a poor coating generated in a negative control experiment (i.e., without the use of a surface amine amplification step). A conformal coating generated with the aid of a surface amine amplification step is shown in Figure 1f of the *J. Mater. Chem.* paper cited.

News of the Week: "Cannibalism on ice" (16 December 2011, p. 1479). The incident in the photograph occurred on 21 July 2010, not in August 2008, as stated.

Reports: "The intraepithelial T cell response to NKG2D-ligands links lymphoid stress surveillance to atopy" by J. Strid *et al*. (2 December 2011, p. 1293). Three confocal images printed in this Report contained minor artifacts. In an early version of the image processing software Imaris, individual z-stack planes were manually loaded for processing, as opposed to current versions in which they load directly from the microscope. Hence, imprecise usage of the early version had a potential for image misalignment and even duplication during subsequent z-stack compression that regrettably occurred in the images in question. They are the "WT" panel in Fig. 2B, the "dox on" panel in Fig. 2C, and the "BTg" panel in fig. S1B. The authors have provided appropriately compressed raw data files for these panels along with paired control images, and they apologize for any confusion caused by these errors. All other images in the Report were already presented as compressed raw data, accurately reflecting each image plane captured on the microscope. The artifacts in the three panels do not in any way affect the paper's findings. A labeling error in the "WT" panel of fig. S4 was also noted and the figure corrected. The Report's conclusions stand.



TECHNICAL COMMENT ABSTRACTS

Comment on "Abiotic Pyrite Formation Produces a Large Fe Isotope Fractionation"

Andrew D. Czaja, Clark M. Johnson, Kosei E. Yamaguchi, Brian L. Beard

Guilbaud *et al*. (Reports, 24 June 2011, p. 1548) suggest that the geologic record of Fe isotope fractionation can be explained by abiological precipitation of pyrite. We argue that a detailed understanding of the depositional setting, mineralogy, and geologic history of Precambrian sedimentary rocks indicates that the Fe isotope record dominantly reflects biological fractionations and Fe redox processes.

Full text at www.sciencemag.org/cgi/content/full/335/6068/538-c

Response to Comment on "Abiotic Pyrite Formation Produces a Large Fe Isotope Fractionation"

Romain Guilbaud, Ian B. Butler, Rob M. Ellam

Czaja *et al*. assert that Guilbaud *et al*. claim that "the geologic record of Fe isotope fractionation can be explained by abiological precipitation of pyrite." At no point did we suggest this. We reported a previously underestimated Fe isotope fractionation that contributes to the sedimentary Fe isotope signal.

Full text at www.sciencemag.org/cgi/content/full/335/6068/538-d

Downloaded from www.sciencemag.org on February 2, 2012

Published by AAAS

of Biological Sciences, The University of Queensland, St. Lucia, QLD 4072, Australia. [11]National Institute of Aquatic Resources, Technical University of Denmark, Charlottenlund Slot, Jægersborg Allé 1, Charlottenlund, Denmark. [12]School of Biological Sciences, ARC Centre of Excellence for Coral Reef Studies, University of Queensland, Brisbane, QLD 4072, Australia. [13]Farallon Institute for Advanced Ecosystem Research, P.O. Box 750756, Petaluma, CA 94975, USA. [14]Institute of Biological, Environmental and Rural Sciences, Aberystwyth University, Aberystwyth, SY23 3DA, UK. [15]Centre for Marine Ecosystems Research, Edith Cowan University, Perth, 6027, Australia. [16]Museum für Naturkunde at Humboldt University, 10115 Berlin, Germany. [17]Climate Adaptation Flagship, CSIRO Marine and Atmospheric Research, Ecosciences Precinct, GPO Box 2583, Brisbane, QLD 4001, Australia. [18]Centre for Applications in Natural Resource Mathematics (CARM), School of Mathematics and Physics, University of Queensland, St. Lucia, QLD 4072, Australia.

*To whom correspondence should be addressed. E-mail: mtb@sams.ac.uk

Letters to the Editor

Letters (~300 words) discuss material published in *Science* in the past 3 months or matters of general interest. Letters are not acknowledged upon receipt. Whether published in full or in part, Letters are subject to editing for clarity and space. Letters submitted, published, or posted elsewhere, in print or online, will be disqualified. To submit a Letter, go to www.submit2science.org.

References

1. C. Parmesan, G. Yohe, *Nature* **421**, 37 (2003).
2. W. W. L. Cheung *et al.*, *Fish Fish.* **10**, 235 (2009).
3. C. S. Kolar, D. M. Lodge, *Trends Ecol. Evol.* **16,** 199 (2001).
4. A. L. Angert *et al.*, *Ecol. Lett.* **14**, 677 (2011).
5. J. L. Hierro *et al.*, *J. Ecol.* **9**, 35 (2005).
6. B. L. Webber, J. K. Scott, *Global Ecol. Biogeogr.*, 10.1111/j.1466-8238.2011.00684.x (2011).
7. E. McDonald-Madden, M. C. Runge, H. P. Possingham, T. G. Martin, *Nat. Clim. Change* **1,** 261 (2011).

Proceed with Planning Despite Multiple Models

IN HIS NEWS FOCUS STORY "TIME TO ADAPT TO A warming world, but where's the science?" (25 November 2011, p. 1052), R. A. Kerr reports on the frustration expressed at a recent meeting in Denver about the lack of "actionable science" that can be used as a basis for planning adaptation to climate change. Understandably, people planning new storm drain systems with a 75-year lifetime, for example, would like to know the maximum flow of water they will need to accommodate over that period. The general expectation seems to be that if we can just get more accurate and more granular climate models, then we can provide definitive answers to this type of question.

Unfortunately, even if we can deal with the tremendous complexity of the physical and biological mechanisms involved, as Lempert *et al*. have pointed out, predicting the future is fundamentally impossible, as it will be influenced by people's future actions, which are currently unknown (*1*). It is productive to consider multiple scenarios of plausible futures (as the Intergovernmental Panel on Climate Change has done) and formulate plans and strategies that provide acceptable outcomes across a broad range of possibilities, rather than to try to find an optimum solution based on a single forecast of future climate. Better climate models will certainly play a key role in making the scenarios more realistic, but we will not enjoy the luxury of having definitive forecasts on which to base our adaptation planning.

ROBERT DICKINSON

President, Climate Strategy Advisors, LLC, 8 Siskiyou Place, Menlo Park, CA 94025, USA. E-mail: bob@climatestrategyadvisors.com

Reference

1. R. Lempert *et al.*, *Shaping the Next One Hundred Years* (RAND Corporation, MR-1626, 2003).

Science Classic



The complete *Science* archive 1880–1996

Fully integrated with *Science* Online (1997–today)

Available to institutional customers through a site license. Contact ScienceClassic@aaas.org for a quote.

Information: **www.sciencemag.org/classic**

Science Classic AAAS

© 2007 JupiterImages Corporation

Downloaded from www.sciencemag.org on February 2, 2012

Comment on "Abiotic Pyrite Formation Produces a Large Fe Isotope Fractionation"

Andrew D. Czaja,[1,2]* Clark M. Johnson,[1,2] Kosei E. Yamaguchi,[2,3] Brian L. Beard[1,2]

Guilbaud *et al*. (Reports, 24 June 2011, p. 1548) suggest that the geologic record of Fe isotope fractionation can be explained by abiological precipitation of pyrite. We argue that a detailed understanding of the depositional setting, mineralogy, and geologic history of Precambrian sedimentary rocks indicates that the Fe isotope record dominantly reflects biological fractionations and Fe redox processes.

Interpreting the origin of isotopic variations preserved in the rock record requires consideration of geologic, petrographic, and geochemical contexts. Guilbaud *et al*. (*1*) described a kinetic Fe isotope fractionation factor for abiological production of pyrite from aqueous and solid FeS, which potentially provides important insight into Fe isotope compositions of sulfides in the rock record. These authors suggest that negative δ^{56}Fe values measured in pyrite from the geologic record could have been produced by this process, implying that Fe isotopes cannot be used to trace ancient biologically or abiologically mediated redox processes. We find such an interpretation to be faulty for three reasons: (i) The authors ignore evidence for biological and abiological redox processes contained in the diversity of Precambrian samples studied to date; (ii) the authors do not fully discuss the limited amount of low-δ^{56}Fe pyrite produced in their model; and (iii) the isotopic fractionations favored by the authors reflect extreme conditions produced in the laboratory and are unlikely to be representative of natural processes.

We first address the Fe isotope record for Neoarchean and Paleoproterozoic marine sedimentary rocks because it bears on the Fe redox processes that Guilbaud *et al*. (*1*) dismiss. Fig. 1A shows Fe isotope compositions of Fe oxides and Fe carbonates in banded iron formations (BIFs), Fe-rich shales, and Fe-rich and Fe-poor Ca-Mg carbonates. In all of these samples, pyrite Fe comprises <20% of the total Fe budget, and for most samples, especially BIFs, pyrite is insignificant or absent. The model proposed by (*1*) cannot, therefore, explain low-δ^{56}Fe values in such samples. Many Fe-poor, Ca-Mg carbonates have very negative δ^{56}Fe values that have been interpreted to reflect the Fe isotope composition of a marine photic zone with low amounts of aqueous ferrous Fe [$Fe(II)_{aq}$] after extensive Fe oxidation and precipitation of Fe oxide/hydroxides (*2*). The Fe-rich BIFs that were deposited coevally in the same basins have average δ^{56}Fe values that provide sufficient mass balance to the Fe-poor Ca-Mg carbonate inventory, providing an example of an Fe redox couple (Fig. 1A). Indeed, as discussed in the references cited in Fig. 1, combining Fe isotope analyses with other geochemical evidence, notably carbon isotopes, indicates that the redox processes of microbial dissimilatory iron reduction (DIR) and Fe oxidation are likely means by which a >3 per mil (‰) range in δ^{56}Fe values was produced.

We next turn to pyrite-bearing shales to test the relationship of δ^{56}Fe and pyrite abundance predicted by the Guilbaud *et al*. (*1*) model. The model involves precipitation of ~10% of marine $Fe(II)_{aq}$ to form FeS, followed by reaction of FeS to pyrite; the maximum decrease in δ^{56}Fe values for pyrite occurs when small amounts (<20%) of FeS are converted to pyrite, equivalent to ~2% pyritization of the initial marine $Fe(II)_{aq}$ inventory [~98% removal of $Fe(II)_{aq}$]. Such signals are unlikely to be found in bulk shales, in which much of the record of negative δ^{56}Fe values in Precambrian rocks lies, because a negative-δ^{56}Fe signal for pyrite would generally be diluted by Fe-bearing silicates ($\delta^{56}Fe_{silicates} \sim 0$‰). The low-$\delta^{56}$Fe signal proposed by (*1*) would be most likely detected in rocks that have low total Fe contents and large proportions of Fe as pyrite and is possibly recorded in less than 10% of the samples plotted in Fig. 1B that have such a combination. In contrast, the numerous Fe-rich shales that have low proportions of their Fe inventory in pyrite and negative δ^{56}Fe values (Fig. 1B) cannot be explained by this model. Additionally, virtually all of the measured low-δ^{56}Fe shales of Neoarchean and Paleoproterozoic age are enriched in Fe [Fe_T/Al_T greater than 0.5, the value of average Archean shale (*3*)], and there is no correlation between Fe enrichment, δ^{56}Fe value, and the proportion of pyrite in the Fe inventories of these samples (Fig. 1C). Focusing on samples that have >20% of their Fe inventory in pyrite, Fe_T/Al_T–δ^{56}Fe variations suggest the presence of pyrite that has a very low δ^{56}Fe value (Fig. 1C). The fact that the majority of these rocks have Fe_T/Al_T ratios equal to or greater than that of average Archean shale suggests, however, that the low-δ^{56}Fe pyrite component is unlikely to reflect a process that occurred by the ~98% $Fe(II)_{aq}$ removal that is required by the model of Guilbaud *et al*. (*1*) and more likely reflects Fe addition. DIR has been recognized as an efficient "pump" for explaining net addition of low-δ^{56}Fe Fe to deep sections of marine basins [e.g., (*4*)].

Next, we turn to the experimental results obtained by (*1*). Guilbaud *et al*. chose an initial kinetic isotope fractionation for precipitation of FeS from $Fe(II)_{aq}$ that was measured for FeS precipitated over time scales of minutes to hours (*5*, *6*), and the very large kinetic fractionation between FeS and pyrite they measured was obtained over periods of hours. Although many experimental studies indicate that pyrite can be formed rapidly, studies of modern marine environments indicate rates of pyrite formation that are orders-of-magnitude slower than those of laboratory experiments (*7*). Kinetically induced stable isotope fractionations can depend upon rates [e.g., (*8*)], and yet this critical point is not discussed by (*1*). Thus, we contend that the fractionation factors used by (*1*) represent laboratory conditions that may not be reflective of natural conditions, especially considering that 65 to 77% isotopic reequilibration occurs between FeS and $Fe(II)_{aq}$ in 2 to 4 days at 25°C (*9*). Indeed, the lack of correlation in the experiments between percent pyritization and the measured Fe isotope fractionation factor [figure 1 in (*1*)] suggests that these data may largely represent experimentally induced kinetic effects.

We conclude that the Fe isotope compositions of Neoarchean and Paleoproterozoic marine sedimentary rocks are the result of numerous processes, including abiological and biological Fe redox processes. It is possible that some low-Fe samples preserve the signal proposed by (*1*), although their model is not a likely explanation for many low-δ^{56}Fe samples from the rock record, and their model does not address the temporal changes in the Fe isotope compositions of Precambrian sedimentary rocks.

[1]Department of Geoscience, 1215 West Dayton Street, University of Wisconsin, Madison, WI 53706, USA. [2]NASA Astrobiology Institute, USA. [3]Department of Chemistry, Toho University, 2-2-1 Miyama, Funabashi, Chiba 274-8510, Japan.

*To whom correspondence should be addressed. E-mail: aczaja@geology.wisc.edu

References and Notes

1. R. Guilbaud, I. B. Butler, R. M. Ellam, *Science* **332**, 1548 (2011).
2. A. D. Czaja *et al*., *Earth Planet. Sci. Lett.* **292**, 170 (2010).
3. S. R. Taylor, S. M. McLennan, *The Continental Crust: Its Composition and Evolution*. A. Hallam, Ed. (Blackwell Scientific Publications, Oxford, 1985).
4. T. F. Anderson, R. Raiswell, *Am. J. Sci.* **304**, 203 (2004).
5. I. B. Butler, C. Archer, D. Vance, A. Oldroyd, D. Rickard, *Earth Planet. Sci. Lett.* **236**, 430 (2005).
6. R. Guilbaud, I. B. Butler, R. M. Ellam, D. Rickard, *Earth Planet. Sci. Lett.* **300**, 174 (2010).
7. M. T. Hurtgen, T. W. Lyons, E. D. Ingall, A. M. Cruse, *Am. J. Sci.* **299**, 556 (1999).
8. J. L. Skulan, B. L. Beard, C. M. Johnson, *Geochim. Cosmochim. Acta* **66**, 2995 (2002).

Downloaded from www.sciencemag.org on February 2, 2012

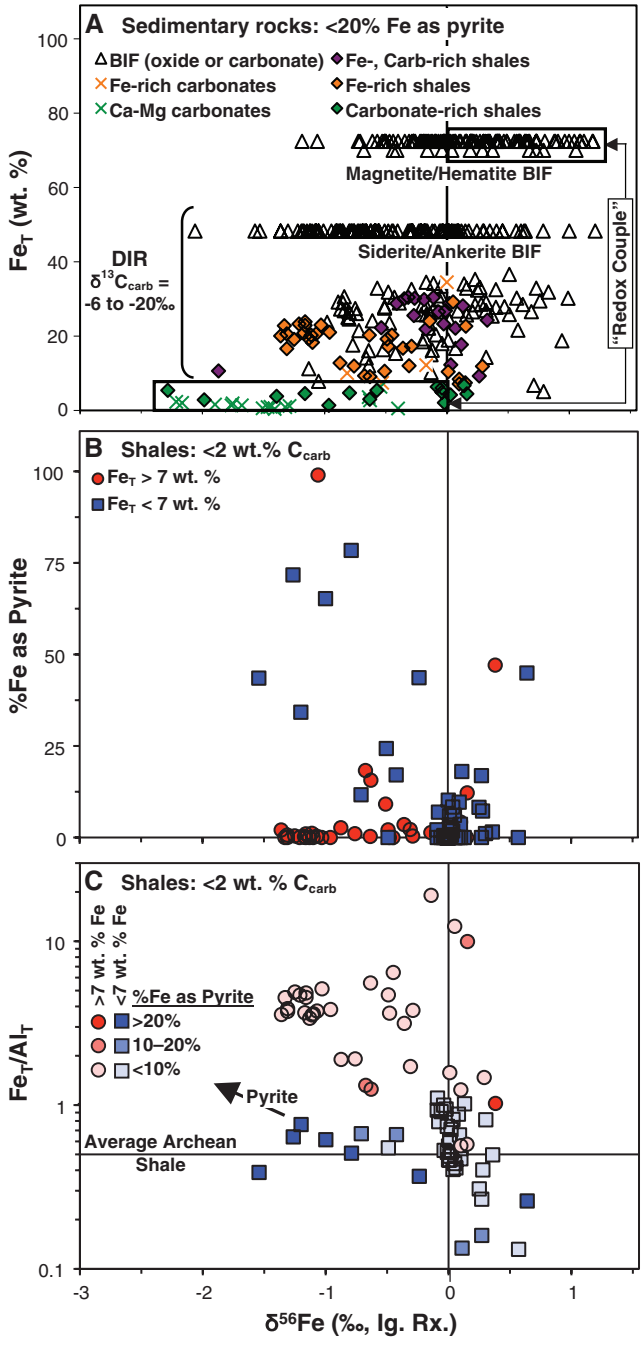


Fig. 1. Fe isotope and chemical compositions of shales, BIFs, and carbonates of Neoarchean and Paleoproterozoic age. δ^{56}Fe values are defined relative to the average of igneous rocks. (**A**) δ^{56}Fe versus total Fe contents (Fe_T) for various types of sedimentary rocks for which pyrite Fe comprises <20% of the total Fe budget. Magnetite and hematite BIF samples, as well as many of the siderite BIF samples (*10*–*12*), were collected from monomineralic layers, and thus their Fe_T values assume stoichiometries of Fe_3O_4 (magnetite), Fe_2O_3 (hematite), and $FeCO_3$ (siderite) [72.4 weight percent (wt %) Fe, 70.0 wt % Fe, and 48.3 wt % Fe, respectively]. Total Fe values of all other samples (*2*, *13*–*15*) were measured from bulk rock digestions. All samples are from the Hamersley and Transvaal basins. (**B**) δ^{56}Fe versus the percent of Fe that is pyrite Fe for shales that have low carbonate contents (<2 wt % C_{carb}). Samples that contain low-δ^{56}Fe pyrite formed by the model proposed by (*1*) would necessarily have low total Fe contents and a high percentage of Fe as pyrite (blue squares in the upper left region of plot) for such a signal to be detected in the bulk sample. All shale samples were analyzed as bulk rock digestions (*2*, *13*, *14*). It is important to note that the relations in Fig. 1B are cast in terms of percentage of Fe in pyrite, rather than the degree of pyritization, the latter of which references pyrite abundance to "reactive" (HCl-extractable) Fe, which may be problematic because of alterations to the reactive Fe pools during even small extents of metamorphism. (**C**) δ^{56}Fe versus the ratio of Fe_T to total Al (Al_T) for low-C_{carb} shales [the samples from (B) for which Al_T data are available] separated by the percentage of Fe that is pyrite Fe and by total Fe contents. These samples are shales that contain siliciclastic Fe, which will dilute any negative δ^{56}Fe values contained in pyrite or other minerals (indicated schematically by the arrow). The Fe_T/Al_T of average Archean shale is that of Taylor and McLennan (*3*).

9. R. Guilbaud, I. B. Butler, R. M. Ellam, D. Rickard, A. Oldroyd, *Geochim. Cosmochim. Acta* **75**, 2721 (2011).
10. C. M. Johnson, B. L. Beard, N. J. Beukes, C. Klein, J. M. O'Leary, *Contrib. Mineral. Petrol.* **144**, 523 (2003).
11. C. M. Johnson, B. L. Beard, C. Klein, N. J. Beukes, E. E. Roden, *Geochim. Cosmochim. Acta* **72**, 151 (2008).
12. P. R. Craddock, N. Dauphas, *Earth Planet. Sci. Lett.* **303**, 121 (2011).
13. K. E. Yamaguchi, thesis, Pennsylvania State University (2002).
14. K. E. Yamaguchi, C. M. Johnson, B. L. Beard, H. Ohmoto, *Chem. Geol.* **218**, 135 (2005).
15. A. Heimann *et al.*, *Earth Planet. Sci. Lett.* **294**, 8 (2010).

Acknowledgments: This work was supported by the NASA Astrobiology Institute.

27 July 2011; accepted 20 December 2011
10.1126/science.1211804

Downloaded from www.sciencemag.org on February 2, 2012

Response to Comment on "Abiotic Pyrite Formation Produces a Large Fe Isotope Fractionation"

Romain Guilbaud,[1,2]*† Ian B. Butler,[1,2] Rob M. Ellam[2,3]

Czaja *et al*. assert that Guilbaud *et al*. claim that "the geologic record of Fe isotope fractionation can be explained by abiological precipitation of pyrite." At no point did we suggest this. We reported a previously underestimated Fe isotope fractionation that contributes to the sedimentary Fe isotope signal.

Czaja *et al*. (*1*) underline the danger of using Fe isotopes as a unique tool to interpret ancient ocean biochemistry without consideration of geological and petrographic contexts. This philosophical position, with which we entirely agree, inspired our original work (*2*) when we noted that interpretations of the Fe isotope composition of sedimentary pyrite lacked any experimental calibration of the Fe isotope fractionation possible during pyrite formation. Indeed, the assumption that pyrite is a passive recorder of the Fe isotope reservoirs from which it was formed is tacit throughout much of the published literature.

The discussion by (*1*) regarding independent evidence for microbial activity in banded iron formations and Ca-Mg carbonates is entirely relevant for a review on sedimentary Fe isotope signatures, but our paper focused specifically on the process of pyrite formation. In light of our data, ^{56}Fe-depleted pyrite is not sufficient evidence on its own for past microbial activity and therefore emphasizes the necessity to use diverse geochemical and geological tools. Czaja *et al*. note that in bulk black shales with high [Fe] and a low degree of pyritization, negative pyrite δ^{56}Fe signal would generally be diluted by other Fe-bearing phases. We entirely agree, and it seemed intuitive that where pyrite is a minor species, the bulk composition will not reflect the fractionation associated with its formation but another mechanism. The Fe isotope values plotted in figure 3 of our paper represent pyrite grains and nodules from (*3*) and not bulk black shales. We noted that the difference in Fe isotope composition between Archean seawater and the mean sedimentary pyrite grains is similar to the fractionation we find in our abiotic experiments. Although this does not preclude the involvement of any other processes, it makes it difficult to deconvolve each of the contributing Fe isotope signatures. Furthermore, studies that have isolated each different highly reactive Fe pool (*4*, *5*) support that δ^{56}Fe pyrite signatures are dependent upon the degree of Fe utilization as pyrite. We strongly encourage researchers to continue such signal extraction before interpreting bulk black shale compositions.

Czaja *et al*. show some degree of confusion over pyrite-formation mechanism and the presence of FeS in our experiments when they assert that our results are only valid under conditions in which the degree of pyritization is "~2%...of the initial marine $Fe(II)_{aq}$ inventory." Initially, there is the kinetic [not equilibrium, as Johnson *et al*. (*6*) incorrectly suggest] isotope fractionation associated with the exchange of water and sulfide ligands and shift from octahedral to tetrahedral coordination as Fe^{2+}_{aq} reacts to form FeS_m. This fractionation produces a ^{56}Fe-depleted condensed phase. Where $\Sigma Fe(II)_{aq}$ exceeds ΣS(-II)aq, or where the Ion Activity Product only marginally exceeds Ksp_{FeSm}, there is the opportunity for progression toward isotope exchange equilibrium, for which a small ^{56}Fe enrichment is associated with the condensed phase (*7*). However, the kinetics of this Fe isotope exchange are asymptotic to a metastable disequilibrium value in which the condensed phase is still ^{56}Fe- depleted compared with its aqueous counterpart (*8*). Czaja *et al*. take great issue with this fractionation process. In fact, compared with the fractionation associated with pyrite, it is a minor contributor to the overall fractionation, and the difference between the initial FeS_m precipitate and one that has undergone Fe isotope exchange is on the order of 0.5 to 0.6‰. The third and most important contributor to Fe isotope fractionation is pyrite formation with a mean fractionation factor of $\Delta^{56}Fe_{Fe(II)RES\text{-}pyrite}$ ~ 2.2‰. Therefore, the amount of Fe use as pyrite should not be <2% to produce ^{56}Fe-depleted pyrite, as Czaja *et al*. assert, but can be as large as 50% (*2*). We should clarify that in figure 2 in (*2*), the 10% in column B does not refer to the requirements of a model but refers to the fact that the fractionation presented was recorded in experiments in which 10% of Fe was precipitated by sulfide (*8*, *9*).

Czaja *et al*. contend that measured fractionations are experimentally induced kinetic effects and note that associated fractionations may be rate dependent. The experimental methodology used has been applied previously to investigations of the kinetics and mechanism of FeS_2 formation (*10*) and has been shown to be robust. The example quoted is for a reversible isotope exchange reaction and is invalid for the unidirectional pyrite-forming reaction. It is unfortunate that Czaja *et al*. choose a paper documenting "anomalous" FeS accumulations to support their assertion that pyrite formation in sediments is uniformly slow. They do not discriminate between the distinct processes of pyrite nucleation, which initiates pyrite formation, and subsequent pyrite growth, which accounts for most of pyrite formation. The most recent authoritative critical review of the chemistry of the Fe-S system (*11*) notes that whereas pyrite crystal growth is relatively fast, pyrite nucleation is slow and rate limiting. The causes of variable pyrite nucleation rates in sedimentary environments are diverse and have been reviewed in detail by (*12*). It is plain from these detailed critical reviews that pyrite-formation rates in modern sediments cannot be summed up by the simple flat assertion that (*1*) make. Given that, similar speculation on rates in the Archean and Palaeoproterozoic are conjectural.

We conclude that our experimental approach is valid and the results pertinent to the question of Fe isotope fractionation during sedimentary pyrite formation. We do not attribute the geologic Fe isotope record to pyrite formation alone, and we have always recognized that in combination with other isotope data, there is evidence for redox and microbial involvement in the early sedimentary Fe cycle. We reemphasize that a large fractionation can be associated with pyrite formation, and this potential fractionation pathway must be taken into account when interpreting Fe isotope signatures of sedimentary pyrite.

[1]School of GeoSciences, University of Edinburgh, Grant Institute, EH9 3JW, UK. [2]ECOSSE (Edinburgh Collaborative of Subsurface Science and Engineering), a Joint Research Institute of the Edinburgh Research Partnership in Engineering and Mathematics, Edinburgh EH9 3JW, UK. [3]Scottish Universities Environmental Research Centre, Rankine Avenue, East Kilbride G75 0QF, UK.

*To whom correspondence should be addressed. E-mail: romain.guilbaud@ncl.ac.uk

†Present address: School of Civil Engineering and Geosciences, Newcastle University, NE1 7RU, UK.

References and Notes

1. A. D. Czaja, C. M. Johnson, K. E. Yamaguchi, B. L. Beard, *Science* **335**, 538 (2012); www.sciencemag.org/cgi/content/full/335/6068/538-c.
2. R. Guilbaud, I. B. Butler, R. M. Ellam, *Science* **332**, 1548 (2011).
3. O. J. Rouxel, A. Bekker, K. J. Edwards, *Science* **307**, 1088 (2005).
4. S. Severmann, C. M. Johnson, B. L. Beard, J. McManus, *Geochim. Cosmochim. Acta* **70**, 2006 (2006).
5. S. Severmann, T. W. Lyons, A. Anbar, J. McManus, G. Gordon, *Geology* **36**, 487 (2008).
6. C. M. Johnson, B. L. Beard, E. E. Roden, *Annu. Rev. Earth Planet. Sci.* **36**, 457 (2008).

Downloaded from www.sciencemag.org on February 2, 2012

7. R. Guilbaud, I. B. Butler, R. M. Ellam, D. Rickard, A. Oldroyd, *Geochim. Cosmochim. Acta* **75**, 2721 (2011).
8. R. Guilbaud, I. B. Butler, R. M. Ellam, D. Rickard, *Earth Planet. Sci. Lett.* **300**, 174 (2010).
9. I. B. Butler, C. Archer, D. Vance, A. Oldroyd, D. Rickard, *Earth Planet. Sci. Lett.* **236**, 430 (2005).
10. D. Rickard, *Geochim. Cosmochim. Acta* **61**, 115 (1997).
11. D. Rickard, G. W. Luther 3rd, *Chem. Rev.* **107**, 514 (2007).
12. D. Rickard, J. W. Morse, *Mar. Chem.* **97**, 141 (2005).

Acknowledgments: This work was funded by an ECOSSE Ph.D. studentship to R.G. and Natural Environment Research Council research grant N E/E003 958/1 to I.B.B.

5 October 2011; accepted 20 December 2011
10.1126/science.1213032

Downloaded from www.sciencemag.org on February 2, 2012

BIOSECURITY

Have We "Met the Enemy"?

David A. Relman



A great deal has been written about the 2001 anthrax mailings in the United States, the resulting deaths, and the subsequent investigations. One might legitimately ask whether more is needed. In *American Anthrax*, Jeanne Guillemin walks us through the chronology of events that began with the mailings of *Bacillus anthracis* spores and associated cases of anthrax and the resulting nine-year criminal investigation. Guillemin (a medical anthropologist and security specialist at the Massachusetts Institute of Technology) offers a colorful, well-written account that integrates the social, personal, political, and scientific dimensions of the case. Importantly, it also highlights the plight of the U.S. postal workers, whose story has received less attention. But the book is more a retelling of the saga than an analysis of it. And with respect to the latter, there are some weaknesses. These include the limited and superficial treatment of the science used in the case and the limited consideration of the nature of biological threats.

We learned at least two critical lessons from the aftermath of the 2001 anthrax mailings: Microbial forensic science, if deployed in a careful, well-controlled, and creative manner, can generate important, novel, useful leads in criminal cases involving the deliberate use of a biological agent. However, science can only get us so far; alone, it cannot reveal attribution. Our expectations about the value of microbial forensics were not well defined or managed in the so-called Amerithrax investigation. To this day and in this book, the formulation of scientific conclusions continues to be misleading.

American Anthrax
Fear, Crime, and the Investigation of the Nation's Deadliest Bioterror Attack
by Jeanne Guillemin
Times Books, New York, 2011. 336 pp. $27, C$31. ISBN 9780805091045.

By 2010, when the Amerithrax investigation was closed by the U.S. Department of Justice, there were two components of the case: the possible linkage between the material in the letters and a flask of *B. anthracis* spores at the U.S. Army Medical Research Institute of Infectious Diseases (USAMRIID) in Fort Detrick, Maryland, and the assessment about who might have used the contents of the flask to prepare and send the letters. Had the case gone to trial, the strengths of the two components would have been weighed and integrated by the prosecution and then challenged by the defense. But because the lead suspect, Bruce Ivins (a microbiologist at USAMRIID), committed suicide, we do not have the benefit of court proceedings. Without such, we must refrain from trying this man in the courtroom of public opinion. Guillemin tracks Ivins from prior to 2001 until his suicide seven years later, builds a case against him and his institution, and suggests to the reader that she views him as guilty.

In early 2011, the U.S. National Academy of Sciences released the results of a 20-month review of the science used to build the first component of the case along with nearly 10,000 pages of supporting documents previously held by the Department of Justice (*1*). The National Research Council (NRC) committee found that it is impossible to arrive at a definitive conclusion about the origin of the letter spores based on the available scientific evidence alone. The scientific data generated by and on behalf of the Federal Bureau of Investigation (FBI) provided leads as to a possible source (flask RMR-1029) but did not rule out other sources. In contrast, the Department of Justice's Amerithrax Investigative Summary states conclusively that the flask was the source of the spores in the letters. Likewise, Guillemin refers to "solid scientific proof that the spores in the anthrax letters matched those in a flask" and fails to acknowledge all of the major criticisms of the science. There were problems with the representativeness of the FBI repository of *B. anthracis* samples against which the letter material was compared. The FBI failed to aggressively pursue an alternative explanation: that some of the mutations in the letters might have arisen by parallel evolution rather than by derivation from the flask. Similar kinds of mutations are known to occur with large-scale production of anthrax spores using bulk serial passaging (*1*). Guillemin also ignores other NRC criticisms, including questions about the reliability of the genetic assays used to look in the repository for the mutations found in the letters. In addition, she describes some of the details of the science-based investigation incorrectly, such as the number of positive samples from a clandestine effort to assess a possible overseas source of the spores and the number of collection missions that yielded positive samples. Although seemingly minor, these incorrect descriptions of the scientific findings may lend credence to the Department of Justice's overstated conclusions, which in the long run will harm public trust in the U.S. government, an outcome that Guillemin rightfully bemoans.

Her limited treatment of the science and presumption of guilt lead Guillemin to focus on the insider threat, the role of USAMRIID, and what she sees as an associated problem: the U.S. biodefense agenda. While there is merit in some of her claims, I worry that undue emphasis on physical control measures and bean (cell) counting for work with naturally occurring, self-replicating pathogens distracts from more important efforts, such as establishing a culture of responsibility among scientists. There are many other potential enemies besides the biodefense establishment insider and a short list of known biological agents (*2*).

Ultimately, I agree with Guillemin that we need to shift future discussion to "how best to protect the public against bioterrorism." From a science-based perspective, we face a number of major challenges. The population struc-

The reviewer is at Stanford University and the Veterans Affairs Palo Alto Health Care System, Palo Alto, CA 94304, USA. E-mail: relman@stanford.edu

CREDIT: JOE SUTLIFF/WWW.CDAD.COM/JOE

Downloaded from www.sciencemag.org on February 2, 2012

Published by AAAS

ture and genetics of the next attack agent may be more complex, less well understood, or both than they are for *B. anthracis*. The agent may be genetically modified and not found in nature. It may be much less easily cultivated than *B. anthracis*, rendering detection and characterization more difficult. And unlike the Amerithrax case, a direct sample of the attack material may not be available, which means that environmental and clinical samples, with their greater inherent challenges, will be even more important. A strategy for microbial forensics proposed by the U.S. government (*3*) outlines an approach and key goals, but the details remain to be developed.

To riff on the famous line from the Pogo comic strip (*4*), there are, in fact, multiple potential enemies—including naturally emerging infectious disease agents, laboratory-engineered biological agents, and humans of widely varying motivations who misuse and/or create these agents. And whether or not Guillemin's *American Anthrax* correctly identifies the perpetrator(s) in the Amerithrax case, we have not met them all.

References

1. National Research Council, "Review of the scientific approaches used during the FBI's investigation of the 2001 anthrax letters" (National Academies Press, Washington, DC, 2011); www.nap.edu/catalog.php?record_id=13098.
2. A. Casadevall, D. A. Relman, *Nat. Rev. Microbiol.* **8**, 149 (2010).
3. National Science and Technology Council, "National research and development strategy for microbial forensics" (Executive Office of the President, Washington, DC, 2009).
4. W. Kelly, *I Go Pogo* (Simon and Schuster, New York, 1952).

10.1126/science.1213942

ETHICS

When Do Incentives Corrupt?

Tyler Cowen

We're used to relying on incentives. Academics face an incentive to publish papers, hedge fund managers have incentives to earn money for their clients, and if we don't pay our taxes we face the threat of sanctions, fines, and jail.

The contribution of Ruth W. Grant (a political scientist at Duke University) in *Strings Attached* is to question the morality of these arrangements and their ubiquity in our lives. Construing incentives as "an exercise of power," she offers an apparently straightforward argument. Incentives seem innocuous because people have a choice, but "[t]hey are one of the means employed to get people to do what they otherwise would not." She argues that while in the short run incentives rest on voluntary compliance, in the longer run they construct and reinforce power relations. The exercise of this power does not always treat people with dignity.

It's easy enough to sympathize with this argument, and indeed most of us have felt unjustly manipulated by incentives. But compared to what? Incentives are always present, and the notion of an incentiveless situation is a nonstarter. What Grant calls "incentives" is very often just adding cash (or some bartered reward) to incentives of esteem, long-term reputation, power, sex, salvation, and conscience, among the other contenders for our attention. It's one set of manipulations against another, and suddenly the cash payments don't seem so obnoxious any more. In terms of the broader sweep of history, a greater scope for cash incentives has coincided with social mobility, the decline of nobilities and aristocracies, and the ability to buy oneself a degree of freedom from oppressive social conventions. It is good that American corporations have an incentive not to offend, or even to please, their gay customers.

Strings Attached
Untangling the Ethics of Incentives
by Ruth W. Grant
Russell Sage Foundation, New York, and Princeton University Press, Princeton, NJ, 2012. 220 pp. $24.95, £16.95. ISBN 9780691151601.

Grant seems most worried about incentives when the transacting parties do not have equal power. I doubt if that is the relevant dividing line. The parties with weak bargaining power are those who need the money the most, and so we should be happy rather than wary if I hire a maid or invest capital in a poor country, as were Hong Kong and Singapore several decades ago.

When it comes to science, there is a core worry—namely, researchers who pursue profit rather than truth. Still, if we evaluate cash incentives for scientists as a general phenomenon, they helped bring us the inventions of the Industrial Revolution, the marketing and application of antibiotics, and the modern-day Internet revolution (including Google). Because ideas are often a "public good"—eventually open to use by all at zero charge—arguably a lot of scientists don't have strong enough cash incentives. We still need a stronger principle of individuation to pin down the problem. There is the well-known point that the battles in academia are so bitter and destructive precisely because the stakes are so small.

In the chapter "Ethical and not so ethical incentives," Grant portrays legitimacy of purpose, voluntariness, and effects on character as characteristics of good incentives, but how far does that bring us? The first standard seems to beg the question. As for coercive incentives, however unpleasant they can be, they are a bedrock of civil society and political order, with bankrupt Greece as a warning for us all. And why should investing in character be a priority above other values? I would gladly have more venal businessmen opening up shop to serve the poor, whether with cell phones or better grocery stores, even if doing so made them greedier. Similarly, a reading of *The Double Helix* indicates that the fame-greedy James D. Watson was not in every way a fine fellow. We very much need to worry about the numerous instances of scientific (and other) corruption, but we are still looking for the deeper structural principles to separate right incentives from wrong incentives.

There is a self-correcting feature to bad incentives—at least under the right institutions—and often current American management philosophy is in tune with some of Grant's concerns. Wages can remain sticky for long periods of time, and many workers do not receive bonuses or pecuniary demerits at all, because incentives do not always motivate well. Often employees are evaluated periodically rather than regularly, in part to insulate them from the demoralizing effects of too-frequent negative feedback. People commonly assume personal ownership over their work projects exactly when they feel apart from incentives and instead in charge of their own destiny.

Even then, it is hardly the case that businesses are walking away from incentives or cash incentives altogether. More accurately, they are trying to trick people into forgetting about broader incentives to focus on their own empowering autonomy. Often the trick works.

Grant would not put it this way, but *Strings Attached* indicates she wants society to use more of these tricks. That's a defensible point of view, but we still haven't gotten very far toward understanding the sources of our current problems with corruption, scientific or otherwise.

10.1126/science.1217670

The reviewer is at the Department of Economics, George Mason University, 4400 University Drive, 3G4, Fairfax, VA 22030, USA. E-mail: tcowen@gmu.edu

Downloaded from www.sciencemag.org on February 2, 2012

Published by AAAS

SCIENTIFIC PUBLICATIONS

Coercive Citation in Academic Publishing

Many journal editors appear to strategically target authors and papers to pressure them into citing the editors' journals.

Allen W. Wilhite*† and Eric A. Fong*

Despite their shortcomings (*1*–*4*), impact factors continue to be a primary means by which academics "quantify the quality of science" (*5*). One side effect of impact factors is the incentive they create for editors to coerce authors to add citations to their journal. Coercive self-citation does not refer to the normal citation directions, given during a peer-review process, meant to improve a paper. Coercive self-citation refers to requests that (i) give no indication that the manuscript was lacking in attribution; (ii) make no suggestion as to specific articles, authors, or a body of work requiring review; and (iii) only guide authors to add citations from the editor's journal. This quote from an editor as a condition for publication highlights the problem: "you cite *Leukemia* [once in 42 references]. Consequently, we kindly ask you to add references of articles published in *Leukemia* to your present article" (*6*). Gentler language may be used, but the message is clear: Add citations or risk rejection.

To explore the extent and nature of such coercive self-citation, we analyzed 6672 responses from a survey sent to researchers in economics, sociology, psychology, and multiple business disciplines (marketing, management, finance, information systems, and accounting) (*7*), as well as data from 832 journals in those same disciplines. We find that coercion is uncomfortably common and appears to be practiced opportunistically. As editors game the system and authors acquiesce, the integrity of academic publications suffers. We conclude by recommending some steps that can be taken to reduce or eliminate the incentive to engage in coercive self-citation.

Inappropriate But Persistent

Our survey asked respondents about their experiences with, and opinions of, such coercion (see the chart) [see supporting online material (SOM) for details]. They also identified 175 journals as coercers, many identified multiple times, with the worst offender being named by 49 different respondents. To put this in context, our respondents reported a total of 45,955 accepted articles, an average of 55.2 articles per journal. By that calculation, the most flagrant offenders may be coercing most of their contributors. However, this rough calculation does not account for variation in the number of articles in journals, references per article, or disciplines. In our regression analyses, we control for those attributes to get a more accurate picture.

Although 86% of our respondents view coercion as inappropriate, 81% agree that coercion reduces a journal's prestige, and 64% even say they are less likely to submit to a coercive journal, the majority (57%) still say they would add superfluous citations before submitting to a journal known to coerce. More fine-grained analyses suggest that there are differences across academic ranks and disciplines (tables S7 and S8). Lower-ranking scholars are more likely to continue submitting to coercive journals and are more willing to add extraneous citations before submission.

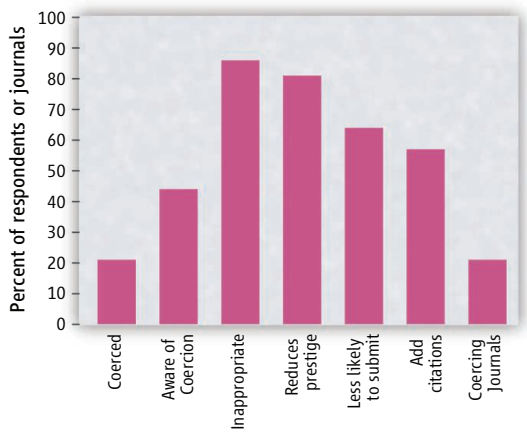
Authors in most of the business disciplines appear more likely to continue submitting to coercive journals than those in economics and sociology. Senior faculty members are more likely to resist coercive demands, whereas junior faculty members are more likely to acquiesce. Finally, we find that familiarity coexists with acceptance. Scholars in disciplines that more frequently practice coercion see it as less inappropriate. And while the direction of causality is unknown, academics who have added citations in response to their editors' urging view the journal's reputation less negatively than those without such experiences.

Strategic Incentives to Coerce

Editors' incentive to inflate impact factors through self-citation is damped by the negative reaction of scholars who disapprove of coercion and think its practice tarnishes a journal's prestige (see the chart). Consequently, editors face a dilemma and must choose. Their decision is complicated by a strategic component; if one journal coerces and improves its ranking, then other journals are relatively worse off.

To further understand the factors seeming to influence the practice of coercive self-citation, we analyzed the survey data using linear probability models. Of the 6672 responses reflected in the chart, only 4920 contained complete responses needed for our regression analysis. We also modeled the journal data to corroborate some findings from the survey data and also to explore potential influences of publisher type. The journal-based data come from Sciverse, a collection of more than 18,000 journals in all fields of academic study. We selected journals for inclusion on the basis of their content coverage as reflected by the All Science Journal Classification (ASJC) code number.

Modeling the editor's strategic decision-making as a game, we can hypothesize the following: First, coercers may try to soften the negative backlash of their actions by



Survey results reflecting the extent, and opinions, of coercion. Percentages of respondents who (i) have been coerced, (ii) are aware of coercion, (iii) think coercion is inappropriate, and agree or strongly agree that (iv) coercion reduces the prestige of a journal, (v) they are less likely to submit to a coercive journal, and (vi) they are likely to add journal-specific citations before submission. The percentage of journals in the study identified as coercers is also shown. See SOM for details.

College of Business Administration, University of Alabama in Huntsville, Huntsville, AL 35899, USA.

*Authors contributed equally to this work.
†Author for correspondence. E-mail: wilhitea@uah.edu

Downloaded from www.sciencemag.org on February 2, 2012

Published by AAAS

focusing on scholars of lower academic rank who are less likely to question or resist an editor's wishes. Second, editors might target manuscripts with fewer authors, so they confront fewer individuals.

Third, the strategic nature of coercion suggests that editors are more likely to coerce if other journals in their discipline coerce; thus, we expect the practice to be concentrated in disciplines as opposed to randomly dispersed across fields. In our analyses, economics is selected as the reference discipline because it stands at the boundary of these disparate fields with one foot in business and the other in the classic social sciences.

Fourth, because a journal's editorial policies can be influenced by its parent publisher, we expect commercial, for-profit publishers to place greater value on the advertising opportunities afforded by a rising impact factor and to be more open to coercion. University-based publishers are expected to put greater emphasis on their long-term reputation.

Our model results support these hypotheses. The table summarizes the central results of the survey-based data, in which the unit of observation is the individual, and of the journal-based data. Editors are more likely to coerce assistant and associate professors than professors and to target manuscripts with fewer authors. Coercion differs significantly across disciplines, with results fairly consistent from both survey and journal data. Relative to economics, coercion is more prevalent in most of the business disciplines and no more prevalent, or even less prevalent, in psychology and sociology.

The type of publisher appears to be influential, as hypothesized; journals published by commercial, for-profit companies show significantly greater use of coercive tactics than journals from university presses. Academic societies also coerce more than university presses.

The journal-based data also allow us to test whether there is a relation between journal rank and coercion. Somewhat surprisingly, the results (tables S2 and S4) suggest that more highly ranked journals are more likely to coerce. Our data cannot discern a direction of causality because some top journals may use coercion to maintain their position, whereas other journals may have attained their lofty position through coercion. But either situation is unsettling. Narrowing our focus to include only the top 30 journals in each discipline yields consistent results (table S6).

So authors are coerced, but how often does it happen? Studying the frequency of coercion yields similar results (table S5 and S6): Author academic rank, author and journal discipline, the number of authors on a paper, and the type of publisher are significantly related to the frequency of coercion.

In addition, our results (table S7) suggest that familiarity coexists with acceptance. Disciplines that more frequently practice coercion see it as less inappropriate, and those academics who have added citations in response to an editor's urging view the journal's reputation less negatively than those without such experiences.

PERCENT CHANGE IN PROBABILITY OF COERCION (SE)

Hypothesized effect	Survey data	Journal data
Academic rank		
Associate professor	4.3** (1.4)	
Assistant professor	5.5** (1.5)	
Lecturer	−5.6 (3.1)	
Graduate student	−0.4 (2.55)	
Confrontation avoidance		
Number of coauthors	−2.0** (0.5)	
Academic discipline		
Sociology	−5.7** (2.1)	−6.5 (9.6)
Psychology	−9.0** (1.9)	1.6 (8.2)
Marketing	20.1** (2.1)	43.1** (11.2)
Management	15.9** (2.0)	31.9** (7.8)
Finance	18.6** (2.7)	37.7** (11.4)
Information systems	18.9** (2.2)	71.8** (13.8)
Accounting	4.4 (2.8)	29.3* (13.5)
Publisher type		
Commercial		9.2* (4.5)
Academic society		12.4* (5.5)

* $P < 0.05$, ** $P < 0.01$

Model results exploring strategic-coercion hypotheses. Independent variables to explore each hypothesis are academic rank (professor as the reference category); number of coauthors on the most recently coerced paper in the last 5 years or, if not coerced, on the most recently accepted paper; academic discipline (economics as the reference category); and publisher type (university presses as the reference category). For example, being an assistant professor instead of a professor adds 5.5% to the chances of being coerced, and each additional author subtracts 2.0% from the chance of being coerced. See SOM for details.

Conclusions

Overall, the empirical results from the author survey and the journal-based data tell a consistent story. Coercive self-citation exists and is more common in the business disciplines than in economics, sociology, and psychology. Additionally, some editors seem to target specific articles and authors.

The American Psychological Association Publication Manual states, "Cite the work of those individuals whose ideas, theories, or research *have directly influenced your work*" (emphasis added) (*8*). The requests studied here do not heed that advice. Although most of our respondents condemn coercion, less than 7% thought an author would refuse to add superfluous citations if coerced to do so. Thus, an author can become both a victim and a coconspirator in the self-citation game; they are rewarded for acquiescing because their manuscript is published, and their gratuitous citations help to boost the impact factor of the journal in which they published.

Although this behavior is less common in economics, psychology, and sociology, these disciplines are not immune—every discipline reported multiple instances of coercion. And there are published references to coercion in fields beyond the social sciences (*3*, *4*, *6*). Future research could help elucidate whether and how these patterns extend to fields across the physical and biological sciences.

Without action, the situation is likely to deteriorate, because the strategic nature of coercion continues to put pressure on editors to coerce. Academic associations could help by officially condemning the practice. Their action would raise the cost of coercion to editors and might help persuade organizations that promote impact factors to remove self-citations from those calculations, which would eliminate the coercive motive.

References and Notes

1. R. Monastersky, The number that's devouring science. *Chron. Higher Ed.*, 14 October 2005. http://chronicle.com/article/The-Number-That-s-Devouring/26481
2. P. A. Lawrence, *Nature* **422**, 259 (2003).
3. N. Romano, *Comm. Assoc. Inform. Syst.* **25**, 41 (2009).
4. P. O. Seglen, *BMJ* **314**, 497 (1997).
5. Editorial, *Nature* **435**, 1003 (2005).
6. R. Smith, *BMJ* **314**, 461 (1997).
7. Survey details are available in the SOM. The survey remains open for participation: www.surveymonkey.com/s/cites
8. APA, Publication Manual of the APA (American Psychological Association, Washington, DC, 2010).

9. The authors thank A. Baldwin, H. Eguchi, S. Wilhite, and University of Alabama in Huntsville Research Seminar participants.

Supporting Online Material

www.sciencemag.org/cgi/content/full/335/6068/542/DC1

10.1126/science.1212540

Downloaded from www.sciencemag.org on February 2, 2012

Published by AAAS

ECONOMICS

Ready, Steady, Compete

Women's willingness to compete can be increased through appropriate affirmative action.

Marie Claire Villeval



The educational attainments of women exceed those of men in most developed countries, yet women continue to lag behind in access to top corporate jobs (*1*, *2*). Women are also underrepresented in politics (*3*). Without dismissing the role of discrimination, recent research has implicated a lower preference of women for competition. On page 579 of this issue, Balafoutas and Sutter (*4*) show how affirmative action policies can increase the willingness of women to compete without affecting the chances of highly skilled men to succeed and while preserving postcompetition cooperation between individuals.

Labor economists have traditionally explained the occupational gender gap by the role of women in the family or by demand-side factors such as discrimination by employers. More recently, behavioral economists have explored other hypotheses. In particular, the lower preferences of women for risks (*5*, *6*) could explain why women are less likely to start up their own business than men. Women differ from men in their attitudes toward negotiation and in social preferences, which could lead them to choose occupations offering fewer career opportunities than those chosen by men (*7*).

One dimension has retained the attention of behavioral economists: Compared with men, women tend to have different attitudes toward competition. The performance of men in a gender-neutral task tends to increase as the environment becomes more competitive, whereas that of women tends to remain stable (*8*). The same difference is observed in running races: Boys tend to outperform girls when racing against someone else, but not when running alone (*9*). These results have initiated studies on how individuals self-select when they can choose between receiving a payment based on relative versus absolute performance. Women are much less likely than men to choose a competitive compensation scheme, even after accounting for risk preferences, relative ability, and beliefs about relative performance (*10*).

This gap in competitiveness seems to be embedded in culture. Women are more likely than men to compete in matriarchal societies, whereas the opposite is observed in patriarchal tribes (*11*). The gender gap emerges from the age of five; below this age, boys and girls show no difference in competitiveness (*12*). Girls from single-sex schools tend to be more willing to compete than girls from coeducational schools (*13*). This does not mean, however, that biological factors are absent. In an experiment involving math and word tasks, women in the low-hormone phase of the menstrual cycle were less likely to enter tournaments than those in a higher-hormone phase, although their average performance was not affected by hormonal fluctuations (*14*).

Holding the lower competitiveness of women responsible for their lower performance in the labor market should influence the design of policies aimed at breaking the glass ceiling. Policy interventions that increase the monetary incentives associated with competitive pay schemes relative to individual pay or that allow individuals to choose the gender of their potential competitors both entice more women to compete. This shows that women are not rejecting competition systematically. However, these interventions also increase men's competitiveness and, therefore, fail to narrow the gender gap in competitiveness (*15*).

Affirmative action can be more effective, as shown, for example, by Niederle, Segal, and Vesterlund (*16*), who introduced a gender quota that guaranteed women equal representation among the winners of an ability-based tournament involving a math task. Without affirmative action, a competitor won the tournament if his/her performance exceeded that of at least four of the five other group members. With affirmative action, the two winners were the best-performing woman and the highest performer of the remaining five participants. In the latter case the entry rate of high-performing women into the competition rose, whereas that of men fell.

The authors attribute this change to two main elements: Quotas distort the objective probability of women to win the competition, but they also improve the confidence of women in their ability to succeed while reducing men's overconfidence. If affirmative action only changed the objective probability of women to win tournaments, this might have created reverse discrimination, as high-ability men could be passed by less able women. The authors find little evidence of such reverse discrimination, because the quotas attracted more able women in the competition. It remains to be shown whether this result holds for other policy interventions.

Balafoutas and Sutter compare three different affirmative action policies: quotas forcing a gender balance among winners, two forms of preferential treatment that artificially increase the performance of women, and a repetition of the competition unless a sufficient number of women compete. In their experiment, participants had to choose between an individual piece-rate scheme and a tournament pay scheme before performing a calculation task, first in the absence of policy intervention and then after one of the various policy interventions had been introduced. Comparison of these competition-entry choices reveals that men compete twice as often as women in the absence of policy intervention but that all the policy interventions reduce the gender gap in competitiveness (or even reverse it). In addition, the interventions do not affect men's choices significantly, whereas they motivate high-ability women to enter the competition.

University of Lyon, 69007 Lyon, France; CNRS, GATE Lyon St Etienne 69130 Ecully, France. E-mail: villeval@gate.cnrs.fr

CREDIT: JOE SUTLIFF/WWW.CDAD.COM/JOE

Downloaded from www.sciencemag.org on February 2, 2012

Published by AAAS

As in (*16*) but for a wider range of policies, Balafoutas and Sutter find that, with very few exceptions, the most able men are not overtaken by less able women. Thus, the policies reduce the competitiveness gap without causing reverse discrimination or reducing efficiency.

Affirmative action may thus ensure fairness if its main effect is to motivate talented but shy women to enter more frequently into competitive schemes. Still, men who think that affirmative action creates unfair competition may be less willing to cooperate with women after competing under affirmative action. In the last part of Balafoutas and Sutter's experiment, participants play a two-player coordination game with each other group member. The authors find that policy interventions do not harm postcompetition cooperation, a hitherto unexplored aspect of affirmative action programs.

These studies (*4*, *16*) explore supply-side effects of affirmative action, whereas labor economists have tended to focus on its demand-side effects (*17*). A more complete picture would require looking at both effects in combination to measure how a higher competitiveness of women will change the demand for labor and affect discrimination. Modification of compensation packages should also be explored further as a route to increasing the proportion of women in top-level occupational positions.

References

1. Organisation for Economic Co-operation and Development, *Employment Outlook* (OECD, Paris, 2002).
2. M. Bertrand, K. F. Hallock, *Ind. Labor Relat. Rev.* **55**, 3 (2001).
3. S. Palmieri, *Gender-Sensitive Parliaments: A Global Review of Good Practice.* Reports and Documents no. 65 (Inter-Parliamentary Union, Geneva, 2011)
4. L. Balafoutas, M. Sutter, *Science* **335**, 579 (2012).
5. R. Croson, U. Gneezy, *J. Econ. Lit.* **47**, 448 (2009).
6. C. C. Eckel, P. J. Grossman, in *Handbook of Experimental Economics Results*, C. R. Plott, V. L. Smith, Eds. (North-Holland, Amsterdam, 2008), pp. 1061–1073.
7. M. Bertrand, in *Handbook of Labor Economics vol. 4B*, O. Ashenfelter, D. Card, Eds. (Elsevier, Amsterdam, 2011), pp. 1545–1592.
8. U. Gneezy, M. Niederle, A. Rustichini, *Q. J. Econ.* **118**, 1049 (2003).
9. U. Gneezy, A. Rustichini, *Am. Econ. Rev. (P&P)* **94**, 2, 377 (2004).
10. M. Niederle, L. Vesterlund, *Q. J. Econ.* **122**, 1067 (2007).
11. U. Gneezy, K. L. Leonard, J. A. List, *Econometrica* **77**, 1637 (2009).
12. M. Sutter, D. Rützler, "Gender differences in competition emerge early in life: Three-year old girls compete as much as boys, but older girls don't," IZA Discussion Paper 5015, IZA, Bonn (2010); available at http://ftp.iza.org/dp5015.pdf.
13. A. L. Booth, P. J. Nolen, "Choosing to compete: How different are girls and boys?" IZA Discussion Paper 4027, IZA, Bonn (2009); available at http://ftp.iza.org/dp4027.pdf.
14. D. Wozniak, W.T. Harbaugh, U. Mayr, "The menstrual cycle and performance feedback alter gender differences in competitive choice," University of Oregon Working Paper, available at http://harbaugh.uoregon.edu/Papers/Menstruation_Wozniak_201010.pdf.
15. N. Datta Gupta, A. Poulsen, M. C. Villeval, *Econ. Inq.* (2012). 10.1111/j.1465-7295.2011.00378.x
16. M. Niederle, C. Segal, L. Vesterlund, "How costly is diversity? Affirmative action in the light of gender differences in competitiveness," Stanford University Working Paper, available at www.stanford.edu/~niederle/AAPaper.pdf.
17. H. Holzer, D. Neumark, *J. Econ. Lit.* **38**, 483 (2000).

10.1126/science.1218000

EVOLUTION

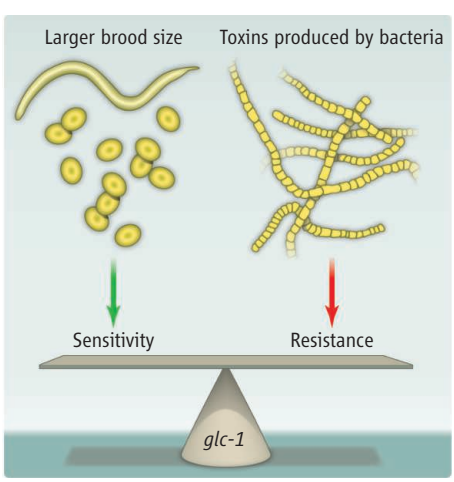
Surviving in a Toxic World

Natural variations in a single gene of wild *C. elegans* populations confer resistance to the bacterial toxin avermectin.

Adrian J. Wolstenholme

The world can be a dangerous place. Although the nematode *Caenorhabditis elegans* is probably best known as a model organism thriving in the undemanding environment of research laboratories, in nature it lives in the soil, exposed to many toxic compounds that are often produced by the microorganisms on which it feeds. One group of these compounds, the avermectins, are produced by the soil bacterium, *Streptomyces avermitilis* (*1*). On page 574 of this issue, Ghosh *et al*. (*2*) report that a natural variation in a *C. elegans* gene, *glc-1*, confers resistance to the avermectins and also to *S. avermitilis*. Because avermectin resistance is a serious problem in veterinary medicine (*3*), and ivermectin (a semisynthetic avermectin) is used to control human parasitic diseases such as river blindness (*4*), this result has wider implications for effective parasite control and human health.

Avermectins activate ligand-gated chloride channels on nerve and muscle cells, blocking their electrical activity and causing paralysis. In nematodes, the most important avermectin receptors are the glutamate-gated chloride channels (GluCls), which in *C. elegans* are encoded by six genes, including *glc-1* (*5*). In laboratory strains of *C. elegans*, high-level avermectin resistance is polygenic, requiring mutations in several genes (*6*). However, despite considerable effort, the genetic basis for resistance in parasitic nematodes is not well understood.



Balancing act. Balancing selection pressures on *glc-1*. Exposure to avermectins produced by soil bacteria select for the resistance allele, but increased brood sizes tend to select against this allele in the absence of toxins.

CREDIT: P. HUEY/*SCIENCE*

Ghosh *et al*. looked for avermectin resistance in wild *C. elegans* populations. They found a Hawaiian isolate, CB4856, which is resistant to both abamectin (a synthetic avermectin derivative) and ivermectin, at concentrations that almost completely paralyzed the normal laboratory strain, N2. Simple genetics suggested that the resistance trait was recessive, and the subsequent quantitative trait locus analysis examining the drug sensitivity of 210 inbred lines generated from crosses between N2 and CB4856 narrowed the likely resistance gene down to *glc-1*. The sequence of *glc-1* had 77 nucleotide differences between the two strains, plus a small deletion in CB4856. Introducing the N2 version of *glc-1* into CB4856 made the resistant worms drug-sensitive. When several of the differences in *glc-1* between the two strains were studied in isolation, only the four–amino acid deletion failed to rescue the phenotype, showing that this small deletion in *glc-1* is by itself enough to cause resistance. Consistent with

Department of Infectious Diseases and Center for Tropical and Emerging Global Diseases, University of Georgia, Athens, GA 30602, USA. E-mail adrianw@uga.edu

Downloaded from www.sciencemag.org on February 2, 2012

Published by AAAS

this, the authors studied *glc-1* in 53 wild isolates of *C. elegans* and found that the deletion was strongly associated with resistance. However, the deletion was not present in all the resistant isolates, and some of those carrying the deletion were drug-sensitive, meaning that other genes must be involved. This may reflect the genetic complexity that is believed to underlie avermectin resistance in parasites (*7*, *8*).

This story turned out to have an additional twist, which might shed some light on why multiple mechanisms of resistance may have evolved. In *C. elegans*, *glc-1* is far more divergent between N2 and CB4856 strains than other GluCl-encoding genes, and this is probably due to long-term balancing selection. As *S. avermitilis* lives in soil, exposure to it could be one of the selective forces for this balancing selection—the other could be loss of optimal GluCl function resulting from the resistance-associated polymorphisms. Consistent with this, although *S. avermitilis* has a detrimental effect on both strains, the effect on CB4856 was smaller and reversed by the expression of the N2 *glc-1*. By contrast, in the absence of *S. avermitilis*, N2 produced more progeny than CB4856, suggesting that N2 *glc-1* confers greater fitness (see the figure).

The study by Ghosh *et al*. provides an excellent illustration of the phenomenon of balancing selection, an important process for maintaining multiple alleles at high frequency within species (*9*). Balancing selection is often invoked to explain the persistence of apparently deleterious alleles in the population, such as those that cause recessive genetic disorders in humans; they may confer resistance to specific environmental threats. One well-known example of this is alleles affecting hemoglobin that protect against malaria. In this case, it suggests that the production of toxins by soil bacteria is a major selection pressure on other organisms. Do similar balancing selections apply to parasitic nematodes, and does this have any relevance to their avermectin resistance? Parasites live in very different environments and have only recently been exposed to high levels of avermectins. Population genetics studies have suggested that GluCl-encoding genes are under selection in resistant isolates of parasitic nematodes (*10*, *11*), and some polymorphisms and changes in gene expression have been found (*12*, *13*). Despite this, no specific resistance-associated mutations have been confirmed, nor do resistant isolates revert to sensitivity in the absence of drug pressure, which balancing selection might predict. However, Ghosh *et al*. clearly show that changes in GluCls can result in drug resistance.

Recently, the structure of GLC-1 complexed with ivermectin was solved. The drug was found to bind to the carboxyl-terminal channel region of GLC-1, between two adjacent subunits (*14*). However, the resistance-associated deletion is at the amino terminus of the protein, some distance away from this binding site. Interpretation of this observation is complicated, as crystallization of GLC-1 required removal of the amino-terminal 40 amino acids, including those deleted in CB4856. It is possible that the deleted amino acids make up an additional component of the drug-binding pocket, though it is perhaps more likely that this deletion causes changes in the three-dimensional structure of the channels that affects the drug's binding site. Indeed, ligand-gated ion channels are well-known for their allosteric properties (*15*), and this deletion might provide another example of this.

It is the mark of good science that it provokes new research directions and ideas in a variety of fields. In this case, Ghosh *et al*. provide insights into genetic mechanisms by which organisms cope with environmental challenges and the possible evolution of drug resistance in pathogens, and also pose questions about drug interactions with a major family of neurotransmitter receptors.

References

1. W. C. Campbell, M. H. Fisher, E. O. Stapley, G. Albers-Schönberg, T. A. Jacob, *Science* **221**, 823 (1983).
2. R. Ghosh, E. C. Andersen, J. A. Shapiro, J. P. Gerke, L. Kruglyak, *Science* **335**, 574 (2012).
3. A. J. Wolstenholme, I. Fairweather, R. K. Prichard, G. von Samson-Himmelstjerna, N. C. Sangster, *Trends Parasitol.* **20**, 469 (2004).
4. U. Amazigo, *Ann. Trop. Med. Parasitol.* **102** (Suppl. 1), 19 (2008).
5. A. J. Wolstenholme, A. T. Rogers, *Parasitology* **131**, (Suppl.), S85 (2005).
6. J. A. Dent, M. M. Smith, D. K. Vassilatis, L. Avery, *Proc. Natl. Acad. Sci. U.S.A.* **97**, 2674 (2000).
7. R. K. Prichard, A. Roulet, *Parasitology* **134**, 1123 (2007).
8. S. McCavera, T. K. Walsh, A. J. Wolstenholme, *Parasitology* **134**, 1111 (2007).
9. T. Mitchell-Olds, J. H. Willis, D. B. Goldstein, *Nat. Rev. Genet.* **8**, 845 (2007).
10. W. J. Blackhall, J. F. Pouliot, R. K. Prichard, R. N. Beech, *Exp. Parasitol.* **90**, 42 (1998).
11. S. G. Forrester, R. K. Prichard, R. N. Beech, *Biochem. Pharmacol.* **63**, 1061 (2002).
12. A. I. Njue, J. Hayashi, L. Kinne, X.-P. Feng, R. K. Prichard, *J. Neurochem.* **89**, 1137 (2004).
13. A. El-Abdellati *et al*., *Int. J. Parasitol.* **41**, 951 (2011).
14. R. E. Hibbs, E. Gouaux, *Nature* **474**, 54 (2011).
15. A. Taly, P.-J. Corringer, D. Guedin, P. Lestage, J.-P. Changeux, *Nat. Rev. Drug Discov.* **8**, 733 (2009).

10.1126/science.1218166

NEUROSCIENCE

To Stop or Not to Stop?

Nora D. Volkow and Ruben D. Baler

Does chronic drug abuse cause brain abnormalities, or do they develop before the onset of dependence?

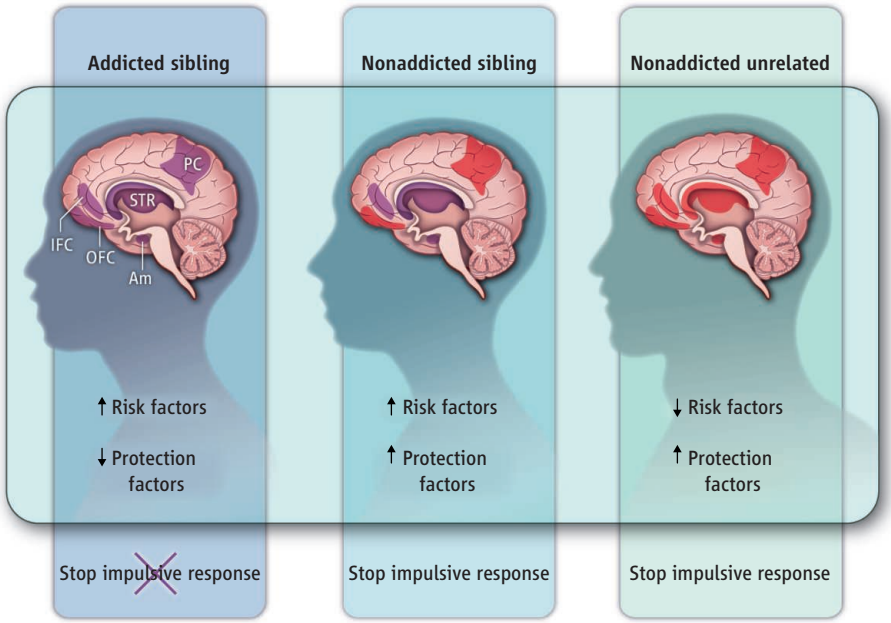
The traffic light turns from green to yellow. With just one car between you and the intersection, your brain sprints into action, calculating distances and relative velocities; checking for hurried pedestrians; simulating the mental processes of the driver in front of you; and readying every muscle in preparation for a split-second decision that could literally change your life: Which pedal? So many of our mental processes, at any given moment, rely upon this constant, "high stakes" computation involving powerful impulses on one hand and inhibitory control on the other. This balancing act of neuronal signals is at the core of complex human behaviors and thus, its malfunction could have a range of adverse medical and social consequences. On page 601 of this issue, Ersche *et al*. (*1*) identify common abnormalities in fronto-striatal brain systems associated with poorer self-control in both drug-dependent individuals and their nonaddicted siblings.

The balance between activating and inhibitory signals in the brain is so central to a successful life that the level of childhood self-control is predictive of a wide range of long-term outcomes, including physical and mental health, substance abuse, financial independence, criminal behavior (*2*), and even mortality. The ability to control this balance is strongly influenced by genetic background, environmental conditions, and their interactions. Therefore, uncovering individual differences in the function and organization of the brain circuits underlying the ability to exert self-control should help

National Institute on Drug Abuse, 6001 Executive Boulevard, Rockville, MD 20857, USA. E-mail: nvolkow@nida.nih.gov

Downloaded from www.sciencemag.org on February 2, 2012

Published by AAAS



Risk and protective factors in balance. As a result of genetic, developmental, and environmental interactions, each of the brain regions shown contributes differentially toward the net balance between adaptive or maladaptive factors. Affected (addicted) and unaffected (nonaddicted) siblings shared several vulnerability (purple) features. The presence of discordant (red) regions renders the unaffected siblings phenotypically closer to unrelated controls (nonaddicted unrelated) with regard to the overall balance between risk and protective factors. The balance between these factors determines whether or not an individual will be able to stop an inappropriate impulse to act. Personality traits that either increase risk include high impulsivity, stress reactivity, novelty seeking, conditioning/habits, negative emotionality, and poor interoceptive awareness; protective factors include positive emotionality, robust inhibitory control and executive functions, balanced reward sensitivity, strong coping skills, and frustration management. Right inferior frontal cortex (IFC), orbitofrontal cortex (OFC), striatum (STR), amygdala (Am), precuneus (PC).

us better understand disorders characterized by "impaired control," not only substance use disorders (including addiction) but also conditions such as obesity, pathological gambling, attention deficit hyperactivity disorder, and obsessive-compulsive disorders.

Ersche *et al*. identify abnormalities in the connectivity between drive and control circuits in the brain that are associated with poorer behavioral control of prepotent responses not only in addicted individuals but also in their nonaddicted siblings as compared to a control group of unrelated healthy individuals. The authors assessed the density (by fractional anisotropy) of white matter fiber tracts, which are the axonal fibers that transmit neural signals between brain regions. They found a correlation between the density of tracts adjacent to the right inferior frontal cortex, which is a key region involved with inhibitory control (*3*), and performance in a classical test of inhibitory control called the "stop signal reaction time," which provides a measure of self-control. Notably, the fiber tract density and self-control deficits—compared to a control group—were as pronounced in stimulant-dependent individuals as in their non-dependent siblings. This finding is important for it suggests not only that dysfunctions in the fronto-striatal circuits that handicap self-control [and are a hallmark of addiction] are influenced by genetics, but also that the increased vulnerability for substance use disorders engendered by these dysfunctions can be overcome. But why did one sibling become addicted while the other did not? Possibly, different environmental exposures contributed to their different trajectories, even though most sibling pairs had a shared childhood environment, at least until adolescence. Alternatively, the nonaddicted sibling may have benefited from resilience factors not present in the addicted one that buffered his or her risk for a substance abuse disorder.

Indeed, comparison of the brain structural differences between the addicted and the nonaddicted siblings with the non-related controls showed that there were shared abnormalities in gray matter volumes between siblings (increases in putamen and amygdala and decreases in posterior insula), but also some differences. Most striking were differences in the volume of the medial orbitofrontal cortex (corresponding to medial Brodmann Area 11) and the precuneus (medial Brodmann area *7*), which were smaller in the afflicted siblings relative to the nonafflicted siblings. The orbitofrontal cortex is implicated in salience attribution and enables behavioral flexibility in response to changing contexts. Smaller volumes and reduced activity in the orbitofrontal cortex of drug-addicted individuals may confer vulnerability to compulsive and inflexible behaviors (*4*, *5*). In addicted subjects, reduced activity in the orbitofrontal cortex (as well as in anterior cingulate gyrus) has been shown to be associated with reduced amounts of dopamine D2 receptors in the striatum (*6*–*8*), which are linked to a greater risk for impulsivity and compulsive drug administration (*9*, *10*). By contrast, subjects who had a high familial risk for alcoholism but were not alcoholics showed an increased number of dopamine D2 receptors in the striatum, which was associated with higher activity in the orbitofrontal cortex (and also in the anterior cingulate gyrus) (*11*). Increased activity in the orbitofrontal cortex (and also in the anterior cingulate gyrus) has been associated with higher scores in positive emotionality, a personality trait that is considered to protect against substance use disorders (*12*) both in individuals at high genetic risk for alcoholism (*11*) and in non–drug-abusing healthy volunteers (*13*). Unlike their nonaddicted siblings, addicted siblings also had smaller volumes in the precuneus, which is involved with self-referential processing and like the middle orbitofrontal cortex also plays an important role in the evaluation of social stimuli. Both metabolic activity and concentration of cannabinoid type 1 receptors in the precuneus are negatively correlated with high-sensation or novelty-seeking behavior (*14*, *15*), a personality trait that increases the risk for substance use disorder. Thus, differences in the balance between the number and severity of vulnerability factors (e.g., poor self-control and traits such as novelty-seeking and reward dependency) versus that of resilience factors (e.g., positive emotionality) may have contributed to the divergent trajectories between siblings, regarding substance use disorders, despite the shared poor self-control (see the figure).

The similarity of the structural changes in striatal and prefrontal brain regions of drug-dependent and nonaddicted siblings is hardly surprising considering the high heritability of global brain volumes particularly in the frontal lobe areas (*16*). The findings of Ersche *et al*. are also consistent with genetic studies showing that polymorphisms that influence behavioral measures of inhibitory

CREDIT: B. STRAUCH/SCIENCE

Downloaded from www.sciencemag.org on February 2, 2012

Published by AAAS

control are mediated by their impact on prefrontal-striatal circuitry. Indeed, preclinical studies have started to clarify the molecular mechanisms that modulate prefrontal-striatal communication during risky decision-making (*17*). For example, in the prefrontal cortex of rodents, dopamine D1 receptor signaling mediates working memory in a nonlinear fashion such that performance is degraded not only during insufficient (aging) but also during excessive (acute stress) transmission. Similarly, in the striatum, dopamine D2 receptor signaling relates to performance through an inverted U-shape function, because both suboptimal as well as supraoptimal dopamine signaling can lead to maladaptive excessive or deficient risk-taking, respectively.

The finding by Ersche *et al*. that decreased connectivity in the right inferior frontal lobe is linked to poor self-control has clinical implications, for it provides a potential biomarker that can be targeted for interventions to strengthen it. Indeed, several childhood and adolescent interventions can improve executive function and self-control, although studies have not yet assessed whether they strengthen frontostriatal connectivity. In more general terms, a deeper, endophenotype-based understanding of personality traits that can promote resiliency and their degree of malleability may help prevent adverse trajectories such as those leading to substance use disorder or other conditions with underlying deficits in self-control.

References

1. K. D. Ersche *et al*., *Science* **335**, 601 (2012).
2. T. E. Moffitt *et al*., *Proc. Natl. Acad. Sci. U.S.A.* **108**, 2693 (2011).
3. A. R. Aron, T. W. Robbins, R. A. Poldrack, *Trends Cogn. Sci.* **8**, 170 (2004).
4. N. D. Volkow, J. S. Fowler, *Cereb. Cortex* **10**, 318 (2000).
5. T. R. Franklin *et al*., *Biol. Psychiatry* **51**, 134 (2002).
6. N. D. Volkow *et al*., *Synapse* **14**, 169 (1993).
7. N. D. Volkow *et al*., *Am. J. Psychiatry* **158**, 2015 (2001).
8. N. D. Volkow *et al*., *J. Neurosci.* **27**, 12700 (2007).
9. B. J. Everitt *et al*., *Philos. Trans. R. Soc. Lond. B Biol. Sci.* **363**, 3125 (2008).
10. B. Lee *et al*., *J. Neurosci.* **29**, 14734 (2009).
11. N. D. Volkow *et al*., *Arch. Gen. Psychiatry* **63**, 999 (2006).
12. T. A. Wills *et al*., *Dev. Psychol.* **37**, 283 (2001).
13. N. D. Volkow *et al*., *Mol. Psychiatry* **16**, 818 (2011).
14. Y. Hakamata *et al*., *Neurosci. Lett.* **396**, 33 (2006).
15. K. Van Laere *et al*., *Arch. Gen. Psychiatry* **66**, 196 (2009).
16. J. S. Peper *et al*., *Hum. Brain Mapp.* **28**, 464 (2007).
17. N. W. Simon *et al*., *J. Neurosci.* **31**, 17660 (2011).

10.1126/science.1218170

CLIMATE CHANGE

Marching in Near Lock-Step

A cave record from Peru closely matches climate patterns seen in cores from Greenland and the North Atlantic Ocean.

Donald T. Rodbell

Over the past ~100,000 years, intervals of gradual climate cooling have repeatedly been followed by abrupt warming events. Collectively known as Dansgaard/Oeschger (D/O) cycles (*1*), these ~1500-year-long cycles are recorded in the oxygen isotope record of Greenland ice cores and in layers of iceberg-rafted sediments in the North Atlantic Ocean known as Heinrich layers (*2*) that record collapses of the Northern Hemisphere ice sheets. On page 570 of this issue, Kanner *et al*. (*3*) report a stunning new archive of the oxygen isotopic composition of tropical precipitation recorded in the deposits of Pacupahuain Cave (see the figure, panel A), located high on the eastern side of the Peruvian Andes, that matches the North Atlantic/Greenland records in striking detail. The results help to elucidate how climate change—both past and future—in one region of the globe may drive climate changes in far-flung regions.

The North Atlantic/Greenland record is based on ice and sediment cores that are tens to hundreds of meters in length, far longer than the 15-cm-long Peruvian speleothem studied by Kanner *et al*. (see the figure, panel B). But the diminutive Peruvian speleothem satisfies a critical prerequisite for close climate comparisons: precise radiometric age control. The calcium carbonate in caves is ideally suited to the uranium-thorium dating method, often yielding a higher age precision than any other dating method applicable to the time window in question; typical age uncertainties are less than ±1%. Indeed, this precision exceeds that of the proxy climate records from the North Atlantic/Greenland region that contain D/O cycles and Heinrich layers. Kanner *et al*. therefore suggest that their Peruvian archive can be used to improve the dating of the very records to which they are comparing.

Cave records from Northern Hemisphere sites have shown clearly that the climate patterns seen in the North Atlantic/Greenland records were followed at sites as far away as east central China and the northwestern Indian Ocean (*4*, *5*). At these sites, the abrupt warmings that mark the end of D/O cycles are recorded as abrupt negative departures in oxygen isotope values—the opposite direction of the changes seen in the Greenland ice cores. Southern Hemisphere cave records show a somewhat more muted Northern Hemisphere influence, but the oxygen isotopic composition of cave calcite generally tracks in the same direction as the Greenland ice cores.

The key to understanding these differences lies in the climatic implications of isotopic shifts in precipitation. At high latitudes, the primary driver of the isotopic composition of precipitation is the temperature of condensation (*6*), with colder temperatures resulting in lower $^{18}O/^{16}O$ ratios in precipitation. At low latitudes, where atmospheric convection dominates, the main control on the isotopic composition of precipitation is the amount of precipitation, with greater convection driving increased precipitation and lower $^{18}O/^{16}O$ ratios, and vice versa.

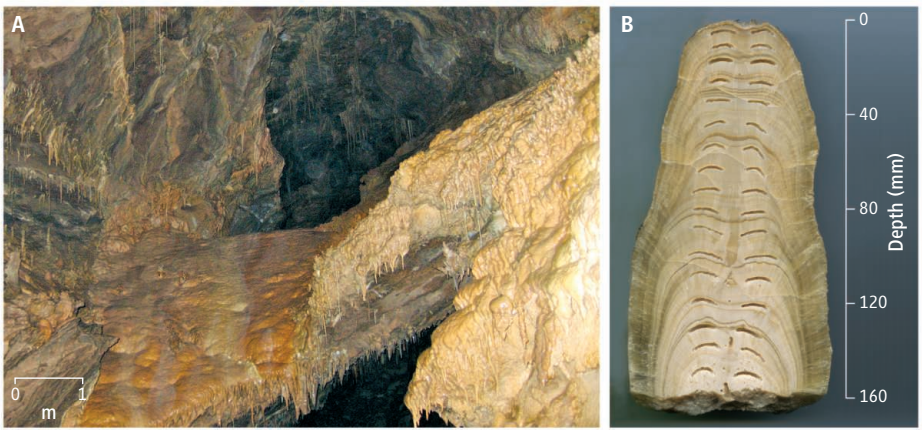
Thus, warm events in the Greenland region correspond with wet events in the low latitudes of the Northern Hemisphere but dry events in the low latitudes of the Southern Hemisphere. The Pacupahuain Cave record shows this with greater fidelity than any other tropical Southern Hemisphere terrestrial record yet: It clearly shows 12 of the 13 major abrupt warming events that mark the end of D/O cycles between 16,000 and 50,000 years ago in Greenland as positive departures in the oxygen isotopic composition of cave calcite. Conversely, cooling of the North Atlantic Ocean during Heinrich events corresponds with increased precipitation over the Peruvian Andes and negative departures in the $^{18}O/^{16}O$ ratio of cave calcite. Several other climate proxy records have shown a close correspondence between the timing of Heinrich events and the advance of Peruvian glaciers (*7*) and expansion of Bolivian lakes (*8*), but until now no single tropical Southern Hemisphere record has recorded the complete sequence with such dating precision.

The interhemispheric precipitation seesaw evident in the network of cave records

Geology Department, Union College, Schenectady, NY 12308, USA. E-mail: rodbelld@union.edu

Downloaded from www.sciencemag.org on February 2, 2012

Published by AAAS



High-resolution climate record from a tropical cave. Pacupahuain Cave (**A**) is located on the eastern side of the Peruvian Andes. Kanner *et al*. used uranium-thorium dating of one speleothem from the cave (**B**) to determine how the precipitation in this region has changed between 16,000 and 50,000 years ago. They show that this record closely tracks ice-core records from Greenland and sediment cores from the North Atlantic, providing insights into long-distance climate connections.

PHOTO CREDITS: (LEFT) CARLOS MORALES-BERMUDEZ/CENTRO DE EXPLORACIONES SUBTERRÁNEAS DEL PERÚ; (RIGHT) LISA KANNER

reflects changes in the vigor of the monsoons in response to variations in the position of the Intertropical Convergence Zone (ITCZ) over the oceans. The sea surface temperature gradient of the North Atlantic may affect the position of the ITCZ, thereby determining which hemisphere is to have a protracted interval of strong monsoons. A cold North Atlantic appears to cause a steep sea surface temperature gradient, a southward migration of the ITCZ, and an enhanced South American summer monsoon. Tropical cave records show that the monsoon seesaw has cycled dozens of times in the past ~50,000 years.

One of the curiosities of the precipitation seesaw is the degree to which it is controlled by temperature cycles in the North Atlantic/Greenland region, and the relatively minor role played by Antarctic temperature cycles. The latter precede those in Greenland by 1500 to 3000 years (*9*). Kanner *et al*.'s precisely dated Pacupahuain Cave record may delineate the competing influence of the two poles. Over two intervals in which the influence of both poles can be seen in the record, the Northern Hemisphere appears to dominate. Speleothem records from caves at higher latitudes in the Southern Hemisphere could delineate the regions within which the influence of the South Pole is dominant. The large size of the region that has climatically marched in near lock-step with the North Atlantic illustrates the remarkable effectiveness with which atmospheric teleconnections can operate.

References

1. W. Dansgaard *et al*., *Nature* **364**, 218 (1993).
2. H. Heinrich, *Quat. Res.* **29**, 142 (1988).
3. L. C. Kanner, S. J. Burns, H. Cheng, R. L. Edwards, *Science* **335**, 570 (2012).
4. Y. J. Wang *et al*., *Science* **294**, 2345 (2001).
5. S. J. Burns, D. Fleitmann, A. Matter, J. Kramers, A. A. Al-Subbary, *Science* **301**, 1365 (2003).
6. W. Dansgaard, *Tellus* **16**, 436 (1964).
7. J. A. Smith, D. T. Rodbell, *J. Quat. Sci.* **25**, 243 (2010).
8. P. A. Baker *et al*., *Nature* **409**, 698 (2001).
9. T. Blunier, E. J. Brook, *Science* **291**, 109 (2001).

10.1126/science.1218365

PHYSICS

Seeing the Superfluid Transition of a Gas

The universal thermodynamic functions of a superfluid formed from a fermion gas of strongly interacting lithium atoms have been measured precisely.

Wilhelm Zwerger

An important characteristic of a superfluid is the critical temperature T_c, below which it forms from an ordinary fluid, but a more detailed understanding comes from measuring other thermodynamic and quantum-mechanical parameters. For systems in which the superfluid is created by pairing fermions (for example, the electron superfluid in superconductors), T_c is often very low compared to another characteristic temperature of mobile fermions, their Fermi temperature T_F. Thus, superconductivity has not been observed at room temperature. On page 563 of this issue, Ku *et al*. (*1*) present precise measurements of thermodynamic quantities of an ultracold gas of lithium-6 atoms—fermions—with strong attractive interactions that explicitly show the superfluid transition through changes in the compressibility and the heat capacity. The absolute temperatures here are on the order of only 100 nK, but this Fermi gas provides an example of a high-temperature superfluid: No other system has ever been observed with a transition temperature as high as ~16% of T_F. Scaled to the density of electrons in metals, T_c would occur far above room temperature.

In classical physics, no phase transitions occur within the gas phase itself. The situation is quite different in quantum physics. Indeed, Einstein showed in 1925 that even a gas of noninteracting particles can undergo a transition to a quite unusual gaseous phase, a Bose-Einstein condensate (BEC), provided that the particles obey Bose statistics (any number of particles can occupy the same quantum state). The realization of this transition with ultracold gases in the sub-microkelvin regime in 1995 opened up a new and still expanding field of atomic and molecular physics (*2*, *3*).

Atoms that obey Fermi statistics (in which only one particle can occupy a quantum state), like lithium-6, undergo a transition to a condensate phase by forming composite particles that act like bosons. For this to happen, interactions are necessary. In the simplest case, a weak attraction arises between two fermions of opposite spin. As realized by Bardeen, Cooper, and Schrieffer (BCS) in 1957 (*4*), this attraction can be arbitrarily weak. The resulting T_c is typically less than 1% of T_F. Stated differently, the pair size in this weak coupling limit is much larger than average interparticle spacing—by an order of 10^3 in conventional superconductors. Within the volume occupied by a single pair, there are thus about a billion other ones.

The BCS theory of fermionic superfluids has proven to be widely applicable. Beyond conventional superconductors, it describes

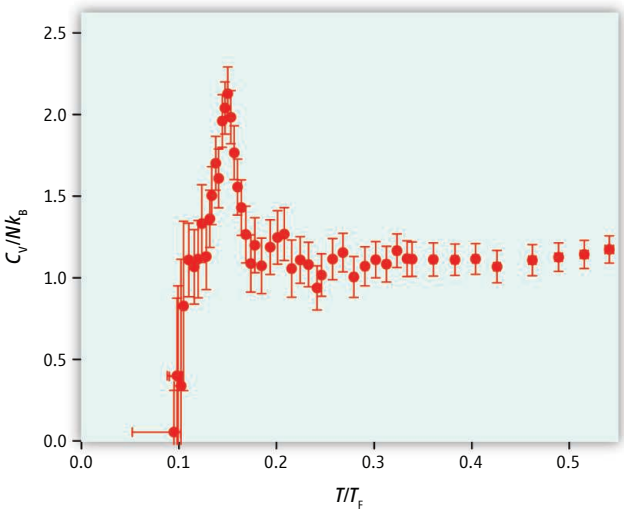
Department of Physics, Technical University Munich, 85748 Garching, Germany. E-mail: zwerger@ph.tum.de

Downloaded from www.sciencemag.org on February 2, 2012

Published by AAAS

the complex kind of pairing that occurs in superfluid helium-3, in atomic nuclei, or in quark matter at high densities. There is an important class of Fermionic superfluids that do not follow the weak-coupling BCS paradigm. These are the high-temperature superconductors, which have electron pairs whose size is of the same order as the interparticle spacing (*5*). Unfortunately, these materials are far too complex to be described by a model that starts from a Fermi gas of electrons.

In recent years, however, a completely new class of neutral Fermi gases have become accessible—trapped ultracold atoms, whose interaction strength can be tuned by a magnetic field. Ku *et al*. study a gas of lithium-6 atoms that contains a 50:50 mixture of the two lowest hyperfine energy states (which are closely spaced energy states created by the interaction of the electron and nuclear magnetic moments). In the ultracold limit, only s-wave, or head-on collisions, occur. The Pauli exclusion principle forbids s-wave collisions between identical fermions. Thus, the only interactions are between atoms in different hyperfine states.



Running hot and cold. Specific heat (heat capacity C_v divided by number of atoms N) of the unitary Fermi gas of lithium-6 atoms as a function of the normalized temperature T/T_F. In the nondegenerate limit $T \rightarrow T_F$, the specific heat per particle approaches the value 3/2 k_B predicted by the equipartition theorem, where k_B is Boltzmann's constant. At very low temperatures, it is expected to vanish as T^3 (because of sound waves) in the superfluid, a dependence that is not resolved experimentally. The superfluid transition at $T_c/T_F \sim 0.16$ shows up as very sharp peak.

At very low temperatures, this interaction is completely characterized by one parameter, the scattering length a. In order to reach the regime of strong coupling, a must be much larger than the average interparticle spacing $1/k_F$. At the low densities typical for ultracold gases, with Fermi wavelengths of almost 1 μm, scattering lengths must be huge compared to atomic dimensions. Such large scattering lengths can be achieved near Feshbach resonances, which occur when the collision energy matches the energy of a closed-channel bound state that mediates the strong interaction (but is not the bound pair state that condenses) (*6*). The energy of this bound state can be shifted with an external magnetic field, so the strength of the interaction can be tuned. Such a two-component Fermi gas with large scattering length and strong short-range interactions is called a unitary Fermi gas.

The unitary Fermi gas is a strongly interacting many-body problem that lies just halfway between the well-understood BCS and BEC limits [for a detailed review, see (*7*)], and for which $1/k_F$ is the only relevant length scale and T_F the only relevant energy scale. As a result, the ground-state energy or pressure is just a pure number times its value in the noninteracting Fermi gas. Similarly, T_c is necessarily a universal fraction of T_F. The challenge to determine these numbers was first formulated by Bertsch in 1999 (*8*), even before ultracold Fermi gases were available. The difficulty of doing precision thermometry on a trapped ultracold gas, which is completely isolated from its environment, had precluded reliable measurements of the universal functions and numbers.

The results of Ku *et al*. are a milestone in the quantitative analysis and understanding of this problem. Their measurement of the equation of state—how pressure, volume, and temperature relate to each other—relies on determining the local gas density $n(x)$ as a function of the local confining potential $V(x)$ from in situ absorption images. Assuming only local thermodynamic equilibrium, they determined the equation of state and the compressibility with unprecedented precision. In particular, they determined the temperature of the gas by integrating the relation between volume and pressure up to the ideal gas limit. This novel method for thermometry of ultracold gases considerably improved the accuracy compared to previous experiments (*9*–*11*), and also allowed the observation of the superfluid transition in a direct manner (see the figure).

The work of Ku *et al*. provides precise values of universal numbers, such as the Bertsch parameter, which is the ratio of the ground-state pressure of the unitary gas with respect to that of the noninteracting Fermi gas or the transition temperature in units of T_F, which have remained controversial for many years. Indeed, the experimental results are now accurate enough to benchmark novel theoretical methods for the fermionic many-body problem. Moreover, as suggested by Bertsch, a precise knowledge of the thermodynamics of the unitary gas realized with ultracold atoms at typical densities ~10^{-12} cm^{-3} has implications for understanding the equation of state of neutron stars at densities that are about 25 orders of magnitude larger than for the unitary Fermi gas (*12*).

In addition, the measurements shed new light on the interpretation of the normal state of the unitary gas in terms of either a Fermi liquid (*13*) or a pseudogap phase (*14*); neither model is substantiated by the present results. Indeed, a detailed understanding of the nontrivial normal phase above the superfluid transition along the crossover from BCS pairing to a BEC of tightly bound dimers is still on open issue. Reliable results on this problem might help us understand the still controversial normal phase of high-temperature superconductors. In this sense, cold atoms can serve as a kind of quantum simulator that allows solving problems that are intractable otherwise.

References

1. M. J. H. Ku, A. T. Sommer, L. W. Cheuk, M. W. Zwierlein, *Science* **335**, 563 (2012); 10.1126/science.1214987.
2. E. A. Cornell, C. E. Wieman, *Rev. Mod. Phys.* **74**, 875 (2002).
3. W. Ketterle, *Rev. Mod. Phys.* **74**, 1131 (2002).
4. J. Bardeen, L. N. Cooper, J. R. Schrieffer, *Phys. Rev.* **108**, 1175 (1957).
5. M. Randeria, in *Bose-Einstein Condensation*, A. Griffin, D. W. Snoke, S. Stringari, Eds. (Cambridge Univ. Press, Cambridge, UK, 1995), pp. 355–392
6. C. Chin, R. Grimm, P. Julienne, E. Tiesinga, *Rev. Mod. Phys.* **82**, 1225 (2010).
7. W. Zwerger, Ed., *The BCS-BEC Crossover and the Unitary Fermi Gas, Lecture Notes in Physics* (Springer, Berlin, Heidelberg, 2012).
8. G. Bertsch, *Proceedings of the 10th International Conference on Recent Progress in Many-Body Theories*, R. F. Bishop *et al.*, Eds. (World Scientific, Singapore, 2000); www.worldscibooks.com/physics/4434.html.
9. J. Kinast *et al.*, *Science* **307**, 1296 (2005).
10. M. Horikoshi, S. Nakajima, M. Ueda, T. Mukaiyama, *Science* **327**, 442 (2010).
11. S. Nascimbène, N. Navon, K. J. Jiang, F. Chevy, C. Salomon, *Nature* **463**, 1057 (2010).
12. A. Schwenk, C. J. Pethick, *Phys. Rev. Lett.* **95**, 160401 (2005).
13. S. Nascimbène *et al.*, *Phys. Rev. Lett.* **106**, 215303 (2011).
14. J. P. Gaebler *et al.*, *Nat. Phys.* **6**, 569 (2010).

10.1126/science.1218074

Downloaded from www.sciencemag.org on February 2, 2012

Published by AAAS

Nanoscopy in a Living Mouse Brain

Sebastian Berning,[1] Katrin I. Willig,[1]* Heinz Steffens,[1] Payam Dibaj,[2] Stefan W. Hell[1]*

Cells, the functional units of life, are best studied in vivo. This is particularly true for neurons, which perform their basic function of information processing by connecting with their neighbors. Therefore, unraveling the inner workings of the brain requires the imaging of neurons in the living animal. Although confocal and multiphoton microscopy can visualize neurons tagged with fluorescent proteins in transgenic living systems, they cannot discern features closer than half the wavelength of light (200 to 300 nm) (*1*). By causing such features to fluoresce sequentially, stimulated emission depletion (STED) microscopy and other emerging superresolution techniques have now overcome this barrier (*2*). Whereas these techniques have been applied throughout the life sciences, in vivo nanoscale imaging of cells in higher animals has remained elusive. We used STED microscopy to superresolve neurons and their subtle dynamics in the cerebral cortex of a living mouse.

We developed an upright scanning STED fluorescence microscope with a 1.3–numerical aperture (NA) lens focusing a 80-MHz train of 70-ps excitation pulses of 488-nm wavelength on the animal brain (Fig. 1A). To visualize neurons, we used heterozygous TgN(Thy1-EYFP) mice expressing enhanced yellow fluorescent protein (EYFP) as a nonfusion protein in neuronal cytoplasm (*3*), which is under the control of the regulatory element from the *thy1* gene. The focused excitation pulses were coaligned and synchronized with doughnut-shaped 592-nm STED pulses of 300-ps duration and 25-mW focal power for silencing the EYFP. The fluorescence was imaged onto a confocal detector so that 600-nm-thick layers inside the brain could be discriminated. Optical access was provided by a cover glass–sealed hole in the skull, exposing the mouse's somatosensory cortex. The anaesthetized mouse was artificially ventilated and controlled for its vital functions, such as body temperature, ventilation, blood oxygenation, and heart function [by recording the electrocardiogram]. Rigid construction and keeping the optical paths short protected our setup from external vibrations. Thus, the images could be recorded without active vibration compensation or numerical image processing. Cardiovascular and respiratory motion was suppressed by an optimized surgical preparation procedure, which was particularly important for recording potential movements of the dendritic spines. Although such movements have been observed in hippocampal organotypical slices of 5- to 7-day-old mice (*4*, *5*) and during de novo growth in the developing cortex (*6*), until now it has remained unclear whether they can occur in the adult animal brain.

The STED image in Fig. 1B shows a dendritic process within the molecular layer of the somatosensory cortex of a TgN(Thy1-EYFP) mouse, located 10 to 15 μm below the surface. The STED images show structures of <70 nm in size (Fig. 1D), indicating that the resolution is at least of that order. Recording images every 7 to 8 min revealed that adult dendritic spines can undergo morphologic changes and movements (Fig. 1C, 0 to 30 min, and movie S1) on the time scale of minutes. These movements were repeatedly observed in all six individuals imaged. The mice were aged between 66 and 205 days. To exclude random defocus from being mistaken for movement, we rendered each image by a maximum intensity projection of a stack of five images with 600-nm-depth spacing. Although the dendrite of origin retained largely the same shape throughout the experiments, morphological changes were found at the head and neck regions of the dendritic spines, potentially reflecting alterations in the connectivity of the neural network, as is seen in the immature brain. Apparently, dendritic spines can alter their morphology in the intact somatosensory cortex of the adult mouse.

Although absorption of the 592-nm STED beam by EYFP is negligible, adverse absorption in the tissue may occur at this wavelength. Indeed, slight local swellings have occasionally been observed for relatively thick dendritic processes featuring many mitochondria. However, we did not observe degradation or disaggregation of dendritic processes as known to occur right after cell death or exitus. A remedy should be the use of red fluorescent proteins calling for STED beams of wavelengths >700 nm, where absorption by mitochondrial metabolites is negligible. Another option is to use transgenic animals tagged with reversibly switchable fluorescent proteins, enabling the STED-like nanoscopy called RESOLFT (reversible saturable optical fluorescence transitions) that requires far lower light intensities than STED (*7*). Future long-term in vivo studies should solve central aspects of brain development and, using mouse models, also of brain disease. Altogether, we expect in vivo optical nanoscopy to assume a major role in the quest for deciphering our primary organ.

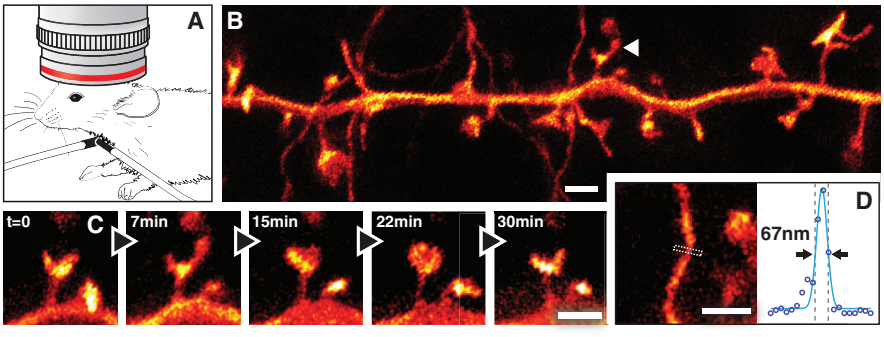


Fig. 1. STED microscopy in the molecular layer of the somatosensory cortex of a mouse with EYFP-labeled neurons. (**A**) Anesthetized mouse under the objective lens (63×, NA 1.3, glycerol immersion) with tracheal tube. (**B**) Projected volumes of dendritic and axonal structures reveal (**C**) temporal dynamics of spine morphology with (**D**) an approximately fourfold improved resolution compared with diffraction-limited imaging. Curve is a three-pixel-wide line profile fitted to raw data with a Gaussian. Scale bars, 1 μm.

References and Notes

1. T. Misgeld, M. Kerschensteiner, F. M. Bareyre, R. W. Burgess, J. W. Lichtman, *Nat. Methods* **4**, 559 (2007).
2. S. W. Hell, *Science* **316**, 1153 (2007).
3. G. P. Feng *et al.*, *Neuron* **28**, 41 (2000).
4. U. V. Nägerl, K. I. Willig, B. Hein, S. W. Hell, T. Bonhoeffer, *Proc. Natl. Acad. Sci. U.S.A.* **105**, 18982 (2008).
5. N. T. Urban, K. I. Willig, S. W. Hell, U. V. Nägerl, *Biophys. J.* **101**, 1277 (2011).
6. H. B. Kwon, B. L. Sabatini, *Nature* **474**, 100 (2011).
7. T. Grotjohann *et al.*, *Nature* **478**, 204 (2011).

Acknowledgments: The experiments were performed according to the ethics guidelines of national law regarding animal protection procedures and were authorized by the ethics committee of the Max Planck Institute for Biophysical Chemistry and by the responsible authorities, the Niedersächsisches Landesamt für Verbraucherschutz. We thank A. Schönle for the software Imspector. S.W.H. holds patents on STED microscopy: German patent DE 4416 558 C2 and U.S. Patent US5731588A.

Supporting Online Material

www.sciencemag.org/cgi/content/full/335/6068/551/DC1
Materials and Methods
Figs. S1 and S2
Movie S1

17 October 2011; accepted 15 December 2011
10.1126/science.1215369

[1]Department of NanoBiophotonics, Max Planck Institute (MPI) for Biophysical Chemistry, Am Fassberg 11, 37077 Göttingen, Germany. [2]MPI for Experimental Medicine, Hermann-Rein-Strasse 3, 37075 Göttingen, Germany.

*To whom correspondence should be addressed. E-mail: kwillig@gwdg.de (K.I.W.); shell@gwdg.de (S.W.H.)

Downloaded from www.sciencemag.org on February 2, 2012

High-Resolution View of the Yeast Meiotic Program Revealed by Ribosome Profiling

Gloria A. Brar,[1] Moran Yassour,[2,3,4] Nir Friedman,[4,5] Aviv Regev,[2,3] Nicholas T. Ingolia,[1]*† Jonathan S. Weissman[1]†

Meiosis is a complex developmental process that generates haploid cells from diploid progenitors. We measured messenger RNA (mRNA) abundance and protein production through the yeast meiotic sporulation program and found strong, stage-specific expression for most genes, achieved through control of both mRNA levels and translational efficiency. Monitoring of protein production timing revealed uncharacterized recombination factors and extensive organellar remodeling. Meiotic translation is also shifted toward noncanonical sites, including short open reading frames (ORFs) on unannnotated transcripts and upstream regions of known transcripts (uORFs). Ribosome occupancy at near-cognate uORFs was associated with more efficient ORF translation; by contrast, some AUG uORFs, often exposed by regulated 5′ leader extensions, acted competitively. This work reveals pervasive translational control in meiosis and helps to illuminate the molecular basis of the broad restructuring of meiotic cells.

Sexual reproduction is enabled by meiosis, a strongly conserved cell division that generates haploid progeny from a diploid precursor. Meiosis has been studied for over a century, including extensive analyses in the budding yeast *Saccharomyces cerevisiae* [reviewed in (*1*, *2*)], where it is linked to spore formation. These efforts have provided a wealth of knowledge about the movement and changes in organization of meiotic chromosomes. Far less is known about the molecular basis of the remodeling events that have an impact on other aspects of meiotic cellular physiology. Pioneering microarray studies (*3*) provided a basic framework of molecular changes accompanying yeast meiotic progression but failed to capture many dynamic processes, in part because of extensive posttranscriptional regulation, including specific instances of functionally significant translational control [reviewed in (*2*); see also (*4*)]. Whether translational control plays a general role in meiotic protein production, however, is unclear.

Ribosome profiling, based on deep sequencing of ribosome-protected mRNA fragments, allows monitoring of translation with scale, speed, and accuracy that rivals approaches for following mRNA levels (*5*, *6*). Applying this method to sporulating *S. cerevisiae* cells allowed us to follow the molecular events underlying meiosis with unprecedented depth.

A high-resolution atlas of meiotic mRNA abundance and new protein synthesis. Our studies relied on three critical features: optimized meiotic synchrony, dense time points that oversampled meiotic transitions, and in-depth staging of each time point. We collected samples through two separate meiosis experiments (Fig. 1, A and B, and fig. S1A). The first used an optimized version of traditional synchronization procedures and focused on early meiotic stages. The second time course used an estrogen-activatable derivative of the Ndt80 transcription factor (*4*, *7*), which allowed synchronous progression through the meiosis I and II (MI and MII) chromosome segregation stages (*4*). Each time point was staged in detail (Fig. 1B and figs. S2 and S3), and we selected 25 of them, chosen for comprehensive meiotic coverage, along with two cycling vegetative samples, for ribosome profiling and mRNA sequencing (Fig. 1A and fig. S1A). Use of time points that oversampled meiotic stages allowed for synthesis of the data into a master time course (Fig. 1A and fig. S1B) and selective pooling, which collapsed meiotic progression into nine categories for some analyses (fig. S4).

Staging revealed a high degree of synchrony and provided a cytological framework to anchor expression data (Fig. 1B and figs. S2 and S3). Examination of ribosome footprints for specific genes showed that the sample synchrony was reflected in sharp, discrete translation patterns (Fig. 1C). The large majority (6134 out of 6708) of genes were translated at some point in meiosis, and most showed strong temporal regulation. In addition to a large shift in expression patterns between vegetative cells and cells entering meiosis, 66% of meiotically expressed genes varied by at least 10-fold in protein synthesis level through meiotic progression itself, a range that far exceeded measurement errors (Fig. 2A and fig. S5, A to D). These changes were due largely to the meiotic program itself rather than the nutrient deprivation conditions that accompany sporulation (fig. S6).

Expression clustering to probe meiotic cell biology and gene function. Clustering of the time points by genome-wide protein synthesis patterns precisely recapitulated their order (figs. S1B and S6A). Thus, dynamic control of protein synthesis results in unique expression signatures throughout the meiotic program. Accordingly, grouping of all genes by protein synthesis pattern through meiosis revealed numerous multifaceted clusters (Fig. 2A).

Many clusters emerged from groups of functionally related genes. This was seen prominently for genes involved in translation, mitochondrial function, mitochondrial translation, nutrient uptake, proteasome function, and redox reactions (Fig. 2A, numbered in the middle panel, and tables S1 and S2). Furthermore, a tight cluster of 27 proteins that were synthesized at the onset of DNA replication was predominantly composed of critical DNA replication and chromosome structure factors [Fig. 2A, top, and table S2; (*8*)]. Similarly, genes involved in recombination and synaptonemal complex (SC) formation were expressed precisely when these processes occurred, and they emerged as a discrete group containing 46 genes from unbiased clustering of the full data set (Fig. 2A, bottom, and table S2). Notably, this cluster included the large majority of meiotic genes with characterized roles in double-strand–break formation, crossover-noncrossover choice, and SC structure [reviewed in (*9*–*11*)].

Several uncharacterized genes were found in the recombination and SC cluster, which suggested that they are involved in these intensely studied processes (*1*). Indeed, loss of either *YDR506C* or *YLR445W* delayed nuclear division, consistent with a role for these factors in prophase, when recombination and SC formation occur (Fig. 2, B and C, and fig. S7A). *ydr506c*Δ and *ylr445w*Δ cells showed distinct, specific defects in SC morphogenesis (fig. S7, B and C), and in both cases, the meiotic progression delay was largely alleviated when the recombination checkpoint was bypassed by deletion of *SPO11* (Fig. 2, B and C, and fig. S7A). The strong delay in *ylr445w*Δ cells, however, was not fully dependent on Spo11 (Fig. 2C and fig. S7A), which implied that this gene has additional functions.

Evidence for cellular remodeling. Whereas our ability to observe precise temporal regulation allowed specific coclustering of some genes, there were prominent cases in which genes with a common function or localization showed highly disparate expression patterns. For example, we found tightly controlled but distinct patterns of expression among endoplasmic reticulum (ER) proteins, which suggested major ER remodeling events (fig. S8 and table S3). A strong down-regulation (relative to vegetative cells) of a set of ER genes, including

[1]Howard Hughes Medical Institute, Department of Cellular and Molecular Pharmacology, University of California, San Francisco, and California Institute for Quantitative Biosciences, San Francisco, CA 94158, USA. [2]Broad Institute of Massachusetts Institute of Technology and Harvard, Cambridge, MA 02142, USA. [3]Howard Hughes Medical Institute, Department of Biology, Massachusetts Institute of Technology, Cambridge, MA 02139, USA. [4]School of Engineering and Computer Science, Hebrew University, Jerusalem 91904, Israel. [5]Alexander Silberman Institute of Life Sciences, Hebrew University, Jerusalem 91904, Israel.

*Present address: Department of Embryology, Carnegie Institution for Science, Baltimore, MD 21218, USA.

†To whom correspondence should be addressed. E-mail: ingolia@ciwemb.edu (N.T.I.); weissman@cmp.ucsf.edu (J.S.W.)

Downloaded from www.sciencemag.org on February 2, 2012

ergosterol biosynthesis components, occurred before meiotic induction. After meiotic entry, a broad group of ER genes was induced, including glycosylation factors (table S3). Finally, after MI, a subset of folding factors, sphingolipid biosynthetic genes, and trafficking components were up-regulated. This last remodeling phase is accompanied by induction of the unfolded protein response (UPR) (*12*, *13*) (Fig. 1C, see also Fig. 3F below).

Autophagy components also showed discrete patterns of expression, which suggested dynamic control of distinct autophagic processes during sporulation [fig. S9A and table S4; (*14*)]. *ATG8*, a gene central to many branches of autophagy (*15*), was highly expressed from early in the meiotic program, and its deletion caused an early and profound meiotic defect (fig. S9, B and C). By contrast, *ATG32*, a mitophagy-specific factor (*16*, *17*), showed low expression until the meiotic divisions (fig. S9B). Delayed onset of mitophagy may ensure full mitochondrial function, which is needed to power early meiotic stages (*18*). Consistently, *atg32*Δ cells progressed normally past prophase but showed delayed meiotic completion (fig. S9D).

Translational control in meiosis. Control of protein production reflects both regulation of mRNA levels and the efficiency with which these messages are translated into proteins. Measuring translation rates and mRNA levels allowed us to evaluate their relative contributions. Much transcriptional regulation was observed, but translational control also regulated the magnitude and timing of protein production in meiotic cells. An example of this interplay is provided by the adjacent *SPS1* and *SPS2* genes (Fig. 3A). mRNA for both genes accumulated late in prophase and persisted through the meiotic divisions, consistent with their transcriptional control by *NDT80* (*19*). By contrast, *SPS1*, but not *SPS2*, was strongly translationally regulated, which resulted in delayed Sps1 protein synthesis until MII (Fig. 3, A and B).

To quantitatively evaluate the role of translational control, we calculated relative translation efficiencies [TEs; ribosome footprint RPKM/mRNA RPKM; where RPKM is reads per kilobase of coding sequence per million mapped reads, as in (*6*)] for messages across our time course. Replicates indicated high TE reproducibility (error <20%), which allowed sensitive measurement of dynamic translational control [fig. S5, E and F; (*6*)]. This approach confirmed, both in timing and degree, the strong MI-specific translational repression that regulates the B-type cyclin, *CLB3* [(*4*), Fig. 3C]. At least 10 genes showed a pattern of translational regulation highly similar to that of *CLB3*—including *SPS1* (Fig. 3A), *GIP1*, and *SPO20*—which, like *CLB3*, have known roles only late in meiosis (*20*–*22*).

Genome-wide analysis revealed that meiotic translational regulation is both pervasive and nuanced (Fig. 3D). As seen for vegetative cells (*6*), meiotic cells showed strong basal differences in translation rates among genes (Fig. 3D). Globally, we observed a net decrease in translation, relative to vegetative cells in their exponential growth phase, that was most pronounced at the very earliest and latest time points (fig. S10). Further, gene-specific translational regulation was widely used to dynamically tune gene expression. For example, 24% of genes during the "core meiotic" period showed greater than threefold TE changes, a period during which net translation capacity appears stable (fig. S10). More than 200 genes in the full time course and 66 in the core meiotic period exhibited a dynamic range in TE that was comparable to the ~10-fold changes seen for *GCN4*, an archetype of strong translational regulation (*23*).

Changes in TE frequently correlated with timing of gene function (Fig. 3E). The DNA replication factor *ORC1* (*24*), for example, showed strong translational repression at later meiotic stages when cells do not replicate DNA. Zip1, an SC component (*25*), specifically showed poor translation in vegetative cells and spores, consistent with the lack of SC in either state. Chitin deposition factor Rcr1 (*26*) is translated efficiently only at late time points, concomitant with new cell wall generation. Finally, *HAC1*, the central UPR mediator (*12*, *13*), showed transient translational activation shortly upon transfer of cells to nutrient-limited conditions, followed by a later, stronger translational activation

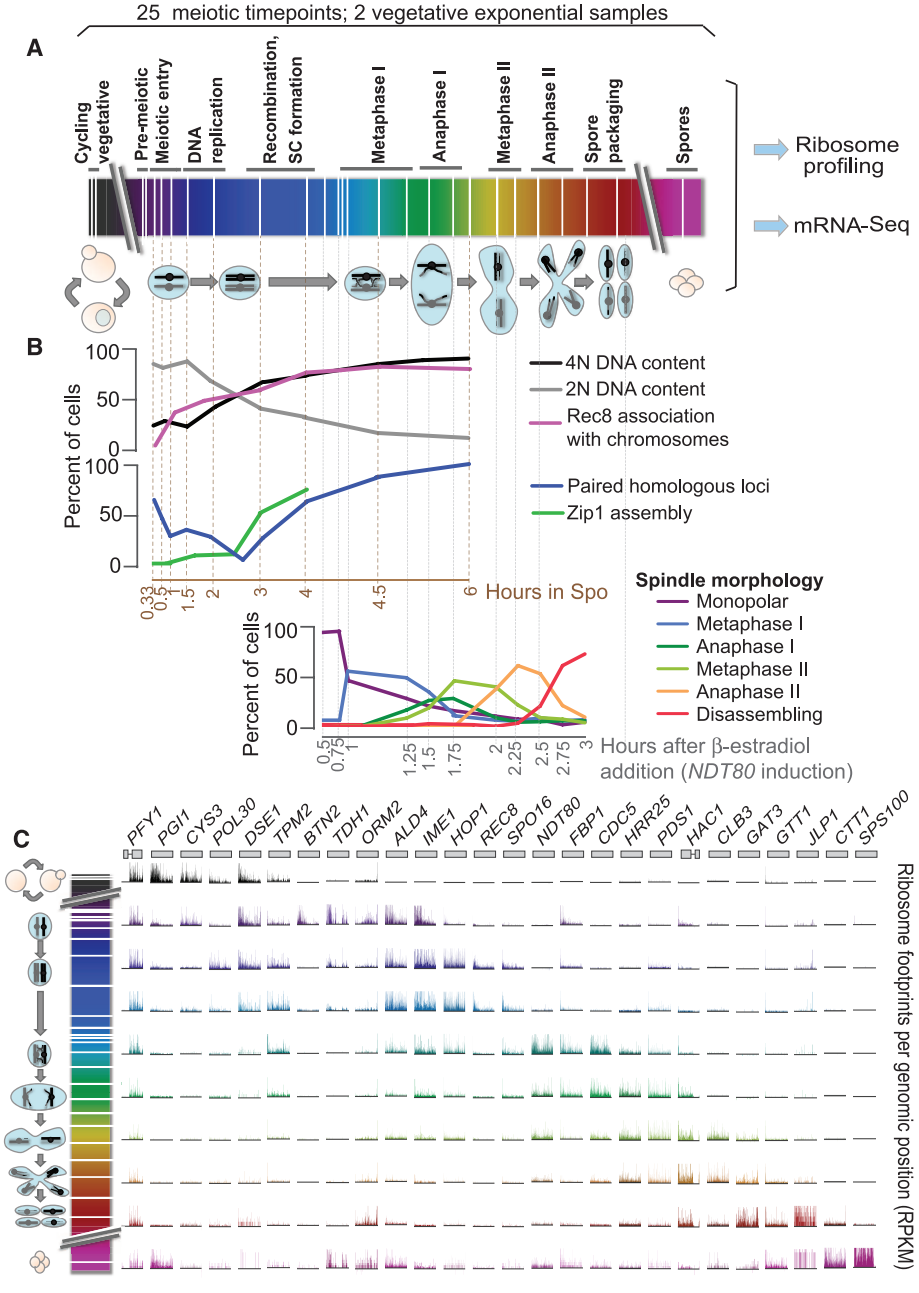


Fig. 1. Ribosome profiling through meiosis. (**A**) Time points (white lines) were taken through two overlapping time courses. Cartoon representations of meiotic stages are below. (**B**) A subset of staging controls. Positions of staging plots correspond to time points in (A). (**C**) Ribosome footprints across specific genes are shown for categories in fig. S4. Scales on the *y* axis are independent by gene.

Downloaded from www.sciencemag.org on February 2, 2012

during the meiotic divisions, as cells are synthesizing new membrane and spore walls (Fig. 3F). *HAC1* is regulated translationally through cytoplasmic splicing of its message (*27*). Consistently, *HAC1* mRNA splicing mirrored TE measurements, both in timing and degree (Fig. 3F). The UPR has been heavily studied in yeast using harsh inhibitors of ER folding (e.g., dithiothreitol). This study reveals a novel physiological setting to follow UPR induction.

Noncanonical translation. Beyond translational control of canonical open reading frames (ORFs), we also observed a shift toward noncanonical translation during the meiotic program. Whereas vegetative cells exhibited ~5% of ribosome footprints mapping outside annotated ORFs, in meiotic cells, up to ~30% of footprints mapped outside of these regions (Fig. 4A). These footprints largely mapped to discrete novel translation sites with well-defined AUG starts and stop codon stops. We systematically annotated translation units by exploiting the strong peak in ribosome density seen at translation initiation sites to identify utilized start codons [fig. S11, (*6*)]. This strategy was sensitive, which allowed de novo identification of start codons for most known ORFs (fig. S12A) and specific, strongly enriching for ORFs initiating at AUG (fig. S13).

Novel ORFs were found on noncanonical mRNAs, including transcripts antisense to known ORFs, alternate transcripts at canonical loci, and transcripts in regions thought to be intergenic (Fig. 4, B and C, and figs. S12A, S14, and S15A). We also identified instances of genome misannotation (e.g., fig. S15B). Many newly annotated ORFs were on stable transcripts, similar to those predicted as noncoding in a meiotic tiling array study [(*28*), fig. S14]. Our empirical strategy found translation of short ORFs (sORFs) (fig. S12A) that were well-expressed (fig. S12, B and C) and highly regulated (fig. S16) but below the cutoff of 80 to 100 amino acids used historically to computationally identify yeast ORFs.

Recent studies have identified cellular functions for short peptides (*29*, *30*), although the function of these meiotic sORFs remains an open question. Minimally, our data suggest the export of many novel transcripts into the cytoplasm, allowing translation by ribosomes. Conversely, this data set facilitates identification of transcripts that act at the RNA level. For example, most antisense transcripts are poorly translated, including *RME2* and *RME3* (antisense to *IME4* and *ZIP2*, respectively), which are known to act through direct cis-transcriptional interference of their sense counterpart [figs. S12C and S17, A, B, and D; (*31*, *32*)]. By contrast, a transcript antisense to *YFL012W* that shows no transcriptional interference activity contained prominent regions of translation [(*31*), fig. S17, C and D].

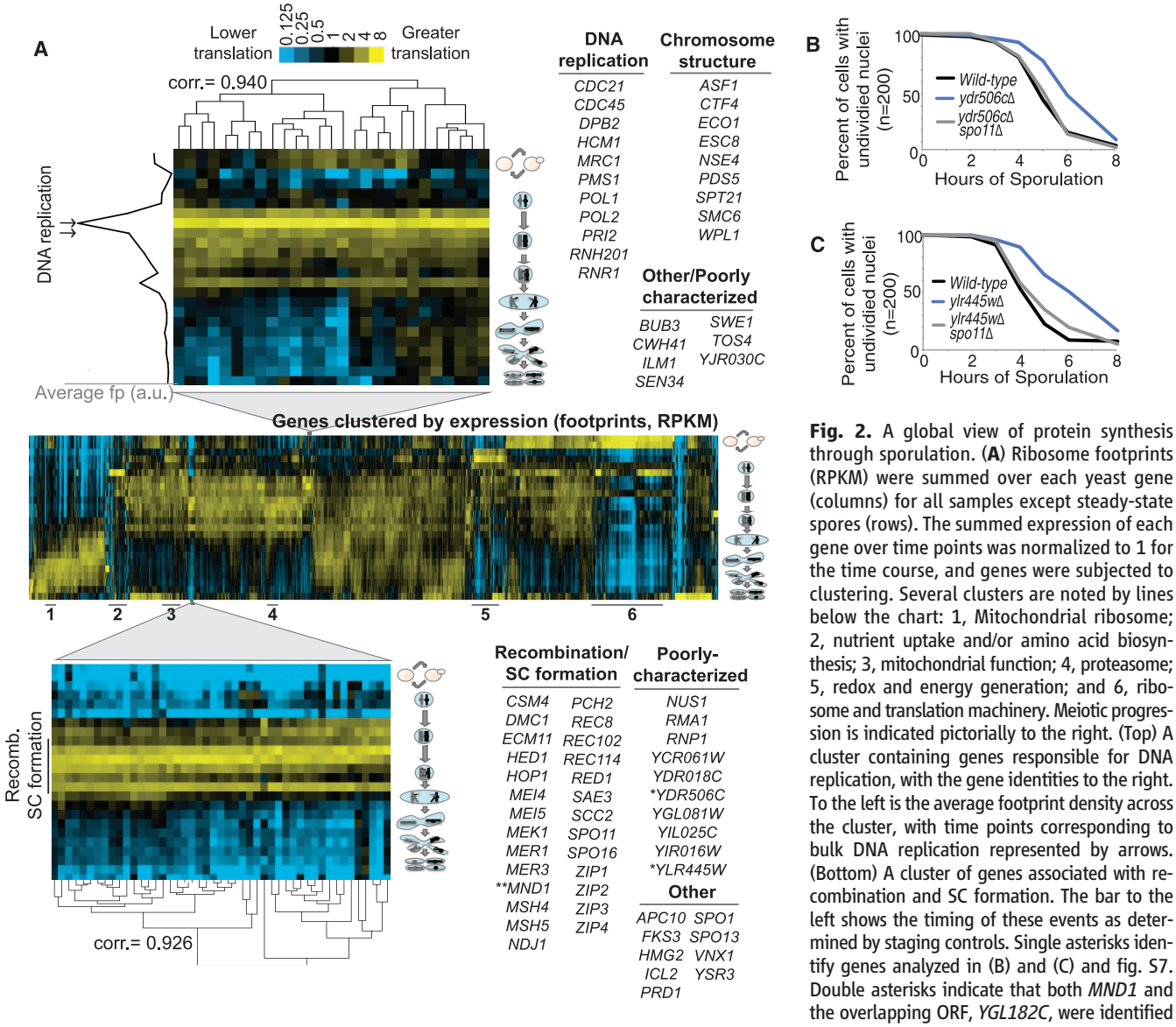


Fig. 2. A global view of protein synthesis through sporulation. (**A**) Ribosome footprints (RPKM) were summed over each yeast gene (columns) for all samples except steady-state spores (rows). The summed expression of each gene over time points was normalized to 1 for the time course, and genes were subjected to clustering. Several clusters are noted by lines below the chart: 1, Mitochondrial ribosome; 2, nutrient uptake and/or amino acid biosynthesis; 3, mitochondrial function; 4, proteasome; 5, redox and energy generation; and 6, ribosome and translation machinery. Meiotic progression is indicated pictorially to the right. (Top) A cluster containing genes responsible for DNA replication, with the gene identities to the right. To the left is the average footprint density across the cluster, with time points corresponding to bulk DNA replication represented by arrows. (Bottom) A cluster of genes associated with recombination and SC formation. The bar to the left shows the timing of these events as determined by staging controls. Single asterisks identify genes analyzed in (B) and (C) and fig. S7. Double asterisks indicate that both *MND1* and the overlapping ORF, *YGL182C*, were identified in this cluster. (**B**) Wild-type, *ydr506c*Δ, and *ydr506c*Δ*spo11*Δ cells were induced to sporulate. At indicated times, samples were scored for nuclear division. (**C**) Wild-type, *ylr445w*Δ, and *ylr445w*Δ *spo11*Δ cells were induced to sporulate and were treated as in (B).

Downloaded from www.sciencemag.org on February 2, 2012

uORFs in meiosis. The second major source of novel meiotic ribosome density was leader sequences [commonly called 5′ untranslated regions (5′UTRs)], situated upstream of canonical ORFs (Fig. 4D and fig. S18A). We saw no general meiotic increase in footprints in 3′UTRs, which argues against a non-specific increase in translational background noise. Examination of individual gene leaders revealed short footprint spans that started at either AUGs or near-cognate codons and generally spanned the region until the next stop codon (Fig. 4D and fig. S18A). Nearly 300 of such upstream ORFs (uORFs) have been identified in yeast under starvation conditions [(*6*), reviewed in (*33*)], but we found them to be far more common in meiosis.

We annotated 10,226 meiotic uORFs, present in the leaders of 3026 genes (fig. S11). These uORFs contained a density of ribosome footprints far greater than the ribosome footprint density in non-uORF leader regions, which suggested that our annotation approach was thorough and specific (fig. S19, A and B). Ribosome occupancy at uORFs was higher in meiotic than vegetative cells (Fig. 4D and figs. S18A and S19, B and C), and most of this effect derives from the meiotic program itself rather than the starvation conditions that accompany sporulation (fig. S19D). As expected, AUG, when present, was efficiently used for uORF translation initiation. The near-cognate codons that showed most efficient initiation, UUG and CUG (fig. S18, B and C), have also been shown to be most efficient in mammalian cells and in vitro (*5*, *34*).

uORFs have been implicated in translational regulation, although no universal functional role has emerged. uORFs that have been well-characterized through reporter studies show diverse effects: enhancing, decreasing, or having little impact on downstream ORF translation [reviewed in (*33*)]. Three features of our study ideally positioned us to evaluate the role of uORFs in translation. First, we annotated many uORFs, which allowed us to distill general principles. Second, we collected data for each time point on mRNA abundance and rates of translation, which provided instantaneous quantification of TE for each downstream ORF, whereas traditional approaches require TE inference by steady-state protein abundance. Finally, our analysis of numerous sequential points through a dynamic process permitted us to detect temporal trends. Comparison of ribosome occupancy of leaders and TE of their corresponding downstream ORFs over 10 time points (see fig. S4) typically revealed a strong positive correlation (Fig. 4, E and F). However, a subset of leaders containing at least one AUG uORF showed a negative correlation, which suggested competition between uORF and ORF translation in these cases (Fig. 4F and fig. S20; see Fig. 5E below).

Leader extensions and competitive uORFs. For some messages, we found that enriched footprint occupancy of leaders was caused by a programmed change in the transcript length during meiosis. Systematic analysis identified 192 genes with regulated leader length (Fig. 5, A to C; fig. S21; and table S5). For example, *ORC1* showed an extended leader after prophase. This extension revealed a number of well-translated uORFs (Fig. 5B) and was accompanied by a concurrent decrease in translation of the *ORC1* coding region (Figs. 3E and 5, B and D). Of genes with regulated leaders, a prominent subset showed a similar negative correlation, often corresponding well with known gene function. Orc1 and Ndj1, for example, have no characterized function late in meiosis (*24*, *35*), and *RED1*, a key meiotic prophase factor (*36*), is translationally repressed exclusively in vegetative cells (Fig. 5D).

For genes with leader extensions containing one or more AUG uORF, at least half showed a strong negative correlation between the ribosome occupancy of the leader and TE of the ORF (Fig. 5E). By contrast, for leaders containing uORFs starting only with near-cognate, non-AUG codons, this correlation was strongly positive (Fig. 5E). Regulated leaders have been observed in budding yeast and mammalian cells, with longer forms often associated with poor ORF translation (*37*, *38*). Here, we have observed a far broader and more nuanced role for leader extensions in providing temporal translational control to many meiotic genes.

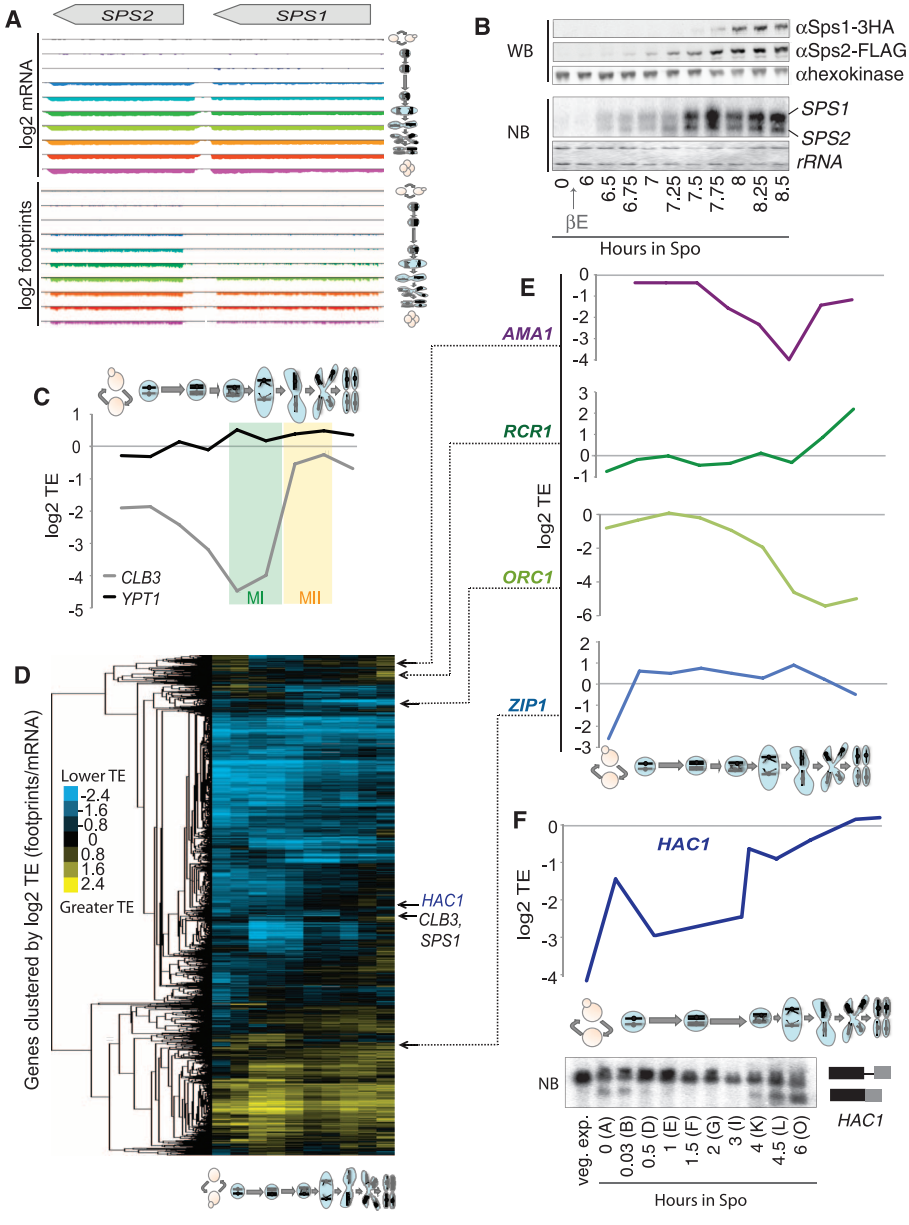


Fig. 3. Widespread dynamic translational control in meiosis. (**A**) Log_2 mRNA and footprints (RPKM) for a region containing *SPS1* and *SPS2* over pooled time points (fig. S4). (**B**) *SPS1-3HA* and *SPS2-FLAG* cells carrying an estrogen-inducible *NDT80* allele were induced to sporulate. At 6 hours, β-estradiol was added. Samples from indicated times were subjected to Western blotting (WB) and Northern blotting (NB). (**C**) Log_2 TE values for *CLB3* and *YPT1* for pooled time points (fig. S4). MI and MII are indicated by colored shading as boxes. (**D**) Cluster analysis of log_2 TE through meiosis for pooled categories (fig. S4) for all genes. (**E**) Log_2 TEs are plotted as in (C) for *AMA1*, *RCR1*, *ORC1*, and *ZIP1*. (**F**) Log_2 TEs are plotted as in (C) for *HAC1*. Below, total RNA from the original time course (see fig. S1) was subjected to Northern blotting for *HAC1*.

Downloaded from www.sciencemag.org on February 2, 2012

More generally, our analyses point to disparate roles for AUG and near-cognate uORFs (Figs. 4F and 5E). A fraction of AUG uORFs appear to competitively down-modulate ORF expression. By contrast, near-cognate uORFs are more common and show a generally strong positive correlation with expression of their downstream ORF, which may allow cells to divert limited resources to an important subset of messages. Whether uORFs directly prime translation of their downstream ORF is unclear. Nonetheless, genes with the strongest positive correlation between leader ribosome occupancy and ORF TE are highly enriched for known function in sporulation (table S6), which suggests physiological relevance of this regulation. The broad monitoring of gene expression by genomics has underscored the importance of quantitative modulation, beyond a model of binary on-off control. MicroRNAs provide a prominent example of developmental control through subtle regulation of broad sets of genes. uORFs may similarly allow condition-specific tuning of protein synthesis for a large portion of the genome.

The preponderance of uORFs suggests a shift of the translation initiation mechanism in meiotic cells from the predominant mechanism in which initiation factors recognize the mRNA cap and the initiation complex scans the message for the first AUG to commence translation [reviewed in (*23*)]. A link between alternative translation initiation mechanisms and the use of uORFs is suggested by analysis of messages that were shown to support cap-independent translation in nitrogen-starved yeast cells (*YMR181C*, *GPR1*, *BOI1*, *FLO8*, *NCE102*, *MSN1*, and *GIC1*) (*39*). We found that all had leaders with well-translated near-cognate uORFs and a strong positive correlation between leader ribosome occupancy and ORF translation (Fig. 4F; fig. S22, excluding *BOI1* as it has a complicating leader extension; table S5).

Perspective. We find that even in the extensively studied yeast, *S. cerevisiae*, genome coding has a complexity not captured by existing annotations. Ribosome profiling also captured a layer of regulation that is invisible to mRNA measurements alone and which revealed extensive and dynamic translational regulation of canonical ORFs. Transcription studies have enabled the identification of cis- and trans-transcriptional elements that control diverse cellular processes, whereas a similarly broad understanding of the importance and mechanisms of translational control remains elusive. This data set provides a valuable foundation for identifying such cis- and trans-translational regulators.

This study also gives a holistic view of the metabolic and cellular reorganization seen through the yeast meiotic program that extends beyond a traditional chromosome-centric picture. Previous studies suggested that meiotic transcriptional control was limited to a few discrete waves (*3*, *40*). Our data reveal multifaceted control of protein production, enabled by the tightly timed induction of many translational and transcriptional programs, including those driving translation factors, the proteasome, and the UPR. Indeed, the view of such responses as environmentally controlled stress pathways may reflect the historical context of their discovery rather than their sole physiological role.

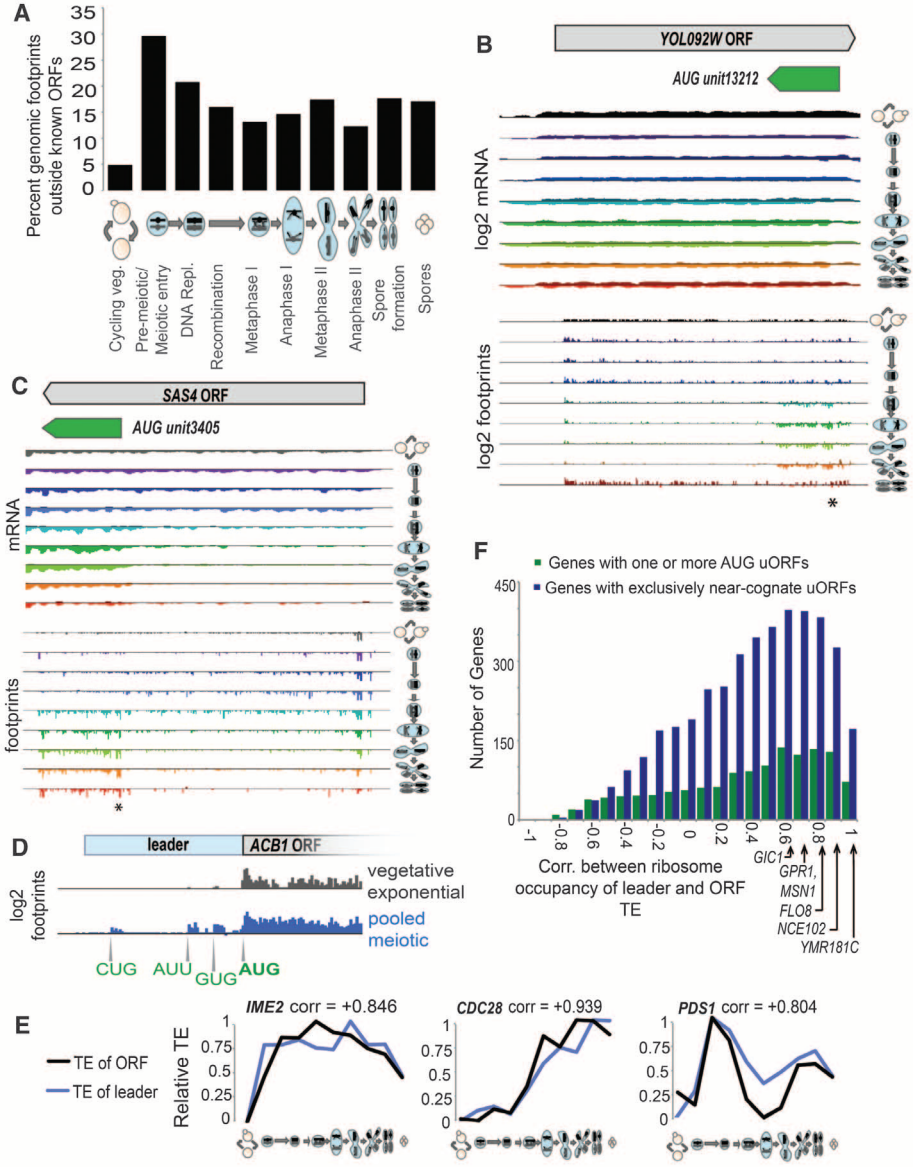


Fig. 4. Noncanonical translation is pervasive in meiotic cells. (**A**) Footprints from pooled time points (see fig. S4) were mapped. The percentage of these footprints outside of known ORF annotations is plotted. (**B**) mRNA and ribosome occupancy profiles around *YOL092W*, with sense above the line for each time point and antisense below. Single asterisk denotes the sORF start site. The "AUG unit" (sORF) was annotated by the strategy shown in fig. S11. (**C**) The region around *SAS4* is displayed as in (B), with truncated ORF start denoted by a single asterisk. (**D**) Ribosome occupancy profile for vegetative cells in exponential growth phase and meiotic cells over the leader of *ACB1*. (**E**) For pooled time points (see fig. S4), TEs are plotted for ORFs and for leaders (see SOM for a discussion of leader TE determination) for *IME2*, *CDC28*, and *PDS1*. Values are normalized to the same range for both plots. (**F**) Correlation coefficients [determined from plots as in (E)] were determined for each gene with uORFs for leaders with only near-cognate uORFs and at least one AUG uORF. The positions of six genes that support cap-independent translation (*39*) are noted.

References and Notes

1. D. Zickler, N. Kleckner, *Annu. Rev. Genet.* **33**, 603 (1999).
2. A. L. Marston, A. Amon, *Nat. Rev. Mol. Cell Biol.* **5**, 983 (2004).
3. S. Chu *et al.*, *Science* **282**, 699 (1998).
4. T. M. Carlile, A. Amon, *Cell* **133**, 280 (2008).
5. N. T. Ingolia *et al.*, *Cell* **147**, 789 (2011).
6. N. T. Ingolia *et al.*, *Science* **324**, 218 (2009).
7. K. R. Benjamin, C. Zhang, K. M. Shokat, I. Herskowitz, *Genes Dev.* **17**, 1524 (2003).
8. P. T. Spellman *et al.*, *Mol. Biol. Cell* **9**, 3273 (1998).
9. A. Lynn *et al.*, *Chromosome Res.* **15**, 591 (2007).
10. S. Keeney, M. J. Neale, *Biochem. Soc. Trans.* **34**, 523 (2006).
11. S. L. Page, R. S. Hawley, *Annu. Rev. Cell Dev. Biol.* **20**, 525 (2004).
12. J. S. Cox, P. Walter, *Cell* **87**, 391 (1996).
13. K. Mori *et al.*, *Genes Cells* **1**, 803 (1996).

Note added in proof: YDR506C and *YLR445W* are now named *GMC1* and *GMC2*, respectively.

Downloaded from www.sciencemag.org on February 2, 2012

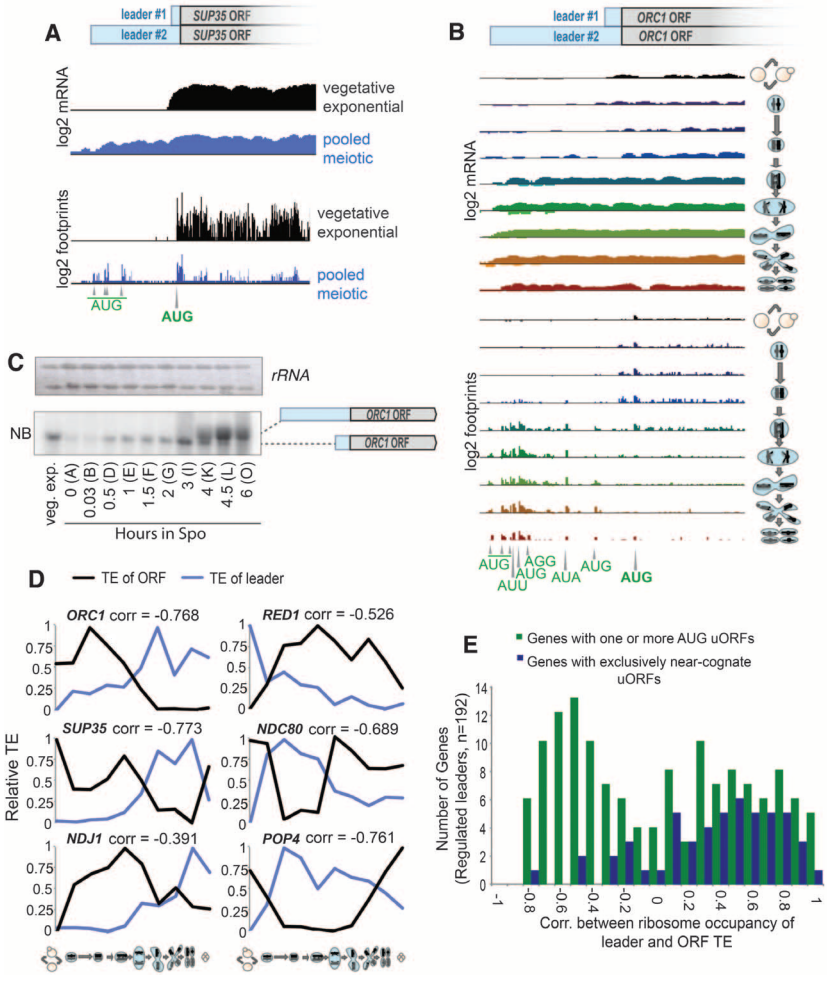


Fig. 5. Regulated transcript extensions expose novel regulatory uORFs. (**A**) mRNA and ribosome occupancy profiles around *SUP35*. (**B**) *ORC1* region displayed as in Fig. 4B. (**C**) Total RNA from the original time course (see fig. S1) was subjected to Northern blotting (NB) for *ORC1*. (**D**) Analysis as in Fig. 4E for *ORC1*, *SUP35*, *NDJ1*, *RED1*, *NDC80*, and *POP4*. (**E**) Analysis as in Fig. 4F for genes with regulated leader extension (table S5).

14. I. Piekarska *et al.*, *Eur. J. Cell Biol.* **89**, 780 (2010).
15. Z. Xie, D. J. Klionsky, *Nat. Cell Biol.* **9**, 1102 (2007).
16. T. Kanki *et al.*, *Dev. Cell* **17**, 98 (2009).
17. K. Okamoto *et al.*, *Dev. Cell* **17**, 87 (2009).
18. A. Jambhekar, A. Amon, *Curr. Biol.* **18**, 969 (2008).
19. S. Chu, I. Herskowitz, *Mol. Cell* **1**, 685 (1998).
20. A. M. Neiman, *J. Cell Biol.* **140**, 29 (1998).
21. H. Tachikawa *et al.*, *J. Cell Biol.* **155**, 797 (2001).
22. H. Friesen *et al.*, *Genes Dev.* **8**, 2162 (1994).
23. N. Sonenberg, A. G. Hinnebusch, *Cell* **136**, 731 (2009).
24. S. P. Bell *et al.*, *Science* **262**, 1844 (1993).
25. M. Sym *et al.*, *Cell* **72**, 365 (1993).
26. K. Imai *et al.*, *J. Biol. Chem.* **280**, 8275 (2005).
27. C. Sidrauski, J. S. Cox, P. Walter, *Cell* **87**, 405 (1996).
28. A. Lardenois *et al.*, *Proc. Natl. Acad. Sci. U.S.A.* **108**, 1058 (2011).
29. T. Kondo *et al.*, *Science* **329**, 336 (2010).
30. Y. Xu, D. Ganem, *J. Virol.* **84**, 5465 (2010).
31. B. Gelfand *et al.*, *Mol. Cell. Biol.* **31**, 1701 (2011).
32. C. F. Hongay *et al.*, *Cell* **127**, 735 (2006).
33. H. M. Hood *et al.*, *Annu. Rev. Microbiol.* **63**, 385 (2009).
34. S. E. Kolitz, J. E. Takacs, J. R. Lorsch, *RNA* **15**, 138 (2009).
35. H. Y. Wu, S. M. Burgess, *Curr. Biol.* **16**, 2473 (2006).
36. B. Rockmill, G. S. Roeder, *Proc. Natl. Acad. Sci. U.S.A.* **85**, 6057 (1988).
37. J. Badhai *et al.*, *PLoS ONE* **6**, e17672 (2011).
38. G. L. Law *et al.*, *Genome Biol.* **6**, R111 (2005).
39. W. V. Gilbert *et al.*, *Science* **317**, 1224 (2007).
40. A. P. Mitchell, *Microbiol. Rev.* **58**, 56 (1994).

Acknowledgments: We thank E. Ünal, A. Amon, and members of the Weissman laboratory for critical reading of this manuscript; C. Chu for sequencing assistance; J. Dunn for protocol development assistance; F. Van Werven for the MATa/a strain; and F. Klein for the the Zip1 antibody. G.A.B. is supported by American Cancer Society Postdoctoral Fellowship 117945-PF-09-136-01-RMC. M.Y. is supported by a Clore Fellowship. This work was supported by a grant from the U.S.-Israel Binational Science Foundation (N.F. and A.R.), an NIH P01 award (AG10770; N.T.I.), a Ruth L. Kirschstein National Research Service Award (GM080853; N.T.I.), and Howard Hughes Medical Institute funding (J.S.W. and A.R.). A patent on the ribosome profiling approach has been assigned to the University of California. Supporting files are in the SOM and at www.ncbi.nlm.nih.gov/geo/ with series accession no. GSE34082.

Supporting Online Material

www.sciencemag.org/cgi/content/full/science.1215110/DC1
Materials and Methods
Figs. S1 to S22
Tables S1 to S7
References (*41*–*57*)
Files S1 and S2

11 October 2011; accepted 13 December 2011
Published online 22 December 2011;
10.1126/science.1215110

Downloaded from www.sciencemag.org on February 2, 2012

The Southern Ocean's Role in Carbon Exchange During the Last Deglaciation

Andrea Burke[1,2]* and Laura F. Robinson[2,3]

Changes in the upwelling and degassing of carbon from the Southern Ocean form one of the leading hypotheses for the cause of glacial-interglacial changes in atmospheric carbon dioxide. We present a 25,000-year-long Southern Ocean radiocarbon record reconstructed from deep-sea corals, which shows radiocarbon-depleted waters during the glacial period and through the early deglaciation. This depletion and associated deep stratification disappeared by ~14.6 ka (thousand years ago), consistent with the transfer of carbon from the deep ocean to the surface ocean and atmosphere via a Southern Ocean ventilation event. Given this evidence for carbon exchange in the Southern Ocean, we show that existing deep-ocean radiocarbon records from the glacial period are sufficiently depleted to explain the ~190 per mil drop in atmospheric radiocarbon between ~17 and 14.5 ka.

The transition between the Last Glacial Maximum [LGM; ~22 to 18 ka (thousand years ago)] and the warm climate of the Holocene was accompanied by an ~80 parts per million rise in atmospheric CO_2 (*1*) and a substantial reduction in the ratio of radiocarbon (^{14}C) to ^{12}C in the atmosphere (*2*). Of particular interest is the large and rapid drop in atmospheric radiocarbon during the first pulse of CO_2 rise at the last deglaciation (*3*). One hypothesis that has been proposed to explain the rise in atmospheric CO_2 and the concurrent fall in atmospheric radiocarbon content is the "isolated reservoir" hypothesis, which calls for ventilation of a carbon-rich, radiocarbon-depleted water mass that was isolated from the atmosphere during the glacial period (*4*). Increased

[1]Massachusetts Institute of Technology/Woods Hole Oceanographic Institution Joint Program in Oceanography, Mailstop 24, Woods Hole, MA 02543, USA. [2]Department of Marine Chemistry and Geochemistry, Woods Hole Oceanographic Institution, Mailstop 25, Woods Hole, MA 02543, USA. [3]School of Earth Sciences, University of Bristol, Wills Memorial Building, Queen's Road, Bristol BS8 1RJ, UK.

*To whom correspondence should be addressed. E-mail: aburke@whoi.edu

upwelling in the Southern Ocean has been suggested as a potential route for CO_2 outgassing to the atmosphere during the last deglaciation (*5*). In this study, we generate reconstructions of Southern Ocean radiocarbon to provide new insights into the storage and release of carbon from the deep ocean.

Radiocarbon is a useful tracer of carbon cycle processes because it is produced in the atmosphere and then is transferred to other carbon reservoirs, where it decays with a half-life of 5730 years. Isolation of deep-water masses allows time for decay of radiocarbon and sequestration of carbon. However, evidence for the presence and subsequent release of a carbon-rich and radiocarbon-depleted glacial water mass remains controversial due to the challenges associated with producing reliable radiocarbon records. Radiocarbon reconstructions require accurate measurement of the $^{14}C/^{12}C$ ratio and, crucially, accurate and precise determinations of absolute (calendar) age. Deep-ocean radiocarbon records have been made using benthic foraminifera (*6*), but dissolution of carbonate, low abundances of benthic foraminifera, and the susceptibility of low sedimentation rate cores to the mixing effects of bioturbation limit the availability of appropriate samples in deep water. Absolute-age models in sediment cores often rely on radiocarbon analyses of planktic foraminifera, which can be strongly influenced by large variations in surface reservoir ages (*7*, *8*). Additionally, variations in foraminiferal abundance or species composition through time can cause biases in benthic-planktic age offsets (*9*, *10*).

In spite of these difficulties, much effort has been made to identify an isolated carbon reservoir in the glacial ocean, but direct evidence remains elusive. Broecker (*3*) has argued that the similarity between planktic-benthic radiocarbon age offsets from today and the LGM from a suite of cores in the Pacific has limited the potential volume for an abyssal isolated reservoir, requiring it to be thin, deep, and extremely radiocarbon-depleted. Skinner *et al.* (*8*) recently suggested the presence of a 4000-year-old water mass in the deep South Atlantic (3770 m) during the LGM. Although an intriguing result, the spatial extent of this water mass is not well constrained, and the associated age model requires large changes in the surface reservoir age.

A series of recent papers showing evidence for extreme radiocarbon depletions at intermediate depths during periods of deglacial CO_2 rise (*11*–*13*) have also sparked interest in this isolated reservoir hypothesis. These papers invoke the transfer of old carbon from a deep isolated reservoir to intermediate depths via upwelling in the Southern Ocean and transport by Antarctic Intermediate Water (AAIW) to locations in the Northern Hemisphere.

Here we provide a glacial and deglacial time series of radiocarbon from deep-sea corals collected from sites in the Southern Ocean at depths corresponding to modern-day Upper Circumpolar Deep Water (UCDW) and AAIW. Uranium-thorium (U-Th) dating is used to provide an independent calendar age that does not depend on reservoir ages or stratigraphic correlation. The location of our samples in the Drake Passage allows us to examine direct links between the deep ocean and the atmosphere because it is a region of mixing and upwelling of major deep-water masses.

Sample description and results. Forty solitary deep-sea corals (37 *Desmophyllum dianthus*, two *Balanophyllia malouinensis*, and one *Flabellum curvatum*) were selected for this study from a suite of dredge-collected corals from Burdwood Bank and seamounts in the Drake Passage (Fig. 1) (*14*, *15*). Coral samples were screened to identify glacial and deglacial specimens by radiocarbon reconnaissance dating (*14*), and these samples were then U-Th dated. Precise radiocarbon measurements (*16*) were made on the corals with ages within the time period of 0 to 35 ka to calculate past $\Delta^{14}C$ values (*17*) of dissolved inorganic carbon (DIC) at depths bathed today by AAIW and UCDW (*18*). Here we refer to the radiocarbon records by the names of the water masses at those depths today, while recognizing that different water masses could have occupied those depths in the past.

The reconstructed $\Delta^{14}C$ values for corals at depths corresponding today to AAIW follow the atmospheric $\Delta^{14}C$ curve (*2*) at an offset [$\Delta\Delta^{14}C$, supporting online material (SOM)] ranging from –80 to –190‰ (Fig. 2), with modern corals reflecting the $\Delta^{14}C$ of ambient seawater DIC (*19*). The largest radiocarbon offsets in AAIW occurred at 13.3 ± 0.1 and 13.7 ± 0.1 ka during the Bølling-Allerød/Antarctic Cold Reversal (BA/ACR; ~14.6 to 12.8 ka).

The reconstructed $\Delta^{14}C$ values for corals from depths bathed today by UCDW follow atmospheric $\Delta^{14}C$ throughout the Holocene, with offsets from the contemporaneous atmosphere ranging from –110 to –155‰, consistent with nearby water column $\Delta^{14}C$ measurements (*19*). During the LGM, radiocarbon in UCDW was 230‰ depleted from the contemporaneous atmosphere, ~80‰ lower than values observed at these sites today. UCDW was even more depleted from the contemporaneous atmosphere before the LGM at 25.6 ± 0.3 ka during Heinrich Stadial 2 (HS2; ~27 to 24 ka), with an offset of –370‰, and also during Heinrich Stadial 1 (HS1; ~18 to 14.6 ka), with offsets of –250 to –300‰. A marked increase in UCDW $\Delta^{14}C$ occurred at the start of the BA/ACR, giving $\Delta\Delta^{14}C$ values of only –140‰. The offsets of UCDW $\Delta^{14}C$ from the contemporaneous atmosphere then remained relatively constant until the modern day, with the exception of slightly enriched radiocarbon values ($\Delta\Delta^{14}C$ = –87 to –105‰) immediately after the end of the Younger Dryas (YD; 12.8 to 11.5 ka) (Fig. 2).

Discussion. Large radiocarbon depletions in the glacial Southern Ocean could be caused by a reduction in air-sea gas exchange (*20*–*22*) [for instance, by an increase in sea-ice cover (*23*) at deep-water formation sites] or by increased stratification within the Southern Ocean (*24*). Additionally, global ocean changes in stratification (*25*) could contribute to lower $\Delta^{14}C$ values in the glacial deep ocean by reducing mixing between the abyssal ocean and better-ventilated water masses above. A reduction in the flux of well-ventilated (radiocarbon-enriched)

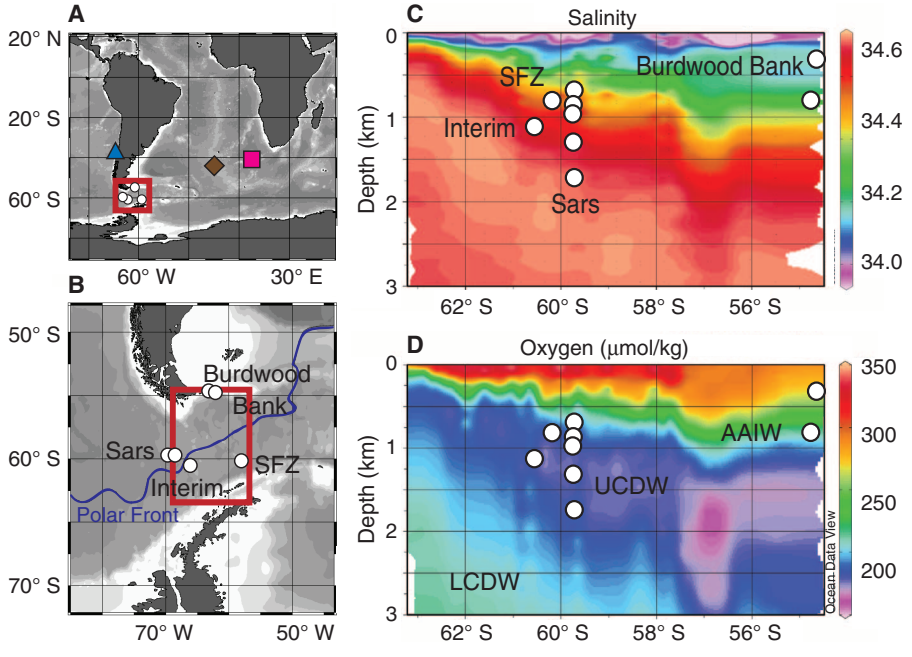


Fig. 1. (**A**) Locations of dredging sites (white circles) and sediment cores. Core SO161-SL22 [36.2°S, 73.7°W, 1000 m; (*28*)] is indicated by a blue triangle, core MD07-3076 CQ [44.1°S, 14.2°W, 3770 m; (*8*)] is indicated by a brown diamond, and core TN057-21 [41.1°S, 7.8°E, 4981 m; (*27*)] is indicated by a pink square. (**B**) Map of the dredging sites (white circles). The Polar Front is indicated by a blue line (*38*). SFZ, Shackleton Fracture Zone. Depth-latitude sections of salinity (**C**) and oxygen (**D**) from the GLODAP data set for the latitudinal transect indicated by the red box from (B) (*19*). Corals (white circles) come from depths bathed today by Antarctic Intermediate Water (AAIW) and Upper Circumpolar Deep Water (UCDW). LCDW, Lower Circumpolar Deep Water.

Downloaded from www.sciencemag.org on February 2, 2012

northern-source waters to the Southern Ocean could also lead to more depleted radiocarbon in UCDW. We explore the potential of these mechanisms to explain the features that we observe in the Southern Ocean radiocarbon records, with reference to additional published records from the global ocean.

Polar stratification has been suggested to play a fundamental role in lowering atmospheric CO_2 during glacial times by reducing the ventilation of CO_2 from the deep ocean (*26*). The depleted radiocarbon values that we detect in glacial UCDW are indeed consistent with reduced ocean ventilation during the last glacial period and imply that carbon at these depths was more isolated from the atmosphere than it is today. To examine the extent of this isolation and depletion, we compare our Drake Passage data to two deep radiocarbon records from benthic foraminifera from the South Atlantic (Figs. 1 and 2) (*8*, *27*). The deeper record [4981 m in modern-day Antarctic Bottom Water (AABW) (*27*)] is broadly consistent with our UCDW data during the deglaciation, suggesting common influences on the radiocarbon values in the Southern Ocean regions of UCDW and AABW formation. The second record [3770 m in modern-day Lower Circumpolar Deep Water (LCDW) (*8*)] is quite different during the glacial, with $\Delta^{14}C$ values up to 500‰ lower than those in the atmosphere, or 290‰ lower than those in UCDW and AABW (Fig. 2). This 500‰ radiocarbon depletion from the atmosphere may have been caused by an increase in the proportion of recirculated deep water from the Pacific. Some of the offset between the two South Atlantic foraminiferal radiocarbon records may arise from the large differences in surface reservoir ages used for their respective age models (SOM). However, even allowing for changes to the sediment core age models, the records from UCDW, LCDW, and AABW suggest that there was a geochemical gradient between deep Southern Ocean water masses at the LGM, consistent with reduced vertical mixing across water-mass boundaries (*25*).

At the end of the glacial period and during HS1, the $\Delta^{14}C$ of UCDW, LCDW, and AABW became more similar, as the $\Delta^{14}C$ of UCDW and AABW decreased and that of LCDW increased (Fig. 2). These changes suggest increased deep mixing in the Southern Ocean and a breakdown of the deep vertical stratification that appears to characterize the LGM. This breakdown of stratification is consistent with evidence for increased nutrient upwelling from opal accumulation records (Fig. 3), hypothesized to result from a southern shift in the westerly winds (*5*). The timing of this event is concurrent with the initial deglacial rise in atmospheric CO_2 (Fig. 3) (*1*) and lends support to the idea that upwelling of deep carbon-rich waters to shallow depths in the Southern Ocean was a major cause of deglacial atmospheric CO_2 rise. The AAIW radiocarbon records from Burdwood Bank and off the coast of Chile (*28*) were more enriched than the other Southern Ocean water masses during HS1, indicating that there was a substantial influence of atmospheric and surface-ocean radiocarbon on AAIW $\Delta^{14}C$ and that AAIW was well ventilated over this time interval.

Before the LGM, at around the time of HS2 (25.6 ka), Drake Passage UCDW had a radiocarbon-depleted signature similar to that of the LCDW site ($\Delta\Delta^{14}C = -370$‰; Fig. 2). This similarity between $\Delta^{14}C$ in UCDW and LCDW during HS2 is also observed during HS1, suggesting a systematic link between Heinrich stadials and changes in circulation and carbon ventilation in the Southern Ocean (*29*).

By the start of the BA/ACR, the offset of UCDW $\Delta^{14}C$ from the atmosphere was similar to that observed through the Holocene (Fig. 2). This decrease in the magnitude of $\Delta\Delta^{14}C$ is caused by the combined effect of the large drop in atmospheric $\Delta^{14}C$ coupled with a rise in the $\Delta^{14}C$ of UCDW (Figs. 2 and 3). An increase in marine $\Delta^{14}C$ is also observed in records from the deep North Atlantic (*30*) and deep South Atlantic (*8*, *27*), suggesting widespread deep ventilation of these regions (Figs. 2 and 3). In contrast to the Atlantic, the $\Delta^{14}C$ in the deep North Pacific remains relatively constant (*6*). However, the drop in atmospheric $\Delta^{14}C$ causes these deep North Pacific waters to appear relatively less radiocarbon depleted from the contemporaneous atmosphere by the BA/ACR (Fig. 2). The increase in the $\Delta^{14}C$ (and decrease in the magnitude of $\Delta\Delta^{14}C$) of UCDW at the start of the BA/ACR is likely due to higher $\Delta^{14}C$ values in the deep waters that are upwelled in the Southern Ocean to form UCDW (*8*). This change may be caused by a deepening of North Atlantic Deep Water supplying a greater flux of well-ventilated (radiocarbon-enriched) waters to the deep Atlantic and Southern Oceans (*27*).

In contrast, the $\Delta\Delta^{14}C$ of AAIW is more depleted during the BA/ACR, with values similar to those in UCDW (Figs. 2 and 3). This decrease in the radiocarbon offset between AAIW and UCDW indicates a reduced influence of surface waters and the atmosphere on AAIW $\Delta^{14}C$ relative to the deep ocean. This change may be achieved by increased stratification between surface and intermediate waters. Increased surface stratification is also supported by lower opal accumulation fluxes south of the Polar Front, which are interpreted as a reduction in the supply of nutrients to the surface at this time (Fig. 3) (5). An increase in Southern Ocean surface stratification could be associated with an increase in sea-ice cover (*23*) and may contribute to the deglacial pause in atmospheric CO_2 rise. AAIW then returns to a more ventilated state during the YD, further supporting the link between enhanced exchange between the upper Southern Ocean and the atmosphere during periods of atmospheric CO_2 rise (Fig. 3).

Lack of extreme ^{14}C depletion in Antarctic Intermediate Water. Our Southern Ocean AAIW data follow the atmospheric radiocarbon record at relatively constant offsets, with absolute values similar to those of the sediment core record from the Chile Margin (Figs. 1 and 2) (*28*). Additionally, there is no evidence for large (>300‰) radiocarbon depletions in any of the deep South Atlantic (*8*, *27*) or Southern Ocean water masses after 14.6 ka. These results are in apparent contradiction with several studies that have invoked an extremely radiocarbon-depleted AAIW to explain the observations at intermediate depths in the North Pacific, South Atlantic, Arabian Sea, and high-latitude North Atlantic (*11*–*13*, *31*). Our new data from the Atlantic sector of

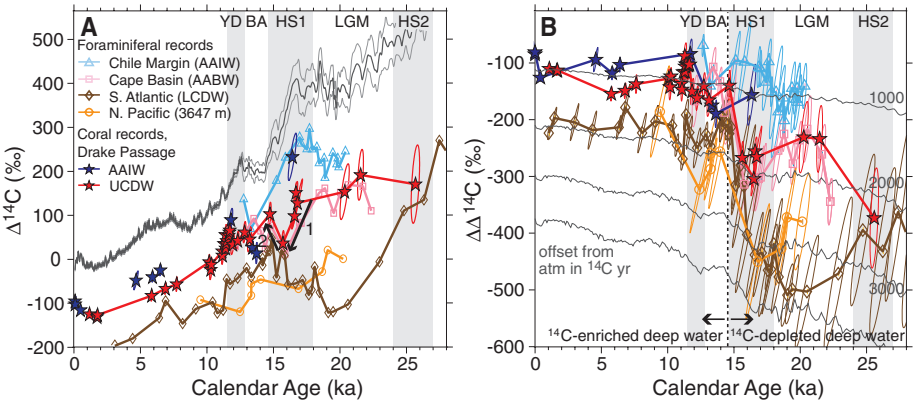


Fig. 2. (**A**) $\Delta^{14}C$ reconstructed from Drake Passage deep-sea corals bathed today by AAIW (dark blue stars) and UCDW (red stars). Uncertainties are represented by 2σ error ellipses. Two previously dated corals from Sars Seamount (*39*, *40*) with ages of ~16.5 and 16.6 ka are included in the UCDW group. Also shown are reconstructed $\Delta^{14}C$ records from benthic foraminifera from cores in the South Atlantic (brown diamonds) (8), North Pacific (gold circles) (*6*), Cape Basin (pink squares) (*27*), and Chilean margin (light blue triangles) (*28*). Atmospheric radiocarbon (IntCal09) (*2*) is shown by the gray lines (±2σ). Arrow 1 marks the drop in UCDW radiocarbon over the HS1/Mystery Interval that parallels the drop in the atmospheric record. Arrow 2 marks the increase in UCDW radiocarbon after the HS1/Mystery Interval. (**B**) Offset of reconstructed deep-sea coral $\Delta^{14}C$ from contemporaneous atmosphere ($\Delta\Delta^{14}C$) for AAIW (dark blue stars) and UCDW (red stars) corals (this study) (*39*, *40*). Also included are the offsets of the reconstructed benthic foraminiferal $\Delta^{14}C$ from the same records as shown in (A). All ellipses are 2σ. Contours of constant radiocarbon age offset from the contemporaneous atmosphere are shown as gray lines to illustrate the effect of the changing atmospheric radiocarbon inventory on $\Delta\Delta^{14}C$ values (SOM). Dashed line at 14.6 ka divides the plot between the relatively radiocarbon-depleted waters of the glacial period and the relatively radiocarbon-enriched waters post–Mystery Interval.

Downloaded from www.sciencemag.org on February 2, 2012

the Southern Ocean make an extremely radiocarbon-depleted AAIW increasingly unlikely. Although our UCDW data do support a Southern Ocean mechanism for the release of carbon during the deglaciation, the radiocarbon-depleted signature does not appear to be transported to the Northern Hemisphere by AAIW. Recent modeling work (*32*) suggests that propagating the signature of an extremely radiocarbon-depleted water mass to the North Pacific via AAIW is improbable, because the signal would be rapidly dissipated and diluted by the carbon in the rest of the ocean and the atmosphere. Thus, it appears that although there is a widespread distribution of extreme radiocarbon depletions at intermediate depths, they are unlikely to be caused by a common radiocarbon-depleted water mass that was transported over large distances.

The Mystery Interval. One of the more intriguing features of the atmospheric radiocarbon record is the ~190‰ drop in radiocarbon beginning at ~17 ka and ending at the beginning of the BA/ACR at ~14.5 ka (*2*). Production records from paleomagnetic and ^{10}Be reconstructions can explain, at maximum, 40‰ of this drop (*33*–*35*). Broecker and Barker (*4*) have suggested that this drop in atmospheric Δ^{14}C requires a very large, or extremely depleted, oceanic radiocarbon reservoir. In the absence of evidence for such a widespread, old radiocarbon reservoir, this event remains unexplained (the "Mystery Interval") (*36*). However, because the atmospheric carbon reservoir is so small compared to that of the ocean, we suggest that a direct outgassing of CO_2 from the ocean to the atmosphere would not require an extremely depleted radiocarbon reservoir to force the atmospheric Δ^{14}C drop, allowing it to be explained with available marine radiocarbon records (fig. S5). We use existing records to constrain the deep-water Δ^{14}C values, and we use Southern Ocean radiocarbon records as evidence for the direct transfer of old carbon to the atmosphere during this time period. During the interval between 16.6 and 15.6 ka, the radiocarbon in the atmosphere decreased at a rate similar to the rate of change in the UCDW Δ^{14}C record, whereas the radiocarbon content of the deep South Atlantic (LCDW) (8) increased (Fig. 2). This convergence of the UCDW and LCDW radiocarbon records is consistent with the ventilation of the deep ocean via the Southern Ocean.

If we assume that the glacial ocean deeper than 2500 m has a $\Delta\Delta^{14}$C of at least –300‰ (~2000 radiocarbon years offset from atmosphere) as observed in the western equatorial Pacific (*37*), or that the glacial ocean deeper than 3700 m has a $\Delta\Delta^{14}$C of at least –430‰ (~3000 radiocarbon years offset from atmosphere) as observed in the deep South Atlantic (*8*) and deep North Pacific (*6*), then only 3% of the carbon from those depths is needed to outgas directly to the atmosphere to decrease atmospheric Δ^{14}C by 190‰. The process of driving down atmospheric Δ^{14}C through outgassing of old carbon in the Southern Ocean would result in an ocean that would be apparently "younger" or less radiocarbon-depleted from the coeval atmosphere than before the Mystery Interval, as the data suggest (Fig. 2). In this case, "old" carbon would be added directly to the atmosphere rather than mixing through the entire ocean, forcing atmospheric Δ^{14}C to fall faster than the Δ^{14}C of most of the ocean.

A major caveat to this calculation is that it is not a transient experiment; hence, we have not taken into account the time scales over which the carbon could be released and subsequently taken up by the ocean. Nonetheless, it provides a possible explanation for the drop in atmospheric radiocarbon over the Mystery Interval that is consistent with available radiocarbon data from the intermediate and deep oceans. This calculation does not require the deep ocean to be as radiocarbon-depleted (old) as a previous calculation done by Broecker and Barker (*4*), which required the ocean deeper than 2500 m to have a radiocarbon age offset of ~6000 years, or the ocean deeper than 3700 m to have a radiocarbon age offset of ~14,000 years. The reason for this large difference is that Broecker and Barker assume that the nonisolated ocean maintains a constant radiocarbon age offset from the atmosphere after the Mystery Interval. This requirement forces oceanic radiocarbon to drop by ~150‰, which is a result that is not supported by available marine radiocarbon data. Thus, the large radiocarbon age offsets required by the calculation of Broecker and Barker are likely an overestimate of the deep-ocean isolation required to explain the atmospheric drop over the Mystery Interval. Our radiocarbon results from UCDW support the idea of a radiocarbon-depleted glacial ocean that is ventilated directly through the Southern Ocean. By the end of the Mystery Interval and the onset of the BA/ACR, the ocean as a whole is better ventilated, and there is no evidence for the large radiocarbon depletions found in glacial times.

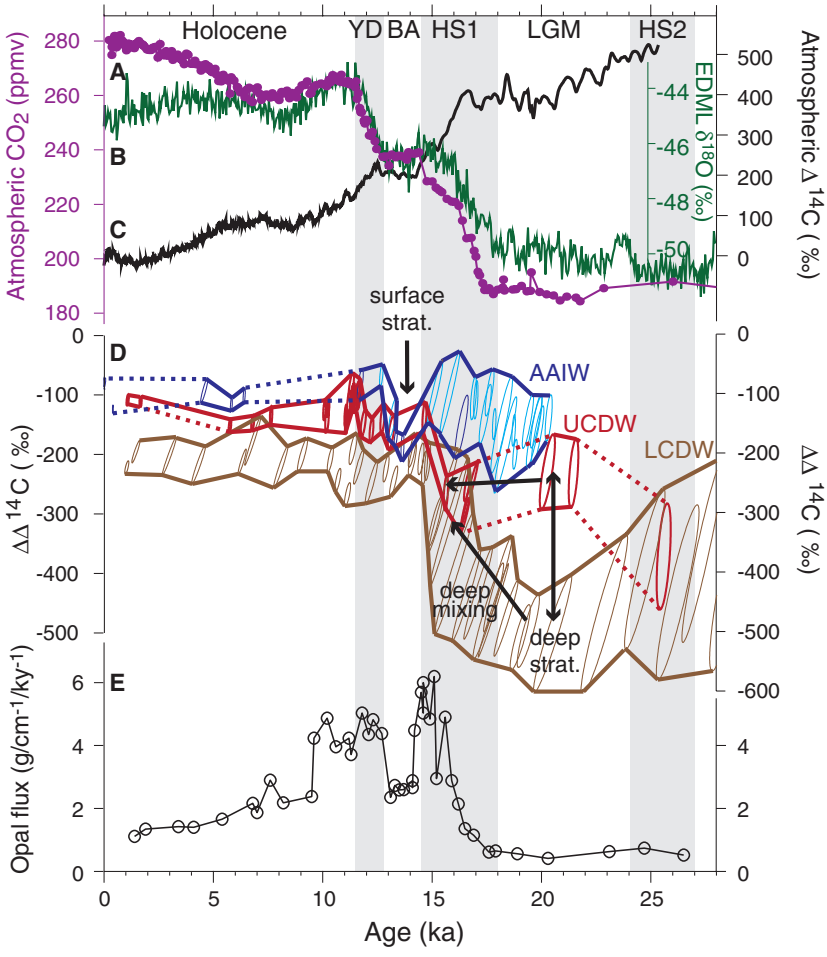


Fig. 3. (**A**) Atmospheric CO_2 (parts per million by volume) from EPICA Dome C (*1*) for data <22 ka on the time scale of Lemieux-Dudon *et al.* (*41*) and from Vostok ice core (*42*) for the data points >22 ka. (**B**) δ^{18}O record from the EDML ice core (*43*), also on the time scale of Lemieux-Dudon *et al.* (*41*). (**C**) Atmospheric Δ^{14}C (‰) from IntCal09 (*2*). (**D**) Offset (‰) of reconstructed Δ^{14}C from that in the contemporaneous atmosphere ($\Delta\Delta^{14}$C) for AAIW (blue), UCDW (red), and LCDW (brown). Error ellipses represent 2σ. (**E**) Opal flux (g cm^{-1} ky^{-1}) south of the Polar Front in the Indian Ocean sector of the Southern Ocean (core TN057-13-4PC; 53.2°S, 5.1°E) as a proxy for Southern Ocean nutrient upwelling (*5*).

References and Notes

1. E. Monnin *et al.*, *Science* **291**, 112 (2001).
2. P. J. Reimer *et al.*, *Radiocarbon* **51**, 1111 (2009).
3. W. Broecker, *Radiocarbon* **51**, 109 (2009).
4. W. S. Broecker, S. Barker, *Earth Planet. Sci. Lett.* **256**, 90 (2007).
5. R. F. Anderson *et al.*, *Science* **323**, 1443 (2009).
6. E. D. Galbraith *et al.*, *Nature* **449**, 890 (2007).

Downloaded from www.sciencemag.org on February 2, 2012

7. E. L. Sikes, C. R. Samson, T. P. Guilderson, W. R. Howard, *Nature* **405**, 555 (2000).
8. L. C. Skinner, S. Fallon, C. Waelbroeck, E. Michel, S. Barker, *Science* **328**, 1147 (2010).
9. A. L. Magana *et al.*, *Paleoceanography* **115**, PA4102 (2010).
10. T.-H. Peng, W. S. Broecker, *Nucl. Instrum. Methods Phys. Res. B* **5**, 346 (1984).
11. S. P. Bryan, T. M. Marchitto, S. J. Lehman, *Earth Planet. Sci. Lett.* **298**, 244 (2010).
12. T. M. Marchitto, S. J. Lehman, J. D. Ortiz, J. Flückiger, A. van Geen, *Science* **316**, 1456 (2007).
13. D. J. R. Thornalley, S. Barker, W. S. Broecker, H. Elderfield, I. N. McCave, *Science* **331**, 202 (2011).
14. A. Burke *et al.*, *Deep Sea Res. Part I Oceanogr. Res. Pap.* **57**, 1510 (2010).
15. R. G. Waller, K. M. Scanlon, L. F. Robinson, *PLoS ONE* **6**, e16153 (2011).
16. Materials and methods are available as supporting material on *Science* Online.
17. ^{14}C is a measure of the relative difference between the radiocarbon activity of an absolute international standard and that of a sample, after correction for both age and ^{13}C.
18. M. Stuiver, H. Polach, *Radiocarbon* **19**, 355 (1977).
19. R. M. Key *et al.*, *Global Biogeochem. Cycles* **18**, GB4031 (2004).
20. B. B. Stephens, R. F. Keeling, *Nature* **404**, 171 (2000).
21. M. Butzin, M. Prange, G. Lohmann, *Earth Planet. Sci. Lett.* **235**, 45 (2005).
22. A. Schmittner, *Earth Planet. Sci. Lett.* **213**, 53 (2003).
23. H. Fischer *et al.*, *Earth Planet. Sci. Lett.* **260**, 340 (2007).
24. R. Francois *et al.*, *Nature* **389**, 929 (1997).
25. D. C. Lund, J. F. Adkins, R. Ferrari, *Paleoceanography* **26**, PA1213 (2011).
26. D. M. Sigman, M. P. Hain, G. H. Haug, *Nature* **466**, 47 (2010).
27. S. Barker, G. Knorr, M. J. Vautravers, P. Diz, L. C. Skinner, *Nat. Geosci.* **3**, 567 (2010).
28. R. De Pol-Holz, L. Keigwin, J. Southon, D. Hebbeln, M. Mohtadi, *Nat. Geosci.* **3**, 192 (2010).
29. J. Ahn, E. J. Brook, *Science* **322**, 83 (2008).
30. L. C. Skinner, N. J. Shackleton, *Paleoceanography* **19**, PA2005 (2004).
31. A. Mangini *et al.*, *Earth Planet. Sci. Lett.* **293**, 269 (2010).
32. M. P. Hain, D. M. Sigman, G. H. Haug, *Geophys. Res. Lett.* **38**, L04604 (2011).
33. C. Laj *et al.*, *Earth Planet. Sci. Lett.* **200**, 177 (2002).
34. M. Frank *et al.*, *Earth Planet. Sci. Lett.* **149**, 121 (1997).
35. R. Muscheler *et al.*, *Earth Planet. Sci. Lett.* **219**, 325 (2004).
36. G. H. Denton, W. S. Broecker, R. B. Alley, *Pages News* **14**, 14 (2006).
37. W. Broecker *et al.*, *Paleoceanography* **22**, PA2206 (2007).
38. A. H. Orsi, T. Whitworth III, W. D. Nowlin Jr., *Deep Sea Res. Part I Oceanogr. Res. Pap.* **42**, 641 (1995).
39. S. J. Goldstein, D. W. Lea, S. Chakraborty, M. Kashgarian, M. T. Murrell, *Earth Planet. Sci. Lett.* **193**, 167 (2001).
40. L. F. Robinson, T. van de Flierdt, *Geology* **37**, 195 (2009).
41. B. Lemieux-Dudon *et al.*, *Quat. Sci. Rev.* **29**, 8 (2010).
42. J. R. Petit *et al.*, *Nature* **399**, 429 (1999).
43. C. Barbante *et al.*; EPICA Community Members, *Nature* **444**, 195 (2006).

Acknowledgments: This research was funded by NSF grants 0636787, 0944474, 0902957, 0338087, and 0819714. The data reported in this study are tabulated in the supporting online material. We acknowledge R. Waller and the science parties of cruises LMG06-05 and NBP08-05 for supplying samples used in this study. We also thank the crews of the R/V *Nathaniel B. Palmer* and R/V *Laurence M. Gould*, NOSAMS staff, the WHOI plasma facility, J. Blusztajn, M. Auro, and two anonymous reviewers for help with this project.

Supporting Online Material

www.sciencemag.org/cgi/content/full/science.1208163/DC1
Materials and Methods
Figs. S1 to S5
Tables S1 to S3
References (*44*–*56*)

10 May 2011; accepted 30 November 2011
Published online 15 December 2011;
10.1126/science.1208163

Spin-Down of Radio Millisecond Pulsars at Genesis

Thomas M. Tauris

Millisecond pulsars are old neutron stars that have been spun up to high rotational frequencies via accretion of mass from a binary companion star. An important issue for understanding the physics of the early spin evolution of millisecond pulsars is the impact of the expanding magnetosphere during the terminal stages of the mass-transfer process. Here, I report binary stellar evolution calculations that show that the braking torque acting on a neutron star, when the companion star decouples from its Roche lobe, is able to dissipate >50% of the rotational energy of the pulsar. This effect may explain the apparent difference in observed spin distributions between x-ray and radio millisecond pulsars and help account for the noticeable age discrepancy with their young white dwarf companions.

Millisecond pulsars (MSPs) are rapidly spinning, strongly magnetized neutron stars. They form as the result of stellar cannibalism, where matter and angular momentum flow from a donor star to an accreting neutron star (*1*, *2*). During this process the system is detectable as an x-ray source (*3*). In some cases, x-ray pulsations reveal a fast spinning neutron star (*4*); the 13 known accreting x-ray MSPs (AXMSPs) have an average spin period of $\langle P \rangle_{\rm AXMSP} = 3.3$ ms (*5*). These AXMSPs are thought to be the evolutionary progenitors of radio MSPs. When the donor star decouples from its Roche lobe (*6*) and the mass transfer generating the x-rays ceases, the radio emission is activated (*7*). Until now more than 200 recycled radio MSPs have been detected in our galaxy, both in the field and in globular clusters, with spin periods between 1.4 and 20 ms. These MSPs, which are observed after the Roche-lobe decoupling phase (RLDP), have $\langle P \rangle_{\rm MSP} = 5.5$ ms (*5*) [see (*8*) for a critical discussion on selection effects and statistics]. It is unknown whether this spin difference is caused by the role of the RLDP or subsequent spin-down from magnetodipole radiation during the lifetime of the radio MSPs.

The interplay between the magnetic field of a neutron star and the conducting plasma of the accreted material is known to provide the accretion torque necessary to spin up the pulsar (*9*–*11*). However, these interactions can also lead to a torque reversal under certain conditions (*12*), especially when the mass-transfer rate decreases (*13*). Similarly, detailed studies of low-mass x-ray binaries (LMXBs) using stellar evolution codes have demonstrated (*14*–*17*) that these systems undergo a long, stable phase of mass transfer, which provides sufficient mass to spin up the accreting neutron star to spin periods of milliseconds. However, these previous studies did not combine such numerical stellar evolution calculations with computations of the resulting accretion torque at work. Here, I compute this torque during the termination of the mass-transfer phase by integrating these two methods, using the time-dependent mass-transfer rate to follow its effect on the pulsar spin rate.

The computation of an LMXB donor star detaching from its Roche lobe is shown in Fig. 1 [see further details in (*8*)]. The full length of the mass-transfer phase was about 1 billion years (Gy); the RLDP happened in the past 200 million years (My) when the mass-transfer rate decreased rapidly. The original mass of the donor star was 1.0 $M_\odot$, and by the time it entered the final stage of the RLDP it had lost 99% of its envelope mass, encapsulating a core of 0.24 $M_\odot$ (i.e., the mass of the hot white dwarf being formed after the RLDP). The orbital period at this stage was 5.1 days, and the MSP had a mass of 1.53 $M_\odot$. By using the received mass-transfer rate, $\dot{M}(t)$, from my stellar models, the radius of the magnetospheric boundary of the pulsar, located at the inner edge of the accretion disk, can be written as $r_{\rm mag} = \varphi \cdot r_{\rm A}$ [with $r_{\rm A}$, the Alfvén radius (*18*), calculated (*8*) following standard prescriptions in the literature (*11*, *19*)]. Knowledge of the relative location of $r_{\rm mag}$, the corotation radius, $r_{\rm co}$, and the light cylinder radius, $r_{\rm lc}$, enabled a computation of the accretion torque acting on the pulsar (*8*) (fig. S1). After a long phase of mass transfer as an LMXB, the pulsar was spinning at its equilibrium period when entering the RLDP. The rapid torque reversals (unresolved in the center panel of Fig. 1; see also fig. S1) originated from successive, small episodes of spin-up or spin-down depending on the relative location of $r_{\rm co}$ and $r_{\rm mag}$, which reflects the small fluctuations in $\dot{M}(t)$. However, this equilibrium was broken when $\dot{M}(t)$ decreased substantially on a short time scale. That resulted in $r_{\rm mag}$ increasing on a time scale ($t_{\rm RLDP}$) faster than the spin-relaxation

Argelander-Institut für Astronomie, Universität Bonn, Auf dem Hügel 71, 53121 Bonn, Germany. Max-Planck-Institut für Radioastronomie, Auf dem Hügel 69, 53121 Bonn, Germany. E-mail: tauris@astro.uni-bonn.de

Downloaded from www.sciencemag.org on February 2, 2012

time scale, t_{torque}, on which the torque would transmit the effect of deceleration to the neutron star, and therefore $r_{mag} > r_{co}$. In this propeller phase (*12*), a centrifugal barrier arose and expelled material entering the magnetosphere, whereby a braking torque acted to slow down the spin rate of the pulsar even further (see bottom panel in Fig. 1 and fig. S2). The spin-relaxation time scale is given by $t_{torque} \simeq J/N$, which yields:

$$t_{torque} \simeq 50\ \mathrm{My} \cdot B_8^{-8/7} \left(\frac{\dot{M}}{0.1\dot{M}_{Edd}}\right)^{-3/7} \left(\frac{M}{1.4M_\odot}\right)^{17/7} \quad (1)$$

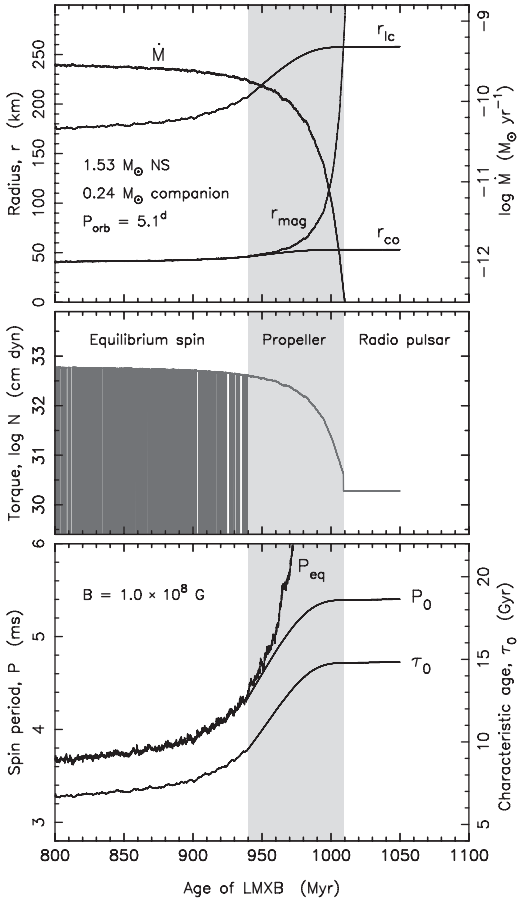


Fig. 1. Final stages of mass transfer in an LMXB. The gradual decoupling of the donor star from its Roche lobe causes the received mass-transfer rate, $\dot{M}$ (i.e., the ram pressure of the inflowing material), to decrease, whereby the magnetospheric boundary of the neutron star, r_{mag}, moves outward relative to the corotation radius, r_{co}, and the light cylinder radius, r_{lc} (**top**). The alternating spin-up/spin-down torques during the equilibrium spin phase are replaced by a continuous spin-down torque in the propeller phase ($r_{co} < r_{mag} < r_{lc}$), until the pulsar activates its radio emission and the magnetodipole radiation remains as the sole braking mechanism [**center**; see also (*8*) and figs. S1 and S2]. After an initial phase of spin-down, the spin equilibrium is broken, which limits the loss of rotational energy of the pulsar and sets the value of the spin period, P_0, of the radio MSP at birth (**bottom**). Also shown in the bottom panel is the resulting characteristic age, $\tau_0 \propto P_0^2$, of the recycled radio MSP, assuming a constant B field of 10^8 G during the RLDP. The gray shaded regions indicate the propeller phase.

where the spin angular momentum of the neutron star is $J = 2\pi I/P$ and the braking torque at the magnetospheric boundary is roughly given by $N \sim \dot{M}\sqrt{GMr_{mag}}$ (*8*). Here, G is the gravitational constant; M and I are the neutron star mass and moment of inertia, respectively; and B_8 is the surface magnetic flux density in units of 10^8 G. In addition to this torque, the magnetic field drag on the disk (*20*) was included in the model, although this effect is usually less dominant. In these calculations, I assumed that the strength of the neutron star B field has reached a constant, residual level before the propeller phase, a reasonable assumption given that less than 1% of the donor star envelope mass remained to be transferred. The propeller phase was terminated when $r_{mag} > r_{lc}$. At this point, the MSP activated its radio emission and turned on a plasma wind, which then inhibited any further accretion onto the neutron star (*13*, *21*). The duration of the RLDP in this example was $t_{RLDP} > 100$ My (including early stages before the propeller phase), which is a substantial fraction of the spin-relaxation time scale, $t_{torque} \approx 200$ My, calculated by using Eq. 1 at the onset of the propeller phase. For this reason, the RLDP has an important effect on the spin rate, P_0, and the characteristic age of the radio MSP at birth, τ_0. In the case reported here, the radio MSP was born (recycled) with $P_0 \approx 5.4$ ms and an initial so-called characteristic age $\tau_0 \equiv P_0/2\dot{P}_0 \approx 15$ Gy. The spin period before the RLDP was about 3.7 ms, implying that this MSP lost more than 50% of its rotational energy during the RLDP. If the pulsar had not broken its spin equilibrium during the RLDP, it would have been recycled with a slow spin period of $P_0 \approx 58$ ms and thus not become an MSP (*22*).

Radio pulsars emit magnetic dipole radiation as well as a plasma wind (*19*, *23*). These effects cause rotational energy to be lost, and hence radio MSPs

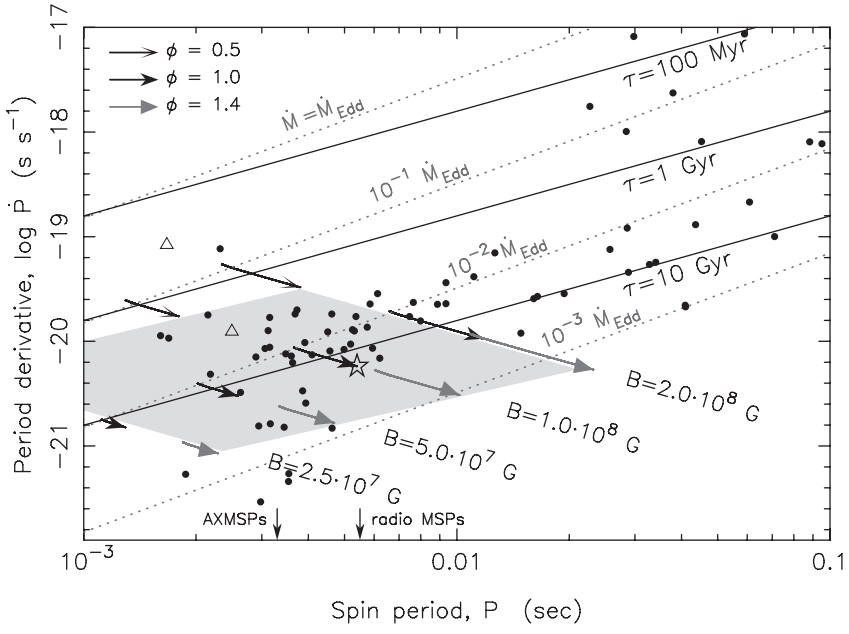


Fig. 2. Evolutionary tracks during the RLDP. Computed tracks are shown as arrows in the $P\dot{P}$ diagram, calculated by using different values of the neutron star B-field strength. The various types of arrows correspond to different values of the magnetospheric coupling parameter, φ. The gray-shaded area indicates all possible birth locations of recycled MSPs calculated from one donor star model. The solid lines represent characteristic ages, τ, and the dotted lines are spin-up lines calculated for a magnetic inclination angle, $\alpha = 90°$. The star indicates the radio MSP birth location for the case presented in Fig. 1. The two triangles indicate approximate locations (*36*) of the AXMSPs SWIFT J1756.9−2508 (upper) and SAX 1808.4−3658 (lower). Observed MSPs in the Galactic field are shown as dots [data taken from the *ATNF Pulsar Catalogue*, December 2011]. All the measured $\dot{P}$ values are corrected for the Shklovskii effect, a kinematic projection effect that affects the apparent value of $\dot{P}$ for pulsars (*37*). If the transverse velocity of a given pulsar was unknown, I used a value of 72 km s^{-1}, the median value of the 44 measured MSP velocities. The average spin periods of AXMSPs and radio MSPs are indicated with arrows at the bottom of the diagram (*8*).

Downloaded from www.sciencemag.org on February 2, 2012

will slow down their spin rates with time after the RLDP. However, they cannot explain the apparent difference in spin distributions between AXMSPs and radio MSPs, because radio MSPs, which have weak surface magnetic field strengths, could not spin down by the required amount even in a Hubble time. The true age of a pulsar (*23*) is given by $t = P/((n-1)\dot{P})[1-(P_0/P)^{n-1}]$. Assuming an evolution with a braking index $n = 3$ and $B = 1.0\times 10^8$ G, the time scale t is larger than 10 Gy, using $P_0 = \langle P\rangle_{\mathrm{AXMSP}} = 3.3$ ms and $P(t) = \langle P\rangle_{\mathrm{MSP}} = 5.5$ ms. To make things worse, one has to add the main-sequence lifetime of the LMXB donor star, which is typically 3 to 12 Gy, thereby reaching unrealistic large total ages. Although the statistics of AXMSPs still has its basis in small numbers and care must be taken for both detection biases (such as eclipsing effects of radio MSPs) and comparison between various subpopulations (*8*), it is evident from both observations and theoretical work that the RLDP effect presented here plays an important role for the spin distribution of MSPs.

The RLDP effect may also help explain a few other puzzles, for example, why characteristic (or spin-down) ages of radio MSPs often largely exceed cooling age determinations of their white dwarf companions (*24*). It has been suggested that standard cooling models of white dwarfs may not be correct (*25*–*27*), particularly for low-mass helium white dwarfs. These white dwarfs avoid hydrogen shell flashes at early stages and retain thick hydrogen envelopes, at the bottom of which residual hydrogen burning can continue for several billion years after their formation, keeping the white dwarfs relatively hot (~10^4 K) and thereby appearing much younger than they actually are. However, it is well known that the characteristic age is not a trustworthy measure of true age (*28*), and the RLDP effect exacerbates this discrepancy even further. In the model calculation presented in Fig. 1, it was assumed that $B = 1.0\times 10^8$ G and $\varphi = 1.0$. However, P_0 and τ_0 depend strongly on both B and φ. This is shown in Fig. 2, where I have calculated the RLDP effect for different choices of B and φ by using the same stellar donor model [i.e., same $\dot{M}(t)$ profile] as before. The use of other LMXB donor star masses, metallicities, and initial orbital periods would lead to other $\dot{M}(t)$ profiles (*16*, *17*) and hence different evolutionary tracks. The conclusion is that recycled MSPs can basically be born with any characteristic age. Thus, we are left with the cooling age of the white dwarf companion as the sole reliable, although still not accurate, measure as an age indicator.

A final puzzle is why no sub-millisecond pulsars have been found among the 216 radio MSPs detected in total so far. Although modern observational techniques are sensitive enough to pick up sub-millisecond radio pulsations, the fastest spinning known radio MSP, J1748−2446ad (*29*), has a spin frequency of only 716 Hz, corresponding to a spin period of 1.4 ms. This spin rate is far from the expected minimum equilibrium spin period (*8*) and the physical mass shedding limit of about 1500 Hz. It has been suggested that gravitational wave radiation during the accretion phase halts the spin period above a certain level (*30*, *31*). The RLDP effect presented here is a promising candidate for an alternative mechanism, in case a sub-millisecond AXMSP is detected (*8*).

References and Notes

1. M. A. Alpar, A. F. Cheng, M. A. Ruderman, J. Shaham, *Nature* **300**, 728 (1982).
2. D. Bhattacharya, E. P. J. van den Heuvel, *Phys. Rep.* **203**, 1 (1991).
3. L. Bildsten *et al.*, *Astrophys. J. Suppl. Ser.* **113**, 367 (1997).
4. R. Wijnands, M. van der Klis, *Nature* **394**, 344 (1998).
5. J. W. T. Hessels *et al.*, *AIP Conf. Proc.* **1068**, 130 (2008).
6. The Roche lobe of a binary star is the innermost equipotential surface passing through the first Lagrangian point, L1. If a star fills its Roche lobe, the unbalanced pressure at L1 will cause mass transfer to the other star (*2*).
7. A. M. Archibald *et al.*, *Science* **324**, 1411 (2009); 10.1126/science.1172740.
8. Materials and methods are available as supporting material on *Science* Online.
9. F. K. Lamb, C. J. Pethick, D. A. Pines, *Astrophys. J.* **184**, 271 (1973).
10. P. Ghosh, F. K. Lamb, *NATO Sci. Ser.* **377**, 487 (1992).
11. J. Frank, A. King, D. J. Raine, *Accretion Power in Astrophysics* (Cambridge Univ. Press, Cambridge, 2002).
12. A. F. Illarionov, R. A. Sunyaev, *Astron. Astrophys.* **39**, 185 (1975).
13. M. Ruderman, J. Shaham, M. Tavani, *Astrophys. J.* **336**, 507 (1989).
14. R. F. Webbink, S. Rappaport, G. J. Savonije, *Astrophys. J.* **270**, 678 (1983).
15. S. Rappaport, Ph. Podsiadlowski, P. C. Joss, R. Di Stefano, Z. Han, *Mon. Not. R. Astron. Soc.* **273**, 731 (1995).
16. T. M. Tauris, G. J. Savonije, *Astron. Astrophys.* **350**, 928 (1999).
17. Ph. Podsiadlowski, S. Rappaport, E. D. Pfahl, *Astrophys. J.* **565**, 1107 (2002).
18. The magnetospheric coupling parameter, $0.5 < \varphi < 1.4$ is a numerical factor of order unity depending on the accretion flow, the disk model, and the magnetic inclination angle of the pulsar (*10*, *11*, *32*–*34*).
19. S. L. Shapiro, S. A. Teukolsky, *Black Holes, White Dwarfs, and Neutron Stars: The Physics of Compact Objects* (Wiley-Interscience, New York, 1983).
20. S. A. Rappaport, J. M. Fregeau, H. C. Spruit, *Astrophys. J.* **606**, 436 (2004).
21. L. Burderi *et al.*, *Astrophys. J.* **560**, L71 (2001).
22. This "turn-off problem" has previously been debated elsewhere (*13*, *33*, *35*).
23. R. N. Manchester, J. H. Taylor, *Pulsars* (Freeman, San Francisco, CA, 1977).
24. D. R. Lorimer, A. G. Lyne, L. Festin, L. Nicastro, *Nature* **376**, 393 (1995).
25. F. Alberts, G. J. Savonije, E. P. J. van den Heuvel, O. R. Pols, *Nature* **380**, 676 (1996).
26. L. A. Nelson, E. Dubeau, K. A. MacCannell, *Astrophys. J.* **616**, 1124 (2004).
27. M. H. van Kerkwijk, C. G. Bassa, B. A. Jacoby, P. G. Jonker, in *Binary Radio Pulsars*, F. A. Rasio, I. H. Stairs, Eds. [Astronomical Society of the Pacific (ASP) Conference Series, San Francisco, CA, 2005], vol. 328, pp. 357–370.
28. This is the case if the pulsar spin period, P, is close to its initial spin period, P_0.
29. J. W. T. Hessels *et al.*, *Science* **311**, 1901 (2006).
30. L. Bildsten, *Astrophys. J.* **501**, L89 (1998).
31. D. Chakrabarty *et al.*, *Nature* **424**, 42 (2003).
32. Y.-M. Wang, *Astrophys. J.* **475**, L135 (1997).
33. F. Lamb, W. Yu, in *Binary Radio Pulsars*, F. A. Rasio, I. H. Stairs, Eds. (ASP Conference Series, San Francisco, CA, 2005), vol. 328, pp. 299–310.
34. C. R. D'Angelo, H. C. Spruit, *Mon. Not. R. Astron. Soc.* **406**, 1208 (2010).
35. M. Ruderman, J. Shaham, M. Tavani, D. Eichler, *Astrophys. J.* **343**, 292 (1989).
36. A. Patruno, *Astrophys. J.* **722**, 909 (2010).
37. I. S. Shklovskii, *Sov. Astron.* **13**, 562 (1970).

Acknowledgments: I gratefully thank N. Langer and M. Kramer for discussions and funding and without whom these results would not be possible and R. Eatough for helpful comments on the SOM. This work was partly supported by the Cluster of Excellence proposal EXC 1076, "The nature of forces and matter," at the University of Bonn. Radio pulsar data has been obtained from the *ATNF Pulsar Catalogue* (www.atnf.csiro.au/research/pulsar/psrcat/).

Supporting Online Material

www.sciencemag.org/cgi/content/full/335/6068/561/DC1
Materials and Methods
SOM Text
Figs. S1 and S2
References (*38*–*54*)

8 November 2011; accepted 6 January 2012
10.1126/science.1216355

Revealing the Superfluid Lambda Transition in the Universal Thermodynamics of a Unitary Fermi Gas

Mark J. H. Ku, Ariel T. Sommer, Lawrence W. Cheuk, Martin W. Zwierlein*

Fermi gases, collections of fermions such as neutrons and electrons, are found throughout nature, from solids to neutron stars. Interacting Fermi gases can form a superfluid or, for charged fermions, a superconductor. We have observed the superfluid phase transition in a strongly interacting Fermi gas by high-precision measurements of the local compressibility, density, and pressure. Our data completely determine the universal thermodynamics of these gases without any fit or external thermometer. The onset of superfluidity is observed in the compressibility, the chemical potential, the entropy, and the heat capacity, which displays a characteristic lambda-like feature at the critical temperature $T_c/T_F = 0.167(13)$. The ground-state energy is $\frac{3}{5}\xi N E_F$ with $\xi = 0.376(4)$. Our measurements provide a benchmark for many-body theories of strongly interacting fermions.

Phase transitions are ubiquitous in nature: Water freezes into ice, electron spins suddenly align as materials turn into magnets, and metals become superconducting. Near the transitions, many systems exhibit critical behavior, reflected by singularities in thermodynamic quantities: The magnetic susceptibility diverges at a ferromagnetic transition, and the specific heat

Downloaded from www.sciencemag.org on February 2, 2012

shows a jump at superconducting and superfluid transitions (*1*, *2*), resolved as the famous lambda peak in ^{4}He (*3*). A novel form of superfluidity has been realized in trapped, ultracold atomic gases of strongly interacting fermions, particles with half-integer spin (*4*–*7*). Thanks to an exquisite control over relevant system parameters, these gases have recently emerged as a versatile system well suited to solve open problems in many-body physics (*7*).

Initial measurements on the thermodynamics of strongly interacting Fermi gases have focused on trap-averaged quantities (*8*–*10*) in which the superfluid transition is inherently difficult to observe. The emergence of the condensate of fermion pairs in a spin-balanced Fermi gas is accompanied by only minute changes in the gas density (*5*). Quantities that involve integration of the density over the local potential, such as the energy E (*11*) and the pressure P (*12*), are only weakly sensitive to the sudden variations in the thermodynamics of the gas expected near the superfluid phase transition (*13*).

For a neutral gas, thermodynamic quantities involving the second derivative of the pressure P are expected to become singular at the second-order phase transition into the superfluid state. An example is the isothermal compressibility $\kappa = \frac{1}{n}\frac{\partial n}{\partial P}|_T$, the relative change of the gas density n due to a change in the pressure P. Because the change in pressure is related to the change in chemical potential μ of the gas via $dP = n\,d\mu$ at constant temperature, $\kappa = \frac{1}{n^2}\frac{\partial^2 P}{\partial \mu^2}|_T$ is a second derivative of the pressure, and thus should reveal a clear signature of the transition.

The general strategy to determine the thermodynamic properties of a given substance is to measure an equation of state (EoS), such as the pressure $P(\mu,T)$ as a function of the chemical potential μ and the temperature T. Equivalently, replacing the pressure by the density $n = \frac{\partial P}{\partial \mu}|_T$, one can determine the density EoS $n(\mu,T)$. We directly measure the local gas density $n(V)$ as a function of the local potential V from in situ absorption images of a trapped, strongly interacting Fermi gas of ^{6}Li atoms at a Feshbach resonance (*5*). The trapping potential is cylindrically symmetric, with harmonic confinement along the axial direction; this symmetry allows us to find the three-dimensional (3D) density through the inverse Abel transform of the measured column density (*14*, *15*). The local potential is directly determined from the atomic density distribution and the accurately known harmonic potential along the axial direction.

The compressibility κ follows as the change of the density n with respect to the local potential V experienced by the trapped gas. The change in the local chemical potential is given by the negative change in the local potential, $d\mu = -dV$, and hence the local compressibility is $\kappa = -\frac{1}{n^2}\frac{dn}{dV}|_T$. We can then replace the unknown chemical potential μ in the density EoS $n(\mu,T)$ by the known variation of n with μ in the atom trap, given by κ. Instead of the a priori unknown temperature T, we determine the pressure $P(V) = \int_{-\infty}^{\mu} d\mu' n(\mu') = \int_V^{\infty} dV' n(V')$ given by the integral of the density over the potential (*16*). The resulting equation of state $n(\kappa,P)$ contains only quantities that can be directly obtained from the density distribution. This represents a crucial advance over previous methods that require the input of additional thermodynamic quantities, such as the temperature T and the chemical potential μ, whose determination requires the use of a fitting procedure or an external thermometer, as in (*11*, *12*).

We normalize the compressibility and the pressure by the respective quantities at the same local density for a noninteracting Fermi gas at $T = 0$, $\kappa_0 = \frac{3}{2}\frac{1}{nE_F}$, and $P_0 = \frac{2}{5}nE_F$, where $E_F = \frac{\hbar^2(3\pi^2 n)^{2/3}}{2m}$ is the local Fermi energy and m is the particle mass, yielding $\tilde{\kappa} \equiv \kappa/\kappa_0$ and $\tilde{p} \equiv P/P_0$. For dilute gases at the Feshbach resonance, the scattering length diverges and is no longer a relevant length scale. In the absence of an interaction-dependent length scale, the thermodynamics of such resonant gases are universal (*17*), and $\tilde{\kappa}$ is a universal function of $\tilde{p}$ only. Every experimental profile $n(V)$, irrespective of the trapping potential, the total number of atoms, or the temperature, must produce the same universal curve $\tilde{\kappa}$ versus $\tilde{p}$. By averaging many profiles, one obtains a low-noise determination of $\tilde{\kappa}(\tilde{p})$.

Our method has been tested on the noninteracting Fermi gas that can be studied in two independent ways: in spin-balanced gases near the zero-crossing of the scattering length and in the wings of highly imbalanced clouds at unitarity, where only one spin state is present locally. Both determinations yield the same noninteracting compressibility EoS (Fig. 1).

Figure 1 also shows the compressibility equation of state $\tilde{\kappa}(\tilde{p})$ for the unitary Fermi gas. In the high-temperature ($\tilde{p} >> 1$) regime, the pressure, and hence all other thermodynamic quantities, allow for a Virial expansion in terms of the fugacity $e^{\beta\mu}$ (*18*): $P\,\beta\lambda^3 = 2\sum_j b_j\, e^{j\beta\mu}$, with the nth-order Virial coefficients b_n. It is known that $b_1 = 1$, $b_2 = 3\sqrt{2}/8$, and $b_3 = -0.29095295$ (*18*); our data show good agreement with the third-order Virial expansion. Fixing b_2 and b_3, our measurement yields a prediction for $b_4 = +0.065(10)$, in agreement with (*12*), but contradicting a recent four-body calculation that gives a negative sign (*19*).

At degenerate temperatures ($\tilde{p} \lesssim 1$), the normalized compressibility rises beyond that of a noninteracting Fermi gas, as expected for an attractively interacting gas. A sudden rise of the compressibility at around $\tilde{p} = 0.55$, followed by a decrease at lower temperatures marks the superfluid transition. The expected singularity of the compressibility at the transition is rounded off by the finite resolution of our imaging system. Below the transition point, the decrease of the compressibility is consistent with the expectation from Bardeen-Cooper-Schrieffer (BCS) theory, in which

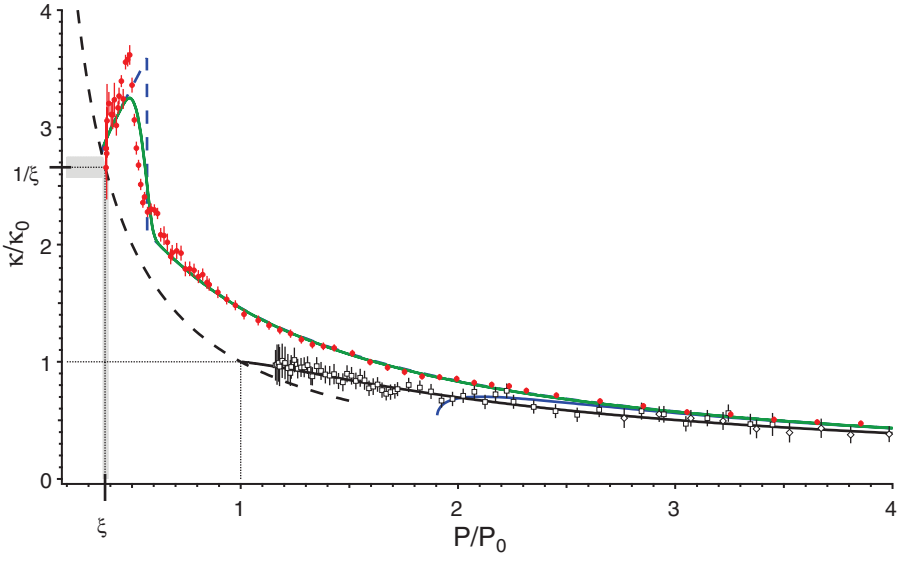


Fig. 1. Normalized compressibility κ/κ_0 versus normalized pressure P/P_0 of the unitary Fermi gas (red solid circles). Each data point is the average of between 30 and 150 profiles. The error bars show mean ± SD, including systematic errors from image calibration (*13*). Blue solid line: third-order Virial expansion. Black open squares (black open diamonds): data for a noninteracting Fermi gas obtained with a highly spin-imbalanced mixture at the Feshbach resonance (spin-balanced gas near zero-crossing of the scattering length). Black solid curve: theory for a noninteracting Fermi gas. Black dashed curve: the relation $\tilde{\kappa} = 1/\tilde{p}$ that must be obeyed at zero temperature both for the noninteracting gas ($\tilde{\kappa} = 1/\tilde{p} = 1$) and the unitary gas ($\tilde{\kappa} = 1/\tilde{p} = 1/\xi$) (dotted lines). Gray band: the uncertainty region for the $T = 0$ value of $\tilde{\kappa} = 1/\xi$ and $\tilde{p} = \xi$. Blue dashed curve: model for the EoS of the unitary Fermi gas [above T_c: interpolation from the Monte Carlo calculation (*34*); below T_c: BCS theory, including phonon and pair-breaking excitations]. Green solid curve: effect of 2 μm optical resolution on the model EoS.

Department of Physics, Massachusetts Institute of Technology (MIT), MIT Harvard Center for Ultracold Atoms, and Research Laboratory of Electronics, MIT, Cambridge, MA 02139, USA.

*To whom correspondence should be addressed. E-mail: zwierlein@mit.edu

Downloaded from www.sciencemag.org on February 2, 2012

single-particle excitations freeze out and pairs form (see model in Fig. 1).

As $T \to 0$, the Fermi energy E_F is the only intensive energy scale, so the chemical potential must be related to E_F by a universal number, $\mu = \xi E_F$, where ξ is known as the Bertsch parameter (*6*, *7*). It follows that at $T = 0$, $\tilde{\kappa} = 1/\tilde{p} = 1/\xi$ (*13*). The extrapolation of the low-temperature experimental data for $\tilde{\kappa}(\tilde{p})$ toward the curve $\tilde{\kappa} = 1/\tilde{p}$ gives $\xi = 0.37(1)$, a value that we find consistently for the normalized chemical potential, energy, and free energy at our lowest temperatures.

From the universal function $\tilde{\kappa}(\tilde{p})$, we obtain all other thermodynamic quantities of the unitary gas. First, to find the normalized temperature T/T_F (where $k_B T_F = E_F$), note that the change in pressure with T/T_F at constant temperature is related to the compressibility. One finds $\frac{d\tilde{p}}{d(T/T_F)} = \frac{5}{2}\frac{T_F}{T}\left(\tilde{p} - \frac{1}{\tilde{\kappa}}\right)$, so by integration (*13*)

$$\frac{T}{T_F} = \left(\frac{T}{T_F}\right)_i exp\left\{\frac{2}{5}\int_{\tilde{p}_i}^{\tilde{p}} d\tilde{p}\,\frac{1}{\tilde{p} - \frac{1}{\tilde{\kappa}}}\right\} \qquad (1)$$

where $(T/T_F)_i$ is the normalized temperature at an initial normalized pressure $\tilde{p}_i$ that can be chosen to lie in the Virial regime validated above.

Thanks to the relation $E = \frac{3}{2}PV$, valid at unitarity (*17*), we can also directly obtain the heat capacity per particle at constant volume V (*13*),

$$\frac{C_V}{k_B N} \equiv \frac{1}{k_B N}\frac{\partial E}{\partial T}\Big|_{N,V} = \frac{3}{5}\frac{d\tilde{p}}{d(T/T_F)} = \frac{3}{2}\frac{T_F}{T}\left(\tilde{p} - \frac{1}{\tilde{\kappa}}\right) \qquad (2)$$

Figure 2 shows the normalized compressibility and the specific heat as a function of T/T_F. At high temperatures, the specific heat approaches that of a noninteracting Fermi gas and eventually $C_V = \frac{3}{2} N k_B$, the value for a Boltzmann gas. A dramatic rise is observed for T/T_F at around 0.16, followed by a steep drop at lower temperatures. Such a λ-shaped feature in the specific heat is characteristic of second-order phase transitions, as in the famous λ transition in ^{4}He (*3*). Jumps in the specific heat are well known from superconductors (*1*) and ^{3}He (*2*). In experiments on atomic gases, such jumps had only been inferred from derivatives to fit functions that implied a jump (*20*, *21*). We do not expect to resolve the critical behavior very close to T_c. Because of the spatially varying chemical potential in our trapped sample, the critical region is confined to a narrow shell.

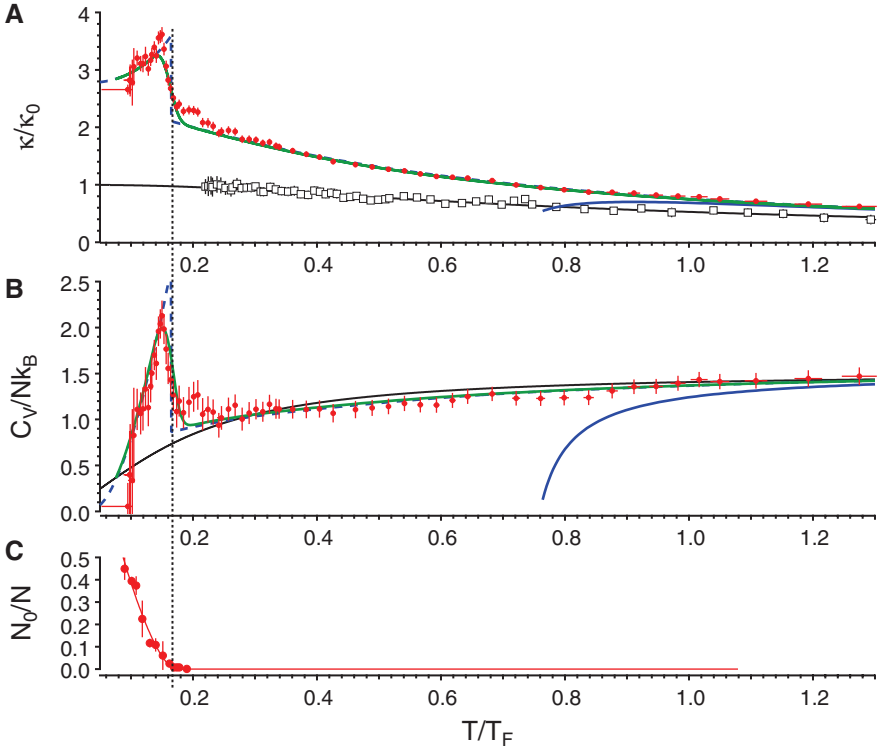


Fig. 2. (**A**) Normalized compressibility $\tilde{\kappa} = [2/3]\kappa\, n\, E_F$ and (**B**) specific heat per particle C_V/Nk_B of a unitary Fermi gas as a function of reduced temperature T/T_F (solid red circles). Black solid curve: theory for a noninteracting Fermi gas. Blue solid curve: third-order Virial expansion for the unitary gas. Black open squares: data for the normalized compressibility as a function of T/T_F of a noninteracting Fermi gas (combining data from both highly imbalanced gases at unitarity and balanced gases near zero-crossing). Blue dashed (green solid) curve: model from Fig. 1, excluding (including) the effect of finite imaging resolution. (**C**) Global condensate fraction at unitarity as determined from a rapid ramp to the molecular side of the Feshbach resonance, plotted as a function of local T/T_F at the trap center. The onset of condensation coincides with the sudden rise of the specific heat. Error bars, mean ± SD.

Based on the estimate in (*22*), the thickness of the critical shell is 1% of the cloud size. The finite resolution of our imaging system (2 μm or about 5% of the cloud size in the radial direction) suffices to explain the rounding of the singularity expected from criticality. The rounding also reduces the observed jump in the heat capacity at the transition. We obtain a lower bound $\Delta C/C_n \equiv (C_s - C_n)/C_n \geq 1.0^{+4}_{-1}$, where C_s/N (C_n/N) is the specific heat per particle at the peak (the onset of the sudden rise). Considering the strong interactions, this is surprisingly close to the BCS value of 1.43 (*1*). Below T_c, the specific heat is expected to decrease as $\sim \exp(-\Delta_0/k_B T)$ due to the pairing gap Δ_0. At low temperatures, $T << T_c$, the phonon contribution $\propto T^3$ dominates (*23*). This behavior is consistent with our data, but the phonon regime is not resolved.

To validate our in situ measurements of the superfluid phase transition, we have employed the rapid ramp method to detect fermion pair condensation (*24*, *25*). The results (Fig. 2C) show that the onset of condensation and the sudden rise in specific heat and compressibility all occur at the same critical temperature, within the error bars. Unlike previous experimental determinations of T_c/T_F for the homogeneous unitary Fermi gas (*11*, *12*), we determine T_c/T_F directly from the density profiles, finding a sudden rise in the specific heat and the onset of condensation at $T_c/T_F = 0.167(13)$. This value is determined as the midpoint of the sudden rise, and the error is assessed as the shift due to the uncertainty of the Feshbach resonance (*13*). This is in very good agreement with theoretical determinations, such as the self-consistent T-matrix approach that gives $T_c/T_F \approx 0.16$ (*23*), and Monte Carlo calculations that give $T_c/T_F = 0.171(5)$ (*26*) and 0.152(7) (*27*). There is a current debate on the possibility of a pseudogap phase of preformed pairs above T_c (*12*, *28*). A pairing gap for single-particle excitations above the transition should be signaled by a downturn of the specific heat above T_c, which is not observed in our measurements.

From the definition of the compressibility $\kappa = \frac{1}{n^2}\frac{\partial n}{\partial \mu}\big|_T$, we can obtain the reduced chemical potential μ/E_F as a function of the T/T_F (Fig. 3A) (*13*). This function is here obtained from measured quantities, rather than from numerical derivatives of data that involved uncontrolled thermometry (*11*). In the interval of T/T_F from around 0.25 to 1, the chemical potential is close to that of a noninteracting Fermi gas, shifted by $(\xi_n - 1)E_F$ because of interactions present in the normal state, with $\xi_n \approx 0.45$. Unlike a normal Fermi gas, the chemical potential attains a maximum of $\mu/E_F = 0.42(1)$ at $T/T_F = 0.171(10)$, and then decreases at lower temperatures, as expected for a superfluid of paired fermions (*23*). As the temperature is increased from zero in a superfluid, first the emergence of phonons (sound excitations) and then the breaking of fermion pairs contribute to increasing the chemical potential. At T_c, the singular compressibility implies a sharp change in slope for μ/E_F, in agreement with our observa-

Downloaded from www.sciencemag.org on February 2, 2012

tion and theory (*23*). At low temperatures, the reduced chemical potential μ/E_F saturates to the universal value ξ. As the internal energy E and the free energy F satisfy $E(T) > E(0) = \frac{3}{5}N\xi E_F = F(0) > F(T)$ for all T, the reduced quantities $f_E \equiv \frac{5}{3}\frac{E}{NE_F} = \tilde{p}$ and $f_F \equiv \frac{5}{3}\frac{F}{NE_F} = \frac{5}{3}\frac{\mu}{E_F} - \frac{2}{3}\tilde{p}$ (Fig. 3A) provide upper and lower bounds for ξ (*29*). Taking the coldest points of these three curves and including the systematic error due to the effective interaction range, we find $\xi = 0.376(4)$. The uncertainty in the Feshbach resonance is expected to shift ξ by at most 2% (*13*). This value is consistent with a recent upper bound $\xi < 0.383(1)$ from (*30*), is close to $\xi = 0.36(1)$ from a self-consistent T-matrix calculation (*23*), and agrees with $\xi = 0.367(9)$ from an epsilon expansion (*31*). It lies below earlier estimates $\xi = 0.44(2)$ (*32*) and $\xi = 0.42(1)$ (*33*) from fixed-node quantum Monte Carlo calculation that provides upper bounds on ξ. Our measurement agrees with several less accurate experimental determinations (*6*) but disagrees with the most recent experimental value 0.415(10) that was used to calibrate the pressure in (*12*).

From the energy, pressure, and chemical potential, we can obtain the entropy $S = \frac{1}{T}(E + PV - \mu N)$, and hence the entropy per particle $S/Nk_B = \frac{T_F}{T}\left(\tilde{p} - \frac{\mu}{E_F}\right)$ as a function of T/T_F (Fig. 3B). At high temperatures, S is close to the entropy of an ideal Fermi gas at the same T/T_F. Above T_c, the entropy per particle is nowhere small compared with k_B. Also, the specific heat C_V is not linear in T in the normal phase. This shows that the normal regime above T_c cannot be described in terms of a Landau Fermi Liquid picture, although some thermodynamic quantities agree surprisingly well with the expectation for a Fermi liquid [see (*12*) and (*13*)]. Below about $T/T_F = 0.17$, the entropy starts to strongly fall off compared with that of a noninteracting Fermi gas, which we again interpret as the freezing out of single-particle excitations as a result of the formation of fermion pairs. Far below T_c, phonons dominate. They only have a minute contribution to the entropy (*23*), less than 0.02 k_B at $T/T_F = 0.1$, consistent with our measurements. At the critical point, we obtain $S_c = 0.73(13)$ Nk_B, in agreement with theory (*23*). It is encouraging for future experiments with fermions in optical lattices that we obtain entropies less than 0.04 $N k_B$, far below critical entropies required to reach magnetically ordered phases.

From the chemical potential μ/E_F and $T/T_F = \frac{1}{(3\pi^2)^{2/3}(n\lambda^3)^{2/3}}$, we finally obtain the density EoS $n(\mu,T) \equiv \frac{1}{\lambda^3}f_n(\beta\mu)$, with the de Broglie wavelength $\lambda = \sqrt{\frac{2\pi\hbar^2}{mk_BT}}$. The pressure EoS follows as $P(\mu,T) \equiv \frac{k_BT}{\lambda^3}f_P(\beta\mu)$, with $f_P = \frac{2}{5}\frac{T_F}{T}\tilde{p}f_n(\beta\mu)$. Figure 4 shows the density and pressure normalized by their noninteracting counterparts at the same chemical potential and temperature. For the normal state, a concurrent theoretical calculation employing a new Monte Carlo method agrees excellently with our data (*34*). Our data deviate from a previous experimental determination of the pressure EoS (*12*) that was calibrated with an independently measured value of $\xi = 0.415(10)$ (*35*) and disagree with the energy measurement in (*11*) that used a thermometry inconsistent with the Virial expansion (*10*). Around

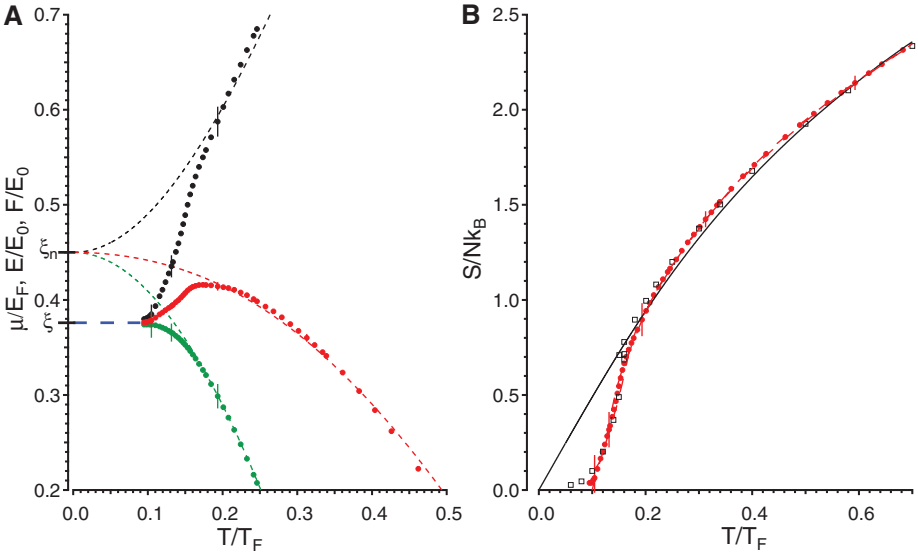


Fig. 3. (**A**) Chemical potential μ, energy E, and free energy F of the unitary Fermi gas versus T/T_F. μ (red solid circles) is normalized by the Fermi energy E_F, and E (black solid circle) and F (green solid circle) are normalized by $E_0 = \frac{3}{5}N E_F$. At high temperatures, all quantities approximately track those for a noninteracting Fermi gas, shifted by $\xi_n - 1$ (dashed curves). The peak in the chemical potential signals the onset of superfluidity. In the deeply superfluid regime at low temperatures, μ/E_F, E/E_0, and F/F_0 all approach ξ (blue dashed line). (**B**) Entropy per particle. At high temperatures, the entropy closely tracks that of a noninteracting Fermi gas (black solid curve). The open squares are from the self-consistent T-matrix calculation (*23*). A few representative error bars are shown, representing mean ± SD.

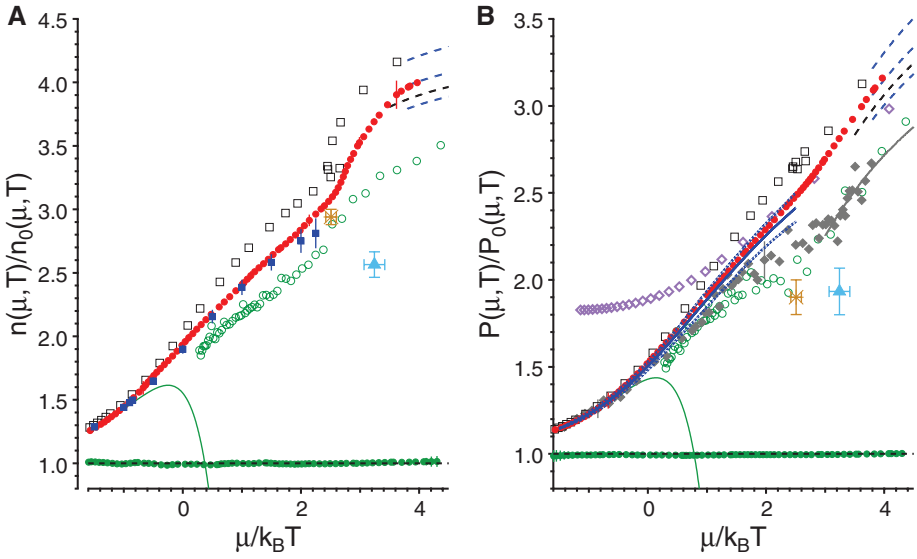


Fig. 4. (**A**) Density and (**B**) pressure of a unitary Fermi gas versus μ/k_BT, normalized by the density and pressure of a noninteracting Fermi gas at the same chemical potential μ and temperature T. Red solid circles: experimental EoS. Blue dashed curves: low-temperature behavior with $\xi = 0.364$ (upper), 0.376 (middle), and 0.388 (lower). Black dashed curve: low-temperature behavior with ξ at upper bound of 0.383 from (*30*). Green solid circles (black fine dashed line): MIT experimental data (theory) for the ideal Fermi gas. Blue solid squares (blue curve): diagrammatic Monte Carlo calculation (*34*) for density (pressure, with blue dashed curves denoting the uncertainty bands). Solid green line: third-order Virial expansion. Open black squares: self-consistent T-matrix calculation (*23*). Open green circles: lattice calculation (*36*). Orange star and blue triangle: critical point from the Monte Carlo calculations (*26*) and (*27*), respectively. Solid diamonds: Ecole Normale Supérieure experiment (*12*). Purple open diamonds: Tokyo experiment (*11*).

Downloaded from www.sciencemag.org on February 2, 2012

the critical point, the density shows a strong variation, whereas the pressure, the integral of the density over μ at constant T, is naturally less sensitive to the superfluid transition.

In conclusion, we have performed thermodynamic measurements of the unitary Fermi gas across the superfluid phase transition at the level of uncertainty of a few percent, without any fits or input from theory, enabling validation of theories for strongly interacting matter. Similar unbiased methods can be applied to other systems, for example, two-dimensional Bose and Fermi gases or fermions in optical lattices.

References and Notes

1. M. Tinkham, *Introduction to Superconductivity* (Dover, Mineola, New York, ed. 2, 2004).
2. D. Vollhardt, P. Wölfle, *The Superfluid Phases of Helium 3* (Taylor & Francis, London, 1990).
3. J. A. Lipa, J. A. Nissen, D. A. Stricker, D. R. Swanson, T. C. P. Chui, *Phys. Rev. B* **68**, 174518 (2003).
4. M. W. Zwierlein, J. R. Abo-Shaeer, A. Schirotzek, C. H. Schunck, W. Ketterle, *Nature* **435**, 1047 (2005).
5. W. Ketterle, M. Zwierlein, *Riv. Nuovo Cim.* **31**, 247 (2008).
6. S. Giorgini, L. P. Pitaevskii, S. Stringari, *Rev. Mod. Phys.* **80**, 1215 (2008).
7. I. Bloch, J. Dalibard, W. Zwerger, *Rev. Mod. Phys.* **80**, 885 (2008).
8. J. Kinast *et al*., *Science* **307**, 1296 (2005).
9. J. T. Stewart, J. P. Gaebler, C. A. Regal, D. S. Jin, *Phys. Rev. Lett.* **97**, 220406 (2006).
10. L. Luo, B. Clancy, J. Joseph, J. Kinast, J. E. Thomas, *Phys. Rev. Lett.* **98**, 080402 (2007).
11. M. Horikoshi, S. Nakajima, M. Ueda, T. Mukaiyama, *Science* **327**, 442 (2010).
12. S. Nascimbène, N. Navon, K. J. Jiang, F. Chevy, C. Salomon, *Nature* **463**, 1057 (2010).
13. Materials and methods are available as supporting material on *Science* Online.
14. Y. Shin, M. W. Zwierlein, C. H. Schunck, A. Schirotzek, W. Ketterle, *Phys. Rev. Lett.* **97**, 030401 (2006).
15. G. B. Partridge *et al*., *Phys. Rev. Lett.* **97**, 190407 (2006).
16. C.-H. Cheng, S.-K. Yip, *Phys. Rev. B* **75**, 014526 (2007).
17. T.-L. Ho, *Phys. Rev. Lett.* **92**, 090402 (2004).
18. X.-J. Liu, H. Hu, P. D. Drummond, *Phys. Rev. Lett.* **102**, 160401 (2009).
19. D. Rakshit, K. M. Daily, D. Blume, Thermodynamics of two-component Fermi gas with large scattering length: Fourth- and higher-order virial coefficients, preprint arXiv:1106.5958; available at http://arxiv.org/abs/1106.5958.
20. J. R. Ensher, D. S. Jin, M. R. Matthews, C. E. Wieman, E. A. Cornell, *Phys. Rev. Lett.* **77**, 4984 (1996).
21. L. Luo, J. Thomas, *J. Low Temp. Phys.* **154**, 1 (2009).
22. L. Pollet, N. V. Prokof'ev, B. V. Svistunov, *Phys. Rev. Lett.* **104**, 245705 (2010).
23. R. Haussmann, W. Rantner, S. Cerrito, W. Zwerger, *Phys. Rev. A* **75**, 023610 (2007).
24. C. A. Regal, M. Greiner, D. S. Jin, *Phys. Rev. Lett.* **92**, 040403 (2004).
25. M. W. Zwierlein *et al*., *Phys. Rev. Lett.* **92**, 120403 (2004).
26. O. Goulko, M. Wingate, *Phys. Rev. A* **82**, 053621 (2010).
27. E. Burovski, N. Prokof'ev, B. Svistunov, M. Troyer, *Phys. Rev. Lett.* **96**, 160402 (2006).
28. J. P. Gaebler *et al*., *Nat. Phys.* **6**, 569 (2010).
29. Y. Castin, F. Werner, *The BCS-BEC Crossover and the Unitary Fermi Gas*, W. Zwerger, ed. (Springer-Verlag, Berlin, 2012), chap. 5.
30. M. M. Forbes, S. Gandolfi, A. Gezerlis, *Phys. Rev. Lett.* **106**, 235303 (2011).
31. P. Arnold, J. E. Drut, D. T. Son, *Phys. Rev. A* **75**, 043605 (2007).
32. J. Carlson, S.-Y. Chang, V. R. Pandharipande, K. E. Schmidt, *Phys. Rev. Lett.* **91**, 050401 (2003).
33. G. E. Astrakharchik, J. Boronat, J. Casulleras, A. S. Giorgini, *Phys. Rev. Lett.* **93**, 200404 (2004).
34. K. Van Houcke *et al*., Feynman diagrams versus Fermi-gas Feynman quantum emulator, preprint arXiv:1110.3747 (2011); available at http://arxiv.org/abs/1110.3747.
35. S. Nascimbène, Thermodynamics of ultracold Fermi gases, thesis, Ecole Normale Supérieure, Paris (2010).
36. A. Bulgac, J. E. Drut, P. Magierski, *Phys. Rev. Lett.* **96**, 090404 (2006).

Acknowledgments: We thank B. Svistunov, N. Prokof'ev, and F. Werner for fruitful discussions; Z. Hadzibabic for a critical reading of the manuscript; the authors of (*11*, *12*, *23*, *26*, *27*, *36*) for kindly providing us with their data; and André Schirotzek for help during the early stages of the experiment. M.J.H.K. acknowledges financial support from NSERC. This work was supported by the NSF, Air Force Office of Scientific Research (AFOSR) - Multidisciplinary Research Program of the University Research Initiative (MURI), Army Research Office (ARO) - MURI, Office of Naval Research, Defense Advanced Research Projects Agency (DARPA) Young Faculty Award, a grant from the ARO with funding from the DARPA Optical Lattice Emulator program, an AFOSR Presidential Early Career Award in Science and Engineering, the David and Lucile Packard Foundation, and the Alfred P. Sloan Foundation.

Supporting Online Material

www.sciencemag.org/cgi/content/full/science.1214987/DC1
Materials and Methods
Figs. S1 to S4
References (*37*–*45*)

7 October 2011; accepted 3 January 2012
Published online 12 January 2012;
10.1126/science.1214987

Iron Catalysts for Selective Anti-Markovnikov Alkene Hydrosilylation Using Tertiary Silanes

Aaron M. Tondreau,[1] Crisita Carmen Hojilla Atienza,[1] Keith J. Weller,[2] Susan A. Nye,[2] Kenrick M. Lewis,[3] Johannes G. P. Delis,[4] Paul J. Chirik[1]*

Alkene hydrosilylation, the addition of a silicon hydride (Si-H) across a carbon-carbon double bond, is one of the largest-scale industrial applications of homogeneous catalysis and is used in the commercial production of numerous consumer goods. For decades, precious metals, principally compounds of platinum and rhodium, have been used as catalysts for this reaction class. Despite their widespread application, limitations such as high and volatile catalyst costs and competing side reactions have persisted. Here, we report that well-characterized molecular iron coordination compounds promote the selective anti-Markovnikov addition of sterically hindered, tertiary silanes to alkenes under mild conditions. These Earth-abundant base-metal catalysts, coordinated by optimized bis(imino)pyridine ligands, show promise for industrial application.

Metal-catalyzed olefin hydrosilylation, which forms alkylsilanes by cleaving a silicon-hydrogen bond and adding the fragments across a carbon-carbon double bond (*1*, *2*), finds widespread application in the commercial manufacture of silicone-based surfactants, fluids, molding products, release coatings, and pressure-sensitive adhesives (*3*, *4*). Consequently, hydrosilylation has emerged as one of the largest-scale applications of homogeneous catalysis (*5*–*9*). For more than three decades, precious metal compounds with Pt, Pd, Ru, and Rh have been used almost exclusively as catalysts. Platinum compounds such as Karstedt's and Speier's catalysts, $Pt_2\{[(CH_2{=}CH)SiMe_2]_2O\}_3$ (Me, methyl) and $H_2PtCl_6{\cdot}6H_2O/{}^{i}PrOH$ (${}^{i}Pr$, isopropyl), respectively, are the most widely used industrial catalysts (*1*, *10*–*12*), though they suffer from chemical limitations such as intolerance to amino-substituted olefins and a tendency to catalyze competing isomerization of the terminal alkenes to internal isomers. Undesired isomerization often necessitates subsequent purification steps that are both energy and cost intensive. Furthermore, decomposition of the catalyst to colloidal platinum contributes to unwanted side reactions and also causes discoloration of the final products.

It has been estimated that the worldwide silicone industry consumed ~180,000 troy ounces (5.6 metric tons) of platinum in 2007 and most is not recovered (*13*). The high cost, coupled with the increasing demands on precious metals due to fuel-cell and other emerging technologies, has increased the volatility of the platinum market (*14*). The combination of chemical, economic, and political challenges inspires the exploration of inexpensive and Earth-abundant catalysts using iron, manganese, and cobalt (*15*). At the core of this challenge is suppressing tendencies of first-row transition metals toward one-electron redox processes in favor of the two-electron chemistry associated with the heavier metals that probably make up the fundamental steps in a catalytic cycle for alkene hydrosilylation.

[1]Department of Chemistry, Princeton University, Princeton, NJ 08544, USA. [2]Momentive Performance Materials, 260 Hudson River Road, Waterford, NY 12188, USA. [3]Momentive Performance Materials, 769 Old Saw Mill River Road, Tarrytown, NY 10591, USA. [4]Momentive Performance Materials bv, Plasticslaan 1, 4612PX Bergen op Zoom, Netherlands.

*To whom correspondence should be addressed. E-mail: pchirik@princeton.edu

Downloaded from www.sciencemag.org on February 2, 2012

In addition to cost and environmental advantages, base-metal compounds also offer the prospect of mechanistic distinctions that may overcome some of the deleterious side reactions observed for existing commercial precious metal–catalyzed processes (*16*, *17*). Although many successful iron-catalyzed carbonyl hydrosilylations for the synthesis of alcohols have been realized (*18*–*23*), catalysts that promote industrially practiced Si-H additions to alkenes are rare. Early studies focused on iron carbonyl compounds such as $Fe(CO)_5$ and $Fe_3(CO)_{12}$ as pre-catalysts but these required either high temperatures or ultraviolet light to access the active species (*24*, *25*). In addition to the inconvenient reaction conditions, measurable quantities of side products arising from hydrogenation, alkene isomerization, and dehydrogenative silane coupling accompany the desired Si-H addition process, limiting the utility of this class of catalyst (*26*).

In 2004, the bis(imino)pyridine iron dinitrogen compound, (^{iPr}PDI)Fe(N_2)$_2$ [^{iPr}PDI = 2,6-(2,6-$^{i}Pr_2$-C_6H_3N=CMe)$_2$$C_5H_3$N] (Fig. 1), was reported as an effective precatalyst for the hydrosilylation of unactivated alkenes and alkynes under mild thermal conditions (*27*). Exclusive anti-Markovnikov addition was observed in reactions of α-olefins such as 1-hexene and styrene, with no evidence for side reactions such as dehydrogenative silylation. Despite this favorable selectivity, this catalyst was unreactive toward the tertiary silane, Et_3SiH (Et, ethyl), and unactivated terminal alkenes, representing a barrier to industrial applicability. Tertiary silanes, R_3SiH (R = alkyl, aryl, alkoxide, etc.), are the most commercially relevant silicon hydrides, as products prepared from primary ($RSiH_3$) or secondary (R_2SiH_2) silanes contain residual Si-H bonds, which act as catalyst poisons and decrease the stability and, hence, the utility of the final product. One example of an iron-catalyzed 1,4-addition of a tertiary silane, $(EtO)_3SiH$, to dienes has been reported by Wu *et al*. (*28*), although the substrate scope and application to commercially relevant alkene substrates have not been disclosed. Here, we describe iron compounds for the catalytic hydrosilylation of industrially applicable alkenes using tertiary silanes. Inspiration for these studies was derived, in part, from dramatically improved alkene hydrogenation activity observed with [(^{Et}PDI)Fe(N_2)]$_2$(μ_2-N_2) and [(^{Me}PDI)Fe(N_2)]$_2$(μ_2-N_2) (μ denotes bridging ligand) (*29*). We were curious if reducing the size of the 2,6-aryl substituents from isopropyl to ethyl and methyl would have a similar effect in catalytic alkene hydrosilylation chemistry. In many examples, the new base-metal catalysts offer advantages in both activity and selectivity over currently employed precious compounds.

Our studies commenced with the hydrosilylation of 1-octene as a representative substrate. The product of the anti-Markovnikov addition of $(Me_3SiO)_2MeSiH$ (MD′M) to 1-octene is 3-octyl-1,1,1,3,5,5,5-heptamethyltrisiloxane (Table 1), which is prepared commercially for use as an agricultural adjuvant and as a sensory and performance enhancer in cosmetic formulations (*3*). With 2000 parts per million (ppm) of (^{iPr}PDI)Fe(N_2)$_2$ in the presence of neat 1-octene and MD′M, we observed more than 98% conversion to the anti-Markovnikov product (Table 1). Likewise, we also observed nearly complete conversion when $(EtO)_3SiH$ was used as the silane. In both cases, there was no evidence for any other products. Alkene hydrosilylations with $(EtO)_3SiH$ are of interest because the alkylsilane products find application as filler treatments (*7*). Consistent with the observations made previously in toluene solution with 1-hexene (*27*), we observed negligible turnover with Et_3SiH. We performed each of these reactions, as well as all others reported in this study, under a dinitrogen atmosphere with predried reagents. Although this may appear to be a limitation, many large-scale, commercial reactions are performed in an inert atmosphere for safe practice.

To improve catalytic activity, we evaluated bis(imino)pyridine iron complexes with smaller aryl substituents for the catalytic hydrosilylation of 1-octene. The 2,6-diethyl-substituted compound,

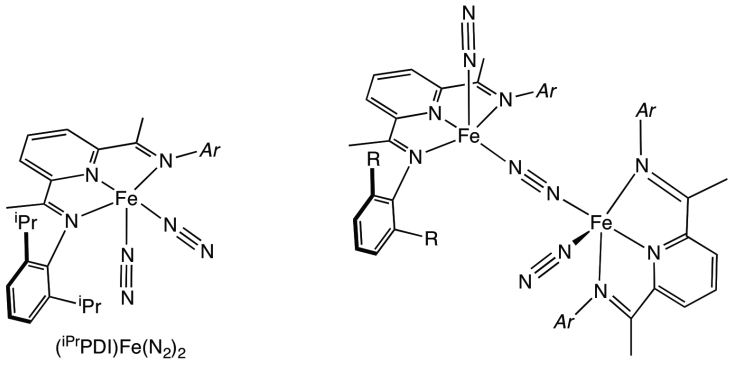
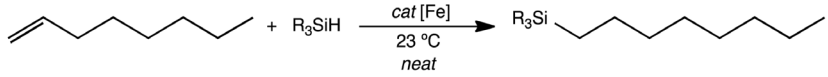


Fig. 1. Bis(imino)pyridine iron dinitrogen complexes used for alkene hydrosilylation. Ar, aryl group.

Table 1. Evaluation of iron precatalysts for the selective hydrosilylation of 1-octene with various tertiary silanes. MD′M, $(Me_3SiO)_2MeSiH$; ^{Et}PDI, 2,6-(2,6-Et_2-C_6H_3N=CMe)$_2$$C_5H_3$N; ^{Me}PDI, 2,6-(2,6-$Me_2$-$C_6H_3$N=CMe)$_2$$C_5H_3$N.



Compound	ppm = mg complex / kg reaction mixture	mol % = (mol complex / mol reaction mixture) x 100	Silane	Time (min)	Yield (GC-FID)
(^{iPr}PDI)Fe(N_2)$_2$	2000*	0.05	MD′M	15	>98%
(^{iPr}PDI)Fe(N_2)$_2$	2000	0.04	$(EtO)_3SiH$	15	96%
(^{iPr}PDI)Fe(N_2)$_2$	2000	0.03	Et_3SiH	60	trace
[(^{Et}PDI)Fe(N_2)]$_2$(μ-N_2)	2000†	0.03	MD′M	15	>98%
[(^{Et}PDI)Fe(N_2)]$_2$(μ-N_2)	2000	0.02	$(EtO)_3SiH$	15	97%
[(^{Et}PDI)Fe(N_2)]$_2$(μ-N_2)	2000	0.02	Et_3SiH	15	9%
[(^{Me}PDI)Fe(N_2)]$_2$(μ-N_2)	200‡	0.004	MD′M	15	>98%
[(^{Me}PDI)Fe(N_2)]$_2$(μ-N_2)	500§	0.007	$(EtO)_3SiH$	15	97%
[(^{Me}PDI)Fe(N_2)]$_2$(μ-N_2)	2000‖	0.02	Et_3SiH	45	>98%

Fe metal concentration: *200 ppm; †200 ppm; ‡20 ppm; §60 ppm; ‖200 ppm.

Downloaded from www.sciencemag.org on February 2, 2012

[(^{Et}PDI)Fe(N_2)]$_2$(μ_2-N_2), exhibited minimal activity for hydrosilylation with Et_3SiH, but fast and selective reactions were observed with $(EtO)_3SiH$ and MD′M (Table 1). Motivations for studying hydrosilylations with Et_3SiH include determining tertiary silane scope as well as potential industrial applications. Further reduction in size of the 2,6-aryl substituents to methyl groups produced the most active hydrosilylation catalysts for 1-octene. Unlike the ^{i}Pr and Et variants, 2000 ppm of [(^{Me}PDI)Fe(N_2)]$_2$(μ_2-N_2) (*29*) resulted in complete conversion of Et_3SiH and the olefin to the anti-Markovnikov product in 45 min at 23°C (Table 1). Monitoring the reaction by gas chromatography as a function of time under these conditions established 60% conversion in 15 min and 88% conversion in 30 min. Successful hydrosilylation was also achieved with 500 ppm of [(^{Me}PDI)Fe(N_2)]$_2$(μ_2-N_2), plateauing at 71% conversion in 2 hours. In all cases, exclusive formation of the anti-Markovnikov product of 1-octene hydrosilylation was detected by gas chromatography and nuclear magnetic resonance (NMR) spectroscopy.

The methyl-substituted compound also exhibited high activity and selectivity for the hydrosilylation of 1-octene with $(EtO)_3SiH$ and MD′M (Table 1). To put the results with the bis(imino)pyridine iron dinitrogen complexes in context, the hydrosilylation of 1-octene with MD′M in the presence of 30 ppm of Karstedt's catalyst proceeds to 80% conversion at 72°C with a detectable quantity (up to 20%) of byproducts arising from alkene hydrogenation, isomerization, and dehydrogenation (*10*). Suppression of these unwanted side reactions has been achieved by using *N*-heterocyclic carbene–supported platinum catalysts (*10*).

The absence of competing olefin isomerization during the hydrosilylation of 1-alkenes and preference for anti-Markovnikov products with the bis(imino)pyridine iron dinitrogen compounds inspired additional study. Hydrosilylation of styrene is often plagued by competing isomerization and sometimes favors silicon addition to the carbon closest to the aryl ring (*30*). Hydrosilylation of this alkene with MD′M in the presence of 200 ppm [(^{Me}PDI)Fe(N_2)]$_2$(μ_2-N_2) exclusively furnished the anti-Markovnikov product in >98% conversion after 30 min (Fig. 2A), highlighting the preference for the iron catalyst to functionalize the terminal position of the alkene. In contrast, (^{iPr}PDI)Fe(N_2)$_2$ produced no turnover at 2000 ppm or higher loadings. Instead, transfer hydrogenation from one of the ligand isopropyl substituents to the substrate to yield ethylbenzene was observed (*31*).

To further probe the regioselectivity, we conducted a deuterium-labeling experiment for the hydrosilylation of 1-octene. If chain-running processes were competitive, deuterium would be found throughout the alkyl chain of the product. Hydrosilylation with $(Me_3SiO)_2MeSiD$ with [(^{Me}PDI)Fe(N_2)]$_2$(μ_2-N_2) yielded the anti-Markovnikov product with deuterium incorporated only in the 2 position of the alkyl chain, demonstrating that chain running is not competitive during catalytic turnover (Fig. 2B).

To screen the compatibility of the iron catalysts with functional groups, we studied the hydrosilylation of amino-substituted olefins, as these substrates often poison platinum catalysts. In the presence of 2000 ppm [0.03 mole percent (mol %); 200 ppm Fe metal] of [(^{Me}PDI)Fe(N_2)]$_2$(μ_2-N_2), the hydrosilylation of *N*,*N*-dimethylallylamine with MD′M reached completion in 15 min, demonstrating the potential compatibility of the bis(imino)pyridine iron catalysts with functionalized alkenes. The more sterically congested (^{iPr}PDI)Fe(N_2)$_2$ (2000 ppm, 0.05 mol %, 200 ppm [Fe] metal) was also active for this reaction, leading to 90% conversion in 15 min at 23°C.

Products arising from the hydrosilylation of methyl- and *tert*-butyl–capped allyl polyethers find application as sensory and performance enhancers in personal-care products, silicone surfactants for the stabilization of polyurethane foams, and agricultural adjuvants (*5*, *6*, *8*, *32*). With industrial platinum catalysts, the reactions are conducted at 85° to 100°C and require a 10 to 30 mol % excess of polyether substrate to compensate for competing isomerization to the propenyl ether that, once formed, is unreactive toward hydrosilylation. In contrast, we observed complete hydrosilylation with a methyl-capped polyether and an equimolar quantity of MD′M in the presence of 7000 ppm of [(^{Me}PDI)Fe(N_2)]$_2$(μ_2-N_2) (0.26 mol %; 700 ppm Fe metal), as judged by ^{1}H NMR spectroscopy (Fig. 2C). No evidence was obtained for competing olefin isomerization. The more sterically hindered iron compound, (^{iPr}PDI)Fe(N_2)$_2$, produced no turnover.

The platinum-catalyzed hydrosilylation of hydrido- and vinyl-functionalized silicone fluids is widely practiced due to the application of the resulting cross-linked silicone polymers as release coatings. Replacing platinum in this specific context is particularly attractive because the viscosity and morphology of the final product

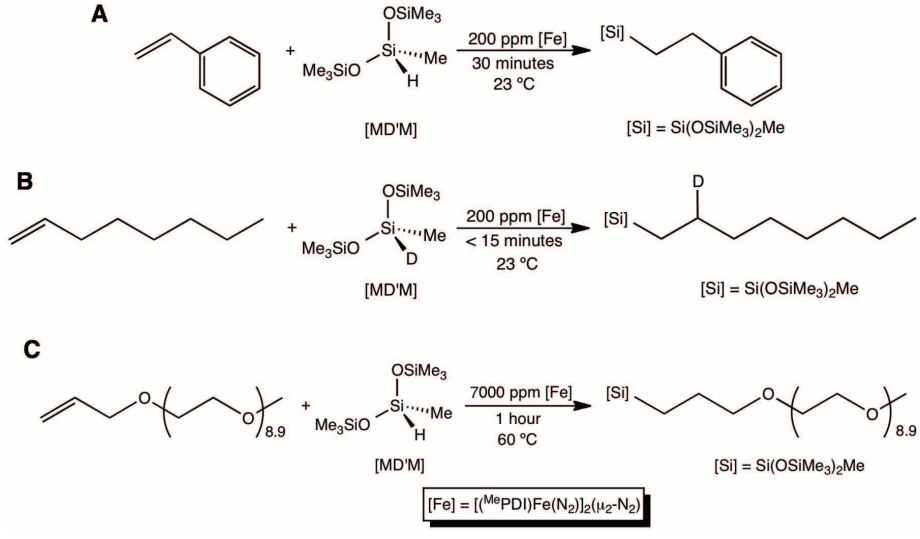


Fig. 2. (**A**) Styrene hydrosilylation catalyzed by [(^{Me}PDI)Fe(N_2)]$_2$(μ_2-N_2). (**B**) Deuterium labeling of 1-octene hydrosilylation. (**C**) Hydrosilylation of an allyl polyether. The 8.9 designation refers to the average number of repeat units.

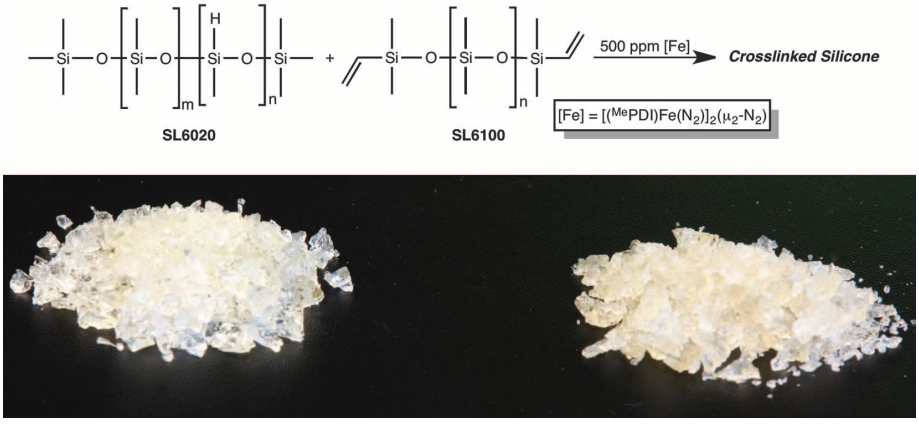


Fig. 3. Cross-linked silicone fluids prepared using the commercial Pt catalyst (left) and the bis(imino) pyridine iron dinitrogen compound [(^{Me}PDI)Fe(N_2)]$_2$(μ_2-N_2) (right).

Downloaded from www.sciencemag.org on February 2, 2012

makes catalyst recovery challenging. We focused our experiments on the cross-linking of two commercial silicone fluids: SilForce SL6100 and SilForce SL6020 (Momentive Performance Materials, Waterford, NY) (Fig. 3). Addition of a toluene solution containing 1000 ppm of (^{iPr}PDI)Fe(N_2)$_2$ to a neat mixture of the two fluids at 23°C resulted in immediate cross-linking. Dissolving the iron compound in a small amount of toluene is necessary because of the low solubility of (^{iPr}PDI)Fe(N_2)$_2$ in the silicone fluids. We also observed immediate cross-linking upon addition of 500 ppm of [(^{Me}PDI)Fe(N_2)]$_2$(μ_2-N_2) in toluene solution. With the more active [(^{Me}PDI)Fe(N_2)]$_2$(μ_2-N_2) compound, cross-linking could be achieved over the course of 2 hours in neat silicone fluid without the addition of toluene. In each case that we studied, the resulting silicone polymer was identical to material prepared commercially using platinum catalysts. Photographs are presented in Fig. 3 for visual comparison.

Collectively, these results demonstrate the potential of Earth-abundant metal complexes to compete with more rare and more expensive precious-metal counterparts. Beyond their high activities, the iron compounds offer functional-group tolerance and, perhaps most importantly, exclusive regioselectivity that obviates the need for separation of unwanted by-products obtained in industrial processes.

References and Notes

1. B. Marciniec, J. Gulinski, W. Urbaniak, Z. W. Kornetka, in *Comprehensive Handbook on Hydrosilylation*, B. Marciniec, Ed. (Pergamon, Oxford, 2002), pp. 3–7.
2. B. Marciniec, *Coord. Chem. Rev.* **249**, 2374 (2005).
3. V. B. Pukhnarevitch, E. Lukevics, L. I. Kopylova, M. Voronkov, *Perspectives of Hydrosilylation* (Institute for Organic Synthesis, Riga, Latvia, 1992).
4. I. Ojima, in *The Chemistry of Organic Silicon Compounds*, S. Patai, Z. Rappoport, Eds. (Wiley Interscience, New York, 1989), pp. 1479–1526.
5. A. K. Roy, *Adv. Organomet. Chem.* **55**, 1 (2007).
6. A. F. Noels, A. J. Hubert, in *Industrial Applications of Homogeneous Catalysis*, A. Mortreux, Ed. (Kluwer, Amsterdam, 1985), pp. 80–91.
7. E. Plueddemann, *Silane Coupling Agents* (Plenum Press, New York, ed. 2, 1991).
8. R. M. Hill, in *Silicone Surfactants, Surfactants Science Series*, vol. 86, R. M. Hill, Ed. (Marcel Dekker, New York, 1999), pp. 1–48.
9. M. Wong, E. Memisha, U.S. Patent 6,805,856 (2004).
10. I. E. Markó *et al.*, *Science* **298**, 204 (2002).
11. O. Buisine *et al.*, *Chem. Commun.* **2005**, 3856 (2005).
12. P. B. Hitchcock, M. F. Lappert, N. J. W. Warhurst, *Angew. Chem. Int. Ed. Engl.* **30**, 438 (1991).
13. A. J. Holwell, *Platin. Met. Rev.* **52**, 243 (2008).
14. C.-J. Yang, *Energy Policy* **37**, 1805 (2009).
15. P. J. Chirik, K. Wieghardt, *Science* **327**, 794 (2010).
16. S. Enthaler, K. Junge, M. Beller, in *Iron Catalysis in Organic Chemistry*, B. Plietker, Ed. (Wiley-VCH, Weinheim, Germany, 2008), pp. 125–142.
17. W. M. Czaplik, M. Mayer, J. Cvengros, A. J. von Wangelin, *ChemSusChem* **2**, 396 (2009).
18. J. Y. Corey, J. Braddock-Wilking, *Chem. Rev.* **99**, 175 (1999).
19. M. Zhang, A. Zhang, *Appl. Organomet. Chem.* **24**, 751 (2010).
20. M. A. Schroeder, M. S. Wrighton, *J. Organomet. Chem.* **128**, 345 (1977).
21. R. D. Sanner, R. G. Austin, M. S. Wrighton, W. D. Honnick, C. U. Pittman, *Inorg. Chem.* **18**, 928 (1979).
22. R. H. Morris, *Chem. Soc. Rev.* **38**, 2282 (2009).
23. P. J. Chirik, in *Catalysis Without Precious Metals* (Wiley-VCH, Weinheim, Germany, 2010), pp. 83–106.
24. B. Marciniec, *Silicon Chem.* **1**, 155 (2002).
25. J. C. Mitchener, M. S. Wrighton, *J. Am. Chem. Soc.* **103**, 975 (1981).
26. F. Kakiuchi, Y. Tanaka, N. Chatani, S. Murai, *J. Organomet. Chem.* **456**, 45 (1993).
27. S. C. Bart, E. Lobkovsky, P. J. Chirik, *J. Am. Chem. Soc.* **126**, 13794 (2004).
28. J. Y. Wu, B. N. Stanzl, T. Ritter, *J. Am. Chem. Soc.* **132**, 13214 (2010).
29. S. K. Russell, J. M. Darmon, E. Lobkovsky, P. J. Chirik, *Inorg. Chem.* **49**, 2782 (2010).
30. J. W. Sprengers, M. de Greef, M. A. Duin, C. J. Elsevier, *Eur. J. Inorg. Chem.* **2003**, 3811 (2003).
31. R. J. Trovitch, E. Lobkovsky, P. J. Chirik, *J. Am. Chem. Soc.* **130**, 11631 (2008).
32. P. J. G. Stevens, *Pestic. Sci.* **38**, 103 (1993).

Acknowledgments: We thank Momentive Performance Materials for financial support. Portions of this work have been published in the following patent applications: US2011/0009573 A1 and U.S. serial no. 13/325,250.

Supporting Online Material

www.sciencemag.org/cgi/content/full/335/6068/567/DC1
SOM Text
Figs. S1 to S14
Tables S1 to S3
References (*33*, *34*)

26 September 2011; accepted 29 November 2011
10.1126/science.1214451

High-Latitude Forcing of the South American Summer Monsoon During the Last Glacial

Lisa C. Kanner,[1]* Stephen J. Burns,[1] Hai Cheng,[2,3] R. Lawrence Edwards[3]

The climate of the Last Glacial period (10,000 to 110,000 years ago) was characterized by rapid millennial-scale climate fluctuations termed Dansgaard/Oeschger (D/O) and Heinrich events. We present results from a speleothem-derived proxy of the South American summer monsoon (SASM) from 16,000 to 50,000 years ago that demonstrate the occurrence of D/O cycles and Heinrich events. This tropical Southern Hemisphere monsoon reconstruction illustrates an antiphase relationship to Northern Hemisphere monsoon intensity at the millennial scale. Our results also show an influence of Antarctic millennial-scale climate fluctuations on the SASM. This high-resolution, precisely dated, tropical precipitation record can be used to establish the timing of climate events in the high latitudes of the Northern and Southern Hemispheres.

Dansgaard/Oeschger (D/O) and Heinrich events have been recognized in many terrestrial and marine records, particularly from the Northern Hemisphere. First observed in oxygen isotope ratios of ice cores from Greenland (*1*), the D/O cycles are interpreted as large abrupt warmings (interstadials) followed by more gradual cooling to stadial conditions. The D/O cycles are particularly well expressed in tropical Northern Hemisphere speleothem records, where cold and warm periods in Greenland are coincident with dry and wet periods, respectively, in the East Asian and Indian summer monsoons (EASM and ISM) (*2*–*4*). The presence of D/O cycles in the Southern Hemisphere, or their relation to Southern Hemisphere monsoons, has not been established, however. Heinrich events are pronounced cold intervals (~500 ± 250 years in duration) marked by horizons of ice-rafted debris in ocean sediment cores from mid-latitudes in the Atlantic Ocean (*5*–*7*). Although an interhemispheric antiphased relation has been observed for the Heinrich (H1 to H6) events, the specific timing and duration are less well constrained because of uncertainties in ocean reservoir ages (*8*) and changes in sediment accumulation rates. Here we present a high-resolution, precisely dated, speleothem reconstruction of South American summer monsoon (SASM) intensity for the Last Glacial period. This record demonstrates the presence of D/O cycles in the SASM, where an intensified SASM is associated with stadial events in Greenland. In addition, we identify millennial-scale climate events that resulted from the interplay between rapid Antarctic warming and cool North Atlantic Heinrich events. Finally, we use the signature of the major D/O cycles to propose possible constraints on the timing and duration of Heinrich events H4 and H5.

We collected stalagmite P09-PH2 from Pacupahuain Cave (11.24°S, 75.82°W; 3800 m above sea level) in the central Peruvian Andes (fig. S1). Pacupahuain Cave was formed in a Triassic dolomitic limestone massif (*9*) and in an area where glacial landforms are not present. P09-PH2 is a calcite stalagmite 16 centimeters tall and was collected in the cave's main gallery about 500 m from the entrance. The speleothem was halved along the growth axis and subsampled along growth layers for radiometric dating, using uranium-thorium (U-Th) techniques by

[1]Department of Geosciences, University of Massachusetts, Amherst, MA 01002, USA. [2]Institute of Global Environmental Change, Xi'an Jiaotong University, Xi'an 710049, China. [3]Department of Geology and Geophysics, University of Minnesota, Minneapolis, MN 55455, USA.

*To whom correspondence should be addressed. E-mail: lkanner@geo.umass.edu

Downloaded from www.sciencemag.org on February 2, 2012

multicollector inductively coupled plasma mass spectroscopy (MC-ICP-MS) (*10*, *11*). Seventeen ^{230}Th dates, all in stratigraphic order, have analytical errors <0.4% (fig. S2 and table S1). An age model was developed based on linear interpolation between adjacent age measurements, yielding an age range for the sample of 16,020 to 49,470 years before the present (yr B.P., with the present = 1950).

Stable oxygen and carbon isotope ratios (δ^{18}O and δ^{13}C) were measured on 1076 micromilled samples taken along the growth axis. The average sampling resolution is approximately 30 years. The very low correlation (coefficient of determination $r^2 = 0.1$) between δ^{13}C and δ^{18}O values along the growth axis (fig. S3) indicates that kinetic fractionation did not significantly influence speleothem isotopic variability (*11*, *12*). P09-PH2 δ^{18}O values range from –14 per mil (‰) to –17.5‰ between 16 and 50 thousand yr B.P. (ky B.P.) (Fig. 1). The δ^{18}O record is characterized by high-amplitude millennial-scale events, with rapid increases of up to 2.5‰ occurring over a century or less. The decline to local δ^{18}O minima occurred more gradually, over periods ranging from a few centuries to a few millennia. The lowest values in the record occur over an extended period of time between 28.8 to 30.3 ky B.P. The highest values are attained over very brief intervals at 16, 37, 38, and 47 ky B.P.

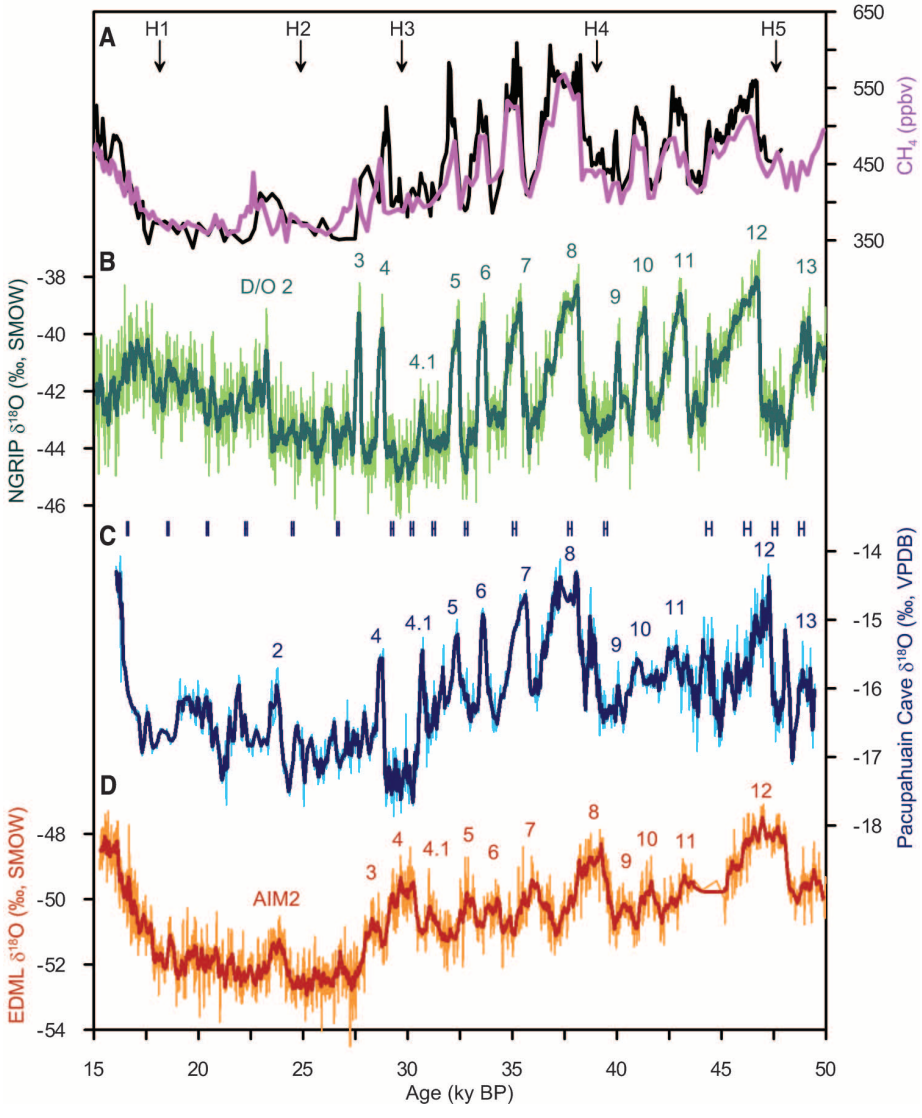


Fig. 1. The δ^{18}O reconstruction of stalagmite P09-PH2 compared to high-latitude ice core δ^{18}O and CH_4 concentrations. SMOW, standard mean ocean water standard; ppbv, parts per billion by volume; VPDB, Vienna Pee Dee belemnite standard. (**A**) GRIP and NGRIP CH_4 (black) (*24*, *25*) and EDML CH_4 (purple) (*23*) concentrations. (**B**) NGRIP ice core δ^{18}O (dark green, 7-point running mean) (*22*). (**C**) Speleothem P09-PH2 δ^{18}O time series with U/Th dates with 2σ uncertainty bars (dark blue, 3-point running mean). (**D**) EDML ice core δ^{18}O (red, 7-point running mean) (*23*). The age models for Greenland and Antarctica δ^{18}O and NGRIP and EDML CH_4 concentrations from (*22*) are shown. GRIP CH_4 concentrations are shown on the Greenland Ice Sheet Project 2 time scale from (*25*). The time scale of P09-PH2 is given on its own age model (fig. S2). The Heinrich events are depicted by the vertical arrows, and age estimations are from (*4*, *7*). The numbers indicate Greenland interstadials and Antarctic AIM events.

The primary climatic control on rainfall δ^{18}O for tropical South America is the amount of precipitation (*13*). Consistent with the "amount effect" (*14*) and Rayleigh-type fractionation during rainout, a stronger SASM leads to lower δ^{18}O values in tropical South American rainfall (*15*). Similar correlations have been made for other parts of the tropical Andes, where local precipitation δ^{18}O is strongly anticorrelated to rainfall amount upstream in the Amazon Basin rather than at the study site (*16*, *17*). Rayleigh distillation and moisture recycling in the Amazon Basin (*18*) preserve the isotopic signal of the monsoon along the moisture path from eastern Amazonia up to the central Peruvian Andes (*15*). On interannual time scales, the SASM is influenced by sea surface temperatures (SSTs) in the Atlantic and Pacific Oceans (*19*) and on orbital time scales by changes in insolation (*20*, *21*). These studies demonstrate that rainfall δ^{18}O in the central Andes records changes in the intensity of large-scale continental atmospheric convection, with more negative rainfall δ^{18}O values being indicative of enhanced SASM activity and increased rainout.

Comparison of the millennial-scale variability in the Pacupahuain Cave record to the isotopic fluctuations from Greenland (Fig. 1) shows that all D/O cycles are also found in our record of SASM intensity, with the sole exception of D/O event 3, which for unknown reasons is not present. The identification of D/O events is based on comparison to the North Greenland Ice Core Project (NGRIP) oxygen isotope record, using the ice core age model of (*22*) (Fig. 1) and the MSD speleothem record from Hulu Cave, China, using its own precise chronology (fig. S4) (*4*, *11*). Abrupt increases in NGRIP $\delta^{18}O_{ice}$, which characterize the onset of the D/O events, are clearly associated with rapid increases in $\delta^{18}O_{calcite}$ for P09-PH2. The relationship between D/O events in the NGRIP record and our results demonstrates that warm events in Greenland correspond to intervals of decreased SASM intensity. The timing of millennial-scale variability is synchronous within the independent age model errors.

Figure 1 also includes the record of atmospheric methane (CH_4) concentrations from Greenland and Antarctic ice cores (*23*–*25*). The origin

Downloaded from www.sciencemag.org on February 2, 2012

of millennial-scale variations in atmospheric CH_4 is not certain, although they are thought to arise from changes in the flux from global wetlands (*26*, *27*) rather than from the release of CH_4 from marine clathrates (*28*) or changes in CH_4 removal via oxidation in the troposphere (*26*). Whether source flux changes derive from tropical wetlands or boreal forests has not been established. We observe that increases in global atmospheric CH_4 occur contemporaneously with increases in P09-PH2 $\delta^{18}O$ and reduced SASM intensity (Fig. 1). Thus, the Southern Hemisphere South American tropics are unlikely to be a source of increased atmospheric CH_4, via wetland expansion, during Greenland interstadials. The interhemispheric antiphasing of the tropical monsoon systems during D/O events, however, indicates that rapid northward shifts of the Intertropical Convergence Zone (ITCZ) and intensification of the EASM and ISM might lead to wetland expansion and increased CH_4 production in the Northern Hemisphere tropics during warm Greenland intervals.

In addition to the millennial-scale D/O events, each Heinrich event (H1 through H5) can also be identified in the P09-PH2 reconstruction by periods of enhanced SASM activity (Fig. 1) and by correlation to decreased Asian monsoon intensity based on the Hulu Cave record (fig. S4) (*4*, *11*). Previous paleoclimate studies of the SASM, which reconstructed precipitation intensity during the Last Glacial period but at lower resolution than presented here, also identified Heinrich events as particularly wet intervals (*29*, *30*). Increased Heinrich event precipitation over tropical South America is supported by evidence of substantial lateral advancement of central Andean glaciers during H1 and H2 (*31*) and increases in precipitation over northeast Brazil for H1 through H5 (*30*, *32*, *33*).

The expression of D/O cycles and Heinrich events in SASM variability is antiphased with Northern Hemisphere monsoon precipitation reconstructions over the Last Glacial period. Our record indicates a weak SASM during D/O interstadials, but reconstructions of Indian Ocean climate (*2*) and EASM intensity (*4*) demonstrate very wet intervals for interstadial phases. Although previous work has demonstrated such antiphase behavior for orbital-scale climate variability in the tropics (*21*) and for Heinrich events (*30*), it had not been unequivocally determined for D/O scale variability. Such antiphase behavior can be explained by latitudinal shifts of the ITCZ driven by rapid Northern Hemisphere temperature fluctuations. Modeling data demonstrate ITCZ migration away from the hemisphere with high-latitude cooling and added ice cover (*34*). During pronounced North Atlantic cold events, southward migration of the ITCZ can alter Hadley cell circulation, increase subsidence (dry conditions) for the northern branch, and intensify uplift (wet conditions) of the southern branch (*35*, *36*). As a result, the ISM and EASM weaken and the SASM intensifies. Although our record is short relative to precessional-scale insolation changes, insolation appears to be only weakly expressed in our record (fig. S5).

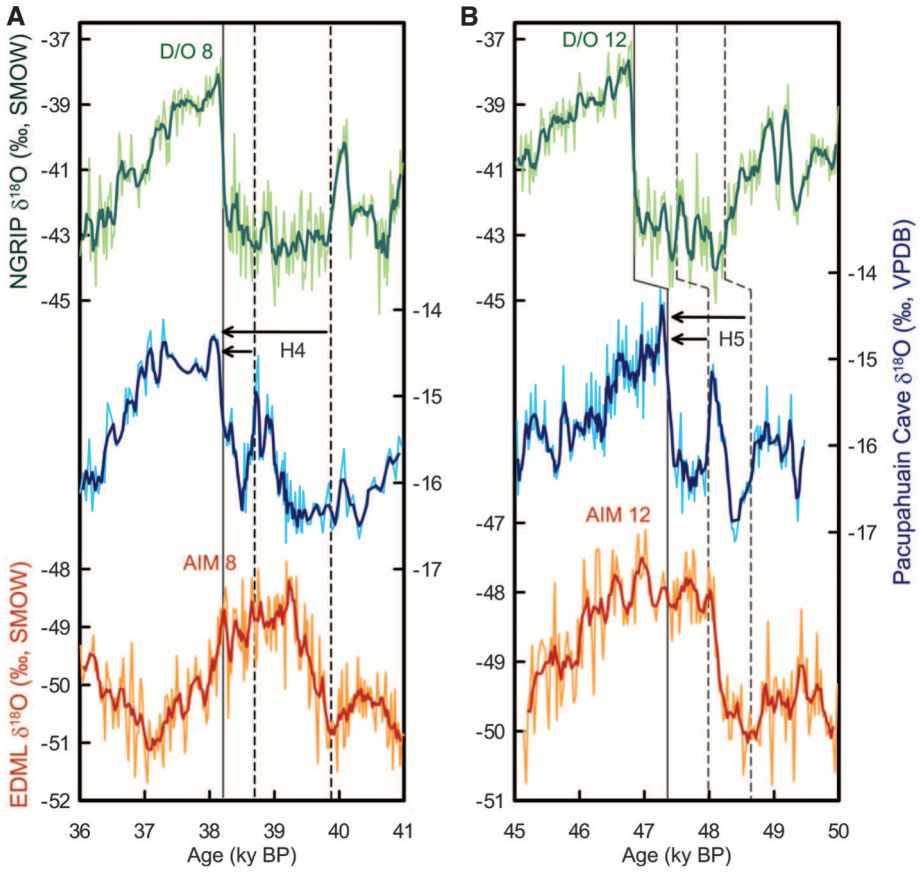


Fig. 2. Detailed view of the $\delta^{18}O$ records from Pacupahuain Cave (blue) and Greenland (green) and Antarctic (red) ice cores during (**A**) Heinrich event 4 and D/O and AIM events 8 and (**B**) Heinrich event 5 and D/O and AIM events 12. The solid black vertical line indicates the end of Heinrich events H4 and H5, and the dashed black vertical lines indicate two possible onsets for Heinrich events H4 and H5. Isotope records and corresponding age models are the same as in Fig. 1.

In addition to demonstrating the presence of D/O and Heinrich variability in the SASM, our record reveals additional rapid, millennial-scale climate reversals in the tropical climate record. These events appear to arise from the interplay between Northern and Southern Hemisphere high-latitude climate change. The reversals are most clearly expressed at 38.75 and 48 ky B.P. during extended Greenland stadials (Fig. 2). We propose that the onset of these events coincides with the onset of Antarctic Isotope Maxima (AIM) events 8 and 12 in the EPICA (European Project for Ice Coring in Antarctica) Dronning Maud Land (EDML) ice core record (*22*). Prolonged Greenland cold phases have been linked with intensification and southward displacement of the Southern Hemisphere westerlies, enhanced upwelling in the Southern Ocean, rising atmospheric CO_2, and Antarctic warming (*37*, *38*). Specifically, the opal flux reconstruction presented in (*38*) demonstrates that ocean upwelling and CO_2 rises were largest during H4 and H5 as compared to more recent Heinrich events. Thus, we propose that enhanced changes in Southern Ocean climate specific to H4 and H5 can explain why our record shows reversals in SASM vigor at H4 and H5 and not for the later Heinrich events.

The precise relation between these transient millennial-scale events and the ice-rafted components of Heinrich events H4 and H5, which occurred at approximately the same time period, is less clear. It is well established that the endings of H4 and H5 occur with Greenland warming at D/O events 8 and 12, respectively, but the beginnings of H4 and H5 are less well constrained. One interpretation based on our record is that the onset of Heinrich events H4 and H5 began with the sharp increase in SASM intensity that follows the decrease associated with Antarctic warming. An abrupt increase in SASM intensity associated with Heinrich events has been recognized in marine (*32*, *33*) and terrestrial (*29*, *30*) records. This sequence of events would restrict the duration of H4 and H5 events to <400 years, which has previously been suggested for H4 (*39*). It would also indicate that Antarctic warming precedes the start of Heinrich events 4 and 5. Antarctic warming has previously been proposed as a trigger for H1 (*40*). A second possibility,

Downloaded from www.sciencemag.org on February 2, 2012

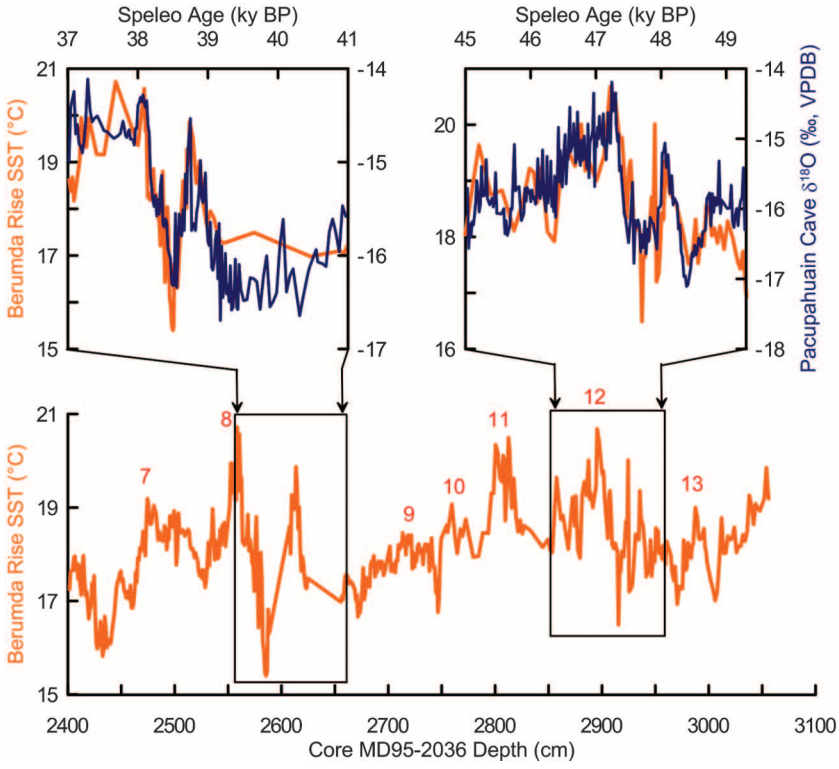


Fig. 3. Bermuda Rise SSTs (orange) shown to depth in core MD95-2036 (*41*). D/O events were identified on the basis of visual correlation to the Greenland isotope temperature record as in (*41*). An expanded view of results from our P09-PH2 record (blue) and subtropical Atlantic SSTs (orange) using our revised age model (*11*) is shown for the intervals of H4 (left) and H5 (right).

however, is that H4 and H5 may have begun before the weakening of the SASM and Antarctic warming and thus lasted throughout the extended Greenland cold phase. Although in this case we have no explanation for why the SASM suddenly strengthened.

One final aspect of the SASM reversals before D/O events 8 and 12 is unusual. High northern latitude warming is associated with an intensification of the Northern Hemisphere monsoons. By analogy, high southern latitude warming might be expected to result in intensification of the SASM, but the opposite is observed. This seeming contradiction can be reconciled by comparison of our record to a high-resolution SST record based on alkenone paleothermometry from the Bermuda Rise (33.69°N, 57.56°W) (*41*). Core MD95-2036 shows large, rapid, warm intervals (warmer by 3° to 5°C) immediately before D/O events 8 and 12, which were originally interpreted as instabilities during the rapid transitions of the largest Greenland interstadials. Based on visual comparison, we establish tie points between the Bermuda Rise SST record and our $\delta^{18}O$ record and provide a revised age model for these two oscillations in Bermuda Rise SSTs (*11*) (Fig. 3). The original marine core chronology was based on maximizing the correlation to the Greenland ice core record and its chronology at the time of publication (*11*, *42*). Our revised chronology for the two intervals of MD95-2036 places the warm intervals 600 ± 100 years earlier, relative to an updated Greenland chronology, which is well within the thousand-year uncertainty of the original marine core age model. Thus, Antarctic warming at AIM events 8 and 12 may be associated with a weakened SASM as described above (Fig. 2), as well as a warmer subtropical North Atlantic Ocean (Fig. 3) (*41*). Similar temperature reversals within H4 and H5 have been identified in a deep water record from the Iberian Margin (*43*). It is not clear why Antarctic warming is associated with warming in the subtropical North Atlantic, although one result of the latter could be a northward shift of the ITCZ in the Atlantic Ocean sector (*44*) due to a weakening of the subtropical Atlantic gyre. The association between warm SSTs in the Bermuda Rise region, a weakening of the SASM, and a more northerly position of the ITCZ, as we have described for the D/O events, could also be applied to the additional reversals identified in Fig. 3.

References and Notes

1. W. Dansgaard *et al.*, *Nature* **364**, 218 (1993).
2. S. J. Burns, D. Fleitmann, A. Matter, J. Kramers, A. A. Al-Subbary, *Science* **301**, 1365 (2003).
3. Y. Wang *et al.*, *Nature* **451**, 1090 (2008).
4. Y. J. Wang *et al.*, *Science* **294**, 2345 (2001).
5. H. Heinrich, *Quat. Res.* **29**, 142 (1988).
6. G. Bond *et al.*, *Nature* **360**, 245 (1992).
7. S. R. Hemming, *Rev. Geophys.* **42**, RG1005 (2004).
8. T. F. Stocker, *Radiocarbon* **40**, 359 (1998).
9. E. J. Cobbing *et al.*, in *The Geology of the Western Cordillera of Northern Peru* (Great Britian Institute of Geological Sciences, Natural Environment Research Council, London, 1981), p. 143.
10. H. Cheng *et al.*, *Geology* **37**, 1007 (2009).
11. Information on materials and methods is available as supporting material on *Science* Online.
12. C. H. Hendy, *Geochim. Cosmochim. Acta* **35**, 801 (1971).
13. M. Vuille, R. S. Bradley, M. Werner, R. Healy, F. Keimig, *J. Geophys. Res.* **108**, 4174 (2003).
14. W. Dansgaard, *Tellus* **16**, 436 (1964).
15. M. Vuille, M. Werner, *Clim. Dyn.* **25**, 401 (2005).
16. F. Vimeux, R. Gallaire, S. Bony, G. Hoffmann, J. Chiang, *Earth Planet. Sci. Lett.* **240**, 205 (2005).
17. G. Hoffmann *et al.*, *Geophys. Res. Lett.* **30**, 1179 (2003).
18. R. L. Victoria, L. A. Martinelli, J. Mortatti, J. Richey, *Ambio* **20**, 384 (1991).
19. M. Vuille, R. S. Bradley, F. Keimig, *J. Geophys. Res.* **105**, 12447 (2000).
20. G. Seltzer, D. Rodbell, S. Burns, *Geology* **28**, 35 (2000).
21. F. W. Cruz Jr. *et al.*, *Nature* **434**, 63 (2005).
22. B. Lemieux-Dudon *et al.*, *Quat. Sci. Rev.* **29**, 8 (2010).
23. C. Barbante *et al.*; EPICA Community Members, *Nature* **444**, 195 (2006).
24. J. Flückiger, *Global Biogeochem. Cycles* **18**, GB1020 (2004).
25. T. Blunier, E. J. Brook, *Science* **291**, 109 (2001).
26. J. Chappellaz *et al.*, *Nature* **366**, 443 (1993).
27. A. Dällenbach *et al.*, *Geophys. Res. Lett.* **27**, 1005 (2000).
28. M. Bock *et al.*, *Science* **328**, 1686 (2010).
29. X. Wang *et al.*, *Quat. Sci. Rev.* **25**, 3391 (2006).
30. X. F. Wang *et al.*, *Nature* **432**, 740 (2004).
31. J. A. Smith, D. T. Rodbell, *J. Quat. Sci.* **25**, 243 (2010).
32. A. Jaeschke, C. Ruhlemann, H. Arz, G. Heil, G. Lohmann, *Paleoceanography* **22**, PA4206 (2007).
33. T. C. Jennerjahn *et al.*, *Science* **306**, 2236 (2004).
34. J. C. H. Chiang, C. M. Bitz, *Clim. Dyn.* **25**, 477 (2005).
35. R. Zhang, T. L. Delworth, *J. Clim.* **18**, 1853 (2005).
36. A. C. Clement, L. C. Peterson, *Rev. Geophys.* **46**, RG4002 (2008).
37. G. H. Denton *et al.*, *Science* **328**, 1652 (2010).
38. R. F. Anderson *et al.*, *Science* **323**, 1443 (2009).
39. D. Roche, D. Paillard, E. Cortijo, *Nature* **432**, 379 (2004).
40. A. J. Weaver, O. A. Saenko, P. U. Clark, J. X. Mitrovica, *Science* **299**, 1709 (2003).
41. J. P. Sachs, S. J. Lehman, *Science* **286**, 756 (1999).
42. E. A. Boyle, *Proc. Natl. Acad. Sci. U.S.A.* **94**, 8300 (1997).
43. L. C. Skinner, H. Elderfield, *Paleoceanography* **22**, PA1205 (2007).
44. A. J. Broccoli, K. A. Dahl, R. J. Stouffer, *Geophys. Res. Lett.* **33**, L01702 (2006).

Acknowledgments: This work is supported by NSF grant ATM-1003466 to S.J.B., NSF grants 0502535 and 1103403 to R.L.E. and H.C., and Geological Society of America Student Award 9308-10 to L.C.K. We thank C. Morales-Bermudez for his invaluable assistance in the field. Comments from two anonymous reviewers substantially improved the manuscript. The data in this paper are tabulated in the supporting online material and are archived online at ftp://ftp.ncdc.noaa.gov/pub/data/paleo.

Supporting Online Material

www.sciencemag.org/cgi/content/full/science.1213397/DC1
Materials and Methods
Figs. S1 to S5
Table S1
References (*45*–*51*)

31 August 2011; accepted 4 January 2012
Published online 12 January 2012;
10.1126/science.1213397

Downloaded from www.sciencemag.org on February 2, 2012

Natural Variation in a Chloride Channel Subunit Confers Avermectin Resistance in *C. elegans*

Rajarshi Ghosh, Erik C. Andersen, Joshua A. Shapiro, Justin P. Gerke,* Leonid Kruglyak†

Resistance of nematodes to anthelmintics such as avermectins has emerged as a major global health and agricultural problem, but genes conferring natural resistance to avermectins are unknown. We show that a naturally occurring four-amino-acid deletion in the ligand-binding domain of GLC-1, the alpha-subunit of a glutamate-gated chloride channel, confers resistance to avermectins in the model nematode *Caenorhabditis elegans*. We also find that the same variant confers resistance to the avermectin-producing bacterium *Streptomyces avermitilis*. Population-genetic analyses identified two highly divergent haplotypes at the *glc-1* locus that have been maintained at intermediate frequencies by long-term balancing selection. These results implicate variation in glutamate-gated chloride channels in avermectin resistance and provide a mechanism by which such resistance can be maintained.

Avermectins are secondary metabolites of the cosmopolitan soil bacterium *Streptomyces avermitilis* (*1*) that are used for management of agricultural and parasitic nematode infestations. Abamectin (a mixture of avermectin B1a and B1b) is an agricultural pesticide, and ivermectin (a synthetic derivative of avermectin B1a and B1b) is a veterinary and human anthelmintic (*2*). Responses to avermectins by nematodes are thought to be dependent on a diverse set of molecules, including glutamate-gated chloride channels and P-glycoproteins (*3*). Widespread resistance of nematodes to these drugs is a global concern for agriculture and health (*4*), but the genetic basis of natural resistance to avermectins has remained elusive (*4*, *5*).

To investigate the genetic basis of natural avermectin resistance, we used a swimming assay (*6*) to quantify the ability of avermectins to induce paralysis (*7*) in strains of the nematode *Caenorhabditis elegans* isolated from different geographical locations. We found that a Hawaiian wild isolate of *C. elegans*, CB4856, was resistant to abamectin and ivermectin, while the laboratory strain, N2, was sensitive under identical conditions; for example, exposure to 0.5 μg/ml of abamectin for 30 min resulted in paralysis of 98% of N2 worms but only 17% of CB4856 worms (Fig. 1, A and B, and figs. S1A and S2). As a comparison, ivermectin reduces worm load by 100% in cattle infected with ivermectin-sensitive parasitic nematode *Cooperia oncophora* and by 70% in cattle infected with ivermectin-resistant *C. oncophora* (*8*). F1 heterozygotes from reciprocal crosses between N2 and CB4856 were as sensitive to abamectin as the N2 parent (Fig. 1, A and B), which suggests that abamectin resistance may be a recessive trait caused by a loss-of-function allele in CB4856.

To identify the gene(s) responsible for the observed difference in abamectin response, we carried out quantitative trait locus (QTL) mapping in a panel of recombinant inbred advanced intercross lines (RIAILs) generated from crosses between the N2 and CB4856 strains (*9*). We measured the frequency of body bends, as well as the probability of animals being paralyzed after 30 min in 0.5 μg/ml abamectin, for 210 RIAILs. The traits were not normally distributed and were significantly correlated with each other (fig. S3A). Nonparametric interval-mapping (*10*) for all measures of response to abamectin revealed a major QTL on chromosome V (Fig. 2A and fig. S3B). RIAILs bearing the CB4856 allele at this locus exhibited higher mean frequency of body bends and lower probability of being paralyzed after 30 min of exposure to

Lewis-Sigler Institute for Integrative Genomics, Department of Ecology and Evolutionary Biology, and Howard Hughes Medical Institute, Princeton University, Princeton, NJ 08544, USA.

*Present address: Pioneer Hi-Bred International, A DuPont Business, Johnston, IA 50131, USA

†To whom correspondence should be addressed. E-mail: leonid@genomics.princeton.edu (L.K.)

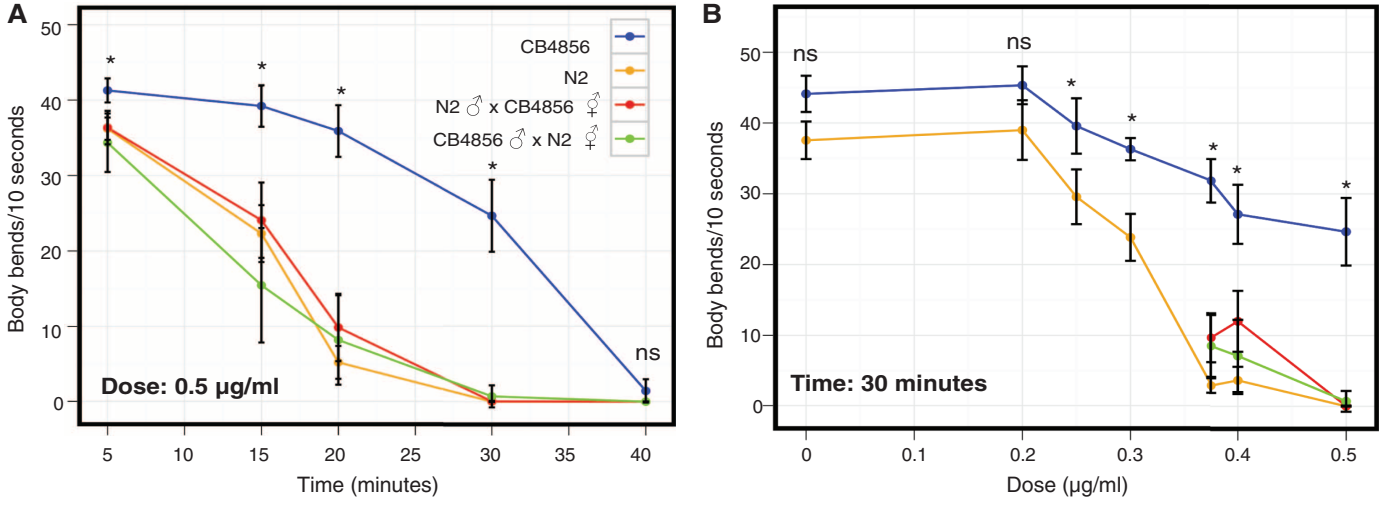


Fig. 1. Sensitivity to abamectin differs between N2 and CB4856. (**A**) Time course of frequency of body bends ($n \geq 20$ animals for each strain). *, significantly different from CB4856 ($P < 0.01$). The legend depicts the strains and their respective colors in (A) and (B). (**B**) Frequency of body bends at 30 min plotted against different doses of abamectin for N2 (orange, $n \geq 12$ animals at each dose); CB4856 (blue, $n \geq 12$ animals at each dose); F1 progeny from crosses between N2 males and CB4856 hermaphrodites (red, $n \geq 18$ animals at each dose); and F1 progeny from crosses between CB4856 males and N2 hermaphrodites (green, $n \geq 28$ animals at each dose). Heterozygotes were scored only at 0.375 μg/ml, 0.4 μg/ml, and 0.5 μg/ml abamectin. Error bars, mean ± SEM for each strain. ns, nonsignificant difference. *, $P < 0.01$. P values are from Mann-Whitney tests for concentrations of 0 to 0.3 μg/ml. For the higher concentrations, where more than two groups were involved, a Kruskal-Wallis test followed by Dunn's multiple comparison test was performed.

Downloaded from www.sciencemag.org on February 2, 2012

abamectin (Fig. 2C), but not all RIAILs with this allele were resistant, which suggests that additional loci are likely involved. Analysis of abamectin response as a binary trait (*6*) revealed a second QTL on chromosome III (fig. S3, C and D). Joint QTL analysis of the loci on chromosomes V and III indicated that they act additively and explain ~26% and ~6% of the phenotypic variance, respectively (*6*) (table S1).

Genotyping of additional markers in RIAILs followed by transgenic rescue with fosmids identified an 11.4-kb segment of N2 DNA that abolished abamectin resistance in CB4856 (Fig. 2, B and D to G, and fig. S5, A to C). This region contained six genes, one of which, *glc-1*, encodes the alpha subunit of a glutamate-gated chloride channel (*11*–*13*), a known target of avermectins (*11*, *12*). A 4.5-kb N2 genomic fragment containing two genes, including *glc-1*, significantly reduced abamectin resistance of CB4856 (Fig. 2, F and G, and fig. S5D), supporting *glc-1* as a candidate causal gene. Crossing CB4856 with the *glc-1(pk54)* mutant strain, which harbors a presumptive loss-of-function allele of *glc-1* in the N2 background (*12*), resulted in F1 progeny resistant to abamectin, in contrast to F1 progeny from crosses between N2 and *glc-1(pk54)*, which were sensitive (Fig. 3A). Introgression of the *glc-1* region from N2 into CB4856 restored sensitivity to abamectin, whereas introgression of this region with the *glc-1(pk54)* mutation resulted in abamectin resistance comparable to CB4856 (Fig. 3A). These and additional results (*6*) (fig. S4) are consistent with a loss-of-function CB4856 allele of *glc-1* conferring abamectin resistance in this genetic background (*6*).

To identify the underlying functional polymorphism(s), we sequenced the N2 and CB4856 alleles of *glc-1*. Relative to N2, CB4856 had 77 single-nucleotide polymorphisms (SNPs) in the coding region, 32 of which resulted in amino-acid changes, as well as a four-amino-acid deletion in exon two (fig. S6A). Despite the multiple coding polymorphisms, the predicted secondary structure and membrane topology of GLC-1 from N2 and CB4856 were similar (*6*) (fig. S6, B and C). Alignment of the predicted structure of CB4856 GLC-1 with the three-dimensional structure (*14*) of homomeric GLC-1 bound to ivermectin and glutamate revealed no obvious changes in the overall structure of GLC-1 (fig. S6C). Based on structure and annotation, we selected three candidate polymorphisms for further analysis. A threonine-to-alanine substitution at position 346 may weaken binding to avermectins by eliminating one of three hydrogen bonds between GLC-1 and ivermectin (fig. S6C), an alanine-to-threonine change at position 20 may reduce the cleavage probability of the signal peptide (*6*), and a four-amino-acid deletion in the ligand-binding domain of GLC-1 may interfere with the kinetics of glutamate binding. Comparison with the closest homolog of *glc-1* in *C. elegans, avr-15*, showed that the CB4856 deletion allele is likely derived (fig. S7A).

To determine whether any of these polymorphisms confer resistance to abamectin in CB4856, we transformed CB4856 with N2 *glc-1* cDNA constructs driven by a 1.1-kb *glc- 1* promoter,

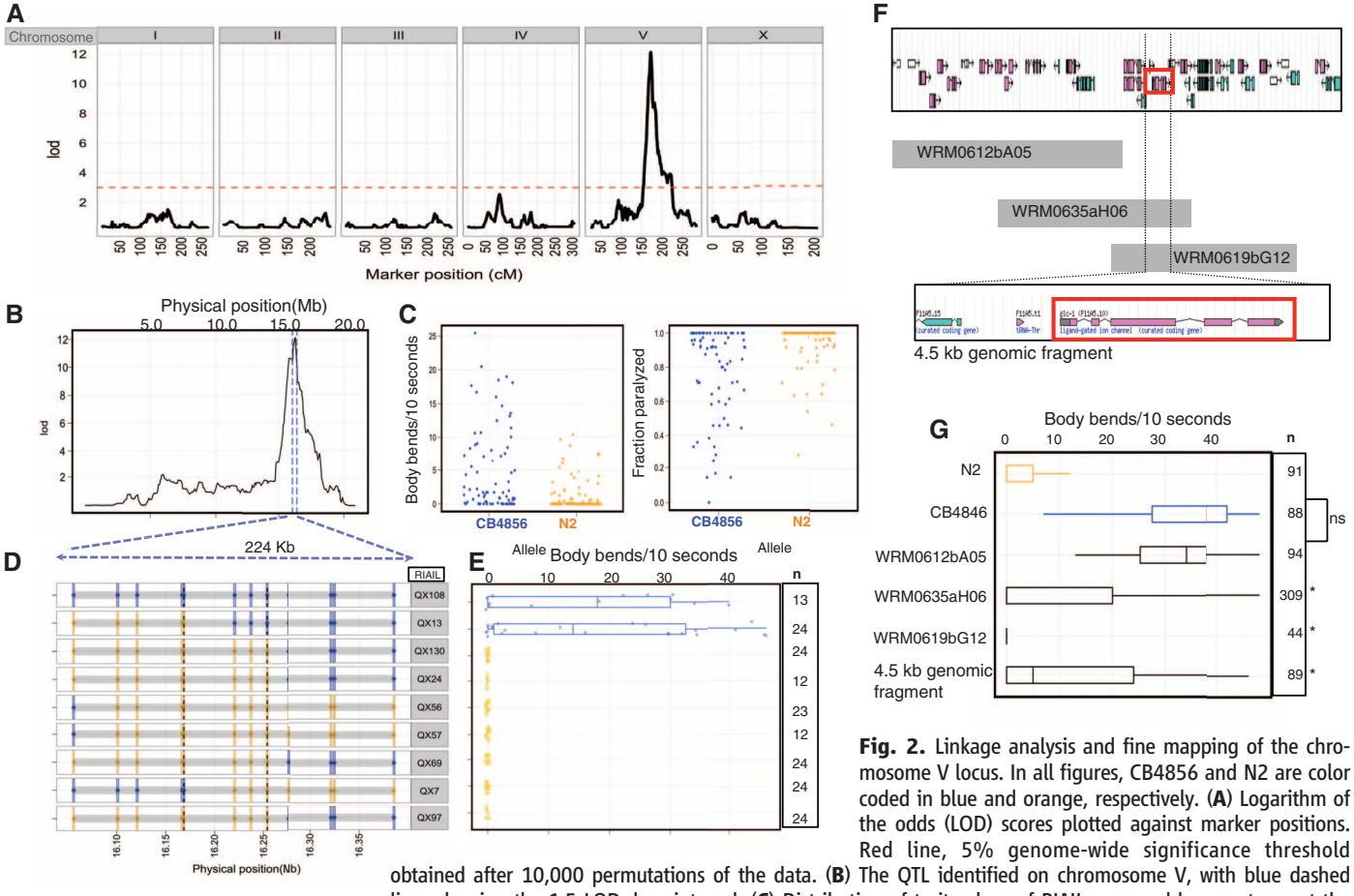


Fig. 2. Linkage analysis and fine mapping of the chromosome V locus. In all figures, CB4856 and N2 are color coded in blue and orange, respectively. (**A**) Logarithm of the odds (LOD) scores plotted against marker positions. Red line, 5% genome-wide significance threshold obtained after 10,000 permutations of the data. (**B**) The QTL identified on chromosome V, with blue dashed lines showing the 1.5 LOD-drop interval. (**C**) Distribution of trait values of RIAILs grouped by genotypes at the marker corresponding to the maximum LOD score on chromosome V. (**D**) Genotypes of RIAILs with breakpoints within the QTL interval. Vertical bars with dots are genotyped markers. (**E**) Box plots of body-bend frequency of RIAILs. Each dot represents a single individual. (**F**) (Top) 107-kb genomic interval within the QTL on chromosome V. (Middle) Horizontal gray bars depict the region of the genome (upper panel) covered by each fosmid. The bottom pull-out shows the 4.5-kb N2 genomic fragment. (**G**) Box plots of the frequency of body bends in abamectin of parental and transgenic strains in CB4856 background harboring indicated N2 fosmids and a genomic clone. Pooled data of rescue lines for each fosmid or genomic fragment are plotted (individual lines are shown in fig. S3). ns, nonsignificant difference. *, $P < 0.001$ from CB4856.

Downloaded from www.sciencemag.org on February 2, 2012

separately harboring each of these three sequence changes observed in CB4856. The N2 *glc-1* cDNA induced sensitivity to abamectin in the otherwise resistant CB4856 strain (Fig. 3B and fig. S5, I and J). Similar results were obtained when CB4856 worms were transformed with N2 *glc-1* cDNA harboring the amino-acid substitutions in the signal peptide (A20T) or in the avermectin binding domain (T346A) (Fig. 3B and fig. S5, L to N). However, the construct harboring the deletion in the ligand-binding domain failed to induce sensitivity to abamectin in

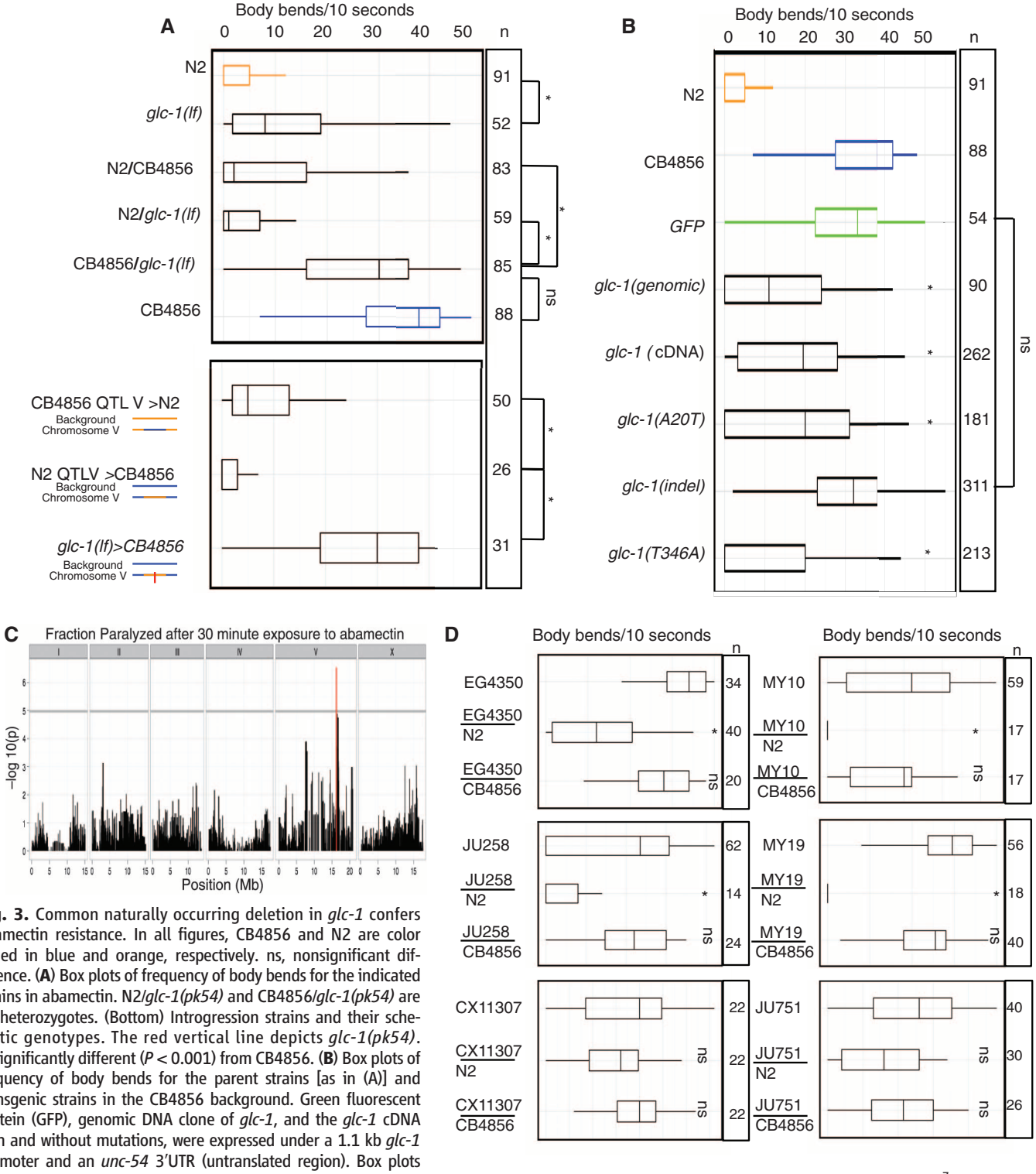


Fig. 3. Common naturally occurring deletion in *glc-1* confers abamectin resistance. In all figures, CB4856 and N2 are color coded in blue and orange, respectively. ns, nonsignificant difference. (**A**) Box plots of frequency of body bends for the indicated strains in abamectin. N2/*glc-1(pk54)* and CB4856/*glc-1(pk54)* are F1 heterozygotes. (Bottom) Introgression strains and their schematic genotypes. The red vertical line depicts *glc-1(pk54)*. *, significantly different ($P < 0.001$) from CB4856. (**B**) Box plots of frequency of body bends for the parent strains [as in (A)] and transgenic strains in the CB4856 background. Green fluorescent protein (GFP), genomic DNA clone of *glc-1*, and the *glc-1* cDNA with and without mutations, were expressed under a 1.1 kb *glc-1* promoter and an *unc-54* 3′UTR (untranslated region). Box plots show pooled data of individual lines shown in fig. S3. CB4856 was transformed with *glc-1* cDNA harboring the following mutations: *glc-1(A20T)*, *glc-1(indel)*, and *glc-1(T346A)*. *, $P < 0.001$ significant difference from GFP. (**C**) Genome-wide association mapping for fraction of worms paralyzed in abamectin. Significantly associated markers ($P < 3 \times 10^{-7}$) are indicated by red lines. (**D**) Box plots of body bends per 10 s in 0.375 μg/ml abamectin are plotted for each wild isolate and the indicated F1 heterozygotes. *, significantly different from the corresponding wild isolate ($P < 0.01$).

Downloaded from www.sciencemag.org on February 2, 2012

CB4856, demonstrating that the four-amino-acid deletion alone is sufficient to generate resistance to abamectin (Fig. 3B and fig. S5K). We cannot rule out the possibility that other polymorphic residues also contribute to abamectin resistance.

A genome-wide association study measuring abamectin resistance in a diverse worldwide collection of 97 wild *C. elegans* isolates identified nine SNPs that were significantly associated ($P < 3 \times 10^{-7}$) with the fraction of worms paralyzed in abamectin (Fig. 3C). These SNPs all fell within a ~47-kb region of linkage disequilibrium that includes *glc-1* (fig. S9). We sequenced *glc-1* in 53 diverse wild isolates and found that 16 carried CB4856-like alleles, including the four-amino-acid deletion, and 37 carried N2-like alleles lacking the deletion. As expected, the presence of the deletion was significantly associated (Pearson's $r = 0.62$, $P < 0.0001$) with abamectin resistance (fig. S8). However, some isolates with the deletion were sensitive, and some isolates lacking it were resistant, indicating that other genetic factors influence abamectin response. We crossed six resistant wild isolates carrying CB4856-like *glc-1* alleles to N2 and CB4856 and measured the abamectin response of the F1 cross-progeny (Fig. 3D). F1 progeny from crosses of MY10, JU258, EG4350, and MY19 to N2 were sensitive,

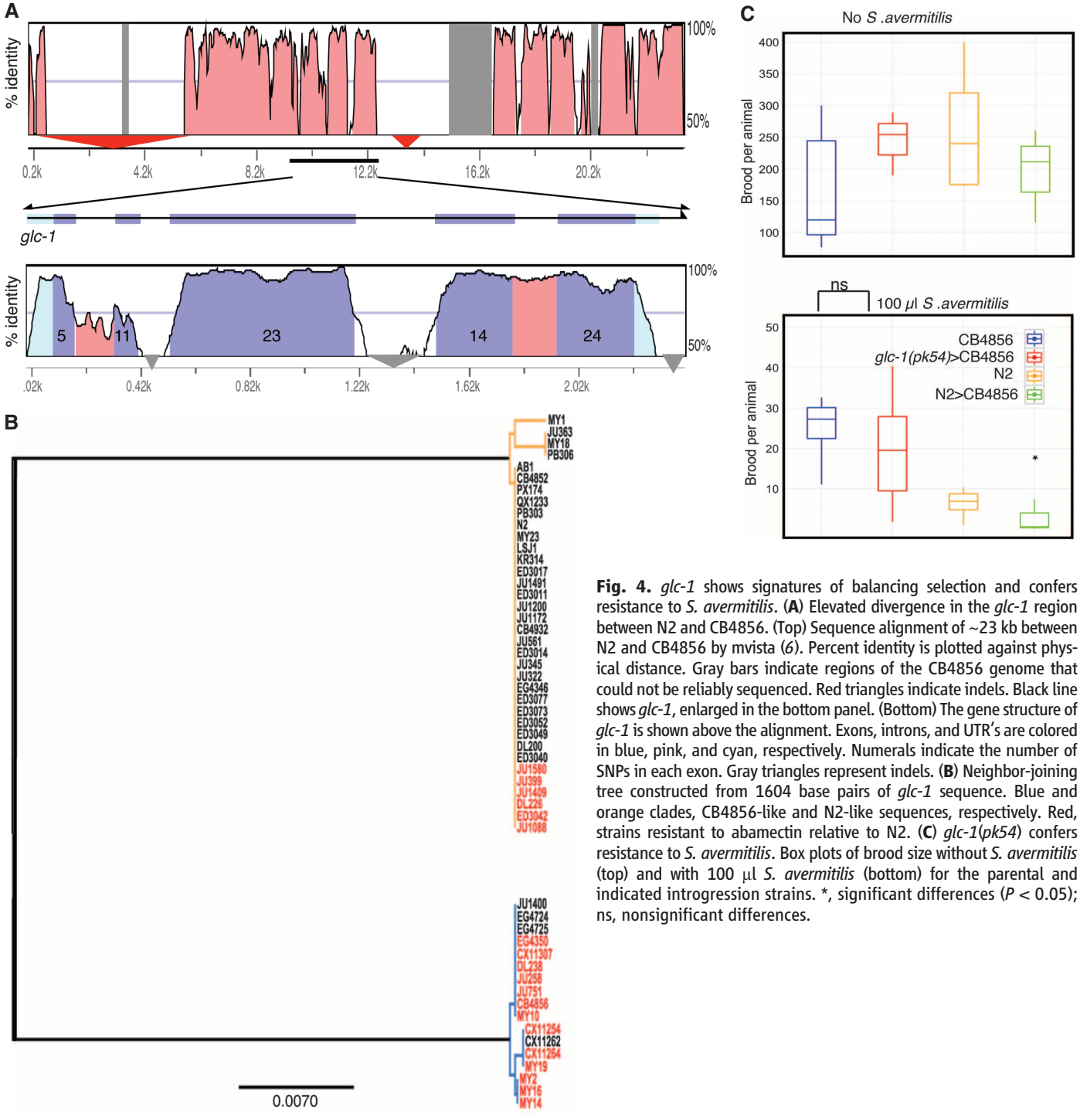


Fig. 4. *glc-1* shows signatures of balancing selection and confers resistance to *S. avermitilis*. (**A**) Elevated divergence in the *glc-1* region between N2 and CB4856. (Top) Sequence alignment of ~23 kb between N2 and CB4856 by mvista (*6*). Percent identity is plotted against physical distance. Gray bars indicate regions of the CB4856 genome that could not be reliably sequenced. Red triangles indicate indels. Black line shows *glc-1*, enlarged in the bottom panel. (Bottom) The gene structure of *glc-1* is shown above the alignment. Exons, introns, and UTR's are colored in blue, pink, and cyan, respectively. Numerals indicate the number of SNPs in each exon. Gray triangles represent indels. (**B**) Neighbor-joining tree constructed from 1604 base pairs of *glc-1* sequence. Blue and orange clades, CB4856-like and N2-like sequences, respectively. Red, strains resistant to abamectin relative to N2. (**C**) *glc-1*(*pk54*) confers resistance to *S. avermitilis*. Box plots of brood size without *S. avermitilis* (top) and with 100 µl *S. avermitilis* (bottom) for the parental and indicated introgression strains. *, significant differences ($P < 0.05$); ns, nonsignificant differences.

Downloaded from www.sciencemag.org on February 2, 2012

whereas F1 progeny from crosses of these isolates to CB4856 were resistant, consistent with abamectin resistance in these strains also arising from loss of *glc-1* function. However, F1 progeny from crosses of CX11307 and JU751 to both CB4856 and N2 were resistant, despite the same *glc-1* sequence, suggesting the presence of a second, dominant resistance factor in these isolates (Fig. 3D). Taken together, these results imply that variation in *glc-1* plays a major role in shaping abamectin resistance among *C. elegans* isolates, but the trait also involves other loci.

The *glc-1* region exhibited high sequence divergence between N2 and CB4856 (Fig. 4A), with 178 SNPs in ~5 kb, a polymorphism rate ~30 times higher than the genome-wide average of one SNP per 840 bases (*15*). Sequences of five other glutamate-gated chloride channel subunit genes differed very little between N2 and CB4856 (fig. S7B). Multiple lines of evidence suggested that the elevated level of polymorphism in *glc-1* is due to long-term balancing selection, rather than an elevated mutation rate or population subdivision. Elevated sequence diversity is not consistent with relaxed constraint on one *glc-1* allele, because the ratio of nonsynonymous to synonymous substitutions was 0.27, indicative of purifying selection (table S2). The *glc-1* sequences obtained from 53 wild isolates fall into two divergent clades (Fig. 4B). We observed 105 segregating sites among the isolates, but only six distinct haplotypes, fewer than expected for sequences evolving neutrally [$P < 0.0001$; (*6*), table S2]. The SNPs in the region surrounding *glc-1* were in complete linkage disequilibrium (fig. S9). We also observed a significant positive Tajima's D (*16*) (3.22; $P < 0.0001$) (table S2), which is expected under balancing selection. Population subdivision is unlikely to explain these observations because both N2-like and CB4856-like haplotypes are observed globally, without any apparent geographic structure (fig. S10). The extent of sequence divergence between the two haplotype clades was used to estimate that both haplotype classes have likely existed for 7.6×10^6 generations (*6*), which is older than typical coalescence times for neutral sequences in *C. elegans*. The observed molecular signatures in this region are analogous to the *zeel-1/peel-1* region involved in a genetic incompatibility, where two ancient, highly diverged haplotype clades are also maintained by balancing selection (*17*).

Because avermectins are metabolites of *S. avermitilis*, a ubiquitous soil bacterium (*1*), exposure to *S. avermitilis* may represent a selective force for this balancing selection. *S. avermitilis* significantly reduced the brood size (Fig. 4C and fig. S11) and induced uncoordinated movement in both CB4856 and N2. However, in the presence of *S. avermitilis*, the median brood size of CB4856 was about five times higher than N2. By contrast, in the absence of *S. avermitilis,* the median brood size of CB4856 was about half that of N2 (Fig. 4C). The strain with the *glc-1* region from N2 introgressed into CB4856 showed a brood size reduction similar to N2 when exposed to *S. avermitilis*, whereas the introgression strain harboring the *glc-1(pk54)* mutation did not (Fig. 4C). These data are consistent with the hypothesis that a loss-of-function allele of *glc-1* in the CB4856 background is responsible for generating resistance to *S. avermitilis*, most likely through its effect on avermectin resistance. Thus, the CB4856 *glc-1* allele may confer resistance to *S. avermitilis* but reduce fitness in the absence of this bacterium, perhaps due to pleiotropy of *glc-1*. *glc-1* has been implicated in shaping the normal foraging pattern in N2 (*18*) and is likely to form heteromeric channels with other glutamate-gated chloride channel subunits (*2*, *3*, *19*) that are critical for multiple physiological processes (*3*, *20*). *glc-1* is expressed in multiple tissues from the embryo through the adult stage, consistent with a role in diverse biological functions (fig. S12).

Although diverse molecules have been identified as targets of avermectins (*3*), only a few studies have examined natural resistance, with glutamate-gated chloride channels implicated in some (*21*, *22*) but not others (*23*, *24*). We have identified a naturally occurring four-amino-acid deletion in the ligand-binding domain of GLC-1 that plays a major role in avermectin resistance in the global *C. elegans* population. In the standard laboratory N2 strain, loss of function of three distinct glutamate-gated chloride channel subunits is required for resistance to avermectins as measured both by growth (*13*) and by our swimming assay (fig. S4). In contrast, we show that the loss of function of one channel subunit is sufficient for resistance in some wild isolates. The observed differences in resistance are modest compared with those in some species (*25*), which suggests that other mechanisms may be involved in generating greater resistance. The *glc-1* variant that confers resistance to avermectins appears to be ancient and maintained by balancing selection, possibly due to a trade-off between resistance to common soil bacteria and a cost in their absence. Although we did not detect any obvious effect of this *glc-1* variant on brood size in laboratory conditions in the absence of *S. avermitilis*, it is possible that in the wild, the effect of a *glc-1* loss-of-function allele on multiple physiological processes may lead to lower fecundity or higher mortality. Analogous trade-offs have been observed for pathogen resistance genes in *Arabidopsis* (*26*–*28*). Because many nematodes, including parasitic ones, spend part of their life cycle in soil, resistance to avermectins in the phylum may be common.

References and Notes

1. R. W. Burg *et al.*, *Antimicrob. Agents Chemother.* **15**, 361 (1979).
2. S. McCavera, T. K. Walsh, A. J. Wolstenholme, *Parasitology* **134**, 1111 (2007).
3. A. J. Wolstenholme, A. T. Rogers, *Parasitology* **131** (suppl.), S85 (2005).
4. A. J. Wolstenholme, I. Fairweather, R. Prichard, G. von Samson-Himmelstjerna, N. C. Sangster, *Trends Parasitol.* **20**, 469 (2004).
5. J. S. Gilleard, R. N. Beech, *Parasitology* **134**, 1133 (2007).
6. Materials and methods are available as supporting material on *Science* Online.
7. J. P. Arena *et al.*, *J. Parasitol.* **81**, 286 (1995).
8. A. I. Njue, R. K. Prichard, *Parasitol. Res.* **93**, 419 (2004).
9. M. V. Rockman, L. Kruglyak, *PLoS Genet.* **5**, e1000419 (2009).
10. L. Kruglyak, E. S. Lander, *Genetics* **139**, 1421 (1995).
11. D. F. Cully *et al.*, *Nature* **371**, 707 (1994).
12. D. K. Vassilatis *et al.*, *J. Biol. Chem.* **272**, 33167 (1997).
13. J. A. Dent, M. M. Smith, D. K. Vassilatis, L. Avery, *Proc. Natl. Acad. Sci. U.S.A.* **97**, 2674 (2000).
14. R. E. Hibbs, E. Gouaux, *Nature* **474**, 54 (2011).
15. S. R. Wicks, R. T. Yeh, W. R. Gish, R. H. Waterston, R. H. Plasterk, *Nat. Genet.* **28**, 160 (2001).
16. F. Tajima, *Genetics* **123**, 585 (1989).
17. H. S. Seidel, M. V. Rockman, L. Kruglyak, *Science* **319**, 589 (2008).
18. A. Cook *et al.*, *Mol. Biochem. Parasitol.* **147**, 118 (2006).
19. A. Etter, D. F. Cully, J. M. Schaeffer, K. K. Liu, J. P. Arena, *J. Biol. Chem.* **271**, 16035 (1996).
20. J. A. Dent, M. W. Davis, L. Avery, *EMBO J.* **16**, 5867 (1997).
21. A. I. Njue, J. Hayashi, L. Kinne, X. P. Feng, R. K. Prichard, *J. Neurochem.* **89**, 1137 (2004).
22. D. H. Kwon, K. S. Yoon, J. M. Clark, S. H. Lee, *Insect Mol. Biol.* **19**, 583 (2010) (Aug).
23. A. El-Abdellati *et al.*, *Int. J. Parasitol.* **41**, 951 (2011).
24. S. McCavera, A. T. Rogers, D. M. Yates, D. J. Woods, A. J. Wolstenholme, *Mol. Pharmacol.* **75**, 1347 (2009).
25. R. M. Kaplan *et al.*, *Int. J. Parasitol.* **37**, 795 (2007).
26. M. Todesco *et al.*, *Nature* **465**, 632 (2010).
27. E. A. Stahl, G. Dwyer, R. Mauricio, M. Kreitman, J. Bergelson, *Nature* **400**, 667 (1999).
28. D. Tian, M. B. Traw, J. Q. Chen, M. Kreitman, J. Bergelson, *Nature* **423**, 74 (2003).

Acknowledgments: We thank F. Albert, I. Ehrenreich, M. Rockman, and H. Seidel for critical reading of the manuscript and members of the Kruglyak laboratory for suggestions, K. Chattopadhyay for advice regarding protein structure analysis, and P. McGrath for sharing unpublished sequence information of the MY14 strain. Supported by a Merck fellowship of the Life Science Research Foundation (J.P.G.), NIH Ruth L. Kirschstein National Research Service Award (E.C.A.), James S. McDonnell Foundation Centennial Fellowship, Howard Hughes Medical Institute, NIH grants R01-HG004321 and R37- MH59520 (L.K.), and NIH grant P50-GM071508 to the Center for Quantitative Biology at the Lewis-Sigler Institute of Princeton University. Some of the *C. elegans* strains used were obtained from the Caenorhabditis Genetics Center. GenBank sequence accession numbers for the sequences are JN983734 to JN983793.

Supporting Online Material

www.sciencemag.org/cgi/content/full/335/6068/574/DC1
Materials and Methods
Figs. S1 to S12
Tables S1 and S2
References (*29*–*46*)

22 September 2011; accepted 30 November 2011
10.1126/science.1214318

Downloaded from www.sciencemag.org on February 2, 2012

Affirmative Action Policies Promote Women and Do Not Harm Efficiency in the Laboratory

Loukas Balafoutas[1] and Matthias Sutter[1,2]*

Gender differences in choosing to enter competitions are one source of unequal labor market outcomes concerning wages and promotions. Given that studying the effects of policy interventions to support women is difficult with field data because of measurement problems and potential lack of control, we evaluated, in a set of controlled laboratory experiments, four interventions: quotas, where one of two winners of a competition must be female; two variants of preferential treatment, where a fixed increment is added to women's performance; and repetition of the competition, where a second competition takes place if no woman is among the winners. Compared with no intervention, all interventions encourage women to enter competitions more often, and performance is at least equally good, both during and after the competition.

Affirmative action programs try to promote an equal representation of women in upper-level positions, both in business and in politics, as well as among members of the academic and scientific community (*1*). The reason for the existence of such programs is that, despite improvements over the past decades, there are still substantial gender differences in labor markets, both in the private sector and in the public sector, including the underrepresentation of women in the sciences. Of particular concern with respect to gender equality in labor markets are wage differentials between men and women and fewer opportunities for career advancement of women (*2*–*4*). Such gender differences are often attributed to differences in preferences regarding the type of employment, rank or position, problems in combining family and career, or to discrimination against women (*5*, *6*). A recent line of research has highlighted the contribution of another important factor—namely, the weaker inclination of women to participate in competitions (*7*–*15*). These studies provide evidence that, in general, men increase their performance in competitive environments more than women, and women more often opt out of competition, even when they are equally qualified. As a consequence of gender differences in competitive behavior, women may get fewer promotion opportunities and subsequently receive lower wages than men.

Policy interventions to support the promotion of women often face the criticism that they are inefficient in assigning the best available candidates, irrespective of gender, to a particular job when several candidates compete for it (*16*). While this is difficult to measure in the field because it is hard to exactly identify a candidate's qualifications, laboratory-based economic experiments allow for an unambiguous assessment of the efficiency of affirmative action programs in promoting the best candidates, although this is measured in the artificial context of a well-controlled, quantitative task. We evaluate and compare four alternative types of policy interventions within a unified experimental framework, examining whether they actually induce more women to compete and whether the performance of the selected winners is harmed by policy interventions. We also look at competitive behavior and teamwork after the competition ends. Competition within firms often means that one member of a working group receives a promotion but that he or she still needs to work together with the other group members afterwards, so that efficient teamwork requires the successful coordination of activities of the losers and winners of the competition. It is open to investigation, however, whether policy interventions in the spirit of affirmative action programs might backfire by spoiling the willingness of losers to coordinate efficiently in subsequent tasks.

We examine the following types of policy interventions: (i) Quotas that guarantee a certain minimum fraction of winners to be female (*1*). For instance, many European parliaments have quotas on parliamentary seats that are reserved for women. (ii) Two variants of preferential treatment of women. Preferential treatment schemes are often encountered in practice as a means to increase the participation of women in leading positions. A weak variant of preferential treatment can be a tie-breaking rule that favors women in case of equal performance or qualifications. In a stronger variant, preferential treatment may imply discrimination against better-performing men. (iii) Repetition of the competition unless a critical number of female winners is reached in the first attempt. For instance, in competitions for academic jobs (and, more generally, for jobs in the public sector) in many continental European countries—for example, in Austria—it is possible for the process of filling a vacant position to be nullified and reset to the start if no woman is shortlisted for the position. This is then equivalent to repeating the competition.

The experiment was run with 360 undergraduate students from various academic backgrounds (N = 360). Subjects were randomly assigned into groups of three men and three women [see the notes on the experimental procedure in the supporting online material (SOM)]. All groups went through several stages. The experimental task in each of the stages 1 to 4 was to add as many sets of five two-digit numbers as possible within 3 minutes (*1*). The task in stage 5 was a simple coordination game.

In stage 1 (piece rate), each subject receives €0.50 for each correct calculation. In stage 2 (tournament), group members compete against each other. The two members who solve the most calculations correctly are paid €1.50 per calculation. The other four group members receive nothing. In stage 3 (choice), subjects choose whether they want to solve the calculations under a piece-rate scheme or a tournament scheme. If the tournament is chosen, a subject's performance in stage

Table 1. Payoff matrix in the coordination game (stage 5). Each group member plays the two-person coordination game illustrated in Table 1 with each of the other five group members. This game has seven Nash equilibria that are Pareto-ranked along the diagonal. Before picking a number from 1 to 7, a subject is informed about the gender of the other player and whether this player has won or lost in the tournament of stage 4. With this information, each subject has to choose five times a number for the interaction with each of the other group members. All decisions are made simultaneously. If a subject wishes to obstruct efficient coordination, she should pick a low number. This decreases total payoffs and at the same time makes it likely that the subject has a higher payoff than her paired member. For instance, a choice of 1 guarantees the subject's own payoff of €3.50, while it implies a payoff of at most €3.50 for the other player. On the contrary, choices of high numbers create the potential for a large payoff for both subjects, provided that both coordinate on choosing a high number.

		Other person's number						
		7	6	5	4	3	2	1
Your number	7	€6.50	€5.50	€4.50	€3.50	€2.50	€1.50	€0.50
	6	€6.00	€6.00	€5.00	€4.00	€3.00	€2.00	€1.00
	5	€5.50	€5.50	€5.50	€4.50	€3.50	€2.50	€1.50
	4	€5.00	€5.00	€5.00	€5.00	€4.00	€3.00	€2.00
	3	€4.50	€4.50	€4.50	€4.50	€4.50	€3.50	€2.50
	2	€4.00	€4.00	€4.00	€4.00	€4.00	€4.00	€3.00
	1	€3.50	€3.50	€3.50	€3.50	€3.50	€3.50	€3.50

[1]University of Innsbruck, Department of Public Finance, Innsbruck, Austria. [2]University of Gothenburg, Department of Economics, Gothenburg, Sweden.

*To whom correspondence should be addressed. E-mail: matthias.sutter@uibk.ac.at

Downloaded from www.sciencemag.org on February 2, 2012

3 is compared with the other group members' performance in stage 2 (*17*). In this stage, we vary the competition rules across five treatments to examine the effects of different types of policy interventions. The treatments are described below. In stage 4 (tournament with policy intervention), all subjects compete (against each other's performance in stage 4) and the competition rules vary according to the policy intervention that is applied in each treatment. At the end of stage 4, we inform subjects about the outcome of the competition, but not about the performance of competitors, before moving on to the coordination task in stage 5 (*17*). Each winner in stage 4 receives an additional €5 as an initial endowment in stage 5, and each loser receives only €2. The reason for this unequal payment is to introduce a clear distinction between winners and losers before starting with the postcompetition stage.

The rules for determining the winners in stages 3 and 4 differ across treatments as follows: In the control treatment (CTR), the winners are the two group members with the largest numbers of correct calculations, regardless of gender. In the minimum quota treatment (QUO), there has to be at least one woman among the two winners of the tournament, irrespective of the ordinal ranking of group members' performances. This implies that the best-performing woman is always a winner. In preferential treatment 1 (PT1), each woman's performance is automatically increased by one unit (i.e., one correct calculation), whereas in preferential treatment 2 (PT2), each woman receives two extra units as a head start. Finally, in repetition of the competition (REP), the competition is repeated once if there is not at least one woman among the two winners. In this case, the rules of the repeated competition are the same as in the control treatment.

Postcompetition stage 5 (coordination game) is identical in all treatments. Each group member plays a two-person coordination game with each of the other five group members. The outcome of this coordination game, which is described in detail in Table 1, depends on players' cooperativeness and on their expectations about the cooperative choices of other players (*18*–*20*).

Figure 1 presents the average performance of men and women across all treatments as the number of correctly solved calculations in stages 1 to 4. The main pattern emerging from Fig. 1 is similar to earlier experimental evidence on the performance of men and women (*1*, *13*). On average, we find that men perform better than women, but the difference is not statistically significant (except in the tournament of stage 2; Mann-Whitney test, $z = -2.16$, $P = 0.031$). The relatively strong increase in performance from stage 1 to stage 2 is probably due to competition in stage 2, although parts of this increase might also be driven by learning effects, because Fig. 1 indicates an upward trend in performance.

Figure 2 shows the relative frequency with which men and women choose to compete in stage 3 (instead of choosing the piece-rate scheme). We find that in the control treatment CTR men compete about twice as often as women, which is consistent with the existing literature (*13*). However, the four different policy interventions reduce, and even reverse, this gender gap. The relative frequency of women opting for competition increases from 30.6% in CTR to 38.9% in REP, 52.8% in QUO, 58.3% in PT1, and 69.4% in PT2. Bilateral comparisons with the control treatment CTR reveal that the frequency of competing women is significantly higher in PT1 [$\chi^2(1) = 5.62$, $P = 0.018$] and PT2 [$\chi^2(1) = 10.89$, $P = 0.001$], whereas the increase is not quite significant in QUO [$\chi^2(1) = 3.66$, $P = 0.056$]. Repetition of the competition (REP) is the only policy intervention that has no significant effect on women's entry choices.

Although the fraction of men choosing competition is slightly affected by interventions (see Fig. 2), there is no significant difference across treatments [$\chi^2(4) = 2.67$, $P = 0.614$]. Hence, the main impact of the different policy interventions is on the choices of women and not on those of men. For a more formal analysis of the determinants of tournament entry choices and the effects of policy interventions, we have run a number of probit regressions, which confirm all of our main findings (see SOM).

Interventions that promote the entry of women may have two opposing effects on the overall efficiency in selecting the best candidates as winners. On the one hand, any intervention that gives an advantage to women may yield efficiency losses by passing over better-performing men for the sake of promoting women. On the other hand, interventions may induce more high-performing women to choose competition instead of going for the piece rate, leading to efficiency gains.

Figure 3 shows for each treatment the average ability level (measured in terms of performance) of those subjects who have entered and won the competition in stage 3 (*21*). The winners' average ability is higher than in the control treatment in two out of the four treatments with a policy intervention (QUO and PT1). However, all differences compared with the control treatment are statistically insignificant (pairwise Mann-Whitney tests, $P > 0.4$). These findings suggest that the two opposing effects discussed above cancel out in the aggregate, so that interventions do not entail efficiency costs.

Next, we examined how the various interventions affect the profile of candidates who choose to compete. We found that our four different interventions increase the likelihood of weak and strong performers entering the competition—always

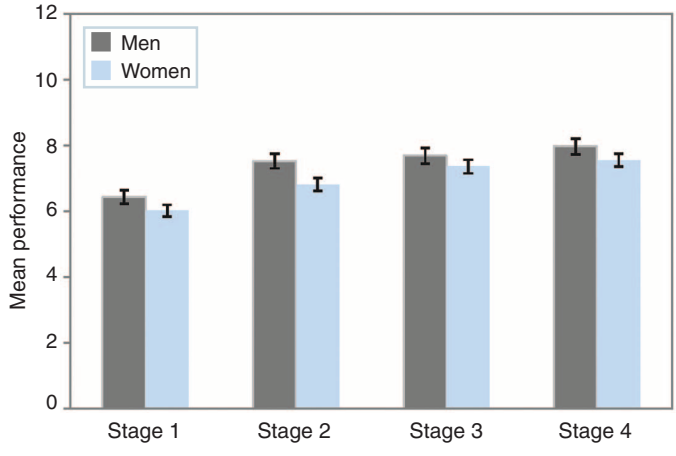


Fig. 1. Performance in the experimental task, by gender ($N = 360$ subjects). Each bar shows the average performance of participants (number of correctly solved calculations) in a particular stage, across all five treatments. Performance in treatments PT1 and PT2 excludes the extra units given to competing women. Error bars, mean ± SEM.

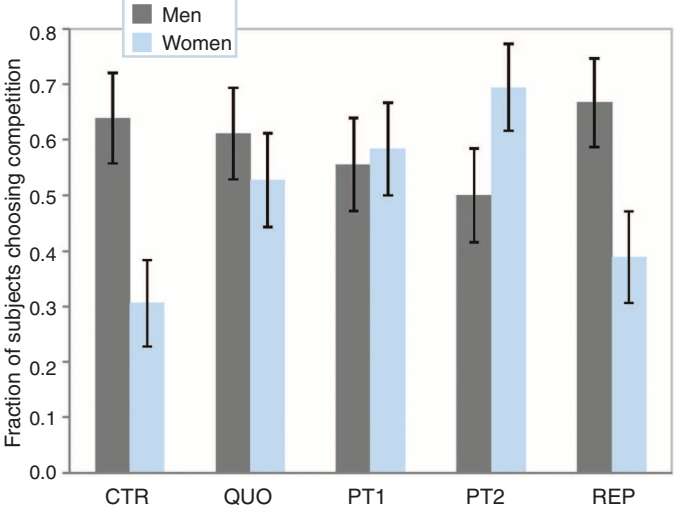


Fig. 2. Proportion of subjects choosing competition ($N = 360$ subjects; 72 per treatment). The bars show, for each treatment, the proportion of subjects (between 0 and 1) who chose the tournament compensation scheme in stage 3. Error bars, mean ± SEM.

Downloaded from www.sciencemag.org on February 2, 2012

compared with the control as a benchmark—whereas they have no effect on intermediate performers (see fig. S1). In particular, the large increase in competition entry by strong female performers shows the potential of policy interventions to improve the quality of participants. It is also encouraging to observe that strong male performers do not respond to policy interventions in a negative way.

The absence of an efficiency-decreasing selection effect is largely due to the fact that hardly any better-qualified men were passed over as a result of interventions. In treatment REP, there was no single instance in which the competition had to be repeated in stage 4, meaning that no better-qualified men could have been passed over. In treatment QUO, there were five cases where a man performed better but lost to a woman. Finally, in only one case in PT1 (PT2) a man performed better by one unit (two units) and lost.

We evaluated post-competition outcomes by means of a group's total payoff from the coordination game in stage 5, expressed as a fraction of the highest possible group payoff of €195 (Fig. 4). This measure can be considered an indicator of efficiency in a coordination task. Although efficiency differs slightly across treatments—fluctuating between 73 and 79%—the differences are not statistically significant [Kruskal-Wallis test comparing across treatments, $\chi^2(4) = 2.67$, $P = 0.614$]. Moreover, when comparing the individual choices of the winners and losers from stage 4, we do not find significant differences between the two groups in any of our treatments; this indicates that the losers of the competition do not react by obstructing efficient coordination after the competition. Nor do we detect significant gender differences in postcompetition behavior or differences between those who entered the competition in stage 3 and those who did not. We thus conclude that, in the aggregate, introducing any of our policy measures does not entail efficiency losses in a coordination task after the competition has been completed.

Studying the effects of different policy interventions on competitive behavior of men and women, both in the course of a competition and after it, is important for companies and politicians alike. Of course, companies and their human resource departments have a general interest in selecting the best candidates for a job, irrespective of gender. However, the gender composition of a company's workforce can have implications for a company's success as well (*22*). Therefore, companies may want to consider the gender of competitors in various ways, and also how different policy interventions affect postcompetition behavior. Likewise, politicians may want to provide an institutional and legal framework for a level playing field of men and women on labor markets. This requires comparing different alternative measures and their effects on behavior and efficiency, something that is difficult to examine in a controlled way with field data. Laboratory experiments are an attractive alternative methodology for the study of these issues (*23*). We provide controlled laboratory evidence on the behavioral consequences and the efficiency of different intervention schemes to promote women in competition and on how intervention schemes may affect postcompetition behavior.

The results of this study allow us to draw some lessons regarding the effects of certain affirmative action programs on individual incentives. In particular, we have looked at incentives to enter into and perform under competitive environments, as well as at incentives to coordinate efficiently in the aftermath of a competition. On the basis of our findings, we conclude that strong preferential treatment is the most successful intervention in terms of encouraging women—and, in particular, high-performing women—to enter competition. Weak preferential treatment and quotas have quantitatively similar effects in this respect, whereas repetition of the competition appears to generate the weakest incentives. Moreover, our policy interventions of minimum quotas, weak or strong preferential treatment, and repetition of the tournament do not entail any efficiency losses, neither in terms of the selection of winners in a competition nor in the postcompetition stage.

Of course, many other aspects of affirmative action schemes need to be considered in policy discussions. Our study focuses on output (in stage 1 to 4) and total payoffs (in stage 5) as a measure of individual and group performance, something that companies will put great emphasis on, but it remains largely agnostic about the welfare implications of affirmative action policies because these are difficult to assess without imposing any welfare functions on individuals. Furthermore, our study has not been able to address the proper scope and extent of affirmative action policies. These aspects refer to issues such as whether affirmative action policies should apply to the public sector and the private sector to the same extent or whether governments might go too far by imposing them on private sector companies.

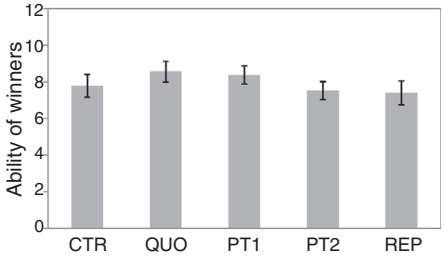


Fig. 3. Average ability of the winners in stage 3, by treatment (N = 360 subjects; 72 per treatment). The bars show, for each treatment, the average stage 1 performance (number of correct calculations) of those subjects who entered and won the tournament in stage 3. Error bars, mean ± SEM.

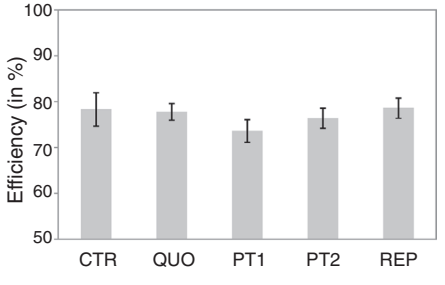


Fig. 4. Efficiency in the coordination game of stage 5 (N = 360 subjects; 72 per treatment). The bars show, for each treatment, the efficiency achieved on average by all groups. Efficiency is defined as the ratio of the average total group payoff in stage 5 to the maximum possible total group payoff of €195, which would emerge if all group members always chose an effort level of 7. Error bars, mean ± SEM.

References and Notes

1. M. Niederle, C. Segal, L. Vesterlund, How costly is diversity? Affirmative action in light of gender differences in competitiveness (Stanford University Working Paper, 2011); available at www.stanford.edu/~niederle/AAPaper.pdf.
2. F. Blau, M. Ferber, A. Winkler, *The Economics of Women, Men and Work* (Prentice Hall, Englewood Cliffs, NJ, 2010).
3. M. Bertrand, K. F. Hallock, *Ind. Labor Relat. Rev.* **55**, 3 (2001).
4. D. Weichselbaumer, R. Winter-Ebmer, *Econ. Policy* **22**, 235 (2007).
5. J. Altonji, R. Blank, in *Handbook of Labor Economics*, O. Ashenfelter, D. E. Card, Eds. (Elsevier, 1999), vol. 3, pp. 3143–3259.
6. C. Goldin, C. Rouse, *Am. Econ. Rev.* **90**, 715 (2000).
7. B. Bartling, E. Fehr, M. Maréchal, D. Schunk, *Am. Econ. Rev.* **99** (no. 2), 93 (2009).
8. R. Croson, U. Gneezy, *J. Econ. Lit.* **47**, 448 (2009).
9. N. Datta Gupta, A. Poulsen, M. C. Villeval, *Econ. Inq.* (2012); available at http://onlinelibrary.wiley.com/doi/10.1111/j.1465-7295.2011.00378.x/abstract.
10. U. Gneezy, K. Leonard, J. List, *Econometrica* **77**, 1637 (2009).
11. U. Gneezy, M. Niederle, A. Rustichini, *Q. J. Econ.* **118**, 1049 (2003).
12. U. Gneezy, A. Rustichini, *Am. Econ. Rev.* **94** (no. 2), 377 (2004).
13. M. Niederle, L. Vesterlund, *Q. J. Econ.* **122**, 1067 (2007).
14. M. Niederle, L. Vesterlund, *J. Econ. Perspect.* **24**, 129 (2010).
15. D. Wozniak, W. T. Harbaugh, U. Mayr, The menstrual cycle and performance feedback alter gender differences in competitive choices (University of Oregon Working Paper, 2010); available at http://harbaugh.uoregon.edu/Papers/Menstruation_Wozniak_201010.pdf.
16. R. G. J. Fryer Jr., G. C. Loury, *J. Econ. Perspect.* **19** (no. 3), 147 (2005).
17. See SOM for details on this procedure.
18. J. Brandts, D. J. Cooper, *Am. Econ. Rev.* **96**, 669 (2006).
19. G. Charness, M. Jackson, *J. Econ. Theory* **136**, 417 (2007).
20. In stage 5, we have kept the hierarchy flat in the sense that the winners of stage 4 do not have superior power over losers. This is motivated by the observation that teamwork, even if there is a formal hierarchy, depends crucially on the successful coordination of activities of team members, be they former losers or winners in the competition stage. We were particularly interested in coordination in groups after a tournament has been concluded.
21. We have used the winners' performances in stage 1 as an appropriate measure of a subject's ability, because this performance is unaffected by competition and any policy intervention.
22. A. Weber, C. Zulehner, *Am. Econ. Rev.* **100** (no. 2), 358 (2010).
23. A. Falk, J. J. Heckman, *Science* **326**, 535 (2009).

Acknowledgments: Financial support from the Austrian Science Foundation (FWF Project P22772) and the D. Swarovski & Co. Förderfonds of the University of Innsbruck is gratefully

Downloaded from www.sciencemag.org on February 2, 2012

acknowledged. We thank G. Charness, N. Feltovich, U. Gneezy, M. Kocher, P. Kuhn, and P. Rey-Biel, as well as seminar participants at the University of Arizona at Tucson, the University of California at Santa Barbara, and the University of Athens and participants at the Economic Science Association meetings in Innsbruck and Melbourne, the Markets, Organization and Votes in Economics meeting in Barcelona, and the Behavioral and Experimental Economics Symposium in Maastricht, for valuable comments.

Supporting Online Material
www.sciencemag.org/cgi/content/full/335/6068/579/DC1
Materials and Methods
SOM Text
Fig. S1
Tables S1 to S3

14 July 2011; accepted 15 December 2011
10.1126/science.1211180

Female Leadership Raises Aspirations and Educational Attainment for Girls: A Policy Experiment in India

Lori Beaman,[1]* Esther Duflo,[2]* Rohini Pande,[3]* Petia Topalova[4]*

Exploiting a randomized natural experiment in India, we show that female leadership influences adolescent girls' career aspirations and educational attainment. A 1993 law reserved leadership positions for women in randomly selected village councils. Using 8453 surveys of adolescents aged 11 to 15 and their parents in 495 villages, we found that, relative to villages in which such positions were never reserved, the gender gap in aspirations closed by 20% in parents and 32% in adolescents in villages assigned a female leader for two election cycles. The gender gap in adolescent educational attainment was erased, and girls spent less time on household chores. We found no evidence of changes in young women's labor market opportunities, which suggests that the impact of women leaders primarily reflects a role model effect.

Quotas are an increasingly common response to the enduring underrepresentation of women in various domains, from science and politics to the corporate boardroom. Around 100 countries have adopted gender quotas in politics—mostly since the United Nations' Fourth World Conference on Women in 1995 (*1*)—and in 2004 Norway became the first country to mandate the presence of women on corporate boards, with a 40% quota. Policy-makers hope that quotas will have long-term effects on women's labor market outcomes over and above the immediate impact on leaders' gender balance, because the first women who become leaders may shape both parents' and children's beliefs about what women can achieve, through their policies and/or through a direct role model effect. In turn, this may raise their aspirations and shape educational and career choices. We present experimental evidence from a field setting in India that supports this view.

The idea that gender identity is at least partially a social construction is widely acknowledged in sociology (*2*) and social cognitive theory (*3*). These literatures identify belief in one's own ability (self-efficacy) as a key mechanism for personal agency and show that this belief is highly correlated with educational aspirations and subsequent occupational choices (*4*). Interventions affecting these beliefs have been shown to influence long-term behavior—for example, effort and performance in schools (*5*). Gender disparities in efficacy beliefs, in turn, are cited as an important factor behind the difference in male and female aspirations (*6*), especially in leadership (*7*, *8*). Role incongruity is often emphasized as the source of the gap in beliefs (*9*, *10*), raising the possibility that role models can challenge prevalent stereotypes and help to reduce this gap. Studies show that girls may be less likely to aspire to become scientists because there are few female scientists (*11*–*14*). Exposure to own-gender experts can provide such role models, break stereotypes regarding gender roles (*15*), and improve individual women's aspirations and propensity to enter traditionally male-dominated areas (*15*–*17*).

Several open questions remain. These include whether role model effects can counteract potential backlash (*18*) and whether other social and economic constraints prevent aspirational improvements from enabling achievement gains. Further, much of the existing evidence comes from observational studies, where beliefs or actions of individuals exposed to different role models are compared (*19*–*22*), or from laboratory or short-term school-based experiments, where individuals are exposed to different role models either in person or on paper (*11*, *16*, *23*). In observational studies, people exposed to alternative role models may themselves have different preferences or opportunities. In the laboratory or school setting, data on beliefs and aspirations are often gathered after a brief exposure to a role model (*24*); this may not reflect real life, where exposure is more enduring. Similarly, the consequences of psychological processes on behavior are generally followed over a brief period [see (*5*) for an exception].

In this study, we took advantage of a large-scale randomized natural experiment in India, which quickly increased the number of women in leadership positions at the village level. Exploiting a rule that requires the random selection of villages where only women could compete for this position, we compared the aspirations of parents for their sons and daughters aged 11 to 15, as well as the aspirations of adolescents for themselves across villages with female and male leaders. We next examined whether changes in girls' aspirations were accompanied by changes in educational outcomes and time spent on domestic chores. Finally, we investigated the potential channels for this effect.

Since 1993, when India adopted gender quotas for elected positions on village councils, the gender balance of village leadership has markedly altered: Across India, the fraction of elected local leaders who are female has risen from less than 5% in 1992 to more than 40% by 2000 (*25*). In West Bengal, our area of study, as in most Indian states, one-third of village councils are randomly selected to be reserved for a woman chief councilor (or "pradhan") in every election. Random selection of reserved councils enables us to identify the causal relationship between the election of female leaders and villagers' aspirations: There should be no other difference between villagers living in councils reserved once or twice versus unreserved councils. Moreover, because of concurrent reservations for historically disadvantaged groups (scheduled caste and scheduled tribes), seats are not set aside to women by pure rotation: Between 1998 when the system was implemented in West Bengal and 2007 when we collected our data, a village council could have been reserved for a female pradhan once (in 1998 or 2003), twice (in 1998 and 2003), or never (*26*), giving us the opportunity to study the "dose response" in exposure to a female leader. Previous research has shown that women leaders invest in goods preferred by women, such as drinking water (*27*), and improve men's perception of women's leadership abilities (*28*).

Our survey team collected data in 2006 and 2007 in one West Bengal district, Birbhum, a rural and poor district located about 200 km from Kolkata. Our survey covered a random sample of 495 villages in Birbhum's 165 village councils. Tables S1 and S2 compare 1991 census data (before reservation) and household survey data according to reservation status of the council. Because of the randomization, councils have very similar characteristics. We interviewed 15 randomly selected households per village, administering separate questionnaires to the youngest married couple in each household and to all adolescents (aged 11 to 15) residing in the household. The final sample of respondents with adolescent children consisted of 2335 male and 2438 female respon-

[1]Department of Economics, Northwestern University, Evanston, IL 60208, USA. [2]Department of Economics, Massachusetts Institute of Technology (MIT), Cambridge, MA 02142, USA. [3]Harvard Kennedy School, Harvard University, Cambridge, MA 02138, USA. [4]International Monetary Fund, Washington, DC 20434, USA.

*To whom correspondence should be addressed. E-mail: l-beaman@northwestern.edu (L.B.); eduflo@mit.edu (E.D.); rohini_pande@ksg.harvard.edu (R.P.); ptopalova@imf.org (P.T.)

Downloaded from www.sciencemag.org on February 2, 2012

dents, which covered 3257 adolescents. Among adolescents our sample was slightly bigger, consisting of 1852 girls and 1828 boys (*29*).

The household roster had information on educational attainment, from which we constructed three variables: 1 if ever attended school, 1 if can read and write, and last grade completed. We report results using the normalized average across these three outcomes as the dependent variable [as in (*30*, *31*)]. A time-use module asked adults and adolescents about time spent on 16 agricultural or household activities during the past 24 hours. We constructed time spent on domestic chores as minutes spent getting water, cooking, cleaning, providing child care, collecting fuel, and doing laundry.

The adult questionnaire covered parents' aspirations for adolescents with four questions concerning desired educational attainment, desired age of marriage, preferred occupation at the age of 25, and whether the parent wished for the child to become pradhan. We constructed five indicator variables to capture aspirations: 1 if the parent would like the child to at least graduate from secondary school (grade 12); 1 if the parent wishes the child to marry at an age above 18; 1 if the preferred occupation is different from housewife or what the in-laws prefer; 1 if the answer is doctor, engineer, scientist, teacher, or a legal career; and 1 if the parent desires the child to become pradhan. For adolescents, we administered the same aspiration questions and coded them in an identical manner.

These five variables are good measures of aspirations, because they are future-oriented and predictive of current behavior (*4*). However, they cover separate spheres of aspirations, and therefore, they could be differently affected by any intervention. Validation tests show that the first four have a fairly high degree of correlation (Cronbach's α = 0.66 for parents, 0.55 for teenagers), whereas the wish to be pradhan is less correlated with any of the others. Thus, in addition to the individual variables, we report the effect of the standardized average across the first four outcomes.

To investigate whether changed opportunities for young women underlie aspirational changes, we examined educational and occupational outcomes of young adults (aged 16 to 30). Using the household roster, we constructed educational variables identical to those for adolescents, along with two indicator variables for occupation (1 if the respondent is not a housewife, 1 if the respondent has a high-education job) and the standardized average of the two variables. Finally, to gauge whether female leadership affected schooling quality, we examined scores on a math and reading test administered to 9-year-old school-enrolled children (*26*).

Tables 1 and 2 present findings on how the election of female leaders shapes parent and adolescent aspirations, and Fig. 1 provides a graphic representation. Both tables show, for each variable, the mean of parents' aspirations for boys and girls in never-reserved villages, as well as regression-adjusted difference in means by reservation status (*26*). The fifth column shows the effect across the standardized measure of the four previous outcomes, and the rightmost column shows aspirations about becoming pradhan.

Parents have higher aspirations for boys than for girls: On average, in villages that have never been reserved for a woman pradhan, parents' aspirations for girls are 0.68 standard deviation lower than for boys ($P < 0.001$, t test). For example, parents are 14 percentage points (45%) less likely to state that they would like their girl

Table 1. Parents' aspirations for their children. The first set of values consists of means and standard deviations (in brackets) of the variable in the column heading in never-reserved village councils. The coefficients in the remainder of the table are ordinary least-squares results for the dependent variable in the column heading and measure the difference in aspirations for boys and girls relative to the never-reserved sample. The row denoted "Gap" for never-reserved village councils shows the gap in aspirations between boys and girls. The subsequent "Difference in gap" rows show the gap in aspirations for boys and girls relative to the gap in the never-reserved sample. For example, the last number in column 5 says that the gap in overall aspirations for girls versus boys has shrunk by 0.136 standard deviation (more than 20%) in twice-reserved village councils relative to never-reserved ones. Standard errors corrected for heteroskedasticity and clustering at the village council level are shown below the coefficients in parentheses. The sample size is 6140. The normalized average is computed across the four outcomes (columns 1 to 4), which are first normalized by subtracting the mean for never-reserved village councils and dividing by the standard deviation in the never-reserved sample. All estimates control for village characteristics described in table S1 and for respondent gender.

	Does not wish child to be housewife or whatever in-laws prefer	Wishes child to have a high-education job	Wishes child to marry after age 18	Wishes child to graduate or get higher education	Normalized average	Wishes child to be pradhan
Means and SDs in never-reserved village councils						
Boys	0.991	0.068	0.992	0.318	0.329	0.688
	[0.092]	[0.252]	[0.089]	[0.466]	[0.446]	[0.463]
Girls	0.242	0.039	0.756	0.176	−0.357	0.588
	[0.429]	[0.193]	[0.430]	[0.381]	[0.654]	[0.492]
Coefficients						
Never reserved						
Gap	−0.747	−0.028	−0.238	−0.140	−0.684	−0.093
	(0.018)	(0.009)	(0.012)	(0.019)	(0.025)	(0.020)
Reserved once						
Boys	−0.005	0.016	−0.004	0.003	0.013	−0.041
	(0.009)	(0.014)	(0.006)	(0.025)	(0.027)	(0.025)
Girls	−0.015	0.020	−0.021	−0.015	−0.011	0.000
	(0.023)	(0.009)	(0.014)	(0.020)	(0.031)	(0.029)
Difference in gap	−0.010	0.003	−0.017	−0.018	−0.024	0.041
	(0.025)	(0.015)	(0.016)	(0.026)	(0.035)	(0.029)
Reserved twice						
Boys	−0.033	−0.012	−0.018	0.003	−0.042	0.008
	(0.018)	(0.016)	(0.010)	(0.044)	(0.039)	(0.043)
Girls	0.064	0.012	0.021	0.051	0.093	0.101
	(0.028)	(0.014)	(0.025)	(0.036)	(0.050)	(0.044)
Difference in gap	0.097	0.025	0.038	0.048	0.136	0.092
	(0.036)	(0.020)	(0.026)	(0.048)	(0.059)	(0.049)

Downloaded from www.sciencemag.org on February 2, 2012

to graduate or study beyond the secondary school level ($P < 0.001$, t test).

The gender gap in aspirations in villages with a female leader for two election cycles drops by 0.14 standard deviation ($P < 0.03$, t test) relative to places that never had one. As parental aspirations for boys are unchanged, the entire decline in the gap is accounted for by improvements for girls. Moreover, the largest changes occur for occupation-related aspirations. For example, the fraction of parents who believe that a daughter's, but not a son's, occupation should be determined by her in-laws declines from 76 to 65%. Previous research suggests that women have more subjective identification with women role models than men (*17*), implying that the effect may be larger for mothers than fathers. Indeed, mothers' aspirations over education and occupation are altered more broadly, whereas fathers primarily increase their desire for their daughters to become pradhan (*26*). This last result is consistent with previous research showing that men's (but not women's) perception of women's ability to lead improved in reserved village councils (*28*).

Similarly, the aspirations of adolescents themselves were affected by the presence of a female leader in the second cycle (Fig. 1, center panel, and Table 2). Although boys are more ambitious than girls, the gender gap among adolescents residing in unreserved village councils is smaller than among the parents. In never-reserved villages, the gender gap in adolescent aspirations is 0.51 standard deviation ($P < 0.001$, t test). The gender gap in the desire to graduate or more is 10 percentage points (32%; $P < 0.001$, t test). The decline in the gap in twice-reserved councils (average effect: 0.17 standard deviation, $P < 0.01$, t test) is very similar in magnitude for parents and adolescents, so girls' and boys' own aspirations remain more similar to one another than parents' aspirations for their daughters versus sons. Here again, the decline in the gap is entirely driven by an increase in girls' aspirations, not by a decrease in boys'. Adolescent girls are more likely to not want to be a housewife or have their occupation determined by their in-laws (8.3 percentage points; $P = 0.053$, t test), to want to marry after 18 (8.8 percentage points; $P = 0.034$, t test), and to want a job that requires an education (8.6 percentage points; $P = 0.02$, t test). In the last case, the gender gap reverses.

Paralleling the changes in aspirations, the presence of female leaders also alters educational attainment and time use (Fig. 1, right panel, and Table 3). Relative to girls, adolescent boys in never-reserved councils are 6% more likely to attend school ($P < 0.01$, t test) and have a 4% higher likelihood of being able to read and write ($P < 0.01$, t test). Like elsewhere in the developing world, adolescent girls spend more time on domestic chores than their male counterparts (79 min more per day in never-reserved villages; $P < 0.001$, t test). The presence of female leaders did not affect educational and time-use outcomes for adolescent boys, but it improved the outcomes for girls. By the second cycle of female leadership, the gender gap in educational outcomes is completely erased (and even reversed), and girls spend less time on household activities (the gender gap in time spent on household activities declines by 18 min relative to never-reserved councils; $P = 0.05$, t test).

In all cases, the gender gap starts shrinking only during the second electoral mandate held by a woman. Results in table S6 confirm that this is a "dose response" rather than a "length since first exposure" effect (*26*).

Women in leadership positions can change aspirations of girls through two main channels: first, by undertaking policies that make it easier for women to succeed, thus changing beliefs on what is possible for girls; and second, by providing a role model of a successful woman. In any setting where actual female leadership is affected [as opposed to situations where female role models are briefly introduced (*14*, *32*)], the two effects may coexist. No experiment can completely distinguish between the two. The trade-off is that only experiments in these settings can shed light on the impact of real-world changes in leadership.

For India, previous research has found that women leaders invest in public goods that are more in line with female preferences, in particular water infrastructure (*27*, *33*). This may explain the reduction in time spent on domestic chores by adolescent girls. Furthermore, if female leaders invested differentially in schooling for girls, this may also underlie the change in educational outcomes we observe. We now provide several pieces of evidence suggesting that in this context, the role model effect of female leaders is an important channel (perhaps the most important) in changing parents' and girls' aspirations.

Table 2. Adolescents' aspirations. Data are presented as in Table 1. The sample size is 3680. All estimates control for village characteristics described in table S1.

	Does not wish to be housewife or whatever in-laws prefer	Wishes to have a high-education job	Wishes to marry after age 18	Wishes to graduate or get higher education	Normalized average	Wishes to be pradhan
Means and SDs in never-reserved village councils						
Boys	0.998	0.157	0.980	0.296	0.248	0.499
	[0.048]	[0.364]	[0.141]	[0.457]	[0.447]	[0.500]
Girls	0.600	0.166	0.660	0.195	−0.260	0.485
	[0.490]	[0.373]	[0.474]	[0.396]	[0.758]	[0.500]
Coefficients						
Never reserved						
Gap	−0.398	0.008	−0.319	−0.099	−0.507	−0.017
	(0.026)	(0.020)	(0.025)	(0.018)	(0.034)	(0.026)
Reserved once						
Boys	−0.008	0.053	−0.004	0.038	0.050	−0.013
	(0.011)	(0.022)	(0.013)	(0.026)	(0.029)	(0.035)
Girls	−0.031	0.062	0.010	0.035	0.045	−0.010
	(0.034)	(0.021)	(0.031)	(0.022)	(0.045)	(0.039)
Difference in gap	−0.023	0.009	0.014	−0.003	−0.005	0.003
	(0.036)	(0.028)	(0.034)	(0.028)	(0.052)	(0.039)
Reserved twice						
Boys	0.008	−0.014	0.003	0.034	0.017	0.057
	(0.017)	(0.034)	(0.021)	(0.047)	(0.048)	(0.056)
Girls	0.083	0.086	0.088	0.035	0.182	0.049
	(0.043)	(0.036)	(0.041)	(0.035)	(0.056)	(0.055)
Difference in gap	0.075	0.099	0.085	0.001	0.166	−0.008
	(0.042)	(0.051)	(0.049)	(0.045)	(0.057)	(0.053)

Downloaded from www.sciencemag.org on February 2, 2012

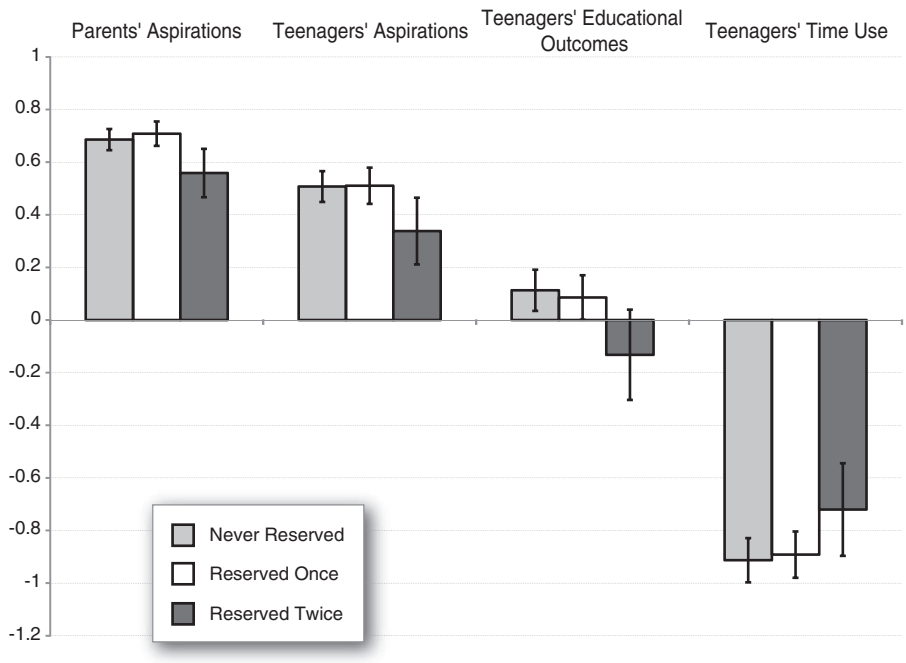


Fig. 1. Gap in aspirations, educational outcomes, and time use. The gray, white, and black bars represent difference in the normalized average of aspirations of parents for their adolescent boys and girls (left-most panel) and the difference in normalized average of aspirations, educational outcomes, and time spent on domestic chores between adolescent boys and girls themselves in village councils that have never been reserved, have been reserved only once, and have been reserved twice for a female leader, respectively. The error bars represent the 95% confidence interval.

In Fig. 2, table S5, and (*26*), we find no evidence that female reservation influenced the careers, education, or labor market outcomes of young adults (aged 16 to 30), a group that adolescent girls and their parents are likely to look to when forming expectations about their future (*34*). The gender gap in the educational outcomes of young adults is not smaller in twice-reserved villages ($P > 0.6$, t test). There is no impact on the probability that young women in villages reserved twice are housewives ($P > 0.8$, t test), have jobs requiring high education ($P > 0.2$, t test), or have access to employment-generating schemes ($P > 0.5$, t test). Finally, neither these young women ($P > 0.5$, t test) nor other women in the household ($P > 0.4$, t test) spend less time on domestic chores in villages.

Moreover, there is no evidence that female leaders made improvements in educational infrastructure that could have benefited girls more than boys. Young girls are as likely as young boys to be in school, and there is no difference in test scores (*26*). The reduction in the gender gap in education of adolescents is thus not due to a change in the environment. It is also probably not due to an 18-min reduction in time spent on domestic chores. It is most likely a consequence of the change in aspirations. In turn, the reduction in time spent on chores may reflect parents giving girls time to study.

Finally, the timing of the effect (starting in the second cycle) suggests that female leaders' image underlies the change in aspiration and

Table 3. Adolescents' educational outcomes and time use. Data are presented as in Table 1. The sample size is 3680. All estimates control for village characteristics described in table S1.

	1 if attends school	1 if can read and write	Grade completed	Normalized average	Total time on domestic chores (minutes per day)
Means and SDs in never-reserved village councils					
Boys	0.744	0.947	5.538	0.055	29.298
	[0.436]	[0.225]	[2.166]	[0.760]	[50.841]
Girls	0.684	0.908	5.409	−0.058	108.231
	[0.465]	[0.289]	[2.386]	[0.898]	[96.884]
Coefficients					
Never reserved					
Gap	−0.060	−0.038	−0.132	−0.112	78.954
	(0.019)	(0.014)	(0.113)	(0.041)	(4.845)
Reserved once					
Boys	0.005	−0.020	0.019	−0.020	−5.095
	(0.022)	(0.013)	(0.117)	(0.042)	(3.719)
Girls	0.010	−0.002	−0.002	0.004	−6.844
	(0.026)	(0.015)	(0.138)	(0.051)	(7.178)
Difference in gap	0.005	0.018	−0.021	0.024	−1.748
	(0.029)	(0.021)	(0.153)	(0.058)	(6.475)
Reserved twice					
Boys	0.005	−0.012	−0.094	−0.025	2.869
	(0.044)	(0.031)	(0.247)	(0.100)	(6.881)
Girls	0.098	0.050	0.587	0.223	−14.772
	(0.049)	(0.029)	(0.237)	(0.102)	(10.153)
Difference in gap	0.093	0.062	0.681	0.248	−17.641
	(0.051)	(0.033)	(0.243)	(0.102)	(8.971)

Downloaded from www.sciencemag.org on February 2, 2012

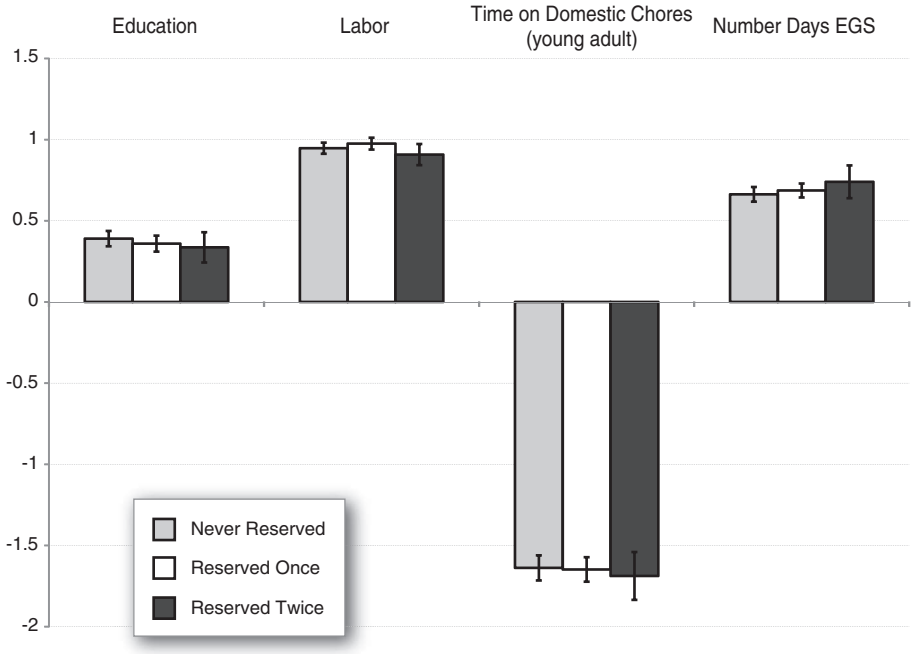


Fig. 2. Potential channels: gap in young adult educational outcomes, young adult labor market outcomes, young adult time use, and access to public services. The gray, white, and black bars represent the gender gap in normalized average of young adults' educational and labor market outcomes, adult time use, and access to employment generation schemes in village councils that have never been reserved, have been reserved only once, and have been reserved twice for a female leader, respectively. The error bars represent the 95% confidence interval.

educational outcomes for two reasons: (i) The changes in infrastructure provision, especially greater investment in water-related facilities, occur in the first electoral cycle after reservation. In the second cycle, there is no discernible difference in infrastructure provision across once- and twice-reserved villages (*27*, *28*). (ii) Previous work (*28*) has shown that in the first cycle, voters have a comparatively low opinion of their female leaders. However, with exposure, their beliefs change progressively: first, their opinion about the ability of women to lead in general (as captured by responses to vignettes in which the gender of the politician is experimentally altered) and then, by the second cycle, their opinion about their own leader's abilities. Voters in twice-reserved villages have as positive a view of their female leader as villagers in never-reserved areas (almost all of whom have male leaders). Voters are also more likely to elect women for unreserved seats in councils that have been reserved twice for a female leader. The timing of the effect on aspirations and education is consistent with the time it takes for female leaders to be seen in a positive light.

Women in leadership positions have long been thought to have the potential to pave the way for long-term changes by influencing aspirations; our study demonstrates their impact in a nationwide policy experiment in India. We present evidence suggesting that this impact exceeds their (relatively limited) ability to change the concrete situation of women and girls in the short run through direct policy actions. It is their presence as positive role models for the younger generation that seems to underlie observed changes in aspirations and educational outcomes of adolescent girls.

These results show that laws can help to create role models by opening opportunities that were previously unavailable to a group, and that this increased opportunity does not diminish the aspirations of those outside the group. The ability of affirmative action to create role models has been subject to debate: Although the policy allows members of disadvantaged groups to access positions of prestige and power, it may also cause a backlash if it creates the perception that the achievement was not due to merit. Our study shows that in the Indian context, the positive effect of exposure to a female leader dominated any possible backlash, probably because it gave women a chance to demonstrate that they are capable leaders. And, perhaps most important, our study establishes that the role model effect reaches beyond the realm of aspirations into the concrete, with real educational and time-use impacts.

References and Notes

1. M. Krook, *Quotas for Women in Politics: Gender and Candidate Selection Reform Worldwide* (Oxford Univ. Press, New York, 2009).
2. A. Eagly, *Sex Differences in Social Behavior: A Social Role Interpretation* (Erlbaum, Hillsdale, NJ, 1987).
3. A. Bandura, *Annu. Rev. Psychol.* **52**, 1 (2001).
4. A. Bandura, C. Barbaranelli, G. V. Caprara, C. Pastorelli, *Child Dev.* **72**, 187 (2001).
5. G. L. Cohen, J. Garcia, V. Purdie-Vaughns, N. Apfel, P. Brzustoski, *Science* **324**, 400 (2009).
6. K. Bussey, A. Bandura, *Psychol. Rev.* **106**, 676 (1999).
7. H. M. Lips, *Psychol. Women Q.* **24**, 39 (2000).
8. H. M. Lips, *J. Soc. Issues* **57**, 799 (2001).
9. A. H. Eagly, S. J. Karau, *Psychol. Rev.* **109**, 573 (2002).
10. L. A. Rudman, J. E. Phelan, *J. Soc. Psychol.* **41**, 192 (2010).
11. M. Gardiner, M. Tiggemann, J. Kearns, K. Marshall, *High. Educ. Res. Dev.* **26**, 425 (2007).
12. M. M. Nauta, D. L. Epperson, J. H. Kahn, *J. Couns. Psychol.* **45**, 483 (1998).
13. L. S. Richman, M. van Dellen, W. Wood, *J. Soc. Issues* **67**, 492 (2011).
14. W. Smith, T. Erb, *J. Res. Sci. Teach.* **23**, 667 (1986).
15. S. Asgari, N. Dasgupta, N. G. Cote, *Soc. Psychol.* **41**, 202 (2010).
16. P. Lockwood, *Psychol. Women Q.* **30**, 36 (2006).
17. J. G. Stout, N. Dasgupta, M. Hunsinger, M. McManus, *J. Pers. Soc. Psychol.* **100**, 255 (2011).
18. L. A. Rudman, J. E. Phelan, *J. Soc. Psychol.* **41**, 192 (2010).
19. L. A. Nixon, M. D. Robinson, *Demography* **36**, 185 (1999).
20. J. C. Wright *et al.*, *Child Dev.* **66**, 1706 (1995).
21. B. J. Canes, H. S. Rosen, *Ind. Labor Relat. Rev.* **48**, 486 (1995).
22. C. Wolbrecht, D. Campbell, *Am. J. Pol. Sci.* **51**, 921 (2007).
23. A. Greene, H. Sullivan, K. Beyard-Tyler, *J. Educ. Psychol.* **74**, 393 (1982).
24. For example, in one of the studies in (*17*), women's perceptions of their role in mathematics and their actual performance on a math test are analyzed after exposure to a brief interaction with a same-sex expert in the laboratory, while another study had laboratory participants read biographies of engineers that were randomly varied to represent women or men, and (*23*) examines the change in college students' self-perceptions relative to a control group after reading an article about hypothetical female or male role models.
25. S. Kaul, S. Sahni, *Stud. Home Comm. Sci.* **3**, 29 (2009).
26. See supporting material on *Science* Online.
27. R. Chattophadhyay, E. Duflo, *Econometrica* **72**, 1409 (2004).
28. L. Beaman *et al.*, *Q. J. Econ.* **124**, 1497 (2009).
29. The survey team interviewed all adolescents in a household. Adult respondents were asked only about their own biological children. There were cases in which adolescents were interviewed whose biological parents were not interviewed, thereby generating a larger sample of adolescents.
30. J. Kling, J. Liebman, L. Katz, *Econometrica* **75**, 83 (2007).
31. D. Karlan, J. Zinman, *Science* **332**, 1278 (2011).
32. T. Nguyen, Information, role models, and perceived returns to education: Experimental evidence from Madagascar. *Mimeo MIT* (2008); www.povertyactionlab.org/sites/default/files/documents/Nguyen%202008.pdf.
33. L. Beaman, E. Duflo, R. Pande, P. Topalova, *India Policy Forum. Brookings and NCAER* **7**, 159 (2010-11).
34. R. Jensen, Economic opportunities and gender differences in human capital: An experimental test for India. *NBER Working Paper 16021* (2010).

Acknowledgments: We thank R. Chattopadhyay, with whom we initiated this research agenda and we collaborated on previous studies, and P. Chakraborthy and SRG Consulting for data collection. The views expressed in this paper are those of the authors and do not implicate the International Monetary Fund, its management, or its executive board. Supported by Ash Institute Harvard, Nike Foundation, MIT, National Institute of Child Health and Human Development grant R01 HD039922-06, Yale University, and UNICEF. The data are accessible at the Harvard-MIT data center Web site: http://dvn.iq.harvard.edu/dvn/dv/mit/faces/StudyListingPage.xhtml?mode=1&collectionId=24.

Supporting Online Material

www.sciencemag.org/cgi/content/full/science.1212382/DC1
Materials and Methods
SOM Text
Tables S1 to S6
References (*35*, *36*)

8 August 2011; accepted 30 December 2011
Published online 12 January 2012;
10.1126/science.1212382

Downloaded from www.sciencemag.org on February 2, 2012

Untangling Genomes from Metagenomes: Revealing an Uncultured Class of Marine Euryarchaeota

Vaughn Iverson, Robert M. Morris, Christian D. Frazar, Chris T. Berthiaume, Rhonda L. Morales, E. Virginia Armbrust*

Ecosystems are shaped by complex communities of mostly unculturable microbes. Metagenomes provide a fragmented view of such communities, but the ecosystem functions of major groups of organisms remain mysterious. To better characterize members of these communities, we developed methods to reconstruct genomes directly from mate-paired short-read metagenomes. We closed a genome representing the as-yet uncultured marine group II *Euryarchaeota*, assembled de novo from 1.7% of a metagenome sequenced from surface seawater. The genome describes a motile, photo-heterotrophic cell focused on degradation of protein and lipids and clarifies the origin of proteorhodopsin. It also demonstrates that high-coverage mate-paired sequence can overcome assembly difficulties caused by interstrain variation in complex microbial communities, enabling inference of ecosystem functions for uncultured members.

Abundant and diverse populations of microbes shape every marine environment on Earth (*1*, *2*). Most environmental microbes are uncultured and resistant to laboratory-based physiological and genomic investigations (*3*, *4*). The importance of this uncultured majority cannot be overstated because microbial life plays a critical role in the biogeochemical cycling of elements, maintaining the chemical state of the oceans (*5*). How these communities may respond to remediate or exacerbate human impacts is unclear because their ecosystem function remains poorly understood.

Glimpses into the genomes of uncultured microbes are provided by environmental genomic approaches such as single-cell genomics (*6*) and the sequencing of long segments [10 to 60 kilo–base pairs (kbp)] of DNA cloned directly from environmental samples (*7*). Shotgun metagenomics bypasses manual isolation of individual sequences and instead yields large catalogs of randomly sampled environmental genes (*8*–*11*). Connecting these genes to specific taxonomic groups has been problematic except for groups previously sequenced or those with relative abundances exceeding ~20% (*12*, *13*). The greater sequencing depth provided by next-generation technologies (*14*) has recently been exploited to partially assemble multiple genomes from cow rumen microbiomes (*15*). Several of these assemblies were estimated to exceed 90% completeness, although all originated from taxonomic orders of Bacteria with cultured and sequenced representatives. We used mate-paired next-generation sequencing of two marine metagenomic samples to reveal the genome sequences of organisms constituting small minorities (<10%) of the total populations, including an uncultured marine group II *Euryarchaeote* genome.

School of Oceanography, University of Washington, Box 357940, Seattle, WA 98195, USA.

*To whom correspondence should be addressed. E-mail: armbrust@uw.edu

We collected cells (<0.8 μm) from surface waters of Puget Sound in October 2008 and May 2009 (*16*). Each sample harbored communities of marine bacteria and archaea present at ~10^6 cells per ml (table S1). Massively parallel sequencing (*14*) with a SOLiD DNA analyzer (Life Technologies Corporation, Carlsbad, California) produced a total of 58.5 gigabases of 50-base mate-paired reads (table S2). Analysis of metagenomic 16*S* ribosomal DNA (rDNA) sequence revealed diverse communities, with most family-level taxonomic groups present at less than 10% [figs. S1 to S9 and supporting online material (SOM) text]. Mismatch-tolerant alignments with the Global Ocean Sampling (GOS) (*10*) and RefSeq (*17*) databases recruited about 10 and 2% of reads, respectively (tables S2 and S3), highlighting the substantial proportion of previously unsequenced populations in our samples.

De novo assembly of the metagenomic reads produced ~300 megabases of contigs that recruited about threefold more metagenomic reads (~30%) than the GOS database (table S2). High-coverage mate-pairing information was exploited to link the assembled contigs (spanning short unassembled sequences), creating metagenomic assembly graphs (Fig. 1 and figs. S10 and S11). These connection graphs were split heuristically by using mate-pairing bit scores, nucleotide composition, and read-coverage statistics, producing parsimonious linear scaffolds. Scaffolds were binned by using tetra-nucleotide statistics into candidate genomes, which were taxonomically profiled by using mate-pair connections to informative 16*S* rDNA regions. Fourteen candidate genomes were produced, each representing 4 to 10% of a sampled community, including representatives of *Euryarchaeota*, *Thaumarchaeota*, *Flavobacteria*, and alpha-, beta-, and gamma-*Proteobacteria*. We selected one candidate genome from each sample for more detailed analysis.

A nearly complete genome closely related to the cultured and sequenced *Rhodobacterales* bacterium strain HTCC2255 was reconstructed entirely de novo from a population composing ~6.3% of the October sample (see *Thalassobacter*, fig. S6).

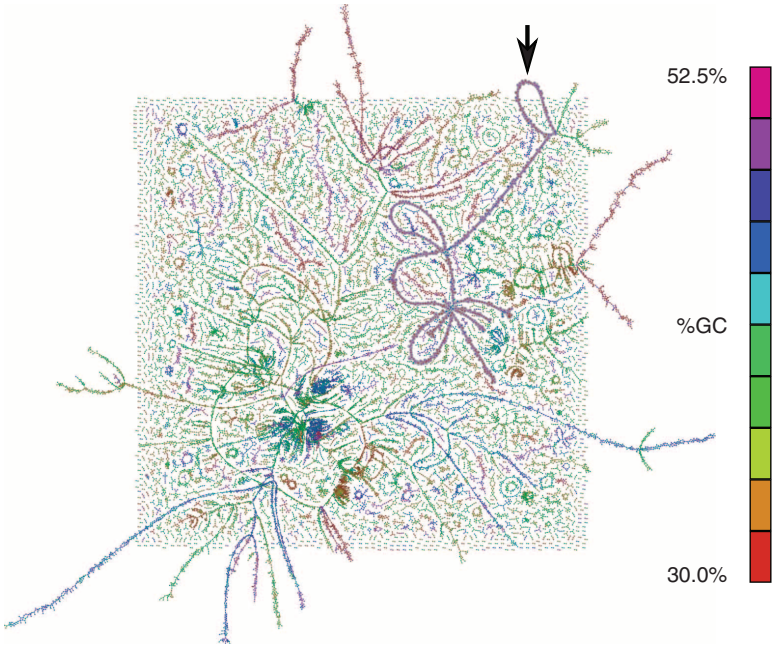


Fig. 1. Mate-pair connection graph illustrating the May 2009 metagenome de novo assembly. Lines represent contigs with mate-pair connections scoring greater than 750 bits (n = 30,945). Long strands represent prokaryote genome sequences, and small circular strands show likely virus or plasmid sequences. Contigs aligning with the MG-II genome assembly are indicated (black arrow, gray shading).

Downloaded from www.sciencemag.org on February 2, 2012

Nucleotide alignments of the binned scaffolds to the HTCC2255 reference genome show all 41 scaffolds aligning, with gaps reflecting the lack of metagenomic reads from the October sample recruiting to those regions of the reference genome (figs. S10 and S12). The remarkable level of agreement between the assembled and reference genomes demonstrates the robustness of our approach.

A closed genome (designated herein as MG-II) representing the marine group II *Euryarchaeota* was reconstructed via de novo assembly of 11 mate-pair connected scaffolds with highly correlated sequence statistics (Fig. 1 and fig. S13) from a population composing ~7.5% of the May sample (fig. S9). A small hypervariable region (HVR) was insufficiently covered for complete automated assembly. Two variants with coverage of ~20× were partially reconstructed, and one of these (~14 kbp) was finished by using Sanger sequencing to fill remaining gaps. The resulting circular chromosome of 2.06 megabases recruited ~5 million aligned reads (1.7% of the May metagenome), yielding 118-fold read coverage and 2194-fold physical coverage by mate-pair inserts (figs. S14 and S15). The proportion of coverage of the two HVR variants to the genome average and analysis of 16*S* rDNA sequences (fig. S16) each predict that five or more strains of marine group II euryarchaeota were present in the May sample. Our assembly therefore represents a "majority rules" consensus, with possible genomic rearrangements at scaffold boundaries in some strains.

The mesophilic marine group II euryarchaeota have a cosmopolitan distribution and are relatively abundant during summer months (*18*, *19*). The metabolism of this uncultured group has been mysterious, with only a handful of sequenced environmental clones containing definitive phylogenetic markers (16*S* and 23*S* rDNA) available to infer its biogeochemical role (fig. S16) (*20*–*23*). To evaluate the correspondence of the MG-II genome to known environmental sequences and identify additional sequences not previously ascribed to this group, we performed six-frame translated alignments of GenBank environmental sequences to the MG-II genome. Sixty-seven environmental clones and 2894 metagenomic assemblies were identified that covered 36 and 96%, respectively, of predicted MG-II protein coding sequences (Fig. 2A). Clones derived from globally distributed marine samples revealed significant conservation

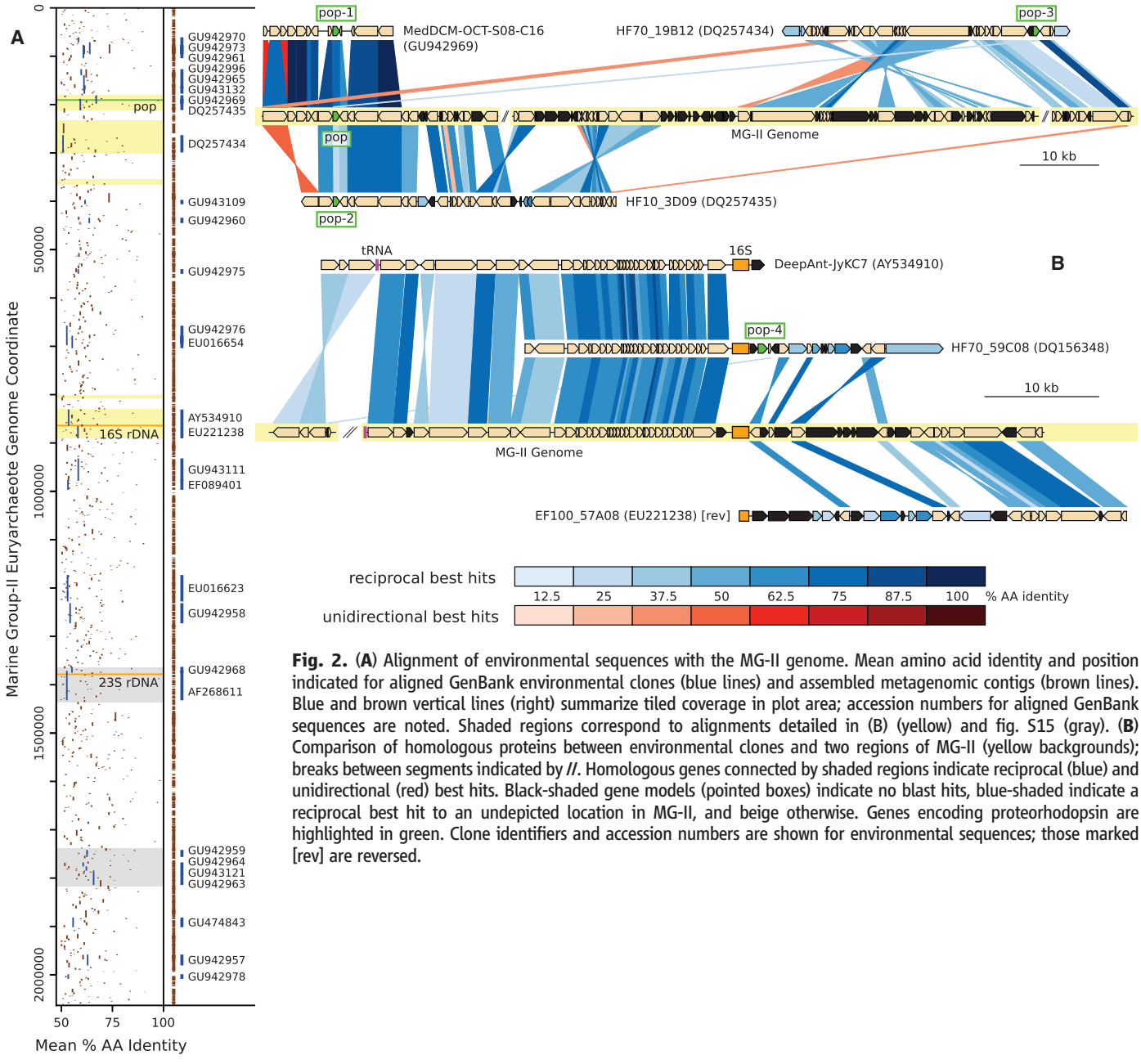


Fig. 2. (**A**) Alignment of environmental sequences with the MG-II genome. Mean amino acid identity and position indicated for aligned GenBank environmental clones (blue lines) and assembled metagenomic contigs (brown lines). Blue and brown vertical lines (right) summarize tiled coverage in plot area; accession numbers for aligned GenBank sequences are noted. Shaded regions correspond to alignments detailed in (B) (yellow) and fig. S15 (gray). (**B**) Comparison of homologous proteins between environmental clones and two regions of MG-II (yellow backgrounds); breaks between segments indicated by //. Homologous genes connected by shaded regions indicate reciprocal (blue) and unidirectional (red) best hits. Black-shaded gene models (pointed boxes) indicate no blast hits, blue-shaded indicate a reciprocal best hit to an undepicted location in MG-II, and beige otherwise. Genes encoding proteorhodopsin are highlighted in green. Clone identifiers and accession numbers are shown for environmental sequences; those marked [rev] are reversed.

Downloaded from www.sciencemag.org on February 2, 2012

of gene order with the MG-II genome assembly (Fig. 2B and fig. S17), reaffirming the group's cosmopolitan distribution.

Of particular interest is the single-copy proteorhodopsin (*pop*) gene present in the MG-II genome, which encodes key active-site residues shared with the light-driven proton-pumping rhodopsin found in *Exiguobacterium sibiricum* (*24*). Environmental marine group II euryarchaeal *pop* genes appear in at least three MG-II genetic contexts: the position originally detected by Frigaard *et al*. (*22*) (pop-4, Fig. 2B); that of the MG-II *pop* gene (pop, Fig. 2B), confirmed by two environmental clones (pop-1 and pop-2, Fig. 2B); and that found in an environmental clone aligning with a third region of the MG-II genome (pop-3, Fig. 2B). These five *pop* genes cluster phylogenetically into two distinct clades that also contain 42 *pop* genes identified in metagenomic assemblies aligning with positions in the MG-II genome. Clade A shares a common ancestor with proteorhodopsins from *Proteobacteria* (*22*), whereas clade B is diverged from all known bacterial proteorhodopsins (*25*) (Fig. 3 and fig. S18). The only synteny shared by *pop* genes from both clades ($n = 22$; in red, Fig. 3 and fig. S18) is the genetic context seen in the MG-II genome (pop, pop-1, and pop-2; Fig. 2B), indicating that the most parsimonious origin of clade A is a euryarchaeal ancestor shared with clade B. Thus, the proteorhodopsin of marine *Proteobacteria* appears to have originated in marine group II *Euryarchaeota*.

The MG-II genome sequence reveals 1781 predicted proteins, single copies of each of the four ribosomal RNA genes, and a typical number of tRNAs and noncoding RNAs (table S4). The MG-II 16*S* rDNA gene clusters with the group II.a clade of marine group II *Euryarchaeota* (*26*) (fig. S16). An analysis using 31 conserved archaeal proteins (table S5) places the marine group II *Euryarchaeota* in the most deeply rooted position of a clade containing primarily thermoacidophiles, including *Aciduliprofundum boonei* (*27*) and members of order *Thermoplasmata* (fig. S19A). The MG-II genome shares the same complement of ribosomal proteins found in *A. boonei* with complete conservation of gene order within multigene clusters (table S6), indicating *A. boonei* is the most closely related sequenced organism to marine group II euryarchaeota.

Core MG-II archaeal metabolic genes include those encoding glycolysis and gluconeogenesis pathways, a complete tricarboxylic acid cycle, and oxidative phosphorylation complexes. Genes dedicated to performing autotrophy or methanogenesis using known pathways are absent. MG-II encodes proteins potentially requiring and transporting cobalamin (vitamin B_{12}) and biotin (vitamin B_7) but does not appear to possess pathways to synthesize these compounds de novo. Additionally it does not appear to possess enzymes to reduce nitrate or sulfate, implying a dependence on reduced forms of N and S. An operon containing genes for archaeal flagellar proteins similar in gene order to those identified in *A. boonei* (*27*) strongly suggests the capacity for motility. We interpret these observations to indicate a motile heterotrophic lifestyle.

Among the MG-II genes are many large putative peptidases (table S7), which are overrepresented in the genome relative to those in the known protein degrader *A. boonei* (*27*) (5.7 versus 4.8% of coding sequence; table S4). This adds considerable new evidence to previous speculation (*20*, *21*) that consumption of protein may be an important metabolic activity shared in common with the peripherally related *Thermoplasmata* (*28*). Unexpectedly, we identified enzymes most similar to bacterial proteins that form a complete fatty acid degradation pathway (table S8), suggesting that marine group II euryarchaeota may catabolize straight chain lipids. The degradation of protein and lipid suggests that particles may be an important growth substrate, and MG-II codes for proteins with a variety of adhesion domains, as well as type II/IV secretion systems to transport such proteins to the cell surface.

We identified enzymes necessary to synthesize precursors for archaeal ether-linked lipids and also identified several putative acyl-carrier-protein fatty-acid synthesis enzymes and enzyme homologs for glycerolipid biosynthesis, most similar to bacterial proteins (table S8) and without homologs among the sequenced Archaea. The exclusive use of ether-linked isoprenoid lipids is considered a signature trait of nearly all Archaea (*29*), so the possible production and function of Bacteria-like ester-linked lipids requires further examination. Overall, MG-II contains 332 genes (~18.6%) with nearest homologs in the genomes of Bacteria, higher than the 119 genes (~7.7%) similarly classified in *A. boonei* (figs. S19 and S20, tables S9 and S10, and SOM text). These genes (including those for ester-linked lipid metabolism) are distributed across all of the well-supported scaffolds in the MG-II assembly (fig. S15), suggesting that marine group II euryarchaeota share many genetic adaptations with Bacteria.

Marine group II euryarchaeota are likely motile photo-heterotrophs focused on protein and lipid degradation. Proteorhodopsin, which appears to be a euryarchaeal innovation, may provide beneficial supplemental energy for propulsion to cells traversing relatively large distances in search of food particles (*30*). De novo assembly and analysis of the MG-II genome from high-coverage mate-paired metagenomic sequence demonstrates the power of this approach to provide insights into the roles uncultured microbes play in a changing global environment.

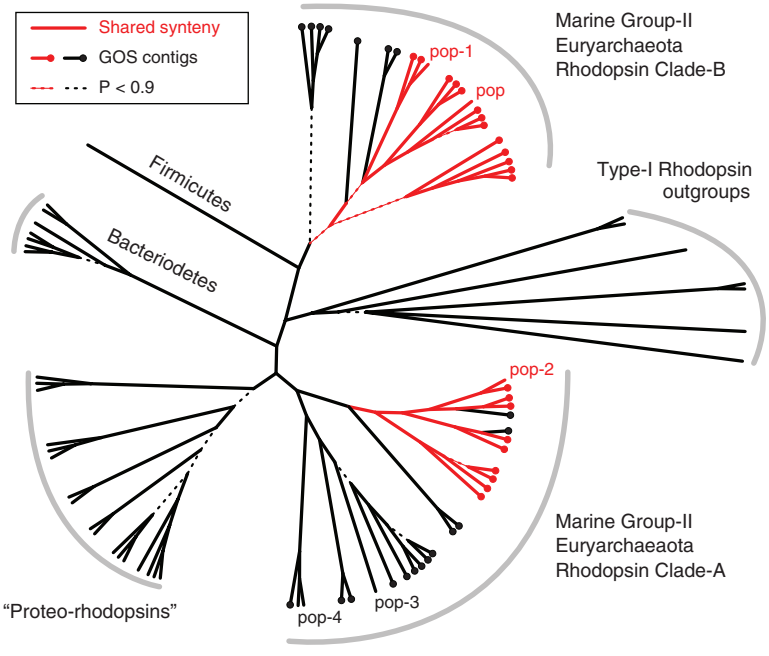


Fig. 3. Unrooted cladogram depicting Bayesian phylogeny of selected rhodopsin proteins. Major clades are labeled taxonomically, with "Proteo-rhodopsins" denoting those found in marine *Proteobacteria* (genomes and environmental clones). Out groups include bacterial and archaeal "bacteriorhodopsins," archaeal halorhodopsins, and sensory rhodopsins. The MG-II rhodopsin (pop), and four proteins from marine group II *Euryarchaeota* environmental clones (pop-1 to pop-4) are identified.

References and Notes

1. D. M. Karl, *Nat. Rev. Microbiol.* **5**, 759 (2007).
2. F. Azam, F. Malfatti, *Nat. Rev. Microbiol.* **5**, 782 (2007).
3. J. T. Staley, A. Konopka, *Annu. Rev. Microbiol.* **39**, 321 (1985).
4. M. S. Rappé, S. J. Giovannoni, *Annu. Rev. Microbiol.* **57**, 369 (2003).
5. P. G. Falkowski, T. Fenchel, E. F. Delong, *Science* **320**, 1034 (2008).
6. R. Stepanauskas, M. E. Sieracki, *Proc. Natl. Acad. Sci. U.S.A.* **104**, 9052 (2007).
7. O. Béjà, *Curr. Opin. Biotechnol.* **15**, 187 (2004).
8. J. C. Venter *et al*., *Science* **304**, 66 (2004); 10.1126/science.1093857.

Downloaded from www.sciencemag.org on February 2, 2012

9. E. F. DeLong *et al.*, *Science* **311**, 496 (2006).
10. D. B. Rusch *et al.*, *PLoS Biol.* **5**, e77 (2007).
11. S. Yooseph *et al.*, *PLoS Biol.* **5**, e16 (2007).
12. D. A. Walsh *et al.*, *Science* **326**, 578 (2009).
13. D. B. Rusch, A. C. Martiny, C. L. Dupont, A. L. Halpern, J. C. Venter, *Proc. Natl. Acad. Sci. U.S.A.* **107**, 16184 (2010).
14. E. R. Mardis, *Trends Genet.* **24**, 133 (2008).
15. M. Hess *et al.*, *Science* **331**, 463 (2011).
16. Materials and methods are available as supporting material on *Science* Online.
17. K. D. Pruitt, T. Tatusova, D. R. Maglott, *Nucleic Acids Res.* **35**, D61 (2007).
18. A. Pernthaler, C. M. Preston, J. Pernthaler, E. F. DeLong, R. Amann, *Appl. Environ. Microbiol.* **68**, 661 (2002).
19. L. Herfort *et al.*, *FEMS Microbiol. Ecol.* **62**, 242 (2007).
20. O. Béjà *et al.*, *Environ. Microbiol.* **2**, 516 (2000).
21. D. Moreira, F. Rodríguez-Valera, P. López-García, *Environ. Microbiol.* **6**, 959 (2004).
22. N.-U. Frigaard, A. Martinez, T. J. Mincer, E. F. DeLong, *Nature* **439**, 847 (2006).
23. A.-B. Martin-Cuadrado *et al.*, *ISME J.* **2**, 865 (2008).
24. L. E. Petrovskaya *et al.*, *FEBS Lett.* **584**, 4193 (2010).
25. R. Ghai *et al.*, *ISME J.* **4**, 1154 (2010).
26. P. E. Galand, C. Gutiérrez-Provecho, R. Massana, J. M. Gasol, E. O. Casamayor, *Limnol. Oceanogr.* **55**, 2117 (2010).
27. A.-L. Reysenbach, G. E. Flores, *Geobiology* **6**, 331 (2008).
28. A. Ruepp *et al.*, *Nature* **407**, 508 (2000).
29. Y. Koga, H. Morii, *Microbiol. Mol. Biol. Rev.* **71**, 97 (2007).
30. J. M. Walter, D. Greenfield, C. Bustamante, J. Liphardt, *Proc. Natl. Acad. Sci. U.S.A.* **104**, 2408 (2007).

Acknowledgments: We thank D. Kingsbury and T. Hunkapiller for helpful conversations about experimental design; W. Martens-Habbena, D. Stahl, and J. Baross for reviewing draft protein annotations; Q. Wang for providing the RDP classifier training set data; D. Schruth for technical support; and A. Ingalls and J. Baross for valuable comments on the draft manuscript. We are grateful to Life Technologies, Incorporated, for SOLiD sequencing of the October 2008 sample. This study was supported by a Gordon and Betty Moore Foundation Marine Microbiology Investigator Award and NSF grant OCE-0723866. Sequences reported in this study have been deposited in the National Center for Biotechnology Information (NCBI) Sequence Read Archive under accession no. SRA047968 and in GenBank under accession nos. JF965490 to JF965492 and JN591771 to JN592031. The Whole Genome Shotgun project has been deposited at DNA Data Bank of Japan/European Molecular Biology Laboratory/GenBank under the accession AHCG00000000. The version described in this paper is the first version, AHCG01000000. Information regarding the custom software developed for use in this research is available at http://armbrustlab.ocean.washington.edu/software.

Supporting Online Material

www.sciencemag.org/cgi/content/full/335/6068/587/DC1
Materials and Methods
SOM Text
Figs. S1 to S20
Tables S1 to S10
References (*31*–*65*)

15 August 2011; accepted 14 December 2011
10.1126/science.1212665

Sequential Signaling Crosstalk Regulates Endomesoderm Segregation in Sea Urchin Embryos

Aditya J. Sethi,[1] Radhika M. Wikramanayake,[2] Robert C. Angerer,[1] Ryan C. Range,[1] Lynne M. Angerer[1]*

The segregation of embryonic endomesoderm into separate endoderm and mesoderm fates is not well understood in deuterostomes. Using sea urchin embryos, we showed that Notch signaling initiates segregation of the endomesoderm precursor field by inhibiting expression of a key endoderm transcription factor in presumptive mesoderm. The regulatory circuit activated by this transcription factor subsequently maintains transcription of a canonical Wnt (cWnt) ligand only in endoderm precursors. This cWnt ligand reinforces the endoderm state, amplifying the distinction between emerging endoderm and mesoderm. Before gastrulation, Notch-dependent nuclear export of an essential β-catenin transcriptional coactivator from mesoderm renders it refractory to cWnt signals, insulating it against an endoderm fate. Thus, we report that endomesoderm segregation is a progressive process, requiring a succession of regulatory interactions between cWnt and Notch signaling.

Early endomesoderm induction and subsequent segregation of endoderm from mesoderm are fundamental processes in animal development. Although initial endomesoderm specification has been studied extensively (*1*, *2*), its separation in deuterostomes is poorly understood. In several deuterostomes including vertebrates such as zebrafish and *Xenopus* and echinoderms such as sea urchins and sea stars (*3*–*7*), Notch signaling induces the expression of endoderm- or mesoderm-specific markers within an endomesoderm field. Although Notch might regulate endomesoderm segregation, it is unknown whether it alters the early endomesoderm signaling milieu, a change that is probably required to stabilize lineage identities. Canonical Wnt (cWnt) signaling probably establishes that precursor environment, given its ancestral role in specifying early endomesoderm (*8*). Elucidating the mechanisms underlying such a Notch-cWnt interaction would substantially advance our understanding of the progressive specialization of the endomesoderm.

Like other deuterostomes, sea urchin embryos are enriched asymmetrically in the cWnt signaling effector nuclear β-catenin (nβ-catenin) (*9*), which specifies endomesoderm precursors in three ways. First, it establishes an early endoderm regulatory state in a tier of vegetal blastomeres (veg_2, Fig. 1A) at cleavage stages (*9*–*11*). Second, in micromere descendants located immediately adjacent to the veg_2 tier (Fig. 1A), nβ-catenin induces expression of the ligand Delta (*12*–*14*), which signals through the Notch receptor in veg_2 blastomeres and activates mesoderm gene expression (*5*, *6*, *13*, *15*). Third, cWnt also makes veg_2 cells competent to receive the micromere Delta signal (*12*). Thus, specification of both endoderm and mesoderm is initiated by the blastula stage throughout veg_2 blastomeres (Fig. 1A) (*6*, *9*, *11*, *16*, *17*).

By the hatching blastula (HB) stage, veg_2 progeny form outer and inner rings of cells (Fig. 1A). Only inner veg_2 daughters adjacent to Delta-expressing micromere progeny can transduce the cell contact–dependent Notch signal and continue expressing mesoderm markers (*17*). Transcripts encoded by endoderm regulatory genes, in turn, are detected in outer veg_2 daughters by this time (*11*, *17*). Notch is required for this restriction because it inhibits expression of the endoderm markers *foxa*, *blimp1b*, and *dac* in inner veg_2 daughters (*17*–*19*). During cleavage and HB stages, nβ-catenin is detected throughout the veg_2 endomesoderm precursor field (*9*). By the mesenchyme blastula (MB) stage, 6 to 8 hours after endoderm marker expression first clears from inner veg_2 daughters, nβ-catenin is down-regulated in these mesoderm precursors through a process requiring Notch (*9*, *20*, *21*). Thus, Notch probably plays a substantial role in endomesoderm segregation beyond merely activating mesoderm regulatory genes. However, several major questions remain unanswered. First, how does Notch restrict endoderm fate to a subset of the endomesoderm progenitor field? Second, how does Notch inhibit endomesoderm-inducing cWnt in presumptive mesoderm (*9*, *21*) 6 to 8 hours after initial endoderm marker expression has disappeared? Third, are these Notch-dependent events mechanistically linked?

To understand initial Notch-dependent restriction of endoderm potential from mesoderm, we used Notch-deficient embryos to systematically assess the expression of each gene in the early endoderm gene regulatory network (GRN) (fig. S1A), which represents cWnt-induced endoderm specification until the HB stage (*10*, *11*). We found that *hox11/13b*, *brachyury*, *blimp1b*, and *foxA* transcripts accumulated ectopically in

[1]National Institute of Dental and Craniofacial Research, National Institutes of Health, Bethesda, MD, USA. [2]Department of Public Health, University of Oxford, Oxford, UK.

*To whom correspondence should be addressed. E-mail: langerer@mail.nih.gov

Downloaded from www.sciencemag.org on February 2, 2012

inner veg_2 descendants when Notch was knocked down (fig. S1, B to E and I to L). Because only part of the cWnt-activated early endoderm GRN is thus subject to Notch inhibition (fig. S1, F to H and M to O), Notch does not initially modulate upstream cWnt signaling. Instead, it probably inhibits an intermediate endoderm GRN factor(s) activated in endomesoderm precursors by the earlier cWnt input. Such a mechanism would also allow mesoderm induction in veg_2 progeny, which require cWnt for competence to transduce the Notch signal (*12*). Furthermore, because *brachyury*, *blimp1b*, and *foxA* are Hox11/13b target genes (Fig. 1, B to I) (*11*), we hypothesized that Notch could initiate endoderm restriction simply by suppressing *hox11/13b* expression in mesoderm. We confirmed this through two observations. First, *brachyury*, *foxa*, and *blimp1b* are not expressed ectopically in inner veg_2 descendants (Fig. 1, K to M versus O to Q) in Notch-deficient embryos that also lack Hox11/13b. Second, Notch-suppressed endoderm genes still accumulate ectopically in inner veg_2 descendants in double morphants that lack both Notch and any one of Brachyury, FoxA or Blimp1b (figs. S2 to S4). Thus, Notch initially suppresses mesodermal accumulation of a single endoderm transcription factor, Hox11/13b. This prevents ectopic activation of the Hox11/13b-dependent regulatory circuit, consisting of Brachyury, Blimp1b, and FoxA, despite the presence of nβ-catenin in the mesoderm (*9*).

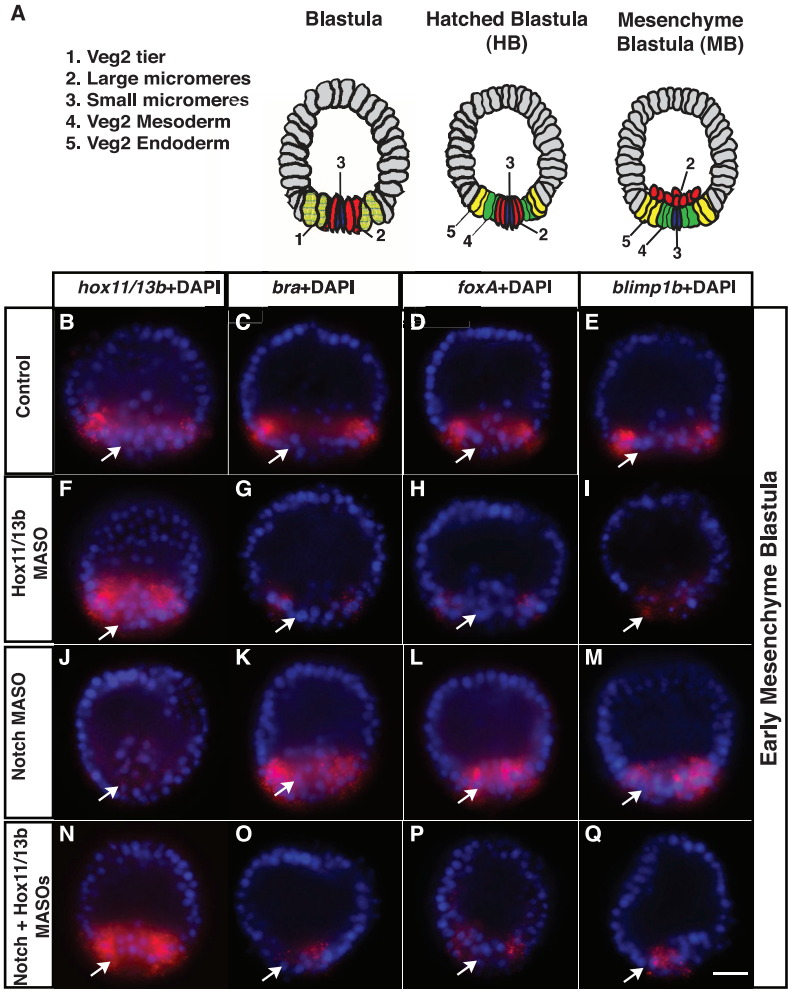


Fig. 1. Notch inhibits a Hox11/13b-dependent regulatory circuit in mesoderm. (**A**) Diagram of endomesoderm blastomeres: Large (red) micromere progeny are adjacent to veg_2 cells in which early cWnt activates endoderm and mesoderm specification (hatched light green) in early blastulae. By the HB stage, veg_2 descendants form outer (presumptive endoderm, yellow) and inner (presumptive mesoderm, green) rings. Large micromere progeny (red) ingress by the MB stage. (**C** to **E**) versus (**G** to **I**) Endodermal *brachyury (bra)*, *foxa*, and *blimp1b* transcripts are down-regulated in Hox11/13b morphants (MASO). Arrows indicate inner veg_2 cells (presumptive mesoderm). DAPI, 4′,6-diamidino-2-phenylindole stain. (**B**), (**F**), and (**N**) *hox11/13b* mRNA is up-regulated in Hox11/13b morphants because Hox11/13b represses its own transcription (*11*). (**K**) to (**M**) Ectopic expression of *brachyury (bra)*, *foxa*, and *blimp1b* mRNA occurs in inner veg_2 cells of Notch morphants. (**J**) *hox11/13b* mRNA concentration is low through autorepression by ectopic Hox11/13b protein (*11*). (**O**) to (**Q**) In Notch+Hox11/13b double morphants, ectopic expression of Hox11/13b target genes in inner veg_2 cells (arrows) is significantly lower (Q). Scale bar, 20 μm.

We hypothesized that Notch clears nβ-catenin from mesoderm by the MB stage (*9*, *21*) by inhibiting expression of a cWnt ligand in this lineage, and we identified *wnt1* as a candidate through two observations: First, like nβ-catenin, *wnt1* mRNA is detected throughout veg_2 endomesoderm (fig. S5) between the HB and MB stages, and is down-regulated through Notch in mesoderm by the MB stage (Fig. 2, A to D) (*9*, *21*). Second, at the MB stage, Wnt1 stimulates nβ-catenin activity, as revealed by cWnt-dependent TOPFLASH (*22*) luciferase reporter assays (Fig. 2E). Because *wnt1* expression is restricted to the endoderm 6 to 8 hours after Notch confines the expression of Hox11/13b-activated regulatory genes to this lineage, we assessed the potential linkage between these events. Both endodermal *wnt1* expression in normal embryos at the MB stage and its persistence in mesoderm in the absence of Notch require Hox11/13b and its target, Brachyury (Fig. 2, F to K). These *wnt1* regulators are also essential for normal levels of cWnt activity at this time (Fig. 2E). Thus, by inhibiting mesodermal *hox11/13b* expression at the HB stage, Notch indirectly restricts *wnt1* accumulation to the endoderm, where it probably contributes to maintaining cWnt activity.

Because the endoderm GRN depends on cWnt (*11*, *18*, *23*), we hypothesized that ligands activating cWnt signaling stabilize the endoderm regulatory state and amplify its distinction from mesoderm. Consistent with this idea, two different Wnt1 morpholinos interfere with endodermal expression of *hox11/13b*, *brachyury*, *foxa*, and *blimp1b* (Fig. 2, L to S, and fig. S6) at the MB stage and substantially delay gastrulation (fig. S7). Additionally, Notch-mediated *wnt1* down-regulation could help deplete nβ-catenin in the mesoderm (*9*), leading to repression of cWnt-sensitive endoderm genes through its transcriptional binding partner T cell factor (TCF) (*24*). This would further reinforce endomesoderm segregation, because TCF represses at least one endoderm factor, FoxA, in the mesoderm at the MB stage (*18*). Other Wnt ligands, including Wnt6 and Wnt8, which are required for endoderm specification (*25*–*27*), might also contribute to endomesoderm separation by increasing cWnt signaling. Consistent with the timing of its restriction to endoderm, Wnt1 reinforces endoderm segregation only at the MB stage. It does not affect its initial restriction at the HB stage because Notch-deficient embryos lacking Wnt1 protein still show ectopic expression of Hox11/13b target genes in inner veg_2 descendants (fig. S8).

Delta-Notch signaling can also inhibit cWnt activity in sea urchin embryos by activating Nemo-like kinase (NLK) expression in veg_2 descendants (*28*). In other systems, NLK, a MAP kinase, modulates cWnt signaling by phosphorylating β-catenin's essential transcriptional coactivator, TCF, and promoting its nuclear export (*29*). The

Downloaded from www.sciencemag.org on February 2, 2012

loss of TCF could eliminate cWnt signaling via any Wnt ligand in the mesoderm. We detected TCF protein in all nuclei until the late MB stage (fig. S9, A to C). However, just before gastrulation begins, 4 hours after the MB stage, TCF clears specifically from mesoderm nuclei (fig. S9) in a Notch- and NLK-dependent manner (Fig. 3, A to I), which strongly antagonizes cWnt in these cells.

In this study, we elucidated sequential Notch-dependent mechanisms that precisely regulate endomesoderm segregation (steps 1 to 3 in Fig. 3J). Notch initially restricts a transcription factor(s) to the endodermal daughters of endomesoderm precursors, where it subsequently activates cWnt. Such a mechanism could be shared with other deuterostomes, because Notch affects expression of *brachyury* and *foxA* during endomesoderm segregation in both echinoderm and vertebrate embryos (*3*, *4*, *7*, *17*–*19*). The regulatory device through which Notch indirectly modifies

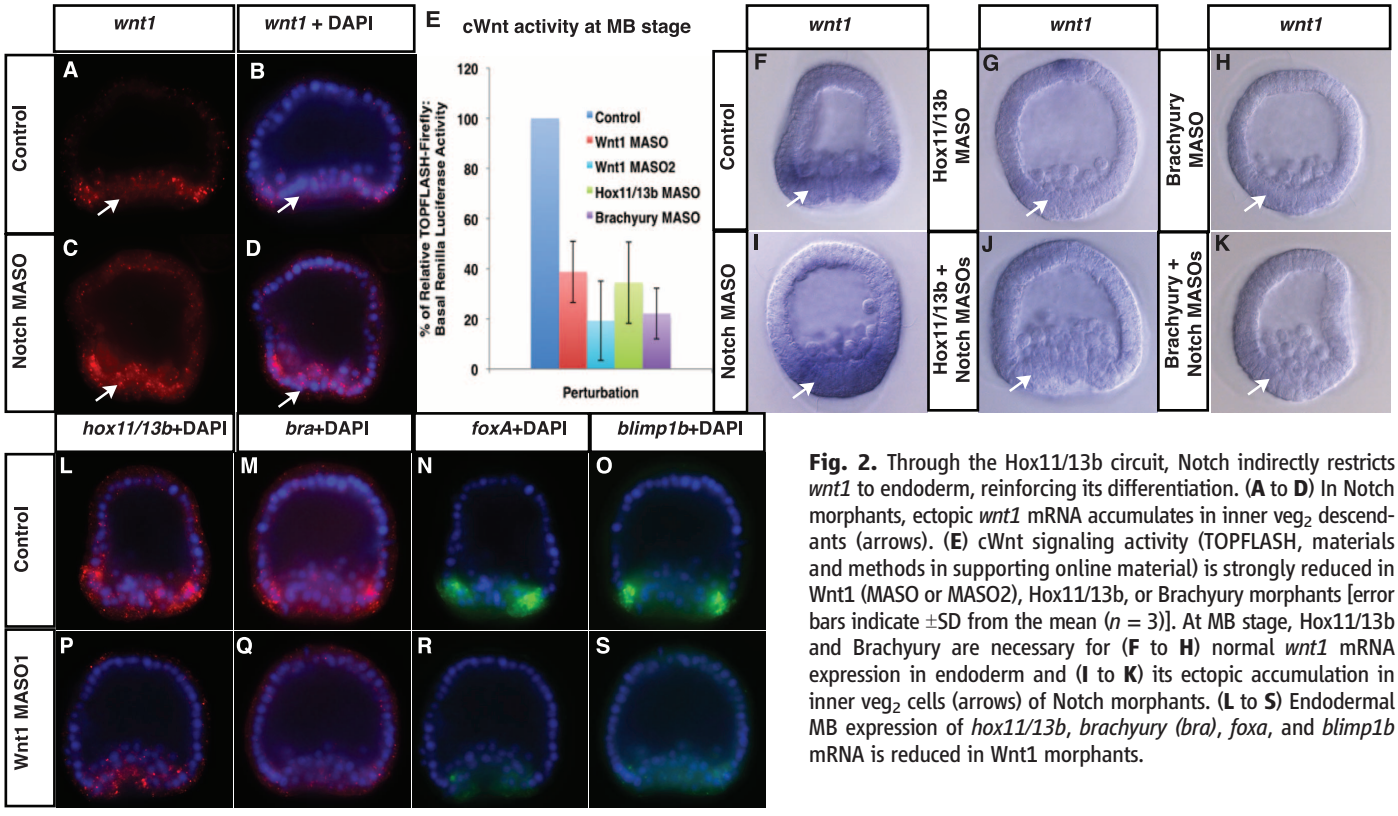


Fig. 2. Through the Hox11/13b circuit, Notch indirectly restricts *wnt1* to endoderm, reinforcing its differentiation. (**A** to **D**) In Notch morphants, ectopic *wnt1* mRNA accumulates in inner veg_2 descendants (arrows). (**E**) cWnt signaling activity (TOPFLASH, materials and methods in supporting online material) is strongly reduced in Wnt1 (MASO or MASO2), Hox11/13b, or Brachyury morphants [error bars indicate ±SD from the mean (n = 3)]. At MB stage, Hox11/13b and Brachyury are necessary for (**F** to **H**) normal *wnt1* mRNA expression in endoderm and (**I** to **K**) its ectopic accumulation in inner veg_2 cells (arrows) of Notch morphants. (**L** to **S**) Endodermal MB expression of *hox11/13b*, *brachyury (bra)*, *foxa*, and *blimp1b* mRNA is reduced in Wnt1 morphants.

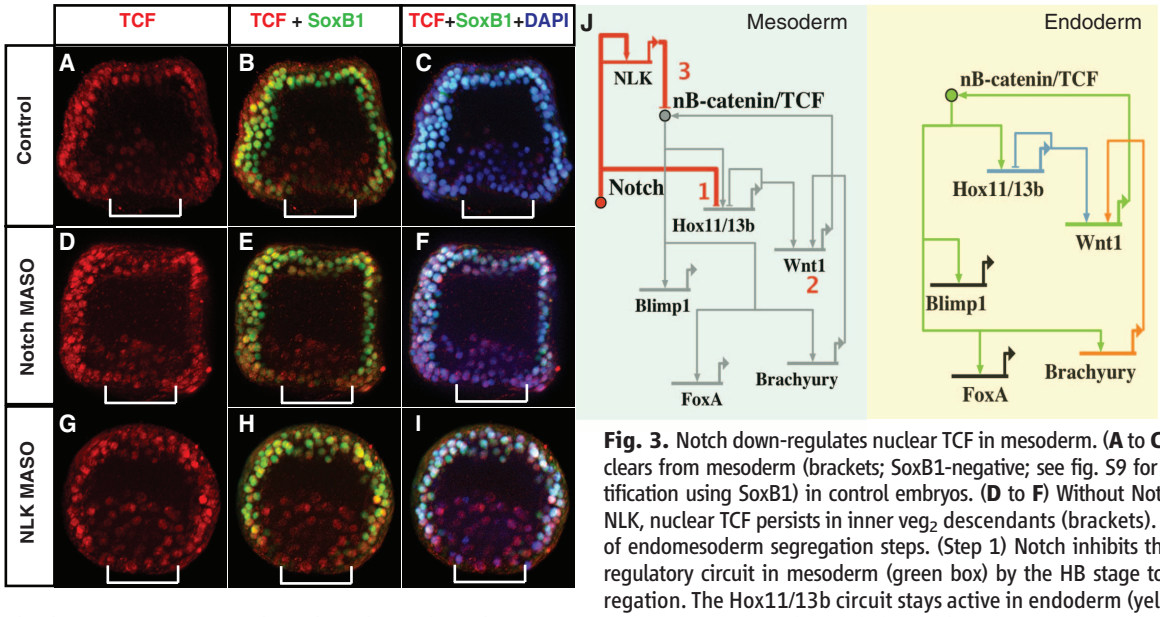


Fig. 3. Notch down-regulates nuclear TCF in mesoderm. (**A** to **C**) Nuclear TCF clears from mesoderm (brackets; SoxB1-negative; see fig. S9 for lineage identification using SoxB1) in control embryos. (**D** to **F**) Without Notch or (**G** to **I**) NLK, nuclear TCF persists in inner veg_2 descendants (brackets). (**J**) Summary of endomesoderm segregation steps. (Step 1) Notch inhibits the Hox11/13b regulatory circuit in mesoderm (green box) by the HB stage to initiate segregation. The Hox11/13b circuit stays active in endoderm (yellow). (Step 2) Consequently, by the MB stage, Hox11/13b- and Brachyury-dependent expression of *wnt1* is restricted to endoderm, where it reinforces cWnt signaling and endoderm fate. (Step 3) By the pre-gastrula stage, a Notch-NLK pathway clears nuclear TCF from mesoderm, making it unresponsive to cWnt. The endoderm retains nuclear TCF and cWnt sensitivity.

Downloaded from www.sciencemag.org on February 2, 2012

the early endomesoderm cWnt signaling state could also be conserved, because Brachyury maintains transcription of cWnt ligands in both zebrafish and sea urchin embryos (*30*). Restricting Brachyury expression to either endoderm or mesoderm would also confine cWnt signaling. This could, in turn, reinforce lineage segregation, as seen with the Brachyury→Wnt1→endoderm and the Brachyury→cWnt→posterior mesoderm pathways in sea urchins and zebrafish, respectively (*30*). More generally, similar Notch-dependent mechanisms could modulate additional pathways such as Nodal/transforming growth factor–β that induce endomesoderm in vertebrate embryos (*31*). Finally, it is unknown whether Notch also insulates mesoderm or endoderm from incident cWnt signals through NLK activity in vertebrate embryos. We thus have uncovered a remarkable timing buffer that uses a cell contact–dependent signal to separate regulatory states within a broadly induced endomesoderm field without immediately altering its signaling milieu. This preserves the competence of each lineage and correctly institutes its specification. Individual lineage choices are then reinforced and cemented through successive signaling state changes.

References and Notes

1. D. Kimelman, K. J. Griffin, *Curr. Opin. Genet. Dev.* **10**, 350 (2000).
2. A. Rodaway, R. Patient, *Cell* **105**, 169 (2001).
3. Y. Kikuchi *et al.*, *Dev. Dyn.* **229**, 756 (2004).
4. D. R. Revinski, A. R. Paganelli, A. E. Carrasco, S. L. López, *Dev. Biol.* **339**, 477 (2010).
5. D. R. Sherwood, D. R. McClay, *Development* **124**, 3363 (1997).
6. D. R. Sherwood, D. R. McClay, *Development* **126**, 1703 (1999).
7. V. F. Hinman, E. H. Davidson, *Proc. Natl. Acad. Sci. U.S.A.* **104**, 19404 (2007).
8. C. P. Petersen, P. W. Reddien, *Cell* **139**, 1056 (2009).
9. C. Y. Logan, J. R. Miller, M. J. Ferkowicz, D. R. McClay, *Development* **126**, 345 (1999).
10. E. H. Davidson *et al.*, *Dev. Biol.* **246**, 162 (2002).
11. I. S. Peter, E. H. Davidson, *Dev. Biol.* **340**, 188 (2010).
12. D. R. McClay, R. E. Peterson, R. C. Range, A. M. Winter-Vann, M. J. Ferkowicz, *Development* **127**, 5113 (2000).
13. H. C. Sweet, M. C. Gehring, C. A. Ettensohn, *Development* **129**, 1945 (2002).
14. P. Oliveri, D. M. Carrick, E. H. Davidson, *Dev. Biol.* **246**, 209 (2002).
15. H. C. Sweet, P. G. Hodor, C. A. Ettensohn, *Development* **126**, 5255 (1999).
16. A. H. Wikramanayake, L. Huang, W. H. Klein, *Proc. Natl. Acad. Sci. U.S.A.* **95**, 9343 (1998).
17. J. C. Croce, D. R. McClay, *Development* **137**, 83 (2010).
18. S. B. de-Leon, E. H. Davidson, *Proc. Natl. Acad. Sci. U.S.A.* **107**, 10103 (2010).
19. I. S. Peter, E. H. Davidson, *Nature* **474**, 635 (2011).
20. S. W. Ruffins, C. A. Ettensohn, *Development* **122**, 253 (1996).
21. D. R. Sherwood, D. R. McClay, *Development* **128**, 2221 (2001).
22. V. Korinek *et al.*, *Science* **275**, 1784 (1997).
23. J. Smith, E. Kraemer, H. Liu, C. Theodoris, E. Davidson, *Dev. Biol.* **313**, 863 (2008).
24. S. Hoppler, C. L. Kavanagh, *J. Cell Sci.* **120**, 385 (2007).
25. J. Croce *et al.*, *Development* **138**, 3297 (2011).
26. A. H. Wikramanayake *et al.*, *Genesis* **39**, 194 (2004).
27. J. Smith, C. Theodoris, E. H. Davidson, *Science* **318**, 794 (2007).
28. E. Röttinger *et al.*, *Development* **133**, 4341 (2006).
29. M. C. Lo, F. Gay, R. Odom, Y. Shi, R. Lin, *Cell* **117**, 95 (2004).
30. B. L. Martin, D. Kimelman, *Dev. Cell* **15**, 121 (2008).
31. A. F. Schier, *Annu. Rev. Cell Dev. Biol.* **19**, 589 (2003).

Acknowledgments: The authors thank D. Adams and R. Benabentos for their comments. Funding was provided by the Intramural Program at the National Institute of Dental and Craniofacial Research, NIH.

Supporting Online Material

www.sciencemag.org/cgi/content/full/335/6068/590/DC1
Materials and Methods
Figs. S1 to S9
References (*32*–*36*)

18 August 2011; accepted 22 December 2011
10.1126/science.1212867

Growth of Western Australian Corals in the Anthropocene

Timothy F. Cooper,[1]* Rebecca A. O'Leary,[1] Janice M. Lough[2]

Anthropogenic increases of atmospheric carbon dioxide lead to warmer sea surface temperatures and altered ocean chemistry. Experimental evidence suggests that coral calcification decreases as aragonite saturation drops but increases as temperatures rise toward thresholds optimal for coral growth. In situ studies have documented alarming recent declines in calcification rates on several tropical coral reef ecosystems. We show there is no widespread pattern of consistent decline in calcification rates of massive *Porites* during the 20th century on reefs spanning an 11° latitudinal range in the southeast Indian Ocean off Western Australia. Increasing calcification rates on the high-latitude reefs contrast with the downward trajectory reported for corals on Australia's Great Barrier Reef and provide additional evidence that recent changes in coral calcification are responses to temperature rather than ocean acidification.

Coral growth is measurably influenced by the physical and chemical properties of the marine environment (*1*), which are changing rapidly owing to human interference in the global climate system (*2*–*4*). Emissions of CO_2 into the atmosphere from the combustion of fossil fuels, deforestation, and altered land use have resulted in current-day atmospheric CO_2 levels of around 390 parts per million (ppm), an increase of about 40% since preindustrial times. Increased concentrations of atmospheric CO_2 (along with other greenhouse gases) are associated with positive radiative forcing, which leads to a warming of the global climate system (*5*); about one-third of this extra CO_2 is taken up by the world's oceans (*6*). Oceanic uptake of anthropogenic CO_2 alters the seawater carbonate equilibrium by reducing both the pH and carbonate saturation states in the upper ocean layers (*2*, *7*) in a process known as ocean acidification (*8*). Reduced carbonate saturation state is expected to have profound effects on the calcification rates of a diverse range of marine calcifers, including reef-building corals (*4*, *9*–*11*). Warming of the tropical oceans is predicted to increase the frequency and severity of mass coral-bleaching events (*3*). Such changes in the marine environment are, therefore, likely to compromise coral calcification (facilitated by the coral-algal symbiosis), which forms the backbone of tropical coral reef ecosystems (*4*).

Annual density banding in certain massive corals allows retrospective analysis of historical calcification rates and inferences to be made about past environmental conditions and growth responses, including those before instrumental observations (*12*). Our study focused on coral reefs spanning an 11° latitudinal range in the southeast Indian Ocean to learn whether there have been any significant changes during the past 110 years in calcification rates on Australia's western coral reefs and how any observed changes relate to known changes in sea surface temperature (SST).

Twenty-seven long cores were collected, between October 2008 and September 2010, from massive *Porites* sp. colonies at six locations covering about 1000 km off the coast of Western Australia. Although some cores extend back to the 18th century, we focused on the period from 1900 to 2010, which was common to the majority (70%) of cores, to provide sufficient replication at each location and overlap with instrumental SST observations. The sampling locations included two reefs in the Rowley Shoals, Clerke Reef (17°16'S, 119°22'E) and Imperieuse Reef (17°31'S, 118°58'E); three locations within the Ningaloo Reef Tract, Bundegi (21°50'S, 114°11'E), Tantabiddi (21°54'S, 113°58'E), and Coral Bay (23°2'S, 113°49'E); and the Houtman Abrolhos Islands (28°28'S, 113°46'E) (Fig. 1). All sampled colonies were ≥2 m in height and selected from the leeward side of the reef or island at depths < 6 m below the lowest astronomical tide. Spatial and temporal variations in three annual coral growth parameters—annual extension (linear distance between adjacent density minima, cm $year^{-1}$), skeletal density (g cm^{-3}), and calcification

[1]Australian Institute of Marine Science, University of Western Australia Oceans Institute, Crawley 6009, Australia. [2]Australian Institute of Marine Science, Townsville, Queensland 4810, Australia.

*To whom correspondence should be addressed. E-mail: t.cooper@aims.gov.au

Downloaded from www.sciencemag.org on February 2, 2012

rate (the product of skeletal density and annual extension, g cm^{-2} $year^{-1}$)—were examined, as measured by gamma densitometry using standard procedures (*13*).

Annual calcification rates for each core were converted to calcification anomalies calculated as the percent difference between the annual calcification rate and the long-term average for the period 1900–2010. Average calcification anomalies were then calculated for each of the six locations and for all 27 coral cores. Average monthly SST were obtained from the HadISST 1.1 database (*14*). Given the close proximity of some of the sampling locations, the same SST series was applied to Imperieuse and Clerke Reefs (Rowley Shoals) and Tantabiddi and Bundegi (Ningaloo Reef). SSTs were expressed as annual anomalies relative to the 1900–2010 average.

Linear regression (generalized linear model) and nonlinear regression (generalized additive models) models were used to examine the influence of time, SST, and location on the calcification average and anomaly data (*15*). First, both models were used to explore the relationship between average annual SST and calcification of massive *Porites* sampled across the six locations. Second, the models were used to test the relationship between decadal anomalies in SST and calcification to allow for high interannual variability in coral growth rates (*12*). Finally, both models were used to examine the relationship between calcification and year over the period 1900–2010 at each location. All models were analyzed by using the statistical package R (*16*, *17*).

Significant warming of the tropical southeast Indian Ocean during the 20th century (Fig. 2A) is comparable to that recorded on the Great Barrier Reef (GBR) (*18*) and for tropical oceans globally (*19*). Average annual SSTs (1900–2010) at the sampling locations ranged from 27.6°C (Rowley Shoals; Clerke/Imperieuse), 25.2°C (northern Ningaloo; Tantabiddi/Bundegi), and 24.0°C (southern Ningaloo; Coral Bay) to 21.5°C (Houtman Abrolhos Islands). This corresponds to an environmental gradient for reef growth comprising "typical" SST conditions at the Rowley Shoals moving closer to "marginal" SST conditions (*20*) at the high-latitude Houtman Abrolhos Islands [although high summer calcium carbonate production rates have been reported at this location (*21*)]. In recent decades, positive SST anomalies have become a dominant feature for the southeast Indian Ocean. Since 1980, there have only been 3 years (1986, 1987, and 1993) with SSTs cooler than the long-term average (Fig. 2A). Warming of SSTs averaged across all locations was significant from 1900–2010 (linear regression, $P < 0.001$, $R^2 = 0.40$). There was, however, no significant change (linear regression, $P = 0.158$, $R^2 = 0.02$) in calcification rates averaged across the 27 coral cores over the same period (Fig. 2B). There are, however, spatial differences along Australia's tropical coasts in the magnitude of recent observed SST warming (*18*). SST warming rates were



Fig. 1. Map showing locations of six coral reef locations sampled for long coral cores along the West Australian coast.

Table 1. Results of generalized linear models testing the relationship between decadal SST and calcification anomalies in massive *Porites* for six coral reefs in Western Australia. Significant *P* values denoted with asterisks.

Location	Slope	SE	*t*	*P*
Clerke Reef	16.704	8.164	2.046	0.0711
Imperieuse Reef	5.039	4.744	1.062	0.3160
Bundegi	−14.442	6.515	−2.217	0.0539
Tantabiddi	8.113	3.043	2.666	0.0258*
Coral Bay	10.572	4.316	2.449	0.0368*
Houtman Abrolhos Islands	28.734	6.780	4.238	0.0022*

Table 2. Results of generalized linear models testing the relationship between calcification anomalies in massive *Porites* at each location and year over the period 1900–2010. Significant *P* values denoted with asterisks.

Location	Slope	SE	*P*	% Change over study period
Clerke Reef	0.022	0.034	0.5110	2.5
Imperieuse Reef	−0.038	0.028	0.1869	−4.1
Bundegi	−0.106	0.036	0.0038*	−11.6
Tantabiddi	−0.030	0.028	0.2811	−3.3
Coral Bay	0.056	0.025	0.0290*	6.2
Houtman Abrolhos Islands	0.216	0.046	<0.0001*	23.7

0.02°C/decade (Rowley Shoals), 0.06°C/decade (northern Ningaloo; Tantabiddi/Bundegi), and 0.08°C/decade (southern Ningaloo; Coral Bay) to 0.10°C/decade (Houtman Abrolhos Islands) during the period 1900–2010.

Warmer-than-average decadal SSTs were associated with significant increases in calcification in massive *Porites* located in the cool southern waters of Western Australia. At the Houtman Abrolhos Islands, increases in SST anomalies resulted in increased calcification rates of 23.5% (Fig. 3). Similar trends occurred at Coral Bay and Tantabiddi, where warmer SST anomalies were associated with 8.7 and 4.9% increases in decadal calcification rates, respectively. Smaller trends for increasing calcification rates were apparent at the northern Clerke and Imperieuse Reefs, where the decadal increase in SST was the least pronounced (Table 1). These positive responses contrasted with massive *Porites* at Bundegi, where above-average decadal SSTs resulted in a declining trend in calcification rates (Table 1).

Annual calcification anomalies at the six locations showed contrasting temporal variability between 1900 and 2010. There was no significant relationship between calcification anomalies and time for corals at the two most northern reefs of Clerke and Imperieuse Reefs (Fig. 4, A and B,

Downloaded from www.sciencemag.org on February 2, 2012

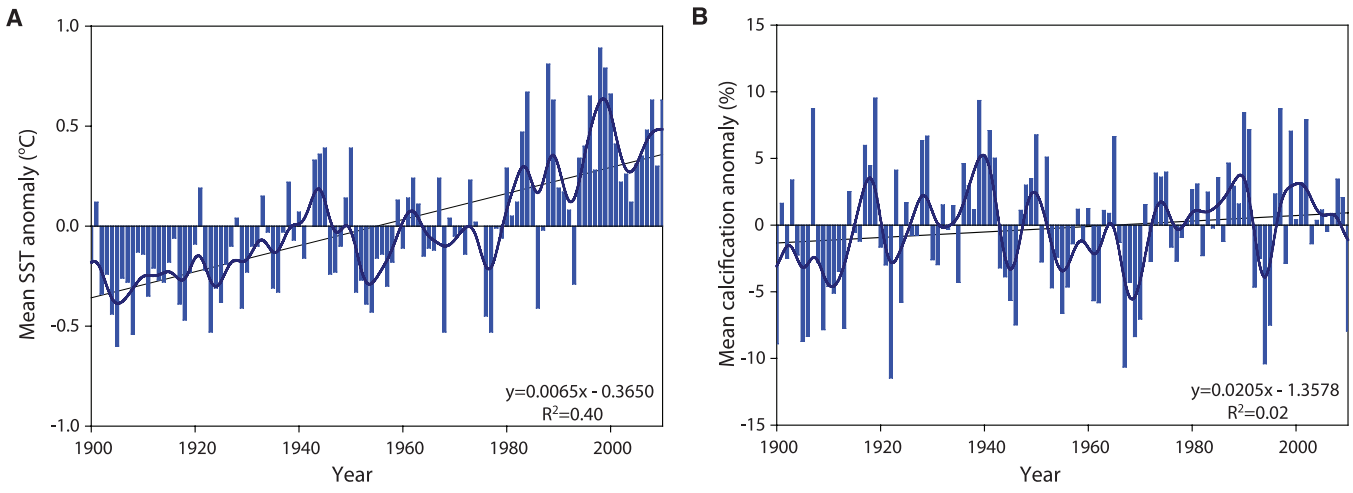


Fig. 2. Annual anomalies in (**A**) average SST (°C from 1900–2010 mean) and (**B**) average calcification (% of 1900–2010 mean) for six coral reef locations in the southeast Indian Ocean, Western Australia. Thick solid line is the 10-year Gaussian filter, and a linear regression is also given.

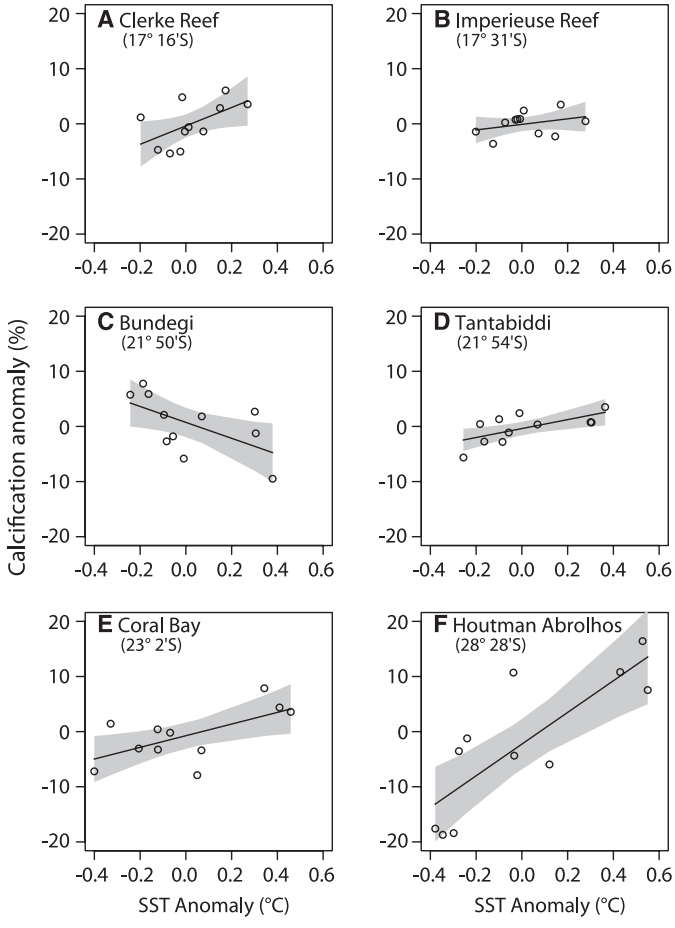


Fig. 3. Relationships between decadal SST and calcification (cal) anomalies (anom.) for (**A**) Clerke Reef (change in cal anom. is 7.5%; range of SST anom., −0.20 to 0.27; n = 5 cores), (**B**) Imperieuse Reef (cal anom., 2.4%; SST anom., −0.20 to 0.28; n = 4), (**C**) Bundegi (cal anom., −8.6%; SST anom., −0.39 to 0.38; n = 4), (**D**) Tantabiddi (cal anom., 4.9%; SST anom., −0.29 to 0.36; n = 7), (**E**) Coral Bay (cal anom., 8.7%; SST anom., −0.40 to 0.46; n = 4), and (**F**) Houtman Abrolhos Islands (cal anom., 23.5%; SST anom., −3.8 to 0.55; n = 3). Raw data are shown as open circles, solid line is the model fit to the data, and gray area is 95% confidence interval.

and Table 2). For the two locations in the northern Ningaloo Reef, there was a significant decline in calcification rates at Bundegi (Fig. 4C) but no significant change at Tantabiddi (Fig. 4D and Table 2). This contrasted with the two southernmost sampling locations. At Coral Bay, there was a significant increase in calcification rate of 6% over the period 1900–2010 (Fig. 4E; and Table 2). At the Houtman Abrolhos Islands, calcification rates increased significantly, by 23.7% between 1900 and 2010 (Fig. 4F and Table 2). In summary, the two most southerly locations, where recent SST warming was greatest, show a significant increase in calcification rates. This contrasts with the two most northerly locations in the Rowley Shoals, where there was no significant change in calcification rates and a much lower rate of SST warming. Only one location, Bundegi in Exmouth Gulf, showed a significant decline in calcification rates since 1900.

Emerging evidence of declines in coral calcification rates in an era of rapid environmental change is of great concern. On the GBR off eastern Australia, growth rates of massive *Porites* have declined about 14 to 21% (*22*, *23*) since 1990. Although the exact causes are not known, suggestions have been made that large-scale processes, such as ocean acidification, could be a possible driver (*23*, *24*). Others have attributed recent declines in coral growth rates to increasing thermal stress either because of setbacks in growth from coral-bleaching events (*25*) or to exceeding a thermal threshold for sustained calcification rates (*26*, *27*).

Annual density banding represents a valuable tool for retrospective monitoring of calcification rates in massive corals. However, owing to highly variable growth rates (*12*), replication is essential to obtain robust estimates of spatial and temporal variability and change. Our analysis of massive coral growth parameters spanned 11° latitude along Australia's western coast, an area of the southeast Indian Ocean that has warmed significantly during the past century. Overall, we found no widespread and consistent pattern of decline in calcification rates of Western Australian massive corals over time (table S1). Relationships between calcification rates and average SSTs and SST anomalies varied depending on location and were driven by the influence of these parameters on annual extension (table S2) rather than skeletal density (table S3). Where SST warming was minimal (Rowley Shoals; 0.02°C/decade), there was no significant change in calcification rates. This is consistent with Helmle *et al.* (*28*), who found a similar noncorrelation for the massive coral *Montastraea faveolata* in the Florida Keys between 1937 and 1996, when there was no significant SST warming. However, at our two most southerly locations, where a relatively large SST warming has occurred (e.g., 0.10°C/decade at Houtman Abrolhos Islands), we found evi-

Downloaded from www.sciencemag.org on February 2, 2012

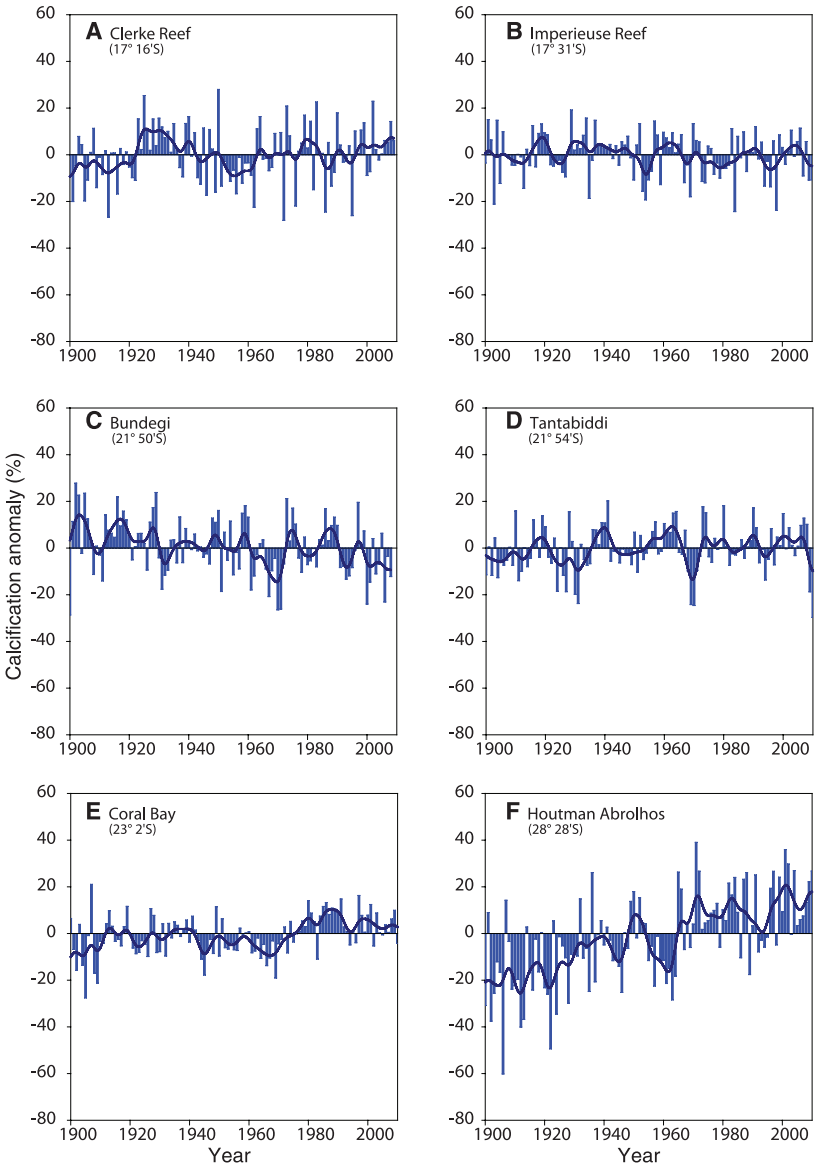


Fig. 4. Average annual calcification anomalies, 1900–2010, for (**A**) Clerke Reef, (**B**) Imperieuse Reef, (**C**) Bundegi, (**D**) Tantabiddi, (**E**) Coral Bay, and (**F**) Houtman Abrolhos Islands. Solid line is the 10-year Gaussian filter.

dence that massive corals have increased their calcification rates. Lough and Barnes (*29*) documented a similar positive correlation, suggesting that calcification rates may, at least initially, increase with global warming. Our findings suggest that the large-scale phenomenon of ocean acidification is not currently limiting calcification on coral reefs uniformly at a global scale. The influence of ocean acidification is expected to occur first at higher latitudes that inherently have lower seawater saturation states with respect to carbonate minerals due to their increased solubility at lower water temperatures (*10*, *30*). However, the significant recent above–long-term–average calcification anomalies recorded at the Houtman Abrolhos Islands lends support to the view that thermal changes are likely to be the principal immediate climate-change threat to the calcification potential of reef-building corals.

Seawater carbon chemistry is a key determinant of coral calcification, and the potential for future anthropogenic-influenced declines in carbonate saturation state, and hence coral calcification, is cause for serious concern (*2*, *4*, *7*). However, we conclude that the rate of change in the thermal environment of coral reefs is currently the primary driver of change in coral calcification rates. Warming SSTs are resulting in (i) increased calcification rates reported here in the southeast Indian Ocean, where marginal reefs have taken advantage of warmer conditions, and (ii) recent declines reported elsewhere for more typical reef environments where thermal optima for calcification have been exceeded or resulted in setbacks in growth as a result of thermally induced bleaching. Whether the former is sustainable as oceans continue to warm is another question.

References and Notes

1. R. W. Buddemeier, R. A. Kinzie, *Oceanogr. Mar. Biol. Annu. Rev.* **14**, 183 (1976).
2. J. A. Kleypas *et al.*, *Science* **284**, 118 (1999).
3. O. Hoegh-Guldberg, *Mar. Freshw. Res.* **50**, 839 (1999).
4. O. Hoegh-Guldberg *et al.*, *Science* **318**, 1737 (2007).
5. K. E. Trenberth *et al.*, in *Climate Change 2007: The Physical Science Basis. Contribution of Working Group I to the Fourth Assessment Report of the Intergovernmental Panel on Climate Change*, S. Solomon *et al.*, Eds. (Cambridge Univ. Press, Cambridge, 2007), pp. 235–336.
6. C. L. Sabine *et al.*, *Science* **305**, 367 (2004).
7. R. A. Feely *et al.*, *Science* **305**, 362 (2004).
8. K. Caldeira, M. E. Wickett, *Nature* **425**, 365 (2003).
9. J. P. Gattuso, M. Frankignoulle, R. Wollast, *Annu. Rev. Ecol. Syst.* **29**, 405 (1998).
10. S. C. Doney, V. J. Fabry, R. A. Feely, J. A. Kleypas, *Annu. Rev. Mar. Sci.* **1**, 169 (2009).
11. J. M. Guinotte, V. J. Fabry, *Ann. N. Y. Acad. Sci.* **1134**, 320 (2008).
12. J. M. Lough, T. F. Cooper, *Earth Sci. Rev.* **108**, 170 (2011).
13. B. E. Chalker, D. J. Barnes, *Coral Reefs* **9**, 11 (1990).
14. N. A. Rayner *et al.*, *J. Geophys. Res.* **108**, 4407 (2003).
15. J. C. Pinheiro, D. M. Bates, *Mixed-Effects Models in S and S-Plus* (Springer-Verlag, New York, 2000).
16. R Development Core Team (R Foundation for Statistical Computing, Vienna, Austria, 2011); http://cran.r-project.org/.
17. For further details see supporting material on *Science* Online.
18. J. M. Lough, *Geophys. Res. Lett.* **35**, L14708 (2008).
19. C. M. Eakin, J. M. Lough, S. F. Heron, in *Coral Bleaching: Patterns, Processes, Causes and Consequences*, M. J. H. van Oppen, J. M. Lough, Eds. (Springer-Verlag, 2009), vol. 205, pp. 41–67.
20. J. A. Kleypas, J. W. McManus, L. A. B. Menez, *Am. Zool.* **39**, 146 (1999).
21. S. V. Smith, *Limnol. Oceanogr.* **26**, 612 (1981).
22. T. F. Cooper, G. De'ath, K. E. Fabricius, J. M. Lough, *Glob. Change Biol.* **14**, 529 (2008).
23. G. De'ath, J. M. Lough, K. E. Fabricius, *Science* **323**, 116 (2009).
24. D. P. Manzello, *Coral Reefs* **29**, 749 (2010).
25. J. E. Carilli, R. D. Norris, B. A. Black, S. M. Walsh, M. McField, *PLoS ONE* **4**, e6324 (2009).
26. J. T. I. Tanzil, B. E. Brown, A. W. Tudhope, R. P. Dunne, *Coral Reefs* **28**, 519 (2009).
27. N. E. Cantin, A. L. Cohen, K. B. Karnauskas, A. M. Tarrant, D. C. McCorkle, *Science* **329**, 322 (2010).
28. K. P. Helmle, R. E. Dodge, P. K. Swart, D. K. Gledhill, C. M. Eakin, *Nature Communications* **2**, 215 (2011).
29. J. M. Lough, D. J. Barnes, *J. Exp. Mar. Biol. Ecol.* **245**, 225 (2000).
30. J. C. Orr *et al.*, *Nature* **437**, 681 (2005).

Acknowledgments: We thank N. Jeeves, K. Cook, T. Hyndes, P. Tinkler, G. Suosaari, M. Depczynski, and the crew of the RV *Solander* for support in collecting the cores; E. Matson for assistance in planning the sample collection, sample preparation, and undertaking the density measurements; and B. Radford for advice on the statistical analyses. An earlier version of the manuscript benefited from comments provided by A. Heyward and two anonymous reviewers. The coral calcification data used in this study has been archived in the AIMS Data Centre. This study was supported by the Australian Institute of Marine Science and BHP Billiton.

Supporting Online Material

www.sciencemag.org/cgi/content/full/335/6068/593/DC1
Materials and Methods
SOM Text
Tables S1 to S3
References

27 September 2011; accepted 23 November 2011
10.1126/science.1214570

Downloaded from www.sciencemag.org on February 2, 2012

Innate Response Activator B Cells Protect Against Microbial Sepsis

Philipp J. Rauch,[1]* Aleksey Chudnovskiy,[1]* Clinton S. Robbins,[1]*† Georg F. Weber,[1] Martin Etzrodt,[1] Ingo Hilgendorf,[1,6] Elizabeth Tiglao,[1] Jose-Luiz Figueiredo,[1] Yoshiko Iwamoto,[1] Igor Theurl,[1,3,7] Rostic Gorbatov,[1] Michael T. Waring,[4] Adam T. Chicoine,[4] Majd Mouded,[5] Mikael J. Pittet,[1] Matthias Nahrendorf,[1] Ralph Weissleder,[1,2] Filip K. Swirski[1]†

Recognition and clearance of a bacterial infection are fundamental properties of innate immunity. Here, we describe an effector B cell population that protects against microbial sepsis. Innate response activator (IRA) B cells are phenotypically and functionally distinct, develop and diverge from B1a B cells, depend on pattern-recognition receptors, and produce granulocyte-macrophage colony-stimulating factor. Specific deletion of IRA B cell activity impairs bacterial clearance, elicits a cytokine storm, and precipitates septic shock. These observations enrich our understanding of innate immunity, position IRA B cells as gatekeepers of bacterial infection, and identify new treatment avenues for infectious diseases.

Sepsis is characterized by whole-body inflammation in response to overwhelming infection (*1*). Over the past 30 years, the incidence of sepsis has risen, indicating the need for a better understanding of its complex pathophysiology (*2*, *3*). The growth factor granulocyte-macrophage colony-stimulating factor (GM-CSF) elicits multiple changes in cells expressing its cognate receptor. Yet, despite GM-CSF's multiple functions and known relationship with innate leukocytes, its in vivo cellular source and role in sepsis remain uncertain (*4*).

Profiling GM-CSF expression by flow cytometry led to a surprising observation. Among the organs, the bone marrow and spleen contained

[1]Center for Systems Biology, Massachusetts General Hospital and Harvard Medical School, Boston, MA 02114, USA. [2]Department of Systems Biology, Harvard Medical School, Boston, MA 02115, USA. [3]Program in Membrane Biology and Division of Nephrology, Massachusetts General Hospital and Harvard Medical School, Boston, MA 02114, USA. [4]Ragon Institute Imaging Core, Massachusetts General Hospital and Harvard Medical School, Boston, MA 02114, USA. [5]Division of Pulmonary, Allergy, and Critical Care Medicine, University of Pittsburgh School of Medicine, Pittsburgh, PA 15213, USA. [6]Department of Cardiology, University Hospital Freiburg, 79106 Freiburg, Germany. [7]Department of General Internal Medicine, Clinical Immunology and Infectious Diseases, University Hospital of Innsbruck, A-6020 Innsbruck, Austria.

*These authors contributed equally to this work.
†To whom correspondence should be addressed. E-mail: fswirski@mgh.harvard.edu (F.K.S.); robbins.clinton@mgh.harvard.edu (C.S.R.)

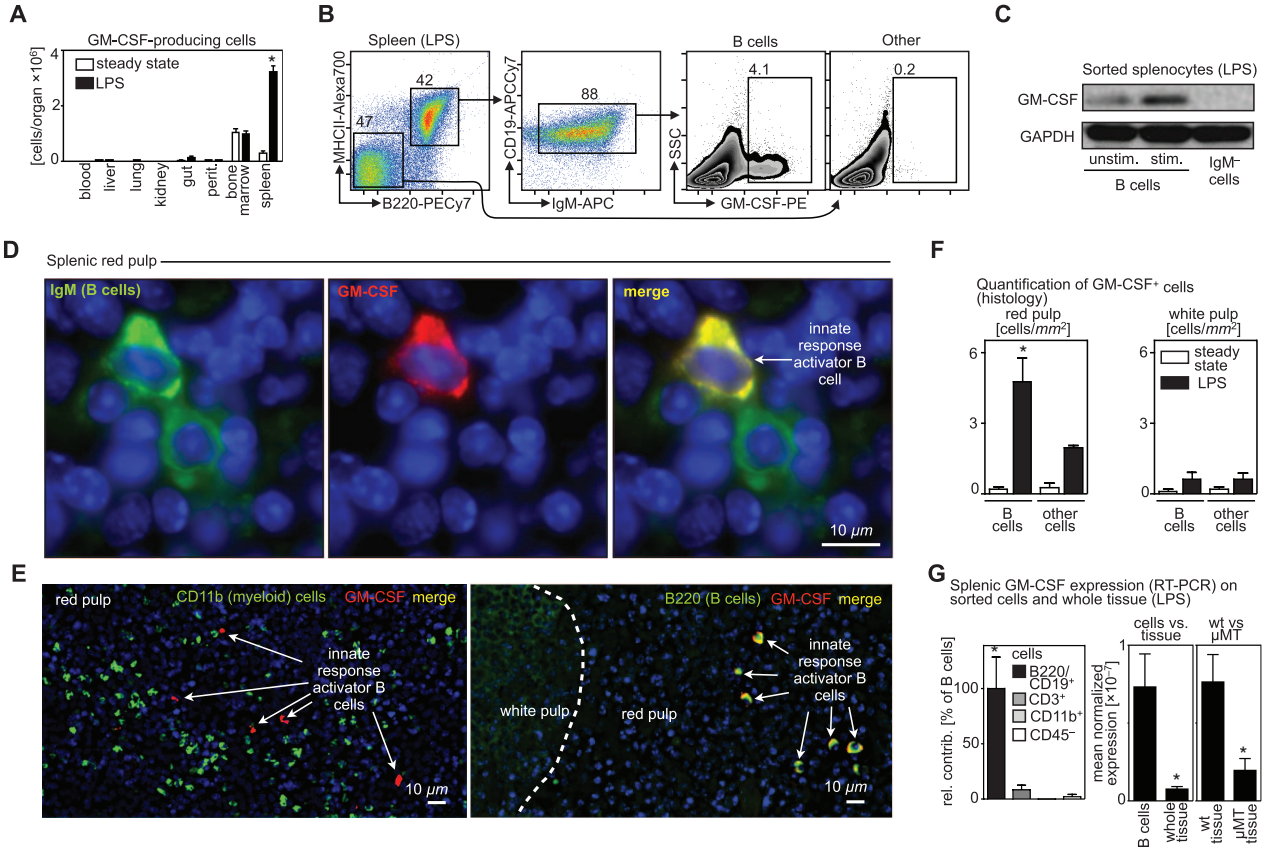


Fig. 1. IRA B cells are GM-CSF–producing B cells that increase in number during inflammation. (**A**) Quantification of GM-CSF–producing cells retrieved from tissues in the steady state and in response to four daily intraperitoneal injections of LPS (means ± SEM, n = 3 to 5 mice). *P < 0.05. (**B**) Identification of GM-CSF–producing cells in the spleen. Representative plots show percentage of B cells and their production of GM-CSF retrieved from spleens during inflammation. Data represent at least 10 independent experiments. (**C**) Western blot for GM-CSF conducted on sorted cells. One of three independent experiments is shown. GAPDH, glyceraldehyde-3-phosphate dehydrogenase. (**D**) Colocalization of representative GM-CSF–producing cells with IgM. (**E**) Red pulp sections with markers against CD11b (green) and GM-CSF (red) (left panel) and B220 (green) and GM-CSF (red) (right panel). Colocalization of green and red cells is shown in yellow. The dashed white curve indicates the border between white and red pulp. (**F**) Quantification of GM-CSF$^+$ B cells and other cells on histological sections of the spleen in the red pulp and white pulp in the steady state and after LPS (means ± SEM, n = 3 to 4). *P < 0.05. (**G**) Splenic GM-CSF expression detected by RT-PCR and conducted on sorted cells and on unprocessed spleen tissue taken from WT and B cell knockout (μMT) mice (means ± SEM, n = 3 to 4). *P < 0.05.

Downloaded from www.sciencemag.org on February 2, 2012

the majority of GM-CSF$^+$ cells in the steady state ($1.0 \pm 0.1 \times 10^6$ and $2.9 \pm 0.8 \times 10^5$ cells, respectively) (Fig. 1A) (*5*). In response to lipopolysaccharide (LPS), a component of Gram-negative bacteria, GM-CSF$^+$ cells increased in number preferentially in the spleen ($3.2 \pm 0.2 \times 10^6$ cells) and were predominantly B220$^+$ MHCII$^+$ CD19$^+$ IgM$^+$ B cells (IgM, immunoglobulin M) (Fig. 1B and fig. S1, A and B). This is surprising because GM-CSF is believed to be produced in vivo by nonhematopoietic cells, macrophages, and, in some cases, T cells (*4*, *6*). Nevertheless, B cells constituted the largest GM-CSF$^+$ population under these conditions (fig. S1C), a finding that we confirmed by Western blot analysis (Fig. 1C). We named these B cells innate response activator (IRA) B cells because of GM-CSF's known role in activating innate leukocytes. Numerous IRA B cells accumulated in the spleen in a mouse model of sepsis (fig. S2, A and B) (*7*) and in response to *Escherichia coli* infection (fig. S2C), indicating that IRA B cell expansion is a general feature of the body's response to bacteria. In humans, we detected CD19$^+$ CD20$^+$ IRA B cells expressing varying levels of CD43, CD27 (fig. S2, D and E), and CD284 [Toll-like receptor 4 (TLR4)] (fig. S2F) (*8*). We therefore elected to characterize murine IRA B cells in more detail.

Immunofluorescence of spleen sections from LPS recipients colocalized the GM-CSF signal with round mononuclear cells expressing IgM, B220, PAX5, and CD19 (Fig. 1D and fig. S1D) in the red pulp (Fig. 1, E and F). Reverse transcription polymerase chain reaction (RT-PCR) experiments conducted on sorted cells and unprocessed tissue from wild-type (WT) or B cell–deficient μMT mice indicated that B cells produce GM-CSF (Fig. 1G). Serum GM-CSF levels were negligible (that is, below the 7.8 pg/ml detection limit of the assay), a result that is consistent with the observation that GM-CSF is rapidly removed through receptor-mediated clearance (*9*). Collectively, these data indicate that inflammation expands the IRA B cell population in vivo.

B cells are linked developmentally, reside in different regions, and mediate distinct functions (*10*–*14*). We profiled IRA B cells according to several well-established methods (*13*, *15*, *16*). Our experiments revealed that (CD19$^+$ B220$^+$ MHCII$^+$ GM-CSF$^+$) IRA B cells are phenotypically unique. They are: IgM^{high} CD23^{low} CD43^{high} CD93$^+$ (Fig. 2, A and B, and fig. S3A), IgD^{low} CD21^{low} (fig. S3B), CD138$^+$ VLA4^{high} LFA1^{high} CD284$^+$ (Fig. 2C and fig. S3, C and D), and CD5^{int} (fig. S3, E and F). IRA B cells contain large stores of intracellular IgM (fig. S4A) and spontaneously secrete IgM, but not IgA or IgG1

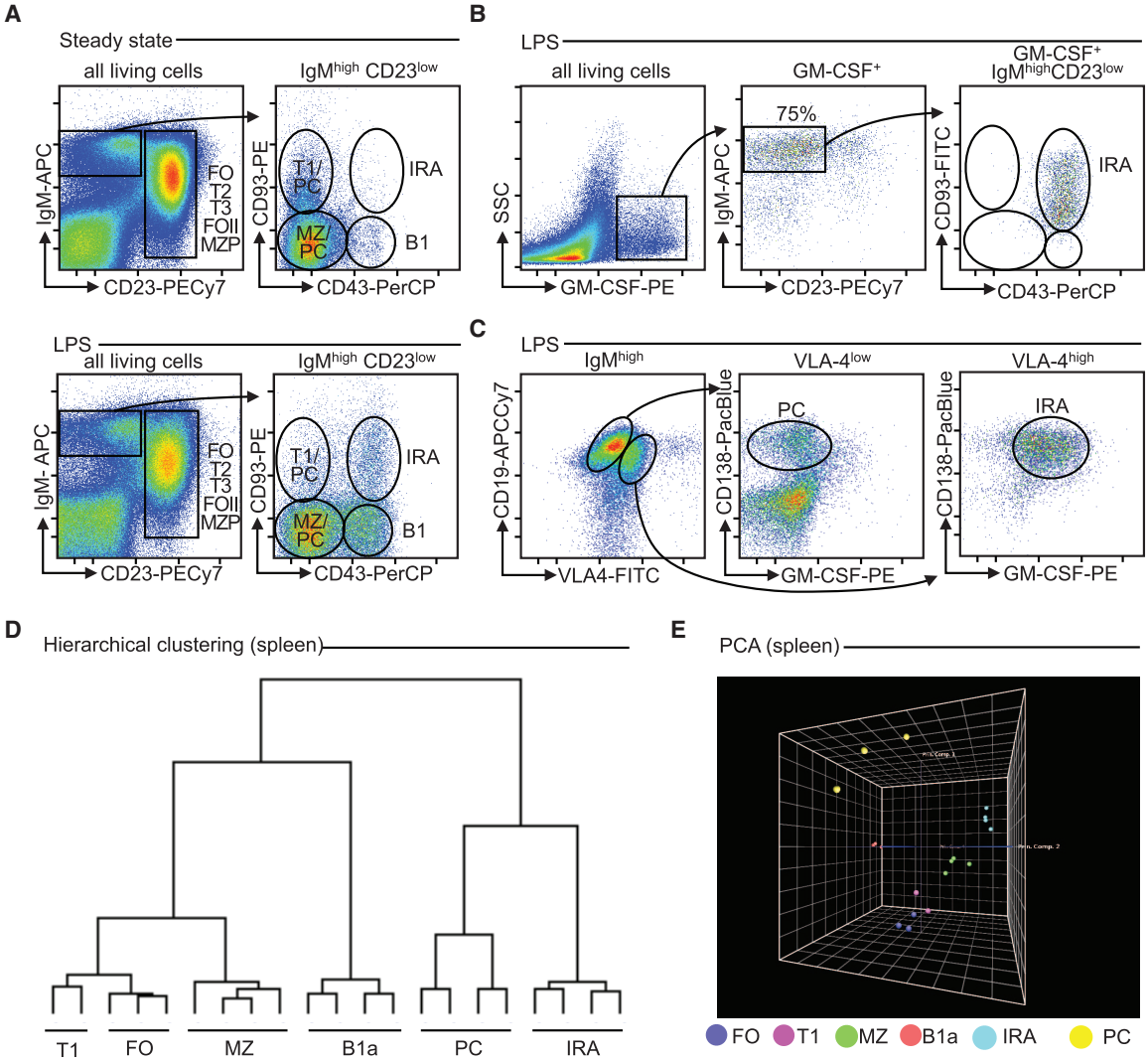


Fig. 2. IRA B cells are a distinct subset with a unique phenotypic signature. (**A**) Flow cytometric analysis of the phenotype of IRA B cells. Plots show B cell phenotypes retrieved from spleens during steady state and inflammation. A representative from $n > 10$ mice is shown. (**B**) Plots show the phenotype of GM-CSF–producing cells in the spleens during inflammation. IRA B cells are IgM^{high}, CD23^{low} CD43$^+$ CD93$^+$. (**C**) Plots show the phenotype of IRA B cells with respect to VLA4 and CD138 expression as determined by flow cytometry. A representative from $n > 5$ is shown. (**D**) Hierarchical clustering dendrogram based on whole-genome microarray data of sorted samples of B cell subsets retrieved from LPS-treated animals and steady-state B1a. (**E**) PCA of the different cell subsets shown in (D).

Downloaded from www.sciencemag.org on February 2, 2012

(fig. S4, B and C). In addition to GM-CSF, IRA B cells produce interleukin-3 (IL-3) but not pro–IL-1β, IL-6, and tumor necrosis factor–α (TNFα) (fig. S4D). We failed to detect IL-10 expression by IRA B cells in any of the conditions. Thus, IRA B cells have a unique B cell phenotype and are functionally distinct from other B cells, including the recently described IL-10–producing B10 B cells (*17*).

Sorting IRA B cells according to their surface phenotype (fig. S5A) allowed us to profile their transcriptome. Unsupervised hierarchical clustering (Fig. 2D) and principal component analysis (PCA) (Fig. 2E) grouped IRA B cells in a separate population from T1, FO, MZ, B1a, and PC. IRA B cells also gave rise to a unique transcriptome signature (fig. S5, B to D, and table S1) and expressed genes relevant to B cell biology (fig. S5D).

To decipher where IRA B cells fit in the B cell lineage, we performed several parabiosis and fate-mapping studies. First, we reasoned that if IRA B cells derive from a circulating precursor, they should have high chimerism in a parabiosis setting. Joining CD45.1$^+$ with CD45.2$^+$ mice revealed high chimerism among IRA B cells (Fig. 3A), T1, and FO B cells (fig. S6A) but markedly lower chimerism for the spleen-resident MZ B cells and their precursors (fig. S6A). Thus, IRA B cells derive from a circulating cell.

Second, to identify the IRA B cell precursor, we adoptively transferred B cell subsets to mice receiving LPS for 3 days (fig. S6, B to E). Among the subsets (splenic T1, FO, MZ, and B1 and peritoneal B1a, B1b, and B2), only peritoneal B1 B cells (Fig. 3B) gave rise to IRA B cells. Of

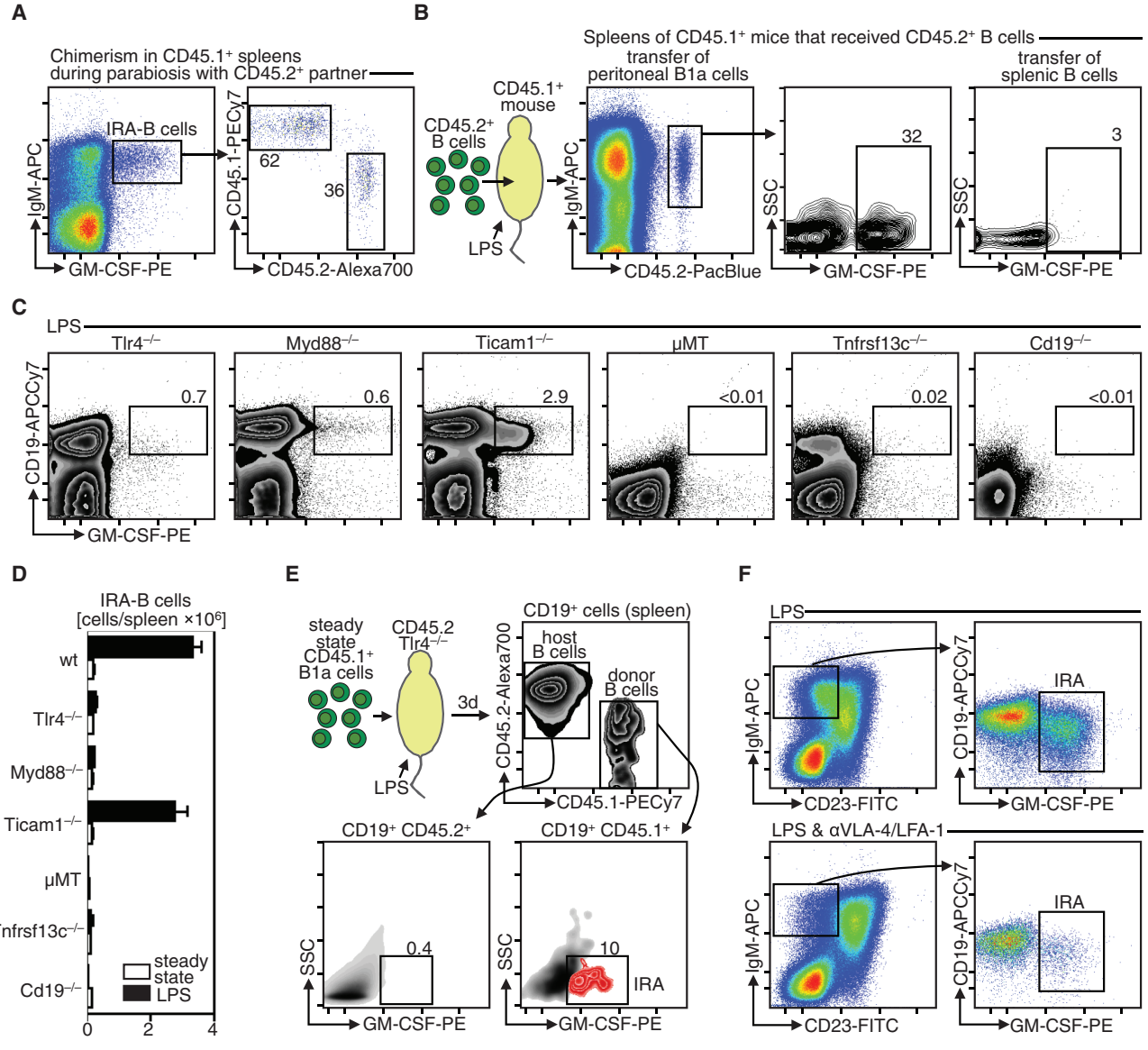


Fig. 3. IRA B cells develop from B1a B cells via TLR4/MyD88 and reside in tissue through LFA-1/VLA-4. (**A**) Flow cytometric analysis of the percent chimerism is shown in spleens of CD45.1$^+$ mice that had been in parabiosis with CD45.2$^+$ mice for 3 weeks before LPS injection. Mice were sacrificed 2 days after LPS injection. Representative plots from two independent experiments are shown. (**B**) Adoptive transfer of peritoneal B1a B cells yields IRA B cells. Cells from steady-state CD45.2$^+$ mice were transferred to CD45.1$^+$ mice that then received LPS for 3 days. Animals were analyzed 72 hours after transfer. Representative plots from flow cytometric analysis of $n = 4$ to 5 mice are shown. (**C**) Flow cytometric analysis of the development of IRA B cells in *Tlr4*$^{-/-}$, *Myd88*$^{-/-}$, *Ticam1*$^{-/-}$ (the gene that encodes TRIF), μMT, *Tnfrsf13c*$^{-/-}$ (the gene that encodes BAFFR), and *Cd19*$^{-/-}$ mice. Representative plots from $n = 4$ mice are shown. (**D**) Enumeration of IRA B cells in steady state and inflammation in WT (C57BL/6) mice and in the mice shown in (C) (means ± SEM, $n = 4$ to 10). *$P < 0.05$. (**E**) Flow cytometric analysis of the adoptive transfer of CD45.1$^+$ B1a cells into congenic *Tlr4*$^{-/-}$ CD45.2$^+$ mice injected with LPS. A representative from $n = 3$ mice is shown. (**F**) Flow cytometric analysis of the effect of blocking VLA-4/LFA-1 on IRA B cell retention in the spleen. A representative from $n = 3$ mice is shown.

Downloaded from www.sciencemag.org on February 2, 2012

these, B1a B cells were the dominant precursor. B1a-derived IRA B cells readily proliferated (fig. S6E) and developed in the spleen after relocating from the peritoneum (fig. S7). These findings confirm that B1a B cells travel to the spleen in response to peritoneal TLR stimuli (*18*, *19*) and indicate that, upon splenic accumulation, B1a B cells can differentiate to IRA B cells.

The ontogenic relationship between B1a and IRA B cells raised the question of whether IRA B cells constitute a distinct subset. To elucidate this, we first placed peritoneal B1a B cells in culture. In response to LPS, B1a B cells separated into three discrete populations: $CD138^-$ cells resembling "unchanged" B1a B cells and two populations of $CD138^+$ cells, one of which was IRA B cells (fig. S8A). In vitro, IRA B cells spontaneously secreted GM-CSF (fig. S8B). We then sorted peritoneal B1a B cells, IRA B cells, and splenic $CD43^+$ $CD138^+$ cells and followed their fate in vivo. B1a B cells gave rise to multiple cell types (fig. S9A), including IRA B and $CD43^+CD138^+$ cells, whereas ($CD43^{high}$ $CD138^+$) IRA B and $CD43^+$ $CD138^+$ cells remained phenotypically segregated (fig. S9, B and C). The data suggest that B1a B cells give rise to distinct cells. IRA B cells are a subset of this group.

Surface phenotype and fate-mapping studies, though important, reveal little about function. How IRA B cells arise was our next question. Expectedly, B cell–deficient μMT (*20*) and $Cd19^{-/-}$ (*21*) mice did not develop IRA B cells (Fig. 3, C and D). Surprisingly, $Tnfrsf13c^{-/-}$ mice lacking the B cell–activating factor receptor (BAFFR) failed to generate IRA B cells; BAFFR is believed to be dispensable to B1 B cells (*22*). At the level of microbial recognition, mice lacking the LPS receptor TLR4 or its adaptor MyD88, but

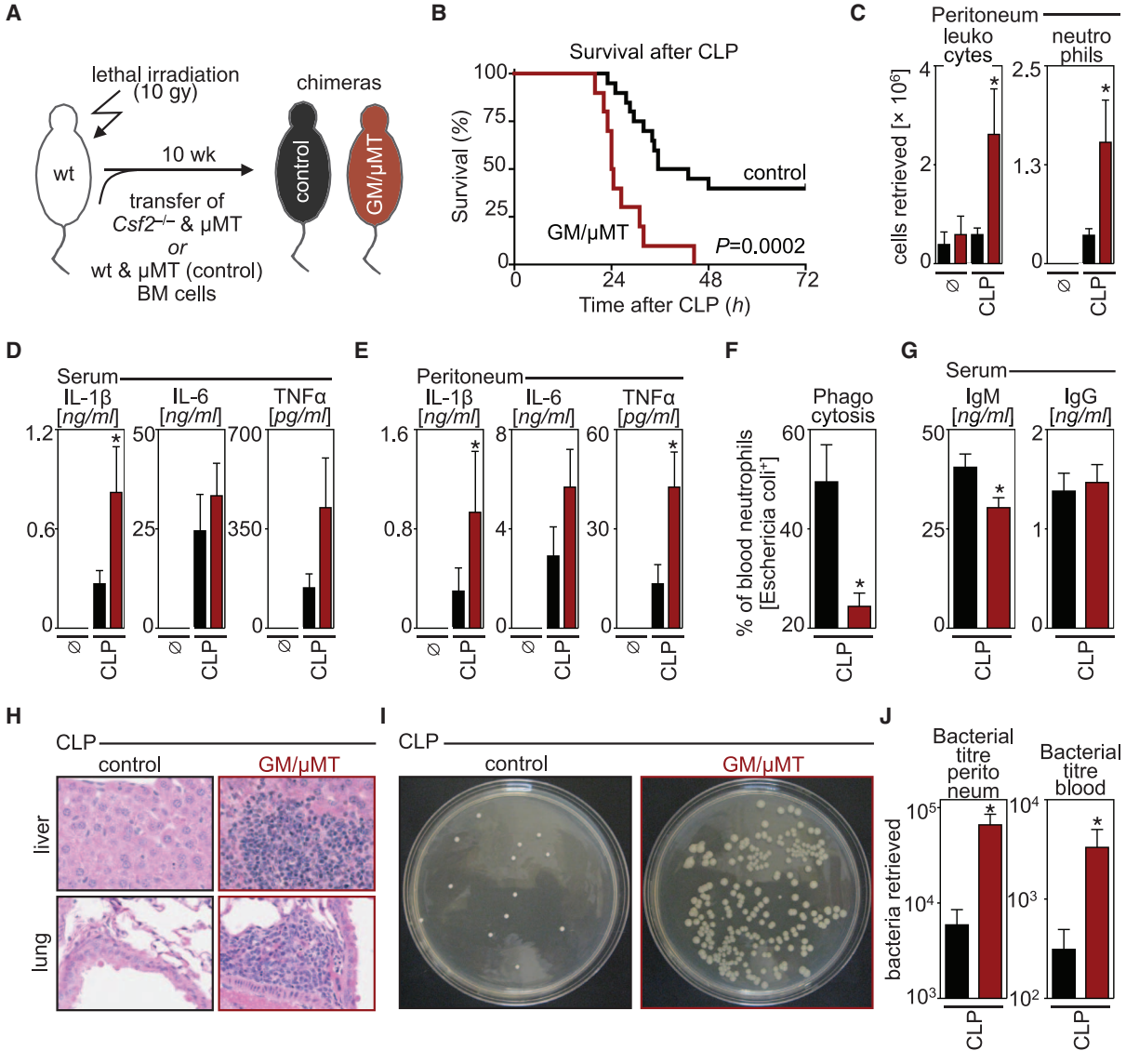


Fig. 4. IRA B cells protect against polymicrobial sepsis. (**A**) Generation of mixed chimeras (GM/μMT). gy, gray; wk, weeks. (**B**) Kaplan-Meier curve showing survival of GM/μMT and control animals after CLP. n = 10 to 20 mice per group. (**C**) Enumeration of total leukocytes and neutrophils in the peritoneum of GM/μMT (dark red bars) and control (black bars) mice 20 hours after CLP. ⦸, steady state. *$P < 0.05$. (**D**) Serum levels and (**E**) peritoneal levels of inflammatory cytokines in GM/μMT (dark red) and control (black) mice 20 hours after CLP. (**F**) Ex vivo phagocytosis assay showing capacity of neutrophils to phagocytose *E. coli* from GM/μMT (dark red) and control (black) mice 20 hours after CLP. (**G**) Serum levels of IgM and IgG 20 hours after CLP in the same groups as above. (**H**) Representative hematoxylin and eosin stain of liver and lung sections 20 hours after CLP in the same groups as above. (**I**) Blood from GM/μMT and control mice 20 hours after CLP was plated for 1 day. Representative plate shows bacterial colonies. (**J**) Enumeration of bacteremia in the peritoneum and blood of GM/μMT (dark red) and control (black) mice 20 hours after CLP. *$P < 0.05$ [means ± SEM, n = 10 to 20 mice per group for (C) to (G) and (J). Four independent experiments were performed and data were grouped].

Downloaded from www.sciencemag.org on February 2, 2012

not TRIF, did not generate IRA B cells (Fig. 3, C and D), indicating a specific MyD88-dependent pathway. The process could depend on direct B1a binding to LPS via TLR4, or on indirect, extrinsic factors such as TLR4-expressing macrophages. To discriminate between these two possibilities, we adoptively transferred B1a B cells from WT mice into *Tlr4*$^{-/-}$ mice (Fig. 3E). B1a WT B cells, but not endogenous *Tlr4*$^{-/-}$ B cells, differentiated to IRA B cells, indicating that direct TLR4 signaling on B1a B cells is sufficient to generate IRA B cells.

To test whether IRA B cells are restricted to TLR4-mediated recognition, we injected TLR ligands Pam3CSK4 (ligand for TLR1/2), Poly(I:C) (TLR3), FLA-ST (TLR5), FSL-1 (TLR2/6), R848 (TLR7/8), and CpG ODN1668 (TLR9). The ligands Pam3CSK4, FSL-1, and R848 yielded IRA B cells (fig. S10A), a finding that we confirmed in vitro (fig. S10B). We also wondered whether GM-CSF can play an autocrine role for B1a–IRA B cell conversion (*23*). B1a cells expressed Csf2Rβ (CD131) (fig. S11A) and, when placed in culture with antibodies against CD131, failed to give rise to IRA B cells (fig. S11, B and C) but remained alive and gave rise to CD43^{+} CD138^{+} cells. Thus, IRA B cells develop via MyD88-dependent pathways and use GM-CSF as an autocrine factor.

The spleen's open circulation (*24*) allows blood leukocytes to enter and exit easily. To reside in the spleen, leukocytes resort to adhesive ligands; MZ B cells, for example, rely on VLA-4 and LFA-1 (*25*). We wondered whether splenic IRA B cells, which express VLA-4 and LFA-1 at high levels, might behave similarly. Injection of neutralizing antibodies to VLA-4 and LFA-1 diminished IRA B cell numbers and revealed that the two integrins are responsible for retention (Fig. 3F).

Are IRA B cells functionally important? To answer this, we focused on the cecal ligation and puncture (CLP) sepsis model (*26*). We generated mixed chimeras by reconstituting lethally irradiated mice with μMT- and GM-CSF–deficient (*Csf2*$^{-/-}$) bone marrow cells. In these mice (called GM/μMT chimeras), the μMT marrow contributed all leukocytes except B cells, whereas the *Csf2*$^{-/-}$ marrow contributed only *Csf2*$^{-/-}$ cells. Consequently, the only population completely lacking the capacity to produce GM-CSF in the reconstituted mice were B cells. We tested the quality of the chimeras and their controls by PCR (fig. S11, A and B) and by flow cytometry (fig. S11, C and D).

In response to severe CLP, 40% of control mice survived and recovered, but every GM/μMT chimera died within 2 days (Fig. 4, A and B). To characterize this phenotype further, we profiled GM/μMT chimeras and controls for several sepsis-relevant indices 20 hours after CLP, before any mortalities. Compared with IRA B cell–containing controls (fig. S11E), the peritoneal cavities of GM/μMT chimeras had more leukocytes, mostly neutrophils (Fig. 4C), and experienced a severe IL-1β, IL-6, and TNFα cytokine storm in the serum (Fig. 4D) and peritoneum (Fig. 4E). This inflammatory signature typically associates with a defect in bacterial clearance. Indeed, neutrophils from the GM/μMT chimeras phagocytosed bacteria poorly (Fig. 4F). Moreover, the GM/μMT chimeras had a modest reduction of serum IgM, but not IgG (Fig. 4G), and developed severe liver and lung pathologies (Fig. 4H). Finally, bacterial titer measurements revealed that GM/μMT chimeras were more infected than controls (Fig. 4, I and J). Although it is possible that other bone marrow cells contribute GM-CSF for the protection against sepsis in this setting, the most likely explanation is that IRA B cells protect against septic shock by controlling the organism's ability to clear bacteria.

GM-CSF is a pleiotropic cytokine that influences the production, maturation, function, and survival of its target cells. GM-CSF's role in sepsis has remained elusive because its indiscriminate ablation is protective (*27*), but its supplementation can be beneficial (*28*). The in vivo identification of GM-CSF–producing B cells illustrates a previously unrecognized locational specificity that dictates the cytokine's function. IRA B cells differ from other subsets because their pathogen recognition pathways and tissue distribution license GM-CSF expression. The function is important in sepsis and gives rise to questions as to how IRA B cells participate in other infectious and inflammatory diseases.

References and Notes

1. J. Cohen, *Nature* **420**, 885 (2002).
2. G. S. Martin, D. M. Mannino, S. Eaton, M. Moss, *N. Engl. J. Med.* **348**, 1546 (2003).
3. R. S. Hotchkiss, S. Opal, *N. Engl. J. Med.* **363**, 87 (2010).
4. J. A. Hamilton, *Nat. Rev. Immunol.* **8**, 533 (2008).
5. Materials and methods are available as supporting material on *Science* Online.
6. I. Sonderegger *et al.*, *J. Exp. Med.* **205**, 2281 (2008).
7. D. Rittirsch, M. S. Huber-Lang, M. A. Flierl, P. A. Ward, *Nat. Protoc.* **4**, 31 (2009).
8. D. O. Griffin, T. L. Rothstein, *J. Exp. Med.* **208**, 2591 (2011).
9. D. Metcalf, N. A. Nicola, S. Mifsud, L. Di Rago, *Blood* **93**, 1579 (1999).
10. T. W. LeBien, T. F. Tedder, *Blood* **112**, 1570 (2008).
11. D. Allman, S. Pillai, *Curr. Opin. Immunol.* **20**, 149 (2008).
12. F. Martin, J. F. Kearney, *Nat. Rev. Immunol.* **2**, 323 (2002).
13. S. Pillai, A. Cariappa, *Nat. Rev. Immunol.* **9**, 767 (2009).
14. Z. Hao, K. Rajewsky, *J. Exp. Med.* **194**, 1151 (2001).
15. D. Allman *et al.*, *J. Immunol.* **167**, 6834 (2001).
16. E. Montecino-Rodriguez, K. Dorshkind, *Trends Immunol.* **27**, 428 (2006).
17. K. Yanaba *et al.*, *Immunity* **28**, 639 (2008).
18. S. A. Ha *et al.*, *J. Exp. Med.* **203**, 2541 (2006).
19. T. Kawahara, H. Ohdan, G. Zhao, Y. G. Yang, M. Sykes, *J. Immunol.* **171**, 5406 (2003).
20. D. Kitamura, J. Roes, R. Kühn, K. Rajewsky, *Nature* **350**, 423 (1991).
21. R. C. Rickert, K. Rajewsky, J. Roes, *Nature* **376**, 352 (1995).
22. B. Schiemann *et al.*, *Science* **293**, 2111 (2001).
23. R. J. Harris *et al.*, *J. Immunol.* **164**, 3887 (2000).
24. R. E. Mebius, G. Kraal, *Nat. Rev. Immunol.* **5**, 606 (2005).
25. T. T. Lu, J. G. Cyster, *Science* **297**, 409 (2002).
26. K. Doi, A. Leelahavanichkul, P. S. Yuen, R. A. Star, *J. Clin. Invest.* **119**, 2868 (2009).
27. S. Basu *et al.*, *J. Immunol.* **159**, 1412 (1997).
28. R. Gennari, J. W. Alexander, L. Gianotti, T. Eaves-Pyles, S. Hartmann, *Ann. Surg.* **220**, 68 (1994).

Acknowledgments: This work was supported in part by NIH grants 1R01HL095612 (to F.K.S.), as well as U01 HL080731, P50 CA86355, R24 CA69246, and P01-A154904 (to R.W.). P.J.R. was supported by the Boehringer Ingelheim Fonds; C.S.R. was supported by an American Heart Association postdoctoral fellowship and the MGH Executive Committee on Research (ECOR) Postdoctoral Award; G.F.W. and I.H. were supported by the German Research Foundation; and I.T. was supported by the Max Kade Foundation. We thank K. Rajewsky, D. Scadden, A. Luster, and K. Otipoby (Harvard Medical School) for helpful discussions and critical reading of the manuscript and M. Greene for secretarial assistance. The data reported in this paper are tabulated in the main paper and in the supporting online material. MIAME (minimum information about a microarray experiment)–compliant expression data have been deposited under the accession no. GSE32372.

Supporting Online Material

www.sciencemag.org/cgi/content/full/science.1215173/DC1
Materials and Methods
Figs. S1 to S12
Table S1
References (*29*–*36*)

11 October 2011; accepted 22 December 2011
Published online 12 January 2012;
10.1126/science.1215173

Abnormal Brain Structure Implicated in Stimulant Drug Addiction

Karen D. Ersche,[1]* P. Simon Jones,[1] Guy B. Williams,[1,2] Abigail J Turton,[1] Trevor W. Robbins,[1] Edward T. Bullmore[1,3,4]

Addiction to drugs is a major contemporary public health issue, characterized by maladaptive behavior to obtain and consume an increasing amount of drugs at the expense of the individual's health and social and personal life. We discovered abnormalities in fronto-striatal brain systems implicated in self-control in both stimulant-dependent individuals and their biological siblings who have no history of chronic drug abuse; these findings support the idea of an underlying neurocognitive endophenotype for stimulant drug addiction.

Drug dependence is increasingly recognized as a "relapsing brain disorder" (*1*) and, in support of this view, marked structural changes in striatal and prefrontal brain regions have been reported in people dependent on stimulant drugs (*2*). These reports, however, raise

Downloaded from www.sciencemag.org on February 2, 2012

the question of whether these brain abnormalities may have predated drug-taking, rendering individuals vulnerable for the development of dependence.

Individuals at risk for drug dependence typically have deficits in self-control (*3*, *4*), which may reflect a diminished ability to recruit prefrontal networks for regulating behavior (*5*). Stimulant drugs are highly reinforcing, because they directly affect brain systems implicated in motivated behavior, such as the basal ganglia and the limbic system (*6*), and they modulate control systems in the prefrontal cortex (*7*). Malfunction of these circuitries may increase the susceptibility for stimulant-induced neuroadaptive changes and facilitate the development of drug dependence.

As brain structure is, to a large extent, inherited (*8*) and drug dependence runs in families (*9*), a genetic or epigenetic influence on addictive behaviors seems plausible. Yet, we know very little about the mechanisms through which risks for drug dependence might be inherited. Endophenotypes are quantitative traits, mediating between the predisposing genes (genotypes) and the clinical symptoms (phenotypes) in complex disorders (*10*). As heritable traits, endophenotypes can be measured objectively in both patients and their unaffected first-degree relatives. We compared brain structure and the ability to regulate behavior in 50 biological sibling pairs; within each pair, one sibling satisfied the *Diagnostic and Statistical Manual of Mental Disorders* (DSM-IV) criteria for dependence on stimulant drugs and the other had no history of chronic drug or alcohol abuse (*11*). The sib-pairs were also compared with 50 unrelated healthy volunteers matched for age and intelligence quotient (table S1). Tobacco was smoked by members of all groups, but smoking rates were significantly higher in the sib-pairs than in the unrelated volunteers (table S1), which is not surprising for individuals with a greater-than-normal genetic risk of drug dependence.

We used the stop-signal task (*12*), one of the most widely used measures of inhibitory control, which requires individuals to rapidly suppress an ongoing, well-established response whenever an auditory signal is suddenly presented. The stop-signal reaction time (SSRT) estimates the time that an individual needs to withhold an ongoing response and can predict the onset of substance abuse in vulnerable individuals (*4*). The neural circuitry underlying stop-signal task performance has been well-characterized and there is ample evidence for the association of SSRT with both the functional and structural integrity of brain systems known to be compromised in stimulant drug dependence (*13*, *14*). We observed marked impairments in the regulation of behavior in both drug-dependent individuals and their biological siblings who have no history of chronic drug abuse (Fig. 1A). Indeed, the deficits in SSRT were as pronounced in the nondependent siblings as in the stimulant-dependent patients. Moreover, the variance in SSRT within sib-pairs was significantly smaller than in unrelated sib-pairs (permutation test, $P = 0.033$), which suggests that poor inhibitory control is a familial trait in vulnerable individuals and not a result of long-term drug abuse.

To investigate the relation between inhibitory control and brain structure, we calculated from each individual's diffusion tensor images the fractional anisotropy (FA) values that serve as a general index of the integrity of white matter fiber tracts (*15*) and analyzed them using tract-based spatial statistics (TBSS) implemented in FSL software (*11*). We compared the mean FA values between the groups within a tract-based skeleton (*16*) and found evidence for a significant reduction of FA in the sib-pairs compared with healthy unrelated volunteers (indicated in blue in Fig. 1B). Again, the variance of FA within biological sib-pairs was significantly smaller compared with the variance within unrelated sib-pairs (permutation test, $P = 0.004$), which suggested that the observed white matter abnormalities were shared among members of the same family and may have predisposed them to drug-taking. In the stimulant-dependent individuals, reduced FA was associated with the duration of stimulant abuse (fig. S2A), which suggests that white matter changes can also result from drug-taking (although these effects of drug exposure were less anatomically extensive than the effects of familial risk for dependence).

Previous research shows that stop-signal task performance is subserved by a neural network, including the inferior frontal gyrus (IFG), the basal ganglia (caudate-putamen), and the presupplementary motor area (pre-SMA) (*17*, *18*). On the basis of previous studies, we created a region of interest using Hammer's probabilistic atlas (*19*), as indicated in orange in Fig. 1B. Within this region of interest, we regressed each participant's SSRT score on their white matter FA. Reduced FA in fiber tracts adjacent to the right IFG was significantly associated with poorer inhibitory control and accounted for ~6% of the variance in SSRT (Fig. 1C). The variability of the abnormality in the right prefrontal white matter was significantly similar within biological siblings compared with unrelated sib-pairs (permutation test, $P = 0.004$). Together, these results support the idea that self-control deficits are subserved by white matter disorganization in the right prefrontal lobe; this finding provides an objective vulnerability marker for an increased, possibly inherited, risk for developing stimulant drug dependence.

We also compared the gray matter volume maps of healthy volunteers with those of the drug-dependent individuals (Fig. 2A) and of the non–drug abusing siblings (Fig. 2B) using voxel-based morphometry analysis implemented in FSL software (*11*). The brains of the sib-pairs showed distinct abnormalities relative to the healthy control volunteers. Specifically, key structures previously implicated in addiction, such as the medial temporal lobe (*20*) and the basal ganglia (*21*, *22*), were significantly enlarged in the sib-pairs. We also identified a significant reduction of gray matter volume in the posterior postcentral gyrus and adjacent areas, such as the superior temporal gyrus and the posterior insula, in both drug-dependent individuals and their siblings compared with healthy volunteers (Fig. 2C). The

[1]Behavioural and Clinical Neuroscience Institute and Department of Experimental Psychology and Department of Psychiatry, University of Cambridge, Cambridge, CB2 3EB and CB2 0SZ, UK. [2]Wolfson Brain Imaging Centre, Department of Clinical Neurosciences, University of Cambridge, Cambridge CB2 0QQ, UK. [3]Clinical Unit Cambridge, GlaxoSmithKline, Addenbrooke's Centre for Clinical Investigations, Cambridge CB2 2GG, UK. [4]Cambridgeshire and Peterborough Foundation, National Health Service Trust, Cambridge CB21 5EF, UK.

*To whom correspondence should be addressed. E-mail: ke220@cam.ac.uk

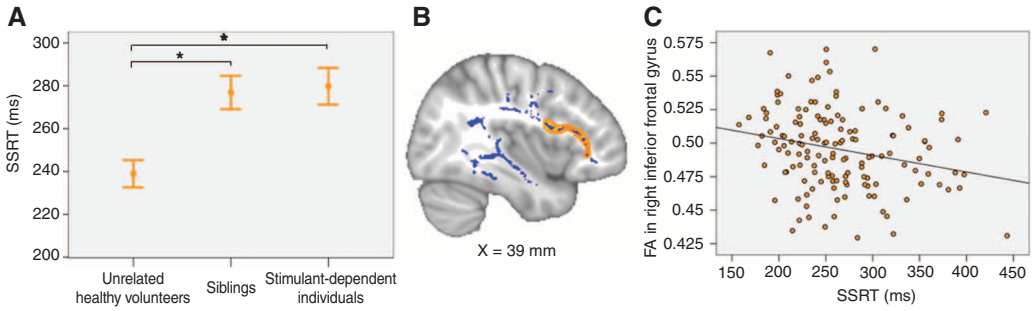
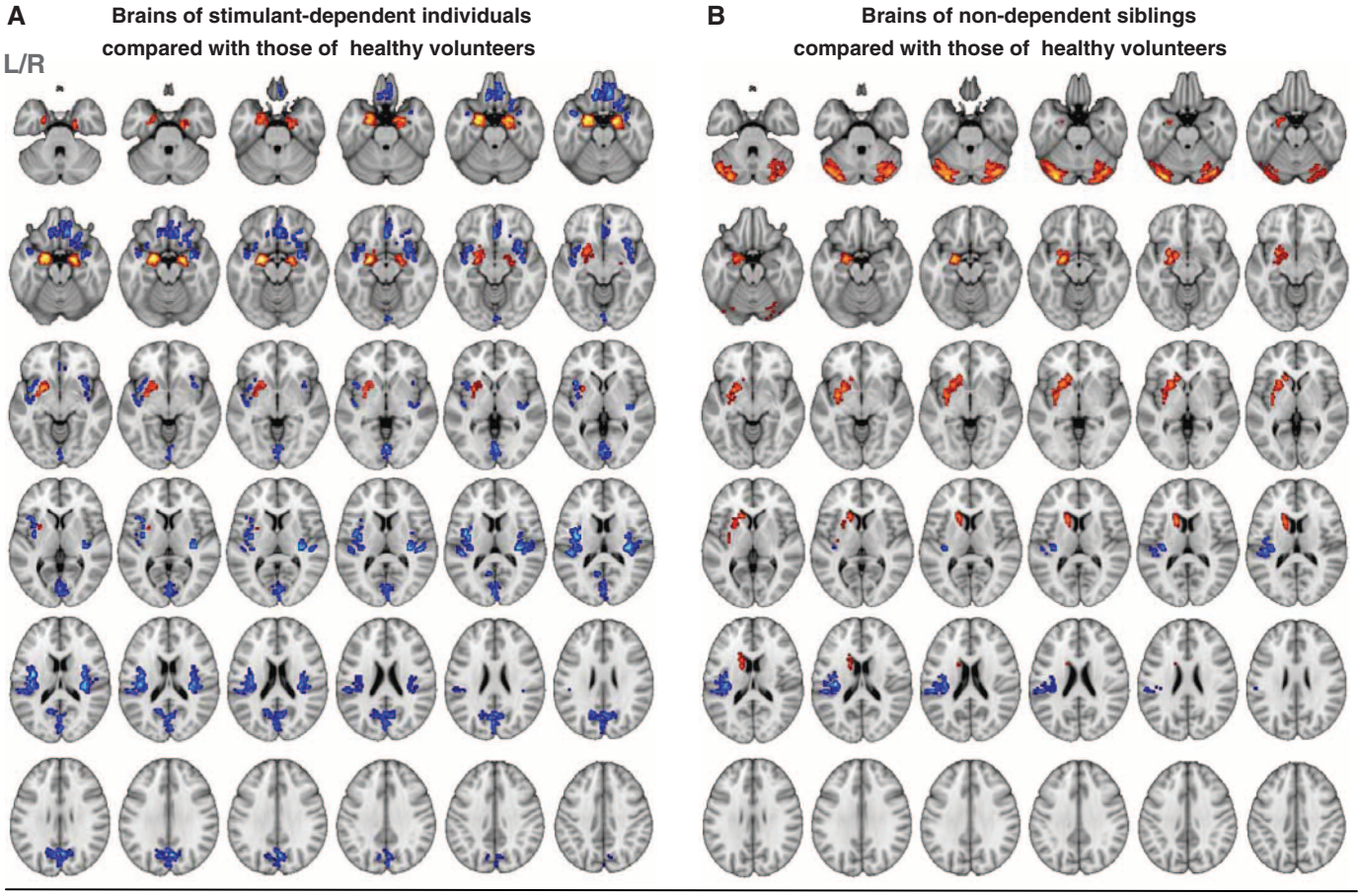


Fig. 1. Deficits of motor inhibitory control and white matter organization in stimulant-dependent individuals and their nondependent siblings. (**A**) SSRT differed significantly between the three groups ($F_{2,141} = 9.9$, $P < 0.001$). SSRT was significantly prolonged in both the stimulant-dependent individuals and their siblings compared with unrelated healthy volunteers (Bonferroni correction, $P \leq 0.005$, for both comparisons). (**B**) The skeleton of group differences in mean FA is colored in blue ($F_{2,141} = 26.3$, $P < 0.001$); on the basis of previous studies, regions of interest were selected within the blue skeleton, which included the IFG and the presupplementary motor area (colored in orange). (**C**) Scatterplot showing that participants with greater mean FA in the right IFG had better inhibitory performance (shorter SSRT) on the stop-signal task (the correlation coefficient, $r = 0.24$; the linear correlation constant, $R^2 = 0.057$, $P < 0.005$).

Downloaded from www.sciencemag.org on February 2, 2012

within-pair variability of the gray matter volume increase in the putamen (permutation test, $P = 0.013$) and of the volume decrease in the posterior insula (permutation test, $P = 0.012$) were both significantly smaller in biological siblings than in randomly paired siblings, which indicated that this abnormality is shared between members of the same family. By contrast, the enlargement of the amygdala in the sib-pairs did not survive the test of familiality (permutation test, $P = 0.144$), which suggested that other, nonfamilial factors may account for this abnormality. Note that higher tobacco exposure in the nondependent siblings is unlikely to explain the pattern of gray matter abnormalities identified as an endophenotype for stimulant dependence, as shown by similar results from a separate analysis restricted to nonsmokers (fig. S1). Moreover, gray matter regions associated with the duration of stimulant drug exposure differed clearly in location from the regions identified as markers of familial risk for stimulant drug dependence (fig. S2B)

The involvement of the putamen is consistent with its implication in fronto-striatal circuits for stop-signal performance and proposed antecedent problems in response control (*23*). However, the additional regions identified as showing changes in the sib-pairs may be related to other psychological processes underlying addiction. Thus, brain abnormalities observed in the sib-pairs in neural systems underlying learning and memory [such as the medial temporal lobe (*24*)], and habit formation [such as the putamen (*25*)] are intriguing, given that some forms of drug addiction are thought to develop through maladaptive acquisition and control of habits (*26*). Enlargement of limbic and striatal structures has been reported previously in patients with obsessive-compulsive disorder (OCD) (*27*), and like addiction, OCD is characterized by dysfunctional habits and "out-of-control" behavior. Our findings may



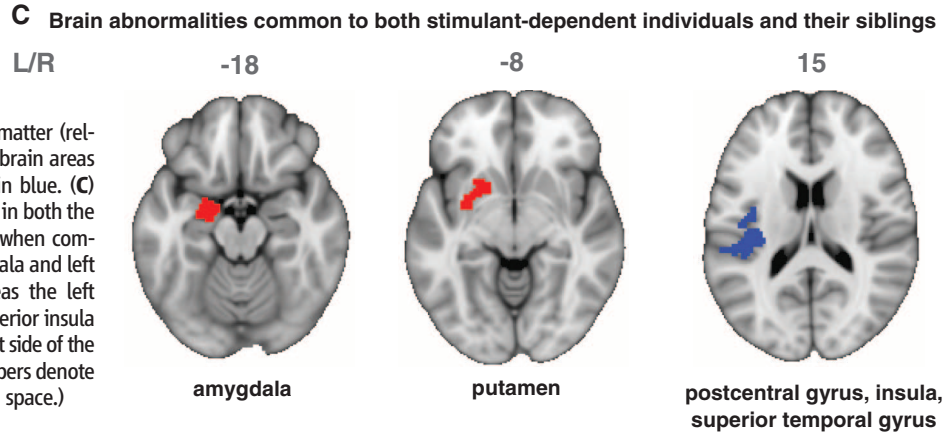


Fig. 2. Similar abnormalities in gray matter brain volume were found in stimulant-dependent individuals (**A**) and in their nondependent siblings (**B**) when separately compared with healthy volunteers. Brain areas of abnormally increased gray matter (relative to healthy volunteers) are colored in red, and brain areas of abnormally decreased gray matter are colored in blue. (**C**) Three clusters of shared abnormality were identified in both the stimulant-dependent individuals and their siblings when compared with unrelated healthy volunteers: left amygdala and left putamen were both significantly enlarged; whereas the left postcentral gyrus, superior temporal gyrus, and posterior insula were significantly reduced in gray matter volume. (Left side of the brain is shown on the left side of each slice; the numbers denote Z coordinates for each slice in standard stereotactic space.)

Downloaded from www.sciencemag.org on February 2, 2012

indicate markers of neural vulnerability for pathological habit formation, which could further facilitate the effects of drugs of abuse by interfering with limbic-striatal functions. Pathological habits in drug addiction typically result in compulsive drug-taking behaviors when prefrontal control fails to regulate behavior (*26*). Our data are also in keeping with preclinical research indicating that impairments in response control are predictive of cocaine reinforcement and dopamine receptor dysfunction in the striatum (*28*). Deficits in inhibitory prefrontal control were evident in both drug-dependent individuals and their siblings who do not abuse drugs, which may reflect an increased risk for out-of-control drug-seeking or drug-taking behaviors, which could pave the way for the development of drug dependence.

The identified profile of familial abnormalities remarkably resembles the developmental changes of brain structure during adolescence, i.e., limbic-striatal structures mature before prefrontal brain systems. This developmental asynchrony has been suggested to create an imbalance between mesolimbic reward and prefrontal control systems, which predisposes adolescents to sensation-seeking and impulsive behavior, rendering them potentially vulnerable to drug-taking (*29*). Our previous data on biological siblings of stimulant-dependent individuals indicated a propensity for increased impulsivity, as measured on the Barratt Impulsivity Scale, contrasting with normal scores on measures of sensation-seeking traits (*30*). The present findings show that even stronger effects in the sib-pairs are observed with an objective measure of impulse control, the SSRT. These findings are also related to changes in brain structure, including the inferior frontal cortex and putamen, which are key nodes in a neural network that mediates response regulation.

Our findings thus indicate that gray matter changes in the dorsal striatum, together with abnormal inferior prefrontal cortical connectivity, underlie an increased risk for developing stimulant drug dependence. However, the almost equivalent impairments in SSRT in both the stimulant-dependent individuals and their unaffected siblings need careful interpretation, as they do not reflect the classic pattern for endophenotypes, i.e., that the first-degree relatives have trait values intermediate between the patients and the unrelated healthy volunteers (*10*). Presumably, the siblings must have some other resilience factors that counteract the familial vulnerability to drug dependence. The identification of these brain and behavioral biomarkers for familial risk of drug dependence demonstrates that an individual's predisposition to become addicted to stimulant drugs may be mediated by brain abnormalities linked to impaired self-control.

References and Notes

1. A. I. Leshner, *Science* **278**, 45 (1997).
2. K. D. Ersche *et al.*, *Brain* **134**, 2013 (2011).
3. R. E. Tarter *et al.*, *Am. J. Psychiatry* **160**, 1078 (2003).
4. J. T. Nigg *et al.*, *J. Am. Acad. Child Adolesc. Psychiatry* **45**, 468 (2006).
5. O. George, G. F. Koob, *Neurosci. Biobehav. Rev.* **35**, 232 (2010).
6. H. C. Breiter *et al.*, *Neuron* **19**, 591 (1997).
7. S. Kroener, A. Lavin, *Neuropsychopharmacology* **35**, 2292 (2010).
8. I. C. Wright, P. Sham, R. M. Murray, D. R. Weinberger, E. T. Bullmore, *Neuroimage* **17**, 256 (2002).
9. K. R. Merikangas *et al.*, *Arch. Gen. Psychiatry* **55**, 973 (1998).
10. I. I. Gottesman, T. D. Gould, *Am. J. Psychiatry* **160**, 636 (2003).
11. Materials and methods are available as supporting material on *Science* Online
12. G. D. Logan, R. J. Schachar, R. Tannock, *Psychol. Sci.* **8**, 60 (1997).
13. G. Tabibnia *et al.*, *J. Neurosci.* **31**, 4805 (2011).
14. C. S. R. Li, V. Milivojevic, K. Kemp, K. Hong, R. Sinha, *Drug Alcohol Depend.* **85**, 205 (2006).
15. D. Le Bihan *et al.*, *J. Magn. Reson. Imaging* **13**, 534 (2001).
16. S. M. Smith *et al.*, *Neuroimage* **31**, 1487 (2006).
17. A. R. Aron, T. E. Behrens, S. Smith, M. J. Frank, R. A. Poldrack, *J. Neurosci.* **27**, 3743 (2007).
18. K. S. Madsen *et al.*, *Neuropsychologia* **48**, 854 (2010).
19. A. Hammers *et al.*, *Hum. Brain Mapp.* **19**, 224 (2003).
20. S. Grant *et al.*, *Proc. Natl. Acad. Sci. U.S.A.* **93**, 12040 (1996).
21. D. Belin, S. Jonkman, A. Dickinson, T. W. Robbins, B. J. Everitt, *Behav. Brain Res.* **199**, 89 (2009).
22. H. H. Yin, B. J. Knowlton, *Nat. Rev. Neurosci.* **7**, 464 (2006).
23. S. Padmala, L. Pessoa, *Neuropsychologia* **48**, 558 (2010).
24. L. R. Squire, S. Zola-Morgan, *Science* **253**, 1380 (1991).
25. A. M. Graybiel, *Curr. Opin. Neurobiol.* **5**, 733 (1995).
26. B. J. Everitt, T. W. Robbins, *Nat. Neurosci.* **8**, 1481 (2005).
27. J. S. Kwon *et al.*, *J. Neurol. Neurosurg. Psychiatry* **74**, 962 (2003).
28. J. W. Dalley *et al.*, *Science* **315**, 1267 (2007).
29. B. J. Casey, R. M. Jones, *J. Am. Acad. Child Adolesc. Psychiatry* **49**, 1189, quiz 1285 (2010).
30. K. D. Ersche, A. J. Turton, S. Pradhan, E. T. Bullmore, T. W. Robbins, *Biol. Psychiatry* **68**, 770 (2010).

Acknowledgments: The authors thank all volunteers for their participation in this study and the clinical study officers at the Mental Health Research Network for their dedicated support with volunteer recruitment. The authors are grateful to the staff at the Wellcome Trust Clinical Research Facility at Addenbrooke's Hospital and the Wolfson Brain Imaging Centre for their help and support throughout the study. This work was funded by the U.K. Medical Research Council (MRC) and conducted within the Behavioral and Clinical Neuroscience Institute at the University of Cambridge, which is jointly funded by the MRC and the Wellcome Trust. K.D.E., P.S.J., and A.J.T. are supported by a research grant of the MRC. T.W.R. and A.J.T. consult for Cambridge Cognition. E.T.B. is employed 50% by GlaxoSmithKline and 50% by the University of Cambridge. K.D.E., P.S.J., and G.B.W. declare that they have no conflicts of interest.

Supporting Online Material

www.sciencemag.org/cgi/content/full/335/6068/601/DC1
Materials and Methods
Figs. S1 to S2
Tables S1 to S3
References (*31*–*42*)

26 September 2011; accepted 29 November 2011
10.1126/science.1214463

Downloaded from www.sciencemag.org on February 2, 2012

New Products

STACKABLE DESICCATORS

Multi-Storey Cubic Desiccators overcome the space inefficiencies of traditional round desiccators which occupy a large bench area while providing only a small circular shelf for actual sample placement. This range of desiccators comprises four multi-shelved stackable cubic desiccators, which are made from highly transparent, noncorrosive, and shatterproof polycarbonate. The internal volumes range from 11 to 45 L with between two and six shelves, and this significantly enhances the storage capacity of the desiccators. Each unit has a full front door that uses a grease-free airtight vacuum seal, which ensures that a vacuum of 1 Torr over 72 hours is held. Also, a vacuum gauge is mounted on the top left hand side of the door while the three-way stopcock mounted on the left hand side of the chamber allows for the removal and replacement of the internal atmosphere as needed. Each unit is available in smoked acrylic to block ultraviolet light.



Medline Scientific
For info: + 44-(0)-1865-400321 | www.medlinescientific.com

INVERTED LIGHT MICROSCOPE

The Axio Vert.A1 is an inverted microscope with extensive performance capabilities. For the first time, a compact cell culture microscope combines all standard contrasting techniques in a single stand. In transmitted light, the Axio Vert.A1 offers brightfield, phase contrast, polarization contrast, PlasDIC, VAREL, and improved Hoffmann modulation contrast (iHMC). The microscope is the only system in its class to also offer differential interference contrast (DIC). This makes it possible to record very fine structures in cells, enabling users to better assess cell cultures. In fluorescence applications, the Axio Vert.A1 uses long-life LED illumination. The entire image field is illuminated homogeneously; no alignment is necessary. As LED excitation light does not contain any undesired ultraviolet components, cell survival rate increases significantly. The Axio Vert.A1 has been specially designed so that it can be positioned directly beside the incubator or the sterile bench. Adapters allow comfortable, upright work in either a seated or standing position.

Carl Zeiss
For info: +49-3641-64-39-49 | www.zeiss.de

PARP1 ENZYME ACTIVITY ASSAY

The PARP1 Enzyme Assay is designed for detection of poly (ADP-ribose) polymerase (PARP) activity and screening of activators and inhibitors. PARPs catalyze the addition of ADP-ribose moieties onto substrate proteins and play a role in DNA repair, chromatin structure, cell cycle, and cell death. The kit is a flexible, homogenous, no-wash assay for quantifying enzymatic activity. Based on patent-pending technology, this assay employs nicotinamidase to measure nicotinamide generated upon cleavage of NAD^+ during PARP-mediated poly-ADP-ribosylation of a substrate, thereby providing a direct, positive signal assessment of the activity of PARP1 and PARP2. The new PARP assay utilizes a novel, patent-pending fluorescently coupled enzyme assay for nicotinamide degradation to permit the use of native NAD^+ substrate and flexibility with peptide/protein acceptor substrates.

EMD Millipore
For info: 800-645-5476 | www.millipore.com

ANTIBODY ARRAY

The Panorama Neurobiology Antibody Array is designed for fast protein expression analysis of hundreds of signaling targets that are indicative of neuronal health and development. The Panorama Neurobiology Antibody Array assesses a broader range of signaling targets, and is expected to provide the most comprehensive view available of the cell signaling and regulation pathways that are key to neuronal development and neurodegenerative disorders. The Panorama Neurobiology Antibody Array enables, within a single day, direct comparisons of neuronal protein expression patterns using a variety of serum, cell, or tissue extracts derived from humans, mice, or rats. The array's 224 polyclonal and monoclonal antibodies are spotted in duplicate, high-density spots on a nitrocellulose-coated slide treated to reduce background fluorescence. Antibodies in the array are also available separately from the Sigma Life Science Antibody catalog of more than 50,000 antibodies.

Sigma Life Science
For info: 800-521-8956 | www.sigma.com

BIOSPECTROMETER

The new Eppendorf BioSpectrometer combines accuracy and sensitivity with outstanding flexibility in a small robust instrument. The Eppendorf BioSpectrometer extends our current detection product line by offering scanning capabilities allowing routine and complex methods such as measuring cytotoxicity, proteins, fluorescent dyes, and more. The BioSpectrometer kinetic model features a temperature-controlled cuvette shaft that requires no additional accessories in order to study enzyme or substrate kinetics. Scanning spectrum as well as individual wavelength measurements can be monitored in the spectral range of 200 to 830 nm. Preprogrammed methods facilitate quick start applications and prevent errors, while a USB port is provided for simple data transfer. No PC is necessary to operate the system and integrated data processing options enable basic data processing directly on the device. Apart from standard cuvettes such as the Eppendorf UVette, the BioSpectrometer can also accommodate micro volume cuvettes.

Eppendorf
For info: 800-645-3050 | www.eppendorfna.com

Electronically submit your new product description or product literature information! Go to **www.sciencemag.org/products/newproducts.dtl** for more information.

Newly offered instrumentation, apparatus, and laboratory materials of interest to researchers in all disciplines in academic, industrial, and governmental organizations are featured in this space. Emphasis is given to purpose, chief characteristics, and availability of products and materials. Endorsement by *Science* or AAAS of any products or materials mentioned is not implied. Additional information may be obtained from the manufacturer or supplier.

Downloaded from www.sciencemag.org on February 2, 2012

Everything you need to measure mitochondrial (dys)function in cells

Webinars On-Demand
See our mitochondrial profiling webinars at seahorsebio.com/science

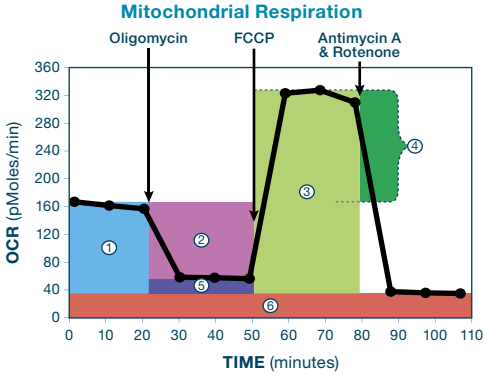


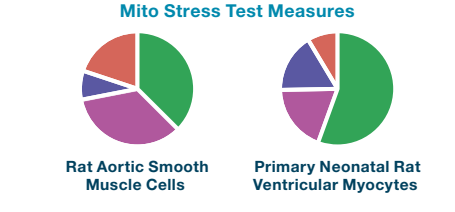
XF Cell Mito Stress Test Kit
for use with the XF Analyzer

With the XF Cell Mito Stress Test Kit and the XF Analyzer you can confidently identify mitochondrial (dys)function, and measure mitochondrial response to stress.

XF Cell Mito Stress Test Kit

- Complete easy-to-use kit, including pre-calibrated, pre-tested reagents for 6 microplates
- Software wizard guides assay optimization, design, and interpretation
- Designed for use with the XF Analyzer
- Provides metrics essential to understanding cancer, aging, and metabolic, cardiovascular, and neurodegenerative diseases





1. Basal Respiration
2. ATP Production
3. Maximal Respiration
4. Spare Respiratory Capacity
5. Proton Leak
6. Non-mitochondrial Respiration

Measuring **cell metabolism** is so easy now!

www.seahorsebio.com/science • +1-978-671-1600 • info@seahorsebio.com
16 Esquire Road, North Billerica, MA 01862, USA

Seahorse *Bioscience*

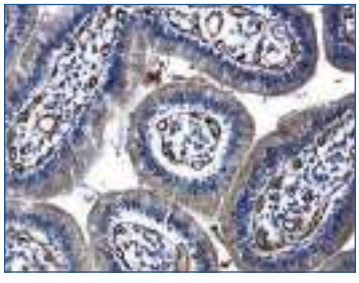
Cancer
Development
Endocrinology
Glycobiology
Immunology
Neuroscience
Proteases
Signal Transduction
Stem Cells



R&D Systems Specialized Tools for Cancer Research

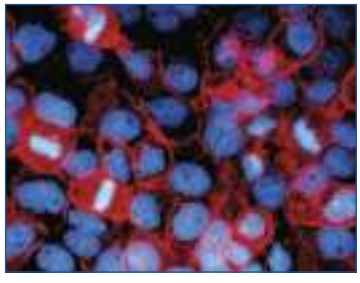
Cancer is a disease of cellular dysfunction involving a range of biological activities that promote unregulated proliferation. To help advance the understanding of this complex disease, R&D Systems offers an expansive selection of quality products, including **high performance antibodies, proteins, ELISAs, & arrays,** for investigating various cancer-related factors. Every product from R&D Systems undergoes rigorous quality control testing to ensure industry leading reliability.

Angiogenesis



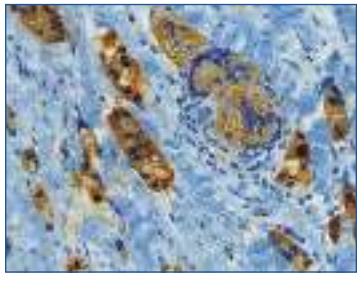
Angiopoietin-2 (Catalog # AF623)
Human Gastrointestinal Cancer Tissue

Epithelial to Mesenchymal Transition



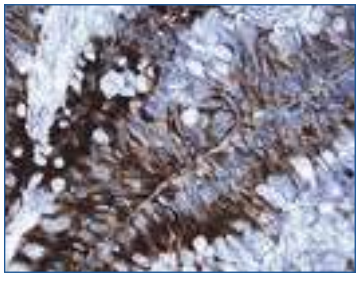
E-Cadherin (Catalog # AF648)
Human Epidermoid Carcinoma Cells

Cancer Biomarkers



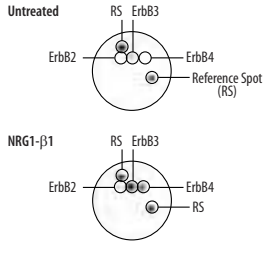
BRCA1 (Catalog # MAB22101)
Human Breast Cancer Tissue

Inflammation



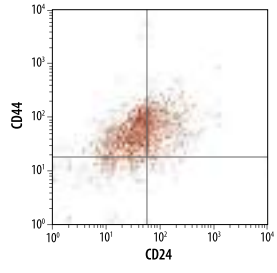
EMAP-II (Catalog # AF1910)
Human Colon Cancer Tissue

Growth Factor/Receptor Signaling



Proteome Profiler™ *96* Phospho-RTK Antibody Array (Catalog # ARZ001)
MDA-MB-453 Cell Line

Cancer Stem Cells



MagCellect $CD24^{-}CD44^{+}$ Breast Cancer Stem Cell Isolation Kit (Catalog # MAGH111)
MCF-7 Cell Line

For more information visit our website at www.RnDSystems.com/go/Cancer

For research use only. Not for use in diagnostic procedures.

R&D Systems, Inc. www.RnDSystems.com
R&D Systems Europe, Ltd. www.RnDSystems.co.uk
R&D Systems China Co., Ltd. www.RnDSystemsChina.com.cn

Determining plant DNA content with the BD Accuri C6®



BD

Helping all people live healthy lives

Flow cytometry within reach.®

The BD Accuri® C6 flow cytometer offers a capable yet simple tool to rapidly identify plant DNA. The affordable, benchtop cytometer can help characterize the DNA content of newly discovered plant species and the impact of environmental changes on genome.

Measuring just 11 x 14.75 x 16.5 inches and weighing just 30 pounds, the BD Accuri C6 gives you the power of flow cytometry when you need it. Best of all, you don't need to be a flow expert because BD CFlow® software's intuitive interface will guide you from sample collection to analysis. For faster throughput, the BD CSampler® option offers reliable and easy-to-use automation with support for 48- and 96-well plates, and 24-tube racks for standard 12 x 75-mm tubes. Setup and maintenance are also simplified to increase availability and up time.

For more information about how you can more easily access the power of flow cytometry in your lab, visit **bdbiosciences.com/go/dna.**

Flow cytometry within reach.®

BD flow cytometers are Class 1 Laser Products.
For Research Use Only. Not for use in diagnostic or therapeutic procedures.
BD, BD Logo and all other trademarks are property of Becton, Dickinson and Company. © 2012 BD
23-13833-00

BD Biosciences
2350 Qume Drive
San Jose, CA 95131
bdbiosciences.com

Now available:
Adaptors & Primers
for Illumina®

NEW ENGLAND
BioLabs® Inc.
enabling technologies in the life sciences

Take the next step.



Library Prep Reagents for Next Gen Sequencing

Isn't it time to break away from the constraints of standard workflows for NGS sample prep? With NEBNext® reagents for DNA and RNA, take advantage of multiple product formats and custom options to tailor solutions for your specific needs.

Available for the leading sequencing platforms, NEBNext reagents allow you to take the next step in designing the workflow that works for you.

www.NEBNext.com

Scan this code to learn more about how NEBNext reagents deliver flexibility to your sample prep workflow

Need a code reader? Go to 2dscan.com from your mobile browser, search for 'ScanLife' in your app store or text SCAN to 43588

Illumina® is a registered trademark of Illumina, Inc.

Accelerating Science:
Concept to Clinic

AACR ANNUAL MEETING 2012

March 31- April 4
McCormick Place West
Chicago, IL



Don't miss the premier forum for the latest breakthroughs

bringing together over 17,000 attendees from over 60 countries. More than 6,000 proffered papers and hundreds of invited talks from leading experts will be presented, covering the full spectrum of cancer research, including basic, translational, clinical, and population research.

NEW in 2012:

- A revised format for the presentation of accepted clinical trials
- New session series titled Current Concepts and Controversies in Diagnostics, Therapeutics, and Prevention
- New poster session on clinical trials in progress
- A regulatory track with sessions on regulatory science and science policy

AACR American Association for Cancer Research

www.aacr.org/AM2012



2012 MRS SPRING MEETING & EXHIBIT

April 9–13
San Francisco, CA

2012 MRS SPRING MEETING SYMPOSIA

*Co-sponsored by the Japan Society of Applied Physics**

ELECTRONICS AND PHOTONICS

- A Amorphous and Polycrystalline Thin-Film Silicon Science and Technology
- B Heterogeneous Integration Challenges of MEMS, Sensor, and CMOS LSI*
- C Interconnect Challenges for CMOS Technology–Materials, Processes, and Reliability for Downscaling, Packaging, and 3D Stacking
- D Nanocontacts–Emerging Materials and Processing for Ohmicity and Rectification
- E Materials and Physics of Emerging Nonvolatile Memories*
- F Phase-Change Materials for Memory and Reconfigurable Electronics Applications
- G Reliability and Materials Issues of III-V and II-VI Semiconductor Optical and Electron Devices and Materials II*
- H Silicon Carbide–Materials, Processing, and Devices
- I Recent Advances in Superconductors, Novel Compounds, and High-T_c Materials*
- J Organic and Hybrid-Organic Electronics
- K Advanced Materials and Processes for "Systems-on-Plastic"*
- L Group IV Photonics for Sensing and Imaging*
- M Optical Interconnects–Materials, Performance, and Applications

MATERIALS SCIENCE AND MATERIALS CHEMISTRY FOR ENERGY

- N One-Dimensional Nanostructured Materials for Energy Conversion and Storage
- O Next-Generation Energy Storage Materials and Systems
- P Advanced Materials and Nanoframeworks for Hydrogen Storage and Carbon Capture
- Q Titanium Dioxide Nanomaterials
- R Bandgap Engineering and Interfaces of Metal Oxides for Energy
- S Design of Materials for Sustainable Nuclear Energy
- T Bio-inspired Materials for Energy Applications
- U Materials for Catalysis in Energy
- V Advanced Materials Processing for Scalable Solar-Cell Manufacturing II
- W Nanostructured Solar Cells
- Y Actinides–Basic Science, Applications, and Technology
- Z Conjugated Organic Materials for Energy Conversion, Energy Storage, and Charge Transport

NANOSTRUCTURED MATERIALS AND DEVICES

- AA Inorganic Nanowires and Nanotubes–Synthesis, Properties, and Device Applications*
- BB Solution Synthesis of Inorganic Films and Nanostructured Materials
- CC Hierarchically Self-assembled Materials–From Molecule to Nano and Beyond
- DD *De Novo* Carbon Nanomaterials
- EE New Functional Nanocarbon Devices*
- FF Nanodiamond Particles and Related Materials–From Basic Science to Applications
- GG Functional Inorganic Nanoparticle-Polymer Composites with Engineered Structures and Coupled Properties
- HH Nanocomposites, Nanostructures, and Heterostructures of Correlated Oxide Systems*
- II Nanoscale Materials Modification by Photon, Ion, and Electron Beams*
- JJ Nanoscale Thermoelectrics–Materials and Transport Phenomena
- KK Plasmonic Materials and Metamaterials
- LL New Trends and Developments in Nanomagnetism
- MM Topological Insulators

BIOLOGICAL, BIOMEDICAL AND BIO-INSPIRED MATERIALS

- NN DNA Nanotechnology
- OO Structure-Function Design Strategies for Bio-enabled Materials Systems
- PP Manipulating Cellular Microenvironments
- QQ Mechanobiology of Cells and Materials
- RR Molecules to Materials–Multiscale Interfacial Phenomena in Biological and Bio-inspired Materials
- SS Structure/Property Relationships in Biological and Biomimetic Materials at the Micro-, Nano-, and Atomic-Length Scales
- TT Interfaces in Materials, Biology, and Physiology
- UU Integration of Natural and Synthetic Biomaterials with Organic Electronics
- VV Nanomedicine for Molecular Imaging and Therapy
- WW Plasma Processing and Diagnostics for Life Sciences*

GENERAL MATERIALS SCIENCE

- XX Computational Materials Design in Heterogeneous Systems
- YY Rare-Earth-based Materials
- ZZ Transforming Education in Materials Science and Engineering
- AAA Synthesis, Fabrication, and Assembly of Functional Particles and Capsules
- BBB Functional Materials and Ionic Liquids
- CCC Local Probing Techniques and *In-Situ* Measurements in Materials Science

X *FRONTIERS OF MATERIALS RESEARCH*

2012 MRS SPRING MEETING CHAIRS

Lara A. Estroff
Cornell University
lae37@cornell.edu

Jun Liu
Pacific Northwest National Laboratory
jun.liu@pnl.gov

Kornelius Nielsch
University of Hamburg
kornelius.nielsch@physik.uni-hamburg.de

Kazumi Wada
University of Tokyo
kwada@material.t.u-tokyo.ac.jp

www.mrs.org/spring2012

DON'T MISS THESE FUTURE MRS MEETINGS!

2012 MRS Fall Meeting & Exhibit ▪ November 26-30, 2012
Hynes Convention Center & Sheraton Boston Hotel ▪ Boston, Massachusetts

2013 MRS Spring Meeting & Exhibit ▪ April 1-5, 2013
Moscone West & San Francisco Marriott Marquis ▪ San Francisco, California

MRS MATERIALS RESEARCH SOCIETY
Advancing materials. Improving the quality of life.
506 Keystone Drive ▪ Warrendale, PA 15086-7573
Tel 724.779.3003 ▪ Fax 724.779.8313
info@mrs.org ▪ www.mrs.org

WEBINAR

APPLYING NEW IMAGING TECHNIQUES TO YOUR RESEARCH

Advice from the Experts

Wednesday, February 29, 2012

12 noon Eastern, 9 a.m. Pacific, 5 p.m. UK

The resolution of light microscopy was long thought to be limited by the wavelength of light, but recent advances have far surpassed this barrier and the most recent technologies are now allowing for the super-resolution imaging of biomolecules at a subcellular level, including the visualizing membrane glycoproteins, observing physical interactions between proteins, and studying cellular processes in 3-D. This webinar will explore how some of the latest technologies can be applied and implemented to advance your research.

Our experts from the NIH Intramural Research Program will:

- Share their experiences using cutting-edge microscopy technologies
- Discuss the advantages, challenges, and limitations of current systems
- Provide advice on how you can best apply these technologies
- Answer questions submitted by you!

SPEAKERS

Hari Shroff, Ph.D.
National Institute of Biomedical Imaging and Bioengineering, NIH
Bethesda, MD

Sriram Subramaniam, Ph.D.
National Cancer Institute, NIH
Bethesda, MD

Clare M. Waterman, Ph.D.
National Heart, Lung and Blood Institute, NIH
Bethesda, MD

All speakers are part of the NIH Intramural Research Program.

REGISTER NOW!
www.sciencemag.org/webinar

Webinar sponsored by

Intramural Research Program
Our Research Changes Lives

Brought to you by the *Science*/AAAS Custom Publishing Office

Science
AAAS

New Products

STACKABLE DESICCATORS

Multi-Storey Cubic Desiccators overcome the space inefficiencies of traditional round desiccators which occupy a large bench area while providing only a small circular shelf for actual sample placement. This range of desiccators comprises four multi-shelved stackable cubic desiccators, which are made from highly transparent, noncorrosive, and shatterproof polycarbonate. The internal volumes range from 11 to 45 L with between two and six shelves, and this significantly enhances the storage capacity of the desiccators. Each unit has a full front door that uses a grease-free airtight vacuum seal, which ensures that a vacuum of 1 Torr over 72 hours is held. Also, a vacuum gauge is mounted on the top left hand side of the door while the three-way stopcock mounted on the left hand side of the chamber allows for the removal and replacement of the internal atmosphere as needed. Each unit is available in smoked acrylic to block ultraviolet light.



Medline Scientific
For info: + 44-(0)-1865-400321 | www.medlinescientific.com

INVERTED LIGHT MICROSCOPE

The Axio Vert.A1 is an inverted microscope with extensive performance capabilities. For the first time, a compact cell culture microscope combines all standard contrasting techniques in a single stand. In transmitted light, the Axio Vert.A1 offers brightfield, phase contrast, polarization contrast, PlasDIC, VAREL, and improved Hoffmann modulation contrast (iHMC). The microscope is the only system in its class to also offer differential interference contrast (DIC). This makes it possible to record very fine structures in cells, enabling users to better assess cell cultures. In fluorescence applications, the Axio Vert.A1 uses long-life LED illumination. The entire image field is illuminated homogeneously; no alignment is necessary. As LED excitation light does not contain any undesired ultraviolet components, cell survival rate increases significantly. The Axio Vert.A1 has been specially designed so that it can be positioned directly beside the incubator or the sterile bench. Adapters allow comfortable, upright work in either a seated or standing position.

Carl Zeiss
For info: +49-3641-64-39-49 | www.zeiss.de

PARP1 ENZYME ACTIVITY ASSAY

The PARP1 Enzyme Assay is designed for detection of poly (ADP-ribose) polymerase (PARP) activity and screening of activators and inhibitors. PARPs catalyze the addition of ADP-ribose moieties onto substrate proteins and play a role in DNA repair, chromatin structure, cell cycle, and cell death. The kit is a flexible, homogenous, no-wash assay for quantifying enzymatic activity. Based on patent-pending technology, this assay employs nicotinamidase to measure nicotinamide generated upon cleavage of NAD^+ during PARP-mediated poly-ADP-ribosylation of a substrate, thereby providing a direct, positive signal assessment of the activity of PARP1 and PARP2. The new PARP assay utilizes a novel, patent-pending fluorescently coupled enzyme assay for nicotinamide degradation to permit the use of native NAD^+ substrate and flexibility with peptide/protein acceptor substrates.

EMD Millipore
For info: 800-645-5476 | www.millipore.com

ANTIBODY ARRAY

The Panorama Neurobiology Antibody Array is designed for fast protein expression analysis of hundreds of signaling targets that are indicative of neuronal health and development. The Panorama Neurobiology Antibody Array assesses a broader range of signaling targets, and is expected to provide the most comprehensive view available of the cell signaling and regulation pathways that are key to neuronal development and neurodegenerative disorders. The Panorama Neurobiology Antibody Array enables, within a single day, direct comparisons of neuronal protein expression patterns using a variety of serum, cell, or tissue extracts derived from humans, mice, or rats. The array's 224 polyclonal and monoclonal antibodies are spotted in duplicate, high-density spots on a nitrocellulose-coated slide treated to reduce background fluorescence. Antibodies in the array are also available separately from the Sigma Life Science Antibody catalog of more than 50,000 antibodies.

Sigma Life Science
For info: 800-521-8956 | www.sigma.com

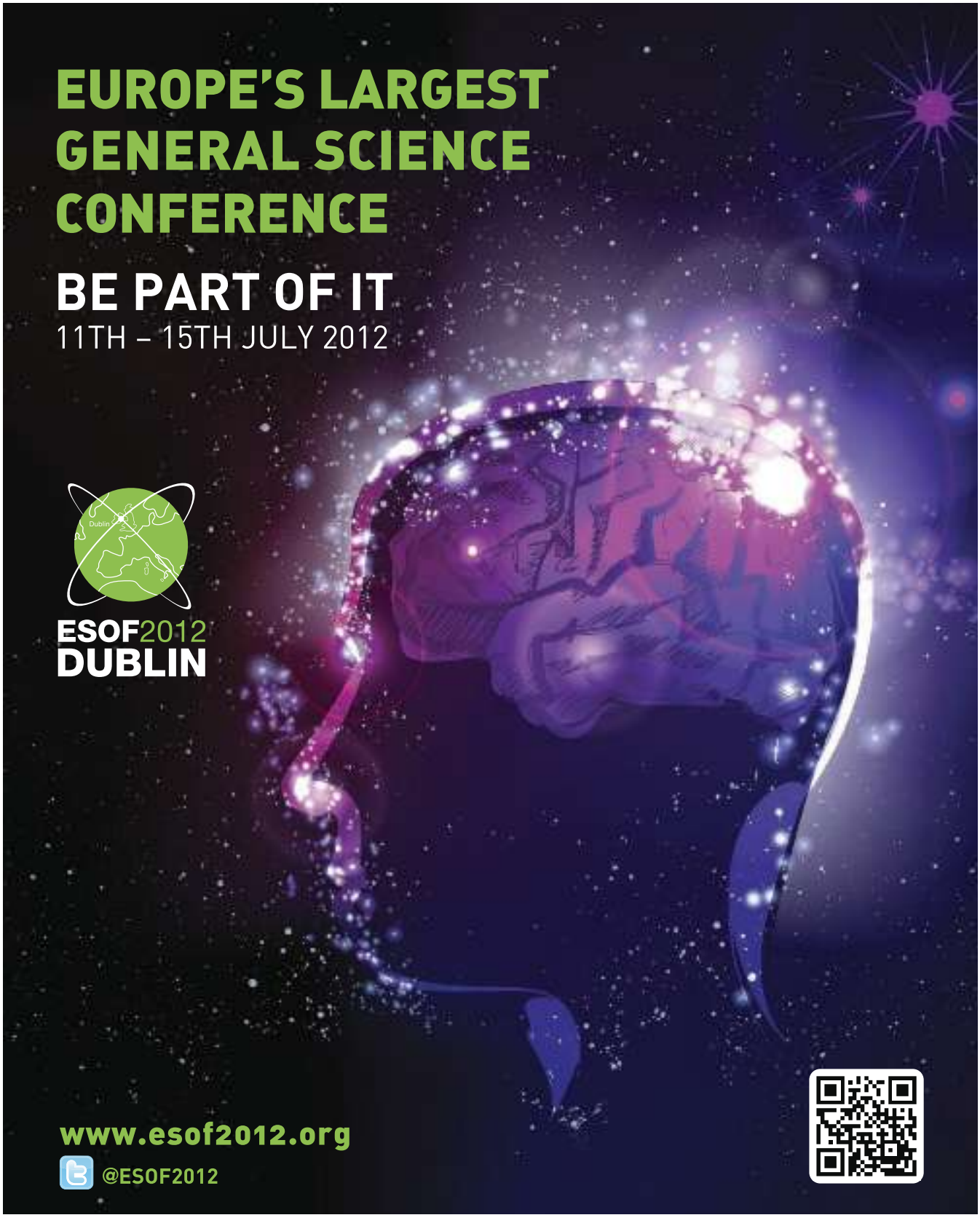
BIOSPECTROMETER

The new Eppendorf BioSpectrometer combines accuracy and sensitivity with outstanding flexibility in a small robust instrument. The Eppendorf BioSpectrometer extends our current detection product line by offering scanning capabilities allowing routine and complex methods such as measuring cytotoxicity, proteins, fluorescent dyes, and more. The BioSpectrometer kinetic model features a temperature-controlled cuvette shaft that requires no additional accessories in order to study enzyme or substrate kinetics. Scanning spectrum as well as individual wavelength measurements can be monitored in the spectral range of 200 to 830 nm. Preprogrammed methods facilitate quick start applications and prevent errors, while a USB port is provided for simple data transfer. No PC is necessary to operate the system and integrated data processing options enable basic data processing directly on the device. Apart from standard cuvettes such as the Eppendorf UVette, the BioSpectrometer can also accommodate micro volume cuvettes.

Eppendorf
For info: 800-645-3050 | www.eppendorfna.com

Electronically submit your new product description or product literature information! Go to **www.sciencemag.org/products/newproducts.dtl** for more information.

Newly offered instrumentation, apparatus, and laboratory materials of interest to researchers in all disciplines in academic, industrial, and governmental organizations are featured in this space. Emphasis is given to purpose, chief characteristics, and availability of products and materials. Endorsement by *Science* or AAAS of any products or materials mentioned is not implied. Additional information may be obtained from the manufacturer or supplier.



European Commission

Robert Bosch Stiftung

intel

sfi Science Foundation Ireland

janssen

IBM

Forfás

An Roinn Post, Fiontar agus Nuálaíochta
Department of Jobs, Enterprise and Innovation

Comhairle Cathrach Bhaile Átha Cliath
Dublin City Council

EIRGRID

Marine Institute
Fóras na Mara

SIGMA-ALDRICH®

SIGMA® Life Science Where bio begins™

Bioelevate.

Let our Cell Design Studio™ experts simplify your custom cell line engineering while you focus on research.

No matter how obscure or exact your specifications, our custom-engineered cell lines are tailored using CompoZr® ZFN and MISSION® shRNA technologies to fit your application perfectly.

sigma.com/biocells





biocells

©2012 Sigma-Aldrich Co. LLC. All rights reserved. SIGMA and SIGMA-ALDRICH are trademarks of Sigma-Aldrich Co. LLC, registered in the US and other countries. CompoZr and MISSION are registered trademarks of Sigma-Aldrich Co. LLC. Where bio begins and Cell Design Studio are trademarks of Sigma-Aldrich Co. LLC.

There's only one
Science



Science Careers Advertising

For full advertising details, go to ScienceCareers.org and click For Employers, or call one of our representatives.

Tracy Holmes
Worldwide Associate Director
Science Careers
Phone: +44 (0) 1223 326525

UNITED STATES & CANADA
E-mail: advertise@sciencecareers.org
Fax: 202-289-6742

Tina Burks
Midwest/West Coast/
South Central/Canada
Phone: 202-326-6577

Elizabeth Early
East Coast & Corporate
Phone: 202-326-6578

Marci Gallun
Sales Administrator
Phone: 202-326-6582

Online Job Posting Questions
Phone: 202-312-6375

EUROPE & REST OF WORLD
E-mail: ads@science-int.co.uk
Fax: +44 (0) 1223 326532

Simone Jux
Phone: +44 (0)1223 326529

Lucy Nelson
Phone: +44 (0)1223 326527

Kelly Grace
Phone: +44 (0) 1223 326528

JAPAN
Makiko Hara
Phone: +81 (0) 90-9853-9982
E-mail: mhara@aaas.org
Fax: +81 (0) 3-6369-4491

CHINA & TAIWAN
Ruolei Wu
Phone: +86-1367-1015-294
E-mail: rwu@aaas.org

All ads submitted for publication must comply with applicable U.S. and non-U.S. laws. *Science* reserves the right to refuse any advertisement at its sole discretion for any reason, including without limitation for offensive language or inappropriate content, and all advertising is subject to publisher approval. *Science* encourages our readers to alert us to any ads that they feel may be discriminatory or offensive.

Science Careers
From the journal *Science* AAAS

UNIVERSITY OF LOUISVILLE

SCIENTIFIC DIRECTOR
Kosair Children's Hospital Research Institute
Department of Pediatrics, University of Louisville School of Medicine

The Department of Pediatrics at the University of Louisville invites competitive applications to fill the position of Scientific Director of the Kosair Children's Hospital Research Institute (KCHRI). The Institute performs basic and translational research on diseases relevant to pediatric patients. KCHRI faculty research is currently focused on two major areas: (1) neurobiology and (2) the neurologic and cardiovascular complications of obesity and diabetes. Additional pediatric relevant basic science research currently occurs in the Cardiovascular Innovation Institute and the James Graham Brown Cancer Center.

The new KCHRI Director will be expected to expand their extramurally funded research program at the University of Louisville while actively leading the expansion of pediatric-relevant basic science research at the University of Louisville. The successful applicant must have demonstrated effective administrative and leadership experience, a strong record of consistent extramural funding, an excellent publication record, and a track record of successfully mentoring clinician-scientists and basic science investigators. The research focus of the new Director and of subsequently recruited faculty would be determined by the new Director. Candidates with an MD, MD/PhD, or PhD will be considered. A tenure-eligible, endowed Chair and substantial financial support are available for the new Director and the continued growth of the KCHRI. The successful candidate will have a primary academic appointment in the Department of Pediatrics and may also have additional joint appointments in basic science and bioengineering departments to facilitate the training of graduate students and faculty. The Director of the KCHRI reports to the Vice-Chair for Research and to the Chairman of the Department of Pediatrics.

The Academic Programs in the Department of Pediatrics at the University of Louisville cover a broad range of basic science, clinical, and translational research topics supported by over 160 faculty, more than 100 residents and fellows, and highly supportive research and administrative staff. Clinical services are provided at the free-standing Kosair Children's Hospital of Norton Healthcare and at regional sites throughout Kentucky. Our pediatric programs have substantial philanthropic support. We have been highly successful in recruiting talented faculty and residents to the University of Louisville and to our very enjoyable community.

Applications will be reviewed until the position is filled with the intent to have a new Director in place by the third quarter of 2012. Please submit a cover letter including a statement of research interests, curriculum vitae, and contact information for three references electronically to **Bradley B. Keller, MD**, **brad.keller @louisville.edu**, Vice Chair for Research, Department of Pediatrics and Kosair Charities Chair and Chief, Division of Pediatric Heart Research, Cardiovascular Innovation Institute, University of Louisville.

The University of Louisville is an Affirmative Action, Equal Opportunity, Americans with Disabilities Employer, committed to diversity, and in that spirit, seeks applications from a broad variety of candidates.

Chair, Department of Cell Biology & Molecular Medicine

UMDNJ-New Jersey Medical School seeks a Chair of the Department of Cell Biology & Molecular Medicine. The Chair will be a dynamic and accomplished scientist and offer leadership and innovative vision for the continued growth of the research, clinical and educational missions of the department, as well as oversee departmental administrative, financial and program components.

The Department of Cell Biology & Molecular Medicine is committed to understanding the molecular mechanisms of disease by bridging the gap between physiology and molecular biology. Current research includes physiology, functional genomics, proteomics, developmental biology, cell biology and cell signaling with a strong concentration in molecular mechanisms of cardiovascular disease. The department is currently in an expansion phase with the creation of a division for cancer research and stem cells, and the recruitment of several new faculty members. In addition to research, the Department is committed to medical and graduate education including the training of postdoctoral fellows, graduate students, and undergraduate medical students. The successful candidate will be an internationally-recognized researcher with a strong record of sustained extramural support. He/she will also have administrative experience in leading basic science research groups and navigating a large university environment.

UMDNJ is the largest health sciences university in the nation and NJMS anchors its largest campus in the city of Newark. The campus is also home to the New Jersey Dental School, School of Health Related Professions, Graduate School of Biomedical Sciences, the School of Nursing and the School of Public Health.

Interested individuals should send a curriculum vitae and cover letter to: **David Perlin, PhD, Chair, Search Committee for the Chair of the Department of Cell Biology & Molecular Medicine, c/o Michael Petti, Executive Assistant to the Dean, UMDNJ-New Jersey Medical School, 185 South Orange Avenue, MSB C-671, Newark, NJ 07101-1709 or email: pettime@umdnj.edu.**

Women and minorities are encouraged to apply. Unless confidentiality is requested in writing, information regarding applicants and nominees must be released upon request. Finalists cannot be guaranteed confidentiality. UMDNJ is an Equal Opportunity and Affirmative Action Employer.

UMDNJ NEW JERSEY MEDICAL SCHOOL
University of Medicine & Dentistry of New Jersey

Lab Is Where The Heart Is?

Trials and Tribulations of Lab Culture



For many grad students, postdocs, and PIs, the lab in which they work represents a type of "home away from home," replete with similar territorial issues, responsibilities, and associated "family dynamics." And just as there are many different types of families, there are many different types of lab cultures. The environment may be competitive or it may be more collaborative. There may be ordered systems of sharing supplies and equipment, or perhaps, as in some families, anarchy reigns. Likewise, members of the "lab family" may enjoy each other's company or spend as much time apart from each other as possible. Regardless of the type of culture, one always exists, so it behooves the PI to try to manage it.

By Emma Hitt



PAUL DOETSCH

SETTING THE TONE

When setting the tone for a lab, a common approach used by principal investigators (PIs) is to clearly state the expectations to lab members when they first start. "When someone is thinking about joining my group I am very up front with what my expectations are," says PI **Paul Doetsch,** professor and distinguished chair in cancer research, at Emory University School of Medicine in Atlanta, Georgia, adding that one major expectation he has for his lab members is a strong work ethic.

"I clearly communicate my philosophy regarding how my lab should run," says PI **Michael Hengartner,** dean of the faculty of science, at the University of Zurich, in Switzerland. "I do not necessarily proselytize, but I do bring it up regularly, particularly when one of my lab members seems to be ignoring my philosophy. I take great pains to make sure that during any recruiting of new lab members, they are informed (or shall I say "warned") of our lab philosophy. I also make sure that current lab members get an opportunity to meet with prospective new lab members, and I make sure to consider their feedback, since a single 'dominant negative' person can kill the good atmosphere of a lab."

The amount of time a PI spends in the lab is also important for setting the work ethic standard, even if it consists of a regular walk around and interaction with the lab members. **Heather Maughan,** a postdoctoral fellow who is now in a laboratory at the University of Toronto, in Canada, observes that when "PIs spend almost no time in the lab, lab members tend to be sloppier and not perform all of their duties, such as lab cleanup and sharing of reagents," she says. "By contrast, PIs who spend a lot of time in the lab tend to run tighter ships."

According to Maughan, when PIs run tighter ships, there is oftentimes more of a feeling of camaraderie among the lab workers. In addition, the lab is better organized, which makes the work easier and more efficient. "By contrast, when the PI is almost completely absent from lab life, workers tend to get along superficially, but may be silently wondering who didn't clean up their mess."

DISHING IT OUT AND TAKING IT

The issue of critiquing each other's work and the way it is done also plays an important role in the culture of a lab. "It is very important to me that people openly constructively critique other lab members' work without the critique being meant or taken personally," Hengartner explains. "Other lab members should be the toughest reviewers for all our manuscripts." He adds that his lab works on several different research problems, and "being able to give constructive input is perhaps one of the most useful skills that my lab members develop—a skill that will become increasingly important the further along they are in academia."

Alan Fersht, a PI at the Medical Research Council Laboratory of Molecular Biology in Cambridge, United Kingdom says he believes in short but frequent contacts rather than lengthier more formal meetings. According to Fersht, wandering around the lab and observing can uncover flaws in techniques and facilitate rapid improvements.

Doetsch says that he tries to maintain a lab culture that provides technicians, students, postdocs, and research faculty a sense of "ownership" of their projects and to give the message everyone is making a significant contribution to the research enterprise, regardless of their specific title or role. "My continued>

UPCOMING FEATURES

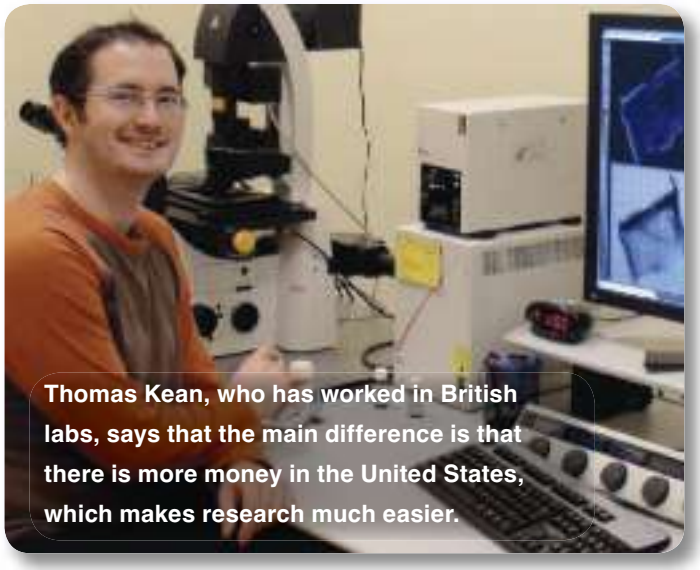
Postdocs: Seeking Funding Resources—March 9

Cancer Research: Vaccine Drug Development—March 23

Bioclusters: Eastern United States—April 6

CREDIT: (LEFT) ISTOCKPHOTO.COM/PICK-UPPATH

Faculty



Thomas Kean, who has worked in British labs, says that the main difference is that there is more money in the United States, which makes research much easier.

position includes heavy administrative duties that preclude me working in the lab," he explains, "but I make it a point to walk around my lab several times a day to chat with my group and hold individual weekly research meetings with each member to get an update of their progress and provide them with direct, constructive feedback on their activities. I always strongly encourage everyone to discuss their results and other issues affecting their project with their lab colleagues and to not hesitate to disagree with me when necessary."

According to Doetsch, the research in his lab is discussed in the context of a weekly meeting shared with several other lab groups with common interests from other local institutions to get another level of feedback. "This multi-pronged approach has worked well for minimizing research bottlenecks and promoting collegial interactions within my group and amongst local colleagues with similar research interests."

Doug Dluzen, currently a graduate student in the Department of Pharmacology at Penn State University, says that he works in a fairly large lab where there are outlets to discuss research problems, and strategies, and "generally there is someone who has stumbled upon a problem before—being able to discuss my issues can be very helpful when troubleshooting an assay or transfection in the early stages of the experiments."

Dluzen says that he has heard of other more competitive labs—in some cases two students or postdocs working on the same project in the same lab—and it is a race to the finish between the two. "I cannot imagine that system of working—having to hide your results and troubles from those around you," he says. "I think an open-atmosphere philosophy fosters more creative and collaborative work that brings scientists together and harbors a larger degree of communication and productivity.

PLAYING WELL TOGETHER

Members of any lab are faced with having to share equipment and supplies, and in most labs, signup sheets for equipment and a common ordering system for supplies can help smooth out any wrinkles that can occur with conducting multiple experiments. Dluzen explains that his lab is fairly big and as a result, there is a lab manager who orders reagents and gets final approval from the PI. "We have an online folder and database with a list we update for needed reagents, and they are ordered generally once a week unless something is needed faster," he says. Equipment such as centrifuges, incubators, and rotating trays are shared routinely by multiple labs, not just the members of an individual lab.

In her lab, says **Amy Dear,** most recently a postdoc in the Department of Biochemistry, at the University of Colorado at Boulder, everyone is responsible for ordering any reagents that continued>

5 WAYS PIs CAN SET THE TONE IN THEIR LAB

1. As Gandhi said, "Be the change you want to see in the world"
While some students and postdocs will be highly motivated regardless of how you act, most will tend to follow your lead. So, if you want the members of your lab to spend extensive time in lab, you should put in as much time as possible there yourself. Even if you feel that you have "done your time in the lab," you can still help promote a strong work ethic by working in your office with the door open and perhaps even conducting a few of your own experiments. A walk around in your lab a couple of times a week, including on weekends and evenings, will help your lab members know that you know they are working.

2. Write and espouse a well-defined mission statement for the lab
As with any business, a lab should have a mission statement that should be made known to the lab members and referred to regularly by the PI. A short, simple statement is often best. An example would be "the mission of this lab is to [insert overarching research goal], and in the process promote the conduct of rigorous science and the development of scientific expertise."

3. Develop a consistent schedule for interacting with lab members
While PIs tend to be extremely busy, a 30-minute to 1-hour meeting per week with each member of the lab may in fact save time since a scheduled opportunity for asking questions can decrease random interruptions during the week. Lab members will appreciate knowing they can have at least a weekly meeting with the PI and this will enhance productivity by providing a hard deadline for them to get their thoughts and work in order.

4. Promote collaboration and critique among lab members
Polite but constructive criticism of lab members' work should be encouraged. A weekly lab meeting where lab members present their work provides an opportunity for this type of discourse.

5. Establish a clear system for ordering supplies and using equipment
Systems for ordering and equipment use will cut down on conflicts among lab members. Every member of the lab should know how to get the supplies they need, whether by ordering them themselves or through a single person. It helps if the person who does the ordering is competent, organized, and approachable and can communicate directly with you when needed. Sign-up sheets should be made available for all major equipment and lab members should be encouraged to clean up after themselves.

CREDIT: PHOTO: DANIELLE L. MACKAY

UNIVERSITY OF BASEL

Professor in Infection Biology

The Biozentrum of the University of Basel in Switzerland invites applications for a professorship in Infection Biology.

The ideal candidate should perform cutting-edge research at the forefront of the field of Infection Biology using innovative approaches and technologies. The research topic should be related to the study of molecular mechanisms of bacterial pathogenesis and/or innate immune responses to infection. With a strong research record and proven communication skills, the successful candidate will strengthen the research portfolio of the Biozentrum and actively participate in teaching at the undergraduate and postgraduate level. In addition, he/she is expected to interact with other departments of the University of Basel, and with other Life Science institutions in the area. Depending on qualifications the position is at the Assistant (Tenure-track), Associate or Full Professor level.

The Biozentrum offers an outstanding scientific environment and an attractive research endowment. Basel is the home of a vibrant international life science community and provides high standard of living and a superb cultural atmosphere.
Applications, including CV, list of publications and a short research summary, should be sent by e-mail (pdf or zip) to Prof. Dr. Martin Spiess, Dean, Faculty of Science, University of Basel, Klingelbergstrasse 50, 4056 Basel, Switzerland, to dekanat-philnat@unibas.ch. For informal enquiries please contact Prof. Dr. Erich A. Nigg (erich.nigg@unibas.ch, phone: +41-61-267 16 56).

The deadline for receipt of applications is March 19, 2012. The University of Basel is an equal opportunity employer and encourages applications from female candidates.

UNI BASEL

UNIVERSITY OF BASEL

Professor in Spatiotemporal Modeling of Biological Processes

The Biozentrum of the University of Basel in Switzerland invites applications for a professorship in modeling of spatiotemporal processes in biology. The position can be filled at the Assistant (Tenure-track), Associate or Full Professor level depending on the qualifications of the applicant.

We are searching for applicants that are at the forefront of research and methods development in the field of spatiotemporal modeling in biology including multiscale modeling. The ideal candidate should combine her/his activity in the development of novel computational modeling and analysis methods with a deep understanding of biology and focus on concrete biological questions from a well-defined area of molecular or cell biology in which spatiotemporal processes play an important role. Areas of interest include, but are not limited to, spatiotemporal patterns of gene expression, morphogenesis, and the dynamics of the cell cycle, of membranes, and of chromatin organization. Applications from candidates that combine cutting-edge computational modeling with wet lab approaches are encouraged. The successful candidate will have a strong research record and communication skills, should complement the research portfolio of the Biozentrum, have a desire to engage in local collaborations, and will actively participate in teaching at the undergraduate and postgraduate level.

The Biozentrum offers an outstanding scientific environment and an attractive research endowment. Basel is the home of a vibrant international life science community and provides a high standard of living and a superb cultural atmosphere.

Applications, including CV, list of publications and a short research summary, should be sent by e-mail (pdf or zip) to Prof. Dr. Martin Spiess, Dean, Faculty of Science, University of Basel, Klingelbergstrasse 50, 4056 Basel, Switzerland, to dekanat-philnat@unibas.ch. For informal inquiries please contact Prof. Dr. Erich A. Nigg (erich.nigg@unibas.ch, phone: +41-61-267 16 56).

The deadline for receipt of applications is March 19, 2012. The University of Basel is an equal opportunity employer and encourages applications from female candidates.

UNI BASEL

Faculty

are needed and for the rest of the lab if they used the last item. "This was an area of conflict in one of the labs I worked in because people often forgot to order supplies when they had used them up," she says. She also recalled being next to a lab with which they shared equipment and supplies and that seemed to take advantage of the setup. "We ended up making them sign off on anything they borrowed, so we knew what they had returned or replaced. They were also very messy and left our equipment dirty, and it was annoying because we had to develop strategies to deal with it."



"On the positive side, [limited resources] makes us devise new ways to strategize, reuse, recycle, and minimize wastage."
—Shobhana Natarajan

Maughan points out that it is very much up to the PI to set down some ground rules about ordering supplies and fair use of equipment. "If the PIs don't set rules, workers are usually good about coming to an agreement so that everyone is happy, but sometimes a lab member will think their work is much more important than anyone else's, and that they deserve to use the equipment/reagents first," she says.

Doetsch explains that as a PI, he addresses the ordering problem by employing a technician-level lab manager with "good diplomatic skills who monitors supply usage, is the point person for ordering, and serves as the gatekeeper for staying within budget." He adds that equipment use is self-policed and any issues are discussed openly in a weekly, brief lab business meeting held 15 minutes prior to the weekly shared research meeting. "This is the forum where problems are brought to everyone's attention and primarily dealt with by the lab members themselves. In these meetings we may focus on a logistical or behavioral problem and its solution although no individual is ever publicly criticized for their actions; we focus on the solution instead, and this has worked very well," he says.

GLOBAL DIFFERENCES

Lab cultures can also be influenced by their geographic location. Labs in the United States are generally different in two major ways to labs elsewhere in the world. The first is that they tend to have more plentiful resources and supplies compared with labs in other countries. This difference may result from differences in funding and also geographic proximity or isolation. In New Zealand, for example, the PIs tend to maintain relationships more actively with overseas labs and develop collaborative projects, according to Dear. "We are more concerned with saving money in New Zealand as well," she says. "We wash and reuse most supplies, whereas my lab in the United States orders disposable supplies," she explains, with the U.S. PI reasoning that he would rather do that than pay his lab members to wash dishes.

The second major difference is that, generally speaking, U.S. labs are much more competitive than labs elsewhere in the world. Hengartner, whose lab is in Zurich, Switzerland, notes that Swiss labs are generally less stressful than U.S. labs—"they are, however, often less dynamic," he says. "I try to bring the best of both cultures together in my lab: 'optimism, blue sky opportunity philosophy, no fear of failure' from the U.S., and 'relaxed atmosphere, willingness to find an appropriate balance between work and family life, joie de vivre' from Europe."

Shobhana Natarajan, who has worked in labs in India and was most recently a postdoc at the Department of Cell Biology, University of Texas, Southwestern Medical Center, in Dallas notes that in general, resources are more limited in India compared with the United States. "On the positive side, this makes us devise new ways to strategize, reuse, recycle, and minimize wastage," she says. "On the negative side, we end up spending more time waiting for resources and planning experiments."

Likewise, **Thomas Kean,** now a senior postdoc at the Benaroya Research Institute at Virginia Mason Hospitals, Seattle, Washington, who has worked in British labs, says that the main difference is that there is more money in the United States, which makes research much easier. There is also better equipment, which is well maintained, and less worry about ordering reagents. However, Fersht points out that in the United Kingdom they seem to have a very enlightened approach. "We are less formal than our other European counterparts, and we put far less pressure on our juniors than they do in the United States," he says. "Many Europeans, especially Germans and Spanish, come to the U.K. and don't want to leave."

Regardless of location, funds, resources, personality, and all the other variables that go into making up a lab culture, however, "In science, if you don't work hard, it is unlikely you are going to be successful," Doetsch says. "Putting in the hours and the ability to overcome setbacks and failures is a great equalizer in research. I tell my students that if they excel in hard work and can 'roll with the punches' they will be successful not only in science but in many other situations in life."

Emma Hitt is a freelance medical and science writer residing in Marietta, Georgia.

DOI: 10.1126/science.opms.r1200114

CREDIT: COURTESY SHOBHANA NATARAJAN

FEATURED PARTICIPANTS

Benaroya Research Institute
www.benaroyaresearch.org

Emory University School of Medicine
www.med.emory.edu

Medical Research Council Laboratory of Molecular Biology
www.mrc-lmb.cam.ac.uk

Penn State University
www.psu.edu

University of Colorado at Boulder
www.colorado.edu

University of Texas Southwestern Medical Center
www.utsouthwestern.edu

University of Toronto
www.utoronto.ca

University of Zurich
www.uzh.ch

UNIVERSITY OF CALIFORNIA
UC RIVERSIDE

Faculty Opportunities

Assistant, Associate or Full Professor Positions in Biomedical Sciences

The Division of Biomedical Sciences within the new School of Medicine at the University of California Riverside is seeking to hire up to four new faculty members at the rank of Assistant, Associate or Full Professor. We are looking for accomplished research scientists in a number of specific areas including **cancer, infectious disease, CNS neurological diseases,** and **cardiovascular and metabolic diseases**. Preference will be given to those individuals examining molecular mechanisms of disease who are committed to a collaborative approach to research, and who are expert in their specific disease model.

The successful candidate will be appointed in the Division of Biomedical Sciences, joining a faculty who have directed a successful M.D. program in collaboration with UCLA, since the late 1970s. The new School of Medicine at UCR will be the sixth University of California Medical School and will serve the rapidly growing and dynamic Inland Southern California region by training a much-needed physician workforce and catalyzing innovations in research, education, and health care delivery that improve the health of medically underserved populations.

Areas of research within the Division include integrative immunology (vaccine development, neuro-immune, endocrine-immune, host- pathogen interactions), glial-neuronal interactions, neurodevelopmental disorders, cancer biology, cardiovascular disease, and diseases of ion transport. Particular strengths on the campus include genetics, epigenetics, genomics/bioinformatics, microRNAs, vector biology, bioengineering and nanotechnology, and synthetic and analytical chemistry.

The Division of Biomedical Sciences sponsors an innovative Ph.D. program that integrates the core medical curriculum with biomedical graduate training and research. The successful candidate will be expected to teach in the medical curriculum and actively participate in the Biomedical Sciences Ph.D. program. As such, preference will be given to candidates who are capable of teaching neuro- and/or general pharmacology, pathology, infectious disease (microbiology/virology), physiology (electrophysiology, renal or respiratory) or genetics.

The University of California, Riverside is situated in an historic citrus growing area surrounded by mountain ranges. Riverside is about an hour away from ski slopes, surfing, or hiking in mountain or desert environments, and housing in the area is very affordable. The campus is also located in a prime position to take advantage of the other universities, research institutes, and biotech industries present in Southern California.

Applicants must hold a Ph.D., M.D., Pharm D., or equivalent degree and qualify for a tenure-track/tenured faculty appointment at the University of California. Applications will be reviewed beginning **February 27, 2012** and the positions will remain open until filled. To apply, please submit the following items:

- Curriculum vitae
- Statement of research accomplishments and goals and teaching expertise
- Names of four individuals who will be asked to provide letters of reference once a short list is developed

Electronic submissions are encouraged. Send the items to: **Violet Vargas, Academic Personnel/HR Analyst, School of Medicine, University of California, Riverside, CA 92521; violet.vargas@ucr.edu**.

UC Riverside is an Equal Opportunity/Affirmative Action Employer.

FACULTY POSITIONS

Institute of Health Sciences

Shanghai Institutes for Biological Sciences of Chinese Academy of Sciences and Shanghai Jiao Tong University School of Medicine

The Institute of Health Sciences (IHS), jointly founded in 1999 by Shanghai Institutes for Biological Sciences (SIBS) of the Chinese Academy of Sciences (CAS) and Shanghai Jiao Tong University School of Medicine (SJTUSM), is devoted to translational biomedical research. Supported by solid basic biomedical research of SIBS and clinical expertise of SJTUSM, IHS strives to accelerate the development of novel therapeutic and diagnostic strategies for critical diseases in China and the world. Currently IHS hosts 28 research groups performing their innovative research in the Basic Research Division, the Clinical Research Division, and the CAS Key Laboratory of Stem Cell Biology.

IHS is seeking outstanding young scholars for multiple professor/PI positions to strengthen its research programs in cancer, immunology, stem cell and biomedical material engineering with strong emphasis on translational research. All positions will be supported by the national "1000 Young Talents Program" or the CAS "100 Talents Program." Applicants must have a Ph.D., M.D./Ph.D., or equivalent graduate degree from reputable educational institutions and have more than 3-5 years of post-doctoral research experience. Special considerations could be offered to individuals with distinguished achievements and expertise.

With a dedicated team of faculty members and administrative staff, IHS has successfully applied for several positions of the "1000 Young Talents Program." In addition to the research fund provided by this prestigious program, IHS also offers competitive packages including salaries, benefits, generous start-up funds, new laboratory space and state-of-art research facility. Successful applicants will have full access to graduate programs both at SIBS and SJTUSM. Scientists at IHS have an outstanding working environment and excellent opportunities to collaborate with colleagues at SIBS, SJTUSM and world-class hospitals in Shanghai.

Interested applicants should forward their curriculum vitae, a statement of research plan and the names of three references to **Ms. Lulu Chen** (**ihs_rs@sibs.ac.cn**). More information of IHS can be found at **http://www.ihs.ac.cn**.

THE GEORGE WASHINGTON UNIVERSITY
WASHINGTON D.C.

Faculty Position in Developmental/Cancer Biology

The Department of Anatomy and Regenerative Biology at The George Washington University School of Medicine and Health Sciences (SMHS) invites applications for a tenure-track or tenured position at the rank of Assistant or Associate Professor. We seek an outstanding candidate with demonstrated significant contributions in the areas of developmental signaling networks and stem cell self-renewal pathways; somatic cell reprogramming which has parallels with malignant transformation; or epithelial-to-mesenchymal transition and tumor-propagating cells.

Basic Qualifications: Applicants must have a Ph.D. and or M.D. degree, a record of top-tier publications, extramural funding and a history of collaborative research.

Current research in the department focuses on normal and malignant aspects of epithelial, hematopoietic and nervous systems; and DNA damage/stress responses in cancer and cancer therapy. The SMHS is centrally located on GW's Foggy Bottom campus; ample opportunities exist to develop new and strengthen ongoing collaborations with cancer researchers in other departments housed within the building; with basic and applied science departments on campus; and with investigators at the NIH, Children's National Medical Center and other universities in the Washington DC metropolitan area.

Competitive salary and start-up funds are available for this position. Faculty rank and salary will be commensurate with experience. **Application Procedure:** Interested applicants must send a complete curriculum vitae, a statement of current and future research interests, and contact information of at least 3 references to **Robert G. Hawley, Ph.D. Professor and Chair, Department of Anatomy and Regenerative Biology, SMHS, The George Washington University** via email to: **anajobs@gwumc.edu**. Review of applications will commence on **March 3, 2012** and continue until the position has been filled.

The George Washington University is an Affirmative Action/Equal Opportunity Employer.

UT COLLEGE OF MEDICINE
THE UNIVERSITY OF TOLEDO

Applications are invited for a tenure-track position at the **Assistant Professor** level in the **Department of Biochemistry and Cancer Biology** at the University of Toledo, College of Medicine (**http://www.utoledo.edu/med/depts/biochem/profiles.html**). Early career scientists working at the cellular, molecular or genetic level on research projects that address cancer development, progression or treatment are encouraged to apply. The University of Toledo College of Medicine is targeting cancer research for strategic emphasis with a competitive start-up package and excellent research facilities available to the successful candidate. Situated on the Health Science Campus, the University of Toledo College of Medicine offers a highly collegial and collaborative academic research environment. Research interests in the department include epigenetics, signal transduction, DNA damage/repair, and the regulation and function of genes involved in cancer cell growth, invasion/metastasis and death. A Ph.D. or M.D. degree, substantial postdoctoral research accomplishments and excellent communication skills are required. The successful candidate will be expected to establish and maintain an active research program with extramural funding and to contribute to the educational missions of the graduate and medical programs.

Applicants must submit (in PDF format) a current CV, a 1-2 page research plan, up to 3 representative publications and arrange for 3 referees to e-mail letters to **BCBFacultySearch@utoledo.edu**.

Review of completed applications will begin immediately with an anticipated start date of August 2012.

The University of Toledo is an Equal Access, Equal Opportunity, Affirmative Action Employer and Educator.

MAYO CLINIC

Faculty Position in Sensory Cilia Biology

Heal the sick, advance the science, share the knowledge.

The Department of Biochemistry and Molecular Biology at Mayo Clinic is searching for a junior-level Ph.D. and/or M.D. scientist with independent NIH funding and an established research program focused on studying sensory cilia in model organisms as they pertain to signal transduction and cystic disease. This candidate is expected to further grow his/her competitive, NIH-funded program through collaborative interactions with NIDDK- and NCI-supported Mayo Centers in gastrointestinal epithelial signaling, cancer and cystic disease. Teaching experience is also required.

Mayo Clinic is a nonprofit organization with over 200 biomedical research laboratories, institutionally supported state-of-the-art animal, molecular, proteomic and microscopy core facilities, a number of unique human disease tissue banks and the opportunities to readily translate discovery to the bedside. Very competitive start-up and sustained intramural funding will be provided.

To apply and learn more about this position, Mayo Clinic and Rochester, MN, please visit **www.mayoclinic.org/scientist-jobs** and reference job posting number **8868BR**. Applications should include a full CV, description of research interests and names/addresses of three references. Specific questions related to the posting should be directed to:

Peter Harris, Ph.D. • Search Committee Chair
Department of Biochemistry and Molecular Biology
Mayo Clinic
200 First Street SW • Rochester, MN 55905
E-mail: harris.peter@mayo.edu

Mayo Foundation is an affirmative action and equal opportunity employer and educator. Post-offer/pre-employment drug screening is required.

WASHINGTON STATE UNIVERSITY

Assistant/Associate/Full Professor of Neuroscience

The Program in Neuroscience at Washington State University, which is housed in the Department of Veterinary and Comparative Anatomy, Pharmacology and Physiology (VCAPP), seeks to fill a tenure-track, full-time, position available in neuroscience at the rank of Assistant/Associate/Full Professor to begin January 2013. This position is a permanent state funded 9-month position with summer funding available for the first two years of appointment. Required: Applicants must have one of the following degrees, a PhD, MD, or DVM degree and at least 2 years post-doctoral research experience. Applicants for associate or full professor positions must provide evidence of an established independent research program (peer-reviewed publications and active external funding). Applicants for an assistant professor position should demonstrate potential to establish an externally-funded program (peer-reviewed publications and developed research agenda).

The successful applicant will be expected to develop and maintain an extramurally funded research program in cellular and molecular neurobiology. The ideal candidate should have a research focus that complements one or more of the following current departmental research interests in drug addiction, feeding and energy homeostasis, sleep and circadian rhythms, synaptic plasticity, neurodegenerative disease, and affective neuroscience. The ideal applicant should also demonstrate a commitment to biomedical education with preference given to those with a demonstrated ability to teach neuroscience. Duties will include classroom instruction of neuroscience graduate or undergraduate students. The ability to support and mentor graduate students and serve on student, departmental, and college committees is required. Salary and rank are dependent upon qualifications. A generous start-up package is available. Laboratory space will be assigned in a newly-built (completion 2012) state-of-the-art research building specifically designed for neuroscience-based research.

Washington State University has a vibrant neuroscience community and is located in a region having a high quality of life for those who enjoy the outdoors, the arts, and collegiality of neighbors. Screening of applications will begin **March 16, 2012**. The application must include a cover letter which states what rank is being applied for, curriculum vitae, description of teaching experience and philosophy, summary of research interests and goals, and names and contact information (including email addresses) for three references. Applications with above attachments accepted at **www.wsujobs.com/applicants/Central?quickFind=56758**. No paper submissions accepted. Direct inquiries by email to **kinslow@vetmed.wsu.edu**. *EEO/AA*

TRANSLATIONAL BIOMEDICAL RESEARCH OPPORTUNITY

Genomic Medicine/Bioinformatics

Sigfried and Janet Weis Center for Research is seeking outstanding independent scientists for full-time research positions at ranks equivalent to Assistant, Associate or Full Professor in the areas of Genomics and Bioinformatics. The Weis Center is a basic and translational research facility of Geisinger Clinic located at Geisinger Medical Center (GMC) in Danville, PA. **Genomic Medicine** is a strategic focus for translational research at Geisinger.

Genomic Medicine is a strategic focus for translational research at Geisinger.

About the position:

- Expertise in laboratory, computational, or statistical genetic approaches
- Expand ongoing research on the genetic basis of disease
- Proven records of innovative research with relevance to human disease
- Collegial environment with collaborative research opportunities

Geisinger Health System's advanced electronic medical record system and health information technology infrastructure allows for electronic capture of clinical data and large biorepository of patient specimens.

Technical resources include instrumentation for confocal, TIRF, and single cell fluorescence imaging, microarray analysis, genotyping, DNA sequencing, and flow cytometry, and an AAALAC-accredited animal facility. Substantial resources are available for start-up, ongoing research support and salary.

Qualified individuals should submit curriculum vitae, statement of research interests and three reference letters to Ms. Kristin Gaul, Weis Center for Research, Geisinger Clinic, via email (kgaul@geisinger.edu). Please refer to position WCR-3638 in the subject line. Applications will be accepted until the positions are filled.

For more information on research programs at Geisinger visit our website at http://www.geisinger.org/professionals/research/wcr.

Geisinger Health System is an Affirmative Action/Equal Opportunity Employer

GEISINGER
HEALTH SYSTEM

REDEFINING THE BOUNDARIES OF MEDICINE

www.mssm.edu

MSSM
MOUNT SINAI SCHOOL OF MEDICINE

INVESTIGATORS/ FACULTY POSITIONS

Metabolism Institute

The Mount Sinai School of Medicine (MSSM) is recruiting exceptional investigators and leading researchers to join its growing Metabolism Institute at the Assistant, Associate, and Full Professor levels. The Mount Sinai Metabolism Institute is one of 14 research Institutes that are rapidly expanding and conducting cutting-edge multi-disciplinary basic and translational research. We invite outstanding researchers to use this opportunity and join the institution's tradition of excellence in basic and translational research in Diabetes and Metabolism. The new recruits will be provided modern and well-equipped prime research space and significant institutional resources.

The Mount Sinai School of Medicine is one of the top research medical schools in the country and is ranked #3 in the nation in NIH funding per investigator. Mount Sinai is currently implementing a $2.25 billion Strategic Plan to enhance its educational, research, and clinical programs. It is known for its outstanding faculty and its innovation, and achievements in research, patient care, and education. The new recruits to the Metabolism Institute are expected to actively collaborate with and utilize the resources of the other MSSM institutes, such as the Institute for Translational Sciences, Cardiovascular Research Institute, Institute for Genomics and Multiscale Biology, and the Experimental Therapeutics Institute, among others.

The prospective candidates should have an outstanding track record of research achievements and strong independent funding. For consideration, please send your CV to: **Ms. Symone Rivera: Symone.Rivera@mssm.edu**

The Mount Sinai Medical Center is an equal opportunity/affirmative action employer. We recognize the power and importance of a diverse employee population and strongly encourage applicants with various experiences and backgrounds.

Mount Sinai Medical Center – An EEO/AA-D/V Employer.

NYU Langone
MEDICAL CENTER

Faculty Position

- Leon H. Charney Division of Cardiology -

http://medicine.med.nyu.edu/cardiology/

- Kimmel Center for Stem Cell Biology -

www.kimmelstem.med.nyu.edu

The Leon H. Charney Division of Cardiology and the Helen L. and Martin S. Kimmel Center for Stem Cell Biology at NYU Langone Medical Center invite applications for tenure-track positions at the assistant, associate or full professor level for a leadership position in a new program in Cardiovascular Regenerative Medicine. We seek applicants with an exceptional record of achievement to facilitate the translation of stem cell discovery related to cardiovascular disease - building on fundamental laboratory investigations to clinical evaluation and application. The Leon H. Charney Division of Cardiology and the Kimmel Center for Stem Cell Biology are highly interdisciplinary, and combine research strengths and clinical trial expertise at the NYU Langone Medical Center and the College of Arts and Sciences.

The NYU Langone Medical Center offers excellent resources to support new faculty, including generous start-up packages and core facilities for siRNA screening, cell sorting, imaging, proteomics, mouse molecular genetics, genomics and structural biology. Successful candidates are expected to maintain vigorous independent research programs that will enrich and be enriched by the highly collaborative environment throughout the NYU research community.

This is an electronic application process only. Please create your application packet by formatting it as a single PDF document. Use the following page order: 1) Cover Letter; 2) Curriculum Vitae; 3) Research Statement, highlighting the most significant research accomplishments and the relevant publications. Email the application packet to **stemcellsearch@med.nyu.edu** by March 31, 2012. Three letters of reference should be sent independently to the same email address. NYU Langone Medical Center was founded in 1841 and is an equal opportunity affirmative action employer. Women and minority candidates are encouraged to apply.

MAYO CLINIC

Researchers in Translational Ophthalmology

Heal the sick, advance the science, share the knowledge.

The Department of Ophthalmology at Mayo Clinic in Rochester is expanding its research division and is seeking scientists and clinicians with established translational programs focused in corneal disease, macular or retinal disease, or glaucoma. The successful applicants must demonstrate a track record of extramural funding, and be willing to collaborate with clinicians and scientists in different subspecialties of ophthalmology. Positions are equivalent to endowed professorships and include a competitive start-up package, and ongoing operating support. Credentials of successful applicants will include an MD or PhD (or equivalent) degree, national/international recognition in the field and a track record of NIH or equivalent peer-reviewed grant funding.

Recognized by *U.S. News and World Report* as one of America's Best Hospitals, Mayo Clinic is an excellent choice for the candidate who is seeking a career with a premier academic medical center, world-renowned for achievements and innovation. Mayo Clinic is a nonprofit organization with approximately 3,800 physicians and scientists across all locations, working in a collaborative environment focused on integrated patient care, research and education.

To apply and learn more about this position, Mayo Clinic and Rochester, MN, please visit **www.mayoclinic.org/scientist-jobs/** and reference job posting number **8120BR**. Applications should include a letter of intent (addressed to Jay Erie, MD, Chair of Ophthalmology) and curriculum vitae and bibliography. Specific questions related to the posting should be directed to:

Jay C. Erie, MD
Chair and Professor of Ophthalmology
Mayo Clinic
200 First Street SW • Rochester, MN 55905
c/o schilbe.jennifer@mayo.edu

Mayo Foundation is an affirmative action and equal opportunity employer and educator. Post-offer/pre-employment drug screening is required.

UC DAVIS

Assistant Professor of Animal Population/ Quantitative Genomicist/Geneticist

The University of California at Davis is pleased to announce recruitment for a tenure-track faculty position in Population/Quantitative Genomicist/ Geneticist. The successful candidate will join the Department of Animal Science in the College of Agricultural and Environmental Sciences at the rank of Assistant Professor. Criteria for appointment include: a Ph.D. or equivalent, a strong interest in Population or Quantitative Genetics of domestic, feral, or wild animals relevant to animal agriculture, a record of excellence in scholarly research, and demonstrable potential to establish a competitively-funded research program relevant to animal genetics, animal breeding, or population genetics of wild animals impacting the production environment. The appointee will be responsible for teaching undergraduate courses including quantitative and population genetics of domestic animals, be actively involved in undergraduate advising, curricular development and department and university service. The appointee is also expected to guide and mentor graduate students and participate in research and outreach programs consistent with the mission of the CA Agricultural Experiment Station.

Applicants should submit materials via the following website: **https://secure.caes.ucdavis.edu/Recruitment/**. Additional inquiries can be directed to **Professor J.D. Murray (530) 752-3179, jdmurray@ucdavis.edu**. The position will remain open until filled but to ensure consideration, applications should be received by **April 1, 2012**.

UC Davis is an Affirmative Action/Equal Employment Opportunity Employer and is dedicated to recruiting a diverse faculty community. We welcome all qualified applicants to apply, including women, minorities, veterans, and individuals with disabilities.

UC DAVIS

Assistant Professor in Animal Epigenetics and Stress Physiology

The University of California at Davis is pleased to announce recruitment for a tenure-track faculty position in Animal Epigentics and Stress Physiology. The successful candidate will join the Department of Animal Science in the College of Agricultural and Environmental Sciences at the rank of Assistant Professor. Criteria for appointment include: a Ph.D. or equivalent, a strong interest in improving sustainable animal production by understanding how environmental, nutritional, hormonal, and behavioral stressors interact with gene expression, a record of excellence in scholarly research, and demonstrable potential to establish a competitively-funded research program relevant to animal stress in sustainable animal agriculture. The appointee will be responsible for teaching an undergraduate course incorporating stress physiology and additional contributions to the departmental curriculum, be actively involved in undergraduate advising, curricular development and department and university service. The appointee is also expected to guide and mentor graduate students and participate in the outreach programs of the department and college.

Applicants should submit materials via the following website: **https://secure.caes.ucdavis.edu/Recruitment/**. Additional inquiries can be directed to **Professor Trish Berger, (530) 752-1267, tberger@ucdavis.edu**. The position will remain open until filled but to ensure consideration, applications should be received by **April 30, 2012**.

UC Davis is an Affirmative Action/Equal Employment Opportunity Employer and is dedicated to recruiting a diverse faculty community. We welcome all qualified applicants to apply, including women, minorities, veterans, and individuals with disabilities.

THE UNIVERSITY OF TEXAS
MD Anderson Cancer Center
Making Cancer History®

Assistant Professor Breast Medical Oncology

John Randall
The University of Texas
MD Anderson Cancer Center
1155 Hermann Pressler, Unit 1354
Houston, TX 77030-4009

The University of Texas MD Anderson Cancer Center, Department of Breast Medical Oncology in Houston, Texas, is recruiting a tenure-track scientist or physician-scientist at the Assistant Professor level to expand and strengthen the translational research capabilities of the department. Research should focus on translating fundamental discoveries made in the laboratory into highly innovative clinical trials. We are especially interested in individuals whose research focuses on breast cancer-relevant growth factor signaling pathways and in developing peptides/small molecules that target this pathway into clinical strategies for patients with various molecular subsets of breast cancer. The department is dedicated to excellence in patient care and education related to breast cancer and the training of graduate students, postdoctoral fellows and clinical fellows in cancer biology and prevention and treatment of breast cancer. The department has had a successful Breast Cancer SPORE grant from the National Cancer Institute, NIH career development awards and major grants from the DOD and multiple foundations.

The successful candidate will also have a background that demonstrates her/his ability to work synergistically with both laboratory based and clinical faculty and be able to translate preclinical findings into clinical trials and biomarker development. A Ph.D. and/or M.D. with a proven track record of sustained external peer-reviewed funding and high quality publications in topics related to breast cancer biology is required. The position includes a competitive salary and a startup package commensurate with previous experience.

Please forward letter of application, indicating position of interest and curriculum vitae along with 3–5 references and a research plan to: JMRandall@mdanderson.org

MD Anderson Cancer Center is an equal opportunity employer and does not discriminate on the basis of race, color, national origin, gender, sexual orientation, age, religion, disability or veteran status except where such distinction is required by law. All positions at The University of Texas MD Anderson Cancer Center are security sensitive and subject to examination of criminal history record information. Smoke-free and drug-free facility.

AMITY UNIVERSITY

India's No. 1 Ranked non-profit Pvt. University

FACULTY POSITIONS

Amity University is part of India's leading global education group with 95,000 brilliant students, over 240 Graduate & Post Graduate degrees and 3,500 faculty comprising distinguished researchers, scientists and industry professionals.

Amity University and its institutions in Biotechnology, Engineering & Telecom have been ranked amongst the top-10 in India by leading surveys on myriad parameters like infrastructure, academic excellence & research.

Focus on Research:

The faculty and scientists at Amity have filed the highest number of patents in the last year, more than any other University in India and are carrying out over 250 Govt. funded research projects. Further, Amity is recognised as a Scientific & Industrial Research Organisation (SIRO) by Govt. of India and has research collaboration with over 80 leading global universities, besides the largest number of Fellowships for Ph.D. and Post Doctoral Research in India.

For its University campus in India and Dubai, Amity invites applications from candidates who enjoy working in a dynamic, growth-oriented environment and with a strong teaching/ research portfolio.

Positions exist in the following disciplines:

Aerospace I Agriculture I Applied Sciences I Biotechnology I Engineering I Environment I Food Tech. I Forensic Sciences I Green Technology I Herbal Research & Studies I Horticulture I Marine Sc. I Medical & Allied Sc. I Microbial Sc. I Nanotechnology I Nuclear Science & Tech. I Pharmacy I Physiotherapy I Post Harvest Tech. & Cold Chain Management I Space Sciences I Telecom I Virology & Immunology. (For complete programme list, visit www.amity.edu)

Faculty interested in teaching at Amity campuses, may e-mail their curriculum vitae to globalfaculty@amity.edu (mentioning the name of the campus they wish to apply to).

BCM
Baylor College of Medicine

Department of Molecular Virology and Microbiology

The Alkek Center for Metagenomics and Microbiome Research (CMMR) and the Department of Molecular Virology and Microbiology at Baylor College of Medicine seek to fill a tenure track faculty position at the **ASSISTANT PROFESSOR** level. We are seeking investigators with promising track records who are emphasizing Microbiome Research in humans and/or model systems in their scientific programs. While specific research interests may vary, preferred candidates will study programs in host-microbe interactions, mucosal immunology, cell signaling, systems biology, metabolomics and related topics.

At Baylor College of Medicine (BCM), you will find a unique collaborative spirit, a dedication to excellence in patient care and an environment that surpasses its reputation as a research powerhouse and educational giant. BCM is located in the heart of the Texas Medical Center (TMC), the largest incorporated medical center in the world with more than 42 member institutions in 100 buildings. The CMMR is building a highly collaborative environment where exciting advances in our understanding of how microbes impact human health and disease will result from synergistic interactions between collaborating faculty, clinicians, centers and institutions. This position features a competitive start-up package and laboratory/office space and will leverage the facilities and resources located in the CMMR and at BCM/TMC, including the Baylor College of Medicine Human Genome Sequencing Center, one of the three NHGRI-funded Large Scale Sequencing Centers with production scale platforms for the latest generation sequencing technologies.

Successful candidates will synergize with our strengths in metagenomics research to delve into the mechanisms by which microbes impact human health. They will maintain an outstanding research program that focuses on solving core problems in this area, and have a commitment to excellence in teaching. Required qualifications include a Ph.D. and a recognized reputation for innovative scholarship, a distinguished track record for research support and publications, leadership experience of students and trainees, and continued faculty development.

Applicants should submit a cover letter, a curriculum vitae including a publication list, a statement of research accomplishments and future research plans, a description of teaching experience and philosophy, and the names and addresses of three potential referees to the address or email below by **March 23, 2012**. **Search Committee, Alkek Center for Metagenomics and Microbiome Research, Baylor College of Medicine, One Baylor Plaza BCM MS385, Houston, Texas 77030; Telephone: 713-798-5867; email: bcm-mvm-facultypos1@bcm.edu**.

Baylor College of Medicine is an Equal Opportunity, Affirmative Action and Equal Access Employer.

CMMr

Perelman School of Medicine
University of Pennsylvania

DIRECTOR OF THE CENTER FOR ORPHAN DISEASE RESEARCH AND THERAPY

The Perelman School of Medicine at the University of Pennsylvania invites applications and nominations for the position of Inaugural Director of the Center for Orphan Disease Research and Therapy. The primary mission of the Center is to expedite the translational science and development of novel therapies for rare and orphan diseases. The Center will achieve this through the promotion of innovative translational research platforms and therapeutic strategies, building on partnerships among investigators, academic institutions, patients and advocacy groups, industry and funding agencies.

The Center provides a truly exciting, one-of-a-kind effort to advance therapies and cures for rare and orphan diseases. The specific Center goals are:

- To unravel the causes and pathophysiology of rare and orphan diseases.
- To unite investigators and clinicians at both Penn and other institutions who are committed to treating and curing rare disorders.
- To extend approaches developed for treatment of one rare disorder to multiple others by enabling technologically advanced basic and clinical research services and platforms.
- To link academicians with both public and private foundations that support biomedical research on rare disorders.
- To provide a facile means for biotech and pharmaceutical companies to engage with academic institutions in rare disease research and therapeutic development.
- To establish a patient-centric advocacy platform, guiding clinical access and empowering donors and foundations to participate in research advances.
- To facilitate communication between academicians and public health authorities who seek to improve the detection and management of orphan diseases.
- To promote funding of orphan disease research from NIH and other federal agencies and to facilitate access of academic investigators to such support.

The Director will report to the Dean of the Perelman School of Medicine. An endowment will be available to provide support for the Director and the Center. Applicants for the position of Director must hold an MD or PhD degree and must be tenure-eligible for faculty appointment as Professor in the standing faculty at the University of Pennsylvania. The faculty appointment will be in an appropriate department in the Perelman School of Medicine. The successful candidate will possess a distinguished research record, strong communication and leadership skills, experience in both clinical and corporate sponsored research, and a strong commitment to advancing orphan disease research and care both as an advocate and consensus builder. Other valuable qualities include demonstrated administrative skills that can promote integration and collaboration across clinical and research domains and that bridge multiple disciplines, schools and universities, visionary thinking and entrepreneurial spirit, and sound financial acumen to build on a foundation of excellence within an interdisciplinary environment.

All interested applicants are invited to send their curriculum vitae and letter of interest to:

Arthur H. Rubenstein, MBBCh, Search Committee Chair, c/o Margaret M. Lizotte,
University of Pennsylvania School of Medicine,
290 John Morgan Building, 3620 Hamilton Walk, Philadelphia, PA 19104-6055

The University of Pennsylvania is an equal opportunity affirmative action employer, and women and minorities are strongly encouraged to apply.

School of Medicine
Temple University

FACULTY POSITIONS
Translational Medical Research

Temple University School of Medicine has recently established a Center for Translational Medicine. We are seeking outstanding scientists for tenure-track faculty positions. Candidates with current funding are preferred but scientists with an excellent track record coming out of a post-doc will be considered. We seek scientists with a research focus in inflammation, stem cell biology, and proteomics. These positions will complement ongoing basic and clinical research programs in the Departments of Pharmacology and Medicine. The Center occupies space on the recently completed 9th floor (over 25,000 sq ft) of the Medical Education and Research Building. Interested candidates should have an MD, PhD or MD/PhD degree, and a strong academic record. Academic appointment is available at all levels with competitive packages.

Please send letters of interest and CV's to:

Walter J. Koch, PhD, Director
Center for Translational Medicine
c/o Nora Baglivo
Temple University School of Medicine
3500 N Broad Street, MERB 941
Philadelphia PA 19140
Email: nora.baglivo@temple.edu

Temple University is an Affirmative Action/ Equal Opportunity Employer and strongly encourages applications from women and minorities.

BENAROYA RESEARCH INSTITUTE
VIRGINIA MASON

FACULTY RECRUITMENT
TRANSLATIONAL RESEARCH

The **Benaroya Research Institute**, in Seattle WA, is recruiting an Assistant/ Associate Member with an MD, PhD, or MD/PhD degree whose research focuses on biomedical translational research. Close collegial interactions with Institute investigators in autoimmune and immune-mediated diseases, as well as interactions with clinical research and clinical trials programs, offer an environment for innovative interdisciplinary research with a human disease focus. Successful candidates will be considered for academic affiliation with the University of Washington School of Medicine.

For an overview of programs see **http://www.benaroyaresearch .org**. Applicants should send a cv, brief statement of research interests, and names of 3 references, prior to **March 1, 2012** to: **jobs@benaroyaresearch .org, Attn: BRI Faculty Search Committee, #12-06**.

EEO/MF

UNIVERSITY OF CALIFORNIA
UCRIVERSIDE

ASSISTANT PROFESSOR OF PLANT PATHOLOGY
Microbial Invasive Species

The Department of Plant Pathology and Microbiology invites applications for a 9-month tenure-track faculty position (research and teaching in the Agricultural Experiment Station), emphasizing the invasion and impacts of microbial (such as bacteria, fungi, viruses) pathogen or symbiont species into agricultural or wildland ecosystems. Applicants studying microbes that regulate invasive plants will also be considered. Approaches could include genetics, genomics, population ecology/evolution, biochemical, bioinformatics, ecoinformatics and/or modeling. The successful candidate will join a vibrant community of researchers studying microbe-host and microbe-environment interactions, have opportunities to collaborate with researchers in UC's Division of Agriculture and Natural Resources, the Center for Conservation Biology, the Center for Invasive Species Research, the Institute for Integrative Genome Biology, and have access to modern campus facilities in genomics, proteomics, microscopy, ecological sensing technologies and field stations and facilities. Consult **www.plantpath.ucr.edu** for details about the department. Applicants will be expected to pursue vigorous, extramurally-funded research and contribute to undergraduate and graduate teaching in Programs in Microbiology, Plant Pathology, or Genetics, Genomics and Bioinformatics. A Ph.D. and demonstrated excellence in research are required.

E-mail curriculum vitae, statements of research and teaching interests, selected reprints, and three letters of reference to: **Dr. James Borneman, c/o Tiffany Lindsey, Department of Plant Pathology and Microbiology, University of California, Riverside, California 92521-0415; e-mail: PLPAJobs@ucr.edu**. Evaluation of applications will begin **February 17, 2012**, but the position will remain open until filled. Position will be available July 1, 2012.

The University of California is an Affirmative Action/Equal Opportunity Employer.

UCRIVERSIDE
Department of Entomology
College of Agricultural and Natural Sciences

Assistant Professor and Assistant Entomologist in the area of Invasive Species Ecology, University of California, Riverside. Position available July 1, 2012, 9-month appointment, 50% Instruction and Research / 50% Organized Research. Appointment level and salary commensurate with experience. Ph.D. in Entomology, Biology, Ecology or a related discipline is required. The successful candidate must demonstrate evidence of strong training and experience with the biological processes, species attributes and ecological conditions that promote the establishment and potential spread of invasive and/or introduced terrestrial arthropod species. Areas of research emphasis could include the study of invasion processes; the evolution and genetics of invasiveness; the role of habitat quality and diversity on the establishment of invasive and introduced species; the dispersal and spread of these species; and the interactions of such species with established potential hosts, competitors and natural enemies. Hypothesis-driven research that includes theoretical issues relating to propagule size and establishment frequencies; climatic matching; genetic adaptations; and population genetics, dynamics and regulation would also be considered. Applied research consistent with the mission of the Agricultural Experiment Station directed toward managing invasive and introduced (insect or weed) species is expected. Teaching responsibilities include supervision of graduate students, participation in undergraduate instruction in entomology, ecology, and evolution, as well as a graduate course taught in an area of interest. Interactions with the other research groups in interdepartmental programs are encouraged. Participation in the Center for Invasive Species Research and the Center for Conservation Biology and the Institute for Genome Biology is encouraged. Send curriculum vitae, transcripts, statement of research interests, reprints, manuscripts in press, and have four letters of recommendation sent to: **Dr. Richard Stouthamer, Invasive Species Ecologist Search Committee Chair, Department of Entomology, University of California, Riverside, CA 92521; e-mail: Richard.Stouthamer@ucr.edu; phone: 951-827-2422; FAX (951)-827-3086**. Review of applications will begin **March 1, 2012**, but this position will remain open until filled. Information about the Entomology Department and an expanded description can be found on the website: **http://www.entomology.ucr.edu**.

The University of California is an Affirmative Action / Equal Opportunity Employer committed to excellence through diversity, and strongly encourages applications from all qualified applicants, including women and minorities.

Cincinnati Children's

Cincinnati Children's Research Foundation
Division Director of Immunology

Cincinnati Children's Research Foundation (CCRF) of the Cincinnati Children's Hospital Medical Center is currently conducting a search for a Director to lead the combined divisions of Immunobiology and Molecular Immunology. The candidate will lead the development and the scholarly, educational and institutional activities for the new division.

The Director will hold an academic appointment at the University of Cincinnati School of Medicine. The ideal candidate will possess a PhD, MD, or both and a distinguished national and international reputation for research excellence. The candidate should be a recognized leader in the field of immunology and have a demonstrated background of administrative leadership to include; mentoring faculty, pursuit of external funding and leadership in graduate and post graduate training.

CCRF is one of the largest pediatric research programs in the nation ranking 2nd among all pediatric institutions in funding from the National Institutes of Health and 6th among all American hospitals. Cooperation and collaboration transcends all aspects of the institution allowing us to excel in our education, research and clinical care missions.

Interested candidates should send letter of interest along with CV to:
John B. Harley, MD, PhD
Chair, Search Committee
Email: immunologyjobs@cchmc.org

Affirmative Action/Equal Opportunity Institution.
Applications from minority and women candidates are encouraged.



Open Rank Faculty Position
Department of Vision Sciences

The Department of Vision Sciences at the University of Alabama at Birmingham (UAB) invites applications for a full-time faculty position. Scientists with an excellent record of peer-reviewed publications and a currently funded research program are encouraged to apply. The rank and tenure status will be commensurate with the candidate's experience.

UAB is one of America's premier research universities, ranking among the top 25 in funding from the National Institutes of Health. Vision research is especially strong at UAB with 55 faculty from eleven departments constituting the Vision Science Research Center, a university-wide interdisciplinary research center. Research areas include retinal biology/disease, myopia, cataract, glaucoma, anterior segment, ocular genetics, and visual and oculomotor systems neuroscience. However, qualified investigators from all areas of the Vision Sciences are encouraged to apply. The successful candidate will have access to fully-staffed core resources which include electronics, computer, machine shop; histology and molecular biology; transgenic; hybridoma; sequencing; confocal, EM, FRET, and multiphoton microscopy; small animal OCT and ERG. MRI facilities include two 3T human systems, a 9.4T small animal system, and a vertical 4.7T system dedicated to non-human primate research. Vision Sciences faculty actively participate in graduate programs including Vision Science, Graduate Biomedical Sciences, Behavioral Neuroscience and Biomedical Engineering.

Applicants should send their *curriculum vitae* including the names of at least three references, and a statement of research interests to: Dr. Paul D. R. Gamlin, Department of Vision Sciences, The University of Alabama at Birmingham, 924 South 18th Street, Birmingham, AL 35294-4390.

Applications should be received by May 31st to ensure full consideration.

The University of Alabama at Birmingham is an equal opportunity, affirmative action employer with a strong commitment to ethnic and cultural diversity among its faculty, staff, and students. Applications from women, minorities, individuals with disabilities and veterans are encouraged.

University of Colorado Boulder

FACULTY POSITION IN THE LINDA CRNIC INSTITUTE FOR DOWN SYNDROME

The Linda Crnic Institute for Down Syndrome invites applications for a tenure-track **faculty position at any level** in an area of molecular biology, genetics, genomics, cell biology, neuroscience, psychology or physiology research likely to contribute to an understanding of the causes of, and treatments for, the medical and cognitive ill effects associated with Down Syndrome. Applicants must have a Ph.D., M.D., or equivalent; and postdoctoral research experience. The candidate is expected to develop a vigorous and innovative research program, and have enthusiasm for teaching. The successful candidate will also be a member of one of the departments appropriate to his/her area of research, Molecular, Cellular and Developmental Biology, Chemistry and Biochemistry, Psychology and Neuroscience or Integrative Physiology, and could also be a member of the Institute for Behavioral Genetics or the Biofrontiers Institute.

About the Linda Crnic Institute for Down Syndrome

The *Linda Crnic Institute for Down Syndrome* is the first medical and research institute with the mission to provide the best clinical care to people with Down syndrome, and to eradicate the medical and cognitive ill effects associated with the condition. Established in 2008, the Crnic Institute is a partnership between the *University of Colorado School of Medicine*, the *University of Colorado Boulder*, and *Children's Hospital Colorado*. Headquartered on the Anschutz Medical Campus, the Crnic Institute includes the Anna and John J. Sie Center for Down Syndrome at the Children's Hospital Colorado. It partners both locally and globally to provide life-changing research and medical care for individuals with Down syndrome. The Crnic Institute is made possible by the generous support of the Anna and John J. Sie Foundation, and relies on the Global Down Syndrome Foundation for fundraising, education, awareness, and government advocacy. It is a research and medical-based organization without political or religious affiliation or intention.

Review of applications will begin on **15 February 2012** and continue until the position is filled. Application materials are accepted electronically at **https://www.jobsatcu.com**, posting number **816026**, and should include curriculum vitae and concise statements of research and teaching interests. Applicants must also provide the names and e-mail addresses of three professional references, who will be asked to submit their letters electronically.

For questions or concerns on submitting your materials electronically, please contact **mcdbsrch@Colorado.EDU**.

The University of Colorado is an Equal Opportunity Employer.

See www.colorado.edu/ArtsSciences/Jobs/ for full job description.

Bureau International des Poids et Mesures
Job vacancy for the post of Director of the Ionizing Radiation Department

The BIPM is an intergovernmental scientific organization whose mandate is to provide the basis for a coherent system of measurements throughout the world, traceable to the International System of Units (SI). Further information about the BIPM can be found on the website: **www.bipm.org**. The Ionizing Radiation Department provides traceability to the SI for all of the BIPM's Member States, either directly or indirectly, for radionuclide activity measurements and x-ray and gamma-ray dosimetry.

Duties: Reporting directly to the BIPM Director, the Director of the Ionizing Radiation Department will undertake scientific and administrative duties including: Direct and supervise the scientific work and the development of the approved Programme of Work and budget; Participate in the scientific work of the Department, demonstrating active leadership and continuing professional development; Maintain the Department's measurement services in accordance with the requirements of the BIPM's quality management system; Promote metrology, particularly ionizing radiation metrology, including BIPM representational roles to the National Metrology Institutes (NMIs), regional metrology organizations (RMOs), intergovernmental organizations and international bodies with similar objectives to the BIPM; Provide the Executive Secretary role and liaise closely with the President of the Consultative Committee for Ionizing Radiation (CCRI) that meets annually with biennial meetings of its three Sections; Maintain and personally encourage a culture of safe working in accordance with BIPM Health and Safety rules; Manage personnel-related issues in the Department; Participate in the management of the Department's finances and infrastructure through effective budgeting and expenditure control.

Employment conditions: The BIPM offers a full-time permanent appointment with an initial probationary period of 6 months. Salary and conditions of employment are in accordance with the *Regulations, Rules and Instructions applicable to staff members of the BIPM*. The BIPM operates its own contributory pension scheme and subscribes to a private medical insurance plan for its staff and their families.

Qualifications and experience: The successful candidate will be expected to have: a PhD or equivalent qualification; at least 10 years of relevant work experience, experience in an intergovernmental organization would be an asset; specific knowledge of ionizing radiation metrology and general knowledge of the physical sciences; an international scientific reputation attained through relevant publications and committee membership; significant management experience, leadership and diplomatic skills; a PCR or RPA certificate or equivalent experience; fluency in spoken and written English and the ability to communicate in French (following lessons if necessary); the ability to work in a multicultural environment and to maintain good working relations inside and outside the organization.

Applications: Applications should be sent to the **BIPM Director, Dr Michael Kühne, BIPM, Pavillon de Breteuil, F-92312 Sèvres Cedex, France, by 29 February 2012** at the latest with a copy by e-mail to **ldelloro@bipm.org**, including a covering letter, a *curriculum vitae* and a list of publications. Applications should include the names of three referees. Only shortlisted applicants will be invited for interview. Prospective candidates are encouraged to make preliminary contact, in confidence, with either the **Director of the BIPM**, **(mkuehne@bipm.org)** or the **Director of the Ionizing Radiation Department, Dr Allisy-Roberts (allisy-roberts@bipm.org)**.

The BIPM is an Equal Opportunity Employer.

National Jewish Health®
Science Transforming Life®

DIRECTOR OF MYCOBACTERIAL LABORATORY

National Jewish Health attracts thousands of patients each year who team with our expert physicians and renowned experts because *We Never Say Never*. National Jewish Health is one of the world's most highly respected institutions for education, research, and treatment for respiratory, allergic, and immune disorders. National Jewish Health has been ranked the #1 Respiratory Hospital in the U.S. by *U.S. News & World Report* for the past 14 consecutive years.

After a distinguished academic and clinical career Professor Leonid Heifets MD, PhD, DSc has elected to retire from his operational responsibilities within the Advanced Diagnostic Laboratory. The Department of Medicine at National Jewish Health is therefore seeking a dynamic Scientist to head the Mycobacterial Reference Lab. The ideal candidate will have demonstrated excellence in leadership, program development, as well as a strong and successful research track record in Tuberculosis and Non-Tuberculous Mycobacteria (NTM). In addition, the Laboratory Director will be responsible for providing scientific and clinical support to customers (Local, National and International in both commercial, & NGO arenas). Candidates should have at least 7 years of relevant clinical experience in mycobacterial disease research and clinical testing and be eligible to hold an academic rank of Professor or Associate Professor.

Interested applicants should send a CV and cover letter to Andrew Cunningham PhD, Executive Director, ADx Laboratories National Jewish Health, Denver CO 80206. Email care of Jessica Tidball **tidballj@NJHealth.org** or by fax (confidential) **+1-303-398-1669**.



National Jewish Health is an Affirmative Action/Equal Opportunity Employer, and we are committed to hiring a diverse and talented workforce. EOE/AA/M/F/Disabled/Vet/Tobacco Free Campus.

Department of Health and Human Services
National Institutes of Health
National Cancer Institute

Tenure-Track/Tenure-eligible Principal Investigators
Laboratory of Biochemistry and Molecular Biology

The Center of Cancer Research (CCR), National Cancer Institute (NCI), National Institutes of Health (NIH), Department of Health and Human Services (DHHS), is accepting applications for two positions as Principal Investigators in the Laboratory of Biochemistry and Molecular Biology (LBMB) at the Tenure-Track or Tenure-eligible levels. LBMB is a focus of basic research excellence in chromosome and chromatin biology, an area of central importance to cancer biology and the mission of CCR, NCI. LBMB provides a highly interactive environment for scientists and promotes synergistic interactions with intramural and extramural laboratories to promote interdisciplinary research to solve problems of fundamental importance.

We are seeking candidates whose research programs address basic biological problems and who have demonstrated excellence, originality, and productivity in research in the areas of biochemistry, cellular, molecular, and/or developmental biology. We are especially interested in applicants using innovative approaches to topics in the broad areas of chromosome and/or genome function. LBMB research programs are integrated into the NCI Center of Excellence in Chromosome Biology (**https://ccrod.cancer.gov/confluence/display/CECB/Home**), and the excellent research environment at the Bethesda campus of the NIH affords ample opportunities for intellectual interactions and collaborations with basic and clinical scientists. Research activities within LBMB are supported by core facilities including Functional Genomics, Proteomics, Imaging, and Flow Cytometry cores. The successful candidate will perform independent research funded by the NCI Intramural Research Program.

Candidates must have a Ph.D. and/or M.D. degree with a proven ability to conduct innovative research. Salary is commensurate with research experience and accomplishments. To apply, submit a cover letter, curriculum vitae including publication list, statement of research accomplishments and future plans, and three letters of recommendation to **NCILBMBsearch@mail.nih.gov** or **Dr. Shiv Grewal, Chief LBMB, 9000 Rockville Pike, National Institutes of Health, Building 37, Room 6106C, Bethesda, MD 20892**. Electronic submissions are encouraged. This position is not restricted to U.S. citizens only. Review of applications will start on **March 20, 2012** and continue until the positions are filled.

HHS, NIH, and NCI are Equal Opportunity Employers.



TENURE TRACK (CLINICAL) POSITION

Department of Health and Human Services
National Institutes of Health
National Institute on Aging
Intramural Research Program

The Laboratory of Behavioral Neuroscience (LBN) of the National Institute on Aging (NIA) is recruiting a scientist for a Clinical Tenure Track position within its Intramural Research Program (IRP) in Baltimore, MD. This position is 100% research, includes an attractive setup package and operating budget, including access to extensive cognitive and neuroimaging databases, and provides the unique and extensive resources of the NIH.

The successful candidate will have a strong background and extensive experience in the neurobiology of dementia and/or age-related cognitive decline, including familiarity with human neuroimaging paradigms. The incumbent will play a major role in training staff and postdoctoral fellows and maintaining research continuity within the laboratory, as well as developing a network of intra- and extramural collaborations. An M.D. or equivalent degree is required and the candidate must be Boarded or Board Eligible.

Salary is commensurate with research experience and accomplishments, and a full Civil service package of benefits (including retirement, health, life and long term care insurance, Thrift Savings Plan participation, etc.) is available. Additional information regarding the NIA, IRP, and the LBN are available at the following website: **http://www.grc.nia.nih.gov**.

To apply: Please send cover letter, curriculum vitae, bibliography, statement of research interest and three letters of recommendation to: **Peggy Grothe, Intramural Program Specialist, Office of the Scientific Director, Vacancy #NIA-IRP-12-02, National Institute on Aging, NIH Biomedical Research Center, 251 Bayview Blvd., Suite 100, Baltimore, Maryland 21224 or e-mail grothep@mail.nih.gov**. Review of applications will begin on or about **April 3, 2012**, but applications will be accepted until the position is filled.

DHHS and NIH are Equal Opportunity Employers. The NIH is dedicated to building a diverse community in its training and employment programs.

MAYO CLINIC

Urologic Cancer Biologist

Heal the sick, advance the science, share the knowledge.

The Department of Urology at Mayo Clinic in Rochester, MN is seeking a talented mid- or senior-level investigator with expertise in the cancer cell and/or molecular biology of urologic cancer. The candidate should have an established track record of publications and sustained extramural funding. Mayo Clinic has an exceptionally strong comprehensive cancer center, over 200 basic and translational biomedical research laboratories, institutionally supported state-of-the-art core facilities and opportunities to readily translate discovery to the bedside. A very competitive start-up package with sustained intramural funding will be provided.

To apply and learn more about this position, Mayo Clinic and Rochester, MN, please visit **www.mayoclinic.org/scientist-jobs/** and reference job posting number **8824BR**. Applications should include a letter of interest, a description of research interests and a curriculum vitae and bibliography.

Specific questions related to the posting should be directed to:

Donald J. Tindall, Ph.D.
Search Committee Chair
Department of Urology
Mayo Clinic
c/o Jennifer Schilbe
E-mail: schilbe.jennifer@mayo.edu

Mayo Foundation is an affirmative action and equal opportunity employer and educator. Post-offer/pre-employment drug screening is required.

Skolkovo Tech

Skolkovo Institute of Science and Technology

The Skolkovo Institute of Science and Technology (SkTech)
and The Massachusetts Institute of Technology (MIT) announce Round One:

Call for International Research Center Proposals

White Paper Deadline: **March 13, 2012**
Invitations to Submit Full Proposal: **April 14, 2012**
Research Awards Announced: **June 30, 2012**

Research Center Proposals:
US $6 million to US $12 million
per center, per year for up to five years

Planning Award Proposals:
US $30,000 for up to one year

Biomedical
Energy
Information
Nuclear
Space

SkTech is a new graduate research university in Russia, launching in collaboration with MIT and the Skolkovo Foundation. SkTech aims to create a pioneering interdisciplinary model for graduate education and research; integrating teaching, research, innovation and entrepreneurship.

Up to 15 research centers will be formed at SkTech. Each research center will be a collaboration among SkTech and both a non-Russian and a Russian participant, and will function as an interdisciplinary international research initiative.

This Call for Proposals is open to Russian and non-Russian universities and research institutions with significant research and educational capacity.

Full details at:
web.mit.edu/SkTech/rc-call

Contact us at:
SkTech-rc-call@mit.edu



POSITIONS OPEN

UNIVERSITY OF ILLINOIS
Hospital & Health Sciences System
Changing medicine. For good.

SECTION CHIEF/DIRECTOR
Hematology & Oncology
College of Medicine,
University of Illinois at Chicago

The Department of Medicine at the University of Illinois at Chicago (UIC) is recruiting a Chief for the Section of Hematology & Oncology. The candidate will lead the clinical Hematology & Oncology Section at the University of Illinois Hospital and Health Sciences System and the Jesse Brown Veterans Affairs Medical Center. We seek an outstanding candidate at or above the **ASSOCIATE PROFESSOR** level with the leadership skills necessary to complement and expand a very strong basic science program with novel clinical translational approaches. There are ample startup funds, research space, administrative offices, and clinical space to expand significantly upon the ongoing programs of excellence within the Section. Please forward your curriculum vitae to: **University of Illinois at Chicago Department of Medicine, Attention: Lauren Walsh, 840 S. Wood Street Room 1023, Chicago, IL 60612** or send as attachment to **e-mail: laurenw@uic.edu.** For additional information on the Section of Hematology & Oncology, please visit **website: http://www.uic.edu/com/dom/hemonc.** *UIC is an Affirmative Action/Equal Opportunity Employer. Women and minorities are encouraged to apply.*

FACULTY—ALL RANKS (CLINICAL)

The Columbia University Center for Motor Neuron Biology and Disease (MNC) and the Eleanor and Lou Gehrig MDA/ALS Research Center seek up to two new faculty members with interests in motor neuron biology and disease, especially amyotrophic lateral sclerosis (ALS). The successful candidate(s) will join a translational program that brings together basic, genetic, clinical, and epidemiological research (**websites: http://www.ColumbiaMNC.org; http://www.cumc.columbia.edu/dept/als; http://www.cumc.columbia.edu/dept/sergievsky**).

For the first position, we are particularly interested in hiring a clinician-scientist who can see ALS patients and in parallel carry out his/her own research program in this area. However, nonclinical candidates with a strong translational program are also invited to apply.

For the second position, we seek a candidate with a strong track record in epidemiology and clinical genetics who is motivated to work on ALS and related disorders.

Appropriate startup packages will be offered. As members of the MNC, faculty will have access to core facilities, including high throughput screening and internal grant programs.

Columbia University has a world-renowned program in neurobiology and behavior and in medical and surgical neurology. Faculty will be affiliated with the Departments of Neurology and/or Pathology and Cell Biology and will interact with other programs and centers, including the Gertrude H. Sergievsky Center.

To apply online, please go to **website: https://academicjobs.columbia.edu/applicants/Central?quickFind=54755.**

Columbia University takes Affirmative Action toward Equal Employment Opportunity.

HARVARD MEDICAL SCHOOL

POSTDOCTORAL POSITION available to study the molecular and cellular mechanisms of Alzheimer's and Parkinson's diseases. Recent Ph.D.s with strong background in molecular biology, biochemistry, or electrophysiology are encouraged to apply. Prior experience in slice physiology, calcium imaging, or mitochondrial analysis is preferred. Send curriculum vitae to **Dr. Jie Shen** (**website: http://www.shenlab.net**) at **e-mail: jshen@rics.bwh.harvard.edu.**

PASTEUR FOUNDATION

POSTDOCTORAL FELLOWSHIPS
Institut Pasteur, Paris, France

Come work in Paris at the Institut Pasteur, the world-renowned, private, biomedical research organization. We invite applications from outstanding Fellowship candidates to any of 130 laboratories within our 10 departments. Areas include: developmental and cell biology, epidemiology, immunology, genomics, genetics, microbiology, neuroscience, structural biology, parasitology, mycology and virology. Next deadline: March 16, 2012. Annual package is $70,000 for three years. *U.S. citizenship required.*

E-mail: pasteurus@aol.com. Website: http://www.pasteurfoundation.org.

FACULTY POSITION
Chemical Biology

The Department of Biochemistry & Molecular Biology at the Drexel University College of Medicine invites applications for a tenure-track faculty position at the **ASSISTANT** or **ASSOCIATE PROFESSOR** level. We seek interactive individuals who are working at the interface of chemistry and biology, using biochemical and/or biophysical approaches to tackle important problems in biology and medicine. Areas of particular interest include protein structure/function, inhibitor/drug design, mechanistic enzymology, metalloproteins, cell signaling, and metabolism. Individuals whose research complements existing strengths in the department (**website: http://www.drexel.edu/med/biochemistry**) are especially encouraged to apply. The Department is conveniently located in Center City Philadelphia, and offers a collegial and stimulating environment with many opportunities for collaboration. Competitive startup funds are available. Successful candidates will have a Ph.D. and/or M.D., relevant postdoctoral experience, and a strong record of research accomplishments. Faculty are expected to establish rigorous, independent, and well-funded research programs and to participate in graduate and medical education.

The Drexel University College of Medicine is the nation's largest private medical school. Drexel University is ranked among the top 100 universities in the nation, and has been named as one of the top "Up-and-Coming" national universities in the 2011 U.S. News College Rankings.

To apply, please submit a single PDF containing curriculum vitae, statement of research interests, statement of teaching philosophy, and names of three references to **e-mail: lucia.boyer@drexelmed.edu;** please include the words "Chemical Biology Search" on the subject line.

DEAN
School of Veterinary Medicine
University of Wisconsin-Madison

The University of Wisconsin-Madison invites applications and nominations for dean of its School of Veterinary Medicine. The dean serves as the chief academic and executive officer of the school with responsibility for faculty and staff development, personnel oversight, fund raising, budget planning and management, curriculum, student academic affairs, clinical resources, facilities development, and has oversight of the Veterinary Medical Teaching Hospital. The school has a budget of $54.5 million, including research expenditures of $20.2 million. Please see **website: http://www.secfac.wisc.edu/searches/VetMedDean/2012/VacancyAnnouncement.htm** for full description and application/nomination information.

Submit electronic applications/nominations to **e-mail: Vet-Med-Dean-Search@secfac.wisc.edu** by 9 March 2012 to ensure consideration.

The University of Wisconsin-Madison is an Equal Opportunity/Affirmative Action Employer.

FACULTY
Department of Cancer Biology

Mayo Clinic in Florida and the Mayo Clinic Comprehensive Cancer Center seek an outstanding investigator in basic cancer research (Ph.D., M.D., or M.D.-Ph.D.) to join the Department of Cancer Biology at the rank of **ASSISTANT, ASSOCIATE,** or **FULL PROFESSOR.** Established in 2003 at the Mayo Clinic in Jacksonville, Florida, the department currently consists of a highly interactive core of NIH-funded faculty working on various aspects of basic and translational tumor biology. Current strengths include expertise in oncogenic signaling mechanisms, molecular mechanisms of carcinogenesis, cancer genomics, oxidative stress signaling, the tumor microenvironment, and molecular mechanisms of invasion and metastasis. The ideal candidate would establish an NCI-funded research program that complements current strengths and expands expertise in cancer stem cell biology, cancer genetics, cell cycle progression and/or mechanisms of cell death, though all qualified candidates will be considered. The Griffin Cancer Research Building is a state-of-the-art facility dedicated to cancer research and provides ample space for future growth. The Mayo Clinic's NCI-designated multi-site Comprehensive Cancer Center facilitates collaborations across all Mayo Clinic sites and provides potential interactions with several associated SPOREs. Interested parties should send a cover letter, curriculum vitae, contact information for three references, and a research program description to **Jenni Bachhofer** (**e-mail: bachhofer.jenni@mayo.edu**), secretary to **Dr. Panos Z. Anastasiadis,** Chair of the Cancer Biology Department. *Mayo Clinic is an Equal Opportunity Employer.*

ASSISTANT PROFESSORSHIP in Neurobiology
Western Washington University

The Biology Department at Western Washington University (WWU), a regional comprehensive university located between Seattle and Vancouver B.C., invites applications for a tenure-track, assistant professor position, beginning September 2012. We seek an individual committed to undergraduate and M.S. education who will establish a vigorous research program that involves students. Ph.D. and postdoctoral experience in neurobiology required. Applicants who can contribute a molecular and cellular approach to our Behavioral Neurosciences program are of particular interest. The applicant must provide evidence of the ability to teach introductory cell and molecular biology and advanced courses in neurobiology and in cell biology or genetics. Review begins February 27, 2012. See full position announcement, including all required qualifications, at **website: http://biol.wwu.edu/biology/.** For application information and instructions, go to the WWU Employment **website: http://www.wwu.edu/jobs.** *Affirmative Action/Equal Opportunity Employer.*

POSTDOCTORAL FELLOWS

The Institute of Marine and Coastal Sciences at Rutgers University is seeking Postdoctoral Fellows in the areas of biological, chemical, geological, and physical oceanography. Prospective candidates should foster creative research avenues and interactions among existing research programs and faculty expertise. These fellowships are one-year renewable appointments. Review of applications will commence on February 15, 2012—applications will continue to be accepted after that time and reviewed on an ongoing basis. To apply, please electronically send curriculum vitae, statement of research interest, and names of three references to **Dr. Richard A. Lutz** (Director, Institute of Marine and Coastal Sciences) **e-mail: postdocsearch@marine.rutgers.edu** (please include "Postdoc" in the subject line).

Fundación BBVA

2012 BBVA Foundation Frontiers of Knowledge Awards

2012 NOMINATIONS NOW OPEN

The **BBVA Foundation Frontiers of Knowledge Awards** are intended to recognize basic research and creative work of excellence, as embedded in theoretical advances, models and fundamental perspectives for an improved understanding of the natural, social and artificial or technological worlds, technological innovations and developments, and the creation of outstanding works or new artistic or interpretative styles in contemporary classical music. Awards also go to significant achievements that advance our understanding or deliver material progress with regard to two key challenges of the global society of the 21st century: climate change and development cooperation.

BBVA Foundation

Plaza de San Nicolás, 4
48005 Bilbao, Spain

Paseo de Recoletos, 10
28001 Madrid, Spain

www.fbbva.es

Categories

— Basic Sciences (Physics, Chemistry, Mathematics)
— Biomedicine
— Ecology and Conservation Biology
— Information and Communication Technologies
— Economics, Finance and Management
— Contemporary Music
— Climate Change
— Development Cooperation

Award content

Awards in each category will comprise €400,000 prize money, a diploma and a commemorative artwork.

Nominations

Nominations can be made by institutions and organizations working in the knowledge areas covered in each category.

Closing date

The closing date for submissions is 23.00 hours GMT on June 30, 2012.

With the collaboration of:
CSIC
CONSEJO SUPERIOR DE INVESTIGACIONES CIENTÍFICAS

More information: www.fbbva.es/awards · awards-info@fbbva.es



Christine - Clinical Research Physician

LILLY IS A EQUAL OPPORTUNITY EMPLOYER

Eli Lilly & Company: *New Lilly China R&D Center in Shanghai*

Biology and Chemistry Leadership Openings for Group Leader and Lab Head Positions

Eli Lilly and Company has an established diabetes franchise with the strategy to commercialize first-in-class and best-in-class treatments to address unmet medical needs. As an integral part of our R&D investment, Lilly has recently established the Lilly China Research & Development Center (LCRDC) in Shanghai, China. The new center will focus primarily on discovering new medicines to treat diabetes and its complications with the aim of improving the health of diabetes patients across the world.

We are seeking seasoned scientific leaders in biology and chemistry who will be involved in building a world-class research organization and who are interested in career development opportunities in China. Requirements include PhD degree and/or MD degree with postdoctoral research experience in relevant fields or at least 5 years of drug hunting experience in metabolic diseases. Strong track record of achievements, excellent communication skills and the ability to work in a team are essential for all positions.

We offer competitive compensation packages and benefits, and provide workforce training and development opportunities.

For application, please send resume and cover letter to YANG_HUI_HY@LILLY.COM

Be connected. Be inspired. **Be a catalyst.**
Visit lilly.com/careers.

Lilly



Nontraditional Careers: Opportunities Away From the Bench

Webinar

Want to learn more about exciting and rewarding careers outside of academic/industrial research? View a roundtable discussion that looks at the various career options open to scientists and strategies you can use to pursue a nonresearch career.

Now Available On Demand
www.sciencecareers.org/webinar

Produced by the *Science*/AAAS Business Office.

Science Careers
From the journal *Science* AAAS

POSITIONS OPEN

BRAZIL FULL PROFESSOR POSITION OPENING
International Institute of Physics

The International Institute of Physics (IIP) together with the Department of Theoretical and Experimental Physics (DFTE) from the Federal University of Rio Grande do Norte (Natal, Brazil) announces the opening of a permanent Full Professor position on the Theory of Emergent Quantum Phenomena in Condensed Matter or in Cold Atoms. This is the first of five permanent IIP/DFTE positions. The selected Full Professor will lead his/her research group and perform his/her research work at the IIP. The IIP has a large number of postdoctoral researchers and visitors and the successful candidate is also encouraged to interact with them. In addition to this, the new Professor will supervise postgraduate students and give regular lecture courses at the DFTE.

The candidates will be selected by the Search Committee: **Konstantin Efetov** (Chair, Bochum University, Germany), **Eduardo Marino** (UFRJ, Brazil), **Dionys Baeriswyl** (University of Fribourg, Switzerland) and **Itamar Procaccia** (Weizmann Institute, Israel).

Application window: from January 16, 2012 until February 24, 2012.

This permanent position entitles the successful candidate to an annual salary of R$ 156.734,00 Brazilian reais (approximately 84.111,84 U.S. dollars) and additional research grants are available from State and National Funding agencies for the participation in scientific meetings in Brazil and abroad.

For more information access our **website: http://www.iip.ufrn.br,** or send enquiries to **e-mail: director@iip.ufrn.br.**

PENN SCHOLARS in Molecular Medicine (Gastroenterology)

The Division of Gastroenterology in the Department of Medicine at the Perelman School of Medicine at the University of Pennsylvania seeks candidates for several **FULL, ASSISTANT,** and/or **ASSOCIATE PROFESSOR** positions in the tenure track. Rank will be commensurate with experience. Applicants must have an M.D or M.D.-Ph.D. degree. B/C, B/E in Internal Medicine.

Through this program, we seek to recruit outstanding physician scientists interested in the interface between basic investigation and translational medicine. Faculty members in the Penn Scholars in Molecular Medicine will have appointments in both the Department of Medicine and the basic science department that most closely corresponds to the investigator's area of research. In addition to providing an environment rich in scientific mentorship and collaboration, appointees to the Penn Scholars in Molecular Medicine program will receive generous start up packages to support the establishment of a robust research program.

The successful applicant will direct a productive, independent basic or translational research program in addition to complementary clinical service and teaching. Applicants are being considered in gastroenterology, hepatology, and related disciplines.

The University of Pennsylvania is an Equal Opportunity/Affirmative Action Employer. Women and minority candidates are strongly encouraged to apply.

Apply for this position online at **website: http://www.med.upenn.edu/apps/faculty_ad/index.php/g/d2833.**

FACULTY POSITIONS
Medical School

The Saint James School of Medicine, an international medical school (**website: http://www.sjsm.org**), invites applications from candidates with teaching and/or research experience in any of the basic medical sciences for its Caribbean campuses.

Senior faculty positions are currently available in Pathology and Anatomy. Applicants must be M.D., D.O., and/or Ph.D.

Teaching experience in the U.S. system is desirable but not required. Retired persons are encouraged to apply. Attractive salary and benefits. Submit curriculum vitae electronically to **e-mail: sjsmcoordinator@sjsm.org** or mail to: **HRDS Inc., 1480 Renaissance Drive. Suite 300, Park Ridge, IL 60068.**

POSITIONS OPEN

ONE ASSISTANT/ASSOCIATE PROFESSOR
Tenure Track
St. John's University College of Pharmacy and Allied Health Professions
Pharmaceutical Sciences

The Department of Pharmaceutical Sciences is seeking applications for the tenure-track position of Assistant/Associate Professor in the Toxicological Sciences with an emphasis in analytical toxicology. An earned Ph.D. is required and postdoctoral experience is preferred. Responsibilities include establishing an active research program that will attract external funding, mentoring students, and teaching graduate and undergraduate students in Toxicology and basic biomedical sciences. The Department has 35 faculty with research interests in medicinal chemistry, toxicology, pharmacology, industrial pharmacy, and biochemistry. The Department offers both the M.S. and Ph.D. degree. Modern instrumentation and AAALAC-accredited facilities are available. This position is subject to a comprehensive background screen, with employment contingent upon satisfactory results. Application letters with curriculum vitae, a statement of teaching philosophy, and three letters of reference should be sent to: **Dr. Louis D. Trombetta, Professor and Chair Department of Pharmaceutical Sciences, St. John's University, 8000 Utopia Parkway, Jamaica, NY 11439. E-mail: trombetl@stjohns.edu.**

St. John's University is an Equal Opportunity Employer and encourages applications from women and minorities.

POSTDOCTORAL FELLOWSHIP
Harvard Medical

We are seeking a motivated individual to join studies on molecular mechanisms of lung injury and repair on animal models of lung disease. We focus on pulmonary hypertension, chronic lung disease, and hypoxic signaling. Current projects explore the therapeutic potential of stem cells on lung disease and the cytoprotective & anti-inflammatory functions of heme oxygenase. The successful candidate will command significant resources to apply cellular, biochemical, and genetic approaches in the study of oxygen-regulated signaling pathways and lung homeostasis. A Ph.D. or equivalent degree is required, and a strong background in molecular biology, biochemistry, or a related discipline is highly desirable. Previous research experience in stem cells, inflammation, or animal models of pulmonary hypertension will complement current research direction. Please mail curriculum vitae and contact information for three references to:

Professor Stella Kourembanas
Department of Pediatrics, Harvard Medical School
Chief, Harvard Division of Neonatology
Children's Hospital Boston
320 Longwood Avenue
Boston, MA 02115

Or send material to **e-mail: sarah.gately@childrens.harvard.edu.**

CHAIR

The Philadelphia College of Pharmacy at University of the Sciences in Philadelphia invites applications for the position of Chair, Department of Pharmaceutical Sciences to begin July 1, 2012. The successful candidate will possess the ability to bring the department to the next level of national recognition and achievement. For a full job description and application details, visit us at **website: http://www.usciences.edu/humanresources/employment.**

Affirmative Action/Equal Opportunity Employer.

MARKETPLACE

Widely Recognized Original & Guaranteed

KlenTaq1

8¢/u Truncated Taq DNA Polymerase Withstand 99°C

US Pat #5,436,149
Call: **Ab Peptides**
Fax: 314•968•8988

e-mail: abpeps@msn.com
1•800•383•3362
www.abpeps.com